REPORT DOCUMENTATION PAGE

AFRL-SR-BL-TR-01-

0432

1. AGENCY USE ONLY (Leave Blank)	2. REPORT DATE 21 May, 2001	3. REPORT TYPE AND DATES COVERED Final Report Oct. 1, 1997 – March 31, 2001

4. TITLE AND SUBTITLE
Identification and Motion Prediction of Tethered Satellite Systems

5. FUNDING NUMBERS
AF-F49620-97-1-0539

6. AUTHOR(S)
David A. Cicci and John E. Cochran, Jr.

7. PERFORMING ORGANIZATION NAME(S) AND ADDRESS(ES)
Auburn University, Aerospace Engineering Dept.,
211 Aerospace Engineering Bldg., Auburn Univ. AL 36849

8. PERFORMING ORGANIZATION REPORT NUMBER

9. SPONSORING / MONITORING AGENCY NAME(S) AND ADDRESS(ES)
Dr. Arje Nachman
AFOSR/NM
801 N. Randolph St.
Room 732
Arlington, VA 22203-1977

10. SPONSORING / MONITORING AGENCY REPORT NUMBER

11. SUPPLEMENTARY NOTES

12 a. DISTRIBUTION / AVAILABILITY STATEMENT

Approved for public release; distribution unlimited.

12 b. DISTRIBUTION CODE

13. ABSTRACT (Maximum 200 words)

This research program addressed the dynamics, estimation, and orbit determination of Tethered Satellite Systems (TSS). In a three year investigation we: (1) considered and reported on the state-of-the-art knowledge regarding TSS identification and motion prediction; (2) reviewed tracking, estimation, and orbit determination algorithms and models currently used by the Air Force; (3) developed algorithms for the detection, quick identification, orbit determination, and tracking of TSS: (4) developed techniques for the accurate prediction of the motions of TSS that have been detected, identified, and tracked; (5) developed methods of detecting changes in the configuration of a TSS; and (6) use the knowledge and experience gained in (1) through (5) above to define and complete additional tasks of interest to the Air Force. Based on the results of both simulated and real data, we have demonstrated that the three-stage orbit determination method developed and presented in this report can indeed be used for the preliminary orbit determination, quick-look identification, and long-term orbit determination and motion prediction of TSS. While the results presented here are encouraging.(cont. P.2)

14. SUBJECT TERMS
Tethered Satellites
Orbit Determination

15. NUMBER OF PAGES
460

16. PRICE CODE

17. SECURITY CLASSIFICATION OR REPORT UNCLASSIFIED	18. SECURITY CLASSIFICATION ON THIS PAGE UNCLASSIFIED	19. SECURITY CLASSIFICATION OF ABSTRACT UNCLASSIFIED	20. LIMITATION OF ABSTRACT UL

20010731 040

GENERAL INSTRUCTIONS FOR COMPLETING SF 298

The Report Documentation Page (RDP) is used for announcing and cataloging reports. It is important that this information be consistent with the rest of the report, particularly the cover and title page. Instructions for filling in each block of the form follow. It is important to **stay within the lines** to meet **optical scanning requirements.**

Block 1. Agency Use Only (Leave blank)

Block 2. Report Date. Full publication date including day, month, and year, if available (e.g. 1 Jan 88). Must cite at least year.

Block 3. Type of Report and Dates Covered. State whether report is interim, final, etc. If applicable enter inclusive report dates (e.g. 10 Jun 87 - 30 Jun 88).

Block 4. Title and Subtitle. A title is taken from the part of the report that provides the most meaningful and complete information. When a report is prepared in more than one volume, repeat the primary title, and volume number, and include subtitle for the specific volume. On classified documents enter the title classification in parentheses.

Block 5. Funding Numbers. To include contract and grant numbers; may include program element number(s) project number(s), task number(s), and work unit number(s). Use the following labels:

C -	Contract	**PR** -	Project
G -	Grant	**TA** -	Task
PE -	Program Element	**WU** -	Work Unit Accession No.

Block 6. Author(s). Name(s) of person(s) responsible for writing the report, performing the research, or credited with the content of the report. If editor or compiler, this should follow the name(s).

Block 7. Performing Organization Name(s) and Address(es). Self-explanatory.

Block 8. Performing Organization Report Number. Enter the unique alphanumeric report number(s) assigned by the organization performing the report.

Block 9. Sponsoring/Monitoring Agency Name(s) and Address(es) Self-explanatory.

Block 10. Sponsoring/Monitoring Agency Report Number. (if known)

Block 11. Supplementary Notes. Enter information not included elsewhere such as; prepared in cooperation with....; Trans. of...; To be published in.... When a report is revised, include a statement whether the new report supersedes or supplements the older report.

Block 12a. Distribution/Availability Statement. Denotes public availability or limitations. Cite any availability to the public. Enter additional limitations or special markings in all capitals (e.g. NORFORN, REL, ITAR).

DOD	-	See DoDD 4230.25, "Distribution Statements on Technical Documents."
DOE	-	See authorities.
NASA	-	See Handbook NHB 2200.2.
NTIS	-	Leave blank.

Block 12b. Distribution Code.

DOD	-	Leave Blank
DOE	-	Enter DOE distribution categories from the Standard Distribution for unclassified Scientific and Technical Reports
NASA	-	Leave Blank.
NTIS	-	Leave Blank.

Block 13. Abstract. Include a brief (*Maximum 200 words*) factual summary of the most significant information contained in the report.

Block 14. Subject Terms. Keywords or phrases identifying major subject in the report.

Block 15. Number of Pages. Enter the total number of pages.

Block 16. Price Code. Enter appropriate price code (NTIS *only*).

Block 17. - 19. Security Classifications. Self-explanatory. Enter U.S. Security Regulations (i.e., UNCLASSIFIED). If form contains classified information, stamp classification on the top and bottom of the page.

Block 20. Limitation of Abstract. This block must be completed to assign a limitation to the abstract. Enter either UL (Unlimited) or SAR (same as report). An entry in this block is necessary if the abstract is to be limited. If blank, the abstract is assumed to be unlimited.

additonal work is clearly needed in order to verify, test, and develop these new techniques to achieve software package which will be operationally useful.

IDENTIFICATION AND MOTION PREDICTION OF TETHERED SATELLITE SYSTEMS

Principal Investigators: Dr. David A Cicci
                             Professor
                             dcicci@eng.auburn.edu

                             Dr. John E. Cochran, Jr.
                             Professor and Head
                             jcochran@eng.auburn.edu

                             Aerospace Engineering Department
                             211 Aerospace Engineering Building
                             Auburn University, AL 36849-5338
                             (334) 844-4874
                             (334) 844-6803 (FAX)

FINAL REPORT
October 1, 1997 – March 31, 2001

(This page was intentionally left blank.)

TABLE OF CONTENTS

(This page was intentionally left blank.)

IDENTIFICATION AND MOTION PREDICTION
OF TETHERED SATELLITE SYSTEMS

RESEARCH PROGRAM

This research program addressed the dynamics, estimation, and orbit determination of Tethered Satellite Systems (TSS). In a three year investigation we proposed to: (1) consider and report on the state-of-the-art knowledge regarding TSS identification and motion prediction; (2) review tracking, estimation, and orbit determination algorithms and models currently used by the U.S. Air Force; (3) develop algorithms for the detection, quick identification, orbit determination, and tracking of TSS; (4) develop techniques for the accurate prediction of the motions of TSS that have been detected, identified, and tracked; (5) develop methods of detecting changes in the configuration of an identified TSS; and (6) use the knowledge and experience gained in (1) through (5) above to define and complete additional tasks of interest to the U.S. Air Force. We have addressed all of the above items.

Motivation for this research came from U.S. Air Force personnel [1], who see immediate and future applicability of the anticipated results. Since it appears certain that there will be more TSS flown by the United States, it is highly foreseeable that future TSS will not belong to the United States. But in all cases, the TSS must be detected, identified, tracked, and their future motion predicted for many reasons, including national defense.

Although the analytical investigations of TSS have been numerous and much has been learned about the dynamic behavior of two-body and multi-body tethered systems, there are still some characteristics of TSS that make their deployment a concern and perhaps a significant problem. The main reason for academic, NASA, and U.S. Air Force interest in TSS is that these dynamical characteristics of TSS are significantly different from those of individual conventional satellites. Some of these characteristics are embodied in the non-Keplerian motion of the members of a two-body TSS orbiting the Earth in a "gravity-gradient" mode. If the motion of the lower satellite is predicted on the basis of conventional observations made over a relatively short period of time, this satellite may appear to be on a re-entry trajectory, when, in reality, it is orbiting with the other members of the system. Depending on the relative sizes of the masses of the satellites, the higher satellite, when considered to be a single satellite, may be traveling at a much greater speed than its altitude would indicate. Thus, in the absence of a priori knowledge that the satellites are tethered, the tracking entity may predict incorrect orbits of the satellites. This incorrect orbit prediction could likely result in the misidentification of a tethered satellite as a ballistic missile. Indeed, this scenario would create significant interest on the part of those responsible for ballistic missile defense activities.

Several investigators have considered the manner in which an unknown tethered condition may lead to anomalous results. Hoots, et al. [2] showed that a "modified" gravitational parameter could cause a tethered satellite to behave as an untethered one might behave. Hence, during the prediction of the orbit of a tethered satellite that is assumed to be untethered using software which only estimates the satellite state, erroneous results may be obtained. Motivated by [2], Kessler and Cicci [3] considered estimation of the gravitational parameter as a means of

determining whether or not a satellite is tethered. Their model was that of a "gravity-gradient stabilized" two-body system with a non-extensible tether. That is, the two satellites always remained along a local vertical. In addition, they found that inclusion of the ballistic coefficient and tether acceleration in the state vector, along with the gravitational parameter, provided a method that could accurately determine the length of the tether as well. In a later work, Cochran, et al. [4], consider the motion of one of the satellites in a two-body TSS being perturbed by the presence of the other. This point of view is necessary if the orbits of the satellites in such a system are to be determined correctly when they are not known a priori to be tethered. Using the observations of a single satellite, but a dynamical model which allows for the possibility of a TSS, the "apparent" gravitational constant was derived in [4] for a non-librating two-body TSS. A two-stage process is subsequently applied to the identification and motion prediction of the two-body TSS.

Additional confusion may arise if a two-body TSS is rotating about its center-of-mass, i.e., the individual satellites exchange lower and higher positions. Very unusual two-body orbits of the individual members of the orbiting, rotating pair may be predicted in such cases. The technical analyses provided in [2-4] are preliminary in nature, but reveal the fact that new methods are needed for detecting, identifying, tracking, and predicting the motions of TSS.

An additional complication to this scenario is that identification of the satellite as part of a TSS must be done very quickly, using observations over a very short time period. This type of "quick-look" orbit determination problem and its associated difficulties are described by Cicci and Hall [5]. The primary difficulty in the solution of this problem arises from the fact that when trying to determine the orbit of a satellite with only a minimum amount of observational data, mathematical ill-conditioning in the problem solution occurs. This ill-conditioning often results in errors in the orbit determination and subsequent identification of the satellite. Advanced orbit determination methods that are termed "ridge-type estimation methods," have been developed by Cicci and Tapley [6] and Cicci [7, 8] which can be applied in order to obtain improved accuracy in ill-conditioned problems. Cicci and Hall [5] have demonstrated the feasibility of these methods in the quick-look orbit determination of non-tethered satellites. In addition, they have shown that the accuracy of the prediction of future motion of such a satellite can be greatly improved over conventional analysis techniques by the use of these ridge-type estimation methods.

Another interesting dynamical characteristic of TSS is that by partially retrieving and deploying the subsatellite of a two-body system in a periodic manner, energy may be pumped into the system in the form of libration, or swinging motion, of the payload. In such a swinging state, the payload will exhibit very non-Keplerian motion. If the tether is cut at the appropriate time in a libration cycle, the payload will enter an orbit with an apogee that is higher than the minimum altitude of the payload in the swinging mode. If the payload has not been identified as a part of a TSS, this type of motion will likely cause a great deal of excitement among those who track objects in Earth orbit. If the proper algorithms are available and the payload has been properly identified, then its new orbit can be readily calculated, and the object can be correctly identified, and informed decisions can be made regarding its purpose.

2

A third scenario should also be considered. The tether may be cut or broken at the primary satellite, leaving the tether, which may have considerable mass, attached to the payload. Warnock and Cochran [9, 10] have shown that the motion of the payload and its tether may be very different from that of the payload alone and hence the current lifetime prediction software used for conventional satellites will not be applicable to such a system. Failure of these currently used methods could again be cause for great concern in the tracking and identification of these objects.

Even though TSS will probably be launched and utilized with increasing frequency in the foreseeable future, it appears that very little work has been undertaken concerning the specific problems described above. In the sections below, we present the results of our effort to provide the tools that will be needed to address these TSS identification and motion prediction problems. This report will, we hope, make it clear that the problems involved in this research program are significantly more complex than the usual type of satellite attitude dynamics and determination problems. They are arguably more complex than those involved in the deployment and retrieval of tethered satellites. The foreseeable number of tethered satellite configurations both planned and accidental and the prospects of having to track TSS for many years make this problem one that will require significant future research efforts in addition to this research program.

RESEARCH OBJECTIVES

The objectives of this research program as originally stated were to:

1. Consider and report on the state-of-the-art knowledge regarding TSS identification and motion prediction.
2. Review tracking and orbit determination algorithms and models currently in use by the U.S. Air Force.
3. Develop algorithms for the detection, quick identification, orbit determination, and tracking of TSS.
4. Develop techniques for the accurate prediction of the motions of TSS that have been detected, identified, and tracked.
5. Develop methods of detecting changes in the configuration of an identified TSS.
6. Use the knowledge and experience gained in Phases 1 through 5 to define and complete additional tasks of interest to the U.S. Air Force.

These objectives were addressed through the research program discussed in the following pages.

ACCOMPLISHMENTS

The major accomplishments towards the objectives of this research program are discussed below. The results of new methodologies described here will be presented in the Research Results section which follows.

Objective 1: State-of-the-art Knowledge in TSS Identification and Motion Prediction

During the first year, we performed an extensive search of the literature on tethered satellites that relates to their dynamics. In our search, we focused on references that deal with the mathematical modeling, motion determination, motion prediction, and identification of unknown system characteristics, such as the masses of the satellites and the tether and the tether length. Although some of the available literature deals with more than two satellites tethered together, our interest was primarily two-satellite systems. References addressing the history of tethered satellites and the mathematical modeling of tethered satellite systems were numerous. Prior to the work performed as part of this project, only a few articles addressed the orbit determination and tracking of tethered satellite systems. The orbit determination procedures discussed in these publications assumed that the object being tracked was known a priori to be part of a tethered satellite system. In addition, these methods used tracking data from both end satellites. No references were found which addressed the solution of the identification problem using real data.

Near the end of this research program, the results obtained from the literature search made during the first year were updated to include any additional relevant references which were published after 1995. In addition, publications generated during this research program have added substantially to the body of literature on the subject, especially in the areas of orbit determination procedures and tethered satellite identification. The original list of reference has subsequently been updated to include these latest pertinent papers, including the ones generated during this study, and is provided in Appendix A.

Objective 2: Review of Current Tracking and Orbit Determination Algorithms and Models Currently Used by the U.S. Air Force

In December of 1997, the Principal Investigators traveled to Colorado Springs, Colorado to participate in a Tethered Satellite Technical Interchange Meeting. Drs. Joseph Liu and Robert Racca of the Space Warfare Center at Schriever Air Force Base were the organizers of the meeting. Briefings were presented by various organizations on the physics of tethers, previous and future tethered satellite research projects, and the problems associated with the detection and tracking of tethered satellites in actual operations. The Principal Investigators presented summaries of their work to date on the motion determination and mathematical modeling of two-satellite tethered systems. The Principal Investigators visited the Cheyenne Mountain installation and discussed current space surveillance operations and procedures.

Objective 3: Develop Algorithms for the Detection, Quick Identification, Orbit Determination, and Tracking of TSS

In addressing this objective, we developed new algorithms for the detection, quick identification, orbit determination, and tracking of two-satellite TSS. This work is part of a three-stage analysis methodology which incorporates preliminary orbit determination methods, quick-look identification and orbit determination methods, and long-term orbit determination and orbit prediction techniques. The first two stages of this methodology address Objective 3, while the third stage addresses Objective 3. This proposed methodology, when implemented, will have the capability to quickly identify an observed satellite as being part of a TSS and to accurately predict its long-term motion. Output generated from the 1st Stage (preliminary orbit determination) is used as input into the 2nd Stage (quick-look identification and orbit determination), and output from the 2nd Stage is subsequently used as input into the 3rd Stage (long-term orbit determination and prediction). This methodology is depicted in Figure 1 below.
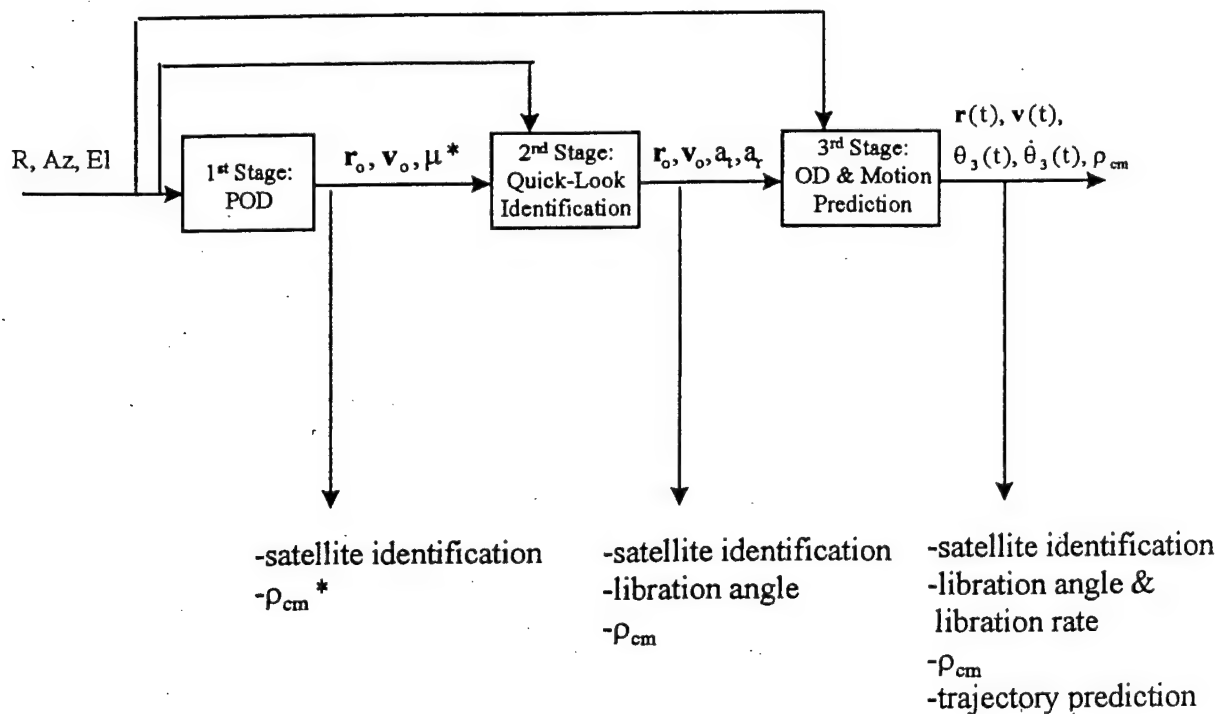

Figure 1. Three stage TSS Identification and Orbit Determination Method

One of the desired outcomes of this research program is the utilization of the algorithms developed in this phase can be implemented in an early warning/detection process for the

identification of orbiting objects which may appear to be on a re-entry trajectory. The concept to accomplish this task can be described using Figure 2 below, which illustrates the tangential and radial tether force components acting on the lower mass of a TSS, with the tether force on the upper mass understood to be oppositely directed.
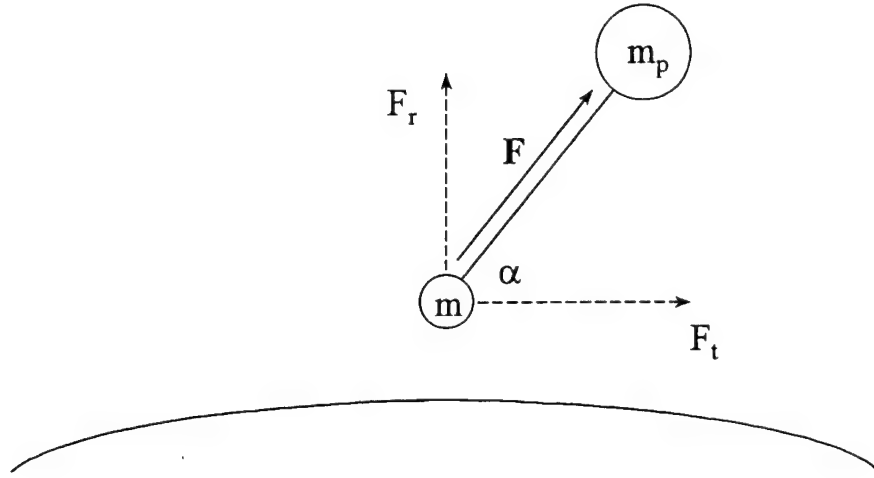
Figure 2. Tethered Satellite System

In [13] a TSS model without libration is used to show how the radial tether force creates an "apparent mu," denoted μ^*, which effectively incorporates all of the radial acceleration due to the tether force into the standard two-body gravitational force. The μ^* for the lower mass of a TSS is less than the conventional μ, while for the upper mass, μ^* is greater than μ. A conventional satellite estimation technique does not account for the tether force, thus it perceives a tethered object as an untethered (Keplerian) body whose orbit is governed by μ^*. Hence, such a method will interpret the lower mass of a TSS as being on a smaller orbit (smaller semi-major axis) than it actually is, and the upper mass as being on an orbit larger than its true orbit. For an identification method equipped with only a conventional filter, this observed mass can be incorrectly identified as being on a re-entry trajectory.

This possible misidentification was illustrated in [2], for the case of circular motion of the center of mass of a TSS with no libration. However, more general motion of the TSS is modeled and investigated here. In the spirit of previous work [14, 21], we desired to generate analytical results, approximate or not, whenever possible. Furthermore, several scenarios were explored wherein the identification method consists of a filtering technique for tethered satellites, rather than a conventional filter. In [11], a classical orbit determination technique was modified for application to a TSS. This method, rather than having a TSS dynamic model embedded within

7

it, employs a simple Keplerian model of an untethered satellite, with the tether effects treated as perturbation accelerations. The technique estimates position and velocity of the mass being observed, as well as the components of tether acceleration tangential and radial to the path of the observed mass. From the radial tether acceleration, the length of the tether from the mass to the center of mass of the TSS was estimated, as well as μ^*. In many cases, this allows the above discrepancy to be avoided. However, since the filter does not contain a full dynamic model of a TSS, certain finer aspects of tethered motion, such as librational motion, cannot be captured. Thus it is important in this analysis to determine what effect libration and other such effects characteristic of tethered systems have on the re-entry discrepancy.

Several particular cases of tethered satellite motion were investigated, assuming an orbit determination method based on a two-body model, as well as one based on a non-librating tethered satellite model. It was found that both the force due to the tether and the librational motion of a TSS can play a significant role in causing a body to appear as though it were on a re-entry path, even though it is not. Consequently, an orbit determination method that includes libration of a tethered system must be used, and over a sufficiently longer period of time, to assure the unambiguous determination of eminent re-entry of a tethered satellite.

A summary of the major accomplishments of this research program in the areas of preliminary orbit determination methods, quick-look orbit determination methods, and long-term orbit determination and orbit prediction is provided below. Actual results of the algorithms' applications to both simulated and TiPS data are presented in the Resuts Section which follows this Accomplishments Section.

1st Stage: Preliminary Orbit Determination

Although there are many preliminary orbit determination (POD) methods in use today, they are unable to distinguish between Keplerian and tethered satellites. In order to address this problem, modifications were made to four POD methods: Herrick-Gibbs [15], ninth-order f and g series [16, 17], iteration on the true anomaly [16-18], and iteration on the semi-parameter, p [16-18]. Current methods require two or more position vectors and their respective times with which to determine the orbital elements. The modifications to the methods still require the same types of input, however both the orbital elements and a modified gravitational parameter are determined in the POD process. This calculated gravitational parameter can then be used to distinguish between a tethered and an untethered satellite.

The POD methods in use today assume Keplerian motion and thus use the standard value for the gravitational parameter. Since the tether force modifies the motion of a satellite, the standard value cannot be used with TSS to determine the motion. To allow for this modified motion, all equations used in the methods were rewritten as functions of the gravitational parameter. These new equations, along with Kepler's equation and a root-finding technique, such as the Secant Method or the Newton-Raphson Method, allow for the calculation of the gravitational parameter as well as the corresponding orbital elements.

The performance of these modified methods was evaluated for cases using simulated Keplerian, tethered, and corrupted tethered data. Results presented by Qualls and Cicci [25]

8

show that the p-iteration technique consistently produced smaller errors than the other POD methods for cases which included small noise levels using a simplified data generation model, i.e., no libration or Earth oblateness effects included. For more realistic dynamical effects including libration and operational levels of noise, the ninth-order f and g series consistently provided more accurate results. This method is therefore the method of choice in the proposed preliminary orbit determination procedure proposed for the 1st-Stage POD procedure resulting from this study.

2nd Stage: Quick-Look Identification and Orbit Determination

The work discussed in this section involves the development of a method for the state estimation of an object that is part of a TSS. This method is developed with capabilities to quickly identify observed objects as being part of a TSS. A simple Keplerian model of an untethered satellite is utilized, with the tether effects treated as perturbational accelerations. Appendix B contains the equations of motion for this model.

In an earlier work [3], the goal was simply to distinguish between Keplerian and modified Keplerian motion. Since that time, the goal was extended, not only to identify a tethered object but to quantify the tether force and possibly extract other information about the TSS, such as tether length, and to do so over as short of a period of time as possible.

Although this batch filter has been developed to identify tethered satellites, its performance has indicated that shorter data arcs produce inaccurate solutions. These inaccurate solutions are due to the fact that the problem becomes more ill-conditioned as the data arcs become shorter. Previous studies of ill-conditioned orbit determination problems have shown that ridge-type estimation methods are able to improve solution accuracy [6, 9].

Ridge-type estimation methods are able to produce more accurate solutions by decreasing the total variance of the estimates. The decrease in the total variance of the estimates is achieved by adding a small amount of bias to the solution. Although this addition of bias results in a poorer data fit, the overall solution accuracy is improved in cases such as those using shorter data arcs. These ridge-type techniques have recently been included in the batch filter as a method of improving solutions obtained using shorter data arcs [5, 8].

Instead of using the conventional minimum variance solution for the state correction, the filter uses a ridge-type estimator solution form. This ridge-type estimator allows the addition of bias to the solution through the use of a diagonal matrix of biasing parameters. The purpose of these biasing parameters is to allow for a more well-conditioned system by increasing the size of each eigenvalue of the normal matrix. This increase will decrease the total variance of the solution while increasing the RMS.

This ridge-type filter has the capability of producing three separate ridge solutions. The three solutions are produced using the following biasing parameter variations:

    a. Single - the averaging of the biasing parameters over all variables comprising the state vector,

9

b. Multiple - individual biasing parameters for each variable comprising the state vector,

c. Variable-type - the averaging of the biasing parameters over different types of model variables.

The resulting filter uses a combination of the single and multiple biasing parameter solutions for stability. This filter was developed in order to estimate the following quantities: x, y, z, v_x, v_y, v_z, a_t, and a_r; where a_t and a_r represent the components of tether acceleration, tangential and radial, respectively, to the path of the daughter mass. Although these components will vary somewhat due to libration, in the current version of the filter they are assumed to be constant during the short observation times considered.

A complete discussion of this filter is given in [26]. Obviously, if a_r and a_t are both equal to zero, to within some specified tolerance, the satellite can be assumed untethered and it can be considered to exhibit Keplerian motion. If a_r and a_t are not equal to zero, the magnitude and direction of the tether force (thus the libration angle) can be determined. In addition, knowledge of a_r allows the determination of the distance from the satellite to the center of mass of the system. This quantity approaches the actual tether length as the ratio of the daughter mass to the parent mass gets small.

To investigate the filter's performance on sample observation data, the "massless rod tether" model was used to simulate several tethered configurations. From these simulation results, position data for the daughter mass was translated into range, azimuth, and elevation data (relative to a tracking station at a chosen location on the Earth) to be utilized by the filter.

In [26], a "baseline" TSS configuration has been defined, in terms of initial orbital and librational states, masses and tether length. From this baseline scenario, a number a different scenarios were constructed for analysis by varying such parameters as: tether length, orientation of the masses, observation time/sampling rate, types of observational quantities utilized, and amount of initial libration. In addition, the baseline observational data was corrupted with various levels of Gaussian noise to simulate tracking station measurement error. The results of this 2nd Stage filter are very encouraging and the solutions show a high degree of accuracy in terms of the RMS of the observation residuals and the estimated tether length to the center-of-mass of the TSS.

The results were compared by studying the solution, RMS, and the calculated value of the length of the tether to the TSS center-of-mass. Analysis of these quantities indicates that ridge-type methods improve minimum variance results for cases with shorter tether lengths, higher noise levels, and shorter observation spans. This improvement is expected because these cases tend to be more ill-conditioned than those with lower noise levels and longer observation spans.

10

Objective 4: Develop Techniques for the Accurate Prediction of the Motions of TSS

This objective was addressed with the development of methods and algorithms which can be used in the prediction of the motion of TSS. While the quick-look filter can accomplish the identification and orbit determination of a TSS using a simplified dynamical model, long-term motion prediction requires the use of a more enhanced dynamical model, including the non-sphericity of the Earth and librational motion. Efforts in satisfying this objective therefore addressed the enhanced modeling for the 3rd Stage of the filtering process, the long-term estimation and motion prediction, and is discussed below

3rd Stage: Long-Term Orbit Determination and Motion Prediction

Once accurate information on the initial conditions and tether specific parameters is obtained from the 2nd Stage filter, a long-term orbit determination filter containing an enhanced dynamical model is used to obtain a more exact solution as well as to predict the future motion of the TSS. Unlike the quick-look filter, which models a single mass with a constant tether force acting on it, the long-term filter models the complete librating two-mass system. This enhanced model is based on that presented in [4, 13] and accounts for both the in-plane libration and libration-rate. Appendix B also contains the equations of motion for this model.

This 3rd Stage process is designed to use a substantial set of observational data encompassing at least one-half of an orbital period or longer. As a result, a standard minimum variance batch filter can be used without the need to incorporate ridge-type estimation methods as was done in the quick-look process described above. The state vector for this filter consists of the initial position and velocity components, the in-plane libration angle, the in-plane libration-rate, and ρ_{cm}. Once these accurate estimates of the initial conditions are obtained in the filtering process, these quantities can subsequently be used in the dynamical model to predict the long-term motion beyond the available observation arcs.

Analytical Approximations

Additional studies have been performed in the development of analytical approximations for the orbital and librational motions of the tethered satellite system [4, 13]. "Restricted tether motion" equations have been obtained that embody the dominant characteristics of the orbital motion of the tethered satellite system by neglecting librational motion in previous reports. An exact analytical solution to the restricted tether motion equations has also been presented. This work was continued and the equations that govern planar motion of a two-satellite tethered system including the librational motion have been investigated [14]. An approximate solution to the restricted tether problem was found by applying the general method of averaging and was used to obtain an approximate solution for small amplitude librational motion. This approximate solution is considered a better mathematical form to use. A combination of analytic methods was used to obtain approximate analytical solution for the librational motion. The analytical solutions were very good approximations to the orbital motion of the tether-perturbed satellite and the libration of the perturbing satellite. Furthermore, an apparent orbit that is a projection of the tethered satellite motion onto an elliptic orbit was introduced. This elliptic orbit was obtained by using the exact solution to the restricted tether motion equation. An apparent semi-

major axis and an apparent eccentricity were introduced to describe the apparent elliptic orbit of a two-satellite tethered system. The solutions provide considerable insight regarding the principal motion of two-satellite tethered systems. The restricted tether motion has been utilized to solve the identification and state determination problem of TSS [20]. Difficulties were caused by the facts that no direct information of the librational motion is provided in the observations and the effects of libration on the observed satellite are often very small

An investigation of an alternative dynamic model of a two-satellite TSS was carried out. The model of a dynamic system used in an estimation process to identify and/or determine the motion of the system can have a significant impact on the success of the estimation process. This study includes the use of the center of mass motion of a two-satellite tethered system for state estimation [21]. The motion of the center of mass of the system of a two-satellite tethered system is much more Keplerian than that of either of the two satellites. The equations of motion include the center of mass and the observed satellite therefore. Numerical and analytical solutions to the equations of motion of the observed satellite referenced from the center of mass of the system were compared with the direct formulation used in previous research. Both formulations may be used to approximate the motion of a two-satellite tethered system for small librational motion. However, the formulation using the center of mass motion provides simpler and more accurate approximate equations that may be solved analytically for small libration angles. On the other hand, both formulations provide practically the same detection/state estimation results for the short observational periods.

Observability Studies

One study which was performed was the analysis of the information $\mathbf{H}^T\mathbf{H}$ matrix generated for each model, for purposes of evaluating the observability of TSS motion in the context of orbit determination. A study of the information matrix was conducted whereby the partial derivatives comprising the $\mathbf{H}$ matrix were calculated numerically rather than analytically. This calculation procedure is described in [12], as well as a full discussion of the numerical sensitivity study of the information matrix. The TSS model used was the "massless rod tether" model, which includes the capability to model the effects of Earth's oblateness as well as drag and is detailed in [4, 13].

For this study, observation data (both range and range-rate) was generated from multiple tracking station locations for the daughter mass of a TSS for one-sixteenth of a period. The data was generated using the model both with and without the effects of oblateness and drag. The estimation vector consisted of various combinations of the orbital and librational states, along with the satellite masses and tether length. As expected, increasing observation time, using multiple tracking stations, using range-rate as well as range measurements, and including drag in the model all tended to improve the conditioning of the information matrix. In addition, when drag was included in the data generation model, the condition number of the complete estimation vector (containing orbital and librational states, both satellite masses, and tether length) took on "reasonable" values. This implies that it may be possible to estimate the satellite masses and tether length independently of one another.

12

Also, a batch estimation routine was used to process the observation data, via numerical calculation of the H matrix as before. Using the model that includes both oblateness and drag, range and range rate data from three tracking stations were processed for one-eighth of a period. The procedure was carried out for three different choices of the estimation vector: orbital states only; orbital plus librational states; and orbital and librational states, plus both masses and tether length. The RMS of the observation residuals takes on a reasonably small value in each case.

Objective 5: Develop Methods for Detecting Changes in the Configuration of TSS

The characteristics of TSS configuration changes were studied to address this objective. As the relative positions of the tethered bodies change within the TSS, the dynamical properties of each of the members will also change. In order to detect changes in the configuration of a TSS, robust estimation methods must be developed. Different estimation models and different types of filters will be required and their performance will be analyzed and compared. Depending on which elements are included in the state vector of the filter, performance regarding the detection of changes in the TSS configuration will vary greatly from one filter to another. Since methods exist for determining the tether length in TSS, one possible filtering concept could take into account the rate-of-change of the tether length. By monitoring the tether length, it may be possible to determine certain aspects of the configuration. Other aspects such as out-of-plane orientation, rotation, and libration must also be determined as discussed in [28].

More importantly, new analysis methods will be able to determine if a tether has been cut or disconnected from the TSS resulting in a new free-flying (non-tethered) satellite. Once it has been determined that a tether has been cut or disconnected, it becomes equally as important to analyze the separate motion of each mass. The work undertaken in addressing this objective deals with studying the dynamics and stability of a mass connected to a trailing tether and is described below. Due to the anticipated complexity of this problem, this research area must be addressed in a much more significant level in a follow-on research program.

Dynamics and Stability of a Satellite and Trailing Tether

The goal of this study was to better understand the dynamics of a satellite trailing a tether. Such a scenario may occur when the tether connecting two satellites is cut as a result of an accident or a planned maneuver. The dynamics of such a system are extremely complicated. However, the relative equilibrium states of the tether trailing satellite can be obtained numerically, and in some cases, even analytically. The problem of predicting the motion of such a system can be significantly aided if the tether trailing satellite was known to admit periodic motions about such states. In this study, the conditions for the existence of such motions were derived analytically.

The main objective here was to apply some recent advances in the theory of nonlinear partial differential equations to an applied problem in dynamics. The well-known Leray-Schauder degree theory [22, 23] was the main tool used in obtaining the results. This theory was first applied in order to prove the existence of solutions of nonlinear PDEs by E. M. Landesman and A. C. Lazer in the 1970's. At first, the theory was used to research elliptic PDEs, which are

13

mostly used to describe chemical processes. However, it was recently implemented [5,24] to prove periodic solvability of parabolic and hyperbolic PDEs, which are widely used in dynamic modeling. The Leray-Schauder degree theory was employed in this study in order to prove the existence of periodic solutions for a system of perturbed hyperbolic PDEs, which model the motion of a linearly extensible tether in a rotating coordinate system. The tethered system was assumed to be influenced by the Earth's gravitational attraction, nonspherical Earth (oblateness) and atmospheric drag.

The primary results of this study was that the modern theory of nonlinear partial differential equations was applied to analyze the dynamics of a tether trailing satellite. Moreover, the gravitational and oblateness forces did not have to be linearized about the relative equilibrium states. Analysis produced several important results:

a. In the case when the system is influenced exclusively by the gravitational and oblateness forces, existence of periodic solutions does not depend on the relative equilibrium state. Existence of such motions depends solely on the physical characteristics of the tether (density, length, flexibility), and the system's rotational speed. It is evident that less flexible, shorter tethers will admit periodic motions about their equilibrium states.

b. If atmospheric drag is influencing the system, then the effects of drag must be bounded for the system to have a periodic motion. In this case, periodic behavior of the tether trailing satellite will heavily depend on the equilibrium state, as well as on tether parameters.

c. The difference in the above results can be easily explained by the fundamental properties of the forces involved. The effect of gravitational and oblateness forces is *uniformly bounded* independently of the position of an object in space. However, the drag forces do not follow the same pattern, and consequently required linearization about the equilibrium states.

d. The mathematical results obtained can be easily generalized in the case of any bounded forcing and/or forces with linear growth. Existence of periiodic motions with bounded forces will depend on tether parameters only, and in the case of unbounded (linear growth) will depend on equilibrium states.

Objective 6: Use the knowledge and experience gained in addressing Objectives 1- 5 to define and complete additional tasks of interest to the U.S. Air Force.

Interaction with Air Force personnel throughout this contract period resulted in many suggestions regarding the direction and focus of this research program. All of these suggestions were considered and implemented, if feasible, in addressing Objectives 1-5 above. Time and budgetary constraints limited examination of tasks of interest of a more complex nature however. The tasks which were identified but could not be addressed in this study are included in the Recommendations for Future Research regarding the further development of identification and

orbit determination methods for tethered satellites. Completion of these tasks is essential for the utilization of the methodologies developed during this research program in an operational environment.

RESEARCH RESULTS

In order to demonstrate the feasibility of this Three-Stage TSS Identification and Orbit Determination Method developed under this research program, test cases using both simulated data and data from an actual TSS were evaluated. The TSS data used for the analysis was a limited about of data obtained from the Tether Physics and Survivability Satellite (TiPS) Experiment [13].

Simulated Data Test Cases

For the test cases using simulated data, the performance of the method was evaluated for a total of 129 TSS scenarios involving differing tether lengths, orientations, observation noise levels, and observation arcs. The value of 10 for the mass ratio m_p/m was used and measurements were provided in the form of range, azimuth angle, and elevation angle for all cases studied. The particular test case combinations which were evaluated are shown in Table 1 below.

Table 1. Simulated Data Test Cases

Tether Lengths (ρ)	0 km, 1 km, 10 km, 50 km, 1 km up, 10 km up
Observation Error (σ), Range/Angles	5 m/0.002° (low), 25 m/0.01°(med), 50 m/0.02° (high)
In-Plane Libration Angle (α)	0°, 5°, 10°
Observation Arc (Δt)	5 min, 10 min, 15 min

The results obtained for these cases are provided in Tables 3-18. These results include the values of ρ_{cm}* for the 1st Stage and the values of Root Mean Square (RMS) error and ρ_{cm} for the 2nd Stage and 3rd Stage filters. The RMS calculations were normalized using the known observation error statistics so that all values approximately equal to 1.0 indicate a good solution fit with the data. The values of ρ_{cm}* and ρ_{cm} reported provide an indication of the overall solution accuracy as well as the ability of each particular phase to identify whether an observed satellite is part of a TSS.

The 1st Stage (POD) filter requires three position vectors which are each 60 to 80 seconds apart in order to obtain the best results. A time span smaller than this is not recommended. As can be seen from the results, there is significant error present in the calculation of ρ_{cm}* and definitive identification is generally not possible. However, the results obtained during the POD stage do provide a sufficiently accurate set of initial conditions input into the 2nd Stage (Quick-Look) filter, which can be used to obtain a substantially more accurate solution.

The 2nd Stage filter was tested using three different time spans: 5, 10, and 15 minutes of observational data. The results show that the filter produces the most accurate results when

using 10 or 15 minutes of data. For the shorter tether lengths a 10 minute time span produces the best result while the 10 km and 50 km tethers require 15 minutes of data when libration is included. The filter is able to produce accurate results regardless of the observation error level or the amount of libration present. Time spans of 5 minutes or less are not recommended due to sufficiently inaccurate results. If at least 10 minutes of data is processed, identification of the tracked satellite as to whether or not it is part of a TSS can almost certainly be made, as can be seen by comparing the calculated value of ρ_{cm} with the actual value. In addition, the RMS of the solution indicates the fit to the observational data is quite good for this phase and provides a substantially improved set of initial conditions for input into the 3rd Stage (Long-Term) filter.

The 3rd Stage filter performs a long-term orbit determination when data beyond the 10-15 minutes used in the 2nd Stage is available. To demonstrate the effectiveness of this stage, data arcs equal to ½ the orbital period and a full orbital period are processed. Results show that, if the initial conditions used were obtained from 10-15 minutes of data during 2nd Stage processing, solution accuracies are quite good for all noise levels and libration angles considered. The state vector, ρ_{cm}, and the libration parameters are accurately determined and the resulting RMS of the fit is quite close to 1.0. The accurate prediction of the future motion of the TSS can subsequently be achieved.

Table 3. Simulated Data: no tether ($\rho_{cm} = 0$ m)

| | POD | | Quick-Look | | Long-Term | | | |
| | | | | | ½ period | | 1 period | |
	ρ_{cm}*(m)	Δt	RMS	ρ_{cm}(m)	RMS	ρ_{cm}(m)	RMS	ρ_{cm}(m)
σ = low:	2856	5 min:	1.021	-116	0.987	19	0.989	0
		10 min:	1.025	310	0.986	16	0.989	2
		15 min:	1.006	152	0.986	16	0.989	2
σ = med:	15679	5 min:	1.042	4246	1.027	5	1.026	-5
		10 min:	1.021	624	1.027	122	1.026	3
		15 min:	1.011	708	1.027	60	1.027	1
σ = high:	46398	5 min:	1.033	4613	1.040	18	0.999	18
		10 min:	1.021	1400	1.010	18	0.999	18
		15 min:	1.009	1493	1.042	18	0.999	18

Table 4. Simulated Data: $\rho = 1$ km ($\rho_{cm} = 909$ m), $\sigma = $ low

| | POD | | Quick-Look | | Long-Term | | | |
| | | | | | ½ period | | 1 period | |
$\underline{\alpha}$	$\underline{\rho_{cm}{}^*(m)}$	$\underline{\Delta t}$	$\underline{RMS}$	$\underline{\rho_{cm}(m)}$	$\underline{RMS}$	$\underline{\rho_{cm}(m)}$	$\underline{RMS}$	$\underline{\rho_{cm}(m)}$
0°	-4487	5 min:	1.022	277	2.196	415	14.300	590
		10 min:	1.022	991	0.986	925	0.989	910
		15 min:	1.007	1077	0.986	925	0.989	910
5°	-4470	5 min:	1.022	230	2.204	472	16.130	518
		10 min:	1.022	943	0.986	925	0.989	910
		15 min:	1.008	1028	0.986	925	0.989	910
10°	-7793	5 min:	1.021	260	0.986	925	0.989	910
		10 min:	1.021	956	0.986	925	0.989	910
		15 min:	1.010	979	0.986	925	0.989	910

Table 5. Simulated Data: $\rho = 1$ km ($\rho_{cm} = 909$ m), $\sigma = $ med

| | POD | | Quick-Look | | Long-Term | | | |
| | | | | | ½ period | | 1 period | |
$\underline{\alpha}$	$\underline{\rho_{cm}{}^*(m)}$	$\underline{\Delta t}$	$\underline{RMS}$	$\underline{\rho_{cm}(m)}$	$\underline{RMS}$	$\underline{\rho_{cm}(m)}$	$\underline{RMS}$	$\underline{\rho_{cm}(m)}$
0°	19974	5 min:	1.020	-1318	1.146	78	3.736	53
		10 min:	1.021	1001	1.084	826	1.027	904
		15 min:	1.008	1521	1.027	821	1.027	904
5°	19999	5 min:	1.020	-1364	1.402	7	2.143	373
		10 min:	1.021	950	1.027	822	1.027	905
		15 min:	1.008	1472	1.027	822	1.027	905
10°	-78347	5 min:	1.021	3381	1.517	-7	4.114	32
		10 min:	1.021	1236	1.027	827	1.027	905
		15 min:	1.010	1416	1.027	827	1.027	905

Table 6. Simulated Data: $\rho = 1$ km ($\rho_{cm} = 909$ m), $\sigma =$ high

| | POD | | Quick-Look | | Long-Term | | | |
| | | | | | ½ period | | 1 period | |
α	$\rho_{cm}{}^*$(m)	Δt	RMS	ρ_{cm}(m)	RMS	ρ_{cm}(m)	RMS	ρ_{cm}(m)
0°	-4371	5 min:	1.015	-892	1.039	87	2.086	-47
		10 min:	1.023	840	1.010	854	1.000	928
		15 min:	1.006	1003	1.010	855	1.000	928
5°	50869	5 min:	1.020	-1432	1.027	822	1.027	905
		10 min:	1.021	1096	1.043	594	1.473	802
		15 min:	1.009	1950	1.010	847	1.000	928
10°	-146423	5 min:	1.021	-8401	1.010	843	1.000	927
		10 min:	1.022	509	1.010	843	1.000	927
		15 min:	1.011	196	1.010	843	1.000	927

Table 7. Simulated Data: $\rho = 10$ km ($\rho_{cm} = 9091$ m), $\sigma =$ low

| | POD | | Quick-Look | | Long-Term | | | |
| | | | | | ½ period | | 1 period | |
α	$\rho_{cm}{}^*$(m)	Δt	RMS	ρ_{cm}(m)	RMS	ρ_{cm}(m)	RMS	ρ_{cm}(m)
0°	3640	5 min:	1.022	8423	0.986	9107	0.989	9092
		10 min:	1.025	9192	0.986	9107	0.989	9092
		15 min:	1.010	9339	0.986	9107	0.989	9092
5°	3834	5 min:	1.021	7948	0.986	9107	0.989	9057
		10 min:	1.025	8714	0.986	9107	0.989	9092
		15 min:	1.065	8845	0.986	9107	0.989	9092
10°	3807	5 min:	1.021	7444	0.986	9107	0.989	9092
		10 min:	1.195	8406	0.986	9107	0.989	9092
		15 min:	1.028	8267	0.986	9107	0.989	9092

Table 8. Simulated Data: $\rho = 10$ km ($\rho_{cm} = 9091$ m), $\sigma =$ med

| | POD | | Quick-Look | | Long-Term | | | |
| | | | | | ½ period | | 1 period | |
$\underline{\alpha}$	$\rho_{cm}{}^*(m)$	$\underline{\Delta t}$	RMS	$\rho_{cm}(m)$	RMS	$\rho_{cm}(m)$	RMS	$\rho_{cm}(m)$
0°	28156	5 min:	1.020	6801	1.027	9001	1.027	9086
		10 min:	1.022	9179	1.027	9001	1.027	9086
		15 min:	1.008	9787	1.027	9001	1.027	9086
5°	28429	5 min:	1.020	6341	1.027	9003	1.027	9087
		10 min:	1.021	8708	1.027	9003	1.027	9087
		15 min:	1.010	9294	1.027	9003	1.027	9087
10°	28473	5 min:	1.020	5842	1.027	9007	1.027	9087
		10 min:	1.022	8274	1.027	9007	1.027	9087
		15 min:	1.016	8855	1.027	9003	1.027	9087

Table 9. Simulated Data: $\rho = 10$ km ($\rho_{cm} = 9091$ m), $\sigma =$ high

| | POD | | Quick-Look | | Long-Term | | | |
| | | | | | ½ period | | 1 period | |
$\underline{\alpha}$	$\rho_{cm}{}^*(m)$	$\underline{\Delta t}$	RMS	$\rho_{cm}(m)$	RMS	$\rho_{cm}(m)$	RMS	$\rho_{cm}(m)$
0°	3738	5 min:	1.015	7211	1.010	9036	1.000	9110
		10 min:	1.023	8992	1.010	9036	1.000	9110
		15 min:	1.006	9225	1.010	9036	1.000	9110
5°	59491	5 min:	1.020	6301	1.010	9030	1.000	9109
		10 min:	1.021	8888	1.010	9031	1.000	9109
		15 min:	1.010	9791	1.010	9032	1.000	9109
10°	59655	5 min:	1.020	5811	1.010	9026	1.000	9109
		10 min:	1.021	8450	1.010	9027	1.000	9109
		15 min:	1.011	9355	1.010	9027	1.000	9108

Table 10. Simulated Data: $\rho = 50$ km ($\rho_{cm} = 45455$ m), $\sigma = $ low

| | POD | | Quick-Look | | Long-Term | | | |
| | | | | | ½ period | | 1 period | |
$\underline{\alpha}$	ρ_{cm}*(m)	$\underline{\Delta t}$	RMS	ρ_{cm}(m)	RMS	ρ_{cm}(m)	RMS	ρ_{cm}(m)
0°	39754	5 min:	1.022	44523	0.986	45471	0.989	45455
		10 min:	1.027	45385	0.986	45471	0.989	45455
		15 min:	1.023	45659	0.986	45471	0.989	45455
5°	41338	5 min:	1.017	42148	0.986	45471	0.989	45455
		10 min:	1.035	42994	0.986	45471	0.989	45455
		15 min:	1.844	43146	0.986	45471	0.989	45455
10°	41783	5 min:	1.016	39625	0.986	45471	0.989	45455
		10 min:	1.105	40795	0.986	45471	0.989	45455
		15 min:	3.202	40910	0.986	45471	0.989	45455

Table 11. Simulated Data: $\rho = 50$ km ($\rho_{cm} = 45455$ m), $\sigma = $ med

| | POD | | Quick-Look | | Long-Term | | | |
| | | | | | ½ period | | 1 period | |
$\underline{\alpha}$	ρ_{cm}*(m)	$\underline{\Delta t}$	RMS	ρ_{cm}(m)	RMS	ρ_{cm}(m)	RMS	ρ_{cm}(m)
0°	64509	5 min:	1.021	42789	1.027	45365	1.027	45451
		10 min:	1.022	45482	1.027	45365	1.027	45451
		15 min:	1.008	46154	1.027	45365	1.027	45451
5°	66681	5 min:	1.019	40517	1.027	45367	1.027	45451
		10 min:	1.021	43138	1.027	45367	1.027	45451
		15 min:	1.054	43703	1.027	45367	1.027	45451
10°	67694	5 min:	1.019	38056	1.027	45370	1.027	45451
		10 min:	1.022	40931	1.027	45370	1.027	45451
		15 min:	1.178	41358	1.027	45370	1.027	45451

Table 12. Simulated Data: $\rho = 50$ km ($\rho_{cm} = 45455$ m), $\sigma = $ high

| | POD | | Quick-Look | | Long-Term | | | |
| | | | | | ½ period | | 1 period | |
α	$\rho_{cm}*$(m)	Δt	RMS	ρ_{cm}(m)	RMS	ρ_{cm}(m)	RMS	ρ_{cm}(m)
0°	95770	5 min:	1.020	42834	1.010	45382	1.000	45471
		10 min:	1.022	45584	1.010	45383	1.000	45471
		15 min:	1.009	46644	1.010	45383	1.000	45471
5°	99001	5 min:	1.019	40629	1.010	45377	1.000	45470
		10 min:	1.021	43221	1.010	45377	1.000	45470
		15 min:	1.022	44137	1.010	45377	1.000	45470
10°	101085	5 min:	1.019	38232	1.010	45374	0.999	45470
		10 min:	1.022	41013	1.010	45374	0.999	45469
		15 min:	1.058	41908	1.010	45374	0.999	45469

Table 13. Simulated Data: $\rho = 1$ km up ($\rho_{cm} = -909$ m), $\sigma = $ low

| | POD | | Quick-Look | | Long-Term | | | |
| | | | | | ½ period | | 1 period | |
α	$\rho_{cm}*$(m)	Δt	RMS	ρ_{cm}(m)	RMS	ρ_{cm}(m)	RMS	ρ_{cm}(m)
0°	-6290	5 min:	1.022	-1532	0.986	-893	0.989	-908
		10 min:	1.022	-833	0.986	-893	0.989	-908
		15 min:	1.006	-761	0.986	-893	0.989	-908
5°	-6307	5 min:	1.022	-1484	0.986	-893	0.989	-908
		10 min:	1.022	-785	0.986	-893	0.989	-908
		15 min:	1.006	-712	0.986	-893	0.989	-908
10°	-6302	5 min:	1.022	-1532	0.986	-893	0.989	-908
		10 min:	1.022	-740	0.986	-893	0.989	-908
		15 min:	1.007	-668	0.986	-893	0.989	-908

Table 14. Simulated Data: $\rho = 1$ km up ($\rho_{cm} = -909$ m), $\sigma = $ med

| | POD | | Quick-Look | | Long-Term | | | |
| | | | | | ½ period | | 1 period | |
$\underline{\alpha}$	$\rho_{cm}{}^*$(m)	$\underline{\Delta t}$	RMS	ρ_{cm}(m)	RMS	ρ_{cm}(m)	RMS	ρ_{cm}(m)
0°	18159	5 min:	1.020	-3121	1.027	-998	1.027	-914
		10 min:	1.021	-809	1.027	-998	1.027	-914
		15 min:	1.008	-318	1.110	-446	1.027	-914
5°	18135	5 min:	1.020	-3074	1.027	-997	1.027	-914
		10 min:	1.021	-757	1.027	-997	1.027	-914
		15 min:	1.009	-269	1.112	-493	1.027	-914
10°	18134	5 min:	1.020	-3025	1.027	-995	1.027	-914
		10 min:	1.021	-709	1.027	-994	1.027	-914
		15 min:	1.008	225	1.010	-964	0.999	-891

Table 15. Simulated Data: $\rho = 1$ km up ($\rho_{cm} = -909$ m), $\sigma = $ high

| | POD | | Quick-Look | | Long-Term | | | |
| | | | | | ½ period | | 1 period | |
$\underline{\alpha}$	$\rho_{cm}{}^*$(m)	$\underline{\Delta t}$	RMS	ρ_{cm}(m)	RMS	ρ_{cm}(m)	RMS	ρ_{cm}(m)
0°	49000	5 min:	1.020	-3194	1.010	-957	0.999	-890
		10 min:	1.021	-683	1.010	-957	0.999	-890
		15 min:	1.009	-155	1.010	-957	0.999	-890
5°	48965	5 min:	1.020	-3149	1.010	-961	0.999	-890
		10 min:	1.021	-637	1.010	-959	0.999	-890
		15 min:	1.009	203	1.031	-453	1.820	-156
10°	48953	5 min:	1.020	-3100	1.010	-964	0.999	-891
		10 min:	1.021	-593	1.010	-962	0.999	-891
		15 min:	1.008	246	1.070	5	1.109	352

Table 16. Simulated Data: ρ = 10 km up (ρ_{cm} = -9091 m), σ = low

| | POD | | Quick-Look | | Long-Term | | | |
| | | | | | ½ period | | 1 period | |
α	ρ_{cm}*(m)	Δt	RMS	ρ_{cm}(m)	RMS	ρ_{cm}(m)	RMS	ρ_{cm}(m)
0°	-6290	5 min:	1.022	-1532	0.986	-9075	0.989	-9090
		10 min:	1.022	-833	0.986	-9075	0.989	9090
		15 min:	1.006	-761	0.986	-9075	0.989	9090
5°	-6307	5 min:	1.022	-1484	0.986	-9075	0.989	-9090
		10 min:	1.022	-785	0.986	-9075	0.989	-9090
		15 min:	1.006	-712	0.986	-9075	0.989	-9090
10°	-6302	5 min:	1.022	-1532	0.986	-9075	0.989	-9090
		10 min:	1.022	-740	0.986	-9075	0.989	-9090
		15 min:	1.007	-668	0.986	-9075	0.989	-9090

Table 17. Simulated Data: ρ = 10 km up (ρ_{cm} = -9091 m), σ = med

| | POD | | Quick-Look | | Long-Term | | | |
| | | | | | ½ period | | 1 period | |
α	ρ_{cm}*(m)	Δt	RMS	ρ_{cm}(m)	RMS	ρ_{cm}(m)	RMS	ρ_{cm}(m)
0°	18159	5 min:	1.020	-3121	1.027	-9179	1.027	-9096
		10 min:	1.021	-809	1.027	-9179	1.027	-9096
		15 min:	1.008	-318	1.027	-9179	1.027	-9096
5°	18135	5 min:	1.020	-3074	1.027	-9178	1.027	-9096
		10 min:	1.021	-757	1.027	-9178	1.027	-9096
		15 min:	1.009	-269	1.027	-9178	1.027	-9096
10°	18134	5 min:	1.020	-3025	1.027	-9175	1.027	-9096
		10 min:	1.021	-709	1.027	-9175	1.027	-9096
		15 min:	1.008	225	1.027	-9175	1.027	-9096

24

Table 18. Simulated Data: $\rho = 10$ km up ($\rho_{cm} = -9091$ m), $\sigma =$ high

α	$\rho_{cm}*$(m)	Δt	RMS	ρ_{cm}(m)	RMS	ρ_{cm}(m)	RMS	ρ_{cm}(m)
			Quick-Look		**Long-Term**			
					½ period		1 period	
0°	49000	5 min:	1.020	-3194	1.010	-9136	0.999	-9072
		10 min:	1.021	-683	1.010	-9136	0.999	-9072
		15 min:	1.009	-155	1.010	-9136	0.999	-9072
5°	48965	5 min:	1.020	-3149	1.010	-9141	0.999	-9072
		10 min:	1.021	-637	1.010	-9141	0.999	-9072
		15 min:	1.009	203	1.010	-9141	0.999	-9072
10°	48953	5 min:	1.020	-3100	1.010	-9145	0.999	-9073
		10 min:	1.021	-593	1.010	-9145	0.999	-9073
		15 min:	1.008	246	1.010	-9145	0.999	-9073

Six additional cases were analyzed consisting of a single satellite, i.e., no tether, on a re-entry trajectory, having low and high levels of measurement error. These cases were run to determine if the Three-Stage methodology developed under this research program could identify a single vehicle traveling on a trajectory which would impact the surface of the Earth. The results of this analysis are presented in Table 19 below. These results show that at least 10 minutes of observational data is required regardless of the level of measurement error in order to properly identify the object as being on a re-entry trajectory. These results are consistent with those for the TSS cases presented above.

Table 19. Simulated Data: no tether ($\rho_{cm} = 0$ m), re-entry trajectory

	$\rho_{cm}*$(m)	Δt	RMS	ρ_{cm}(m)	RMS	ρ_{cm}(m)	RMS	ρ_{cm}(m)
	POD		**Quick-Look**		**Long-Term**			
					15 min		30 min	
$\sigma =$ low:	-85,982	5 min:	1.112	8,878	0.990	13	1.012	1
		10 min:	1.020	-15	0.990	33	1.012	-3
		15 min:	0.999	112	0.992	25	1.012	29
$\sigma =$ high:	-432,356	5 min:	1.018	4,797	0.981	693	0.975	284
		10 min:	1.021	394	0.976	21	0.975	23
		15 min:	0.998	932	0.997	-13	0.972	-13

25

TiPS Experiment Data Cases

The TiPS Experiment is described in [13] and consists of two end masses having the mass ratio m_p/m of 3.65, which are connected by a 4 km tether weighing 12.0 lbs. This geometry results in a value of 3024 m for ρ_{cm}. TiPS was launched in June 1996 into an orbit having an altitude of 1022 km.

A limited amount of TiPS data was made available to us by Air Force personnel for use during this research program. A formal request for additional data was submitted to Mr. Bill Craig of Cheyenne Mountain AFB through Dr. Robert Racca of the SWC/AESA on May 3, 2000 by Dr. Cicci [27]. This additional data was not provided for our use, therefore the performance of the developed methodology on real TSS data could not be thoroughly evaluated.

The six particular cases evaluated consisted of range, azimuth, and elevation angles which were recorded over various observation spans obtained from different tracking stations having differing measurement accuracies. All data used was recorded in mid-to-late 1996. The particular TiPS data test cases evaluated are summarized in Table 20 below.

Table 20. TiPS Data Test Cases

Case	Tracking Stations	Mass Observed	Observation Span	Number of Observations
1	345 and 344	Lower	350 sec	36
2	346	Lower	410 sec	42
3	369	Lower	626 sec	72
4	346	Upper	410 sec	42
5	346 and 344	Upper	540 sec	55
6	345 and 344	Upper	370 sec	38

Results of the analysis are very encouraging and are provided in Table 21 below. While the POD process did not provide accurate results for $\rho_{cm}*$, the Quick-Look results were reasonably accurate, except in cases (4) and (6), and could generally be used to identify whether the tracked satellite was part of a TSS. The Long-Term Orbit Determination results also shown in Table 21 are not seen to be as accurate as the Quick-Look results in most cases. In addition, the low values of the RMS results also presented below (as compared to the normalized value of 1.0) likely indicate that the observations used in the estimation process were of a higher accuracy than the nominal tracking station statistics would indicate.

The inaccuracies present in these results could be caused by erroneous data or data which were incorrectly tagged as being obtained from one satellite when the actual measurement were obtained from the other satellite. This was demonstrated to be a problem in a portion of the TiPS

data used here. Additional error could be the result of short data arcs, as Case (3) below was the only case studied which consisted of at least 10 minutes of measurement data. It is believed that much improved results could be obtained from this methodology if adequate observational data was processed.

Table 21. TiPS Data: $\rho = 4$ km ($\rho_{cm} = 3024$ m)

	POD		Quick-Look		Long-Term (through Δt)	
Case	$\rho_{cm}{}^*$(m)	Δt	RMS	ρ_{cm}(m)	RMS	ρ_{cm}(m)
1	3079	350 sec:	0.375	2169	0.362	-123
2	-426	270 sec:	0.186	1910	0.181	177
3	15303	626 sec:	4.197	7702	4.245	-34
4*	1352	410 sec:	0.171	4300	0.175	3
5*	-1540	540 sec	19.27	-2297	18.69	-145
6*	558	370 sec	0.411	9455	0.408	4469

(*Note: For upper mass observation cases, $\rho_{cm} = -3024$ m.)

CONCLUSIONS

Based on the results of both simulated and real data obtained during the course of this research project, it has been demonstrated that the three-stage orbit determination method developed and presented here can indeed be used for the POD, quick-look identification, and long-term orbit determination and motion prediction of a TSS. While the best results can certainly be obtained using the most accurate data available, several guidelines can be recommended for the use of this proposed methodology. These guidelines are:

a. Observations used in the 1st Stage POD process should be taken 60-80 seconds apart.

b. Observations used in the 2nd Stage Quick-Look Identification process should consist of 10-15 minutes of data taken as often as possible within this time span.

c. Once the satellite has been identified as being part of a TSS in the 2nd Stage process, longer arcs of data on the order of ½ of an orbital period or more should be used to determine the TSS orbit and generate an accurate prediction of the long-term TSS motion.

We have made significant progress in the areas of preliminary orbit determination, filtering techniques, the development of mathematical models for long-term estimation and prediction, and the problem of analyzing the motion of a satellite with a trailing tether. We have provided Dr. Racca with preliminary filtering software so that he could become familiar with the capabilities of the filter and learn about the procedures required for its use. This software transfer took place in the Fall of 1999.

We have also presented the results of our work at technical conferences on a regular basis and have a number of journal articles at various stages of publication. We have gained a great knowledge of the problems we have studied and feel that our work has made a significant contribution to the state-of-the-art of the orbit determination of TSS.

While the results presented are very encouraging, additional work is clearly needed in order to verify, test, and develop the techniques presented in this study to achieve a software package which can be operationally useful. Recommendations for future work are discussed in the following section. An undertaking of this recommended or a similar research program would certainly help to ensure that the identification, orbit determination, and orbit prediction of TSS can be accomplished in the future.

We submitted a second proposal under DEPSCoR in order to request funding for the continuation of this research program. Our proposal was selected as one of the fifteen proposals from the State of Alabama which were submitted to the Department of Defense for funding consideration. Unfortunately, we were not successful at the final stage of the funding process. We believe that this work is sufficiently important and that we have obtained results that should lead to an operational system. We intend to pursue other funding options for completion of this endeavor.

RECOMMENDATIONS FOR FUTURE RESEARCH

The objectives of an appropriate follow-on research program would include:

1. Extensively test the dynamical models and software algorithms which have been developed, i.e., perform parametric studies to quantify model performance in an environment of limited and/or noisy SSN data, investigate the effects of the use of range-rate data on filter/model performance, and investigate the effects of the use of combined data from multiple ground sensors, i.e., stereo viewing, on filter/model performance.
2. Combine the POD, quick-look orbit determination, and long-term motion prediction models into a single, stand-alone, modular program, to be called the Tethered Satellite Analysis Model (TESAM), the requirements of which will be driven by the operational needs and capabilities of the U. S. Air Force.
3. Conduct extensive Verification and Validation (V&V) of the results generated by the TESAM and presentation of all documentation required for consideration for incorporation of the TESAM into the Cheyenne Mountain AFB space surveillance system.
4. Enhance the existing dynamical models to include the incorporation of complex models, e.g., massive tethers, into the prediction and filter models.
5. Investigate and develop additional analysis methods for the detection of configuration changes in TSS.
6. Update the pertinent research literature.
7. Define and complete additional tasks of interest to the Air Force.

The approach to accomplish these objectives is described in detail below.

Objective 1: Testing of the dynamical models and software algorithms

In order to complete the development of a stand-alone software package which has the capability of quickly identifying satellites as being part of TSS, extensive testing of the individual dynamical models, i.e., POD methods, quick-look orbit determination, and long-term motion prediction models and software algorithms must be performed. This will include performing parametric studies which are designed to quantify model performance in an environment of limited and/or noisy SSN data, the investigation of the effects of the use of range-rate data on filter/model performance, the investigation of the effects of the use of combined data from multiple ground sensors, i.e., stereo viewing on filter/model performance. While a portion of these analyses can be carried out using simulated data, the major thrust of the structured testing program will be focused on the use of real data obtained from the TiPS program. This data has been obtained by special request to the Air Force Space Command through the Space Warfare Center located at Schriever AFB, CO. This data will be used in order to perform testing of the performance of the dynamical models and software algorithms which have been developed.

Objective 2: Development of the Tethered Satellite Analysis Model (TESAM)

Upon successful testing of the dynamical models and software algorithms, this phase will consist of the combination of the POD, quick-look orbit determination, and long-term prediction models into a single, stand-alone, modular program, the TESAM. The requirements of TESAM will be driven by the operational needs and capabilities currently existing within the U. S. Air Force. We will work closely with Drs. Joseph Liu and Robert Racca of the Space Warfare Center in order to identify these needs and capabilities to effectively complete this phase of the research program. Issues to be considered will be input types and format, output types and format, language, host platform, and user interfaces. This collaboration will require visitation to Space Warfare Center facilities by the Principal Investigators and one or more graduate students involved in this proposed research program. It is envisioned that TESAM will include all theoretical models, user information, and documentation required for the implementation of our product into the daily operations of the existing space surveillance system.

Objective 3: Verification and Validation of the TESAM

Using both simulated and actual tethered satellite data, we will conduct extensive Verification and Validation (V&V) of the results generated by the TESAM. Data will include both circular and non-circular data and noise levels consistent with data approved by SSN sites. At the end of the contract period, we will deliver the TESAM software and all accompanying documentation, i.e., V&V Report, Theoretical Report, and Users Manual, to HQ, Space Warfare Center, Analysis and Engineering branch for consideration for incorporation into the Cheyenne Mountain space surveillance system.

Objective 4: Enhancement of the dynamical models

Upon the completion of the TESAM, additional effort will be directed to improvement of the dynamical models within TESAM through the incorporation of more complex models, e.g., massive tethers and enhanced modeling, into the long-term prediction filter. As part of this effort, consideration will be given to include modeling of out-of-plane libration and the possibility of electromagnetic tethers which will create additional forces acting within TSS. These additional capabilities in the TESAM will be included in order to construct the TESAM in the most general form possible to obtain as complete of an algorithm as possible.

Objective 5: Investigation and development of additional analysis methods for the detection of configuration changes in TSS

While a limited amount of analysis has been performed [27] thus far in addressing configuration changes of TSS, additional research will be devoted to inclusion of the capability to detect any configuration change in TSS which may occur as the motion is being tracked. Such configuration changes could result from an accidental break or an intentional cut of the tether in order to modify the trajectory of the disengaged body. This could be done for a variety of

reasons, some of which could be cause for great concern among personnel at the organizations responsible for tracking and monitoring space vehicle of this type. It is envisioned that these methods will include an extended sequential (Kalman) filter possessing the capability to quickly detect changes in the estimated state vector of an observed body. Such an algorithm could be incorporated into the TESAM after testing, validation, and verification of its performance has been completed in the context of this research program.

Objective 6: Update of the pertinent research literature

As part of the original DEPSCoR 1997 research program, an extensive and thorough literature search was conducted. The information which was determined to be pertinent to the problem being addressed was incorporated into the knowledge base and was used where appropriate. Since that time, while we have regularly attended technical conferences and read all related information which was published and/or presented in technical forums, we have significantly contributed to, and extended the state-of-the-art body of literature relative to this problem. Still, we shall formally update all pertinent literature provide the complete survey as part of the results of this research program.

Objective 7: Define and complete additional tasks of interest to the U. S. Air Force

Once Objectives (1) through (6) are completed, a presentation and demonstration on the research program will be made to Air Force personnel. Detailed discussions will then take place in order to define any additional tasks which will be of interest. It is conceivable that once the new methods are implemented, other requirements regarding the detection, quick identification, and orbit determination of TSS will become apparent. It is our intent, upon definition of these additional tasks, to undertake further development in order to address these topics. We will work closely with Air Force personnel, as needed, to accomplish the new goals set forth in Recommendation 7 of this research program.

SOFTWARE DESCRIPTION

The following is a description and the required format of the input and output files processed by each of the three algorithms. Examples of each input and output file is included. Complete copies of all software files developed during this project are included in Appendix C.

1st Stage: POD Algorithm

INPUTS:
- pod.in - consists of 3 observation data points containing tracking station #, time (yydddhhmmss.sss), range (km), range covariance, azimuth (deg), azimuth covariance, elevation (deg), and elevation covariance in the following format:

    I3,2X,I2,I3,I2,I2,F6.3,2X,F8.3,2X,F6.2,2X,F8.4,2X,F10.8,2X,F8.4,2X,F10.8

    For example:

    369 96185182650.597 3373.396 104.04 135.9610 0.00004761 3.6390 0.00004761
    369 96185182756.564 3183.705 104.04 128.7020 0.00004761 5.6190 0.00004761
    369 96185182857.353 3048.506 104.04 121.2440 0.00004761 7.1160 0.00004761

    (Note: There must be two spaces between each column in pod.in.)

OUTPUTS:
- pod.out - consists of the following items:
    - initial observation time in seconds, initial value of local siderreal time (radians) found when calculating the Julian date
    - position vector (meters) for first observation time
    - velocity vector (meters/sec) for first observation time
    - tether acceleration components (meters/sec^2)for first observation time
    - estimated distance (meters) from observed mass to the tether's center-of-mass

    For example:

0.0000000000000000 2.2213042198336230	t_o	θ_o
-5.7973958423219470D+006	r_x	
3.7530345202765030D+006	r_y	
2.6601850520098670D+006	r_z	
422.58945778877625000	v_x	
-4463.3106379500100000	v_y	
5817.4423591773510000	v_z	
0.0000000000000000	a_t	
0.0450495903883404	a_r	
15302.5085408019200000	ρ_{cm}	

32

2nd Stage: Quick-Look Algorithm

INPUTS:
- obs.in - consists of a batch of observation data in the same format used in pod.in; for example:

```
369  96185182650.597  3373.896  104.04  135.9610  0.00004761  3.6390  0.00004761
369  96185182705.189  3328.635  104.04  134.3999  0.00004761  4.0950  0.00004761
369  96185182709.139  3316.592  104.04  134.0110  0.00004761  4.2070  0.00004761
369  96185182715.539  3297.376  104.04  133.3209  0.00004761  4.4200  0.00004761
369  96185182720.789  3281.894  104.04  132.7480  0.00004761  4.5820  0.00004761
              ⋮
              ⋮
```

- pod.out (same as for 1st Stage algorithm above)

OUTPUTS:
- qlf.out - consists of estimated values of position coordinates (meters), velocity coordinates (meters/sec), a_t (meters/sec^2), a_r (meters/sec^2), and ρ_{cm} (meters). For example:

```
4.2833101207155030D+006        rx
-5.4159875054842680D+006       ry
2.6598024362644060D+006        rz
1315.3251339551280000          vx
4006.2176511132270000          vy
6007.9024652927640000          vz
-0.0008114425608780            at
0.0254833853712772             ar
8644.3330139343620000          ρcm
```

where the labels are r_x, r_y, r_z, v_x, v_y, v_z, a_t, a_r, ρ_{cm}.

- quick-look.out - provides the data found in qlf.out plus RMS, the tether orientation angle, and a statement of whether the satellite is tethered or not as well as the orientation of the satellite (i.e. whether the satellite is the upper or lower mass of the system). For example:

```
RIDGE-TYPE SOLUTION
4.2833101207155030D+006
-5.4159875054842680D+006
2.6598024362644060D+006
1315.3251339551280000
4006.2176511132270000
6007.9024652927640000
-0.0008114425608780
0.0254833853712772
RMS     4.2026768531638880
```

DISTANCE FROM TETHERED SATELLITE TO THE CM (M)

8644.3330139343620000

TETHER ORIENTATION ANGLE (DEG)

91.8237973440692300

THIS IS A TETHERED SATELLITE.

THE OBSERVED SATELLITE IS THE LOWER MASS OF A TETHERED SATELLITE SYSTEM

3rd Stage: Long-Term Algorithm

INPUTS:
- obs.in (same as for 2nd Stage algorithm above)

- qlf.out (same as for 2nd Stage algorithm above)

OUTPUTS:
- ltf.out - estimated values of position coordinates (meters), velocity coordinates (meters/sec), libration angle (deg), libration rate (rad/sec), and ρ_{cm} (meters), plus RMS residual error. For example:

4392361.887017369000000	r_x
-603231.392820723200000	r_y
5920423.691058521000000	r_z
-3128.725756762024000	v_x
5965.718358200920000	v_y
2928.540421372993000	v_z
-218.582319413363100	α
1.394394047857037E-002	α-dot
23.531254403341700	ρ_{cm}
.437759518702758	RMS

Figure 3 below provides a block-diagram depiction of the three-stage methodology developed during this study.
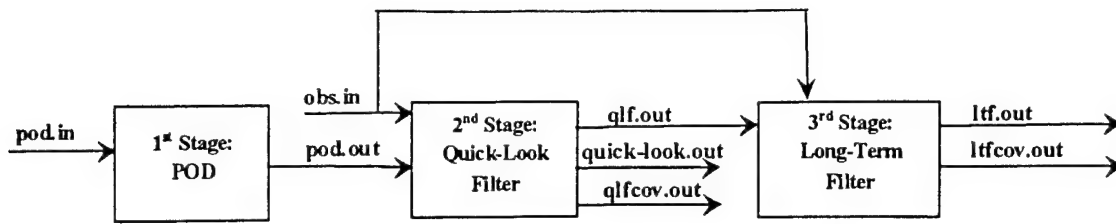
34

Figure 3. Depiction of Three-Stage TSS Identification and Orbit Determination Computational Procedure.

Sample Case

Copies of all pertinent input and output files for a sample case are provided below. The case considered is for Case (6) of the TiPS analysis presented in Table 21. The input file, "obs.in", contains a 370-second batch of observations taken from the database for the TiPS upper mass. The POD result indicates a ρ_{cm} value of 558m, the quick-look filter results indicates an RMS residual error of 0.411 and a value of 9455m for ρ_{cm}, and the long-term filter result gives an RMS of 0.408 and ρ_{cm} of 4469 m.

POD.IN:

```
344   96256003323.159   1166.062   894.01   257.5792   0.00052000   59.4335
0.00039200
345   96256003443.159   1055.110   888.04   329.4737   0.00062000   76.1779
0.00057600
345   96256003603.159   1191.583   888.04    30.4119   0.00062000   57.2229
0.00057600
```

POD.OUT:

```
      0.0000000000000000      6.2652689791188940
  4.4023318519027870D+006
-658082.6354631375000000
  5.9022668690712680D+006
 -3403.6153755342960000
  6006.2993053847880000
  2483.9012980381220000
      0.0000000000000000
      0.0016511273341505
    557.8838244114083000
```

35

OBS.IN:

```
345   96256003323.159   1166.062   894.01   257.5792   0.00052000   59.4335
0.00039200
345   96256003333.159   1139.586   894.01   260.8353   0.00052000   62.3041
0.00039200
345   96256003343.159   1116.354   894.01   264.9759   0.00052000   65.1871
0.00039200
345   96256003353.159   1096.572   894.01   270.3145   0.00052000   68.0188
0.00039200
345   96256003403.159   1080.434   894.01   277.3165   0.00052000   70.7030
0.00039200
345   96256003413.159   1068.105   894.01   286.5744   0.00052000   73.0914
0.00039200
345   96256003423.159   1059.720   894.01   298.6270   0.00052000   74.9660
0.00039200
344   96256003433.159   1055.371   888.04   313.3820   0.00062000   76.0669
0.00057600
344   96256003443.159   1055.110   888.04   329.4737   0.00062000   76.1779
0.00057600
344   96256003453.159   1058.940   888.04   344.6365   0.00062000   7⁵.⧸617
0.00057600
344   96256003503.159   1066.814   888.04   357.2223   0.00062000   73.5128
0.00057600
344   96256003513.159   1078.645   888.04     6.9507   0.00062000   71.2039
0.00057600
344   96256003523.159   1094.301   888.04    14.3168   0.00062000   68.5675
0.00057600
344   96256003533.159   1113.620   888.04    19.9198   0.00062000   65.7634
0.00057600
344   96256003543.159   1136.412   888.04    24.2487   0.00062000   62.8953
0.00057600
344   96256003553.159   1162.472   888.04    27.6641   0.00062000   60.0336
0.00057600
344   96256003603.159   1191.583   888.04    30.4119   0.00062000   57.2229
0.00057600
344   96256003613.159   1223.523   888.04    32.6615   0.00062000   54.4906
0.00057600
344   96256003623.159   1258.075   888.04    34.5365   0.00062000   51.8547
0.00057600
344   96256003633.159   1295.026   888.04    36.1216   0.00062000   49.3237
0.00057600
344   96256003643.159   1334.172   888.04    37.4777   0.00062000   46.9045
0.00057600
344   96256003653.159   1375.324   888.04    38.6525   0.00062000   44.5978
0.00057600
344   96256003703.159   1418.302   888.04    39.6791   0.00062000   42.4005
0.00057600
344   96256003713.159   1462.938   888.04    40.5848   0.00062000   40.3097
0.00057600
344   96256003723.159   1509.087   888.04    41.3897   0.00062000   38.3226
0.00057600
344   96256003733.159   1556.608   888.04    42.1115   0.00062000   36.4342
0.00057600
344   96256003743.159   1605.375   888.04    42.7627   0.00062000   34.6399
0.00057600
```

```
344  96256003753.159  1655.271  888.04  43.3529  0.00062000  32.9335
0.00057600
344  96256003803.159  1706.195  888.04  43.8921  0.00062000  31.3083
0.00057600
344  96256003813.159  1758.051  888.04  44.3842  0.00062000  29.7602
0.00057600
344  96256003823.159  1810.756  888.04  44.8379  0.00062000  28.2843
0.00057600
344  96256003833.159  1864.233  888.04  45.2578  0.00062000  26.8760
0.00057600
344  96256003843.159  1918.411  888.04  45.6482  0.00062000  25.5305
0.00057600
344  96256003853.159  1973.228  888.04  46.0119  0.00062000  24.2434
0.00057600
344  96256003903.159  2028.628  888.04  46.3515  0.00062000  23.0102
0.00057600
344  96256003913.159  2084.559  888.04  46.6701  0.00062000  21.8267
0.00057600
344  96256003923.159  2140.973  888.04  46.9701  0.00062000  20.6910
0.00057600
344  96256003933.159  2197.831  888.04  47.2530  0.00062000  19.5997
0.00057600
```

QLF.OUT:

```
   4.4065349776160330D+006
  -630394.0438157753000000
   5.9022984690315050D+006
     -3109.5082825530830000
      5956.4580839276270000
      2954.5871897991120000
         0.0024007931112876
         0.0279485258221759
      9455.0744685966150000
```

QUICK-LOOK.OUT:

RIDGE-TYPE SOLUTION

```
RX (M)   4.4065349776160330D+006
RY (M)  -630394.0438157753000000
RZ (M)   5.9022984690315050D+006
VX (M/S)    -3109.5082825530830000
VY (M/S)     5956.4580839276270000
VZ (M/S)     2954.5871897991120000
AT (M/S^2)       0.0024007931112876
AR (M/S^2)       0.0279485258221759
RMS          0.4113008135743922
```

DISTANCE FROM TETHERED SATELLITE TO THE CM (M)

```
    9455.0744685966150000
```

TETHER ORIENTATION ANGLE (DEG)

   85.0903146716977800

THIS IS A TETHERED SATELLITE.

THE OBSERVED SATELLITE IS THE LOWER MASS OF A
        TETHERED SATELLITE SYSTEM

LTF.OUT:

    4394564.203803360000000
    -709269.251280797000000
    5902247.150233440000000
      -3002.198031099093000
       6011.603080867935000
       2955.187291830438000
         -2.825406760036377
    8.583524744085534E-004
       4468.548432569249000
    4.077873570369031E-001

REFERENCES

1. Liu, J., Private Communication, February 1993 and May 1995.

2. Hoots, F. R., Roehrich, R., and Szebehely, V., "Space Shuttle Tethered Satellite Analysis," D06 TM 83-5, AFSPACECOM, August 1983.

3. Kessler, S.A., and Cicci, D. A., "Filtering Methods for the Orbit Determination of a Tethered Satellite," *The Journal of the Astronautical Sciences*, Vol. 45, No. 3, pp. 263-278, July-September 1997.

4. Cochran, J. E., Jr., Cho. S. Cheng, Y-M, and Cicci, D. A., "Dynamics and Orbit Determination of Tethered Satellite Systems," *The Journal of the Astronautical Sciences*, Vol. 46, No. 2, pp. 177-194, April-June 1998.

5. Cicci, D. A. and Hall, R. L., "Improved Estimation/Prediction in Quick-Look Orbit Determination," *The Journal of the Astronautical Sciences*, Vol. 40, No. 1, pp. 91-106, January-March 1992.

6. Cicci, D. A. and Tapley, B. D., "Optimal Solutions of Unobservable Orbit Determination Problems," *Celestial Mechanics*, 44, pp. 339-363, December 1988.

7. Cicci, D. A., "Improving Gravity Field Determination in Ill-Conditioned Inverse Problems," *Computer & Geosciences*, Vol. 18, No. 5, pp. 509-516, June 1992.

8. Cicci, D. A., "Optimal Weighting of Apriori Statistics in Quick-Look Orbit Determination Problems," *AIAA Journal of Guidance, Control, and Dynamics*, Vol. 16, No. 5, pp. 988-990, September-October 1993.

9. Warnock, T. W. and Cochran, J. E., Jr., "Orbital Lifetime of Tethered Satellites," *The Journal of the Astronautical Sciences*, Vol. 41, No. 2, April-June, 1993, pp. 165-188.

10. Warnock, T. W. and Cochran, J. E., Jr., "Predicting the Orbital Lifetime of Tethered Satellites," *Acta Astronautica*, Vol. 35, No. 2/3, January-February, 1995, pp. 193-203.

11. Cicci, D. A., Lovell, T. A., and Qualls, C., "A Filtering Method for the Identification of a Tethered Satellite," submitted to *The Journal of the Astronautical Sciences*, August 1999.

12. Cochran, J. E., Jr., Cho, S., Lovell, A., and Cicci, D. A., "On the Information Contained in the Motion of One Satellite of a Two-Satellite Tethered System," submitted to *The Journal of the Astronautical Sciences*, May 1999.

13. Cho, S., Cochran, J. E., Jr., and Cicci, D. A., "Identification and Orbit Determination of Tethered Satellite System", AAS Paper Number 98-101, *Advances in the Astronautical Sciences*, Vol. 99, Part 1, pp. 21-34, proceedings of the AAS/AIAA Space Flight Mechanics Meeting, Monterey, CA, February 9-11, 1998.

14. Cho, S., Cochran, J. E., Jr., Cicci, D. A., "Approximate Solutions for Tethered Satellite Motion," AAS Paper Number 99-193, *Advances in the Astronautical Sciences*, Vol. 102, Part 2, pp. 1345-1360, proceedings of the AAS/AIAA Spaca Flight Mechanics Meeting, Breckenridge, CO, February 7-10, 1999.

15. Tapley, B. D, Schutz, B. E., and Born, G. H., "Satellite Orbit Determination: Fundamentals and Applications," June 1998.

16. Madonna, R. G., *Orbital Mechanics*, Krieger Publishing Co., Florida, 1997.

17. Taff, L. G., *Celestial Mechanics, A Computational Guide for the Practitioner*, John Wiley & Sons, Canada, 1985.

18. Escobal, P. R., *Methods of Orbit Determination*, Krieger Publishing Co., Florida, 1976.

19. Cicci, D. A., "Use of Multiple Observation Types in Ridge-Type Estimation Methods," *The Journal of the Astronautical Sciences*, Vol. 30, No. 2, pp. 215-227, April-June 1990.

20. Cho, S., "Analysis of Orbital Motion of a Tethered Satellite System," Ph.D. Dissertation, Auburn University, 1999.

21. Cochran, J. E., Jr., Cho, S., Lovell, A., and Cicci, D. A., "Modeling Tethered Satellite Systems for Detection and Orbit Determination," AAS Paper Number 99-416, presented at the AAS/AIAA Astrodynamics Specialist Conference, Girdwood, AK, August 16-19, 1999.

22. Deimling, K., *Nonlinear Functional Analysis*, Springer-Verlag, 1985.

23. Lloyd, N., *Degree Theory*, Cambridge University Press, 1978.

24. Grossinho, M. R. and Nkashama, M. N., "Periodic Solutions of Parabolic and Telegraph Equations with Asymmetric Nonlinearities," *Nonlinear Analysis, Theory, Methods and Applications*, 33(2), pp. 187-210, 1998.

25. Qualls, C. and Cicci, D. A., "Preliminary Orbit Determination of a Tethered Satellite," presented as paper number AAS 00-191 at the AAS/AIAA Space Flight Mechanics Meeting, Clearwater, FL, January 23-26, 2000.

26. Cicci, D. A., Cochran, J. E., Jr., Qualls, C., and Lovell, T. A., "Quick-Look Identification and Orbit Determination of a Tethered Satellite," presented as paper number AAS 01-232 at the AAS/AIAA Space Flight Mechanics Meeting, Santa Barbara, CA, February 11-14, 2001.

27. Cicci, D. A., Letter to Mr. Bill Craig, Cheyenne Mountain AFB, requesting additional TiPS observational data for further analysis, May 3, 2000.

28. "A Study of the Re-Entry Orbit Discrepancy Involving Tethered Satellites," T. A. Lovell, S. Cho, J. E. Cochran, Jr., and D. A. Cicci, presented as paper number AAS 00-194 at the AAS/AIAA Space Flight Mechanics Meeting, Clearwater, FL, January 23-26, 2000.

FACULTY AND STUDENTS SUPPORTED

This section summarizes the faculty and student financial support received from this research grant during the period October 1, 1997 through March 31, 2001.

Faculty		**Percent of Full-Time**

John E. Cochran, Jr.

Year 1:	10/1/97 - 8/31/98	9%
Year 2:	9/1/98 - 8/31/99	9%
Year 3:	9/1/99 - 8/31/00	9%
Year 4:	9/1/00 - 10/31/00	4%
	11/1/00 - 3/31/01	0%

David A. Cicci

Year 1:	10/1/97 - 8/31/98	33%
Year 2:	9/1/98 - 8/31/99	33%
Year 3:	9/1/99 - 8/31/00	32%
Year 4:	9/1/00 - 10/31/00	7%
	11/1/00 - 3/31/01	0%

Graduate Students

Sungki Cho

Year 1:	11/1/97 - 6/15/98	33%
	6/16/98 - 8/31/98	100%
Year 2:	9/1/98 - 9/15/98	100%
	9/16/98 - 6/15/99	50%
	6/16/99 - 8/31/99	75%
Year 3:	9/1/99 - 2/29/00	44%

Alan Lovell

Year 1:	11/1/97 - 6/15/98	33%
	6/16/98 - 8/31/98	50%
Year 2:	9/1/98 - 6/15/99	50%
	6/16/99 - 8/31/99	75%
Year 3:	9/1/99 - 9/15/99	78%
	9/16/99 - 5/15/00	50%
	5/16/00 - 8/31/00	87%
Year 4:	9/1/00 - 3/31/01	47%

Cherish Qualls

Year 1:	1/1/98 - 6/15/98	25%
	6/16/98 - 8/31/98	33%
Year 2:	9/1/98 - 6/15/99	33%
	6/16/99 - 8/31/99	50%
Year 3:	9/1/99 - 9/15/99	83%
	9/16/99 - 5/15/00	57%
	5/16/00 - 8/31/00	83%
Year 4:	9/1/00 - 3/31/01	47%

Elena Rossi

Year 2:	3/16/99 - 6/15/99	33%
	6/16/99 - 8/31/99	50%
Year 3:	9/1/99 - 9/15/99	59%
	9/16/99 - 8/31/00	29%

Cheryl Walker

Year 1:	11/1/97 - 6/15/98	33%

DEGREES CONFERRED

The following graduate degrees were conferred to the students listed below during the term of this research program. These students used all or a portion of their research work performed under this grant as the basis of their master's degree theses or doctoral dissertations.

Student	Degree	Year
S. Cho	PhD	2000
E. Rossi	MS	2000
C. Qualls	MS	2000

BUDGET AND EXPENDITURES

This project was originally funded for the period of time from Oct, 1, 1977 through Nov. 13, 2000. A no-cost extension was subsequently requested and granted which extended the end-date of the contract period to March 31, 2001.

The following is a summary of the actual expenditures compared to the original proposed budget for this research project. Costs are separated into DOD Funds provided through the DEPSCoR Program and Auburn University Cost-Share Funds (AU). Complete details of the original proposed budget are provided in Appendix D on a yearly basis as well as by cumulative total.

ITEM	BUDGET DOD	BUDGET AU	TOTAL	ACTUAL DOD	ACTUAL AU	TOTAL
Salary Costs:						
D. A. Cicci	$52,489	$23,358	$75,847	$52,604	$24,352	$76,956
J. E. Cochran, Jr.	17,763	13,322	31,085	17,617	11,932	29,549
Graduate Students	83,200	41,600	106,932	85,195	40,986	126,181
Fringe Benefits	17,563	9,170	26,733	12,842	5,415	18,257
Overhead Costs:	80,893	45,946	126,839	80,893	45,946	126,839
Supplies/Materials:	0	3,000	3,000	0	872	872
Travel Costs:	12,000	6,000	18,000	14,757	11,803	26,560
Publications/Reports:	0	7,500	7,500	0	8,590	8,590
Totals:	$263,908	$149,896	$413,804	$263,908	$149896	$413,804

CUSTOMER CONTACT

Auburn University personnel have had regular contact with personnel from the Space Warfare Center, Analysis and Engineering Directorate (SWC/AE), in the form of telephone calls, teleconferences, FAX's, and status reports.

In addition, the following Technical Interchange Meetings were held during the contract period of the research project:

1. September 18, 1997, Research Program Kickoff Meeting, AFOSR, Washington, DC. Presentations were made by Drs. Cochran and Cicci concerning the research program, objectives, and results achieved thus far. The meeting was attended by personnel from AFOSR, SWC/AES and other invited guests.

2. December 11, 1997, Tether Satellite Working Group (TSWG) Technical Interchange Meeting, Falcon AFM, CO. Presentations were made by Drs. Cochran and Cicci concerning previous and future anticipated tethered satellite research efforts, and the problems associated with the detection and tracking of tethered satellites. The meeting was attended by personnel from AFSPC, 1 CACS, USSPACECOM, SWC, and 21st Space Wing.

3. December 2, 1998, Technical Interchange Meeting at Auburn University, Auburn AL. Drs. Liu and Racca visited the Aerospace Engineering Department for presentations and discussion regarding the current status of the tethered satellite research project. Presentations were made by Drs. Cochran and Cicci, as well as by graduate students S. Cho, A. Lovell, C. Qualls, and E. Rossi.

4. June 9, 1999, Space R&D Technical Interchange Meeting, SAIC Corp., Colorado Springs, CO. Drs. Cochran and Cicci presented updates on the current status of the ongoing tethered satellite research project at Auburn University. The meeting was attended by personnel from Auburn University, the University of Colorado, SWC, DARPA, SAIC, AFOSR, and guests.

PRESENTATIONS

The following presentations related to this research program were made during the term of this research program.

1. September 18, 1997, Research Program Kickoff Meeting, AFOSR, Washington, DC. Presentations were made by Drs. Cochran and Cicci concerning the overall research program, objectives, and plan. The meeting was attended by personnel from AFOSR, SWC/AES and other invited guests.

2. December 11, 1997, Tether Satellite Working Group (TSWG) Technical Interchange Meeting, Falcon AFM, CO. Presentation were made by Drs. Cochran and Cicci concerning previous and future anticipated tethered satellite research efforts, and the problems associated with the detection and tracking of tethered satellites. The meeting was attended by personnel from AFSPC, 1 CACS, USSPACECOM, SWC, and 21st Space Wing.

3. February 9, 1998, AAS/AIAA Space Flight Mechanics Meeting, Monterey, CA. Mr. Cho presented the AAS Paper Number AAS 98-101 entitled, "Identification and Orbit Determination of Tethered Satellite Systems," by S. Cho, J. E. Cochran, Jr., and D. A. Cicci.

4. August 12, 1998, AIAA/AAS Astrodynamics Specialist Conference, Boston, MA. Dr. Cochran presented AIAA Paper Number 98-4555 entitled, "On the Information Contained in the Motion of One Satellite of a Two-Satellite Tethered System," by J. E. Cochran, Jr., S. Cho, A. Lovell, and D. A. Cicci.

5. December 2, 1998, Technical Interchange Meeting at Auburn University, Auburn, AL. Drs. Liu and Racca visited the Aerospace Engineering Department for presentations and discussion regarding the current status of the tethered satellite research project. Presentations were made by Drs. Cochran and Cicci, as well as by graduate students S. Cho, A. Lovell, C. Qualls, and E. Rossi.

6. February 10, 1999, AAS/AIAA Space Flight Mechanics Meeting, Breckenridge, CO. Mr. Cho presented AAS Paper Number 99-193 entitled, "Approximate Solution for Tethered Satellite Motion," by S. Cho, J. E. Cochran, Jr., and D. A. Cicci.

7. February 10, 1999, AAS/AIAA Space Flight Mechanics Meeting, Breckenridge, CO. Mr. Lovell presented AAS Paper Number 99-196 entitled, "A Method for the Identification of a Tethered Satellite," by D. A. Cicci, T. A. Lovell, and C. Qualls.

8.   June 9, 1999, Space R&D Technical Interchange Meeting, SAIC Corp., Colorado Springs, CO. Drs. Cochran and Cicci presented updates on the current status of the ongoing tethered satellite research project at Auburn University. The meeting was attended by personnel from Auburn University, the University of Colorado, SWC, SAIC, DARPA, AFOSR, and several guests.

8.   August 18, 1999, AAS/AIAA Astrodynamics Specialist Conference, Girdwood, AK. Dr. Cicci presented AAS Paper Number 99-415 entitled, "A Look at Tethered Satellite Identification Using Ridge-Type Estimation Methods," by D. A. Cicci, C. Qualls, and T. A. Lovell.

9.   August 18, 1999, AAS/AIAA Astrodynamics Specialist Conference, Girdwood, AK. Dr. Cochran presented AAS Paper Number 99-416 entitled, "Modeling Tethered Satellite Systems for Detection and Orbit Determination," by J. E. Cochran, Jr., S. Cho, A. Lovell, and D. A. Cicci.

10.   January 26, 2000, AAS/AIAA Space Flight Mechanics Meeting, Clearwater, FL. Ms. Qualls presented AAS Paper Number 00-191 entitled, "Preliminary Orbit Determination of a Tethered Satellite," by C. Qualls and D. A. Cicci.

11.   January 26, 2000, AAS/AIAA Space Flight Mechanics Meeting, Clearwater, FL. Mr. Lovell presented AAS Paper Number 00-194 entitled, "Use of Tethered Satellite Filtering Methods in Identifying Re-Entering Objects," by T. A. Lovell, S. Cho, J. E. Cochran, Jr., and D. A. Cicci.

12.   August 16, 2000, AIAA/AAS Astrodynamics Specialist Conference, Denver, CO. Dr. Rossi presented AIAA Paper Number 2000-4347 entitled, "Existence of Periodic Motions of a Tether Trailing Satellite," by E. V. Rossi, D. A. Cicci, and J. E. Cochran, Jr.

13.   February 15, 2001, AAS/AIAA Space Flight Mechanics Meeting, Santa Barbara, CA. Dr. Cicci presented AAS Paper Number 01-232 entitled, "Quick-Look Identification and Orbit Determination of a Tethered Satellite," by D. A. Cicci, J. E. Cochran, Jr., C Qualls, and T. A. Lovell.

TECHNICAL PAPERS

The following papers generated during this research project have been, or are in the process of being published as described below. Copies of all papers are included in Appendix E.

Published

1. "Modeling Tethered Satellite Dynamics for Identification and Orbit Determination," J. E. Cochran, Jr., S. Cho, A. Lovell, and D. A. Cicci, *The Journal of the Astronautical Sciences*, Vol. 48, No. 1, pp. 89-108, January-March 2000. Also published in *Advances in the Astronautical Sciences*, proceedings of the AAS/AIAA Space Flight Mechanics Meeting, Girdwood, AK, August 16-19, 1999.

2. "Evaluation of the Information Contained in the Motion of One Satellite of a Two-Satellite Tethered System," J. E. Cochran, Jr., S. Cho, A. Lovell, and D. A. Cicci, *The Journal of the Astronautical Sciences*, Vol. 48, No. 4, October-December 2000.

3. "Identification and Orbit Determination of a Tethered Satellite System," S. Cho, J. E. Cochran, Jr., and D. A. Cicci, *Applied Mathematics and Computation*, Vol. 117, pp. 301-312, 2001. Also published in *Advances in the Astronautical Sciences*, Vol. 99, Part 1, pp. 21-34, proceedings of the AAS/AIAA Space Flight Mechanics Meeting, Monterey, CA, February 9-11, 1999.

4. "A Look at Tethered Satellite Identification Using Ridge-Type Estimation Methods," D. A. Cicci, C. Qualls and T. A. Lovell, *Applied Mathematics and Computation*, Vol. 119. pp. 297-316, 2001. Also published in *Advances in the Astronautical Sciences*, proceedings of the AAS/AIAA Space Flight Mechanics Meeting, Girdwood, AK, August 16-19, 1999.

Accepted for Publication

5. "Approximate Solution for Tethered Satellite Motion," S. Cho, J. E. Cochran, Jr., and D. A. Cicci, accepted for publication in the *AIAA Journal of Guidance, Control, and Dynamics*, February 2000. Also published in *Advances in the Astronautical Sciences*, Vol. 102, Part 2, pp. 1345-1360, proceedings of the AAS/AIAA Space Flight Mechanics Meeting, Breckenridge, CO, February 7-10, 1999.

6. "A Filtering Method for the Identification of a Tethered Satellite," D. A. Cicci, T. A. Lovell, and C. Qualls, accepted for publication in *The Journal of the Astronautical Sciences*, November 2000. Also published in *Advances in the Astronautical Sciences*, Vol. 102, Part 2, pp. 1399-1418, proceedings of the AAS/AIAA Space Flight Mechanics Meeting, Breckenridge, CO, February 7-10, 1999.

7. "Existence of Periodic Motions of a Tether Trailing Satellite," E. V. Rossi, D. A. Cicci, and J. E. Cochran, Jr., accepted for publication in the *AIAA Journal of Spacecraft and Rockets*, January 2001. Also published in *A Collection of Technical Papers*, pp. 390-396, proceedings of the AIAA/AAS Astrodynamics Specialist Conference, Denver, CO, August 14-17, 2000.

Submitted for Publication

8. "A Study of the Re-Entry Orbit Discrepancy Involving Tethered Satellites," T. A. Lovell, S. Cho, J. E. Cochran, Jr., and D. A. Cicci, submitted for publication to *Acta Astronautica*, July 2000. Also published in *Advances in the Astronautical Sciences*, proceedings of the AAS/AIAA Space Flight Mechanics Meeting, Clearwater, FL, January 23-26, 2000.

To Be Submitted for Publication

9. "Preliminary Orbit Determination of a Tethered Satellite," C. Qualls and D. A. Cicci, to be submitted to *The Journal of the Astronautical Sciences*. Also published in *Advances in the Astronautical Sciences*, proceedings of the AAS/AIAA Space Flight Mechanics Meeting, Clearwater, FL, January 23-26, 2000.

10. "Quick-Look Identification and Orbit Determination of a Tethered Satellite," D. A. Cicci, J. E. Cochran, Jr., C. Qualls, and T. A. Lovell, to be submitted to *The Journal of Astronautical Sciences*. Also published in *Advances in the Astronautical Sciences*, proceedings of the AAS/AIAA Space Flight Mechanics Meeting, Santa Barbara, CA, February 11-15, 2001.

Conference Papers

11. "On the Information Contained in the Motion of One Satellite of a Two-Satellite Tethered System," J. E. Cochran, Jr., S. Cho, A. Lovell, and D. A. Cicci. Published as paper number AIAA 98-4555 in *A Collection of Technical Papers*, pp. 422-431, proceedings of the AIAA/AAS Astrodynamics Specialist Conference, Boston, MA, August 10-12, 1998.

12. "Use of Tethered Satellite Estimation Methods in Identifying Re-Entering Objects," T. A. Lovell, S. Cho. J. E. Cochran, Jr., and D. A. Cicci. Published as paper number AAS 00-194 in *Advances in the Astronautical Sciences*, proceedings of the AAS/AIAA Space Flight Mechanics Meeting, Clearwater, FL, January 23-26, 2000.

Abstracts Accepted for Conference Papers

13. "A Comparison of Orbit Determination and Long-Term Prediction Methods for Tethered Satellite Systems," T. A. Lovell, J. E. Cochran, Jr., and D. A. Cicci, accepted for presentation at the AAS/AIAA Astrodynamics Specialist Conference, Quebec City, Ontario, Canada, July30-Aubust 2, 2001.

APPENDIX A: DOCUMENT LIST

1998 – Present:

1. <u>A Comparison of Orbit Determination and Long-Term Prediction Methods for Tethered Satellite Systems</u>
   AUTHORS: T. A. Lovell, J. E. Cochran, Jr., and D. A. Cicci
   PUBLICATION: To be presented at the AAS/AIAA Astrodynamics Specialist Conference, Quebec City, Ontario, Canada, July 30-August 2, 2001.

2. <u>Quick-Look Identification and Orbit Determination of a Tethered Satellite</u>
   AUTHORS: D. A. Cicci, J. E. Cochran, Jr., C. Qualls, and T. A. Lovell
   PUBLICATION: Presented as paper number AAS 01-232 at the AAS/AIAA Space Flight Mechanics Meeting, Santa Barbara, CA, February 11-14, 2001.

3. <u>Preliminary Orbit Determination of a Tethered Satellite</u>
   AUTHORS: C. Qualls and D. A. Cicci
   PUBLICATION: Presented as paper number AAS 00-191 at the AAS/AIAA Space Flight Mechanics Meeting, Clearwater, FL, January 26-28, 2000.

4. <u>Existence of Periodic Motions of a Tether Trailing Satellite</u>
   AUTHORS: E. V. Rossi, D. A. Cicci, and J. E. Cochran, Jr.
   PUBLICATION: Submitted to the *AIAA Journal of Spacecraft and Rockets*, September 2000. Also presented as paper number AIAA 2000-4347 at the AIAA/AAS Astrodynamics Specialist Conference, Denver, CO, August 14-17, 2000.

5. <u>Use of Tethered Satellite Estimation Methods in Identifying Re-Entering Objects</u>
   AUTHORS: T. A. Lovell, S. Cho, J. E. Cochran, Jr., and D. A. Cicci
   PUBLICATION: Submitted to *Acta Astronautica*, July 2000. Also presented as paper number AAS 00-194 at the AAS/AIAA Space Flight Mechanics Meeting, Clearwater, FL, January 26-28, 2000.

6. <u>A Filtering Method for the Identification of a Tethered Satellite</u>
   AUTHORS: D. A. Cicci, A. Lovell, and C. Qualls
   PUBLICATION: To appear in *The Journal of the Astronautical Sciences*, 2001. Also presented as paper number AAS 99-196 at the AAS/AIAA Space Flight Mechanics Meeting, Breckenridge, CO, Feb. 7-10, 1999.

7. **Approximate Solution for Tethered Satellite Motion**
   AUTHORS: S. Cho, J. E. Cochran, Jr., and D. A. Cicci
   PUBLICATION: To appear in *AIAA Journal of Guidance, Control, and Dynamics*, 2001. Also presented as paper number AAS 99-193 at the AAS/AIAA Space Flight Mechanics Meeting, Breckenridge, CO, Feb. 7-10, 1999.

8. **A Look at Tethered Satellite Identification Using Ridge-Type Estimation Methods**
   AUTHORS: D. A. Cicci, C. Qualls, and T. A. Lovell
   PUBLICATION: *Applied Mathematics and Computation*, Vol. 119, pp. 297-316, 2001. Also presented as paper number AAS 99-415 at the AAS/AIAA Astrodynamics Specialist Conference, Girdwood, AK, August 16-19, 1999.

9. **Identification and Orbit Determination of a Tethered Satellite System**
   AUTHORS: S. Cho, J. E. Cochran, Jr., and D. A. Cicci
   PUBLICATION: *Applied Mathematics and Computation*, Vol. 117, pp. 301-312, 2001. Also presented as paper number AAS 98-101 at the AAS/AIAA Space Flight Mechanics Meeting, Monterey, CA, February 9-11, 1998.

10. **Evaluation of the Information Contained in the Motion of One Satellite of a Two-Satellite Tethered System**
    AITHORS: J. E. Cochran, Jr., S. Cho, A. Lovell and D. A. Cicci
    PUBLICATION: *The Journal of the Astronautical Sciences*, Vol. 48, No. 4, October-December 2000.

11. **Modeling Tethered Satellite Systems for Identification and Orbit Determination**
    AUTHORS: J. E. Cochran, Jr., S. Cho, A. Lovell, and D. A. Cicci
    PUBLICATION: *The Journal of the Astronautical Sciences*, Vol. 48, No. 1, pp. 89-108, January-March 2000. Also presented as paper number AAS 99-416 at the AAS/AIAA Astrodynamics Specialist Conference, Girdwood, AK, August 16-19, 1999.

12. **Tracking the TiPS Tethered Satellite System**
    AUTHORS: W. J. Barnds and S. L. Coffey
    PUBLICATION: AAS 99-417, AAS/AIAA Astrodynamics Specialist Conference, Girdwood, AK, August 16-19, 1999.

13. **Dynamics of the ASTOR Tethered Satellite System**
    AUTHORS: A. P. Mazzoleni and J. H. Hoffman
    PUBLICATION: AAS 99-191, AAS/AIAA Space Flight Mechanics Meeting, Breckenridge, CO, Feb. 7-10, 1999.

14. **On the Information Contained in the Motion of One Satellite of a Two-Satellite Tethered System**

    AUTHOR: J. E. Cochran, Jr., S. Cho, A. Lovell and D. A. Cicci

    PUBLICATION: Presented as paper number AIAA 98-4555 at the AIAA/AAS Astrodynamics Specialist Conference, Boston, MA, Aug. 10-12, 1998.

15. **Tether Deployment and Trajectory Modeling for the OEDIPUS Missions**

    AUTHORS: F. R. Vigneron, F. Schultz, A. M. Jablonski, and G. Tyc

    PUBLICATION: AIAA 98-4553, AIAA/AAS Astrodynamics Specialist Conference, Boston, MA, August 10-12, 1998.

16. **Dynamics and Orbit Determination of Tethered Satellite Systems**

    AUTHORS: J. E. Cochran, Jr., S. Cho, Y-M Cheng, and D. A. Cicci

    PUBLICATION: *The Journal of the Astronautical Sciences*, Vol. 46, No. 2, pp. 177-194, April-June 1998. Also presented as paper number AAS 96-147 at the AAS/AIAA Space Flight Mechanics Conference, Austin, TX, February 12-15, 1996.

17. **Eccentricity Effects on Apparent Earth-Impacting Orbits of Tethered Space Objects**

    AUTHORS: R. A. Racca and J. K. Feldman

    PUBLICATION: Technical Report 98-9, Directorate of Analysis and Engineering, Falcon Air Force Base, CO, April 1998.

18. **Orbit Determination of a Tethered Satellite System Using Laser and Radar Tracking**

    AUTHORS: S. R. Vadali, H. Jung, and K. T. Alfriend

    PUBLICATION: AAS 98-102, AAS Space Flight Mechanics Meeting, Monterey, CA, Feb 1998.

19. **Conditions for Apparent Earth-Impacting Orbits of Tethered Space Objects**

    AUTHORS: R. A. Racca and J. J. F. Liu

    PUBLICATION: Technical Report 97-22, Directorate of Analysis and Engineering, Falcon Air Force Base, CO, January 1998.

1996 - 1997:

20. **Filtering Methods for the Orbit Determination of a Tethered Satellite,**

    AUTHORS: S. A. Kessler and D. A. Cicci

    PUBLICATION: *The Journal of the Astronautical Sciences*, Vol. 45, No. 3, pp. 263-278, July-September 1997. Also presented as paper number AAS 95-350 at the AAS/AIAA Astrodynamics Specialist Conference, Halifax, NS, Canada, August 14-17, 1995.

21. **Results of the TiPS Tethered Satellite Experiment**
     AUTHORS: W. J. Barnds, S. Coffey, W. Purdy, B. Kelm, and M. Davis
     PUBLICATION: AAS 97-600

22. **Experiments in Tether Dynamics Planned for ATEX's Flight**
     AUTHORS: Michael F. Zedd
     PUBLICATION: AAS 97-601

23. **Strategy for the Passive Maneuvering of Tether-Connected Systems**
     AUTHORS: Chu Shi-Sheng and Wang Li-Sheng
     PUBLICATION: *AIAA Journal of Guidance, Control, and Dynamics*, v 20 n 2,
                        March-April 1997.

24. **Periodic Motion in the Tethered Satellite System**
     AUTHORS: Shaohua Yu
     PUBLICATION: *AIAA Journal of Guidance, Control, and Dynamics*, v19 n 5, Sept-
                        Oct 1996, pp. 1195-1197.

25. **General Formulation for N-body Tethered Satellite System Dynamics**
     AUTHORS: M. Keshmiri and A. K. Misra
     PUBLICATION: *AIAA Journal of Guidance, Control, and Dynamics*, v 19, n 1 Jan-
                        Feb 1996, pp. 75-83.

26. **Stability of the Pendular Motion of a Tethered System in Elliptical Orbit**
     AUTHORS: M. Ruiz, J. Pelaez, and E. C. Lorenzini
     PUBLICATION: AAS-96-201, AAS/AIAA Space Flight Mechanics Meeting,
                        Austin, TX, Feb. 12-15, 1996.

1994 - 1995:

27. **On the Inverse Control of Tethered Satellite Systems**
     AUTHORS: S. Pradhan, V. J. Modi, and A. K. Misra
     PUBLICATION: *The Journal of the Astronautical Sciences*, v 43, n 2 April-June
                        1995, pp. 179-193.

28. **Attitude and Orbit Determination of A Tethered Satellite System**
     AUTHORS: K. T. Alfriend, W. J. Barnds, S. L. Coffey, and L. M. Stuhrenberg,
     PUBLICATION: AAS 95-351, AAS/AIAA Astrodynamics Specialist Conference,
                        Halifax, Nova Scotia, CAN, Aug 1995.

29. **Estimation and Control of Tethered Satellite Systems**
     AUTHORS: Ehud Netzer and Thomas R. Kane
     PUBLICATION: *AIAA Journal of Guidance, Control, and Dynamics*, v 18, n 4,
                        July-Aug 1995, pp. 851-858.

30. **On the Dynamics of a Tethered Satellite**
   AUTHORS: Wang Li-Sheng, Chern Shuh-Jye, and Shih Chih-Wen
   PUBLICATION: *Archive for Rational Mechanics and Analysis*, v 127, Iss 4, pp. 297-318, 1994.

31. **Analytical Investigation of the Dynamics of Tethered Constellations in Earth Orbit, Phase 2**
   AUTHORS: E. C. Lorenzini, G. E. Gullahorn, M. L. Cosmo, R. D. Estes, and M. D. Grossi
   PUBLISHED: May 01, 1994, NAS 1.26:196509.

32. **Non-Linear Free Periodic Oscillations of a Tethered Satellite System**
   AUTHORS: A. Luongo and F. Vestroni
   PUBLICATION: *Journal of Sound and Vibration*, Volume: 175 Issue: 3 Page: pp. 299-315, Aug 18, 1994.

33. **Comparison of Predicted and Actual Orbital Lifetimes for the SEDS-2 Mission**
   AUTHORS: Steven W. Evans
   PUBLISHED: Jan 01, 1994, NAS 1.15:111114.

34. **Object Recognition and Pose Estimation of Planar Objects from Range Data**
   AUTHORS: Thomas W. Pendleton, Chiun Hong Chien, Mark L. Littlefield, and Michael Magee
   PUBLICATION: Dual-Use Space Technology Transfer Conference and Exhibition, V 2 Page: 427-434 May 01, 1994.

35. **The Calculation of the Orbital Elements of a Tethered Satellite System After Release**
   AUTHORS: Naigang Liu Cui, Liu Dun, and Naiming Yuhua Qi
   PUBLICATION: AIAA 94-3746

1992 - 1993:

36. **Dynamics of a Tethered Satellite System**
   AUTHORS: Gyounghyun Bae, Eunsup Sim, and Jewel B. Barlow
   PUBLICATION: *Advances in the Astronautical Sciences*, v 82, pt 2 1993, pp. 1297-1310.

37. **Effects of Aerodynamic Lift on the Stability of Tethered Subsatellite System**
   AUTHORS: Mehdi Keshmiri and Arun K. Misra
   PUBLICATION: *Advances in the Astronautical Sciences*, Vol. 82, Pts.1 & 2, 1993.

38. **Orbital Lifetime of Tethered Satellites**
   AUTHORS: Ted Warnock and John E. Cochran, Jr.
   PUBLICATION: *The Journal of the Astronautical Sciences*, v 41, n 2, Apr-Jun 1993.

39. **Space Time Neural Networks for Tether Operations in Space**
    AUTHORS: Robert N. Lea, James A. Villarreal, Yashvant Jani, and
                           Charles Copeland
    PUBLICATION: *Proceedings of the Third International Workshop on Neural
                           Networks and Fuzzy Logic*, Volume 1, pp. 127-168, Jan 01, 1993
                           NAS 1.55:10111.

40. **Precession and Circularization of Elliptical Space-Tether Motion**
    AUTHORS: Jim D. Chapel and Patrick Grosserode
    PUBLICATION: AIAA Guidance, Navigation and Control Conference, Monterey,
                           CA, Aug. 9-11, 1993, Technical Papers. Pt. 1 (A93-51301 22-63),
                           pp. 147-156, AIAA 93-3716.

41. **Tethered Dynamics**
    AUTHORS: R. H. Smith
    PUBLICATION: The Aerospace Corporation, Interoffice Correspondence, 94-5513-
                           RHS-01, 4 Oct. 1993.

42. **Simulation of Single Tether Systems**
    AUTHORS: Theron J. Carter and Michael Greene
    PUBLICATION: *Simulation*, Jan 1992.

43. **Improved Estimation/Prediction in Quick-Look Orbit Determination**
    AUTHORS: David A. Cicci and Roger L. Hall
    PUBLICATION: *The Journal of the Astronautical Sciences*, v 40, n 1, Jan-Mar
                           1992, pp. 91-106.

44. **Dynamics of a Tethered Satellite in Elliptical, Non-Equatorial Orbits**
    AUTHORS: Guido De Matteis
    PUBLICATION: *AIAA Journal of Guidance, Control, and Dynamics*, V 15, N 3, pp.
                           621-626, Jun 01, 1992.

45. **Predicting the Orbital Lifetime of Tethered Satellite Systems**
    AUTHORS: T. W. Warnock and J. E. Cochran, Jr.
    PUBLICATION: 43rd Congress of the International Astronautical Federation, IAF
                           92-0002, 1992.

46. **Planar Motion of a Tethered Satellite-Platform System in a Slightly Elliptic Orbit**
    AUTHORS: Clare Savaglio and Nguyen X. Vinh
    PUBLICATION: AAS PAPER 91-546, Jan 1992.

47. **Tethered Satellite Tracking Using an Adaptive Kalman Filter**
    AUTHORS: Jinkuan Wang and Tadashi Takano
    PUBLICATION: International Symposium on Space Technology and Science, 18th,
                           Vols. 1 & 2. A95-82299, pp. 1871-1876, Jan 1992.

1990-1991:

48. <u>Real Time Estimator for Control of an Orbiting Single Tether System</u>
    AUTHORS: Michael Greene and Thomas S. Denney, Jr.
    PUBLICATION: *IEEE Transactions on Aerospace and Electronic Systems*, v 27, n
                    6, Nov 1991, pp. 880-883.

49. <u>Discretized Model for the Dynamics of a Tethered Satellite System and Applications</u>
    AUTHORS: Guido de Matteis and Luciano M. de Socio
    PUBLICATION: *Advances in the Astronautical Sciences*, v 75, pt 2, 1991, pp. 1029-
                    1051.

50. <u>Navigation of the TSS-1 Mission</u>
    AUTHORS: Timothy C. Jackson
    PUBLICATION: *Advances in the Astronautical Sciences*, v 75, pt 2, 1991, pp. 971-
                    986.

51. <u>On State Estimation for an Orbiting Single Tether System</u>
    AUTHORS: Thomas S. Denney, Jr. and Michael Greene
    PUBLICATION: *IEEE Transactions on Aerospace and Electronic Systems*, July
                    1991.

52. <u>Three-Dimensional Vibrations of a Tethered Satellite System</u>
    AUTHORS: Marcello Pignataro, Angelo Luongo, and Monica Pasca
    PUBLICATION: *AIAA Journal of Guidance, Control, and Dynamics*, Vol 14, No 2,
                    pp.312-320, March 1991.

53. <u>Dynamics of a Tethered Satellite Subjected to Aerodynamic Forces</u>
    AUTHORS: Guido De Matteis, and Luciano M. De Socio
    PUBLICATION: *AIAA Journal of Guidance, Control, and Dynamics*, Volume: 14
                    pp. 1129-113, Dec 1991.

54. <u>A Continuous Discrete Extended Kalman Filter for the Small Expendable Deployment</u>
    <u>System</u>
    AUTHORS: Thomas S. Denney
    PUBLICATION: Auburn University - Theses 1990

55. <u>Newtonian Derivation of the Equations of Motion for a Tethered Satellite System</u>
    AUTHORS: Kenneth D. Kopke, Leland E. Herder, Leland E., Cynthia L.
                    Trowbridge and Thomas J. Eller
    PUBLICATION: AIAA 90-2989, Jan 1990.

56. **Dynamics and Control of Tethered Spacecraft - A Brief Overview**
    AUTHORS: V. J. Modi, P. K. Lakshmanan, and A. K. Misra
    PUBLICATION: AIAA Dynamics Specialists Conference, Long Beach, CA, Apr. 5,
                    6, 1990, Technical Papers (A90-26776 10-39). 1990, p. 42-57.
                    AIAA 90-1195.

1988 - 1989:

57. **Optical Tracker for an Orbiting Tethered System**
    AUTHORS: Michael Greene and Greg Stover
    PUBLICATION: *Proceedings of the 21ˢᵗAnnual Southeastern Symposium on System
                    Theory*, Available - IEEE Service Center Piscataway, NJ, 1989.

58. **Orbit Evolution and Decay of Tether Launched Space Systems**
    AUTHORS: S. Bergamaschi
    PUBLICATION: AIAA PAPER 89-1572, Jan 1989.

59. **A Vectorized Algorithm for 3D Dynamics of a Tethered Satellite**
    AUTHORS: Howard B. Wilson
    PUBLICATION: Alabama Univ., Research Reports: 1989 NASA (ASEE Summer
                    Faculty Fellowship Program) Page: 30 p.

60. **Tethered Satellites - The Orbit Determination Problem and Missile Early Warning
    Systems**
    AUTHORS: T. A. Asher, D. G. Boden, and R. J. Tegtmeyer
    PUBLICATION: AIAA PAPER 88-4284, Jan 1988.

61. **Gravity Gradient Disturbances on Rotating Tethered Systems in Circular Orbit**
    AUTHORS: Anthony B. Decou
    PUBLICATION: International Conference on Tethers in Space - Toward Flight, 3rd
                    Collection of Papers and Abstracts AIAA (A8940176 17-12) pp.
                    343-351, Jan 01, 1989,   AIAA 89-1593.

62. **Optimal State Estimation of a Tethered Satellite System**
    AUTHORS: Robert F. Stengel and Daniel S. Swanson
    PUBLICATION: *Space Tethers for Science in the Space Station Era*; Bologna,
                    Societa Italiana di Fisica, 1988, p. 85-92.

63. **Order of Magnitude Evaluation of the Lifetime of a Free Tether in Orbit**
    AUTHORS: S. Bergamaschi and M. Morana
    PUBLICATION   *Space Tethers for Science in the Space Station Era*; Proceedings of
                    the Second International Conference, Venice, Italy, Oct. 4-8, 1987
                    (A89-43326 18-12). Bologna, Societa Italiana di Fisica, 1988, p.
                    453-460. Jan 01, 1988.

Before 1988:

64. **A Review of Tether Induced Dynamical Features**
    AUTHORS: S. Bergamaschi
    PUBLICATION: NASA, Washington Applications of Tethers in Space: Workshop
                    Proceedings, V 1, pp. 103-116, Jun 01, 1986.

65. **J2 Perturbations on the Motion of Tethered Platforms**
    AUTHORS: S. Bergamaschi and C. Savaglio
    PUBLICATION: NASA, AIAA, and PSN, International Conference on Tethers in
                    Space, Arlington, VA, Sept. 17-19, 1986, Paper. 11 p. Sep 01,
                    1986.

66. **First Integrals of Motion in the Dynamics of Tethered Satellites**
    AUTHORS: Mahesh Rajan and T. J. Anderson
    PUBLICATION: *The Journal of the Astronautical Sciences* (ISSN 0021-9142), vol.
                    34, July-Sept. 1986, pp. 331-339.

67. **Quasi-Analytical Solutions for the Dynamics of a Class of Tethered Satellites with Danby's Aerodynamical Drag**
    AUTHORS: Zvattaro I. Bonzani and M. G. Chiado Piat
    PUBLICATION: *Celestial Mechanic,s* Volume: 37 Page: 371-385 Dec 01, 1985.

68. **On Modeling and Simulation of the Dynamics of Tether Connected Satellite Systems**
    AUTHORS: V. J. Modi, A. K. Misra, amd D. M. Xu
    PUBLICATION: World Congress on System Simulation and Scientific
                    Computation, 10th, Montreal, Canada, August 8-13, 1982,
                    Proceedings. Volume 3 (A84-11828 02- 59). Montreal, 1983.

69. **Space Shuttle Tethered Satellite Analysis**
    AUTHORS: Felix R. Hoots, Ronald L. Roehrich, and Victor G. Szebehely
    PUBLICATION: Directorate of Astrodynamics DCS/Operations, HQ SPACECOM,
                    26 Aug 1983.

70. **Orbital and Relative Motion of a Tethered Satellite System**
    AUTHORS: J. C. Van Der Ha
    PUBLICATION: International Astronautical Federation, International
                    Astronautical Congress, 34th, Oct 1983.

71. **Dynamics and Control of Tether Connected Two-Body Systems -A Brief Review**
    AUTHORS: A. K. Misra and V. J. Modi
    PUBLICATION: International Astronautical Federation, International Astronautical
                    Congress, 33rd, Paris, France, Sept. 27-Oct. 2, 1982, 25 p.

72. **Orbital Perturbations of Tethered Satellite Systems**
    AUTHORS: V. J. Modi and A. K. Misra
    PUBLICATION: *The Journal of the Astronautical Sciences*, vol. 25, July-Sept.
                      1977, pp. 271-278.

73. **Tethered Body Problems and Relative Motion Orbit Determination**
    AUTHORS: J. B. Eades, Jr. and H. Wolf
    PUBLISHED: NASA Technical Report NASA-CR-132780, Aug 01, 1972.

74. **Dynamics of Two Slowly Rotating Point-Mass Vehicles Connected by a Massless Tether and in a Circular Orbit**
    AUTHORS: W. M. Adams, Jr.
    PUBLISHED: NASA Technical Report, NASA-TN-D-5599, Jan 01, 1970.

APPENDIX B: EQUATIONS OF MOTION

The nomenclature used and the equations of motion for the 2nd Stage and 3rd Stage filters are provided below.

Nomenclature

x, y, z	= position coordinates of observed mass (GEC axes)
u, v, w	= velocity coordinates of observed mass (GEC axes)
a_t	= tangential component of tether acceleration
a_r	= radial component of tether acceleration
α	= in-plane libration angle
ω	= in-plane libration rate
ρ_{cm}	= tether length from observed mass to center of mass
r_E	= radius of Earth
μ	= gravitational constant **of the Earth**
J_2	= zonal harmonic gravitational constant of the Earth

2nd STAGE FILTER:

State vector = $[x\ y\ z\ u\ v\ w\ a_t\ a_r]^T$

Equations of motion:

$$\dot{x} = u$$
$$\dot{y} = v$$
$$\dot{z} = w$$
$$\dot{u} = -\frac{\mu}{r^3}x + a_r\frac{x}{r} + a_t\frac{u}{V} + a_{ox}$$
$$\dot{v} = -\frac{\mu}{r^3}y + a_r\frac{y}{r} + a_t\frac{v}{V} + a_{oy}$$
$$\dot{w} = -\frac{\mu}{r^3}z + a_r\frac{z}{r} + a_t\frac{w}{V} + a_{oz}$$

where

$$r = \sqrt{x^2 + y^2 + z^2}$$

$$V = \sqrt{u^2 + v^2 + w^2}$$

$$a_{ox} = -\frac{3}{2}\mu J_2 \frac{r_E^2}{r^5} x(1 - 5\frac{z^2}{r^2})$$

$$a_{oy} = -\frac{3}{2}\mu J_2 \frac{r_E^2}{r^5} y(1 - 5\frac{z^2}{r^2})$$

$$a_{oz} = -\frac{3}{2}\mu J_2 \frac{r_E^2}{r^5} z(3 - 5\frac{z^2}{r^2})$$

3rd STAGE FILTER

State vector $= [x\ y\ z\ \alpha\ u\ v\ w\ \omega\ \rho_{cm}]^T$

<u>Equations of motion</u>:

$$\dot{x} = u$$
$$\dot{y} = v$$
$$\dot{z} = w$$
$$\dot{\alpha} = \omega$$

$$\dot{u} = -\frac{\mu}{r^3}x + a_T(\cos\alpha\frac{x}{r} + \sin\alpha\frac{u}{V}) + a_{ox}$$

$$\dot{v} = -\frac{\mu}{r^3}y + a_T(\cos\alpha\frac{y}{r} + \sin\alpha\frac{v}{V}) + a_{oy}$$

$$\dot{w} = -\frac{\mu}{r^3}z + a_T(\cos\alpha\frac{z}{r} + \sin\alpha\frac{w}{V}) + a_{oz}$$

$$\dot{\omega} = \frac{2\dot{\theta}\dot{r} - a_T\sin\alpha}{r} - \frac{3\mu\cos\alpha\sin\alpha}{r^3}$$

$$+ \frac{1}{\beta\rho_{cm}}[(a_{opx} - a_{ox})(\cos\alpha\frac{u}{V} - \sin\alpha\frac{x}{r}) + (a_{opy} - a_{oy})(\cos\alpha\frac{v}{V} - \sin\alpha\frac{y}{r})$$

$$+ (a_{opz} - a_{oz})(\cos\alpha\frac{w}{V} - \sin\alpha\frac{z}{r})] - \frac{1}{r}(a_{ox}\frac{u}{V} + a_{oy}\frac{v}{V} + a_{oz}\frac{w}{V})$$

where

$$a_T = \rho_{cm}[(\dot{\theta}+\omega)^2 + \frac{\mu}{r^3}(3\cos^2\alpha - 1)] + (a_{opx} - a_{ox})(\cos\alpha\frac{x}{r} + \sin\alpha\frac{u}{V})$$

$$+ (a_{opy} - a_{oy})(\cos\alpha\frac{y}{r} + \sin\alpha\frac{v}{V}) + (a_{opz} - a_{oz})(\cos\alpha\frac{z}{r} + \sin\alpha\frac{w}{V})$$

$$\dot{\theta} = \frac{\sqrt{(yw - zv)^2 + (zu - xw)^2 + (xv - yu)^2}}{r^2}$$

$$a_{opx} = -\frac{3}{2}\mu J_2 \frac{r_E^2}{r_p^5} x_p (1 - 5\frac{z_p^2}{r_p^2})$$

$$a_{opy} = -\frac{3}{2}\mu J_2 \frac{r_E^2}{r_p^5} y_p (1 - 5\frac{z_p^2}{r_p^2})$$

$$a_{opz} = -\frac{3}{2}\mu J_2 \frac{r_E^2}{r_p^5} z_p (3 - 5\frac{z_p^2}{r_p^2})$$

$$x_p = x + \beta\rho_{cm}(\cos\alpha\frac{x}{r} + \sin\alpha\frac{u}{V})$$

$$y_p = y + \beta\rho_{cm}(\cos\alpha\frac{y}{r} + \sin\alpha\frac{v}{V})$$

$$z_p = z + \beta\rho_{cm}(\cos\alpha\frac{z}{r} + \sin\alpha\frac{w}{V})$$

*The constant β is defined as $1 + \frac{m_p}{m}$. Although its value is generally noi known, for the results generated in this report a value of 1 was assumed (i.e. $m_p \gg m$).

APPENDIX C: SOFTWARE

This appendix includes hard copies of the computer programs which have been developed, as well as sample input and output files which are used in the implementation of the proposed methodology. All programs are written in FORTRAN 77. A diskette containing these files, as well as the executable files, POD.EXE, QLF.EXE, and LTF.EXE, is attached to the inside of the back cover of this report. The following files are included in this appendix:

1st Stage: POD Algorithm

POD.IN
POD.FOR
POD.OUT

2nd Stage: Quick-Look Algorithm

OBS.IN
QLF.FOR
QLF.OUT
QUICK-LOOK.OUT

3rd Stage: Long-Term Algorithm

LTF.FOR
LTF.OUT

POD.IN:

```
345   96256003323.159   1166.062   894.01   257.5792   0.00052000   59.4335
0.00039200
344   96256003443.159   1055.110   888.04   329.4737   0.00062000   76.1779
0.00057600
344   96256003603.159   1191.583   888.04    30.4119   0.00062000   57.2229
0.00057600
```

POD.FOR:

```
***********************************************************************
*       THIS PROGRAM USES THREE TIMES/POSITION VECTORS TO FIND AN
*       ESTIMATE OF THE VELOCITY, ACCELERATION, AND TETHER LENGTH OF THE
*       FIRST OBSERVATION TIME. THE NINTH ORDER F & G SERIES IS USED TO
*       ITERATE ON THE MODIFIED GRAVITATIONAL PARAMETER, MU_STAR, IN THE
*       DIFFERENCED KEPLER'S EQUATION.  ONCE THE VALUE OF MU_STAR IS
*    ·  DETERMINED, RHO_CM IS CALCULATED.
*       INPUT: POD.IN
*       OUTPUT: POD.OUT
*
*       THIS PROGRAM WAS WRITTEN BY MEMBERS OF THE TETHER SATELLITE
*       WORKING GROUP (DAVID CICCI, CHERISH QUALLS) AT AUBURN
*       UNIVERSITY. THE POINT OF CONTACT, DAVID A. CICCI CAN BE
*       REACHED AT THE FOLLOWING:
*                                   AEROSPACE ENGINEERING DEPARTMENT
*                                   211 AEROSPACE ENGINEERING BUILDING
*                                   AUBURN UNIVERSITY, AL 36849-5338
*
*                                   PHONE: (334) 844-6820
*                                   FAX: (334) 844-6803
*                                   E-MAIL: DCICCI@ENG.AUBURN.EDU
*
***********************************************************************

        IMPLICIT DOUBLE PRECISION (A-Z)
        DIMENSION A(3,3),TIME(3)
        INTEGER I,SITE,YEAR,DAY,HOUR,MINUTE

        OPEN(100,FILE='POD.IN',STATUS='UNKNOWN')
        OPEN(200,FILE='POD.OUT',STATUS='UNKNOWN')


        PI=2.0D0*DASIN(1.0D0)

***********************************************************************
*       READ IN DATA IN THE FOLLOWING FORMAT: SITE, YYDDDHHMMSS.SSS,
*       RANGE, RANGE COVARIANCE, AZIMUTH, AZIMUTH COVARIANCE, ELEVATION,
*       ELEVATION COVARIANCE
***********************************************************************

        DO I=1,3

        READ(100,12) SITE,YEAR,DAY,HOUR,MINUTE,SECOND,RHO,SIGR,AZ,SIGAZ
      . ,EL,SIGEL
   12   FORMAT(I3,2X,I2,I3,I2,I2,F6.3,2X,F8.3,2X,F6.2,2X,F8.',2X,F10.8,
      . 2X,F8.4,2X,F10.8)
        CALL STATION(SITE,HEIGHTG,LONG,LAT)

***********************************************************************
*       CONVERT YYDDDHHMMSS.SSS TIME FORMAT TO MINUTES FOR USE IN
*       CALCULATING THE JULIAN DATE
***********************************************************************
```

66

```
         DT=(DAY-1)*1440.0D0+HOUR*60.0D0+MINUTE+SECOND/60.0D0

**********************************************************************
*        DETERMINE THE YEAR IN WHICH THE DATA WAS OBTAINED.
**********************************************************************

         IF (YEAR.LT.10) THEN
            YEAR=YEAR+2000.0D0
         ELSE
            YEAR=YEAR+1900.0D0
         END IF

**********************************************************************
*        BEGIN CALCULATING THE JULIAN DATE. JANUARY 1, YEAR IS CONSIDERED
*        AS THE EPOCH START TIME.
**********************************************************************

         JDSTART=367.0D0*YEAR-AINT(7.0D0*(YEAR+AINT((1.0D0+9.0D0)
     .   /12.0D0))/4.0D0)+AINT(275.0D0*1.0D0/9.0D0)+1.0D0+1721013.5D0+
     .   (0.0D0+0.0D0/60.0D0)/1440.0D0+0.0D0/24.0D0

         TU=(JDSTART-2415020.0D0)/36525.0D0
         THETAG0=99.6909833D0+(36000.7689D0*TU)+(.00038708D0*TU**2)

         ANGLE=THETAG0/360.0D0
         THETAG0=DABS(AINT(ANGLE)*360.0D0-THETAG0)

         WE=2.5068447D-1

         THETAG=THETAG0+DT*WE
         ANGLE=THETAG/360.0D0
         THETAG=DABS(AINT(ANGLE)*360.0D0-THETAG)
         THETA=THETAG+LONG*180.0D0/PI
         ANGLE=THETA/360.0D0
         THETA=DABS(AINT(ANGLE)*360.0D0-THETA)

         THETA=THETA*PI/180.0D0

**********************************************************************
*        DETERMINE THE INITIAL THETA VALUE FOR USE IN THE QUICK-LOOK
*        FILTER. THETA IS INCLUDED IN THE QUICK-LOOK FILTER'S INITIAL
*        CONDITIONS FILE.
**********************************************************************

         IF (I.EQ.1) THEN
             THETA1=THETA
         END IF

**********************************************************************
*        USING THE GIVEN LATITUDE AND GEODETIC HEIGHT AND THE CALCULATED
*        THETA - CALCULATE THE POSITION VECTOR OF THE TRACKER IN THE
*        GEOCENTRIC-EQUATORIAL SYSTEM
**********************************************************************

         CALL GEODETIC(LAT,THETA,HEIGHTG,RX,RY,RZ)

**********************************************************************
```

67

```
*        CONVERT TIME FROM MINUTES TO SECONDS AND CONVERT AZIMUTH /
*        ELEVATION FROM DEGREES TO RADIANS FOR USE IN THE F AND G SERIES
**********************************************************************

         TIME(I)=DT*60.0D0
         AZ=AZ*(PI/180.0D0)
         EL=EL*(PI/180.0D0)
         RHO=RHO*1000.0D0
         R=DSQRT(RX**2+RY**2+RZ**2)
         PHI=LAT

**********************************************************************
*        CONVERT RANGE, AZIMUTH, ELEVATION TO GEOCENTRIC-EQUATORIAL
*        POSITION VECTORS
**********************************************************************

         LXH=-DCOS(AZ)*DCOS(EL)
         LYH=DSIN(AZ)*DCOS(EL)
         LZH=DSIN(EL)
         SX=DSIN(PHI)*DCOS(THETA)
         SY=DSIN(PHI)*DSIN(THETA)
         SZ=-DCOS(PHI)
         EX=-DSIN(THETA)
         EY=DCOS(THETA)
         EZ=0.0D0
         ZX=DCOS(THETA)*DCOS(PHI)
         ZY=DCOS(PHI)*DSIN(THETA)
         ZZ=DSIN(PHI)
         LX=SX*LXH+EX*LYH+ZX*LZH
         LY=SY*LXH+EY*LYH+ZY*LZH
         LZ=SZ*LXH+EZ*LYH+ZZ*LZH

         RXX=RX+RHO*LX
         RYY=RY+RHO*LY
         RZZ=RZ+RHO*LZ

**********************************************************************
*        CONVERT POSITION VECTORS FROM METERS TO KILOMETERS
**********************************************************************

         A(I,1)=RXX/1000.0D0
         A(I,2)=RYY/1000.0D0
         A(I,3)=RZZ/1000.0D0

         ENDDO

         T1=TIME(1)
         T2=TIME(2)
         T3=TIME(3)

         R1X=A(1,1)
         R1Y=A(1,2)
         R1Z=A(1,3)
         R2X=A(2,1)
         R2Y=A(2,2)
         R2Z=A(2,3)
         R3X=A(3,1)
```

```
      R3Y=A(3,2)
      R3Z=A(3,3)

************************************************************************
*       CALL FGNINTH SUBROUTINE TO BEGIN ITERATIVE PROCESS.  ONCE
*       STOPPING CRITERIA IS MET INITIAL ESTIMATES OF POSITION,
*       VELOCITY, ACCELERATION, AND TETHER LENGTH ARE WRITTEN TO
*       QLFIC.IN.  THIS FILE IS THEN USED AS AN INPUT INTO THE
*       QUICK-LOOK FILTER.
************************************************************************

      CALL FGNINTH(TJ,R1X,R1Y,R1Z,T2,R2X,R2Y,R2Z,T3,R3X,R3Y,R3Z,
    .     THETA1,SEMIPTR,RHOCM,MUSTAR,A,ECCEN)

      END

************************************************************************
*     THIS SUBROUTINE WILL COMPUTE THE ECEF COORDINATES OF A RECEIVER
*     GIVEN THE GEODETIC LONG.,LAT.,HEIGHT
************************************************************************

      SUBROUTINE GEODETIC(PHIG,LAMBDAG,HEIGHTG,XECEF,YECEF,ZECEF)
      IMPLICIT DOUBLE PRECISION(A-Z)

      A=6378137.0D0
      F=1.0D0/298.257223563D0
      E=DSQRT(2.0D0*F-F**2.0D0)
      R=A/(DSQRT(1.0D0-E**2.0D0*(DSIN(PHIG))**2.0D0))
      XECEF=(R+HEIGHTG)*DCOS(PHIG)*DCOS(LAMBDAG)
      YECEF=(R+HEIGHTG)*DCOS(PHIG)*DSIN(LAMBDAG)
      ZECEF=((1.0D0-E**2.0D0)*R+HEIGHTG)*DSIN(PHIG)

      RETURN
      END


************************************************************************
*       THIS SUBROUTINE CONSISTS OF THE ITERATIVE TECHNIQUE, THE
*       SECANT METHOD. ONCE THE STOPPING CRITERIA (TOL) HAS BEEN MET
*       THE POD STAGE IS COMPLETED AND AN INITIAL CONDITIONS FILE
*       (QLFIC.IN) IS AVAILABLE FOR USE WITH THE QUICK-LOOK FILTER. THE
*       MODIFIED GRAVITATIONAL PARAMETER (MU*) IS ALSO ESTIMATED ALONG
*       WITH THE RADIAL DISTANCE FROM THE OBSERVED SATELLITE TO THE
*       CENTER OF MASS OF THE TETHERED SYSTEM
************************************************************************

      SUBROUTINE FGNINTH(T1,R1X,R1Y,R1Z,T2,R2X,R2Y,R2Z,T3,R3X,R3Y,R3Z,
    .     THETA1,SEMIP,RHOCM,P,A,ECCEN)
      IMPLICIT DOUBLE PRECISION(A-Z)
      INTEGER NO,I

      R1=DSQRT(R1X**2+R1Y**2+R1Z**2)
      R2=DSQRT(R2X**2+R2Y**2+R2Z**2)
      RO=(R2+R1)/2.0D0

      TOL=1.0D-5
      NO=35500
```

69

```
***********************************************************************
*     PO,P1 = INITIAL ESTIMATES OF THE GRAVITATIONAL PARAMETER, MU.
***********************************************************************

         PO=3.98600434D5
         P1=3.98600436D5
         MUSTAND=3.98600436D5
         I=1
         QO=FNINTH(PO,ECCEN,A,NU,E1,E2,T1,T2,T3,R1X,R1Y,R1Z,R2X,R2Y
      .         ,R2Z,R3X,R3Y,R3Z,SEMIP,V1X,V1Y,V1Z)
         Q1=FNINTH(P1,ECCEN,A,NU,E1,E2,T1,T2,T3,R1X,R1Y,R1Z,R2X,R2Y
      .         ,R2Z,R3X,R3Y,R3Z,SEMIP,V1X,V1Y,V1Z)
    5    IF (I.LE.NO) THEN

         P=P1-(Q1*(P1-PO)/(Q1-QO))

         IF (DABS((P-P1)).LT.TOL) THEN

                 RHOCM=(MUSTAND-P)/(2.0D0*MUSTAND+P)*R1
                 AR=(MUSTAND-P)/R1**2

***********************************************************************
*     WRITE DATA TO THE QLFIC.IN FILE FOR USE IN THE SECOND STAGE.
*     ALSO, PRINT QLFIC.IN DATA TO THE SCREEN.
*     CRIT = STOPPING CRITERIA FOR THE QUICK-LOOK FILTER (QLF)
*     DT = TIME STEP USED DURING INTEGRATION IN THE QLF
*     THETA0 = THETA CALCULATED FROM INITIAL LINE OF OBSERVATION DATA
***********************************************************************

                 DT=5.0D0
                 T0=0.0D0
                 THETA0=THETA1
                 AT=0.0D0

                 WRITE(200,*) T0,THETA0
                 WRITE(200,*) R1X*1000.0D0
                 WRITE(200,*) R1Y*1000.0D0
                 WRITE(200,*) R1Z*1000.0D0
                 WRITE(200,*) V1X*1000.0D0
                 WRITE(200,*) V1Y*1000.0D0
                 WRITE(200,*) V1Z*1000.0D0
                 WRITE(200,*) AT*1000.0D0
                 WRITE(200,*) AR*1000.0D0
                 WRITE(200,*) RHOCM*1000.0D0

                 WRITE(*,*) 'R1X (M)   ', R1X*1000.0D0
                 WRITE(*,*) 'R1Y (M)   ', R1Y*1000.0D0
                 WRITE(*,*) 'R1Z (M)   ', R1Z*1000.0D0
                 WRITE(*,*) 'V1X (M/S) ', V1X*1000.0D0
                 WRITE(*,*) 'V1Y (M/S) ', V1Y*1000.0D0
                 WRITE(*,*) 'V1Z (M/S) ', V1Z*1000.0D0
                 WRITE(*,*) 'AT (M/S^2)',  AT*1000.0D0
                 WRITE(*,*) 'AR (M/S^2)',  AR*1000.0D0
                 WRITE(*,*) 'RHO (M)   ', RHOCM*1000.0D0

         ELSE
```

70

```
                I=I+1
                PO=P1
                QO=Q1
                P1=P
                Q1=FNINTH(P,ECCEN,A,NU,E1,E2,T1,T2,T3,R1X,R1Y,R1Z,R2X,
    .           R2Y,R2Z,R3X,R3Y,R3Z,SEMIP,V2X,V2Y,V2Z)
                GOTO 5
            END IF
        END IF

************************************************************************
*       DETERMINE IF METHOD HAS FAILED.  A 'METHOD FAILED' ERROR
*       INDICATES TOO SHORT/LONG OF A TIME SPAN OR 'BAD' DATA. INPUT
*       DATA SHOULD HAVE 60-80 SECONDS IN BETWEEN OBSERVATIONS.
************************************************************************

        IF (I.GT.NO) THEN
            PRINT*,'METHOD FAILED'
            WRITE (200,*) 'METHOD FAILED',P
        END IF
        RETURN
        END


************************************************************************
*       FNINTH FUNCTION IS CALLED BY THE FGNINTH SUBROUTINE. THIS
*       FUNCTION PASSES THE TIMES/POSITION VECTORS TO THE F & G SERIES.
*       ONCE ALL VECTORS HAVE BEEN SENT THROUGH THE F & G SERIES, THE
*       ORBITAL ELEMENTS ARE CALCULATED.  THE ELEMENTS AND TIMES ARE
*       USED IN A DIFFERENCED KEPLER'S EQUATION. THIS EQUATION IS THE
*       ONE USED BY THE SECANT METHOD TO DETERMINE THE MODIFIED
*       GRAVITATIONAL PARAMETER, MU_STAR.
************************************************************************

        FUNCTION FNINTH(MU,ECCEN,A,NU,E1,E2,T1,T2,T3,R1X,R1Y,R1Z,R2X,
    .   R2Y,R2Z,R3X,R3Y,R3Z,P,V2X,V2Y,V2Z)
        IMPLICIT DOUBLE PRECISION(A-Z)

        CALL FGNINE(MU,T1,T2,R1X,R1Y,R1Z,R2X,R2Y,R2Z,V1X,V1Y,V1Z)

        R1=DSQRT(R1X**2+R1Y**2+R1Z**2)
        V1=DSQRT(V1X**2+V1Y**2+V1Z**2)

        CALL RVTOOE(MU,R1X,R1Y,R1Z,R1,V1X,V1Y,V1Z,V1,ECCEN,A,I,OMEGA,NU)

        DEN=DSQRT((1.0D0+ECCEN)/(1.0D0-ECCEN))
        E1=2.0D0*DATAN(DTAN(NU/2.0D0)/DEN)
        N=DSQRT(MU/(A**3))

        CALL FGNINE(MU,T2,T3,R2X,R2Y,R2Z,R3X,R3Y,R3Z,V2X,V2Y,V2Z)

        R2=DSQRT(R2X**2+R2Y**2+R2Z**2)
        V2=DSQRT(V2X**2+V2Y**2+V2Z**2)

        CALL RVTOOE(MU,R2X,R2Y,R2Z,R2,V2X,V2Y,V2Z,V2,ECCEN,A,I,OMEGA,NU)
```

71

```
      DEN=DSQRT((1.0D0+ECCEN)/(1.0D0-ECCEN))
      E2=2.0D0*DATAN(DTAN(NU/2.0D0)/DEN)
      N=DSQRT(MU/(A**3))
      P=A*(1-ECCEN**2)

      FNINTH=N*(T2-T1)-E2+E1-ECCEN*DSIN(E1)+ECCEN*DSIN(E2)

      RETURN
      END


************************************************************************
*         THIS SUBROUTINE CONTAINS THE NINTH-ORDER F & G SERIES.  TWO
*         TIMES/POSITION VECTORS ARE INPUT INTO THE SUBROUTINE.  THE F & G
*         SERIES IS USED TO CALCULATE THE VELOCITY OF THE FIRST TIME/
*         POSITION VECTOR.  THIS VELOCITY IS THEN USED IN THE FNINTH
*         FUNCTION TO CALCULATE THE ORBITAL ELEMENTS.  MU IS SENT TO THIS
*         SUBROUTINE BECAUSE THE F & G SERIES IS A FUNCTION OF MU - AS MU
*         IS CHANGED DURING THE ITERATIVE PROCESS THE NEW VALUE IS USED.
************************************************************************

      SUBROUTINE FGNINE(MU,T1,T2,R1X,R1Y,R1Z,R2X,R2Y,R2Z,V1X,V1Y,V1Z)
      IMPLICIT DOUBLE PRECISION(A-Z)
      INTEGER COUNT

      PI=2.0D0*DASIN(1.0D0)
      COUNT=0
      R1=DSQRT(R1X**2+R1Y**2+R1Z**2)
      R2=DSQRT(R2X**2+R2Y**2+R2Z**2)

      TO=(T1+T2)/2.0D0
      TAU1=(T1-TO)
      TAU2=(T2-TO)

      RO=(R2+R1)/2.0D0
      A=1.0D0-(MU*TAU1**2)/(2.0D0*RO**3)
      B=1.0D0-(MU*TAU2**2)/(2.0D0*RO**3)
      DELTA=A*TAU2-B*TAU1

      ROX=(TAU2/DELTA)*R1X-(TAU1/DELTA)*R2X
      ROY=(TAU2/DELTA)*R1Y-(TAU1/DELTA)*R2Y
      ROZ=(TAU2/DELTA)*R1Z-(TAU1/DELTA)*R2Z

      VOX=(A/DELTA)*R2X-(B/DELTA)*R1X
      VOY=(A/DELTA)*R2Y-(B/DELTA)*R1Y
      VOZ=(A/DELTA)*R2Z-(B/DELTA)*R1Z

  10  COUNT=COUNT+1
      RO=DSQRT(ROX**2+ROY**2+ROZ**2)
      VO=DSQRT(VOX**2+VOY**2+VOZ**2)
      UO=MU/(RO**3)
      PO=(ROX*VOX+ROY*VOY+ROZ*VOZ)/(RO**2)
      QO=(VO**2-RO**2*UO)/(RO**2)

      F1=1.0D0-.5D0*UO*TAU1**2+.5D0*UO*PO*TAU1**3+(1.0D0/24.0D0)*
     . (3.0D0*UO*QO-15.0D0*UO*PO**2+UO**2)*TAU1**4+(1.0D0/8.0D0)*
     . (7.0D0*UO*PO**3-3.0D0*UO*PO*QO-UO**2*PO)*TAU1**5+(1.0D0/720.0D0
```

72

```fortran
      )*(630.0D0*UO*PO**2*QO-24.0D0*UO**2*QO-UO**3-45.0D0*UO*QO**2-
     .945.0D0*UO*PO**4+210.0D0*UO**2*PO**2)*TAU1**6+(1.0D0/5040.0D0)*
     .(882.0D0*UO**2*PO*QO-3150.0D0*UO**2*PO**3-9450.0D0*UO*PO**3*QO+
     .1575.0D0*UO*PO*QO**2+63.0D0*UO**3*PO+10395.0D0*UO*PO**5)*TAU1**
     .7+(1.0D0/40320.0D0)*(1107.0D0*UO**2*QO**2-24570.0D0*UO**2*PO**2*
     .QO-2205.0D0*UO**3*PO**2+51975.0D0*UO**2*PO**4-42525.0D0*UO*PO**
     .2*QO**2+155925.0D0*UO*PO**4*QO+1575.0D0*UO*QO**3+117.0D0*UO**3*
     .QO-135135.0D0*UO*PO**6+UO**4)*TAU1**8

      F2=1.0D0-.5D0*UO*TAU2**2+.5D0*UO*PO*TAU2**3+(1.0D0/24.0D0)*
     .(3.0D0*UO*QO-15.0D0*UO*PO**2+UO**2)*TAU2**4+(1.0D0/C.0D0)*(7.0D0
     .*UO*PO**3-3.0D0*UO*PO*QO-UO**2*PO)*TAU2**5+(1.0D0/720.0D0)*
     .(630.0D0*UO*PO**2*QO-24.0D0*UO**2*QO-UO**3-45.0D0+UO*QO**2-
     .945.0D0*UO*PO**4+210.0D0*UO**2*PO**2)*TAU2**6+(1.0D0/5040.0D0)*
     .(882.0D0*UO**2*PO*QO-3150.0D0*UO**2*PO**3-9450.0D0*UO*PO**3*QO+
     .1575.0D0*UO*PO*QO**2+63.0D0*UO**3*PO+10395.0D0*UO*PO**5)*TAU2**7
     .+(1.0D0/40320.0D0)*(1107.0D0*UO**2*QO**2-24570.0D0*UO**2*PO**2*
     .QO-2205.0D0*UO**3*PO**2+51975.0D0*UO**2*PO**4-42525.0D0*UO*PO**2
     .*QO**2+155925.0D0*UO*PO**4*QO+1575.0D0*UO*QO**3+117.0D0*UO**3*QO
     .-135135.0D0*UO*PO**6+UO**4)*TAU2**8

      G1=TAU1-(1.0D0/6.0D0)*UO*TAU1**3+.25D0*UO*PO*TAU1**4+(1.0D0/
     .120.0D0)*(9.0D0*UO*QO-45.0D0*UO*PO**2+UO**2)*TAU1**5+(1.0D0/
     .360.0D0)*(210.0D0*UO*PO**3-90.0D0*UO*PO*QO-15.0D0*UO**2*PO)*TAU1
     .**6+(1.0D0/5040.0D0)*(3150.0D0*UO*PO**2*QO-54.0D0*UO**2*QO-
     .225.0D0*UO*QO**2-4725.0D0*UO*PO**4+630.0D0*UO**2*PO**2-UO**3)*
     .TAU1**7+(1.0D0/40320.0D0)*(3024.0D0*UO**2*PO*QO-12600.0D0*UO**2
     .*PO**3-56700.0D0*UO*PO**3*QO+9450.0D0*UO*PO*QO**2+62370.0D0*UO*
     .PO**5+126.0D0*UO**3*PO)*TAU1**8

      G2=TAU2-(1.0D0/6.0D0)*UO*TAU2**3+.25D0*UO*PO*TAU2**4+(1.0D0/
     .120.0D0)*(9.0D0*UO*QO-45.0D0*UO*PO**2+UO**2)*TAU2**5+(1.0D0/
     .360.0D0)*(210.0D0*UO*PO**3-90.0D0*UO*PO*QO-15.0D0*UO**2*PO)*TAU2
     .**6+(1.0D0/5040.0D0)*(3150.0D0*UO*PO**2*QO-54.0D0*UO**2*QO-
     .225.0D0*UO*QO**2-4725.0D0*UO*PO**4+630.0D0*UO**2*PO**2-UO**3)*
     .TAU2**7+(1.0D0/40320.0D0)*(3024.0D0*UO**2*PO*QO-12600.0D0*UO**2*
     .PO**3-56700.0D0*UO*PO**3*QO+9450.0D0*UO*PO*QO**2+62_10.0D0*UO*
     .PO**5+126.0D0*UO**3*PO)*TAU2**8

      D=F1*G2-F2*G1

      C1=G2/D
      C2=-G1/D
      DC1=-F2/D
      DC2=F1/D

      ROX=C1*R1X+C2*R2X
      ROY=C1*R1Y+C2*R2Y
      ROZ=C1*R1Z+C2*R2Z
      RO=DSQRT(ROX**2+ROY**2+ROZ**2)

      VOX=DC1*R1X+DC2*R2X
      VOY=DC1*R1Y+DC2*R2Y
      VOZ=DC1*R1Z+DC2*R2Z
      VO=DSQRT(VOX**2+VOY**2+VOZ**2)

      DRO=(ROX*VOX+ROY*VOY+ROZ*VOZ)/RO
```

73

```
        DF1=-UO*TAU1+3.0D0*.5D0*UO*PO*TAU1**2+(1.0D0/6.0D0)*(3.0D0*UO*QO
     .  -15.0D0*UO*PO**2+UO**2)*TAU1**3+(5.0D0/8.0D0)*(7.0D0*UO*PO**3-
     .  3.0D0*UO*PO*QO-UO**2*PO)*TAU1**4+(6.0D0/720.0D0)*(630.0D0*UO*
     .  PO**2*QO-24.0D0*UO**2*QO-UO**3-45.0D0*UO*QO**2-945.0D0*UO
     .  *PO**4+210.0D0*UO**2*PO**2)*TAU1**5+(7.0D0/5040.0D0)*(882.0D0*
     .  UO**2*PO*QO-3150.0D0*UO**2*PO**3-9450.0D0*UO*PO**3*QO+1575.0D0
     .  *UO*PO*QO**2+63.0D0*UO**3*PO+10395.0D0*UO*PO**5)*TAU1**6+(8.0D0
     .  /40320.0D0)*(1107.0D0*UO**2*QO**2-24570.0D0*UO**2*PO**2*QO-
     .  2205.0D0*UO**3*PO**2+51975.0D0*UO**2*PO**4-42525.0D0*UO*PO**2*
     .  QO**2+155925.0D0*UO*PO**4*QO+1575.0D0*UO*QO**3+117.0D0*UO**3*QO
     .  -135135.0D0*UO*PO**6+UO**4)*TAU1**7

        DG1=1.0D0-(3.0D0/6.0D0)*UO*TAU1**2+UO*PO*TAU1**3+(5.0D0/120.0D0)
     .  *(9.0D0*UO*QO-45.0D0*UO*PO**2+UO**2)*TAU1**4+(6.0D0/360.0D0)*
     .  (210.0D0*UO*PO**3-90.0D0*UO*PO*QO-15.0D0*UO**2*PO)*TAU1**5
     .  +(7.0D0/5040.0D0)*(3150.0D0*UO*PO**2*QO-54.0D0*UO**2*QO-225.0D0
     .  *UO*QO**2-4725.0D0*UO*PO**4+630.0D0*UO**2*PO**2-UO**3)*TAU1**6
     .  +(8.0D0/40320.0D0)*(3024.0D0*UO**2*PO*QO-12600.0D0*UO**2*PO**3
     .  -56700.0D0*UO*PO**3*QO+9450.0D0*UO*PO*QO**2+62370.0D0*UO*PO**5
     .  +126.0D0*UO**3*PO)*TAU1**7

        V1X=DF1*ROX+DG1*VOX
        V1Y=DF1*ROY+DG1*VOY
        V1Z=DF1*ROZ+DG1*VOZ
        V1=DSQRT(V1X**2+V1Y**2+V1Z**2)

        RETURN
        END


***********************************************************************
*            THIS SUBROUTINE CONVERTS FROM POSITION/VELOCITY VECTORS TO
*            ORBITAL ELEMENTS
***********************************************************************
        SUBROUTINE RVTOOE(U,RX,RY,RZ,R,VX,VY,VZ,V,E,A,I,OMEGA,NU)
        IMPLICIT DOUBLE PRECISION(A-Z)

        EXI=((((V**2)/U)-(1.0D0/R))*RX)
        EXJ=((1.0D0/U)*((RX*VX)+(RY*VY)+(RZ*VZ))*VX)
        EX=EXI-EXJ
        EYI=((((V**2)/U)-(1.0D0/R))*RY)
        EYJ=((1.0D0/U)*((RX*VX)+(RY*VY)+(RZ*VZ))*VY)
        EY=EYI-EYJ
        EZI=((((V**2)/U)-(1.0D0/R))*RZ)
        EZJ=((1.0D0/U)*((RX*VX)+(RY*VY)+(RZ*VZ))*VZ)
        EZ=EZI-EZJ
        E=DSQRT(EX**2+EY**2+EZ**2)

        HX=(-1.0D0*(RZ*VY)+(RY*VZ))
        HY=(-1.0D0*(RX*VZ)+(RZ*VX))
        HZ=(-1.0D0*(RY*VX)+(RX*VY))
        H=DSQRT(HX**2+HY**2+HZ**2)
        P=(H**2)/U
        A=P/(1.0D0-E**2)

        PI=(2.0D0*DASIN(1.0D0))
```

74

```
        I=DACOS(HZ/H)

        N=DSQRT(((-1.0D0*HY)**2+(HX**2)))
        NI=-1.0D0*HY
        NJ=HX
        OMEGA=DACOS(NI/N)

        IF(NJ.LT.0.0D0)THEN
            OMEGA=2.0D0*PI-OMEGA
        END IF

        NDE=(-1.0D0*HY*EX)+(HX*EY)
        NE=N*E
        PK=(HZ**2)/U

        EDR=(EX*RX)+(EY*RY)+(EZ*RZ)
        ER=E*R
        RDV=(RX*VX)+(RY*VY)+(RZ*VZ)

        NU=DACOS(EDR/ER)

        IF(RDV.LT.0.0D0)THEN
            NU=2.0D0*PI-NU
        END IF

1111    RETURN
        END


*********************************************************************
*       THIS SUBROUTINE SELECTS THE CORRECT HEIGHT, LATITUDE, &
*       LONGITUDE FOR THE TRACKING STATION BEING USED
*********************************************************************

        SUBROUTINE STATION(SITE,HT,LONG,LAT)
        IMPLICIT DOUBLE PRECISION (A-Z)
        INTEGER SITE

        PI=2.0D0*DASIN(1.0D0)

        IF (SITE.EQ.  5) THEN

            HT=    -2.8000000000000

            LONG=    279.31453910000*PI/180.0D0

            LAT=    28.024644600000*PI/180.0D0

        ELSEIF (SITE.EQ.  27) THEN

            HT=    28.900000000000

            LONG=    294.78995470000*PI/180.0D0

            LAT=    46.899465200000*PI/180.0D0
```

```
ELSEIF (SITE.EQ.  28) THEN

    HT=     38.100000000000

    LONG=    17.845735000000*PI/180.0D0

    LAT=     40.640989200000*PI/180.0D0

ELSEIF (SITE.EQ.  200) THEN

    HT=     1511.5000000000

    LONG=    253.34083880000*PI/180.0D0

    LAT=     33.817761800000*PI/180.0D0

ELSEIF (SITE.EQ.  201) THEN

    HT=     38.100000000000

    LONG=    17.845735000000*PI/180.0D0

    LAT=     40.640989200000*PI/180.0D0

ELSEIF (SITE.EQ.  202) THEN

    HT=     1510.7000000000

    LONG=    253.34024570000*PI/180.0D0

    LAT=     33.817951500000*PI/180.0D0

ELSEIF (SITE.EQ.  205) THEN

    HT=     1510.4000000000

    LONG=    253.34067140000*PI/180.0D0

    LAT=     33.818097300000*PI/180.0D0

ELSEIF (SITE.EQ.  206) THEN

    HT=     1510.4000000000

    LONG=    253.34067140000*PI/180.0D0

    LAT=     33.818097300000*PI/180.0D0

ELSEIF (SITE.EQ.  207) THEN

    HT=     1506.5000000000

    LONG=    253.34107320000*PI/180.0D0

    LAT=     33.818430300000*PI/180.0D0

ELSEIF (SITE.EQ.  210) THEN
```

76

```
      HT=      1512.1000000000

      LONG=      253.33984960000*PI/180.0D0

      LAT=      33.817270700000*PI/180.0D0

ELSEIF (SITE.EQ.  211) THEN

      HT=      1512.1000000000

      LONG=      253.33984960000*PI/180.0D0

      LAT=      33.817270700000*PI/180.0D0

ELSEIF (SITE.EQ.  212) THEN

      HT=      1512.1000000000

      LONG=      253.34032520000*PI/180.0D0

      LAT=      33.817270700000*PI/180.0D0

ELSEIF (SITE.EQ.  213) THEN

      HT=      1512.1000000000

      LONG=      253.34026670000*PI/180.0D0

      LAT=      33.817050700000*PI/180.0D0

ELSEIF (SITE.EQ.  215) THEN

      HT=      1512.1000000000

      LONG=      253.33984960000*PI/180.0D0

      LAT=      33.617270700000*PI/180.0D0

ELSEIF (SITE.EQ.  220) THEN

      HT=      786.20000000000

      LONG=      128.60802220000*PI/180.0D0

      LAT=      35.744033900000*PI/180.0D0

ELSEIF (SITE.EQ.  221) THEN

      HT=      786.20000000000

      LONG=      128.60802220000*PI/180.0D0

      LAT=      35.744083900000*PI/180.0D0

ELSEIF (SITE.EQ.  222) THEN
```

```
      HT=      786.20000000000

      LONG=      128.60850890000*PI/180.0D0

      LAT=      35.744084800000*PI/180.0D0

ELSEIF (SITE.EQ.  223) THEN

      HT=      786.20000000000

      LONG=      128.60844030000*PI/180.0D0

      LAT=      35.743863900000*PI/180.0D0

ELSEIF (SITE.EQ.  225) THEN

      HT=      786.20000000000

      LONG=      128.60802220000*PI/180.0D0

      LAT=      35.744083900000*PI/180.0D0

ELSEIF (SITE.EQ.  230) THEN

      HT=      3059.6000000000

      LONG=      203.74221670000*PI/180.0D0

      LAT=      20.708049600000*PI/180.0D0

ELSEIF (SITE.EQ.  231) THEN

      HT=      3059.6000000000

      LONG=      203.74221670000*PI/180.0D0

      LAT=      20.708049600000*PI/180.0D0

ELSEIF (SITE.EQ.  232) THEN

      HT=      3059.6000000000

      LONG=      203.74252670000*PI/180.0D0

      LAT=      20.708050700000*PI/180.0D0

ELSEIF (SITE.EQ.  233) THEN

      HT=      3059.7000000000

      LONG=      203.74255390000*PI/180.0D0

      LAT=      20.708530400000*PI/180.0D0

ELSEIF (SITE.EQ.  235) THEN

      HT=      3059.6000000000
```

```
      LONG=     203.74221670000*PI/180.0D0

      LAT=      20.708049600000*PI/180.0D0

ELSEIF (SITE.EQ.  240) THEN

   HT=    -62.300000000000

   LONG=     72.452059500000*PI/180.0D0

   LAT=     -7.4116129000000*PI/180.0D0

ELSEIF (SITE.EQ.  241) THEN

   HT=    -62.300000000000

   LONG=     72.452059500000*PI/180.0D0

   LAT=     -7.4116129000000*PI/180.0D0

ELSEIF (SITE.EQ.  242) THEN

   HT=    -62.400000000000

   LONG=     72.452463600000*PI/180.0D0

   LAT=     -7.4116140000000*PI/180.0D0

ELSEIF (SITE.EQ.  243) THEN

   HT=    -62.400000000000

   LONG=     72.452404200000*PI/180.0D0

   LAT=     -7.4113451000000*PI/180.0D0

ELSEIF (SITE.EQ.  245) THEN

   HT=    -62.300000000000

   LONG=     72.452059500000*PI/180.0D0

   LAT=     -7.4116129000000*PI/180.0D0

ELSEIF (SITE.EQ.  315) THEN

   HT=     892.20000000000

   LONG=  0.*PI/180.0D0

   LAT=     37.905248300000*PI/180.0D0

ELSEIF (SITE.EQ.  329) THEN

   HT= ,  216.80000000000
```

```fortran
         LONG=    210.80717450000*PI/180.0D0

      LAT=    64.291173700000*PI/180.0D0

   ELSEIF (SITE.EQ.   330) THEN

      HT=    302.20000000000

      LONG=    359.33158340000*PI/180.0D0

      LAT=    54.368798000000*PI/180.0D0

   ELSEIF (SITE.EQ.   331) THEN

      HT=    348.20000000000

      LONG=    145.79621670000*PI/180.0D0

      LAT=    15.249145700000*PI/180.0D0

   ELSEIF (SITE.EQ.   333) THEN

      HT=    42.400000000000

      LONG=    167.48284910000*PI/180.0D0

      LAT=    9.3985998000000*PI/180.0D0

   ELSEIF (SITE.EQ.   334) THEN

      HT=    62.800000000000

      LONG=    167.47928830000*PI/180.0D0

      LAT=    9.3954289000000*PI/180.0D0

   ELSEIF (SITE.EQ.   335) THEN

      HT=    57.400000000000

      LONG=    167.48214790000*PI/180.0D0

      LAT=    9.3987474000000*PI/180.0D0

   ELSEIF (SITE.EQ.   337) THEN

      HT=    892.20000000000

      LONG=  0.*PI/180.0D0

      LAT=  0.*PI/180.0D0

   ELSEIF (SITE.EQ.   341) THEN

      HT=    302.20000000000

      LONG=    359.33158340000*PI/180.0D0
```

80

```
        LAT=      54.368798000000*PI/180.0D0

ELSEIF (SITE.EQ.   342) THEN

    HT=      304.60000000000

    LONG=      359.33333140000*PI/180.0D0

    LAT=      54.367176000000*PI/180.0D0

ELSEIF (SITE.EQ.   343) THEN                    .

    HT=      303.30000000000

    LONG=      359.33452700000*PI/180.0D0

    LAT=      54.365857700000*PI/180.0D0

ELSEIF (SITE.EQ.   344) THEN

    HT=      342.00000000000

    LONG=      359.33006780000*PI/180.0D0

    LAT=      54.361922400000*PI/180.0D0

ELSEIF (SITE.EQ.   345) THEN

    HT=      342.00000000000

    LONG=      359.33006780000*PI/180.0D0

    LAT=      54.361922400000*PI/180.0D0

ELSEIF (SITE.EQ.   346) THEN

    HT=      342.00000000000

    LONG=      359.33006780000*PI/180.0D0

    LAT=      54.361922400000*PI/180.0D0

ELSEIF (SITE.EQ.   349) THEN

    HT=      216.80000000000

    LONG=      210.80717450000*PI/180.0D0

    LAT=      64.291173700000*PI/180.0D0

ELSEIF (SITE.EQ.   354) THEN

    HT=      54.900000000000

    LONG=      345.59750780000*PI/180.0D0
```

81

```
        LAT=   -7.9066377000000*PI/180.0D0

ELSEIF (SITE.EQ.  355) THEN

    HT=    140.80000000000

    LONG=   345.59879220000*PI/180.0D0

    LAT=   -7.9725795000000*PI/180.0D0

ELSEIF (SITE.EQ.  359) THEN

    HT=    216.80000000000

    LONG=   210.80717450000*PI/180.0D0

    LAT=   64.291173700000*PI/180.0D0

ELSEIF (SITE.EQ.  360) THEN

    HT=    -16.900000000000

    LONG=   279.33560140000*PI/180.0D0

    LAT=   28.424699800000*PI/180.0D0

ELSEIF (SITE.EQ.  361) THEN


    HT=    -13.400000000000

    LONG=   279.40071280000*PI/180.0D0

    LAT=   28.226391000000*PI/180.0D0

ELSEIF (SITE.EQ.  363) THEN

    HT=    1.2000000000000

    LONG=   298.20748400000*PI/180.0D0

    LAT=   17.143639000000*PI/180.0D0

ELSEIF (SITE.EQ.  369) THEN

    HT=    125.60000000000

    LONG=   288.50910340000*PI/180.0D0

    LAT=   42.617435100000*PI/180.0D0

ELSEIF (SITE.EQ.  370) THEN

    HT=    115.60000000000

    LONG=   288.50876270000*PI/180.0D0
```

```
      LAT=      42.619588900000*PI/180.0D0

ELSEIF (SITE.EQ.  371) THEN

   HT=      105.60000000000

   LONG=     288.50769450000*PI/180.0D0

   LAT=      42.617552600000*PI/180.0D0

ELSEIF (SITE.EQ.  382) THEN

   HT=      775.90000000000

   LONG=     259.44717420000*PI/180.0D0

   LAT=      30.978291500000*PI/180.0D0

ELSEIF (SITE.EQ.  383) THEN

   HT=      775.90000000000

   LONG=     259.44717420000*PI/180.0D0

   LAT=      30.973291500000*PI/180.0D0

ELSEIF (SITE.EQ.  384) THEN

   HT=      88.100000000000

   LONG=     276.43079100000*PI/180.0D0

   LAT=      32.581262500000*PI/180.0D0

ELSEIF (SITE.EQ.  385) THEN

   HT=      88.100000000000

   LONG=     276.43079100000*PI/180.0D0

   LAT=      32.581262500000*PI/180.0D0

ELSEIF (SITE.EQ.  386) THEN

   HT=      82.700000000000

   LONG=     289.46188110000*PI/180.0D0

   LAT=      41.752456600000*PI/180.0D0

ELSEIF (SITE.EQ.  387) THEN

   HT=      82.700000000000

   LONG=     289.46188110000*PI/180.0D0

   LAT=      41.752456600000*PI/180.0D0
```

83

```
ELSEIF (SITE.EQ.  388) THEN

    HT=     118.00000000000

    LONG=    238.64928060000*PI/180.0D0

    LAT=     39.136073700000*PI/180.0D0

ELSEIF (SITE.EQ.  389) THEN

    HT=     118.00000000000

    LONG=    238.64928060000*PI/180.0D0

    LAT=     39.136073700000*PI/180.0D0

ELSEIF (SITE.EQ.  392) THEN

    HT=     94.200000000000

    LONG=    174.09108640000*PI/130.0D0

    LAT=     52.737286700000*PI/180.0D0

ELSEIF (SITE.EQ.  393) THEN

    HT=     94.200000000000

    LONG=    174.09108640000*PI/180.0D0

    LAT=     52.737286700000*PI/180.0D0

ELSEIF (SITE.EQ.  394) THEN

    HT=     428.50000000000

    LONG=    291.70092830000*PI/180.0D0

    LAT=     76.570298800000*PI/180.0D0

ELSEIF (SITE.EQ.  395) THEN

    HT=     428.50000000000

    LONG=    291.70092830000*PI/180.0D0

    LAT=     76.570298800000*PI/180 0D0

ELSEIF (SITE.EQ.  396) THEN

    HT=     350.10000000000

    LONG=    262.10041670000*PI/180.0D0

    LAT=     48.724813700000*PI/180.0D0
```

84

```
ELSEIF (SITE.EQ.  398) THEN
    HT=     36.400000000000
    LONG=     273.78530810000*PI/180.0D0
    LAT=     30.572460800000*PI/180.0D0
ELSEIF (SITE.EQ.  399) THEN
    HT=     36.400000000000
    LONG=     273.78530810000*PI/180.0D0
    LAT=     30.572460800000*PI/180.0D0
ELSEIF (SITE.EQ.  400) THEN
    HT=     892.20000000000
    LONG=     39.993340000000*PI/180.0D0
    LAT=     37.905248300000*PI/180.0D0
ELSEIF (SITE.EQ.  401) THEN
    HT=     892.20000000000
    LONG=     39.993340000000*PI/180.0D0
    LAT=     37.905248300000*PI/180.0D0
ELSEIF (SITE.EQ.  402) THEN
    HT=     892.20000000000
    LONG=     39.993340000000*PI/180.0D0
    LAT=     37.905248300000*PI/180.0D0
ELSEIF (SITE.EQ.  403) THEN
    HT=     892.20000000000
    LONG=     39.993340000000*PI/180.0D0
    LAT=     37.905248300000*PI/180.0D0
ELSEIF (SITE.EQ.  404) THEN
    HT=     892.20000000000
    LONG=     39.993340000000*PI/180.0D0
    LAT=     37.905248300000*PI/180.0D0
ELSEIF (SITE.EQ.  501) THEN
```

85

```
      HT=   -0.60000000000000

      LONG=    70.000153900000*PI/180.0D0

      LAT=     4.0400000000000D-05*PI/180.0D0
ELSEIF (SITE.EQ.   502) THEN

      HT=   -0.60000000000000

      LONG=  0.*PI/180.0D0

      LAT=     4.0400000000000D-05*PI/180.0D0
ELSEIF (SITE.EQ.   503) THEN

      HT=   -0.60000000000000

      LONG=    290.00015390000*PI/180.0D0

      LAT=     4.0400000000000D-05*PI/180.0D0
ELSEIF (SITE.EQ.   620) THEN

      HT=     267.10000000000

      LONG=    239.49460340000*PI/180.0D0

      LAT=     34.825634300000*PI/180.0D0
ELSEIF (SITE.EQ.   622) THEN

      HT=     201.73770470000

      LONG=    5689646.0000000*PI/180.0D0

      LAT=     21.000000000000*PI/180.0D0
ELSEIF (SITE.EQ.   623) THEN

      HT=     193.10000000000

      LONG=    288.36967830000*PI/180.0D0

      LAT=     42.044742100000*PI/180.0D0
ELSEIF (SITE.EQ.   649) THEN

      HT=     271.00000000000

      LONG=    239.49815270000*PI/180.0D0

      LAT=     34.822610000000*PI/180.0D0
ELSEIF (SITE.EQ.   654) THEN
```

86

```
      HT=     429.80000000000

      LONG=     201.75789400000*PI/180.0D0

      LAT=     21.562265000000*PI/180.0D0
   ELSEIF (SITE.EQ.   657) THEN

      HT=     203.30000000000

      LONG=     288.37343750000*PI/180.0D0

      LAT=     42.947821400000*PI/180.0D0
   ELSEIF (SITE.EQ.   660) THEN

      HT=     218.90000000000

      LONG=     144.85604940000*PI/180.0D0

      LAT=     13.615187500000*PI/180.0D0
   ELSEIF (SITE.EQ.   661) THEN

      HT=     560.40000000000

      LONG=     55.477820500000*PI/180.0D0

      LAT=     -4.6717481000000*PI/180.0D0
   ELSEIF (SITE.EQ.   731) THEN

      HT=     62.800000000000

      LONG=     167.47928830000*PI/180.0D0

      LAT=     9.3954289000000*PI/180.0D0
   ELSEIF (SITE.EQ.   732) THEN

      HT=     62.800000000000

      LONG=     167.47928830000*PI/180.0D0

      LAT=     9.3954289000000*PI/180.0D0
   ELSEIF (SITE.EQ.   733) THEN

      HT=     62.800000000000

      LONG=     167.47928830000*PI/180.0D0

      LAT=     9.3954289000000*PI/180.0D0
   ELSEIF (SITE.EQ.   741) THEN

      HT=     121.40000000000
```

87

```
        LONG=      243.02999390000*PI/180.0D0

        LAT=     32.578435700000*PI/180.0D0

ELSEIF (SITE.EQ.   742) THEN

    HT=     1413.0000000000

        LONG=      253.00191390000*PI/180.0D0

        LAT=     33.444385400000*PI/180.0D0

ELSEIF (SITE.EQ.   743) THEN

    HT=     6.2000000000000

        LONG=      268.97919390000*PI/180.0D0

        LAT=     33.145655500000*PI/180.0D0

ELSEIF (SITE.EQ.   744) THEN

    HT=     26.500000000000

        LONG=      278.07745390000*PI/180.0D0

        LAT=     32.043265900000*PI/180.0D0

ELSEIF (SITE.EQ.   745) THEN

    HT=     307.20000000000

        LONG=      261.23709390000*PI/180.0D0

        LAT=     33.553995300000*PI/180.0D0

ELSEIF (SITE.EQ.   746) THEN

    HT=     53.800000000000

        LONG=      266.44976390000*PI/180.0D0

        LAT=     33.331325400000*PI/180.0D0

ELSEIF (SITE.EQ.   747) THEN

    HT=     73.100000000000

        LONG=      276.46387390000*PI/180.0D0

        LAT=     32.289365800000*PI/180.0D0

ELSEIF (SITE.EQ.   750) THEN

    HT=     140.60000000000
```

88

```
      LONG=      284.38765390000*PI/180.0D0

      LAT=       43.148642400000*PI/180.0D0

ELSEIF (SITE.EQ.  888) THEN

   HT=      1869.7000000000

   LONG=      255.83348720000*PI/180.0D0

   LAT=       38.816699900000*PI/180.0D0

ELSEIF (SITE.EQ.  932) THEN

   HT=      301.30000000000

   LONG=      201.73341480000*PI/180.0D0

   LAT=       21.572119700000*PI/180.0D0

ELSEIF (SITE.EQ.  951) THEN

   HT=      3060.5000000000

   LONG=      203.74218470000*PI/180.0D0

   LAT=       20.708522300000*PI/180.0D0

ELSEIF (SITE.EQ.  952) THEN

   HT=      3060.5000000000

   LONG=      203.74264360000*PI/180.0D0

   LAT=       20.708371500000*PI/180.0D0

ELSEIF (SITE.EQ.  961) THEN

   HT=      3059.4000000000

   LONG=      203.74231090000*PI/180.0D0

   LAT=       20.708276800000*PI/180.0D0

END IF

RETURN
END
```

POD.OUT:

```
       0.0000000000000000        6.2656366475895700
 4.3890191239616630D+006
-627437.2187645634000000
 5.9203788438615920D+006
   -3430.1606612317690000
    6011.6733270027260000
    2454.1005600175490000
       0.0000000000000000
       0.0090939762330475
    3078.5938197010790000
```

OBS.IN:

```
345  96256003323.159  1166.062  894.01  257.5792  0.00052000  59.4335
0.00039200
345  96256003333.159  1139.586  894.01  260.8353  0.00052000  62.3041
0.00039200
345  96256003343.159  1116.354  894.01  264.9759  0.00052000  65.1871
0.00039200
345  96256003353.15ᶜ  1096.572  894.01  270.3145  0.00052000  68.0188
0.00039200
345  96256003403.159  1080.434  894.01  277.3165  0.00052000  70.7030
0.00039200
345  96256003413.159  1068.105  894.01  286.5744  0.00052000  73.0914
0.00039200
345  96256003423.159  1059.720  894.01  298.6270  0.00052000  74.9660
0.00039200
344  96256003433.159  1055.371  888.04  313.3820  0.00062000  76.0669
0.00057600
344  96256003443.159  1055.110  888.04  329.4737  0.00062000  76.1779
0.00057600
344  96256003453.159  1058.940  888.04  344.6365  0.00062000  75.2617
0.00057600
344  96256003503.159  1066.814  888.04  357.2223  0.00062000  73.5128
0.00057600
344  96256003513.159  1078.645  888.04    6.9507  0.00062000  71.2039
0.00057600
344  96256003523.159  1094.301  888.04   14.3168  0.00062000  68.5675
0.00057600
344  96256003533.159  1113.620  888.04   19.9198  0.00062000  65.7634
0.00057600
344  96256003543.159  1136.412  888.04   24.2487  0.00062000  62.8953
0.00057600
344  96256003553.159  1162.472  888.04   27.6641  0.00062000  60.0336
0.00057600
344  96256003603.159  1191.583  888.04   30.4119  0.00062000  57.2229
0.00057600
344  96256003613.159  1223.523  888.04   32.6615  0.00062000  54.4906
0.00057600
344  96256003623.159  1258.075  888.04   34.5365  0.00062000  51.8547
0.00057600
344  96256003633.159  1295.026  888.04   36.1216  0.00062000  49.3237
0.00057600
344  96256003643.159  1334.172  888.04   37.4777  0.00062000  46.9045
0.00057600
344  96256003653.159  1375.324  888.04   38.6525  0.00062000  44.5978
0.00057600
344  96256003703.159  1418.302  888.04   39.6791  0.00062000  42.4005
0.00057600
344  96256003713.159  1462.938  888.04   40.5848  0.00062000  40.3097
0.00057600
344  96256003723.159  1509.087  888.04   41.3897  0.00062000  38.3226
0.00057600
344  96256003733.159  1556.608  888.04   42.1115  0.00062000  36.4342
0.00057600
```

```
344   96256003743.159   1605.375   888.04   42.7627   0.00062000   34.6399
0.00057600
344   96256003753.159   1655.271   888.04   43.3529   0.00062000   32.9335
0.00057600
344   96256003803.159   1706.195   888.04   43.8921   0.00062000   31.3083
0.00057600
344   96256003813.159   1758.051   888.04   44.3842   0.00062000   29.7602
0.00057600
344   96256003823.159   1810.756   888.04   44.8379   0.00062000   28.2843
0.00057600
344   96256003833.159   1864.233   888.04   45.2578   0.00062000   26.8760
0.00057600
344   96256003843.159   1918.411   888.04   45.6482   0.00062000   25.5305
0.00057600
344   96256003853.159   1973.228   888.04   46.0119   0.00062000   24.2434
0.00057600
344   96256003903.159   2028.628   888.04   46.3515   0.00062000   23.0102
0.00057600
344   96256003913.159   2084.559   888.04   46.6701   0.00062000   21.8267
0.00057600
344   96256003923.159   2140.973   888.04   46.9701   0.00062000   20.6910
0.00057600
344   96256003933.159   2197.831   888.04   47.2530   0.00062000   19.5997
0.00057600
```

QLF.FOR:

```
*****************************************************************************
**
*         5/10/01: UTILIZES RANGE/AZ/EL DATA
*
*         THIS PROGRAM ESTIMATES THE TETHER POSITION, VELOCITY, AND TETHER
*         TETHER FORCE COMPONENTS IN ORDER TO DETERMINE WHETHER THE OBSERVED
*         SATELLITE IS PART OF A TETHERED PAIR.
*
*         THIS PROGRAM WAS WRITTEN BY THE TETHER SATELLITE WORKING GROUP
*         (DAVID CICCI,JOHN COCHRAN, SUNGKI CHO, ALAN LOVELL, CHERISH QUALLS)
*         AT AUBURN UNIVERSITY. THE POINT OF CONTACT, DAVID A. CICCI CAN BE
*         REACHED AT THE FOLLOWING:
*                             AEROSPACE ENGINEERING DEPARTMENT
*                             211 AEROSPACE ENGINEERING BUILDING
*                             AUBURN UNIVERSITY, AL 36849-5338
*
*                             PHONE: (334) 844-6820
*                             FAX: (334) 844-6803
*                             E-MAIL: DCICCI@ENG.AUBURN.EDU
*
*****************************************************************************
**

          IMPLICIT DOUBLE PRECISION (A-Z)

          INTEGER N,I,P,SITE,FLAG, J, ICOUNT, N1, N2, IPAR,
     .    SCOUNT,MCOUNT,VCOUNT,COUNT,ITER, II, JJ

          PARAMETER (N = 8, N1=6, N2=2, IPAR=56, P=3)

          DIMENSION NI(N,P), RINV(P,P), H(P,N), L(N,N), LI(N,N), M(N,1),
     .    HX(P,1), LN(N,N), MN(N,1), XN(N,1), D(N), YVEC(P,1), RES(P,1),
     .    MI(N,1), Y(P,1), X(N,1), HXPSF(N,P), IVEC(IPAR), XSTAR(N),
     .    D1(IPAR), D2(IPAR), D3(IPAR), HD(P,N1), HB(P,N2), DUM16(P,N1),
     .    DUM12(P,N2), PHIDD(N1,N1), PHIDC(N1,N2), XPREV(N,1), REST(1,P),
     .    CQ(P,P), XNR(N,1), XSTARR(N), XSTARMV(N),  XNSING(N,1),
     .    LNSING(N,N), MNSING(N,1), XSTARS(N), XSTARM(N), XNMULT(N,1),
     .    LNMULT(N,N), MNMULT(N,1), YSING(P,1), HSING(P,N), YMULT(P,1),
     .    HMULT(P,N), DSING(N), DMULT(N), YOLDS(P,1), HOLDS(P,N),
     .    DOLDS(N), XSTARSO(N), XNOLDS(N,1), LNOLDS(N,N), MNOLDS(N,1),
     .    YOLDM(P,1), HOLDM(P,N), DOLDM(N), XSTARMO(N), XNOLDM(N,1),
     .    MNOLDM(N,1), LNOLDM(N,N), IVECSO(IPAR), IVECS(IPAR),
     .    IVECMO(IPAR), IVECM(IPAR), IVEC0(IPAR), XSTARRS(N), XSTARRM(N),
     .    XS(N,1), XM(N,1), SIG2VEC(P)

          COMMON/SITEVEC/THETA0, T0

          OPEN(5,  FILE=  'DATA.IN', STATUS='UNKNOWN')
          OPEN(6,  FILE = 'QUICK-LOOK.OUT', STATUS = 'UNKNOWN')
          OPEN(7,  FILE = 'POD.OUT', STATUS = 'UNKNOWN')
          OPEN(8,  FILE = 'QLFCOV.OUT', STATUS = 'UNKNOWN')
          OPEN(10, FILE=  'QLF.OUT', STATUS = 'UNKNOWN')
          OPEN(11, FILE = 'OBS.IN', STATUS = 'UNKNOWN')
```

93

```
*******************************************************************
*        READ IN THE ORIGINAL DATA FILE AND CONVERT THE
*        YEAR/DAY/HOUR/MIN/SEC FORMAT TO ONE WITH TIME IN SECONDS ONLY
*******************************************************************

         CALL TCONVERT

*******************************************************************
*        INITIALIZE VARIABLES AND MATRICES
*******************************************************************

         FLAG = 0
         OLDRMS = 1.0D10

         SCOUNT=0
         MCOUNT=0
         VCOUNT=0
         COUNT=0

         CALL MATZERO (RINV,P,P)
         CALL MATZERO (XPREV, N,1)


*******************************************************************
*        BEGIN MINIMUM VARIANCE ITERATIONS AND CONTINUE INITIALIZING
*        MATRICES
*******************************************************************

 300     TKM1=T0
         COUNT=COUNT+1
         CALL MATZERO (LI, N,N)
         CALL MATZERO (MI, N,1)
         CALL INICOND (IVEC, FLAG, CRIT)

         DO I = 1, N

            IF (FLAG .EQ. 0) THEN
               XSTAR(I) = IVEC(I)
            END IF

            IF (FLAG .EQ. 1) THEN
               XSTAR(I) = XSTAR(I) + X(I,1)
               IVEC(I) = XSTAR(I)
            END IF

         ENDDO

         DO I=1,IPAR
            IVEC0(I)=IVEC(I)
         ENDDO

         RMS = 0.0D0
         RMS2= 0.0D0
         RMS1=0.0D0

         ICOUNT = 0
```

94

```
          CALL MATZERO (X, N,1)


**********************************************************************
*         READ IN OBSERVATION DATA. DATA MUST BE IN THE FOLLOWING ORDER:
*         SITE NUMBER, TIME, RANGE, RANGE COVARIANCE, AZIMUTH, AZIMUTH
*         COVARIANCE, ELEVATION, ELEVATION COVARIANCE
**********************************************************************

          DO I = 1, 10000

   600        READ(5,*,ERR=2000,END=2000)SITE,T,(YVEC(J,1),SIG2VEC(J),J=1,P)

             DO J = 1,P
                RINV(J,J) = 1.0D0/(SIG2VEC(J))
             ENDDO

             ICOUNT = ICOUNT + 1

             DT=T-TKM1

             IF (T-TKM1 .GT. 15.0D0) THEN
                DT=15.0D0
             END IF


**********************************************************************
*         THIS SECTION BEGINS THE QUICK-LOOK IDENTIFICATION PROCESS
**********************************************************************

             CALL RK4 (TKM1, T, DT, IPAR, IVEC, D1, D2, D3)
             CALL HTILDE (IVEC, T, SITE, YVEC, HD, HB, Y)
             CALL MKPHI (IVEC, PHIDD, PHIDC)
             CALL MATMLT (HD, PHIDD, DUM16, P,N1,N1,N1)
             CALL MATMLT (HD, PHIDC, DUM12, P,N1,N1,N2)
             CALL MKH (H, DUM16, DUM12, HB)

             DO II = 1,2

                IF (YVEC(II,1).LT.0.0D0) THEN
                   Y(II,1) = 0.0D0

                   DO JJ = 1,N
                      H(II,JJ) = 0.0D0
                   ENDDO

                ENDIF

             ENDDO

             IF (DABS(YVEC(3,1)).GT.90.0D0) THEN

                Y(3,1) = 0.0D0

                DO JJ = 1,N
                   H(3,JJ) = 0.0D0
                ENDDO
```

95

```fortran
      ENDIF

      CALL MATMLT (H, XPREV, HX, P, N, N, 1)
      CALL MATSUB (Y, HX, RES, P, 1)
      CALL TRANSPOSE(RES,REST,P,1)
      CALL MATMLT(REST,RINV,CQ,1,P,P,P)
      CALL MATMLT(CQ,RES,RMSNEW,1,P,P,1)

      RMS=RMS+RMSNEW

      CALL TRANSPOSE (H, HXPSE, P, N)
      CALL MATMLT (HXPSE, RINV, NI, N,P,P,P)
      CALL MATMLT (NI, H, L, N,P,P,N)
      CALL MATADD (L, LI, LI, N,N)
      CALL MATMLT (NI, Y, M, N,P,P,1)
      CALL MATADD (M, MI, MI, N,1)

      TKM1 = T

      ENDDO
2000  CONTINUE

 634  DO I = 1, N

         IF (LI(I,I) .LE. 0.0D0) THEN
            D(I) = 1.0D0
         ELSE
            D(I) = 1.0D0 / DSQRT (LI(I,I))
         ENDIF

      ENDDO

      DO I = 1, N
         MN(I,1) = D(I) * MI(I,1)
         DO J = 1, N
            LN(I,J) = D(I) * D(J) * LI(I,J)
         ENDDO
      ENDDO

1000  CALL CHOLESKY2(LN,MN,XN)

      DO I = 1, N
         X(I,1) = D(I) * XN(I,1)
      ENDDO

      NORM = 0.D0
      DIFF = 0.D0

      DO I = 1, N
         DIFF = DIFF + (X(I,1)-XPREV(I,1)) * (X(I,1)-XPREV(I,1))
         NORM = NORM + X(I,1) * X(I,1)
         XPREV(I,1) = X(I,1)
      ENDDO

      RMS = DSQRT(RMS/ICOUNT/P)
      NORM = DSQRT(NORM)
```

96

```
          DIFF = DSQRT(DIFF)

          REWIND(6)

          RMSS = ((OLDRMS - RMS)/OLDRMS)

  12      FORMAT (/, 2X,'STATE CORRECTION VECTOR NORM:'
         .     ,1PG35.15,/,2X, 1PG35.15,
         .     /,
         .'****************************************************************',
         .'****************************************************************')

          IF ( DABS(RMSS) .GT. CRIT ) THEN
             FLAG = 1
             REWIND 5
             OLDRMS = RMS


****************************************************************************
*        THIS SECTION INITIALIZES THE MATRICES TO BE USED IN THE RIDGE-TYPE
*        FILTER
****************************************************************************


             CALL SINGMAT(XN,Y,H,D,XSTAR,MN,LN,SCOUNT,IVEC0,YOLDS,
         .     HOLDS,YSING,HSING,DOLDS,XSTARSO,XNOLDS,MNOLDS,LNOLDS,DSING,
         .     XSTARS,XNSING,MNSING,LNSING,IVECSO,IVECS)

             CALL MULTMAT(XN,Y,H,D,XSTAR,MN,LN,MCOUNT,IVEC0,YOLDM,
         .     HOLDM,YMULT,HMULT,DOLDM,XSTARMO,XNOLDM,MNOLDM,LNOLDM,DMULT,
         .     XSTARM,XNMULT,MNMULT,LNMULT,IVECMO,IVECM)

             GOTO 300

          END IF


****************************************************************************
*        CALCULATE THE MINIMUM VARIANCE ESTIMATE
****************************************************************************

          DO I=1,N
             XSTARMV(I)=XSTAR(I)+X(I,1)
          ENDDO


****************************************************************************
*        THIS SECTION CALCULATES THE SINGLE BIASING PARAMETER
*        RIDGE-TYPE SOLUTION
****************************************************************************

          CALL SINGLE(XNSING,XNOLDS,XNR,LNSING,LNOLDS,MNSING,MNOLDS,ITER)

          IF (ITER.EQ.1) THEN

             DO I=1,N
                XS(I,1)=DSING(I)*XNR(I,1)
             ENDDO
```

97

```
            CALL RMSRIDGE(YSING,HSING,XS,RINV,IVECS,RMSNEWRS)

            DO I = 1, N
               XSTARRS(I) = XSTARS(I) + XS(I,1)
            ENDDO

        ELSE

            DO I=1,N
               XS(I,1)=DOLDS(I)*XNR(I,1)
            ENDDO

            CALL RMSRIDGE(YOLDS,HOLDS,XS,RINV,IVECSO,RMSNEWRS)

            DO I = 1, N
               XSTARRS(I) = XSTARSO(I) + XS(I,1)
            ENDDO

        END IF

        CALL RHO(XSTARRS,RHOCMS)


*********************************************************************
*       THIS SECTION CALCULATES THE MULTIPLE BIASING PARAMETER
*       RIDGE-TYPE SOLUTION
*********************************************************************

        CALL MULTIPLE(XNMULT,XNOLDM,XNR,LNMULT,LNOLDM,MNMULT,MNOLDM,ITER)

        IF (ITER.EQ.1) THEN
            DO I=1,N
               XM(I,1)=DMULT(I)*XNR(I,1)
            ENDDO

            CALL RMSRIDGE(YMULT,HMULT,XM,RINV,IVECM,RMSNEWRM)

            DO  I = 1, N
               XSTARRM(I) = XSTARM(I) + XM(I,1)
            ENDDO

        ELSE

            DO I=1,N
               XM(I,1)=DOLDM(I)*XNR(I,1)
            ENDDO

            CALL RMSRIDGE(YOLDM,HOLDM,XM,RINV,IVECMO,RMSNEWRM)

            DO  I = 1, N
               XSTARRM(I) = XSTARMO(I) + XM(I,1)
            ENDDO

        END IF

        CALL RHO(XSTARRM,RHOCMM)
```

98

```
************************************************************************
*          THIS SECTION COMBINES THE SINGLE AND MULTIPLE RIDGE-TYPE RESULTS
*          TO OBTAIN THE FINAL RIDGE SOLUTION
************************************************************************

          WRITE(6,*) 'RIDGE-TYPE SOLUTION'
          WRITE(6,*) ' '

          DO I=1,N
              XSTARR(I)=(XSTARRS(I)+XSTARRM(I))/2.0D0
              WRITE(10,*) XSTARR(I)
              PRINT*,XSTARR(I)
          ENDDO

          WRITE(6,*) 'RX  (M)',XSTARR(1)
          WRITE(6,*) 'RY  (M)',XSTARR(2)
          WRITE(6,*) 'RZ  (M)',XSTARR(3)
          WRITE(6,*) 'VX  (M/S)',XSTARR(4)
          WRITE(6,*) 'VY  (M/S)',XSTARR(5)
          WRITE(6,*) 'VZ  (M/S)',XSTARR(6)
          WRITE(6,*) 'AT  (M/S^2)',XSTARR(7)
          WRITE(6,*) 'AR  (M/S^2)',XSTARR(8)


************************************************************************
*          CALCULATE THE TETHER ORIENTATION ANGLE, ALPHA, AND THE DISTANCE
*          FROM THE OBSERVED SATELLITE TO THE SYSTEM'S CENTER-OF-MASS
************************************************************************

          PI=2.0D0*DASIN(1.0D0)
          RATIO=XSTARR(8)/XSTARR(7)
          ALPHA=DATAN(RATIO)*180.0D0/PI

          IF (RATIO.LT.0.0D0) THEN
             ALPHA=ALPHA+180.0D0
          END IF

          CALL RHO(XSTARR,RHOCM)

          RMSC=(RMSNEWRS+RMSNEWRM)/2.0D0
          WRITE(6,*) 'PMS',RMSC
          WRITE(6,*) 'DISTANCE FROM TETHERED SATELLITE TO THE CM (M)'
          WRITE(6,*) ' '
          WRITE(6,*) RHOCM
          WRITE(10,*) RHOCM
          WRITE(6,*) ' '
          WRITE(6,*) 'TETHER ORIENTATION ANGLE (DEG)'
          WRITE(6,*) ' '
          WRITE(6,*) ALPHA
          WRITE(6,*) ' '
          PRINT*,'RHOCM',RHOCM
          IF (DABS(RHOCM).LT.270.0D0) THEN

             WRITE(6,*) 'THIS IS AN UNTETHERED SATELLITE.'
             WRITE(6,*) ' '
```

```
          ELSE

              WRITE(6,*) 'THIS IS A TETHERED SATELLITE.'
              WRITE(6,*) ' '

              IF(RHOCM.GT.0.0D0) THEN

                 WRITE(6,*) 'THE OBSERVED SATELLITE IS THE LOWER MASS OF A'
                 WRITE(6,*) '          TETHERED SATELLITE SYSTEM'

              ELSE

                 WRITE(6,*) 'THE OBSERVED SATELLITE IS THE UPPER MASS OF A'
                 WRITE(6,*) '          TETHERED SATELLITE SYSTEM'

              END IF

          END IF


*****************************************************************************
*       THIS SECTION WRITES THE FINAL COVARIANCE MATRIX TO THE FILE
*       'COVAR.OUT'
*****************************************************************************

  13      FORMAT (7X, 'XSTAR[',I2, '] = ', 1PG35.15)

          WRITE(8,*)
          WRITE(8,*) 'FINAL COVARIANCE MATRIX [P]:'
          WRITE(8,*)

          DO J = 1,10,3
              WRITE(8,*)
              WRITE(8,*)

              DO I = 1, N
                 WRITE(8,14) LI(I,J), LI(I,J+1), LI(I,J+2)
  14             FORMAT(3(4X,1PG21.10))
              ENDDO
          ENDDO

          STOP
          END


*****************************************************************************
*       THIS SUBROUTINE DETERMINES THE APPROPRIATE MATRICES TO BE USED
*       BY THE SINGLE BIASING PARAMETER RIDGE-TYPE SOLUTION.  MATRICES
*       ARE OBTAINED THROUGH THE MINIMUM VARIANCE CALCULATIONS.
*****************************************************************************

          SUBROUTINE SINGMAT(XN,Y,H,D,XSTAR,MN,LN,SCOUNT,IVEC0,YOLDS,
        . HOLDS,YSING,HSING,DOLDS,XSTARSO,XNOLDS,MNOLDS,LNOLDS,DSING,
        . XSTARS,XNSING,MNSING,LNSING,IVECSO,IVECS)

          IMPLICIT DOUBLE PRECISION(A-Z)
```

```fortran
      INTEGER I,IPAR,J,N,P,SCOUNT
      PARAMETER (N=8,P=3,IPAR=56)
      DIMENSION XN(N,1),Y(P,1),H(P,N),D(N),XSTAR(N),MN(N,1),LN(N,N),
    . IVEC0(IPAR),YOLDS(P,1),HOLDS(P,N),YSING(P,1),HSING(P,N),DOLDS(N)
    . ,XSTARSO(N),XNOLDS(N,1),MNOLDS(N,1),LNOLDS(N,N),DSING(N),
    . XSTARS(N),XNSING(N,1),MNSING(N,1),LNSING(N,N),IVECSO(IPAR),
    . IVECS(IPAR),K(N,N),XNT(1,N),DEN(1,1)

      KMAX=1.0D0/DSQRT(N*1.0D0)

      CALL TRANSPOSE (XN, XNT, 8, 1)
      CALL MATMLT(XNT,XN,DEN,1,N,N,1)
      LILKS=(N*1.0D0)/DEN(1,1)

      KSUM=0.0D0

      DO I=1,N
         K(I,I)=LILKS
         KSUM=KSUM+K(I,I)
      ENDDO

      IF (KSUM.LT.KMAX*8.0D0) THEN
         SCOUNT=SCOUNT+1

         DO I=1,P

            IF (SCOUNT.EQ.1) THEN
               YOLDS(I,1)=Y(I,1)

               DO J=1,N
                  HOLDS(I,J)=H(I,J)
               ENDDO

            ELSE

               YOLDS(I,1)=YSING(I,1)

               DO J=1,N
                  HOLDS(I,J)=HSING(I,J)
               ENDDO

            ENDIF

            YSING(I,1)=Y(I,1)

            DO J=1,N
               HSING(I,J)=H(I,J)
            ENDDO

         ENDDO

         DO I=1,N

            IF (SCOUNT.EQ.1) THEN

               DOLDS(I)=D(I)
               XSTARSO(I)=XSTAR(I)
```

```
                  XNOLDS(I,1)=XN(I,1)
                  MNOLDS(I,1)=MN(I,1)

                  DO J=1,N
                      LNOLDS(I,J)=LN(I,J)
                  ENDDO

            ELSE

                  DOLDS(I)=DSING(I)
                  XSTARSO(I)=XSTARS(I)
                  XNOLDS(I,1)=XNSING(I,1)
                  MNOLDS(I,1)=MNSING(I,1)

                  DO J=1,N
                      LNOLDS(I,J)=LNSING(I,J)
                  ENDDO

            ENDIF

            DSING(I)=D(I)
            XSTARS(I)=XSTAR(I)
            XNSING(I,1)=XN(I,1)
            MNSING(I,1)=MN(I,1)

            DO J=1,N
                LNSING(I,J)=LN(I,J)
            ENDDO

      ENDDO

         DO I=1,IPAR

            IF (SCOUNT.EQ.1) THEN

                IVECSO(I)=IVEC0(I)

            ELSE

                IVECSO(I)=IVECS(I)

            END IF

            IVECS(I)=IVEC0(I)

         ENDDO

      END IF

      RETURN
      END


**********************************************************************
*      THIS SUBROUTINE USES THE SINGLE-BIASING PARAMETER RIDGE-TYPE
*      TECHNIQUE
**********************************************************************
```

102

```fortran
      SUBROUTINE SINGLE(XNC,XNCOLD,XN,LN,LNOLD,MN,MNOLD,ITER)
      IMPLICIT DOUBLE PRECISION(A-Z)
      INTEGER I,N,J,COUNT,ITER
      PARAMETER(N=8)
      DIMENSION XNC(N,1),XN(8,1),LN(N,N),LN1(8,8),MN(N,1),K(8,8),
     .  DEN(1,1),XNT(1,8),XNCOLD(N,1),LNOLD(N,N),MNOLD(N,1)

      ITER=1

      COUNT=0
      KMAX=1.0D0/DSQRT(N*1.0D0)
      CHECKOLD=0.0D0

777   CALL MATZERO(K,N,N)
      CALL TRANSPOSE (XNC, XNT, 8, 1)
      CALL MATMLT(XNT,XNC,DEN,1,N,N,1)
      LILK=(N*1.0D0)/DEN(1,1)

      DO I=1,N
          K(I,I)=LILK
      ENDDO

      CALL MATADD(LN,K,LN1,N,N)
      CALL CHOLESKY2(LN1,MN,XN)

      IF (LILK.GT.KMAX.AND.COUNT.EQ.0) THEN

          CHECKOLD=0.0D0
          ITER=0
          COUNT=COUNT+1
          CALL TRANSPOSE (XNCOLD, XNT, 8, 1)
          CALL MATMLT(XNT,XNCOLD,DEN,1,N,N,1)
          LILK=(N*1.0D0)/DEN(1,1)

          DO I=1,N
              K(I,I)=LILK
              MN(I,1)=MNOLD(I,1)
              DO J=1,N
                  LN(I,J)=LNOLD(I,J)
              ENDDO
          ENDDO

          CALL MATADD(LNOLD,K,LN1,N,N)
          CALL CHOLESKY2(LN1,MNOLD,XN)

      END IF

      CHECK=0.0D0

      DO I=1,N
          CHECK=CHECK+XN(I,1)**2
      ENDDO


      IF (DABS(CHECK-CHECKOLD).GT..01D0*CHECKOLD) THEN
```

103

```
            CHECKOLD=CHECK

            DO I=1,N
               XNC(I,1)=XN(I,1)
            ENDDO

            GOTO 777

         ELSE

            GOTO 888

         END IF

  888    RETURN
         END


*******************************************************************
*       THIS SUBROUTINE DETERMINES THE APPROPRIATE MATRICES TO BE USED
*       BY THE SINGLE BIASING PARAMETER.  MATRICES ARE OBTAINED THROUGH
*       THE MINIMUM VARIANCE CALCULATIONS.
*******************************************************************

         SUBROUTINE MULTMAT(XN,Y,H,D,XSTAR,MN,LN,MCOUNT,IVEC0,YOLDM,
      .  HOLDM,YMULT,HMULT,DOLDM,XSTARMO,XNOLDM,MNOLDM,LNOLDM,DMULT,
      .  XSTARM,XNMULT,MNMULT,LNMULT,IVECMO,IVECM)

         IMPLICIT DOUBLE PRECISION(A-Z)
         INTEGER I,IPAR,J,N,P,MCOUNT
         PARAMETER (N=8,P=3,IPAR=56)
         DIMENSION XN(N,1),Y(P,1),H(P,N),D(N),XSTAR(N),MN(N,1),LN(N,N),
      .  IVEC0(IPAR),YOLDM(P,1),HOLDM(P,N),YMULT(P,1),HMULT(P,N),DOLDM(N)
      .  ,XSTARMO(N),XNOLDM(N,1),MNOLDM(N,1),LNOLDM(N,N),DMULT(N),
      .  XSTARM(N),XNMULT(N,1),MNMULT(N,1),LNMULT(N,N),IVECMO(IPAR),
      .  IVECM(IPAR),K(N,N)

         KMAX=1.0D0/DSQRT(N*1.0D0)
         KSUM=0.0D0

         DO I=1,N
            LILK=1.0D0/(XN(I,1)**2)
            K(I,I)=LILK
            KSUM=KSUM+K(I,I)
         ENDDO

         IF (KSUM.LT.KMAX*8.0D0) THEN

            MCOUNT=MCOUNT+1
            DO I=1,P

               IF (MCOUNT.EQ.1) THEN

                  YOLDM(I,1)=Y(I,1)
                  DO J=1,N
                     HOLDM(I,J)=H(I,J)
                  ENDDO
```

104

```fortran
    ELSE

        YOLDM(I,1)=YMULT(I,1)
        DO J=1,N
            HOLDM(I,J)=HMULT(I,J)
        ENDDO

    END IF

    YMULT(I,1)=Y(I,1)
    DO J=1,N
        HMULT(I,J)=H(I,J)
    ENDDO

ENDDO

DO I=1,N

    IF (MCOUNT.EQ.1) THEN

        DOLDM(I)=D(I)
        XSTARMO(I)=XSTAR(I)
        XNOLDM(I,1)=XN(I,1)
        MNOLDM(I,1)=MN(I,1)
        DO J=1,N
            LNOLDM(I,J)=LN(I,J)
        ENDDO

    ELSE

        DOLDM(I)=DMULT(I)
        XSTARMO(I)=XSTARM(I)
        XNOLDM(I,1)=XNMULT(I,1)
        MNOLDM(I,1)=MNMULT(I,1)

        DO J=1,N
            LNOLDM(I,J)=LNMULT(I,J)
        ENDDO

    END IF

    DMULT(I)=D(I)
    XSTARM(I)=XSTAR(I)
    XNMULT(I,1)=XN(I,1)
    MNMULT(I,1)=MN(I,1)

    DO J=1,N
        LNMULT(I,J)=LN(I,J)
    ENDDO

ENDDO

DO I=1,IPAR

    IF (MCOUNT.EQ.1) THEN
        IVECMO(I)=IVEC0(I)
```

105

```
                  ELSE
                      IVECMO(I)=IVECM(I)
                  END IF

                  IVECM(I)=IVEC0(I)


            ENDDO

      END IF

      RETURN
      END


****************************************************************************
*       THIS SUBROUTINE USES THE MULTIPLE BIASING PARAMETER RIDGE-TYPE
*       TECHNIQUE
****************************************************************************

      SUBROUTINE MULTIPLE(XNC,XNCOLD,XN,LN,LNOLD,MN,MNOLD,ITER)
      IMPLICIT DOUBLE PRECISION(A-Z)
      INTEGER I,N,ITER,J,COUNT
      PARAMETER(N=8)
      DIMENSION XNC(N,1),XN(8,1),LN(N,N),LN1(8,8),MN(N,1),K(8,8),
    . XNCOLD(N,1),LNOLD(N,N),MNOLD(N,1)

      ITER=1
      COUNT=0
      KMAX=1.0D0/DSQRT(N*1.0D0)
      CHECKOLD=0.0D0

  777 KSUM=0.0D0
      CALL MATZERO(K,N,N)

            DO I=1,N

                  LILK=1.0D0/(XNC(I,1)**2)
                  K(I,I)=LILK

                  IF (K(I,I).GT.KMAX) THEN
                      K(I,I)=KMAX
                  END IF

                  KSUM=KSUM+K(I,I)

            ENDDO

      CALL MATADD(LN,K,LN1,N,N)

      CALL CHOLESKY2(LN1,MN,XN)

      IF (KSUM.GT.KMAX*4.0D0.AND.COUNT.EQ.0) THEN

            CHECKOLD=0.0D0
            ITER=0
            COUNT=COUNT+1
```

106

```fortran
      DO I=1,N
         LILK=1.0D0/(XNCOLD(I,1)**2)
         K(I,I)=LILK
      ENDDO

      DO I=1,N
         MN(I,1)=MNOLD(I,1)

         DO J=1,N
            LN(I,J)=LNOLD(I,J)
         ENDDO

      ENDDO

      CALL MATADD(LNOLD,K,LN1,N,N)
      CALL CHOLESKY2(LN1,MNOLD,XN)

   END IF

   CHECK=0.0D0

   DO I=1,N
      CHECK=CHECK+XN(I,1)**2
   ENDDO

   IF (DABS(CHECK-CHECKOLD).GT..01D0*CHECKOLD) THEN

      CHECKOLD=CHECK

      DO I=1,N
         XNC(I,1)=XN(I,1)
      ENDDO

      GOTO 777

   ELSE

      GOTO 888

   END IF

888   RETURN
      END


************************************************************************
*      THIS SUBROUTINE CALCULATES THE RMS OF THE RIDGE-TYPE SOLUTION
************************************************************************

      SUBROUTINE RMSRIDGE(Y,H,X,RINV,IVEC,RMS)
      IMPLICIT DOUBLE PRECISION(A-Z)
      INTEGER ICOUNT,P,N,SITE,N1,N2,IPAR,J,I,II,JJ
      PARAMETER (N=8,P=3,N1=6, N2=2, IPAR=56)
      DIMENSION Y(P,1), H(P,N), X(N,1), RINV(P,P), RES(P,1),REST(1,P),
     .  CQ(1,P), YVEC(P,1), IVEC(IPAR), PHIDD(N1,N1),PHIDC(N1,N2),
     .  HD(P,N1),HB(P,N2),DUM16(P,N1),DUM12(P,N2),D1(IPAR),D2(IPAR),
     .  D3(IPAR),SIG2VEC(P)
```

107

```fortran
        ICOUNT=0
        RMS=0.0D0
        TKM1=0.0D0
        REWIND(5)

        DO I = 1, 10000

600     READ(5,*,ERR=2000,END=2000)SITE,T,(YVEC(J,1),SIG2VEC(J),J=1,P)

        DO J = 1,P
           RINV(J,J) = 1.0D0/(SIG2VEC(J))
        ENDDO

        ICOUNT = ICOUNT + 1

        DT=T-TKM1

        IF (T-TKM1 .GT. 15.0D0) THEN
           DT=15.0D0
        ENDIF

        CALL RK4 (TKM1, T, DT, IPAR, IVEC, D1, D2, D3)
        CALL HTILDE (IVEC, T, SITE, YVEC, HD, HB, Y)
        CALL MKPHI (IVEC, PHIDD, PHIDC)
        CALL MATMLT (HD, PHIDD, DUM16, P,N1,N1,N1)
        CALL MATMLT (HD, PHIDC, DUM12, P,N1,N1,N2)
        CALL MKH (H, DUM16, DUM12, HB)

        DO II = 1,2

           IF (YVEC(II,1).LT.0.0D0) THEN

              Y(II,1) = 0.0D0

              DO JJ = 1,N
                 H(II,JJ) = 0.0D0
              ENDDO

           ENDIF

        ENDDO

        IF (DABS(YVEC(3,1)).GT.90.0D0) THEN

           Y(3,1) = 0.0D0

           DO JJ = 1,N
              H(3,JJ) = 0.0D0
           ENDDO

        ENDIF

        CALL MATMLT (H, X, HX, P, N, N, 1)
        CALL MATSUB (Y, HX, RES, P, 1)
        CALL TRANSPOSE(RES,REST,P,1)
        CALL MATMLT(REST,RINV,CQ,1,P,P,P)
```

108

```
            CALL MATMLT(CQ,RES,RMSNEW,1,P,P,1)
            RMS=RMS+RMSNEW
            TKM1=T
         ENDDO

 2000    CONTINUE

         RMS=DSQRT(RMS/(ICOUNT*P))

         RETURN
         END


*********************************************************************
*        THIS SUBROUTINE CALCULATES THE DISTANCE FROM THE OBSERVED
*        SATELLITE TO THE SYSTEM'S CENTER-OF-MASS
*********************************************************************

         SUBROUTINE RHO(XSTAR,RHOCM)
         IMPLICIT DOUBLE PRECISION(A-Z)
         DIMENSION XSTAR(8)

         TRUEMU=3.98600436D14

         RR=DSQRT(XSTAR(1)**2+XSTAR(2)**2+XSTAR(3)**2)

         MUSTAR=TRUEMU-XSTAR(8)*RR**2

         RHOCM=((TRUEMU-MUSTAR)/(2.0D0*TRUEMU+MUSTAR))*RR

         WRITE(6,*)

         RETURN
         END


*********************************************************************
*        THIS SUBROUTINE PERFORMS CHOLESKY DECOMPOSITION
*********************************************************************

         SUBROUTINE CHOLESKY2(L,M,XH)
         IMPLICIT DOUBLE PRECISION(A-Z)
         INTEGER I,J,N,K
         PARAMETER(N=8)
         DIMENSION L(N,N),S(N,N),M(N,1),Z(N,1),XH(N,1),B(N,N),P(N,N)


*********************************************************************
*        SOLVE FOR Z USING FORWARD ELIMINATION
*********************************************************************

         DO I=1,N

            SUM1=0.0D0

            DO J=1,I-1
               SUM1=S(J,I)*S(J,I)+SUM1
```

109

```
        ENDDO

        S(I,I)=DSQRT(L(I,I)-SUM1)

        DO K=I+1,N

            SUM2=0.0D0

            DO J=1,I-1
                SUM2=S(J,I)*S(J,K)+SUM2
            ENDDO

            S(I,K)=(L(I,K)-SUM2)/S(I,I)

        ENDDO

        SUM3=0.0D0

        DO J=1,I-1
            SUM3=S(J,I)*Z(J,1)+SUM3
        ENDDO

        Z(I,1)=(M(I,1)-SUM3)/S(I,I)

    ENDDO

*********************************************************************
*        SOLVE FOR X USING BACK SUBSTITUTION
*********************************************************************

        DO I=N,1,-1

        SUM4=0.0D0

        DO J=N,I+1,-1
            SUM4=S(I,J)*XH(J,1)+SUM4
        ENDDO

        XH(I,1)=(Z(I,1)-SUM4)/S(I,I)

        DO K=N,I,-1

            IF (K.EQ.I) THEN

                B(I,K)=1.0D0/S(I,K)

            ELSE

                SUM5=0.0D0

                DO J=I+1,K
                    SUM5=S(I,J)*B(J,K)+SUM5
                ENDDO

                B(I,K)=-SUM5/S(I,I)
```

110

```
              ENDIF

              SUM6=0.0D0

                DO J=K,N
                    SUM6=B(I,J)*B(K,J)+SUM6
                ENDDO

                P(I,K)=SUM6
                P(K,I)=P(I,K)

            ENDDO

          ENDDO

          RETURN
          END


**********************************************************************
**
*       THIS SUBROUTINE COMPUTES AND RETURNS THE MATRICES HTILDE-SUB-D AND
*       HTILDE-SUB-B.  IT ALSO COMPUTES AND RETURNS THE RANGE CORRECTION, LIL
*       Y-SUB-I.       (TWW, 18 NOV 90)
**********************************************************************
**

          SUBROUTINE HTILDE (IVEC, T, SITE, YVEC, HD, HB, Y)
          IMPLICIT DOUBLE PRECISION (A-Z)
          INTEGER  P, N1, N2, IPAR, SITE
          PARAMETER ( N1=6, N2=2, IPAR=56, P=3)
          DIMENSION IVEC(IPAR), HD(P,N1), HB(P,N2), Y(P,1), YVEC(P,1)
          COMMON/SITEVEC/THETA0, T0



**********************************************************************
**
*       SET CONSTANTS & FIND CURRENT GST
**********************************************************************
**

          PI=3.141592654D0
          WE = 7.292115147D-05
          THETA = THETA0 + WE*(T-T0)

          CT = DCOS(THETA)
          ST = DSIN(THETA)

          IF (SITE.EQ.  5) THEN

            HT=    -2.8000000000000

            LONG=     279.31453910000*PI/180.0D0

            LAT=      28.024644600000*PI/180.0D0
```

```fortran
ELSEIF (SITE.EQ.   27) THEN

    HT=      28.900000000000

    LONG=     294.78995470000*PI/180.0D0

    LAT=      46.899465200000*PI/180.0D0

ELSEIF (SITE.EQ.   28) THEN

    HT=      38.100000000000

    LONG=     17.845735000000*PI/180.0D0

    LAT=      40.640989200000*PI/180.0D0

ELSEIF (SITE.EQ.  200) THEN

    HT=      1511.5000000000

    LONG=     253.3408388000*PI/180.0D0

    LAT=      33.8177618000CJ*PI/180.0D0

ELSEIF (SITE.EQ.  201) THEN

    HT=      38.100000000000

    LONG=     17.845735000000*PI/180.0D0

    LAT=      40.640989200000*PI/180.0D0

ELSEIF (SITE.EQ.  202) THEN

    HT=      1510.7000000000

    LONG=     253.34024570000*PI/180.0D0

    LAT=      33.817951500000*PI/180.0D0

ELSEIF (SITE.EQ.  205) THEN

    HT=      1510.4000000000

    LONG=     253.34067140000*PI/180.0D0

    LAT=      33.818097300000J*PI/180.0D0

ELSEIF (SITE.EQ.  206) THEN

    HT=      1510.4000000000

    LONG=     253.34067140000*PI/180.0D0

    LAT=      33.818097300000*PI/180.0D0

ELSEIF (SITE.EQ.  207) THEN
```

112

```
      HT=      1506.5000000000

      LONG=     253.34107320000*PI/180.0D0

      LAT=      33.818430300000*PI/180.0D0
ELSEIF (SITE.EQ.  210) THEN

      HT=      1512.1000000000

      LONG=     253.33984960000*PI/180.0D0

      LAT=      33.817270700000*PI/180.0D0
ELSEIF (SITE.EQ.  211) THEN

      HT=      1512.1000000000

      LONG=     253.33984960000*PI/180.0D0

      LAT=      33.817270700000*PI/180.0D0
ELSEIF (SITE.EQ.  212) THEN

      HT=      1512.1000000000

      LONG=     253.34032520000*PI/180.0D0

      LAT=      33.817270700000*PI/180.0D0
ELSEIF (SITE.EQ.  213) THEN

      HT=      1512.1000000000

      LONG=     253.34026670000*PI/180.0D0

      LAT=      33.817050700000*PI/180.0D0
ELSEIF (SITE.EQ.  215) THEN

      HT=      1512.1000000000

      LONG=     253.33984960000*PI/180.0D0

      LAT=      33.617270700000*PI/180.0D0
ELSEIF (SITE.EQ.  220) THEN

      HT=      786.20000000000

      LONG=     128.60802220000*PI/180.0D0

      LAT=      35.744033900000*PI/180.0D0
ELSEIF (SITE.EQ.  221) THEN
```

113

```
        HT=      786.20000000000

     LONG=      128.60802220000*PI/180.0D0

     LAT=       35.744083900000*PI/180.0D0

ELSEIF (SITE.EQ.  222) THEN

     HT=      786.20000000000

     LONG=      128.60850890000*PI/180.0D0

     LAT=       35.744084800000*PI/180.0D0

ELSEIF (SITE.EQ.  223) THEN

     HT=      786.20000000000

     LONG=      128.60844030000*PI/180.0D0

     LAT=       35.743863900000*PI/180.0D0

ELSEIF (SITE.EQ.  225) THEN

     HT=      786.20000000000

     LONG=      128.60802220000*PI/180.0D0

     LAT=       35.744083900000*PI/180.0D0

ELSEIF (SITE.EQ.  230) THEN

     HT=      3059.6000000000

     LONG=      203.74221670000*PI/180.0D0

     LAT=       20.708049600000*PI/180.0D0

ELSEIF (SITE.EQ.  231) THEN

     HT=      3059.6000000000

     LONG=      203.74221670000*PI/180.0D0

     LAT=       20.708049600000*PI/180.0D0

ELSEIF (SITE.EQ.  232) THEN

     HT=      3059.6000000000

     LONG=      203.74252670000*PI/180.0D0

     LAT=       20.708050700000*PI/180.0D0

ELSEIF (SITE.EQ.  233) THEN

     HT=      3059.7000000000
```

```
        LONG=      203.74255390000*PI/180.0D0

        LAT=       20.708530400000*PI/180.0D0

ELSEIF (SITE.EQ.  235) THEN

     HT=      3059.6000000000

     LONG=     203.74221670000*PI/180.0D0

     LAT=       20.708049600000*PI/180.0D0

ELSEIF (SITE.EQ.  240) THEN

     HT=      -62.300000000000

     LONG=      72.452059500000*PI/180.0D0

     LAT=      -7.4116129000000*PI/180.0D0

ELSEIF (SITE.EQ.  241) THEN

     HT=      -62.300000000000

     LONG=      72.452059500000*PI/180.0D0

     LAT=      -7.4116129000000*PI/180.0D0

ELSEIF (SITE.EQ.  242) THEN

     HT=      -62.400000000000

     LONG=      72.452463600000*PI/180.0D0

     LAT=      -7.4116140000000*PI/180.0D0

ELSEIF (SITE.EQ.  243) THEN

     HT=      -62.400000000000

     LONG=      72.452404200000*PI/180.0D0

     LAT=      -7.4118451000000*PI/180.0D0

ELSEIF (SITE.EQ.  245) THEN

     HT=      -62.300000000000

     LONG=      72.452059500000*PI/180.0D0

     LAT=      -7.4116129000000*PI/180.0D0

ELSEIF (SITE.EQ.  315) THEN

     HT=      892.20000000000
```

115

```
          LONG=   0.*PI/180.0D0

          LAT=    37.905248300000*PI/180.0D0

      ELSEIF (SITE.EQ.   329) THEN

          HT=     216.80000000000

          LONG=   210.80717450000*PI/180.0D0

          LAT=    64.291173700000*PI/180.0D0

      ELSEIF (SITE.EQ.   330) THEN

          HT=     302.20000000000

          LONG=   359.33158340000*PI/180.0D0

          LAT=    54.368798000000*PI/180.0D0

      ELSEIF (SITE.EQ.   331) THEN

          HT=     348.20000000000

          LONG=   145.79621670000*PI/180.0D0

          LAT=    15.249145700000*PI/180.0D0

      ELSEIF (SITE.EQ.   333) THEN

          HT=     42.400000000000

          LONG=   167.48284910000*PI/180.0D0

          LAT=    9.3985998000000*PI/180.0D0

      ELSEIF (SITE.EQ.   334) THEN

          HT=     62.800000000000

          LONG=   167.47928830000*PI/180.0D0

          LAT=    9.3954289000000*PI/180.0D0

      ELSEIF (SITE.EQ.   335) THEN

          HT=     57.400000000000

          LONG=   167.48214790000*PI/180.0D0

          LAT=    9.3987474000000*PI/180.0D0

      ELSEIF (SITE.EQ.   337) THEN

          HT=     892.20000000000

          LONG=   0.*PI/180.0D0
```

116

```
      LAT=   0.*PI/180.0D0

  ELSEIF (SITE.EQ.  341) THEN

     HT=     302.20000000000

     LONG=    359.33158340000*PI/180.0D0

     LAT=     54.368798000000*PI/180.0D0

  ELSEIF (SITE.EQ.  342) THEN

     HT=     304.60000000000

     LONG=    359.33333140000*PI/180.0D0

     LAT=     54.367176000000*PI/180.0D0

  ELSEIF (SITE.EQ.  343) THEN

     HT=     303.30000000000

     LONG=    359.33452700000*PI/180.0D0

     LAT=     54.365857700000*PI/180.0D0

  ELSEIF (SITE.EQ.  344) THEN

     HT=     342.00000000000

     LONG=    359.33006780000*PI/180.0D0

     LAT=     54.361922400000*PI/180.0D0

  ELSEIF (SITE.EQ.  345) THEN

     HT=     342.00000000000

     LONG=    359.33006780000*PI/180.0D0

     LAT=     54.361922400000*PI/180.0D0

  ELSEIF (SITE.EQ.  346) THEN

     HT=      342.00000000000

     LONG=    359.33006780000*PI/180.0D0

     LAT=     54.361922400000*PI/180.0D0

  ELSEIF (SITE.EQ.  349) THEN

     HT=     216.80000000000

     LONG=    210.80717450000*PI/180.0D0
```

117

```
        LAT=      64.291173700000*PI/180.0D0

ELSEIF (SITE.EQ.  354) THEN

    HT=      54.900000000000

    LONG=     345.59750780000*PI/180.0D0

    LAT=      -7.9066377000000*PI/180.0D0

ELSEIF (SITE.EQ.  355) THEN

    HT=      140.80000000000

    LONG=     345.59879220000*PI/180.0D0

    LAT=      -7.9725795000000*PI/180.0D0

ELSEIF (SITE.EQ.  359) THEN

    HT=      216.80000000000

    LONG=     210.80717450000*PI/180.0D0

    LAT=      64.291173700000*PI/180.0D0

ELSEIF (SITE.EQ.  360) THEN

    HT=      -16.900000000000

    LONG=     279.33560140000*PI/180.0D0

    LAT=      28.424699800000*PI/180.0D0

ELSEIF (SITE.EQ.  361) THEN

    HT=      -13.400000000000

    LONG=     279.40071280000*PI/180.0D0

    LAT=      28.226391000000*PI/180.0D0

ELSEIF (SITE.EQ.  363) THEN

    HT=      1.2000000000000

    LONG=     298.20748400000*PI/180.0D0

    LAT=      17.143639000000*PI/180.0D0

ELSEIF (SITE.EQ.  369) THEN

    HT=      125.60000000000

    LONG=     288.50910340000*PI/180.0D0
```

```
          LAT=      42.617435100000*PI/180.0D0

ELSEIF (SITE.EQ.   370) THEN

      HT=      115.60000000000

      LONG=      288.50876270000*PI/180.0D0

      LAT=      42.619588900000*PI/180.0D0

ELSEIF (SITE.EQ.   371) THEN

      HT=      105.60000000000

      LONG=      288.50769450000*PI/180.0D0

      LAT=      42.617552600000*PI/180.0D0

ELSEIF (SITE.EQ.   382) THEN

      HT=      775.90000000000

      LONG=      255.44717420000*PI/180.0D0

      LAT=      30.978291500000*PI/180.0D0

ELSEIF (SITE.EQ.   383) THEN

      HT=      775.90000000000

      LONG=      259.44717420000*PI/180.0D0

      LAT=      30.973291500000*PI/180.0D0

ELSEIF (SITE.EQ.   384) THEN

      HT=      88.100000000000

      LONG=      276.43079100000*PI/180.0D0

      LAT=      32.581262500000*PI/180.0D0

ELSEIF (SITE.EQ.   385) THEN

      HT=      88.100000000000

      LONG=      276.43079100000*PI/180.0D0

      LAT=      32.581262500000*PI/180.0D0

ELSEIF (SITE.EQ.   386) THEN

      HT=      82.700000000000

      LONG=      289.46188110000*PI/180.0D0

      LAT=      41.752456600000*PI/180.0D0
```

119

```
      ELSEIF (SITE.EQ.   387) THEN

         HT=     82.700000000000

         LONG=    289.46188110000*PI/180.0D0

         LAT=    41.752456600000*PI/180.0D0

      ELSEIF (SITE.EQ.   388) THEN

         HT=    118.00000000000

         LONG=    238.64928060000*PI/180.0D0

         LAT=    39.136073700000*PI/180.0D0

      ELSEIF (SITE.EQ.   389) THEN

         HT=    118.00000000000

         LONG=    238.64928060000*PI/180.0D0

         LAT=    39.136073700000*PI/180.0D0

      ELSEIF (SITE.EQ.   392) THEN

         HT=     94.200000000000

         LONG=    174.09108640000*PI/180.0D0

         LAT=    52.737286700000*PI/180.0D0

      ELSEIF (SITE.EQ.   393) THEN

         HT=     94.200000000000

         LONG=    174.09108640000*PI/180.0D0

         LAT=    52.737286700000*PI/180.0D0

      ELSEIF (SITE.EQ.   394) THEN

         HT=    428.50000000000

         LONG=    291.70092830000*PI/180.0D0

         LAT=    76.570298800000*PI/180.0D0

      ELSEIF (SITE.EQ.   395) THEN

         HT=    428.50000000000

         LONG=    291.70092830000*PI/180.0D0

         LAT=    76.570298800000*PI/180.0D0
```

120

```
ELSEIF (SITE.EQ.  396) THEN

   HT=    350.10000000000

   LONG=   262.10041670000*PI/180.0D0

   LAT=    48.724813700000*PI/180.0D0

ELSEIF (SITE.EQ.  398) THEN

   HT=    36.400000000000

   LONG=   273.78530810000*PI/180.0D0

   LAT=    30.572460800000*PI/180.0D0

ELSEIF (SITE.EQ.  399) THEN

   HT=    36.400000000000

   LONG=   273.78530810000*PI/180.0D0

   LAT=    30.572460800000*PI/180.0D0

ELSEIF (SITE.EQ.  400) THEN

   HT=    892.20000000000

   LONG=   39.993340000000*PI/180.0D0

   LAT=    37.905248300000*PI/180.0D0

ELSEIF (SITE.EQ.  401) THEN

   HT=    892.20000000000

   LONG=   39.993340000000*PI/180.0D0

   LAT=    37.905248300000*PI/180.0D0

ELSEIF (SITE.EQ.  402) THEN

   HT=    892.20000000000

   LONG=   39.993340000000*PI/180.0D0

   LAT=    37.905248300000*PI/180.0D0

ELSEIF (SITE.EQ.  403) THEN

   HT=    892.20000000000

   LONG=   39.993340000000*PI/180.0D0

   LAT=    37.905248300000*PI/180.0D0

ELSEIF (SITE.EQ.  404) THEN
```

121

```
        HT=      892.20000000000

        LONG=     39.993340000000*PI/180.0D0

        LAT=     37.905248300000*PI/180.0D0

    ELSEIF (SITE.EQ.   501) THEN

        HT=   -0.60000000000000

        LONG=    70.000153900000*PI/180.0D0

        LAT=     4.0400000000000D-05*PI/180.0D0

    ELSEIF (SITE.EQ.   502) THEN

        HT=   -0.60000000000000

        LONG=  0.*PI/180.0D0

        LAT=     4.0400000000000D-05*PI/180.0D0

    ELSEIF (SITE.EQ.   503) THEN

        HT=   -0.60000000000000

        LONG=    290.00015390000*PI/180.0D0

        LAT=     4.0400000000000D-05*PI/180.0D0

    ELSEIF (SITE.EQ.   620) THEN

        HT=      267.10000000000

        LONG=    239.49460340000*PI/180.0D0

        LAT=    34.825634300000*PI/180.0D0

    ELSEIF (SITE.EQ.   622) THEN

        HT=      201.73770470000

        LONG=    5689646.0000000*PI/180.0D0

        LAT=    21.000000000000*PI/180.0D0

    ELSEIF (SITE.EQ.   623) THEN

        HT=      193.10000000000

        LONG=    288.36967830000*PI/180.0D0

        LAT=    42.044742100000*PI/180.0D0

    ELSEIF (SITE.EQ.   649) THEN
```

122

```
    HT=     271.00000000000

    LONG=    239.49815270000*PI/180.0D0

    LAT=     34.822610000000*PI/180.0D0

ELSEIF (SITE.EQ.   654) THEN

    HT=     429.80000000000

    LONG=    201.75789400000*PI/180.0D0

    LAT=     21.562265000000*PI/180.0D0

ELSEIF (SITE.EQ.   657) THEN

    HT=     203.30000000000

    LONG=    288.37343750000*PI/180.0D0

    LAT=     42.947821400000*PI/180.0D0

ELSEIF (SITE.EQ.   660) THEN

    HT=     218.90000000000

    LONG=    144.85604940000*PI/180.0D0

    LAT=     13.615187500000*PI/180.0D0

ELSEIF (SITE.EQ.   661) THEN

    HT=`    560.40000000000

    LONG=    55.477820500000*PI/180.0D0

    LAT=    -4.6717481000000*PI/180.0D0

ELSEIF (SITE.EQ.   731) THEN

    HT=     62.800000000000

    LONG=    167.47928830000*PI/180.0D0

    LAT=     9.3954289000000*PI/180.0D0

ELSEIF (SITE.EQ.   732) THEN

    HT=     62.800000000000

    LONG=    167.47928830000*PI/180.0D0

    LAT=     9.3954289000000*PI/180.0D0

ELSEIF (SITE.EQ.   733) THEN

    HT=     62.800000000000
```

```
        LONG=     167.47928830000*PI/180.0D0

        LAT=      9.3954289000000*PI/180.0D0

    ELSEIF (SITE.EQ.  741) THEN

      HT=     121.40000000000

      LONG=     243.02999390000*PI/180.0D0

      LAT=      32.578435700000*PI/180.0D0

    ELSEIF (SITE.EQ.  742) THEN

      HT=     1413.0000000000

      LONG=     253.00191390000*PI/180.0D0

      LAT=      33.444385400000*PI/180.0D0

    ELSEIF (SITE.EQ.  743) THEN

      HT=     6.2000000000000

      LONG=     268.97919390000*PI/180.0D0

      LAT=      33.145655500000*PI/180.0D0

    ELSEIF (SITE.EQ.  744) THEN

      HT=     26.500000000000

      LONG=     278.07745390000*PI/180.0D0

      LAT=      32.043265900000*PI/180.0D0

    ELSEIF (SITE.EQ.  745) THEN

      HT=     307.20000000000

      LONG=     261.23709390000*PI/180.0D0

      LAT=      33.553995300000*PI/180.0D0

    ELSEIF (SITE.EQ.  746) THEN

      HT=     53.800000000000

      LONG=     266.44976390000*PI/180.0D0

      LAT=      33.331325400000*PI/180.0D0

    ELSEIF (SITE.EQ.  747) THEN

      HT=     73.100000000000
```

124

```fortran
       LONG=     276.46387390000*PI/180.0D0

       LAT=      32.289365800000*PI/180.0D0
   ELSEIF (SITE.EQ.  750) THEN
       HT=       140.60000000000

       LONG=     284.38765390000*PI/180.0D0

       LAT=      43.148642400000*PI/180.0D0
   ELSEIF (SITE.EQ.  888) THEN
       HT=       1869.7000000000

       LONG=     255.83348720000*PI/180.0D0

       LAT=      38.816699900000*PI/180.0D0
   ELSEIF (SITE.EQ.  932) THEN
       HT=       301.30000000000

       LONG=     201.73341480000*PI/180.0D0

       LAT=      21.572119700000*PI/180.0D0
   ELSEIF (SITE.EQ.  951) THEN
       HT=       3060.5000000000

       LONG=     203.74218470000*PI/180.0D0

       LAT=      20.708522300000*PI/180.0D0
   ELSEIF (SITE.EQ.  952) THEN
       HT=       3060.5000000000

       LONG=     203.74264360000*PI/180.0D0

       LAT=      20.708371500000*PI/180.0D0
   ELSEIF (SITE.EQ.  961) THEN
       HT=       3059.4000000000

       LONG=     203.74231090000*PI/180.0D0

       LAT=      20.708276800000*PI/180.0D0
   END IF
   CALL GEODETIC(LAT,LONG,HT,A,B,C)
```

```
************************************************************************
**
*        CALCULATE THE EXPECTED (PREDICTED) RANGE
************************************************************************
**

          R1 = IVEC(1)*CT + IVEC(2)*ST - A
          R2 = - IVEC(1)*ST + IVEC(2)*CT - B
          R3 = IVEC(3) - C

          H1=R1*DSIN(LAT)*DCOS(LONG)+R2*DSIN(LAT)*DSIN(LONG)-R3*DCOS(LAT)
          H2=R2*DCOS(LONG)-R1*DSIN(LONG)
          H3=R1*DCOS(LAT)*DCOS(LONG)+R3*DSIN(LAT)+R2*DCOS(LAT)*DSIN(LONG)

          G = DSQRT(R1*R1 + R2*R2 + R3*R3)
          AZ =-DATAN(H2/H1)*180.0D0/PI

          IF (H1.GT.0.0D0) THEN

             AZ=180.0D0+AZ

          ENDIF

          IF (H2.LT.0.0D0) THEN

             IF (H1.LT.0.0D0) THEN

                AZ=360.0D0+AZ

             ENDIF

          ENDIF

          EL = DASIN(H3/G)*180.0D0/PI
          Y(1,1) = YVEC(1,1) - G

          Y(2,1) = YVEC(2,1) - AZ

          IF (Y(2,1).GT.180.0D0) THEN

             Y(2,1)=Y(2,1)-360.0D0

          ENDIF

          IF (Y(2,1).LT.-180.0D0) THEN

             Y(2,1)=Y(2,1)+360.0D0

          ENDIF

          Y(3,1) = YVEC(3,1) - EL


          H1X=CT*DCOS(LONG)*DSIN(LAT)-DSIN(LONG)*ST*DSIN(LAT)
          H1Y=DCOS(LONG)*ST*DSIN(LAT)+DSIN(LONG)*CT*DSIN(LAT)
          H1Z=-DCOS(LAT)
```

```
          H2X=-DSIN(LONG)*CT-DCOS(LONG)*ST
          H2Y=-ST*DSIN(LONG)+DCOS(LONG)*CT
          H2Z=0.0D0

          H3X=CT*DCOS(LONG)*DCOS(LAT)-DSIN(LONG)*ST*DCOS(LAT)
          H3Y=DCOS(LONG)*ST*DCOS(LAT)+DSIN(LONG)*CT*DCOS(LAT)
          H3Z=DSIN(LAT)


**********************************************************************
**
*         CALCULATE HD MATRIX
**********************************************************************
**

          HD(1,1) = (R1*CT - R2*ST)/G
          HD(1,2) = (R1*ST + R2*CT)/G
          HD(1,3) = (IVEC(3) - C)/G

          HD(2,1) = (-H2X*H1+H1X*H2)/(H1**2+H2**2)*180.0D0/PI
          HD(2,2) = (-H2Y*H1+H1Y*H2)/(H1**2+H2**2)*180.0D0/PI
          HD(2,3) = (-H2Z*H1+H1Z*H2)/(H1**2+H1**2)*180.0D0/PI

          HD(3,1) = (H3X*G-HD(1,1)*H3)/(G*DSQRT(G**2-H3**2))*180.0D0/PI
          HD(3,2) = (H3Y*G-HD(1,2)*H3)/(G*DSQRT(G**2-H3**2))*180.0D0/PI
          HD(3,3) = (H3Z*G-HD(1,3)*H3)/(G*DSQRT(G**2-H3**2))*180.0D0/PI

          HD(1,4) = 0.0D0
          HD(1,5) = 0.0D0
          HD(1,6) = 0.0D0

          HD(2,4) = 0.0D0
          HD(2,5) = 0.0D0
          HD(2,6) = 0.0D0
          HD(3,4) = 0.0D0
          HD(3,5) = 0.0D0
          HD(3,6) = 0.0D0


**********************************************************************
**
*         CALCULATE HB MATRIX
**********************************************************************
**

          HB(1,1) = 0.0D0
          HB(1,2) = 0.0D0
          HB(2,1) = 0.0D0
          HB(2,2) = 0.0D0
          HB(3,1) = 0.0D0
          HB(3,2) = 0.0D0

          RETURN
          END
```

```
************************************************************************
**
*        THIS SUBROUTINE FORMS THE PHI-SUB-DD AND PHI-SUB-DC MATRICES FROM THE
*        INTEGRATION VECTOR, IVEC.   PHIDD(1,1) IS IN IVEC(9), PHIDD(6,6)
*        IS IN IVEC(44), WHILE PHIDC(1,1) IS IN IVEC(45), AND PHIDC(6,2) IS IN
*        IVEC(56).                (25 NOV 90, TWW)
************************************************************************
**

         SUBROUTINE MKPHI (IVEC, PHIDD, PHIDC)
         IMPLICIT DOUBLE PRECISION (A-Z)
         INTEGER N, N1, N2, IPAR
         PARAMETER (N = 8, N1=6, N2=2, IPAR=56)
         DIMENSION IVEC(IPAR), PHIDD(N1,N1), PHIDC(N1,N2)
         INTEGER I,J, CTR

         CTR = N

         DO I = 1,N1

            DO J = 1,N1
               CTR = CTR + 1
               PHIDD(I,J) = IVEC(CTR)
            ENDDO

         ENDDO

         CTR = N+N1*N1

         DO I = 1,N1

            DO J = 1,N2
               CTR = CTR + 1
               PHIDC(I,J) = IVEC(CTR)
            ENDDO

         ENDDO

         RETURN
         END


************************************************************************
**
*        THIS SUBROUTINE PLACES THREE SMALLER MATRICES INTO THE H MATRIX.
*                        (25 NOV 90, TWW)
************************************************************************
**

         SUBROUTINE MKH (H, DUM16, DUM12, HB)
         IMPLICIT DOUBLE PRECISION (A-Z)
         INTEGER N, P, N1, N2
         PARAMETER (N = 8, N1=6, N2=2, P=3)
         DIMENSION H(P,N), DUM16(P,N1), DUM12(P,N2), HB(P,N2)
         INTEGER I,J

         HB(1,1)=HB(1,1)
```

128

```fortran
          DO J = 1,P

             DO I = 1,N1
                H(J,I) = DUM16(J,I)
             ENDDO

             DO I = 1,N2
                H(J, I+N1) = DUM12(J,I)
             ENDDO

          ENDDO

          RETURN
          END
```

```
************************************************************************
**
*       THIS SUBROUTINE PLACES THE PHIDD & PHIDC MATRICES INTO THE
INTEGRATION
*       VECTOR, IVEC.  PHIDD(1,1) IS PLACED AT IVEC(9), & PHIDC(1,1) IS
*       PLACED AT IVEC(4 ).  THE ENTRIES RUN BY COLUMNS, THEN ROWS.
*                       (TWW, 25 NOV 90)
************************************************************************
**
```

```fortran
          SUBROUTINE PHITOIVEC (PHIDD, PHIDC, IVEC)
          IMPLICIT DOUBLE PRECISION (A-Z)
          INTEGER N,  N1, N2, IPAR
          PARAMETER (N = 8, N1=6, N2=2, IPAR=56)
          DIMENSION PHIDD(N1,N1), PHIDC(N1,N2), IVEC(IPAR)
          INTEGER I, J, CTR

          CTR = N

          DO I = 1,N1

             DO J = 1,N1
                CTR = CTR + 1
                IVEC(CTR) = PHIDD(I,J)
             ENDDO

          ENDDO

          CTR = N+N1*N1

          DO I = 1,N1

             DO J = 1,N2
                CTR = CTR + 1
                IVEC(CTR) = PHIDC(I,J)
             ENDDO

          ENDDO

          RETURN
```

129

```
          END


***********************************************************************
**
*         THIS SUBROUTINE CALCULATES AND RETURNS THE TIME DERIVATIVE OF THE
STATE
*         VECTOR.      (TWW, 25 NOV 90)
***********************************************************************
**

          SUBROUTINE DERIV (T, STATE, D)
          IMPLICIT DOUBLE PRECISION (A-Z)
          INTEGER  N1, N2, IPAR
          PARAMETER (N1=6, N2=2, IPAR=56)
          DIMENSION STATE(IPAR),D(IPAR),AD(N1,N1),AC(N1,N2),PHIDD(N1,N1),
     .               PHIDC(N1,N2), PHIDDDOT(N1,N1), PHIDCDOT(N1,N2)

          WE = 7.292115147D-05
          RE = 6378135.0D0
          J2 = 1 082626076D-3
          K = 5.381D-6
          MU = 3.98600436D14
          BETA = 0.0D0



***********************************************************************
**
*         DEFINE CONVENIENCE ITEMS
***********************************************************************
**

          X1 = STATE(1)
          X2 = STATE(2)
          X3 = STATE(3)
          X4 = STATE(4)
          X5 = STATE(5)
          X6 = STATE(6)
          X7 = STATE(7)
          X8 = STATE(8)

          X32 = X3**2
          X33 = X32*X3
          X62 = X6**2
          R = DSQRT(X1**2+X2**2+X3**2)
          V = DSQRT(X4**2+X5**2+X6**2)
          R2 = R**2
          R3 = R2*R
          R4 = R3*R
          R5 = R3*R2
          R7 = R5*R2
          FAC2 = X4 + WE*X2
          FAC3 = X5 - WE*X1
          RE2 = RE**2

          CALL DENSITY (R, RHO)
```

130

```
********************************************************************************
**
*       S/C POSITION TIME DERIVATIVES
********************************************************************************
**


        D(1) = X4
        D(2) = X5
        D(3) = X6



********************************************************************************
**
*       S/C VELOCITY TIME DERIVATIVES
********************************************************************************
**


        D(4) = (X1*MU/R3)*(-1.0D0-1.5D0*J2*RE2/R2+7.5D0*J2*RE2*X32/R4)
    .          - BETA*RHO*DSQRT(FAC2**2+FAC3**2+X62)*FAC2+X8*X1/R+X7*X4/V
        D(5) = (X2*MU/R3)*(-1.0D0-1.5D0*J2*RE2/R2+7.5D0*J2*RE2*X32/R4)
    .          - BETA*RHO*DSQRT(FAC2**2+FAC3**2+X62)*FAC3+X8*X2/R+X7*X5/V
        D(6) = (X3*MU/R3)*(-1.0D0-4.5D0*J2*RE2/R2+7.5D0*J2*RE2*X32/R4)
    .          - BETA*RHO*DSQRT(FAC2**2+FAC3**2+X62)*X6+X8*X3/R+X7*X6/V



********************************************************************************
**
*       SET TIME DERIVATIVES OF CONSTANTS TO ZERO
********************************************************************************
**


        D(7) = 0.D0
        D(8) = 0.D0



********************************************************************************
**
*       CALCULATE TIME DERIVATIVE OF THE STATE TRANSITION MATRIX
********************************************************************************
**


        CALL CALCA (STATE, AD, AC)
        CALL MKPHI (STATE, PHIDD, PHIDC)
        CALL MATMLT (AD, PHIDD, PHIDDDOT, N1,N1,N1,N1)
        CALL MATMLT (AD, PHIDC, PHIDCDOT, N1,N1,N1,N2)
        CALL MATADD (PHIDCDOT, AC, PHIDCDOT, N1,N2)



********************************************************************************
**
*       PUT THE STATE TRANSITION MATRIX TIME DERIVATIVES INTO D
********************************************************************************
**


        CALL PHITOIVEC (PHIDDDOT, PHIDCDOT, D)
```

```
      RETURN
      END


***********************************************************************
**
*         THIS SUBROUTINE CALCULATES THE A(T) MATRICES, AD & AC, GIVEN THE
STATE
*         VECTOR IVEC.  IT REQUIRES THE SUPPORTING SUBROUTINE DENSITY.
*                       (TWW, 20 NOV 90)
***********************************************************************
**

      SUBROUTINE CALCA (IVEC, AD, AC)
      IMPLICIT DOUBLE PRECISION (A-Z)
      INTEGER  N1, N2, IPAR
      PARAMETER (N1=6, N2=2, IPAR=56)
      DIMENSION AD(N1,N1), AC(N1,N2), IVEC(IPAR)


***********************************************************************
**
*         SET CONSTANTS
***********************************************************************
**

      CALL MATZERO(AD, N1, N1)
      CALL MATZERO(AC, N1, N2)
      AD(1,4) = 1.0D0
      AD(2,5) = 1.0D0
      AD(3,6) = 1.0D0
      WE = 7.292115147D-05
      RE = 6378135.0D0
      J2 = 1.082626076D-3
      K = 5.381D-06
      MU = 3.98600436D14
      BETA = 0.0D0


***********************************************************************
**
*         DEFINE CONVENIENCE ITEMS
***********************************************************************
**

      X1 = IVEC(1)
      X2 = IVEC(2)
      X3 = IVEC(3)
      X4 = IVEC(4)
      X5 = IVEC(5)
      X6 = IVEC(6)
      X7 = IVEC(7)
      X8 = IVEC(8)

      R2 = X1*X1 + X2*X2 + X3*X3
      V = DSQRT(X4*X4+X5*X5+X6*X6)
      R = DSQRT(R2)
```

132

```
          R3 = R2 * R
          R4 = R3 * R
          R5 = R4 * R
          R6 = R5 * R
          R7 = R6 * R
          R8 = R7 * R
          R9 = R8 * R
          RE2 = RE * RE
          FAC2 = X4 + WE * X2
          FAC3 = X5 - WE * X1
          FAC4 = DSQRT(FAC2**2 + FAC3**2 + X6**2)
          X12 = X1*X1
          X22 = X2*X2
          X32 = X3*X3


          CALL DENSITY (R, RHO)


********************************************************************
**
*         COMPUTE AD MATRIX
********************************************************************
**

          AD(4,1) = MU*(-1.0D0/R3 - 1.5D0*RE2*J2/R5 + 7.5D0*RE2*J2*X32/R7)
      .           + X12*MU*(3.0D0/R5 + 7.5D0*RE2*J2/R7 - 52.5D0*RE2*J2*
      .           X32/R9) + K*RHO*X1*(BETA/R)*FAC4*FAC2 + RHO*WE*BETA*FAC2
      .           *FAC3/FAC4 + X8/R - X8*X12/R3

          AD(4,2) = X1*X2*MU*(3.0D0/R5 + 7.5D0*RE2*J2/R7 - 52.5D0*RE2*J2
      .           *X32/R9) + K*RHO*X2*(BETA/R)*FAC4*FAC2 - RHO*WE*BETA*FAC2
      .           *FAC2/FAC4 - RHO*WE*BETA*FAC4 - X8*X1*X2/R3
          AD(4,3) = X1*X3*MU*(3.0D0/R5 + 22.5D0*RE2*J2/R7 - 52.5D0*RE2*
      .           J2*X32/R9)+K*RHO*X3*(BETA/R)*FAC4*FAC2-X8*X1*X3/R3
          AD(4,4) = -RHO*BETA*(FAC2**2/FAC4+FAC4)+X7/V-X7*X4*X4/V**3
          AD(4,5) = -RHO*BETA*FAC2*FAC3/FAC4-X7*X5*X4/V**3
          AD(4,6) = -RHO*BETA*FAC2*X6/FAC4-X7*X6*X4/V**3

          AD(5,1) = X1*X2*MU*(3.0D0/R5 + 7.5D0*RE2*J2/R7 - 52.5D0*RE2*X32
      .           *J2/R9) + K*RHO*X1*(BETA/R)*FAC4*FAC3 + RHO*WE*BETA*
      .           FAC3**2/FAC4 + WE*BETA*RHO*FAC4 - X8*X1*X2/R3

          AD(5,2) = MU*(-1.0D0/R3 - 1.5D0*RE2*J2/R5 + 7.5D0*RE2*X3**2*J2
      .           /R7) + X22*MU*(3.0D0/R5 + 7.5D0*RE2*J2/R7 - 52.5D0*RE2*
      .           X32*J2/R9) + K*RHO*X2*(BETA/R)*FAC4*FAC3 - RHO*WE*BETA
      .           *FAC2*FAC3/FAC4+ X8/R - X8*X22/R3

          AD(5,3) = X2*X3*MU*(3.0D0/R5 + 22.5D0*RE2*J2/R7 - 52.5D0*RE2*X32
      .           *J2/R9) + K*RHO*X3*(BETA/R)*FAC4*FAC3 -X8*X2*X3/R3

          AD(5,4) = -RHO*BETA*FAC2*FAC3/FAC4-X7*X4*X5/V**3

          AD(5,5) = -RHO*BETA*FAC3**2/FAC4-RHO*BETA*FAC4+X7/V-X7*X5*X5/
      .           V**3

          AD(5,6) = -RHO*X6*BETA*FAC3/FAC4-X7*X6*X5/V**3
```

133

```
        AD(6,1) = X1*X3*MU*(3.0D0/R5 + 22.5D0*RE2*J2/R7 - 52.5D0*RE2
     .           *X32*J2/R9) + K*RHO*X1*(BETA/R)*FAC4*X6 + RHO*WE*X6*
     .           BETA*FAC3/FAC4 - X8*X1*X3/R3

        AD(6,2) = X2*X3*MU*(3.0D0/R5 + 22.5D0*RE2*J2/R7 - 52.5D0*RE2
     .           *X32*J2/R9) + K*RHO*X2*(BETA/R)*FAC4*X6 - RHO*WE*X6*
     .           BETA*FAC2/FAC4 - X8*X2*X3/R3

        AD(6,3) = MU*(-1.0D0/R3 - 4.5D0*RE2*J2/R5 + 7.5D0*RE2*X32*J2/R7)
     .           + X32*MU*(3.0D0/R5 + 37.5D0*RE2*J2/R7 - 52.5D0*RE2*X32
     .           *J2/R9) + K*RHO*X3*(BETA/R)*FAC4*X6 + X8/R - X8*X32/R3

        AD(6,4) = -RHO*X6*BETA*FAC2/FAC4-X7*X6*X4/V**3

        AD(6,5) = -RHO*X6*BETA*FAC3/FAC4-X7*X6*X5/V**3

        AD(6,6) = -RHO*BETA*FAC4 - RHO*X6*X6*BETA/FAC4+X7/V-X7*X6*X6/
     .           V**3


*****************************************************************************
**
*       COMPUTE AC MATRIX
*****************************************************************************
**

        AC(4,1) = X4/V
        AC(4,2) = X1/R
        AC(5,1) = X5/V
        AC(5,2) = X2/R
        AC(6,1) = X6/V
        AC(6,2) = X3/R

        RETURN
        END


*****************************************************************************
**
*       THIS SUBROUTINE COMPUTES ATMOSPHERIC DENSITY (KG/M^3) GIVEN A
GEOCENTRIC
*       ALTITUDE (M).  IT MODELS THE ATMOSPHERE WITH AN EXPONENTIAL FUNCTION.
*                       (TWW, 20 NOV 90)
*****************************************************************************
**

        SUBROUTINE DENSITY (R, RHO)
        IMPLICIT DOUBLE PRECISION (A-Z)

        R0 = 7278000.0D0
        K = 5.381D-6
        RHO0 = 4.36D-14

        RHO = RHO0 * DEXP(-K*(R - R0))
```

134

```
        RETURN
        END


**********************************************************************
**
*       THIS SUBROUTINE ASSIGNS THE PROPER INITIAL CONDITIONS TO THE
INTEGRATION
*       VECTOR, IVEC.  IF FLAG = 1, THE INCOMING POSN, VELOCITY, & J
COMPONENTS
*       ARE LEFT UNCHANGED.    (TWW, 25 NOV 90)
**********************************************************************
**

        SUBROUTINE INICOND (IVEC, FLAG, CRIT)
        IMPLICIT DOUBLE PRECISION (A-Z)
        INTEGER  N1, N2, IPAR
        PARAMETER (N1=6, N2=2, IPAR=56)
        DIMENSION IVEC(IPAR), PHIDD(N1,N1), PHIDC(N1,N2)
        INTEGER FLAG,I

        IF (FLAG .EQ. 1) THEN

           GOTO 10

        ENDIF


**********************************************************************
··**
*       GIVEN [CARTESIAN] NOMINAL VALUES TO START THE COMPUTATIONS.
**********************************************************************
**

        CRIT=1D-4
        READ(7,*) T0,THETA0

        DO I = 1, 8
           READ(7,*) IVEC(I)
        ENDDO


**********************************************************************
**
*       SET PHIDD(0) TO IDENTITY MATRIX, PHIDC(0) TO NULL MATRIX
**********************************************************************
**

  10    CALL IDENTMAT (PHIDD, N1)
        CALL MATZERO (PHIDC, N1,N2)


**********************************************************************
**
*       PUT MATRIX ELEMENTS INTO INTEGRATION VECTOR
```

135

```
********************************************************************
**

          CALL PHITOIVEC (PHIDD, PHIDC, IVEC)

          RETURN
          END


********************************************************************
**
*         THIS SUBROUTINE MULTIPLIES 2 MATRICES WHOSE DIMENSIONS ARE
*         (M1ROWS, M1COL),(M2ROWS, M2COL).  M1COL MUST = M2ROWS EXACTLY!  THE
*         PRODUCT OF MATRICES A AND B IS RETURNED IN MATRIX C, WHOSE DIMENSION
IS
*         (M1ROWS, M2COL).          (TWW, 22OCT90)
********************************************************************
**

          SUBROUTINE MATMLT (A,B,C, M1ROWS, M1COL, M2ROWS, M2COL)
          IMPLICIT DOUBLE PRECISION (A-H,L,N-Z)
          DIMENSION A(M1ROWS,M1COL), B(M2ROWS, M2COL), C(M1ROWS,M2COL)
          INTEGER I,J,K, M1ROWS, M1COL, M2ROWS, M2COL

          IF (M1COL .NE. M2ROWS) THEN
             WRITE(*,*) 'INVALID MATRIX MULTIPLICATION ATTEMPTED!!'
             RETURN
          ENDIF

          DO I=1,M1ROWS

            DO K = 1,M2COL
               C(I,K) = 0.D0

               DO J=1,M1COL
                  C(I,K) = A(I,J)*B(J,K) + C(I,K)
               ENDDO

            ENDDO

          ENDDO

          RETURN
          END


********************************************************************
**
*         THIS SUBROUTINE ADDS TWO MATRICES, A+B, AND RETURNS THEIR SUM IN
*         MATRIX C.  A & B MUST HAVE THE SAME DIMENSION!
*                 (TWW, 22 OCT90)
********************************************************************
**

          SUBROUTINE MATADD (A,B,C, ROWS, COL)
          IMPLICIT DOUBLE PRECISION (A-Z)
          INTEGER I,J, ROWS, COL
```

136

```
         DIMENSION A(ROWS,COL), B(ROWS,COL), C(ROWS,COL)

         DO I = 1,ROWS

            DO J = 1,COL
               C(I,J) = A(I,J) + B(I,J)
            ENDDO

         ENDDO

         RETURN
         END


**********************************************************************
**
*        THIS SUBROUTINE SUBTRACTS TWO MATRICES, A+B, AND RETURNS THEIR SUM IN
*        MATRIX C.  A & B MUST HAVE THE SAME DIMENSION!
*                (DAC, 25 MAY93)
**********************************************************************
**

         SUBROUTINE MATSUB (A,B,C, ROWS, COL)
         IMPLICIT DOUBLE PRECISION (A-Z)
         INTEGER I,J, ROWS, COL
         DIMENSION A(ROWS,COL), B(ROWS,COL), C(ROWS,COL)

         DO I = 1,ROWS

            DO J = 1,COL
               C(I,J) = A(I,J) - B(I,J)
            ENDDO

         ENDDO

         RETURN
         END


**********************************************************************
**
*        THIS SUBROUTINE COMPUTES THE TRANSPOSE OF MATRIX A, AND RETURNS THE
*        RESULT IN MATRIX AT.
*        (TWW, 22 OCT 90)
**********************************************************************
**

         SUBROUTINE TRANSPOSE (A, AT, ROWS, COLS)
         IMPLICIT DOUBLE PRECISION (A-Z)
         INTEGER I, J, ROWS, COLS
         DIMENSION A(ROWS,COLS), AT(COLS,ROWS)

         DO I = 1,ROWS

            DO J = 1, COLS
               AT(J,I) = A(I,J)
            ENDDO
```

137

```
        ENDDO

        RETURN
        END


*********************************************************************
**
*       THIS SUBROUTINE ASSIGNS ALL ELEMENTS OF MATRIX A (ROWS X COLS) TO BE
*       EQUAL TO ZERO.
*                         (TWW, 22 OCT 90)
*********************************************************************
**

        SUBROUTINE MATZERO (A, ROWS, COLS)
        IMPLICIT DOUBLE PRECISION (A-Z)
        INTEGER ROWS, COLS, I, J
        DIMENSION A(ROWS, COLS)

        DO I = 1, ROWS

          DO J = 1, COLS
             A(I,J) = 0.D0
          ENDDO

        ENDDO

        RETURN
        END


*********************************************************************
**
*       THIS SUBROUTINE FORMS A (ROW X ROW) [SQUARE] IDENTITY MATRIX.
*          (TWW, 25 NOV 90)
*********************************************************************
**

        SUBROUTINE IDENTMAT (MAT, ROWS)
        IMPLICIT DOUBLE PRECISION (A-Z)
        INTEGER I, ROWS
        DIMENSION MAT(ROWS, ROWS)

        CALL MATZERO (MAT, ROWS, ROWS)

        DO I = 1, ROWS
           MAT(I,I) = 1.0D0
        ENDDO

        RETURN
        END


*********************************************************************
**
*       THIS SUBROUTINE ROTATES A 3D VECTOR V THROUGH "ANGLE" ABOUT THE
```

138

```
*        2 ("Y") AXIS.                    (TWW, 25 NOV 90)
*************************************************************************
**

        SUBROUTINE ROT2 (ANGLE, V)
        IMPLICIT DOUBLE PRECISION (A-Z)
        DIMENSION V(3)

        C = DCOS(ANGLE)
        S = DSIN(ANGLE)
        V1 = V(1)
        V2 = V(2)
        V3 = V(3)

        V(1) = C*V1 - S*V3
        V(2) = V2
        V(3) = S*V1 + C*V3

        RETURN
        END



*************************************************************************
**
*      THIS SUBROUTINE ROTATES A 3D VECTOR V THROUGH "ANGLE" ABOUT THE
*        3 ("Z") AXIS.                    (TWW, 25 NOV 90)
*************************************************************************
**

        SUBROUTINE ROT3 (ANGLE, V)
        IMPLICIT DOUBLE PRECISION (A-Z)
        DIMENSION V(3)

        C = DCOS(ANGLE)
        S = DSIN(ANGLE)
        V1 = V(1)
        V2 = V(2)
        V3 = V(3)

        V(1) = C*V1 + S*V2
        V(2) = -S*V1 + C*V2
        V(3) = V3

        RETURN
        END



*************************************************************************
**
*
*   SUBROUTINE RK4
*
*   4TH ORDER RUNGE-KUTTA INTEGRATOR -- FIXED STEP SIZE -- TAKES INTEGRATION
*   STEPS OF SIZE TSTEP OR (TSTOP-T) WHICH EVER IS SMALLER UNTIL THE STOP
*   TIME IS REACHED.  T IS UPDATED TO TSTOP UPON RETURN.
*
*   *** NOTE *** IF T IS GREATER THAN OR "EQAUL TO" TSTOP, THIS ROUTINE
```

```
*                      WILL EXIT IMMEDIATELY -- NO ERROR MESSAGE IS GENERATED
*
*   WRITTEN BY:   CAPT ROGER L. HALL, ASTRO DEPT, 12 NOV 1987
*                 (MODIFIED 21 OCT 1988 TO PERFORM MULTIPLE STEPS
*                  UNTIL TSTOP IS REACHED)
*
*   INPUTS:    DERIV -- THE NAME OF THE STATE DERIVATIVE SUBROUTINE
*                        (TRUE NAME SHOULD BE DECLARED EXTERNAL IN CALLING
*                          ROUTINE)
*              T -- TIME (INDEPENDENT VARIABLE)
*              TSTOP -- STOP TIME (FINAL VALUE FOR INDEPENDENT VARIABLE)
*              TSTEP -- TIME STEP (STEP INCREMENT OF INDEPENDENT VARIABLE)
*              STATE -- STATE VARIABLE ARRAY
*              NSTATE -- NUMBER OF STATES TO BE INTEGRATED
*              D1,D2,D3 -- WORKSPACE ARRAYS -- NEED TO BE DECLARED IN THE
*                           CALLING ROUTINE -- EACH NEEDS TO BE DIMENSIONED
*                           AT LEAST AS LARGE AS THE STATE ARRAY (>=NSTATE)
*
*   OUTPUTS:   T -- TIME (INDEPENDENT VARIABLE) IS UPDATED TO TSTOP
*              STATE -- STATES (MOVED FORWARD TO TIME T)
*
*   EXTERNAL REFERENCES:  SUBROUTINE "DERIV"
*
*********************************************************************************
**

        SUBROUTINE RK4(T,TSTOP,TSTEP,NSTATE,STATE,D1,D2,D3)
        IMPLICIT DOUBLE PRECISION (A-Z)
        INTEGER I,NSTATE
        DIMENSION STATE(1),D1(1),D2(1),D3(1)

*********************************************************************************
**.
*         CHECK FOR TERMINATION -- T >= TSTOP
*********************************************************************************
**

 100   DELTAT = TSTOP-T

        IF ( (DELTAT .LT. 0.0D0) .OR. DABS(DELTAT) .LT. 1.0D-6 ) THEN
           GOTO 999
        END IF

        IF ( DELTAT .GT. TSTEP ) DELTAT = TSTEP


*********************************************************************************
**
*         TAKE ONE INTEGRATION STEP BY DELTAT -- REQUIRES 4 CALLS TO THE DERIV
*********************************************************************************
**

        CALL DERIV(T,STATE,D1)

        DO I = 1,NSTATE
           D1(I) = D1(I)*DELTAT
           D2(I) = STATE(I)+0.5D0*D1(I)
```

140

```fortran
        ENDDO

        TT = T+0.5D0*DELTAT

        CALL DERIV(TT,D2,D3)

        DO I = 1,NSTATE
            D3(I) = D3(I)*DELTAT
            D1(I) = D1(I)+2.0D0*D3(I)
            D2(I) = STATE(I)+0.5D0*D3(I)
        ENDDO

        CALL DERIV(TT,D2,D3)

        DO I = 1,NSTATE
            D3(I) = D3(I)*DELTAT
            D1(I) = D1(I)+2.0D0*D3(I)
            D2(I) = STATE(I)+D3(I)
        ENDDO

        T = T+DELTAT

        CALL DERIV(T,D2,D3)


************************************************************************
**
*       MOVE THE STATES FORWARD 1 INTEGRATION STEP
************************************************************************
**

        DO I = 1,NSTATE
            STATE(I) = STATE(I)+(D1(I)+D3(I)*DELTAT)/6.0D0
        ENDDO

        GOTO 100

999     RETURN
        END


************************************************************************
*       THIS SUBROUTINE WILL COMPUTE THE ECEF COORDINATES OF A RECEIVER
*       GIVEN THE GEODETIC LONG.,LAT.,HEIGHT
************************************************************************

        SUBROUTINE GEODETIC(PHIG,LAMBDAG,HEIGHTG,XECEF,YECEF,ZECEF)
        IMPLICIT DOUBLE PRECISION(A-Z)
        A=6378137.0D0
        F=1.0D0/298.257223563D0
        E=DSQRT(2.0D0*F-F**2.0D0)
        R=A/(DSQRT(1.0D0-E**2.0D0*(DSIN(PHIG))**2.0D0))
        XECEF=(R+HEIGHTG)*DCOS(PHIG)*DCOS(LAMBDAG)
        YECEF=(R+HEIGHTG)*DCOS(PHIG)*DSIN(LAMBDAG)
        ZECEF=((1.0D0-E**2.0D0)*R+HEIGHTG)*DSIN(PHIG)
        RETURN
        END
```

141

```
**********************************************************************
*       THIS SUBROUTINE CONVERTS THE ORIGINAL DATA FILE FROM THE
*       YEAR,DAY,HOUR,MIN,SEC FORMAT TO A FORMAT WITH TIME IN SECONDS
**********************************************************************

        SUBROUTINE TCONVERT
        IMPLICIT DOUBLE PRECISION(A-Z)
        INTEGER YEAR,DAY,HOUR,MINUTE,SITE,I
        DIMENSION DT(500)

        DO I=1,10000

        READ(11,1,ERR=2000,END=2000)SITE,YEAR,DAY,HOUR,MINUTE,SEC,RHO,
    .   SIGR,AZ,SIGAZ,EL,SIGEL

    1   FORMAT(I3,2X,I2,I3,I2,I2,F6.3,2X,F8.3,2X,F6.2,2X,F8.4,2X,F10.8,
    .   2X,F8.4,2X,F10.8)

        DT(I)=DAY*1440.0D0+HOUR*60.0D0+MINUTE+SEC/60.0D0
        DT(I)=DT(I)*60.0D0

        IF (I.EQ.1) THEN
            DT1=0.0D0
        ELSE
            DT(I)=DT(I)-DT(1)
            DT1=DT(I)
        END IF

        WRITE(5,*)SITE,DT1,RHO*1000.0D0,SIGR,AZ,SIGAZ,EL,SIGEL

 2000   CONTINUE
        ENDDO
        REWIND (5)
        RETURN
        END
```

142

QLF.OUT

```
   4.3925931796853460D+006
 -601623.0483765668000000
   5.9204702133240160D+006
  -3131.1078370931020000
   5963.8992351847610000
   2927.5650703629200000
   1.3878646365751700D-004
      0.0064084198932626
   2169.2269005184000000
```

QUICK-LOOK.OUT:

RIDGE-TYPE SOLUTION

```
RX (M)    4.3925931796853460D+006
RY (M)   -601623.0483765668000000
RZ (M)    5.9204702133240160D+006
VX (M/S)    -3131.1078370931020000
VY (M/S)     5963.8992351847610000
VZ (M/S)     2927.5650703629200000
AT (M/S^2)  1.3878646365751700D-004
AR (M/S^2)        0.0064084198932626
```

RMS   0.3747441153648814
DISTANCE FROM TETHERED SATELLITE TO THE CM (M)

      2169.2269005184000000

TETHER ORIENTATION ANGLE (DEG)

        88.7593453762560900

THIS IS A TETHERED SATELLITE.

THE OBSERVED SATELLITE IS THE LOWER MASS OF A
        TETHERED SATELLITE SYSTEM

```
          PROGRAM LONGTERM

***********************************************************************
**
*
*       THIS PROGRAM ESTIMATES THE STATE OF A TETHERED SATELLITE SYSTEM
*       (POSITION, VELOCITY, LIBRATION ANGLE, LIBRATION RATE, & DISTANCE
*       FROM THE OBSERVED MASS TO THE TSS CENTER OF MASS) BASED ON A LONG-
TERM
*       ARC OF OBSERVATION DATA.
*
*       THIS PROGRAM WAS PREPARED BY THE TETHERED SATELLITE WORKING GROUP
*       AT AUBURN UNIVERSITY. THE POINT OF CONTACT, DAVID A. CICCI, CAN BE
*       REACHED AT THE FOLLOWING:
*                               AEROSPACE ENGINEERING DEPARTMENT
*                               211 AEROSPACE ENGINEERING BUILDING
*                               AUBURN UNIVERSITY, AL 36849-5338
*
*                               PHONE: (334) 844-6820
*                               FAX: (334) 844-6803
*                               E-MAIL: DCICCI@ENG.AUBURN.EDU
*
***********************************************************************
**

          IMPLICIT DOUBLE PRECISION (A-Z)
          INTEGER I,N,P,SITE,FLAG,J,ICOUNT,N1,N2,IPAR
          PARAMETER (N = 9, N1=8, N2=1, IPAR=81, P=3)
          DIMENSION NI(N,P), R(P,P), H(P,N), L(N,N), LI(N,N), M(N,1),
     .   HX(P,1),LN(N,N), MN(N,1), XN(N,1), D(N), YVEC(P,1), RES(P,1),
     .           MI(N,1), Y(P,1), X(N,1), HXPSE(N,P), S(N,N), Z(N,1),
     .   IVEC(IPAR), XSTAR(N), D1(IPAR), D2(IPAR), D3(IPAR), HD(P,N1),
     .   HB(P,N2), DUM16(P,N1), DUM12(P,N2), PHIDD(N1,N1), PHIDC(N1,N2),
     .   XPREV(N,1),YXPSE(1,P),RESXPSE(1,P),RMSVEC(1,P),RMS2VEC(1,P)
     .   ,RMSVEC2(1,1),RMS2VEC2(1,1),RMS(1,1),RMS2(1,1),OLDRMS(1,1)
     .,RMSS(1,1),RSIG(3),AZSIG(3),ELSIG(3)
          COMMON/SITEVEC/THETA0, T0

          OPEN(4, FILE = 'OBS.IN', STATUS = 'UNKNOWN')
          OPEN(5, FILE = 'DATA.IN', STATUS = 'UNKNOWN')
          OPEN(6, FILE = 'LTF.OUT', STATUS = 'UNKNOWN')
          OPEN(7, FILE = 'QLF.OUT', STATUS = 'UNKNOWN')
          OPEN(8, FILE = 'POD.OUT', STATUS = 'UNKNOWN')

***********************************************************************
* READ IN THE EPOCH TIME AND GST VALUE AT FIRST OBSERVATION TIME
***********************************************************************

          READ(8,*) T0,THETA0


***********************************************************************
* READ IN THE BATCH OF OBSERVATION DATA AND CONVERT THE
```

145

```
* YEAR,DAY,HOUR,MIN,SEC FORMAT TO A FORMAT WITH TIME IN SECONDS
**********************************************************************

        CALL TCONVERT

**********************************************************************
*         INITIALIZE VARIABLES AND MATRICES
**********************************************************************


        FLAG = 0
        OLDRMS(1,1) = 1.0D10
        CALL MATZERO (R,P,P)
        CALL MATZERO (XPREV,N,1)

**********************************************************************
*         FOLLOWING ARE THE STOPPING CRITERION AND RELAXATION PARAMETER
*         FOR THE DIFFERENTIAL CORRECTIONS PROCESS; EITHER MAY BE CHANGED
*         IF DESIRED
**********************************************************************


        CRIT = 1.0D-2
        STEP = 1.0D-2

**********************************************************************
*         BEGIN MINIMUM VARIANCE ITERATIONS AND CONTINUE INITIALIZING
*         MATRICES
**********************************************************************

  300   TKM1=T0

        CALL MATZERO (LI, N,N)
        CALL MATZERO (MI, N,1)
        CALL INICOND (IVEC, FLAG)
        DO 500 I = 1, N
          IF (FLAG .EQ. 0) THEN
            XSTAR(I) = IVEC(I)
          ENDIF
          IF (FLAG .EQ. 1) THEN
            XSTAR(I) = XSTAR(I) + STEP*X(I,1)
            IVEC(I) = XSTAR(I)
          ENDIF
  500   CONTINUE
          IF (ABS(IVEC(7)).GE.2*3.141592654D0) THEN
            IVEC(7) = MOD(IVEC(7),2*3.141592654D0)
          ENDIF

        RMS(1,1) = 0.0D0
        RMS2(1,1) = 0.0D0
        ICOUNT = 0
        CALL MATZERO (X, N,1)

**********************************************************************
*         READ IN 'CONVERTED' OBSERVATION DATA. DATA MUST BE IN THE FOLLOWING
*         ORDER:  SITE NUMBER, TIME, RANGE, RANGE COVARIANCE, AZIMUTH, AZIMUTH
*         COVARIANCE, ELEVATION, ELEVATION COVARIANCE
```

```
**************************************************************************

          DO 633 I = 1, 10000
  600 READ(5,*,ERR=2000,END=2000)SITE,T,YVEC(1,1),SIG1,YVEC(2,1),SIG2
     *,YVEC(3,1),SIG3
          ICOUNT = ICOUNT + 1
          R(1,1) =      1.0D0/ SIG1
          R(2,2) =      1.0D0/ SIG2
          R(3,3) =      1.0D0/ SIG3
          DT=T-TKM1
          IF (T-TKM1 .GT. 15.0D0) THEN
               DT=15.0D0
            END IF

**************************************************************************
*         CALCULATE PSEUDOINVERSE MATRIX AND RMS RESIDUAL ERROR
**************************************************************************

          CALL RK4 (TKM1, T, DT, IPAR, IVEC, D1, D2, D3)
          CALL HTILDE (IVEC, T, SITE, YVEC, HD, HB, Y)
          CALL MKPHI (IVEC, PHIDD, PHIDC)
          CALL MATMLT (HD, PHIDD, DUM16, P,N1,N1,N1)
          CALL MATMLT (HD, PHIDC, DUM12, P,N1,N1,N2)
          CALL MKH (H, DUM16, DUM12, HB)
          CALL MATMLT (H, XPREV, HX, P, N, N, 1)
          CALL MATSUB (Y, HX, RES, P, 1)
          CALL TRANSPOSE (RES, RESXPSE, P, 1)
          CALL MATMLT (RESXPSE, R, RMS2VEC, 1,P,P,P)
          CALL MATMLT (RMS2VEC, RES, RMS2VEC2, 1,P,P,1)
          CALL TRANSPOSE (Y, YXPSE, P, 1)
          CALL MATMLT (YXPSE, R, RMSVEC, 1,P,P,P)
          CALL MATMLT (RMSVEC, Y, RMSVEC2, 1,P,P,1)
      RMS2(1,1) = RMS2(1,1) + RMSVEC2(1,1)
      RMS(1,1) = RMS(1,1) + RMS2VEC2(1,1)
          CALL TRANSPOSE (H, HXPSE, P, N)
          CALL MATMLT (HXPSE, R, NI, N,P,P,P)
          CALL MATMLT (NI, H, L, N,P,P,N)
          CALL MATADD (L, LI, LI, N,N)
          CALL MATMLT (NI, Y, M, N,P,P,1)
          CALL MATADD (M, MI, MI, N,1)
  633 TKM1 = T
 2000 CONTINUE
C          GOTO 1360

**************************************************************************
*         SOLVE FOR STATE CORRECTIONS VIA CHOLESKY DECOMPOSITION
**************************************************************************

  634 DO 700 I = 1, N
          IF (LI(I,I) .LE. 0.0D0) THEN
             D(I) = 1.0D0
          ELSE
             D(I) = 1.0D0 / DSQRT (LI(I,I))
          ENDIF
  700 CONTINUE
          DO 702 I = 1, N
          MN(I,1) = D(I) * MI(I,1)

                              147
```

```
           DO 702 J = 1, N
  702 LN(I,J) = D(I) * D(J) * LI(I,J)
 1000 CALL CHOLESKY (N, LN, XN, MN, S, Z)
           DO 706 I = 1, N
  706 X(I,1) = D(I) * XN(I,1)

      DO 1050 I = 1, N
 1050    XPREV(I,1) = X(I,1)
           RMS(1,1) = DSQRT(RMS(1,1)/ICOUNT/P)
           RMS2(1,1) = DSQRT(RMS2(1,1)/ICOUNT/P)
      RMSS(1,1) = 100.0D0*((OLDRMS(1,1) - RMS(1,1))/OLDRMS(1,1))
      PRINT*, 'RMS=',RMS
      IF(DABS(RMSS(1,1)).GT.CRIT) THEN
       FLAG = 1
           OLDRMS(1,1) = RMS(1,1)
           REWIND 5
           GOTO 300
         ENDIF
         DO 1200 I = 1, N
           XSTAR(I) = XSTAR(I) + X(I,1)
 1200    CONTINUE
         IF (ABS(XSTAR(7)).GE.2*3.141592654D0) THEN
           XSTAR(7) = MOD(XSTAR(7),2*3.141592654D0)
         ENDIF
         XSTAR(7) = XSTAR(7)/0.01745329251990D0
         IF(XSTAR(7).LT.-180.0D0) THEN
           XSTAR(7) = XSTAR(7)+360.0D0
         ENDIF
         IF(XSTAR(7).GT.180.0D0) THEN
           XSTAR(7) = XSTAR(7)-360.0D0
         ENDIF
         DO 1250 I = 1, N
           WRITE(6,*) XSTAR(I)
 1250    CONTINUE
           WRITE(6,*) RMS(1,1)
 1360         END

C################################################################
#
C   THIS SUBROUTINE COMPUTES AND RETURNS THE MATRICES HTILDE-SUB-D AND HTILDE-
C   SUB-B.  IT ALSO COMPUTES AND RETURNS THE RANGE CORRECTION, LIL Y-SUB-I.
C             (TWW, 18 NOV 90)
C################################################################
#
         SUBROUTINE HTILDE (IVEC, T, SITE, YVEC, HD, HB, Y)
         IMPLICIT DOUBLE PRECISION (A-Z)
         INTEGER N, P, N1, N2, IPAR, SITE
         PARAMETER (N = 9, N1=8, N2=1, IPAR=81, P=3)
         DIMENSION IVEC(IPAR), HD(P,N1), HB(P,N2), Y(P,1), YVEC(P,1)
         COMMON/SITEVEC/THETA0, T0


    ****************************************************************
    **
    *         SET CONSTANTS & FIND CURRENT GST
    ****************************************************************
    **
```

148

```
         PI=3.141592654D0
         WE = 7.292115147D-05
         THETA = THETA0 + WE*(T-T0)

         CT = DCOS(THETA)
         ST = DSIN(THETA)

**********************************************************************
*        BASED ON THE TAG NUMBER OF THE TRACKING STATION, CALCULATE ITS
*        LOCATION COORDINATES (GEOCENTRIC EQUATORIAL)
**********************************************************************

         IF (SITE.EQ.  5) THEN
            HT=    -2.8000000000000
            LONG=    279.31453910000*PI/180.0D0
            LAT=     28.024644600000*PI/180.0D0
         ELSEIF (SITE.EQ.  27) THEN
            HT=     28.900000000000
            LONG=    294.78995470000*PI/180.0D0
            LAT=     46.899465200000*PI/180.0D0
         ELSEIF (SITE.EQ.  28) THEN
            HT=     38.100000000000
            LONG=     17.845735000000*PI/180.0D0
            LAT=     40.640989200000*PI/180.0D0
         ELSEIF (SITE.EQ.  200) THEN
            HT=    1511.5000000000
            LONG=    253.34083880000*PI/180.0D0
            LAT=     33.817761800000*PI/180.0D0
         ELSEIF (SITE.EQ.  201) THEN
            HT=     38.100000000000
            LONG=     17.845735000000*PI/180.0D0
            LAT=     40.640989200000*PI/180.0D0
         ELSEIF (SITE.EQ.  202) THEN
            HT=    1510.7000000000
            LONG=    253.34024570000*PI/180.0D0
            LAT=     33.817951500000*PI/180.0D0
         ELSEIF (SITE.EQ.  205) THEN
            HT=    1510.4000000000
            LONG=    253.34067140000*PI/180.0D0
            LAT=     33.818097300000*PI/180.0D0
         ELSEIF (SITE.EQ.  206) THEN
            HT=    1510.4000000000
            LONG=    253.34067140000*PI/180.0D0
            LAT=     33.818097300000*PI/180.0D0
         ELSEIF (SITE.EQ.  207) THEN
            HT=    1506.5000000000
            LONG=    253.34107320000*PI/180.0D0
            LAT=     33.818430300000*PI/180.0D0
         ELSEIF (SITE.EQ.  210) THEN
            HT=    1512.1000000000
            LONG=    253.33984960000*PI/180.0D0
            LAT=     33.817270700000*PI/180.0D0
         ELSEIF (SITE.EQ.  211) THEN
            HT=    1512.1000000000
            LONG=    253.33984960000*PI/180.0D0
            LAT=     33.817270700000*PI/180.0D0
```

149

```
ELSEIF (SITE.EQ.   212) THEN
   HT=      1512.1000000000
   LONG=      253.34032520000*PI/180.0D0
   LAT=      33.817270700000*PI/180.0D0
ELSEIF (SITE.EQ.   213) THEN
   HT=      1512.1000000000
   LONG=      253.34026670000*PI/180.0D0
   LAT=      33.817050700000*PI/180.0D0
ELSEIF (SITE.EQ.   215) THEN
   HT=      1512.1000000000
   LONG=      253.33984960000*PI/180.0D0
   LAT=      33.617270700000*PI/180.0D0
ELSEIF (SITE.EQ.   220) THEN
   HT=      786.20000000000
   LONG=      128.60802220000*PI/180.0D0
   LAT=      35.744033900000*PI/180.0D0
ELSEIF (SITE.EQ.   221) THEN
   HT=      786.20000000000
   LONG=      128.60802220000*PI/180.0D0
   LAT=      35.744083900000*PI/180.0D0
ELSEIF (SITE.EQ.   222) THEN
   .'T=      786.20000000000
   LONG=      128.60850890000*PI/180.0D0
   LAT=      35.744084800000*PI/180.0D0
ELSEIF (SITE.EQ.   223) THEN
   HT=      786.20000000000
   LONG=      128.60844030000*PI/180.0D0
   LAT=      35.743863900000*PI/180.0D0
ELSEIF (SITE.EQ.   225) THEN
   HT=      786.20000000000
   LONG=      128.60802220000*PI/180.0D0
   LAT=      35.744083900000*PI/180.0D0
ELSEIF (SITE.EQ.   230) THEN
   HT=      3059.6000000000
   LONG=      203.74221670000*PI/180.0D0
   LAT=      20.708049600000*PI/180.0D0
ELSEIF (SITE.EQ.   231) THEN
   HT=      3059.6000000000
   LONG=      203.74221670000*PI/180.0D0
   LAT=      20.708049600000*PI/180.0D0
ELSEIF (SITE.EQ.   232) THEN
   HT=      3059.6000000000
   LONG=      203.74252670000*PI/180.0D0
   LAT=      20.708050700000*PI/180.0D0
ELSEIF (SITE.EQ.   233) THEN
   HT=      3059.7000000000
   LONG=      203.74255390000*PI/180.0D0
   LAT=      20.708530400000*PI/180.0D0
ELSEIF (SITE.EQ.   235) THEN
   HT=      3059.6000000000
   LONG=      203.74221670000*PI/180.0D0
   LAT=      20.708049600000*PI/180.0D0
ELSEIF (SITE.EQ.   240) THEN
   HT=      -62.300000000000
   LONG=      72.452059500000*PI/180.0D0
   LAT=      -7.4116129000000*PI/180.0D0
ELSEIF (SITE.EQ.   241) THEN
```

```fortran
      HT=    -62.300000000000
      LONG=    72.452059500000*PI/180.0D0
      LAT=    -7.4116129000000*PI/180.0D0
ELSEIF (SITE.EQ.  242) THEN
      HT=    -62.400000000000
      LONG=    72.452463600000*PI/180.0D0
      LAT=    -7.4116140000000*PI/180.0D0
ELSEIF (SITE.EQ.  243) THEN
      HT=    -62.400000000000
      LONG=    72.452404200000*PI/180.0D0
      LAT=    -7.4118451000000*PI/180.0D0
ELSEIF (SITE.EQ.  245) THEN
      HT=    -62.300000000000
      LONG=    72.452059500000*PI/180.0D0
      LAT=    -7.4116129000000*PI/180.0D0
ELSEIF (SITE.EQ.  315) THEN
      HT=    892.20000000000
      LONG=  0.*PI/180.0D0
      LAT=    37.905248300000*PI/180.0D0
ELSEIF (SITE.EQ.  329) THEN
      HT=    216.80000000000
      LONG=    210.80717450000*PI/180.0D0
      LAT=    64.291173700000*PI/180.0D0
ELSEIF (SITE.EQ.  330) THEN
      HT=    302.20000000000
      LONG=    359.33158340000*PI/180.0D0
      LAT=    54.368798000000*PI/180.0D0
ELSEIF (SITE.EQ.  331) THEN
      HT=    348.20000000000
      LONG=    145.79621670000*PI/180.0D0
      LAT=    15.249145700000*PI/180.0D0
ELSEIF (SITE.EQ.  333) THEN
      HT=    42.400000000000
      LONG=    167.48284910000*PI/180.0D0
      LAT=    9.3985998000000*PI/180.0D0
ELSEIF (SITE.EQ.  334) THEN
      HT=    62.800000000000
      LONG=    167.47928830000*PI/180.0D0
      LAT=    9.3954289000000*PI/180.0D0
ELSEIF (SITE.EQ.  335) THEN
      HT=    57.400000000000
      LONG=    167.48214790000*PI/180.0D0
      LAT=    9.3987474000000*PI/180.0D0
ELSEIF (SITE.EQ.  337) THEN
      HT=    892.20000000000
      LONG=  0.*PI/180.0D0
      LAT=  0.*PI/180.0D0
ELSEIF (SITE.EQ.  341) THEN
      HT=    302.20000000000
      LONG=    359.33158340000*PI/180.0D0
      LAT=    54.368798000000*PI/180.0D0
ELSEIF (SITE.EQ.  342) THEN
      HT=    304.60000000000
      LONG=    359.33333140000*PI/180.0D0
      LAT=    54.367176000000*PI/180.0D0
ELSEIF (SITE.EQ.  343) THEN
      HT=    303.30000000000
```

151

```
      LONG=    359.33452700000*PI/180.0D0
      LAT=     54.365857700000*PI/180.0D0
ELSEIF (SITE.EQ.  344) THEN
   HT=    342.00000000000
   LONG=    359.33006780000*PI/180.0D0
   LAT=     54.361922400000*PI/180.0D0
ELSEIF (SITE.EQ.  345) THEN
   HT=    342.00000000000
   LONG=    359.33006780000*PI/180.0D0
   LAT=     54.361922400000*PI/180.0D0
ELSEIF (SITE.EQ.  346) THEN
   HT=    342.00000000000
   LONG=    359.33006780000*PI/180.0D0
   LAT=     54.361922400000*PI/180.0D0
ELSEIF (SITE.EQ.  349) THEN
   HT=    216.80000000000
   LONG=    210.80717450000*PI/180.0D0
   LAT=     64.291173700000*PI/180.0D0
ELSEIF (SITE.EQ.  354) THEN
   HT=    54.900000000000
   LONG=    345.5975078^C00*PI/180.0D0
   LAT=    -7.90663770C0^00*PI/180.0D0
ELSEIF (SITE.EQ.  355) THEN
   HT=    140.80000000000
   LONG=    345.59879220000*PI/180.0D0
   LAT=    -7.9725795000000*PI/180.0D0
ELSEIF (SITE.EQ.  359) THEN
   HT=    216.80000000000
   LONG=    210.80717450000*PI/180.0D0
   LAT=     64.291173700000*PI/180.0D0
ELSEIF (SITE.EQ.  360) THEN
   HT=    -16.900000000000
   LONG=    279.33560140000*PI/180.0D0
   LAT=     28.424699800000*PI/180.0D0
ELSEIF (SITE.EQ.  361) THEN
   HT=    -13.400000000000
   LONG=    279.40071280000*PI/180.0D0
   LAT=     28.226391000000*PI/180.0D0
ELSEIF (SITE.EQ.  363) THEN
   HT=    1.2000000000000
   LONG=    298.20748400000*PI/180.0D0
   LAT=     17.143639000000*PI/180.0D0
ELSEIF (SITE.EQ.  369) THEN
   HT=    125.60000000000
   LONG=    288.50910340000*PI/180.0D0
   LAT=     42.617435100000*PI/180.0D0
ELSEIF (SITE.EQ.  370) THEN
   HT=    115.60000000^30
   LONG=    288.50876270000*PI/180.0D0
   LAT=     42.619588900000*PI/180.0D0
ELSEIF (SITE.EQ.  371) THEN
   HT=    105.60000000000
   LONG=    288.50769450000*PI/180.0D0
   LAT=     42.617552600000*PI/180.0D0
ELSEIF (SITE.EQ.  382) THEN
   HT=    775.90000000000
   LONG=    259.44717420000*PI/180.0D0
```

152

```
        LAT=       30.978291500000*PI/180.0D0
ELSEIF (SITE.EQ.   383) THEN
        HT=       775.90000000000
        LONG=      259.44717420000*PI/180.0D0
        LAT=       30.973291500000*PI/180.0D0
ELSEIF (SITE.EQ.   384) THEN
        HT=       88.100000000000
        LONG=      276.43079100000*PI/180.0D0
        LAT=       32.581262500000*PI/180.0D0
ELSEIF (SITE.EQ.   385) THEN
        HT=       88.100000000000
        LONG=      276.43079100000*PI/180.0D0
        LAT=       32.581262500000*PI/180.0D0
ELSEIF (SITE.EQ.   386) THEN
        HT=       82.700000000000
        LONG=      289.46188110000*PI/180.0D0
        LAT=       41.752456600000*PI/180.0D0
ELSEIF (SITE.EQ.   387) THEN
        HT=       82.700000000000
        LONG=      289.46188110000*PI/180.0D0
        LAT=       41.752456600000*PI/180.0D0
ELSEIF (SITE.EQ.   388) THEN
        HT=       118.00000000000
        LONG=      238.64928060000*PI/180.0D0
        LAT=       39.136073700000*PI/180.0D0
ELSEIF (SITE.EQ.   389) THEN
        HT=       118.00000000000
        LONG=      238.64928060000*PI/180.0D0
        LAT=       39.136073700000*PI/180.0D0
ELSEIF (SITE.EQ.   392) THEN
        HT=       94.200000000000
        LONG=      174.09108640000*PI/180.0D0
        LAT=       52.737286700000*PI/180.0D0
ELSEIF (SITE.EQ.   393) THEN
        HT=       94.200000000000
        LONG=      174.09108640000*PI/180.0D0
        LAT=       52.737286700000*PI/180.0D0
ELSEIF (SITE.EQ.   394) THEN
        HT=       428.50000000000
        LONG=      291.70092830000*PI/180.0D0
        LAT=       76.570298800000*PI/180.0D0
ELSEIF (SITE.EQ.   395) THEN
        HT=       428.50000000000
        LONG=      291.70092830000*PI/180.0D0
        LAT=       76.570298800000*PI/180.0D0
ELSEIF (SITE.EQ.   396) THEN
        HT=       350.10000000000
        LONG=      262.10041670000*PI/180.0D0
        LAT=       48.724813700000*PI/180.0D0
ELSEIF (SITE.EQ.   398) THEN
        HT=       36.400000000000
        LONG=      273.78530810000*PI/180.0D0
        LAT=       30.572460800000*PI/180.0D0
ELSEIF (SITE.EQ.   399) THEN
        HT=       36.400000000000
        LONG=      273.78530810000*PI/180.0D0
        LAT=       30.572460800000*PI/180.0D0
```

153

```
ELSEIF (SITE.EQ.  400) THEN
   HT=     892.20000000000
   LONG=    39.993340000000*PI/180.0D0
   LAT=     37.905248300000*PI/180.0D0
ELSEIF (SITE.EQ.  401) THEN
   HT=     892.20000000000
   LONG=    39.993340000000*PI/180.0D0
   LAT=     37.905248300000*PI/180.0D0
ELSEIF (SITE.EQ.  402) THEN
   HT=     892.20000000000
   LONG=    39.993340000000*PI/180.0D0
   LAT=     37.905248300000*PI/180.0D0
ELSEIF (SITE.EQ.  403) THEN
   HT=     892.20000000000
   LONG=    39.993340000000*PI/180.0D0
   LAT=     37.905248300000*PI/180.0D0
ELSEIF (SITE.EQ.  404) THEN
   HT=     892.20000000000
   LONG=    39.993340000000*PI/180.0D0
   LAT=     37.905248300000*PI/180.0D0
ELSEIF (SITE.EQ.  501) THEN
   HT=  -0.60000000000000
   LONG=    70.000153900000*PI/180.0D0
   LAT=     4.04000000000000D-05*PI/180.0D0
ELSEIF (SITE.EQ.  502) THEN
   HT=  -0.60000000000000
   LONG=  0.*PI/180.0D0
   LAT=     4.04000000000000D-05*PI/180.0D0
ELSEIF (SITE.EQ.  503) THEN
   HT=  -0.60000000000000
   LONG=    290.00015390000*PI/180.0D0
   LAT=     4.04000000000000D-05*PI/180.0D0
ELSEIF (SITE.EQ.  620) THEN
   HT=     267.10000000000
   LONG=    239.49460340000*PI/180.0D0
   LAT=     34.825634300000*PI/180.0D0
ELSEIF (SITE.EQ.  622) THEN
   HT=     201.73770470000
   LONG=    5689646.0000000*PI/180.0D0
   LAT=     21.000000000000*PI/180.0D0
ELSEIF (SITE.EQ.  623) THEN
   HT=     193.10000000000
   LONG=    288.36967830000*PI/180.0D0
   LAT=     42.044742100000*PI/180.0D0
ELSEIF (SITE.EQ.  649) THEN
   HT=     271.00000000000
   LONG=    239.49815270000*PI/180.0D0
   LAT=     34.822610000000*PI/180.0D0
ELSEIF (SITE.EQ.  654) THEN
   HT=     429.80000000000
   LONG=    201.75789400000*PI/180.0D0
   LAT=     21.562265000000*PI/180.0D0
ELSEIF (SITE.EQ.  657) THEN
   HT=     203.30000000000
   LONG=    288.37343750000*PI/180.0D0
   LAT=     42.947821400000*PI/180.0D0
ELSEIF (SITE.EQ.  660) THEN
```

154

```
      HT=       218.90000000000
      LONG=      144.85604940000*PI/180.0D0
      LAT=       13.615187500000*PI/180.0D0
ELSEIF (SITE.EQ.   661) THEN
      HT=       560.40000000000
      LONG=      55.477820500000*PI/180.0D0
      LAT=      -4.6717481000000*PI/180.0D0
ELSEIF (SITE.EQ.   731) THEN
      HT=       62.800000000000
      LONG=      167.47928830000*PI/180.0D0
      LAT=       9.3954289000000*PI/180.0D0
ELSEIF (SITE.EQ.   732) THEN
      HT=       62.800000000000
      LONG=      167.47928830000*PI/180.0D0
      LAT=       9.3954289000000*PI/180.0D0
ELSEIF (SITE.EQ.   733) THEN
      HT=       62.800000000000
      LONG=      167.47928830000*PI/180.0D0
      LAT=       9.3954289000000*PI/180.0D0
ELSEIF (SITE.EQ.   741) THEN
      HT=       121.40000000000
      LONG=      243.02999390000*PI/180.0D0
      LAT=       32.578435700000*PI/180.0D0
ELSEIF (SITE.EQ.   742) THEN
      HT=       1413.0000000000
      LONG=      253.00191390000*PI/180.0D0
      LAT=       33.444385400000*PI/180.0D0
ELSEIF (SITE.EQ.   743) THEN
      HT=       6.2000000000000
      LONG=      268.97919390000*PI/180.0D0
      LAT=       33.145655500000*PI/180.0D0
ELSEIF (SITE.EQ.   744) THEN
      HT=       26.500000000000
      LONG=      278.07745390000*PI/180.0D0
      LAT=       32.043265900000*PI/180.0D0
ELSEIF (SITE.EQ.   745) THEN
      HT=       307.20000000000
      LONG=      261.23709390000*PI/180.0D0
      LAT=       33.553995300000*PI/180.0D0
ELSEIF (SITE.EQ.   746) THEN
      HT=       53.800000000000
      LONG=      266.44976390000*PI/180.0D0
      LAT=       33.331325400000*PI/180.0D0
ELSEIF (SITE.EQ.   747) THEN
      HT=       73.100000000000
      LONG=      276.46387390000*PI/180.0D0
      LAT=       32.289365800000*PI/180.0D0
ELSEIF (SITE.EQ.   750) THEN
      HT=       140.60000000000
      LONG=      284.38765390000*PI/180.0D0
      LAT=       43.148642400000*PI/180.0D0
ELSEIF (SITE.EQ.   888) THEN
      HT=       1869.7000000000
      LONG=      255.83348720000*PI/180.0D0
      LAT=       38.816699900000*PI/180.0D0
ELSEIF (SITE.EQ.   932) THEN
      HT=       301.30000000000
```

```
            LONG=      201.73341480000*PI/180.0D0
            LAT=      21.572119700000*PI/180.0D0
        ELSEIF (SITE.EQ.   951) THEN
            HT=      3060.5000000000
            LONG=      203.74218470000*PI/180.0D0
            LAT=      20.708522300000*PI/180.0D0
        ELSEIF (SITE.EQ.   952) THEN
            HT=      3060.5000000000
            LONG=      203.74264360000*PI/180.0D0
            LAT=      20.708371500000*PI/180.0D0
        ELSEIF (SITE.EQ.   961) THEN
            HT=      3059.4000000000
            LONG=      203.74231090000*PI/180.0D0
            LAT=      20.708276800000*PI/180.0D0
        ENDIF

      CALL GEODETIC(LAT,LONG,HT,A,B,C)
****************************************************************************
**
*       CALCULATE THE EXPECTED (PREDICTED) RANGE
****************************************************************************
**

        R1 = IVEC(1)*CT + IVEC(2)*ST - A
        R2 = - IVEC(1)*ST + IVEC(2)*CT - B
        R3 = IVEC(3) - C

        H1=R1*DSIN(LAT)*DCOS(LONG)+R2*DSIN(LAT)*DSIN(LONG)-R3*DCOS(LAT)
        H2=R2*DCOS(LONG)-R1*DSIN(LONG)
        H3=R1*DCOS(LAT)*DCOS(LONG)+R3*DSIN(LAT)+R2*DCOS(LAT)*DSIN(LONG)

        G = DSQRT(R1*R1 + R2*R2 + R3*R3)
        AZ =-DATAN(H2/H1)*180.0D0/PI

        IF (H1.GT.0.0D0) THEN

           AZ=180.0D0+AZ

        ENDIF

        IF (H2.LT.0.0D0) THEN

           IF (H1.LT.0.0D0) THEN

              AZ=360.0D0+AZ

           ENDIF

        ENDIF

        EL = DASIN(H3/G)*180.0D0/PI

        Y(1,1) = YVEC(1,1) - G

        Y(2,1) = YVEC(2,1) - AZ

        IF (Y(2,1).GT.180.0D0) THEN
```

156

```
        Y(2,1)=Y(2,1)-360.0D0

     ENDIF

     IF (Y(2,1).LT.-180.0D0) THEN

        Y(2,1)=Y(2,1)+360.0D0

     ENDIF

     Y(3,1) = YVEC(3,1) - EL


     H1X=CT*DCOS(LONG)*DSIN(LAT)-DSIN(LONG)*ST*DSIN(LAT)
     H1Y=DCOS(LONG)*ST*DSIN(LAT)+DSIN(LONG)*CT*DSIN(LAT)
     H1Z=-DCOS(LAT)

     H2X=-DSIN(LONG)*CT-DCOS(LONG)*ST
     H2Y=-ST*DSIN(LONG)+DCOS(LONG)*CT
     H2Z=0.0D0

     H3X=CT*DCOS(LONG)*DCOS(LAT)-DSIN(LONG)*ST*DCOS(LAT)
     H3Y=DCOS(LONG)*ST*DCOS(LAT)+DSIN(LONG)*CT*DCOS(LAT)
     H3Z=DSIN(LAT)


************************************************************************
**
*      CALCULATE HD AND HB MATRICES
************************************************************************
**

        HD(1,1) = (R1*CT - R2*ST)/G
        HD(1,2) = (R1*ST + R2*CT)/G
        HD(1,3) = (IVEC(3) - C)/G

        HD(2,1) = (-H2X*H1+H1X*H2)/(H1**2+H2**2)*180.0D0/PI
        HD(2,2) = (-H2Y*H1+H1Y*H2)/(H1**2+H2**2)*180.0D0/PI
        HD(2,3) = (-H2Z*H1+H1Z*H2)/(H1**2+H2**2)*180.0D0/PI

        HD(3,1) = (H3X*G-HD(1,1)*H3)/(G*DSQRT(G**2-H3**2))*180.0D0/PI
        HD(3,2) = (H3Y*G-HD(1,2)*H3)/(G*DSQRT(G**2-H3**2))*180.0D0/PI
        HD(3,3) = (H3Z*G-HD(1,3)*H3)/(G*DSQRT(G**2-H3**2))*180.0D0/PI

        HD(1,4) = 0.0D0
        HD(1,5) = 0.0D0
        HD(1,6) = 0.0D0
        HD(1,7) = 0.0D0
        HD(1,8) = 0.0D0
        HD(2,3) = 0.0D0
        HD(2,4) = 0.0D0
        HD(2,5) = 0.0D0
        HD(2,6) = 0.0D0
        HD(2,7) = 0.0D0
        HD(2,8) = 0.0D0
        HD(3,4) = 0.0D0
```

157

```
         HD(3,5) = 0.0D0
         HD(3,6) = 0.0D0
         HD(3,7) = 0.0D0
         HD(3,8) = 0.0D0

         HB(1,1) = 0.0D0
         HB(2,1) = 0.0D0
         HB(3,1) = 0.0D0

         RETURN
         END


C############################################################################
#
C   THIS SUBROUTINE FORMS THE PHI-SUB-DD AND PHI-SUB-DC MATRICES FROM THE
C      INTEGRATION VECTOR, IVEC.  PHIDD(1,1) IS IN IVEC(9), PHIDD(6,6)
C      IS IN IVEC(44), WHILE PHIDC(1,1) IS IN IVEC(45), AND PHIDC(6,2) IS IN
C      IVEC(56).          (25 NOV 90, TWW)
C############################################################################
#
         SUBROUTINE MKPHI (IVEC, PHIDD, PHIDC)
         IMPLICIT DOUBLE PRECISION (A-Z)
         INTEGER N, P, N1, N2, IPAR
         PARAMETER (N = 9, N1=8, N2=1, IPAR=81, P=3)
         DIMENSION IVEC(IPAR), PHIDD(N1,N1), PHIDC(N1,N2)
         INTEGER I,J, CTR

         CTR = N
         DO 20 I = 1,N1
          DO 10 J = 1,N1
            CTR = CTR + 1
 10         PHIDD(I,J) = IVEC(CTR)
 20      CONTINUE

         CTR = N+N1*N1
         DO 40 I = 1,N1
           DO 30 J = 1,N2
             CTR = CTR + 1
 30         PHIDC(I,J) = IVEC(CTR)
 40      CONTINUE

         RETURN
         END


C############################################################################
#
C    THIS SUBROUTINE PLACES THREE SMALLER MATRICES INTO THE H MATRIX.
C                      (25 NOV 90, TWW)
C############################################################################
#
         SUBROUTINE MKH (H, DUM16, DUM12, HB)
         IMPLICIT DOUBLE PRECISION (A-Z)
         INTEGER N, P, N1, N2, IPAR
         PARAMETER (N = 9, N1=8, N2=1, IPAR=81, P=3)
         DIMENSION H(P,N), DUM16(P,N1), DUM12(P,N2), HB(P,N2)
```

158

```
      INTEGER I,J

      HB(1,1)=HB(1,1)
      DO 10 J = 1,P
      DO 20 I = 1,N1
 20   H(J,I) = DUM16(J,I)
      DO 30 I = 1,N2
 30   H(J, I+N1) = DUM12(J,I)
 10   CONTINUE

      RETURN
      END
```

```
C##################################################################
#
C    THIS SUBROUTINE PLACES THE PHIDD & PHIDC MATRICES INTO THE INTEGRATION
C    VECTOR, IVEC.  PHIDD(1,1) IS PLACED AT IVEC(9), & PHIDC(1,1) IS
C    PLACED AT IVEC(45).  THE ENTRIES RUN BY COLUMNS, THEN ROWS.
C                     (TWW, 25 NOV 90)
C##################################################################
#
      SUBROUTINE PHITOIVEC (PHIDD, PHIDC, IVEC)
      IMPLICIT DOUBLE PRECISION (A-Z)
      INTEGER N, P, N1, N2, IPAR
      PARAMETER (N = 9, N1=8, N2=1, IPAR=81, P=3)
      DIMENSION PHIDD(N1,N1), PHIDC(N1,N2), IVEC(IPAR)
      INTEGER I, J, CTR

      CTR = N
      DO 20 I = 1,N1
       DO 10 J = 1,N1
         CTR = CTR + 1
 10      IVEC(CTR) = PHIDD(I,J)
 20   CONTINUE

      CTR = N+N1*N1
      DO 30 I = 1,N1
        DO 25 J = 1,N2
          CTR = CTR + 1
 25      IVEC(CTR) = PHIDC(I,J)
 30   CONTINUE

      RETURN
      END
```

```
C##################################################################
#
C    THIS SUBROUTINE CALCULATES AND RETURNS THE TIME DERIVATIVE OF THE STATE
C    VECTOR.      (TWW, 25 NOV 90)
C##################################################################
#
      SUBROUTINE DERIV (T, STATE, D)
      IMPLICIT DOUBLE PRECISION (A-Z)
      INTEGER N, P, N1, N2, IPAR
      PARAMETER (N = 9, N1=8, N2=1, IPAR=81, P=3)
```

```
              DIMENSION STATE(IPAR),D(IPAR),AD(N1,N1),AC(N1,N2),PHIDD(N1,N1),
       .          PHIDC(N1,N2), PHIDDDOT(N1,N1), PHIDCDOT(N1,N2),
       .          AVEC(3), APVEC(3), E1VEC(3), E2VEC(3), U2VEC(3)

C     ***    SET CONSTANTS    ***
          WE = 7.292115147D-05
          RE = 6378135.0D0
          J2 = 1.082626076D-3
          K = 5.381D-6
          MU = 3.98600436D14
          BETA = 0.0D0

          X1 = STATE(1)
          X2 = STATE(2)
          X3 = STATE(3)
          X4 = STATE(4)
          X5 = STATE(5)
          X6 = STATE(6)
          X7 = STATE(7)
          X8 = STATE(8)
          X9 ·- STATE(9)

          X32 = X3*X3
          X33 = X32*X3
          X62 = X6*X6
          R = DSQRT(X1*X1+X2*X2+X3*X3)
          V = DSQRT(X4*X4+X5*X5+X6*X6)
          R2 = R*R
          R3 = R2*R
          R4 = R3*R
          R5 = R3*R2
          R7 = R5*R2
          FAC2 = X4 + WE*X2
          FAC3 = X5 - WE*X1
          RE2 = RE*RE

C THE FOLLOWING ARE DEFINED FOR OBLATENESS EFFECTS
          ALPHA = 1.0D0/1.0D0
          XP = X1+X9*ALPHA*(DCOS(X7)*X1/R+DSIN(X7)*X4/V)
          YP = X2+X9*ALPHA*(DCOS(X7)*X2/R+DSIN(X7)*X5/V)
          ZP = X3+X9*ALPHA*(DCOS(X7)*X3/R+DSIN(X7)*X6/V)
          ZP2 = ZP*ZP
          RP = DSQRT(XP*XP+YP*YP+ZP*ZP)
          RP2 = RP*RP
          RP5 = RP2*RP2*RP
          AVEC(1)= -1.5D0*MU*J2*RE2/R5*X1*(1-5.0D0*X32/R2)
          AVEC(2)= -1.5D0*MU*J2*RE2/R5*X2*(1-5.0D0*X32/R2)
          AVEC(3)= -1.5D0*MU*J2*RE2/R5*X3*(3-5.0D0*X32/R2)
          APVEC(1)= -1.5D0*MU*J2*RE2/RP5*XP*(1-5.0D0*ZP2/RP2)
          APVEC(2)= -1.5D0*MU*J2*RE2/RP5*YP*(1-5.0D0*ZP2/RP2)
          APVEC(3)= -1.5D0*MU*J2*RE2/RP5*ZP*(3-5.0D0*ZP2/RP2)
          E1VEC(1)= DCOS(X7)*X1/R+DSIN(X7)*X4/V
          E1VEC(2)= DCOS(X7)*X2/R+DSIN(X7)*X5/V
          E1VEC(3)= DCOS(X7)*X3/R+DSIN(X7)*X6/V
          E2VEC(1)= DCOS(X7)*X4/V-DSIN(X7)*X1/R
          E2VEC(2)= DCOS(X7)*X5/V-DSIN(X7)*X2/R
          E2VEC(3)= DCOS(X7)*X6/V-DSIN(X7)*X3/R
```

160

```
            U2VEC(1)= X4/V
            U2VEC(2)= X5/V
            U2VEC(3)= X6/V
        D8J2=0.0D0
        ATJ2=0.0D0
        DO 30 J = 1,3
        D8J2=D8J2+(APVEC(J)-AVEC(J))*E2VEC(J)/X9/ALPHA-AVEC(J)*U2VEC(J)/R
        ATJ2=ATJ2+(APVEC(J)-AVEC(J))*E1VEC(J)
  30    CONTINUE

        RD = (X1*X4+X2*X5+X3*X6)/R
        TERM1 = DSQRT((X2*X6-X3*X5)*(X2*X6-X3*X5)+(X3*X4-X1*X6)*(X3*X4
     .        -X1*X6)+(X1*X5-X2*X4)*(X1*X5-X2*X4))
        THETAD = TERM1/R2
        AT = X9*((X8+THETAD)*(X8+THETAD)+MU/R3*(3.0D0*(DCOS(X7)
     .        *DCOS(X7))-1.0D0))+ATJ2/ALPHA

        CALL DENSITY (R, RHO)

C   ***  S/C POSITION TIME DERIVATIVES   ***
        D'1) = X4
        D(2) = X5
        D(3) = X6
        D(7) = X8

C   ***   S/C VELOCITY TIME DERIVATIVES   ***
        D(4) = (X1*MU/R3)*(-1.0D0-1.5D0*J2*RE2/R2+7.5D0*J2*RE2*X32/R4)
     .        - BETA*RHO*DSQRT(FAC2**2+FAC3**2+X62)*FAC2+AT*DCOS(X7)*X1/R+AT
     .        *DSIN(X7)*X4/V
        D(5) = (X2*MU/R3)*(-1.0D0-1.5D0*J2*RE2/R2+7.5D0*J2*RE2*X32/R4)
     .        - BETA*RHO*DSQRT(FAC2**2+FAC3**2+X62)*FAC3+AT*DCOS(X7)*X2/R+AT
     .        *DSIN(X7)*X5/V
        D(6) = (X3*MU/R3)*(-1.0D0-4.5D0*J2*RE2/R2+7.5D0*J2*RE2*X32/R4)
     .        - BETA*RHO*DSQRT(FAC2**2+FAC3**2+X62)*X6+AT*DCOS(X7)*X3/R+AT
     .        *DSIN(X7)*X6/V
        D(8)=2.D0*THETAD*RD/R-AT*DSIN(X7)/R-1.5D0*MU/R3*DSIN(2.D0*X7)+D8J2

C   ***   SET TIME DERIVATIVES OF CONSTANTS TO ZERO   ***
        D(9) = 0.D0

C   ***  CALCULATE TIME DERIVATIVE OF THE STATE TRANSITION MATRIX   ***
        CALL CALCA (STATE, AD, AC)
        CALL MKPHI (STATE, PHIDD, PHIDC)
        CALL MATMLT (AD, PHIDD, PHIDDDOT, N1,N1,N1,N1)
        CALL MATMLT (AD, PHIDC, PHIDCDOT, N1,N1,N1,N2)
        CALL MATADD (PHIDCDOT, AC, PHIDCDOT, N1,N2)

C   ***  PUT THE STATE TRANSITION MATRIX TIME DERIVATIVES INTO D   ***
        CALL PHITOIVEC (PHIDDDOT, PHIDCDOT, D)

        RETURN
        END


C###############################################################################
#
```

161

```fortran
C  THIS SUBROUTINE CALCULATES THE A(T) MATRICES, AD & AC, GIVEN THE STATE
C   VECTOR IVEC.  IT REQUIRES THE SUPPORTING SUBROUTINE DENSITY.
C                       (TWW, 20 NOV 90)
C#################################################################
#
      SUBROUTINE CALCA (IVEC, AD, AC)
      IMPLICIT DOUBLE PRECISION (A-Z)
      INTEGER N, P, N1, N2, IPAR
      PARAMETER (N = 9, N1=8, N2=1, IPAR=81, P=3)
      DIMENSION AD(N1,N1), AC(N1,N2), IVEC(IPAR),
     .     AVEC(3), APVEC(3), E1VEC(3), E2VEC(3), U2VEC(3)

C   ***    SET CONSTANTS    ***
      CALL MATZERO(AD, N1,N1)
      CALL MATZERO(AC, N1,N2)
      AD(1,4) = 1.D0
      AD(2,5) = 1.D0
      AD(3,6) = 1.D0
      AD(7,8) = 1.D0
      WE = 7.292115147D-05
      RE = 6378135.0D0
      J2 = 1.082626076D-3
      K = 5.381D-06
      MU = 3.98600436D14
      BETA = 0.0D0

      X1 = IVEC(1)
      X2 = IVEC(2)
      X3 = IVEC(3)
      X4 = IVEC(4)
      X5 = IVEC(5)
      X6 = IVEC(6)
      X7 = IVEC(7)
      X8 = IVEC(8)
      X9 = IVEC(9)

      R2 = X1*X1 + X2*X2 + X3*X3
      R = DSQRT(R2)
      R3 = R2 * R
      R4 = R3 * R
      R5 = R4 * R
      R6 = R5 * R
      R7 = R6 * R
      R8 = R7 * R
      R9 = R8 * R
      V = DSQRT(X4*X4+X5*X5+X6*X6)
      V2 = V * V
      V3 = V2 * V
      RE2 = RE * RE
      FAC2 = X4 + WE * X2
      FAC3 = X5 - WE * X1
      FAC4 = DSQRT(FAC2**2 + FAC3**2 + X6**2)
      X12 = X1*X1
      X22 = X2*X2
      X32 = X3*X3
      X42 = X4*X4
      X52 = X5*X5
```

162

```
        X62 = X6*X6

C THE FOLLOWING ARE DEFINED FOR OBLATENESS EFFECTS
        ALPHA = 1.0D0/1.0D0
        XP = X1+X9*ALPHA*(DCOS(X7)*X1/R+DSIN(X7)*X4/V)
        YP = X2+X9*ALPHA*(DCOS(X7)*X2/R+DSIN(X7)*X5/V)
        ZP = X3+X9*ALPHA*(DCOS(X7)*X3/R+DSIN(X7)*X6/V)
        ZP2 = ZP*ZP
        RP = DSQRT(XP*XP+YP*YP+ZP*ZP)
        RP2 = RP*RP
        RP5 = RP2*RP2*RP
        RP7 = RP2*RP5
        RP9 = RP2*RP7
        AVEC(1)= -1.5D0*MU*J2*RE2/R5*X1*(1-5.0D0*X32/R2)
        AVEC(2)= -1.5D0*MU*J2*RE2/R5*X2*(1-5.0D0*X32/R2)
        AVEC(3)= -1.5D0*MU*J2*RE2/R5*X3*(3-5.0D0*X32/R2)
        APVEC(1)= -1.5D0*MU*J2*RE2/RP5*XP*(1-5.0D0*ZP2/RP2)
        APVEC(2)= -1.5D0*MU*J2*RE2/RP5*YP*(1-5.0D0*ZP2/RP2)
        APVEC(3)= -1.5D0*MU*J2*RE2/RP5*ZP*(3-5.0D0*ZP2/RP2)
        E1VEC(1)= DCOS(X7)*X1/R+DSIN(X7)*X4/V
        E1VEC(2)= DCOS(X7)*X2/R+DSIN(X7)*X5/V
        E1VEC(3)= DCOS(X7)*X3/R+DSIN(X7)*X6/V
        E2VEC(1)= DCOS(X7)*X4/V-DSIN(X7)*X1/R
        E2VEC(2)= DCOS(X7)*X5/V-DSIN(X7)*X2/R
        E2VEC(3)= DCOS(X7)*X6/V-DSIN(X7)*X3/R
        U2VEC(1)= X4/V
        U2VEC(2)= X5/V
        U2VEC(3)= X6/V
      ATJ2=0.0D0
      DO 30 J = 1,3
      ATJ2=ATJ2+(APVEC(J)-AVEC(J))*E1VEC(J)
  30    CONTINUE
        AP1=AVEC(1)
        AP2=APVEC(2)
        AP3=APVEC(3)
        A1=AVEC(1)
        A2=AVEC(2)
        A3=AVEC(3)


        RD = (X1*X4+X2*X5+X3*X6)/R
        TERM1 = DSQRT((X2*X6-X3*X5)*(X2*X6-X3*X5)+(X3*X4-X1*X6)*(X3*X4
     .      -X1*X6)+(X1*X5-X2*X4)*(X1*X5-X2*X4))
        THETAD = TERM1/R2
        ATOLD = X9*((X8+THETAD)*(X8+THETAD)+MU/R3*(3.0D0*(DCOS(X7)
     .      *DCOS(X7))-1.0D0))
        AT = ATOLD+ATJ2/ALPHA
      THETADX =(X5*(X1*X5-X2*X4)-X6*(X3*X4-X1*X6))/R2/TERM1
     .      -2.0D0*X1*TERM1/R4
      THETADY =(X6*(X2*X6-X3*X5)-X4*(X1*X5-X2*X4))/R2/TERM1
     .      -2.0D0*X2*TERM1/R4
      THETADZ =(X4*(X3*X4-X1*X6)-X5*(X2*X6-X3*X5))/R2/TERM1
     .      -2.0D0*X3*TERM1/R4
        THETADXD = (X3*(X3*X4-X1*X6)-X2*(X1*X5-X2*X4))/R2/TERM1
        THETADYD = (X1*(X1*X5-X2*X4)-X3*(X2*X6-X3*X5))/R2/TERM1
        THETADZD = (X2*(X2*X6-X3*X5)-X1*(X3*X4-X1*X6))/R2/TERM1
        RDX = (X4*(X2*X2+X3*X3)-X1*(X2*X5+X3*X6))/R3
```

163

```
      RDY = (X5*(X1*X1+X3*X3)-X2*(X1*X4+X3*X6))/R3
      RDZ = (X6*(X1*X1+X2*X2)-X3*(X1*X4+X2*X5))/R3
      RDXD = X1/R
      RDYD = X2/R
      RDZD = X3/R

      A1X = MU*(-1.5D0*RE2*J2/R5 + 7.5D0*RE2*J2*X32/R7)
    .       + X12*MU*(7.5D0*RE2*J2/R7 - 52.5D0*RE2*J2*
    .       X32/R9)

      A1Y = X1*X2*MU*(7.5D0*RE2*J2/R7 - 52.5D0*RE2*J2
    .       *X32/R9)

      A1Z = X1*X3*MU*(22.5D0*RE2*J2/R7 - 52.5D0*RE2*
    . J2*X32/R9)

      A2X = X1*X2*MU*(7.5D0*RE2*J2/R7 - 52.5D0*RE2*X32
    .   *J2/R9)

      A2Y = MU*(-1.5D0*RE2*J2/R5 + 7.5D0*RE2*X3**2*J2
    .       /R7) + X22*MU*(7.5D0*RE2*J2/R7 - 52 5D0*RE2*
    .       X32*J2/R9)

      A2Z = X2*X3*MU*(22.5D0*RE2*J2/R7 - 52.5D0*RE2*X32
    .       *J2/R9)

      A3X = X1*X3*MU*(22.5D0*RE2*J2/R7 - 52.5D0*RE2
    .       *X32*J2/R9)

      A3Y = X2*X3*MU*(22.5D0*RE2*J2/R7 - 52.5D0*RE2
    .       *X32*J2/R9)

      A3Z = MU*(-4.5D0*RE2*J2/R5 + 7.5D0*RE2*X32*J2/R7)
    .       + X32*MU*(37.5D0*RE2*J2/R7 - 52.5D0*RE2*X32
    .       *J2/R9)

      AP1XP = MU*(-1.5D0*RE2*J2/RP5 + 7.5D0*RE2*J2*ZP2/RP7)
    .       + XP2*MU*(7.5D0*RE2*J2/RP7 - 52.5D0*RE2*J2*
    .       ZP2/RP9)

      AP1YP = XP*YP*MU*(7.5D0*RE2*J2/RP7 - 52.5D0*RE2*J2
    .       *ZP2/RP9)

      AP1ZP = XP*ZP*MU*(22.5D0*RE2*J2/RP7 - 52.5D0*RE2*
    . J2*ZP2/RP9)

      AP2XP = XP*YP*MU*(7.5D0*RE2*J2/RP7 - 52 5D0*RE2*ZP2
    .   *J2/RP9)

      AP2YP = MU*(-1.5D0*RE2*J2/RP5 + 7.5D0*RE2*ZP**2*J2
    .       /RP7) + YP2*MU*(7.5D0*RE2*J2/RP7 - 52.5D0*RE2*
    .       ZP2*J2/RP9)

      AP2ZP = YP*ZP*MU*(22.5D0*RE2*J2/RP7 - 52.5D0*RE2*ZP2
    .       *J2/RP9)

      AP3XP = XP*ZP*MU*(22.5D0*RE2*J2/RP7 - 52.5D0*RE2
```

164

```
          *ZP2*J2/RP9)

   AP3YP = YP*ZP*MU*(22.5D0*RE2*J2/RP7 - 52.5D0*RE2
.          *ZP2*J2/RP9)

   AP3ZP = MU*(-4.5D0*RE2*J2/RP5 + 7.5D0*RE2*ZP2*J2/RP7)
.          + ZP2*MU*(37.5D0*RE2*J2/RP7 - 52.5D0*RE2*ZP2
.          *J2/RP9)

   AP1X = AP1XP*(1+ALPHA*X9*DCOS(X7)*(1/R-X12/R3))
.          + AP1YP*ALPHA*X9*DCOS(X7)*(-X1*X2/R3)
.          + AP1ZP*ALPHA*X9*DCOS(X7)*(-X1*X3/R3)

   AP1Y = AP1XP*ALPHA*X9*DCOS(X7)*(-X1*X2/R3)
.          + AP1YP*(1+ALPHA*X9*DCOS(X7)*(1/R-X22/R3))
.          + AP1ZP*ALPHA*X9*DCOS(X7)*(-X2*X3/R3)

   AP1Z = AP1XP*ALPHA*X9*DCOS(X7)*(-X1*X3/R3)
.          + AP1YP*ALPHA*X9*DCOS(X7)*(-X2*X3/R3)
.          + AP1ZP*(1+ALPHA*X9*DCOS(X7)*(1/R-X32/R3))

   AP1XD = AP1XP*ALPHA*X9*DSIN(X7)*(1/V-X42/V3)
.          + AP1YP*ALPHA*X9*DSIN(X7)*(-X4*X5/V3)
.          + AP1ZP*ALPHA*X9*DSIN(X7)*(-X4*X6/V3)

   AP1YD = AP1XP*ALPHA*X9*DSIN(X7)*(-X4*X5/V3)
.          + AP1YP*ALPHA*X9*DSIN(X7)*(1/V-X52/V3)
.          + AP1ZP*ALPHA*X9*DSIN(X7)*(-X5*X6/V3)

   AP1ZD = AP1XP*ALPHA*X9*DSIN(X7)*(-X4*X6/V3)
.          + AP1YP*ALPHA*X9*DSIN(X7)*(-X6*X5/V3)
.          + AP1ZP*ALPHA*X9*DSIN(X7)*(1/V-X62/V3)

   AP1TH3 = AP1XP*ALPHA*X9*(X4/V*DCOS(X7)-X1/R*DSIN(X7))
.          + AP1YP*ALPHA*X9*(X5/V*DCOS(X7)-X2/R*DSIN(X7))
.          + AP1ZP*ALPHA*X9*(X6/V*DCOS(X7)-X3/R*DSIN(X7))

   AP1RHOCM = AP1XP*ALPHA*(X4/V*DSIN(X7)+X1/R*DCOS(X7))
.          + AP1YP*ALPHA*(X5/V*DSIN(X7)+X2/R*DCOS(X7))
.          + AP1ZP*ALPHA*(X6/V*DSIN(X7)+X3/R*DCOS(X7))

   AP2X = AP2XP*(1+ALPHA*X9*DCOS(X7)*(1/R-X12/R3))
.          + AP2YP*ALPHA*X9*DCOS(X7)*(-X1*X2/R3)
.          + AP2ZP*ALPHA*X9*DCOS(X7)*(-X1*X3/R3)

   AP2Y = AP2XP*ALPHA*X9*DCOS(X7)*(-X1*X2/R3)
.          + AP2YP*(1+ALPHA*X9*DCOS(X7)*(1/R-X22/R3))
.          + AP2ZP*ALPHA*X9*DCOS(X7)*(-X2*X3/R3)

   AP2Z = AP2XP*ALPHA*X9*DCOS(X7)*(-X1*X3/R3)
.          + AP2YP*ALPHA*X9*DCOS(X7)*(-X2*X3/R3)
.          + AP2ZP*(1+ALPHA*X9*DCOS(X7)*(1/R-X32/R3))

   AP2XD = AP2XP*ALPHA*X9*DSIN(X7)*(1/V-X42/V3)
.          + AP2YP*ALPHA*X9*DSIN(X7)*(-X4*X5/V3)
.          + AP2ZP*ALPHA*X9*DSIN(X7)*(-X4*X6/V3)
```

```
AP2YD = AP2XP*ALPHA*X9*DSIN(X7)*(-X4*X5/V3)
    .       + AP2YP*ALPHA*X9*DSIN(X7)*(1/V-X52/V3)
    .       + AP2ZP*ALPHA*X9*DSIN(X7)*(-X5*X6/V3)


AP2ZD = AP2XP*ALPHA*X9*DSIN(X7)*(-X4*X6/V3)
    .       + AP2YP*ALPHA*X9*DSIN(X7)*(-X6*X5/V3)
    .       + AP2ZP*ALPHA*X9*DSIN(X7)*(1/V-X62/V3)


AP2TH3 = AP2XP*ALPHA*X9*(X4/V*DCOS(X7)-X1/R*DSIN(X7))
    .        + AP2YP*ALPHA*X9*(X5/V*DCOS(X7)-X2/R*DSIN(X7))
    .        + AP2ZP*ALPHA*X9*(X6/V*DCOS(X7)-X3/R*DSIN(X7))


AP2RHOCM = AP2XP*ALPHA*(X4/V*DSIN(X7)+X1/R*DCOS(X7))
    .          + AP2YP*ALPHA*(X5/V*DSIN(X7)+X2/R*DCOS(X7))
    .          + AP2ZP*ALPHA*(X6/V*DSIN(X7)+X3/R*DCOS(X7))


AP3X = AP3XP*(1+ALPHA*X9*DCOS(X7)*(1/R-X12/R3))
    .      + AP3YP*ALPHA*X9*DCOS(X7)*(-X1*X2/R3)
    .      + AP3ZP*ALPHA*X9*DCOS(X7)*(-X1*X3/R3)


AP3Y = AP3XP*ALPHA*X9*DCOS(X7)*(-X1*X2/R3)
    .      + AP3YP*(1+ALPHA*X9*DCOS(X7)*(1/R-X22/R3))
    .      + AP3ZP*ALPHA*X9*DCOS(X7)*(-X2*X3/R3)


AP3Z = AP3XP*ALPHA*X9*DCOS(X7)*(-X1*X3/R3)
    .      + AP3YP*ALPHA*X9*DCOS(X7)*(-X2*X3/R3)
    .      + AP3ZP*(1+ALPHA*X9*DCOS(X7)*(1/R-X32/R3))


AP3XD = AP3XP*ALPHA*X9*DSIN(X7)*(1/V-X42/V3)
    .       + AP3YP*ALPHA*X9*DSIN(X7)*(-X4*X5/V3)
    .       + AP3ZP*ALPHA*X9*DSIN(X7)*(-X4*X6/V3)


AP3YD = AP3XP*ALPHA*X9*DSIN(X7)*(-X4*X5/V3)
    .       + AP3YP*ALPHA*X9*DSIN(X7)*(1/V-X52/V3)
    .       + AP3ZP*ALPHA*X9*DSIN(X7)*(-X5*X6/V3)


AP3ZD = AP3XP*ALPHA*X9*DSIN(X7)*(-X4*X6/V3)
    .       + AP3YP*ALPHA*X9*DSIN(X7)*(-X6*X5/V3)
    .       + AP3ZP*ALPHA*X9*DSIN(X7)*(1/V-X62/V3)


AP3TH3 = AP3XP*ALPHA*X9*(X4/V*DCOS(X7)-X1/R*DSIN(X7))
    .        + AP3YP*ALPHA*X9*(X5/V*DCOS(X7)-X2/R*DSIN(X7))
    .        + AP3ZP*ALPHA*X9*(X6/V*DCOS(X7)-X3/R*DSIN(X7))


AP3RHOCM = AP3XP*ALPHA*(X4/V*DSIN(X7)+X1/R*DCOS(X7))
    .          + AP3YP*ALPHA*(X5/V*DSIN(X7)+X2/R*DCOS(X7))
    .          + AP3ZP*ALPHA*(X6/V*DSIN(X7)+X3/R*DCOS(X7))


ATJ2X = (AP1X-A1X)*(X1/R*DCOS(X7)+X4/V*DSIN(X7))
    .      +(AP2X-A2X)*(X2/R*DCOS(X7)+X5/V*DSIN(X7))
    .      +(AP3X-A3X)*(X3/R*DCOS(X7)+X6/V*DSIN(X7))
.+((AP1-A1)*X1+(AP2-A2)*X2+(AP3-A3)*X3)*(-X1/R3*DCOS(X7))
.+(AP1-A1)*DCOS(X7)/R


ATJ2Y = (AP1Y-A1Y)*(X1/R*DCOS(X7)+X4/V*DSIN(X7))
    .      +(AP2Y-A2Y)*(X2/R*DCOS(X7)+X5/V*DSIN(X7))
    .      +(AP3Y-A3Y)*(X3/R*DCOS(X7)+X6/V*DSIN(X7))
```

166

```
.+((AP1-A1)*X1+(AP2-A2)*X2+(AP3-A3)*X3)*(-X2/R3*DCOS(X7))
.+(AP2-A2)*DCOS(X7)/R

   ATJ2Z = (AP1Z-A1Z)*(X1/R*DCOS(X7)+X4/V*DSIN(X7))
.         +(AP2Z-A2Z)*(X2/R*DCOS(X7)+X5/V*DSIN(X7))
.         +(AP3Z-A3Z)*(X3/R*DCOS(X7)+X6/V*DSIN(X7))
.+((AP1-A1)*X1+(AP2-A2)*X2+(AP3-A3)*X3)*(-X3/R3*DCOS(X7))
.+(AP3-A3)*DCOS(X7)/R

   ATJ2XD = AP1XD*(X1/R*DCOS(X7)+X4/V*DSIN(X7))
.          +AP2XD*(X2/R*DCOS(X7)+X5/V*DSIN(X7))
.          +AP3XD*(X3/R*DCOS(X7)+X6/V*DSIN(X7))
.+((AP1-A1)*X4+(AP2-A2)*X5+(AP3-A3)*X6)*(-X4/V3*DSIN(X7))
.+(AP1-A1)*DSIN(X7)/V

   ATJ2YD = AP1YD*(X1/R*DCOS(X7)+X4/V*DSIN(X7))
.          +AP2YD*(X2/R*DCOS(X7)+X5/V*DSIN(X7))
.          +AP3YD*(X3/R*DCOS(X7)+X6/V*DSIN(X7))
.+((AP1-A1)*X4+(AP2-A2)*X5+(AP3-A3)*X6)*(-X5/V3*DSIN(X7))
.+(AP2-A2)*DSIN(X7)/V

   ATJ2ZD = AP1ZD*(X1/R*DCOS(X7)+X4/V*DSIN(X7))
..         +AP2ZD*(X2/R*DCOS(X7)+X5/V*DSIN(X7))
.          +AP3ZD*(X3/R*DCOS(X7)+X6/V*DSIN(X7))
.+((AP1-A1)*X4+(AP2-A2)*X5+(AP3-A3)*X6)*(-X6/V3*DSIN(X7))
.+(AP3-A3)*DSIN(X7)/V

   ATJ2TH3 = AP1TH3*(X1/R*DCOS(X7)+X4/V*DSIN(X7))
.           +AP2TH3*(X2/R*DCOS(X7)+X5/V*DSIN(X7))
.           +AP3TH3*(X3/R*DCOS(X7)+X6/V*DSIN(X7))
.+(AP1-A1)*(X4/V*DCOS(X7)-X1/R*DSIN(X7))
.+(AP2-A2)*(X5/V*DCOS(X7)-X2/R*DSIN(X7))
.+(AP3-A3)*(X6/V*DCOS(X7)-X3/R*DSIN(X7))

   ATJ2RHOCM = AP1RHOCM*(X1/R*DCOS(X7)+X4/V*DSIN(X7))
.             +AP2RHOCM*(X2/R*DCOS(X7)+X5/V*DSIN(X7))
.             +AP3RHOCM*(X3/R*DCOS(X7)+X6/V*DSIN(X7))

   D8J2X = ((AP1X-A1X)*(X4/V*DCOS(X7)-X1/R*DSIN(X7))
.          +(AP2X-A2X)*(X5/V*DCOS(X7)-X2/R*DSIN(X7))
.          +(AP3X-A3X)*(X6/V*DCOS(X7)-X3/R*DSIN(X7))
.+((AP1-A1)*X1+(AP2-A2)*X2+(AP3-A3)*X3)*(X1/R3*DSIN(X7))
.-(AP1-A1)*DSIN(X7)/R)/ALPHA/X9+X1/R3*(A1*X4/V+A2*X5/V+A3*X6/V)
.-(A1X*X4/V+A2X*X5/V+A3X*X6/V)/R

   D8J2Y = ((AP1Y-A1Y)*(X4/V*DCOS(X7)-X1/R*DSIN(X7))
.          +(AP2Y-A2Y)*(X5/V*DCOS(X7)-X2/R*DSIN(X7))
.          +(AP3Y-A3Y)*(X6/V*DCOS(X7)-X3/R*DSIN(X7))
.+((AP1-A1)*X1+(AP2-A2)*X2+(AP3-A3)*X3)*(X2/R3*DSIN(X7))
.-(AP2-A2)*DSIN(X7)/R)/ALPHA/X9+X2/R3*(A1*X4/V+A2*X5/V+A3*X6/V)
.-(A1Y*X4/V+A2Y*X5/V+A3Y*X6/V)/R

   D8J2Z = ((AP1Z-A1Z)*(X4/V*DCOS(X7)-X1/R*DSIN(X7))
.          +(AP2Z-A2Z)*(X5/V*DCOS(X7)-X2/R*DSIN(X7))
.          +(AP3Z-A3Z)*(X6/V*DCOS(X7)-X3/R*DSIN(X7))
.+((AP1-A1)*X1+(AP2-A2)*X2+(AP3-A3)*X3)*(X3/R3*DSIN(X7))
.-(AP3-A3)*DSIN(X7)/R)/ALPHA/X9+X3/R3*(A1*X4/V+A2*X5/V+A3*X6/V)
```

167

```fortran
      .-(A1Z*X4/V+A2Z*X5/V+A3Z*X6/V)/R

         D8J2XD = (AP1XD*(X4/V*DCOS(X7)-X1/R*DSIN(X7))
      .          +AP2XD*(X5/V*DCOS(X7)-X2/R*DSIN(X7))
      .          +AP3XD*(X6/V*DCOS(X7)-X3/R*DSIN(X7))
      .+((AP1-A1)*X4+(AP2-A2)*X5+(AP3-A3)*X6)*(-X4/V3*DCOS(X7))
      .+(AP1-A1)*DCOS(X7)/V)/ALPHA/X9
      .+(A1/R*X4+A2/R*X5+A3/R*X6)*X4/V3-A1/R/V

         D8J2YD = (AP1YD*(X4/V*DCOS(X7)-X1/R*DSIN(X7))
      .          +AP2YD*(X5/V*DCOS(X7)-X2/R*DSIN(X7))
      .          +AP3YD*(X6/V*DCOS(X7)-X3/R*DSIN(X7))
      .+((AP1-A1)*X4+(AP2-A2)*X5+(AP3-A3)*X6)*(-X5/V3*DCOS(X7))
      .+(AP2-A2)*DCOS(X7)/V)/ALPHA/X9
      .+(A1/R*X4+A2/R*X5+A3/R*X6)*X5/V3-A2/R/V

         D8J2ZD = (AP1ZD*(X4/V*DCOS(X7)-X1/R*DSIN(X7))
      .          +AP2ZD*(X5/V*DCOS(X7)-X2/R*DSIN(X7))
      .          +AP3ZD*(X6/V*DCOS(X7)-X3/R*DSIN(X7))
      .+((AP1-A1)*X4+(AP2-A2)*X5+(AP3-A3)*X6)*(-X6/V3*DCOS(X7))
      .+(AP3-A3)*DCOS(X7)/V)/ALPHA/X9
      .+(A1/R*X4+A2/R*X5+A3/R*X6)*X6/V3-A3/R/V

         D8J2TH3 = (AP1TH3*(X4/V*DCOS(X7)-X1/R*DSIN(X7))
      .          +AP2TH3*(X5/V*DCOS(X7)-X2/R*DSIN(X7))
      .          +AP3TH3*(X6/V*DCOS(X7)-X3/R*DSIN(X7))
      .+(AP1-A1)*(-X1/R*DCOS(X7)-X4/V*DSIN(X7))
      .+(AP2-A2)*(-X2/R*DCOS(X7)-X5/V*DSIN(X7))
      .+(AP3-A3)*(-X3/R*DCOS(X7)-X6/V*DSIN(X7)))/ALPHA/X9

         D8J2RHOCM = (AP1RHOCM*(X4/V*DCOS(X7)-X1/R*DSIN(X7))
      .          +AP2RHOCM*(X5/V*DCOS(X7)-X2/R*DSIN(X7))
      .          +AP3RHOCM*(X6/V*DCOS(X7)-X3/R*DSIN(X7)))/ALPHA/X9
      .-((AP1-A1)*(X4/V*DCOS(X7)-X1/R*DSIN(X7))
      .          +(AP2-A2)*(X5/V*DCOS(X7)-X2/R*DSIN(X7))
      .     +(AP3-A3)*(X6/V*DCOS(X7)-X3/R*DSIN(X7)))/ALPHA/X9/X9

         ATX = X9*(2.0D0*(X8+THETAD)*THETADX-3.0D0*MU*X1/R5*(3.0D0
      .        *(DCOS(X7)*DCOS(X7))-1.0D0))+ATJ2X
         ATY = X9*(2.0D0*(X8+THETAD)*THETADY-3.0D0*MU*X2/R5*(3.0D0
      .        *(DCOS(X7)*DCOS(X7))-1.0D0))+ATJ2Y
         ATZ = X9*(2.0D0*(X8+THETAD)*THETADZ-3.0D0*MU*X3/R5*(3.0D0
      .        *(DCOS(X7)*DCOS(X7))-1.0D0))+ATJ2Z
         ATXD = X9*2.0D0*(X8+THETAD)*THETADXD+ATJ2XD
         ATYD = X9*2.0D0*(X8+THETAD)*THETADYD+ATJ2YD
         ATZD = X9*2.0D0*(X8+THETAD)*THETADZD+ATJ2ZD
         ATTHETA3 = -6.0D0*MU*X9/R3*DCOS(X7)*DSIN(X7)+ATJ2TH3
         ATTHETA3D = X9*2.0D0*(X8+THETAD)


         CALL DENSITY (R, RHO)
C    ***    COMPUTE AD MATRIX    ***
C    ***    ROW 4   ***
         AD(4,1) = MU*(-1.0D0/R3 - 1.5D0*RE2*J2/R5 + 7.5D0*RE2*J2*X32/R7)
      .            + X12*MU*(3.0D0/R5 + 7.5D0*RE2*J2/R7 - 52.5D0*RE2*J2*
      .            X32/R9) + K*RHO*X1*(BETA/R)*FAC4*FAC2 + RHO*WE*BETA*FAC2
      .            *FAC3/FAC4 + AT*DCOS(X7)/R - AT*DCOS(X7)*X12/R3
```

168

```
     .            + ATX*(DCOS(X7)*X1/R+DSIN(X7)*X4/V)

          AD(4,2) = X1*X2*MU*(3.0D0/R5 + 7.5D0*RE2*J2/R7 - 52.5D0*RE2*J2
     .            *X32/R9) + K*RHO*X2*(BETA/R)*FAC4*FAC2 - RHO*WE*BETA*FAC2
     .            *FAC2/FAC4 - RHO*WE*BETA*FAC4 - AT*DCOS(X7)*X1*X2/R3
     .            + ATY*(DCOS(X7)*X1/R+DSIN(X7)*X4/V)
          AD(4,3) = X1*X3*MU*(3.0D0/R5 + 22.5D0*RE2*J2/R7 - 52.5D0*RE2*
     . J2*X32/R9)+K*RHO*X3*(BETA/R)*FAC4*FAC2- AT*DCOS(X7)*X1*X3/R3
     .            + ATZ*(DCOS(X7)*X1/R+DSIN(X7)*X4/V)
          AD(4,4) = -RHO*BETA*(FAC2**2/FAC4+FAC4)+AT*DSIN(X7)/V-AT
     .            *DSIN(X7)*X4*X4/V3+ ATXD*(DCOS(X7)*X1/R+DSIN(X7)*X4/V)
          AD(4,5) = -RHO*BETA*FAC2*FAC3/FAC4-AT*DSIN(X7)*X5*X4/V3
     .            + ATYD*(DCOS(X7)*X1/R+DSIN(X7)*X4/V)
          AD(4,6) = -RHO*BETA*FAC2*X6/FAC4-AT*DSIN(X7)*X6*X4/V3
     .            + ATZD*(DCOS(X7)*X1/R+DSIN(X7)*X4/V)
          AD(4,7) = AT*(DCOS(X7)*X4/V-DSIN(X7)*X1/R)
     .            + ATTHETA3*(DCOS(X7)*X1/R+DSIN(X7)*X4/V)
          AD(4,8) = ATTHETA3D*(DCOS(X7)*X1/R+DSIN(X7)*X4/V)

C    ***   ROW 5    ***

          AD(5,1) = X1*X2*MU*(3.0D0/R5 + 7.5D0*RE2*J2/R7 - 52.5D0*RE2*X32
     .          *J2/R9) + K*RHO*X1*(BETA/R)*FAC4*FAC3 + RHO*WE*BETA*FAC3**2
     .            /FAC4 + WE*BETA*RHO*FAC4 - AT*DCOS(X7)*X1*X2/R3
     .            + ATX*(DCOS(X7)*X2/R+DSIN(X7)*X5/V)
          AD(5,2) = MU*(-1.0D0/R3 - 1.5D0*RE2*J2/R5 + 7.5D0*RE2*X3**2*J2
     .            /R7) + X22*MU*(3.0D0/R5 + 7.5D0*RE2*J2/R7 - 52.5D0*RE2*
     .            X32*J2/R9) + K*RHO*X2*(BETA/R)*FAC4*FAC3 - RHO*WE*BETA
     .            *FAC2*FAC3/FAC4+ AT*DCOS(X7)/R - AT*DCOS(X7)*X22/R3
     .            + ATY*(DCOS(X7)*X2/R+DSIN(X7)*X5/V)
          AD(5,3) = X2*X3*MU*(3.0D0/R5 + 22.5D0*RE2*J2/R7 - 52.5D0*RE2*X32
     .            *J2/R9) + K*RHO*X3*(BETA/R)*FAC4*FAC3 - AT*DCOS(X7)*X2
     .            *X3/R3 + ATZ*(DCOS(X7)*X2/R+DSIN(X7)*X5/V)
          AD(5,4) = -RHO*BETA*FAC2*FAC3/FAC4-AT*DSIN(X7)*X4*X5/V3
     .            + ATXD*(DCOS(X7)*X2/R+DSIN(X7)*X5/V)
         AD(5,5) = -RHO*BETA*FAC3**2/FAC4-RHO*BETA*FAC4+AT*DSIN(X7)/V-AT
     .            *DSIN(X7)*X5*X5/V3 + ATYD*(DCOS(X7)*X2/R+DSIN(X7)*X5/V)
          AD(5,6) = -RHO*X6*BETA*FAC3/FAC4-AT*DSIN(X7)*X6*X5/V3
     .            + ATZD*(DCOS(X7)*X2/R+DSIN(X7)*X5/V)
          AD(5,7) = AT*(DCOS(X7)*X5/V-DSIN(X7)*X2/R)
     .            + ATTHETA3*(DCOS(X7)*X2/R+DSIN(X7)*X5/V)
          AD(5,8) = ATTHETA3D*(DCOS(X7)*X2/R+DSIN(X7)*X5/V)

C    ***   ROW 6    ***
          AD(6,1) = X1*X3*MU*(3.0D0/R5 + 22.5D0*RE2*J2/R7 - 52.5D0*RE2
     .            *X32*J2/R9) + K*RHO*X1*(BETA/R)*FAC4*X6 + RHO*WE*X6*
     .            BETA*FAC3/FAC4 - AT*DCOS(X7)*X1*X3/R3
     .            + ATX*(DCOS(X7)*X3/R+DSIN(X7)*X6/V)
          AD(6,2) = X2*X3*MU*(3.0D0/R5 + 22.5D0*RE2*J2/R7 - 52.5D0*RE2
     .            *X32*J2/R9) + K*RHO*X2*(BETA/R)*FAC4*X6 - RHO*WE*X6*
     .            BETA*FAC2/FAC4 - AT*DCOS(X7)*X2*X3/R3
     .            + ATY*(DCOS(X7)*X3/R+DSIN(X7)*X6/V)
          AD(6,3) = MU*(-1.0D0/R3 - 4.5D0*RE2*J2/R5 + 7.5D0*RE2*X32*J2/R7)
     .            + X32*MU*(3.0D0/R5 + 37.5D0*RE2*J2/R7 - 52.5D0*RE2*X32
     .            *J2/R9) + K*RHO*X3*(BETA/R)*FAC4*X6 + AT*DCOS(X7)/R
     .            - AT*DCOS(X7)*X32/R3 + ATZ*(DCOS(X7)*X3/R+DSIN(X7)*X6/V)
          AD(6,4) = -RHO*X6*BETA*FAC2/FAC4-AT*DSIN(X7)*X6*X4/V3
```

169

```
         .           + ATXD*(DCOS(X7)*X3/R+DSIN(X7)*X6/V)
         AD(6,5)  = -RHO*X6*BETA*FAC3/FAC4-AT*DSIN(X7)*X6*X5/V3
         .           + ATYD*(DCOS(X7)*X3/R+DSIN(X7)*X6/V)
        AD(6,6)  = -RHO*BETA*FAC4 - RHO*X6*X6*BETA/FAC4+AT*DSIN(X7)/V-AT
         .          *DSIN(X7)*X6*X6/V3 + ATZD*(DCOS(X7)*X3/R+DSIN(X7)*X6/V)
         AD(6,7)  = AT*(DCOS(X7)*X6/V-DSIN(X7)*X3/R)
         .           + ATTHETA3*(DCOS(X7)*X3/R+DSIN(X7)*X6/V)
         AD(6,8)  = ATTHETA3D*(DCOS(X7)*X3/R+DSIN(X7)*X6/V)

      AD(8,1)=2.D0*THETAD*RDX/R-2.0D0*THETAD*RD*X1/R3+2.0D0*THETADX*RD/R
      .+AT*DSIN(X7)*X1/R3+9.0D0*X1*MU*DSIN(X7)*DCOS(X7)/R5-ATX*DSIN(X7)/R
      .+D8J2X
       AD(8,2)=2.D0*THETAD*RDY/R-2.D0*THETAD*RD*X2/R3+2.D0*THETADY*RD/R
      .+AT*DSIN(X7)*X2/R3+9.0D0*X2*MU*DSIN(X7)*DCOS(X7)/R5-ATY*DSIN(X7)/R
      .+D8J2Y
       AD(8,3)=2.D0*THETAD*RDZ/R-2.D0*THETAD*RD*X3/R3+2.D0*THETADZ*RD/R
      .+AT*DSIN(X7)*X3/R3+9.0D0*X3*MU*DSIN(X7)*DCOS(X7)/R5-ATZ*DSIN(X7)/R
      .+D8J2Z
        AD(8,4)  = 2.0D0*THETADXD*RD/R+2.0D0*THETAD*RDXD/R-ATXD*DSIN(X7)/R
      .+D8J2XD
        AD(8,5)  = 2.0D0*THETADYD*RD/R+2.0D0*THETAD*RDYD/R-ATYD*DSIN(X7)/R
      .+D8J2YD
        AD(8,6)  = 2.0D0*THETADZD*RD/R+2.0D0*THETAD*RDZD/R-ATZD*DSIN(X7)/R
      .+D8J2ZD
        AD(8,7)=-ATTHETA3*DSIN(X7)/R-AT*DCOS(X7)/R-3.D0*MU/R3
         .          *DCOS(2.D0*X7)+D8J2TH3
        AD(8,8)  = -ATTHETA3D*DSIN(X7)/R

C    ***    COMPUTE AC MATRIX    ***
C    ***    ROW 4     ***
        AC(4,1)  = (ATOLD/X9+ATJ2RHOCM)*(DCOS(X7)*X1/R+DSIN(X7)*X4/V)
        AC(5,1)  = (ATOLD/X9+ATJ2RHOCM)*(DCOS(X7)*X2/R+DSIN(X7)*X5/V)
        AC(6,1)  = (ATOLD/X9+ATJ2RHOCM)*(DCOS(X7)*X3/R+DSIN(X7)*X6/V)
        AC(8,1)  = -(ATOLD/X9+ATJ2RHOCM)*DSIN(X7)/R+D8J2RHOCM
        RETURN
        END


C###############################################################################
#
C    THIS SUBROUTINE COMPUTES ATMOSPHERIC DENSITY (KG/M^3) GIVEN A GEOCENTRIC
C     ALTITUDE (M).  IT MODELS THE ATMOSPHERE WITH AN EXPONENTIAL FUNCTION.
C                         (TWW, 20 NOV 90)
C###############################################################################
#
        SUBROUTINE DENSITY (R, RHO)
        IMPLICIT DOUBLE PRECISION (A-Z)

        R0 = 7278000.0D0
        K = 5.381D-6
        RHO0 = 4.36D-14

        RHO = RHO0 * DEXP(-K*(R - R0))

        RETURN
        END
```

170

```
C###############################################################
#
C  THIS SUBROUTINE ASSIGNS THE PROPER INITIAL CONDITIONS TO THE INTEGRATION
C    VECTOR, IVEC.  IF FLAG = 1, THE INCOMING STATE VALUES ARE LEFT
UNCHANGED.
C###############################################################
#
      SUBROUTINE INICOND (IVEC, FLAG)
      IMPLICIT DOUBLE PRECISION (A-Z)
      INTEGER N, P, N1, N2, IPAR
      PARAMETER (N = 9, N1=8, N2=1, IPAR=81, P=3)
      DIMENSION IVEC(IPAR), PHIDD(N1,N1), PHIDC(N1,N2)
      INTEGER FLAG,I

      IF (FLAG .EQ. 1) GOTO 10

C   ***   GIVEN [CARTESIAN] NOMINAL VALUES TO START THE COMPUTATIONS.   ***
      DO 4 I = 1, 8
    4 READ(7,*) IVEC(I)

      MU = 3.98600436D14
    . X1 = IVEC(1)
      X2 = IVEC(2)
      X3 = IVEC(3)
      X4 = IVEC(4)
      X5 = IVEC(5)
      X6 = IVEC(6)
      X7 = IVEC(7)
      X8 = IVEC(8)
      R2 = X1*X1 + X2*X2 + X3*X3
      R = DSQRT(R2)
      R3 = R2 * R
      TERM1 = DSQRT((X2*X6-X3*X5)*(X2*X6-X3*X5)+(X3*X4-X1*X6)*(X3*X4
     .     -X1*X6)+(X1*X5-X2*X4)*(X1*X5-X2*X4))
      THETAD = TERM1/R2
      ATETH=DSQRT(X7*X7+X8*X8)
      IVEC(7)=DATAN2(X7,X8)
      IVEC(9)=ABS(X8*R2/(3*MU-X8*R2)*R)
C         IF (X8 .LT. 0.0D0) THEN
C            IVEC(9) = -IVEC(9)
C         ENDIF
      IVEC(8)=DSQRT(ATETH/IVEC(9)-MU/R3*(3.0D0*DCOS(IVEC(7))
     .     *DCOS(IVEC(7))-1.0D0))-THETAD


C   ***   SET PHIDD(0) TO IDENTITY MATRIX, PHIDC(0) TO NULL MATRIX   ***
 10    CALL IDENTMAT (PHIDD, N1)
      CALL MATZERO (PHIDC, N1,N2)

C   ***   PUT MATRIX ELEMENTS INTO INTEGRATION VECTOR   ***

      CALL PHITOIVEC (PHIDD, PHIDC, IVEC)

      RETURN
      END
```

```
C############################################################
#
C  THIS SUBROUTINE SOLVES A LINEAR SYSTEM OF EQUATIONS OF THE FORM LX = Y,
C    USING THE CHOLESKY DECOMPOSITON IN LIEU OF A MATRIX INVERSION.   THE
C    VARIABLE "N" SPECIFIES THE NUMBER OF EQUATIONS INVOLVED.
C                        (TWW, 21 OCT 90)
C############################################################
#
        SUBROUTINE CHOLESKY (N, L, X, Y, S, Z)
        IMPLICIT DOUBLE PRECISION (A-H,L-M,O-Z)
        DIMENSION L(N,N), X(N,1), S(N,N), Z(N,1), Y(N,1)
        INTEGER N, I, J, K


C  COMPUTE UPPER TRIANGULAR MATRIX S.   (LX = Y,   S^T*S = L)
        DO 20 I = 1,N
          SUM = 0.D0
          DO 5 K = 1, (I-1)
 5        SUM = SUM + S(K,I)*S(K,I)
          S(I,I) = DSQRT(L(I,I) - SUM)

          DO 10 J = (I+1), N
            SUM = 0.D0
            DO 7 K = 1, (I-1)
 7          SUM = SUM + S(K,I)*S(K,J)
            S(I,J) = (L(I,J) - SUM) / S(I,I)
 10       CONTINUE

C  SOLVE FOR Z BY FORWARD SUBSTITUTION.   (S^T * Z = Y)
          SUM = 0.D0
          DO 12 K = 1, (I-1)
 12       SUM = SUM + S(K,I)*Z(K,1)

          Z(I,1) = (Y(I,1) - SUM) / S(I,I)
 20     CONTINUE

C  SOLVE FOR X VIA BACKWARD SUBSTITUTION.   (SX = Z)

        X(N,1) = Z(N,1) / S(N,N)
        DO 30 I = (N-1), 1, -1
          SUM = 0.D0
          DO 25 J = N, (I+1), -1
 25       SUM = SUM + S(I,J)*X(J,1)

          X(I,1) = (Z(I,1) - SUM) / S(I,I)
 30     CONTINUE

        RETURN
        END


C############################################################
#
C  THIS SUBROUTINE MULTIPLIES 2 MATRICES WHOSE DIMENSIONS ARE (M1ROWS,
M1COL),
C    (M2ROWS, M2COL).  M1COL MUST = M2ROWS EXACTLY!  THE PRODUCT OF MATRICES
C    A AND B IS RETURNED IN MATRIX C, WHOSE DIMENSION IS (M1ROWS, M2COL).
```

172

```
C                (TWW, 22OCT90)
C###################################################################
#
        SUBROUTINE MATMLT (A,B,C, M1ROWS, M1COL, M2ROWS, M2COL)
        IMPLICIT DOUBLE PRECISION (A-H,L,N-Z)
        DIMENSION A(M1ROWS,M1COL), B(M2ROWS, M2COL), C(M1ROWS,M2COL)
        INTEGER I,J,K, M1ROWS, M1COL, M2ROWS, M2COL

        IF (M1COL .NE. M2ROWS) THEN
          WRITE(*,*) 'INVALID MATRIX MULTIPLICATION ATTEMPTED!!'
          RETURN
        ENDIF

        DO 30 I=1,M1ROWS
          DO 20 K = 1,M2COL
            C(I,K) = 0.D0
            DO 10 J=1,M1COL
 10         C(I,K) = A(I,J)*B(J,K) + C(I,K)
 20     CONTINUE
 30   CONTINUE

        RETURN
        END


C###################################################################
#
C  THIS SUBROUTINE ADDS TWO MATRICES, A+B, AND RETURNS THEIR SUM IN
C   MATRIX C.  A & B MUST HAVE THE SAME DIMENSION!
C               (TWW, 22 OCT90)
C###################################################################
#
        SUBROUTINE MATADD (A,B,C, ROWS, COL)
        IMPLICIT DOUBLE PRECISION (A-Z)
        INTEGER I,J, ROWS, COL
        DIMENSION A(ROWS,COL), B(ROWS,COL), C(ROWS,COL)

        DO 20 I = 1,ROWS
          DO 10 J = 1,COL
 10       C(I,J) = A(I,J) + B(I,J)
 20     CONTINUE

        RETURN
        END


C###################################################################
#
C  THIS SUBROUTINE SUBTRACTS TWO MATRICES, A+B, AND RETURNS THEIR SUM IN
C   MATRIX C.  A & B MUST HAVE THE SAME DIMENSION!
C               (DAC, 25 MAY93)
C###################################################################
#
        SUBROUTINE MATSUB (A,B,C, ROWS, COL)
        IMPLICIT DOUBLE PRECISION (A-Z)
        INTEGER I,J, ROWS, COL
        DIMENSION A(ROWS,COL), B(ROWS,COL), C(ROWS,COL)
```

173

```
      DO 20 I = 1,ROWS
        DO 10 J = 1,COL
10        C(I,J) = A(I,J) - B(I,J)
20    CONTINUE

      RETURN
      END


C##################################################################
#
C  THIS SUBROUTINE COMPUTES THE TRANSPOSE OF MATRIX A, AND RETURNS THE
C    RESULT IN MATRIX AT.
C      (TWW, 22 OCT 90)
C##################################################################
#
      SUBROUTINE TRANSPOSE (A, AT, ROWS, COLS)
      IMPLICIT DOUBLE PRECISION (A-Z)
      INTEGER I, J, ROWS, COLS
      DIMENSION A(ROWS,COLS), AT(COLS,ROWS)

      DO 20 I = 1,ROWS
        DO 10 J = 1, COLS
10        AT(J,I) = A(I,J)
20    CONTINUE

      RETURN
      END


C##################################################################
#
C  THIS SUBROUTINE ASSIGNS ALL ELEMENTS OF MATRIX A (ROWS X COLS) TO BE
C    EQUAL TO ZERO.
C                          (TWW, 22 OCT 90)
C##################################################################
#
      SUBROUTINE MATZERO (A, ROWS, COLS)
      IMPLICIT DOUBLE PRECISION (A-Z)
      INTEGER ROWS, COLS, I, J
      DIMENSION A(ROWS, COLS)

      DO 20 I = 1, ROWS
        DO 10 J = 1, COLS
10        A(I,J) = 0.D0
20    CONTINUE

      RETURN
      END


C##################################################################
#
C     THIS SUBROUTINE FORMS A (ROW X ROW) [SQUARE] IDENTITY MATRIX.
C           (TWW, 25 NOV 90)
```

174

```
C##################################################################
#
          SUBROUTINE IDENTMAT (MAT, ROWS)
          IMPLICIT DOUBLE PRECISION (A-Z)
          INTEGER I, ROWS
          DIMENSION MAT(ROWS, ROWS)

          CALL MATZERO (MAT, ROWS, ROWS)

          DO 10 I = 1, ROWS
   10     MAT(I,I) = 1.0D0

          RETURN
          END


          SUBROUTINE RK4(T,TSTOP,TSTEP,NSTATE,STATE,D1,D2,D3)


*******************************************************************
*
*
*    SUBROUTINE RK4
*
*    4TH ORDER RUNGE-KUTTA INTEGRATOR -- FIXED STEP SIZE -- TAKES INTEGRATION
*    STEPS OF SIZE TSTEP OR (TSTOP-T) WHICH EVER IS SMALLER UNTIL THE STOP
*    TIME IS REACHED.  T IS UPDATED TO TSTOP UPON RETURN.
*
*    *** NOTE *** IF T IS GREATER THAN OR "EQAUL TO" TSTOP, THIS ROUTINE
*                 WILL EXIT IMMEDIATELY -- NO ERROR MESSAGE IS GENERATED
*
*    WRITTEN BY:   CAPT ROGER L. HALL, ASTRO DEPT, 12 NOV 1987
*                  (MODIFIED 21 OCT 1988 TO PERFORM MULTIPLE STEPS
*                   UNTIL TSTOP IS REACHED)
*
*    INPUTS:    DERIV -- THE NAME OF THE STATE DERIVATIVE SUBROUTINE
*                        (TRUE NAME SHOULD BE DECLARED EXTERNAL IN CALLING
*                         ROUTINE)
*               T -- TIME (INDEPENDENT VARIABLE)
*               TSTOP -- STOP TIME (FINAL VALUE FOR INDEPENDENT VARIABLE)
*               TSTEP -- TIME STEP (STEP INCREMENT OF INDEPENDENT VARIABLE)
*               STATE -- STATE VARIABLE ARRAY
*               NSTATE -- NUMBER OF STATES TO BE INTEGRATED
*               D1,D2,D3 -- WORKSPACE ARRAYS -- NEED TO BE DECLARED IN THE
*                           CALLING ROUTINE -- EACH NEEDS TO BE DIMENSIONED
*                           AT LEAST AS LARGE AS THE STATE ARRAY (>=NSTATE)
*
*    OUTPUTS:   T -- TIME (INDEPENDENT VARIABLE) IS UPDATED TO TSTOP
*               STATE -- STATES (MOVED FORWARD TO TIME T)
*
*    EXTERNAL REFERENCES:  SUBROUTINE "DERIV"
*
*******************************************************************
*

          IMPLICIT DOUBLE PRECISION (A-Z)

          INTEGER I,NSTATE,IPAR
```

175

```
        PARAMETER (IPAR=81)
        DIMENSION STATE(IPAR),D1(IPAR),D2(IPAR),D3(IPAR)
CPROJ1
C        OPEN(13, FILE = 'STATE3.OUT')

******************************************
* CHECK FOR TERMINATION -- T >= TSTOP *
******************************************

 100  DELTAT = TSTOP-T

        IF ( (DELTAT .LT. 0.0D0) .OR. ABS(DELTAT) .LT. 1.0D-6 ) RETURN

        IF ( DELTAT .GT. TSTEP ) DELTAT = TSTEP

*******************************************************************************
* TAKE ONE INTEGRATION STEP BY DELTAT -- REQUIRES 4 CALLS TO THE DERIV *
*******************************************************************************

        CALL DERIV(T,STATE,D1)

        DO 101 I = 1,NSTATE
            D1(I) = D1(I)*DELTAT
            D2(I) = STATE(I)+0.5D0*D1(I)
 101  CONTINUE

        TT = T+0.5D0*DELTAT

        CALL DERIV(TT,D2,D3)

        DO 102 I = 1,NSTATE
            D3(I) = D3(I)*DELTAT
            D1(I) = D1(I)+2.0D0*D3(I)
            D2(I) = STATE(I)+0.5D0*D3(I)
 102  CONTINUE

        CALL DERIV(TT,D2,D3)

        DO 103 I = 1,NSTATE
            D3(I) = D3(I)*DELTAT
            D1(I) = D1(I)+2.0D0*D3(I)
            D2(I) = STATE(I)+D3(I)
 103  CONTINUE

        T = T+DELTAT

        CALL DERIV(T,D2,D3)

***************************************************
* MOVE THE STATES FORWARD 1 INTEGRATION STEP *
***************************************************

        DO 104 I = 1,NSTATE
            STATE(I) = STATE(I)+(D1(I)+D3(I)*DELTAT)/6.0D0
 104  CONTINUE
CPROJ1
C        WRITE(13,*)(STATE(J),J=1,8)
```

```
        GOTO 100

        END


****************************************************************
* THIS SUBROUTINE CONVERTS A TRACKING STATION'S LAT, LONG, AND HEIGHT
* (IN RAD AND M) INTO GEOCENTRIC EQUATORIAL X, Y, AND Z COORDINATES (IN M)
****************************************************************
        SUBROUTINE GEODETIC(PHIG,LAMBDAG,HEIGHTG,XECEF,YECEF,ZECEF)
        IMPLICIT DOUBLE PRECISION(A-Z)
        A=6378137.0D0
        F=1.0D0/298.257223563D0
        E=DSQRT(2.0D0*F-F**2.0D0)
        R=A/(DSQRT(1.0D0-E**2.0D0*(DSIN(PHIG))**2.0D0))
        XECEF=(R+HEIGHTG)*DCOS(PHIG)*DCOS(LAMBDAG)
        YECEF=(R+HEIGHTG)*DCOS(PHIG)*DSIN(LAMBDAG)
        ZECEF=((1.0D0-E**2.0D0)*R+HEIGHTG)*DSIN(PHIG)
        RETURN
        END


****************************************************************
* THIS SUBROUTINE CONVERTS THE ORIGINAL DATA FILE FROM THE
* YEAR,DAY,HOUR,MIN,SEC FORMAT TO A FORMAT WITH TIME IN SECONDS
****************************************************************

        SUBROUTINE TCONVERT
        IMPLICIT DOUBLE PRECISION(A-Z)
        INTEGER YEAR,DAY,HOUR,MINUTE,SITE,I
        DIMENSION DT(500)

        DO I=1,10000
        READ(4,1,ERR=2000,END=2000)SITE,YEAR,DAY,HOUR,MINUTE,SEC,RHO,
      . SIGR,AZ,SIGAZ,EL,SIGEL

      1 FORMAT(I3,2X,I2,I3,I2,I2,F6.3,2X,F8.3,2X,F6.2,2X,F8.4,2X,F10.8,
      . 2X,F8.4,2X,F10.8)

        DT(I)=DAY*1440.0D0+HOUR*60.0D0+MINUTE+SEC/60.0D0
        DT(I)=DT(I)*60.0D0

        IF (I.EQ.1) THEN
        DT1=0.0D0
        ELSE
        DT(I)=DT(I)-DT(1)
        DT1=DT(I)
        END IF

        WRITE(5,*)SITE,DT1,RHO*1000.0D0,SIGR,AZ,SIGAZ,EL,SIGEL

      2000 CONTINUE
        ENDDO
        REWIND (5)
        RETURN
        END
```

```
      SUBROUTINE NORMAL(SEED,SIGMA,BIAS,NOISE)

*********************************************************************
*
*   GENERATES A NOISE VALUE BASED UPON A GAUSSIAN (NORMAL) DISTRIBUTION
*   CHARACTERIZED BY A MEAN VALUE "BIAS" AND A STANDARD DEVIATION "SIGMA"
*
*   WRITTEN BY:  CAPT ROGER L. HALL
*
*   INPUTS:    SEED -- UNIFORM RANDOM NUMBER GENERATOR SEED (INIT ONCE...)
*              SIGMA -- STANDARD DEVIATION OF NOISE
*              BIAS -- MEAN VALUE NOISE
*
*   OUTPUTS:   SEED -- UPDATED SEED
*              NOISE -- RANDOM NOISE VALUE
*
*   EXTERNAL REFERENCES:  IMSL SUBROUTINES MDNRIS, MERFI
*
*********************************************************************

      IMPLICIT DOUBLE PRECISION (A-Z)

      INTEGER IER

      CALL RANDOM(SEED,PUNIF)
      CALL MDNRIS(PUNIF,PNORM,IER)

      IF ( IER .NE. 0 ) THEN
          WRITE(*,*)
          WRITE(*,*)'*** IN ROUTINE NORMAL, PUNIF,IER = ',PUNIF,IER
          WRITE(*,*)'    UPON RETURN FROM MDNRIS ***'
          WRITE(*,*)
          STOP '*** ABNORMAL TERMINATION ***'
      END IF

      NOISE = PNORM*SIGMA+BIAS

      RETURN
      END

      SUBROUTINE RANDOM(SEED,P)

*********************************************************************
*
*   PSEUDO-RANDOM NUMBER GENERATOR -- GENERATES A RANDOM NUMBER (BASED
*   UPON A UNIFORM DISTRIBUTION) BETWEEN 0 AND 1 -- SEED VALUE IS CHANGED
*   EACH CALL
*
*   WRITTEN BY:  CAPT ROGER L. HALL (SIMPLIFIED IMSL ROUTINE)
*
*   INPUTS:   SEED -- RANDOM NUMBER GENERATOR SEED
*
*   OUTPUTS:  SEED -- RANDOM NUMBER GENERATOR SEED (UPDATED)
*              P -- RANDOM NUMBER BETWEEN 0 AND 1
```

```
*
*   EXTERNAL REFERENCES:   NONE
*
****************************************************************

      IMPLICIT DOUBLE PRECISION (A-H,O-Z)

*                         D2P31M=(2**31) - 1
*                         D2P31 =(2**31)(OR AN ADJUSTED VALUE)

      DATA                D2P31M/2147483647.D0/
      DATA                D2P31/2147483648.D0/

      SEED = DMOD(16807.D0*SEED,D2P31M)
      P = SEED / D2P31

      RETURN
      END

C   IMSL ROUTINE NAME    - MDNRIS
C
C---------------------------- ----------------------------------------
C
C   COMPUTER             - HARRIS/SINGLE
C
C   LATEST REVISION      - SEPTEMBER 1, 1981
C
C   PURPOSE              - INVERSE STANDARD NORMAL (GAUSSIAN)
C                              PROBABILITY DISTRIBUTION FUNCTION
C
C   USAGE                - CALL MDNRIS (P,Y,IER)
C
C   ARGUMENTS    P       - INPUT VALUE IN THE EXCLUSIVE RANGE (0.0,1.0)
C                Y       - OUTPUT VALUE OF THE INVERSE NORMAL (0,1)
C                              PROBABILITY DISTRIBUTION FUNCTION
C                IER     - ERROR PARAMETER (OUTPUT)
C                          TERMINAL ERROR
C                            IER = 129 INDICATES P LIES OUTSIDE THE LEGAL
C                               RANGE. PLUS OR MINUS MACHINE INFINITY IS
C                               GIVEN AS THE RESULT (SIGN IS THE SIGN OF
C                               THE FUNCTION VALUE OF THE NEAREST LEGAL
C                               ARGUMENT).
C
C   PRECISION/HARDWARE   - SINGLE/ALL
C
C   REQD. IMSL ROUTINES  - MERFI.UERTST,UGETIO
C
C   NOTATION             - INFORMATION ON SPECIAL NOTATION AND
C                              CONVENTIONS IS AVAILABLE IN THE MANUAL
C                              INTRODUCTION OR THROUGH IMSL ROUTINE UHELP
C
C   COPYRIGHT            - 1978 BY IMSL, INC. ALL RIGHTS RESERVED.
C
C   WARRANTY             - IMSL WARRANTS ONLY THAT IMSL TESTING HAS BEEN
C                              APPLIED TO THIS CODE. NO OTHER WARRANTY,
C                              EXPRESSED OR IMPLIED, IS APPLICABLE.
C
```

179

```fortran
C-------------------------------------------------------------------
C
      SUBROUTINE MDNRIS (P,Y,IER)
      IMPLICIT DOUBLE PRECISION (A-H,O-Z)
      DIMENSION D(25)
      DATA              XINF/1.7D+38/
      DATA              SQRT2/1.4142135624D0/
      DATA              EPS/7.28D-12/
      DATA              D(1)/.95667970902D0/
      DATA              D(2)/-.02310700431D0/
      DATA              D(3)/-.00437423610D0/
      DATA              D(4)/-.00057650342D0/
      DATA              D(5)/-.00001096102D0/
      DATA              D(6)/.00002510855D0/
      DATA              D(7)/.00001056234D0/
      DATA              D(8)/.00000275441D0/
      DATA              D(9)/.00000043248D0/
      DATA              D(10)/-.00000002053D0/
      DATA              D(11)/-.00000004389D0/
      DATA              D(12)/-.00000001768D0/
      DAT:.             D(13)/-.00000000399D0/
      DAT A             D(14)/-.00000000019D0/
      TATA              D(15)/.00000000027D0/
      DATA              D(16)/.00000000013D0/
      DATA              D(17)/.00000000003D0/
      DATA              D(18)/.00000000000/
      DATA              D(19)/-.00000000000/
      DATA              D(20)/-.00000000000/
      DATA              D(21)/-.00000000000/
      DATA              D(22)/-.00000000000/
      DATA              D(23)/.00000000000/
      DATA              D(24)/.00000000000/
      DATA              D(25)/.00000000000/
      DATA              H3/-.55945763133D0/
      DATA              H4/2.2879157163D0/
C                                   FIRST EXECUTABLE STATEMENT
      IER = 0
      IF (P .GT. 0.0D0  .AND. P .LT. 1.0D0 ) GO TO 5
      IER = 129
      SIGMA = DSIGN(1.0D0 ,P)
      Y = SIGMA * XINF
      GO TO 9000
    5 IF(P.LE.EPS) GO TO 10
      X = 1.0D0 -(P + P)
      CALL MERFI (X,Y,IER)
      Y = SQRT2 * Y
      GO TO 9005
C                                   P TOO SMALL, COMPUTE Y DIRECTLY
   10 A = P+P
      B = DSQRT(-DLOG(A+(A-A*A)))
      W = H3 * B + H4
      X3 = 1.0D0
      X4 = W
      X6 = D(1)
      DO 15 I=2,25
          X6 = X6 + D(I) * X4
          X5 = X4 * W * 2.D0 - X3
```

180

```
          X3 = X4
          X4 = X5
   15 CONTINUE
      Y = B*X6
      Y = -SQRT2 * Y
      GO TO 9005
 9000 CONTINUE
*     CALL UERTST(IER,6HMDNRIS)
 9005 RETURN
      END
```

```
      SUBROUTINE MERFI (P,Y,IER)

      IMPLICIT DOUBLE PRECISION (A-H,O-Z)

      DIMENSION A(65)

      DATA                A(1),A(2),A(3),A(4),A(5),A(6),A(7),A(8),A(9),
     *                    A(10),A(11),A(12),A(13),A(14),A(15),A(16),
```

181

```
     *                         A(17),A(18),A(19),A(20),A(21),A(22),A(23)
     *                         /.99288537662D0,.12046751614D0,
     *                         .16078199342D-01,.26867044372D-02,
     *                         .49963473024D-03,.98898218599D-04,
     *                         .20391812764D-04,.4327271618D-05,
     *                         .938081413D-06,.206734721D-06,
     *                         .46159699D-07,.10416680D-07,
     *                         .2371501D-08,.543928D-09,
     *                         .125549D-09,.29138D-10,
     *                         .6795D-11,.1591D-11,
     *                         .374D-12,.88D-13,
     *                         .21D-13,.5D-14,
     *                         .1D-14/
      DATA                     A(24),A(25),A(26),A(27),A(28),A(29),A(30),
     *                         A(31),A(32),A(33),A(34),A(35),A(36),A(37),
     *                         A(38),A(39),A(40)
     *                         /.91215880342D00,-.16266281868D-01,
     *                         .43355647295D-03,.21443857007D-03,
     *                         .2625751076D-05,-.302109105D-05,
     *                         -.12406062D-07,.62406609D-07,
     *                         -.5.0125D-09,-.142328D-08,
     *                         .34384D-10,.33585D-10,
     *                         -.1458D-11,-.81D-12,
     *                         .53D-13,.2D-13,
     *                         -.2D-14/
      DATA                     A(41),A(42),A(43),A(44),A(45),A(46),A(47),
     *                         A(48),A(49),A(50),A(51),A(52),A(53),A(54),
     *                         A(55),A(56),A(57),A(58),A(59),A(60),A(61),
     *                         A(62),A(63),A(64),A(65)
     *                         /.95667970902D0,-.023107004309D0,
     *                         -.43742360975D-02,-.57650342265D-03,
     *                         -.10961022307D-04,.25108547025D-04,
     *                         .10562336068D-04,.275441233D-05,
     *                         .432484498D-06,-.20530337D-07,
     *                         -.43891537D-07,-.1768401D-07,
     *                         -.3991289D-08,-.186932D-09,
     *                         .272923D-09,.132817D-09,
     *                         .31834D-10,.1670D-11,
     *                         -.2036D-11,-.965D-12,
     *                         -.22D-12,-.1D-13,
     *                         .13D-13,.6D-14,
     *                         .1D-14/
      DATA                     H1,H2,H3,H4/-1.5488130424D0,
     *                         2.5654901231D0,-.55945763133D0,
     *                         2.2879157163D0/
      DATA                     XINF/1.7D+38/
C                                      FIRST EXECUTABLE STATEMENT
      X = P
      IER = 0
      SIGMA = DSIGN(1.D0,X)
      IF (.NOT.(X.GT.-1.D0.AND.X.LT.1.D0)) GO TO 35
      Z = DABS(X)
      IF(Z.GT..8D0) GO TO 20
      W = Z*Z/.32D0-1.D0
      N = 22
      IPP = 1
      L = 1
```

182

```fortran
    5 LB2 = 1
      X3 = 1.D0
      X4 = W
      X6 = A(IPP)
   10 X6 = X6 + A(IPP+LB2) * X4
      X5 = X4 * W * 2.D0-X3
      X3 = X4
      X4 = X5
      LB2 = LB2 + 1
      IF (LB2 .LE. N) GO TO 10
      GO TO (15,30),L
   15 Y = Z * X6 * SIGMA
      GO TO 9005
   20 B = DSQRT(-DLOG(1.D0-Z*Z))
      IF (Z .GT. .9975D0) GO TO 25
      W = H1*B+H2
      IPP = 24
      L = 2
      N = 16
      GO TO 5
   25 W = H3 * B + H4
      IPP = 41
      N = 24
      L = 2
      GO TO 5
   30 Y = B * X6 * SIGMA
      GO TO 9005
   35 Y = SIGMA*XINF
      IER = 129
 9000 CONTINUE
    *     CALL UERTST(IER,6HMERFI )
 9005 RETURN
      END
```

LTF.OUT:

```
 4394564.203803360000000
 -709269.251280797000000
 5902247.150233440000000
   -3002.198031099093000
    6011.603080867935000
    2955.187291830438000
      -2.825406760036377
 8.583524744085534E-004
    4468.548432569249000
 4.077873570369031E-001
```

APPENDIX D: PROPOSED BUDGET

The budget originally proposed for this research project is provided in this section. This budget is presented for each of the three years of the proposed program as well as a three-year cumulative total budget for the entire project.

C. PROPOSAL BUDGET

ORGANIZATION Auburn University				PROPOSAL NO.	PERIOD OF PERFORMANCE Nov. 14, 1997 - Nov. 13, 1998	
PRINCIPAL INVESTIGATOR/PROJECT DIRECTOR David A. Cicci				AWARD NO.		
Salary Costs: Senior Personnel:PI/PD, Co-PIs, Faculty and Other Sen. Assoc. (List each separately with title; A.6. show number in brackets)	DOD FUNDED PERSON-MOS.			FUNDS REQUESTED FROM DOD	NON-FEDERAL MATCHING FUNDS	TOTAL PROJECT COSTS
	CAL	ACAD	SUM			
1. D. A. Cicci, Associate Professor	0	2.9	0	$17,404	$7,135	$24,539
2. J. E. Cochran, Jr., Professor	0.6	0	0	$5,747	$17,240	$22,987
3.	0	0	0	$0	$0	$0
4.	0	0	0	$0	$0	$0
5. ( )OTHERS (LIST INDIVIDUALS ON BUDGET EXPL. PG)	0	0	0	$0	$0	$0
6. (2)TOTAL SENIOR PERSONNEL (1-5)	0.6	2.9	0	$23,151	$24,375	$47,526
B. OTHER PERSONNEL (SHOW NUMBERS IN BRACKETS)						
1. ( )POST DOCTORAL ASSOCIATES	0	0	0	$0	$0	$0
2. ( )OTHER PROFESSIONALS (TECHNICIAN, ETC.)	0	0	0	$0	$0	$0
3. (3)GRADUATE STUDENTS	18	0	0	$39,000	$0	$39,000
4. ( )UNDERGRADUATE STUDENTS	0	0	0	$0	$0	$0
5. ( )SECRETARIAL-CLERICAL	0	0	0	$0	$0	$0
6. ( )OTHER	0	0	0	$0	$0	$0
TOTAL SALARIES AND WAGES (A+B)				$62,151	$24,375	$86,526
C. FRINGE BENEFITS (IF CHARGED AS DIRECT COSTS) - RATE: 25%				$5,788	$6,094	$11,882
TOTAL SALARIES, WAGES, & FRINGE BENEFITS (A+B+C)				$67,939	$30,469	$98,408

2. OVERHEAD RATE: 44.2%
NEGOTIATED WITH   DHHS   ON September 3, 1996 .
          (AGENCY NAME)   (DATE)
BASE: RATE: 44.2%   BASIS: MTDC
PERIOD OF GRANTEE'S FISCAL YEAR: Oct. 1, 1997 - Sept. 30, 1998

	FUNDS REQUESTED FROM DOD	NON-FEDERAL MATCHING FUNDS	TOTAL PROJECT COSTS
TOTAL OVERHEAD COSTS	$31,797	$15,898	$47,695
3. SUPPLIES AND MATERIALS	$0	$3,500	$3,500
4. EQUIPMENT: Describe any equipment to be acquired & the basis of cost estimates. Costs should be based on recent quotations from manufacturers and distributors.	$0	$0	$0
5. TRAVEL COSTS: List proposed destinations and basis of cost estimates.	$4,000	$2,000	$6,000
6. PUBLICATION AND REPORT COSTS	$0	$0	$0
7. SUBAWARD COSTS: Support the estimate of subaward work by indicating the specific items or portion of the work to be subawarded, type of subaward anticipated, name of subawardee, and a detailed cost summary.	$0	$0	$0
8. CONSULTANT COSTS: State planned daily consultant fee & travel expenses, the nature of the consulting effort, & reason consultants are required.	$0	$0	$0
9. COMMUNICATION COSTS: Estimate communication costs (i.e., long distance phone calls, telegrams, & postage) not included in overhead.	$0	$0	$0
10. OTHER DIRECT COSTS: Itemize other anticipated direct costs such as rental for computers & other equipment. Unusual or expensive items should be fully justified.	$0	$0	$0
11. TOTAL COSTS:	$103,736	$51,867	$155,603
12. COST SHARING PLANS: Construct a table (on attached budget explanation page) showing the matching share committed to DEPSCoR in the following categories: state, institutional, and private sector. In each category show the amount & nature of the matching share (e.g. state appropriation, equipment, new faculty positions, etc.). A signed statement of commitment regarding the matching funds described above should be obtained from the appropriate state, institutional, and private sector officials.			

Alabama EPSCoR - Revised 7/15/95

C. PROPOSAL BUDGET

ORGANIZATION Auburn University				PROPOSAL NO.		PERIOD OF PERFORMANCE Nov. 14, 1998 - Nov. 13, 1999
PRINCIPAL INVESTIGATOR/PROJECT DIRECTOR David A. Cicci				AWARD NO.		

Salary Costs: Senior Personnel: PI/PD, Co-PIs, Faculty and Other Sen. Assoc. (List each separately with title; A.6. show number in brackets)	DOD FUNDED PERSON-MOS.			FUNDS REQUESTED FROM DOD	NON-FEDERAL MATCHING FUNDS	TOTAL PROJECT COSTS
	CAL	ACAD	SUM			
1. D. A. Cicci, Associate Professor	0	2.9	0	$17,702	$7,573	$25,275
2. J. E. Cochran, Jr., Professor	0.6	0	0	$5,919	$17,757	$23,676
3.	0	0	0	$0	$0	$0
4.	0	0	0	$0	$0	$0
5. ( )OTHERS (LIST INDIVIDUALS ON BUDGET EXPL. PG)	0	0	0	$0	$0	$0
6. (2)TOTAL SENIOR PERSONNEL (1-5)	0.6	2.9	0	$23,621	$25,330	$48,951
B. OTHER PERSONNEL (SHOW NUMBERS IN BRACKETS)						
1. ( )POST DOCTORAL ASSOCIATES	0	0	0	$0	$0	$0
2. ( )OTHER PROFESSIONALS (TECHNICIAN, ETC.)	0	0	0	$0	$0	$0
3. (3)GRADUATE STUDENTS	18	0	0	$40,800	$0	$40,800
4. ( )UNDERGRADUATE STUDENTS	0	0	0	$0	$0	$0
5. ( )SECRETARIAL-CLERICAL	0	0	0	$0	$0	$0
6. ( )OTHER	0	0	0	$0	$0	$0
TOTAL SALARIES AND WAGES (A+B)				$64,421	$25,330	$89,751
C. FRINGE BENEFITS (IF CHARGED AS DIRECT COSTS) - RATE: 25%				$5,905	$6,333	$12,238
TOTAL SALARIES, WAGES, & FRINGE BENEFITS (A+B+C)				$70,326	$31,663	$101,989

2. OVERHEAD RATE: 44.2%
NEGOTIATED WITH   DHHS   ON   September 3, 1996   .
          (AGENCY NAME)   (DATE)
BASE: RATE: 44.2%   BASIS: MTDC
PERIOD OF GRANTEE'S FISCAL YEAR: Oct. 1, 1998 - Sept. 30, 1999

	FUNDS REQUESTED FROM DOD	NON-FEDERAL MATCHING FUNDS	TOTAL PROJECT COSTS
TOTAL OVERHEAD COSTS	$32,852	$16,426	$49,278
3. SUPPLIES AND MATERIALS	$0	$3,500	$3,500
4. EQUIPMENT: Describe any equipment to be acquired & the basis of cost estimates. Costs should be based on recent quotations from manufacturers and distributors.	$0	$0	$0
5. TRAVEL COSTS: List proposed destinations and basis of cost estimates.	$4,000	$2,000	$6,000
6. PUBLICATION AND REPORT COSTS	$0	$0	$0
7. SUBAWARD COSTS: Support the estimate of subaward work by indicating the specific items or portion of the work to be subawarded, type of subaward anticipated, name of subawardee, and a detailed cost summary.	$0	$0	$0
8. CONSULTANT COSTS: State planned daily consultant fee & travel expenses, the nature of the consulting effort, & reason consultants are required.	$0	$0	$0
9. COMMUNICATION COSTS: Estimate communication costs (i.e., long distance phone calls, telegrams, & postage) not included in overhead.	$0	$0	$0
10. OTHER DIRECT COSTS: Itemize other anticipated direct costs such as rental for computers & other equipment. Unusual or expensive items should be fully justified.	$0	$0	$0
11. TOTAL COSTS:	$107,178	$53,589	$160,767

12. COST SHARING PLANS: Construct a table (on attached budget explanation page) showing the matching share committed to DEPSCoR in the following categories: state, institutional, and private sector. In each category show the amount & nature of the matching share (e.g. state appropriation, equipment, new faculty positions, etc.). A signed statement of commitment regarding the matching funds described above should be obtained from the appropriate state, institutional, and private sector officials.

Alabama EPSCoR - Revised 7/15/95

187

C. PROPOSAL BUDGET

ORGANIZATION	PROPOSAL NO.	PERIOD OF PERFORMANCE
Auburn University		Nov. 14, 1999 - Nov. 13, 2000
PRINCIPAL INVESTIGATOR/PROJECT DIRECTOR	AWARD NO.	
David A. Cicci		

Salary Costs: Senior Personnel:PI/PD, Co-PIs, Faculty and Other Sen. Assoc. (List each separately with title; A.6. show number in brackets)	DOD FUNDED PERSON-MOS.			FUNDS REQUESTED FROM DOD	NON-FEDERAL MATCHING FUNDS	TOTAL PROJECT COSTS
	CAL	ACAD	SUM			
1. D. A. Cicci, Associate Professor	0	2.9	0	$17,383	$8,650	$26,033
2. J. E. Cochran, Jr., Professor	0.6	0	0	$6,097	$18,290	$24,387
3.	0	0	0	$0	$0	$0
4.	0	0	0	$0	$0	$0
5. ( )OTHERS (LIST INDIVIDUALS ON BUDGET EXPL. PG)	0	0	0	$0	$0	$0
6. (2)TOTAL SENIOR PERSONNEL (1-5)	0.6	2.9	0	$23,480	$26,940	$50,420
B. OTHER PERSONNEL (SHOW NUMBERS IN BRACKETS)						
1. ( )POST DOCTORAL ASSOCIATES	0	0	0	$0	$0	$0
2. ( )OTHER PROFESSIONALS (TECHNICIAN, ETC.)	0	0	0	$0	$0	$0
3. (3)GRADUATE STUDENTS	18	0	0	$45,000	$0	$45,000
4. ( )UNDERGRADUATE STUDENTS	0	0	0	$0	$0	$0
5. ( )SECRETARIAL-CLERICAL	0	0	0	$0	$0	$0
6. ( )OTHER	0	0	0	$0	$0	$0
TOTAL SALARIES AND WAGES (A+B)				$68,480	$26,940	$95,420
C. FRINGE BENEFITS (IF CHARGED AS DIRECT COSTS) - RATE: 25%				$5,870	$6,735	$12,605
TOTAL SALARIES, WAGES, & FRINGE BENEFITS (A+B+C)				$74,350	$33,675	$108,025

2. OVERHEAD RATE: 44.2%			
NEGOTIATED WITH DHHS ON September 13, 1996			
(AGENCY NAME) (DATE)			
BASE: RATE: 44.2% BASIS: MTDC			
PERIOD OF GRANTEE'S FISCAL YEAR: Oct. 1, 1999 - Sept. 30, 2000			
TOTAL OVERHEAD COSTS	$34,631	$17,315	$51,946
3. SUPPLIES AND MATERIALS	$0	$3,500	$3,500
4. EQUIPMENT: Describe any equipment to be acquired & the basis of cost estimates. Costs should be based on recent quotations from manufacturers and distributors.	$0	$0	$0
5. TRAVEL COSTS: List proposed destinations and basis of cost estimates.	$4,000	$2,000	$6,000
6. PUBLICATION AND REPORT COSTS	$0	$0	$0
7. SUBAWARD COSTS: Support the estimate of subaward work by indicating the specific items or portion of the work to be subawarded, type of subaward anticipated, name of subawardee, and a detailed cost summary.	$0	$0	$0
8. CONSULTANT COSTS: State planned daily consultant fee & travel expenses, the nature of the consulting effort, & reason consultants are required.	$0	$0	$0
9. COMMUNICATION COSTS: Estimate communication costs (i.e., long distance phone calls, telegrams, & postage) not included in overhead.	$0	$0	$0
10. OTHER DIRECT COSTS: Itemize other anticipated direct costs such as rental for computers & other equipment. Unusual or expensive items should be fully justified.	$0	$0	$0
11. TOTAL COSTS:	$112,981	$56,490	$169,471

12. COST SHARING PLANS: Construct a table (on attached budget explanation page) showing the matching share committed to DEPSCoR in the following categories: state, institutional, and private sector. In each category show the amount & nature of the matching share (e.g. state appropriation, equipment, new faculty positions, etc.). A signed statement of commitment regarding the matching funds described above should be obtained from the appropriate state, institutional, and private sector officials.

Alabama EPSCoR - Revised 7/15/95

C. PROPOSAL BUDGET

ORGANIZATION Auburn University				PROPOSAL NO.		PERIOD OF PERFORMANCE Nov. 14, 1997 - Nov. 13, 2000	

PRINCIPAL INVESTIGATOR/PROJECT DIRECTOR David A. Cicci				AWARD NO.			

Salary Costs: Senior Personnel:PI/PD, Co-PIs, Faculty and Other Sen. Assoc. (List each separately with title; A.6. show number in brackets)	DOD FUNDED PERSON-MOS.			FUNDS REQUESTED FROM DOD	NON-FEDERAL MATCHING FUNDS	TOTAL PROJECT COSTS
	CAL	ACAD	SUM			
1. D. A. Cicci, Associate Professor	0	8.7	0	$52,489	$23,358	$75,847
2. J. E. Cochran, Jr., Prorfessor	1.8	0	0	$17,763	$53,287	$71,050
3.	0	0	0	$0	$0	$0
4.	0	0	0	$0	$0	$0
5. ( )OTHERS (LIST INDIVIDUALS ON BUDGET EXPL. PG)	0	0	0	$0	$0	$0
6. ( )TOTAL SENIOR PERSONNEL (1-5)	1.8	8.7	0	$70,252	$76,645	$146,897
B. OTHER PERSONNEL (SHOW NUMBERS IN BRACKETS)						
1. ( )POST DOCTORAL ASSOCIATES	0	0	0	$0	$0	$0
2. ( )OTHER PROFESSIONALS (TECHNICIAN, ETC.)	0	0	0	$0	$0	$0
3. ( )GRADUATE STUDENTS	54	0	0	$124,800	$0	$124,800
4. ( )UNDERGRADUATE STUDENTS	0	0	0	$0	$0	$0
5. ( )SECRETARIAL-CLERICAL	0	0	0	$0	$0	$0
6. ( )OTHER	0	0	0	$0	$0	$0
TOTAL SALARIES AND WAGES (A+B)				$195,052	$76,645	$271,697
C. FRINGE BENEFITS (IF CHARGED AS DIRECT COSTS) - RATE: 25%				$17,563	$19,162	$36,725
TOTAL SALARIES, WAGES, & FRINGE BENEFITS (A+B+C)				$212,615	$95,807	$308,422

2. OVERHEAD RATE: 44.2%			
NEGOTIATED WITH DHHS ON September 13, 1996 (AGENCY NAME) (DATE)			
BASE: RATE: 44.2% BASIS: MTDC			
PERIOD OF GRANTEE'S FISCAL YEAR: Oct. 1, 1997 - Sept. 30, 00			
TOTAL OVERHEAD COSTS	$99,280	$49,639	$148,919
3. SUPPLIES AND MATERIALS	$0	$10,500	$10,500
4. EQUIPMENT: Describe any equipment to be acquired & the basis of cost estimates. Costs should be based on recent quotations from manufacturers and distributors.			
	$0	$0	$0
5. TRAVEL COSTS: List proposed destinations and basis of cost estimates.			
	$12,000	$6,000	$18,000
6. PUBLICATION AND REPORT COSTS	$0	$0	$0
7. SUBAWARD COSTS: Support the estimate of subaward work by indicating the specific items or portion of the work to be subawarded, type of subaward anticipated, name of subawardee, and a detailed cost summary.			
	$0	$0	$0
8. CONSULTANT COSTS: State planned daily consultant fee & travel expenses, the nature of the consulting effort, & reason consultants are required.			
	$0	$0	$0
9. COMMUNICATION COSTS: Estimate communication costs (i.e., long distance phone calls, telegrams, & postage) not included in overhead.			
	$0	$0	$0
10. OTHER DIRECT COSTS: Itemize other anticipated direct costs such as rental for computers & other equipment. Unusual or expensive items should be fully justified.			
	$0	$0	$0
11. TOTAL COSTS:	$323,895	$161,946	$485,841
12. COST SHARING PLANS: Construct a table (on attached budget explanation page) showing the matching share committed to DEPSCoR in the following categories: state, institutional, and private sector. In each category show the amount & nature of the matching share (e.g. state appropriation, equipment, new faculty positions, etc.). A signed statement of commitment regarding the matching funds described above should be obtained from the appropriate state, institutional, and private sector officials.			

Alabama EPSCoR - Revised 7/15/95

APPENDIX E: TECHNICAL PAPERS

The following technical papers were written during the contract period. The publication status of each is designated below. All papers are attached at the end of this appendix.

Published

1. "Modeling Tethered Satellite Dynamics for Identification and Orbit Determination," J. E. Cochran, Jr., S. Cho, A. Lovell, and D. A. Cicci, *The Journal of the Astronautical Sciences*, Vol. 48, No. 1, pp. 89-108, January-March 2000. Also published in *Advances in the Astronautical Sciences*, proceedings of the AAS/AIAA Space Flight Mechanics Meeting, Girdwood, AK, August 16-19, 1999.

2. "Evaluation of the Information Contained in the Motion of One Satellite of a Two-Satellite Tethered System," J. E. Cochran, Jr., S. Cho, A. Lovell, and D. A. Cicci, *The Journal of the Astronautical Sciences*, Vol. 48, No. 4, October-December 2000.

3. "Identification and Orbit Determination of a Tethered Satellite System," S. Cho, J. E. Cochran, Jr., and D. A. Cicci, *Applied Mathematics and Computation*, Vol. 117, pp. 301-312, 2001. Also published in *Advances in the Astronautical Sciences*, Vol. 99, Part 1, pp. 21-34, proceedings of the AAS/AIAA Space Flight Mechanics Meeting, Monterey, CA, February 9-11, 1999.

4. "A Look at Tethered Satellite Identification Using Ridge-Type Estimation Methods," D. A. Cicci, C. Qualls and T. A. Lovell, *Applied Mathematics and Computation*, Vol. 119. pp. 297-316, 2001. Also published in *Advances in the Astronautical Sciences*, proceedings of the AAS/AIAA Space Flight Mechanics Meeting, Girdwood, AK, August 16-19, 1999.

Accepted for Publication

5. "Approximate Solution for Tethered Satellite Motion," S. Cho, J. E. Cochran, Jr., and D. A. Cicci, accepted for publication in the *AIAA Journal of Guidance, Control, and Dynamics*, February 2000. Also published in *Advances in the Astronautical Sciences*, Vol. 102, Part 2, pp. 1345-1360, proceedings of the AAS/AIAA Space Flight Mechanics Meeting, Breckenridge, CO, February 7-10, 1999.

6. "A Filtering Method for the Identification of a Tethered Satellite," D. A. Cicci, T. A. Lovell, and C. Qualls, accepted for publication in *The Journal of the Astronautical Sciences*, November 2000. Also published in *Advances in the Astronautical Sciences*, Vol. 102, Part 2, pp. 1399-1418, proceedings of the AAS/AIAA Space Flight Mechanics Meeting, Breckenridge, CO, February 7-10, 1999.

7. "Existence of Periodic Motions of a Tether Trailing Satellite," E. V. Rossi, D. A. Cicci, and J. E. Cochran, Jr., accepted for publication in the *AIAA Journal of Spacecraft and Rockets*, January 2001. Also published in *A Collection of Technical Papers*, pp. 390-396, proceedings of the AIAA/AAS Astrodynamics Specialist Conference, Denver, CO, August 14-17, 2000.

Submitted for Publication

8. "A Study of the Re-Entry Orbit Discrepancy Involving Tethered Satellites," T. A. Lovell, S. Cho, J. E. Cochran, Jr., and D. A. Cicci, submitted for publication to *Acta Astronautica*, July 2000.

To Be Submitted for Publication

9. "Preliminary Orbit Determination of a Tethered Satellite," C. Qualls and D. A. Cicci, to be submitted to *The Journal of the Astronautical Sciences*. Also published in *Advances in the Astronautical Sciences*, proceedings of the AAS/AIAA Space Flight Mechanics Meeting, Clearwater, FL, January 23-26, 2000.

10. "Quick-Look Identification and Orbit Determination of a Tethered Satellite," D. A. Cicci, J. E. Cochran, Jr., C. Qualls, and T. A. Lovell, to be submitted to *The Journal of Astronautical Sciences*. Also published in *Advances in the Astronautical Sciences*, proceedings of the AAS/AIAA Space Flight Mechanics Meeting, Santa Barbara, CA, February 11-15, 2001.

Conference Papers

11. "On the Information Contained in the Motion of One Satellite of a Two-Satellite Tethered System," J. E. Cochran, Jr., S. Cho, A. Lovell, and D. A. Cicci. Published as paper number AIAA 98-4555 in *A Collection of Technical Papers*, pp. 422-431, proceedings of the AIAA/AAS Astrodynamics Specialist Conference, Boston, MA, August 10-12, 1998.

12. "Use of Tethered Satellite Estimation Methods in Identifying Re-Entering Objects," T. A. Lovell, S. Cho. J. E. Cochran, Jr., and D. A. Cicci. Published as paper number AAS 00-194 in *Advances in the Astronautical Sciences*, proceedings of the AAS/AIAA Space Flight Mechanics Meeting, Clearwater, FL, January 23-26, 2000.

Abstract Accepted for Conference Paper

13. "A Comparison of Orbit Determination and Long-Term Prediction Methods for Tethered Satellite Systems," T. A. Lovell, J. E. Cochran, Jr., and D. A. Cicci, accepted for presentation at the AAS/AIAA Astrodynamics Specialist Conference, Quebec City, Ontario, Canada, July30-August 2, 2001.

(This page was intentionally left blank.)

MODELING TETHERED SATELLITE DYNAMICS FOR IDENTIFICATION AND ORBIT DETERMINATION

J. E. Cochran,[*] Jr., S. Cho,[+] T. A. Lovell,[#] and D. A. Cicci[‡]
Auburn University
Auburn. AL 36830

Abstract

This paper investigates methods of detection and orbit determination for a two-satellite tethered system, given observation data for one of the satellites over a relatively short time. Such a task is more difficult when the system has a relatively short tether and/or significant libration. The estimation of the state of the system using the same information is also more difficult under these conditions. Two different formulations of the equations of motion of a tethered satellite system with a massless tether are used to see which results in the best performance of detection and state estimation algorithms. The two formulations involve the use of different state variables. In the first, the position and velocity of the observed satellite are used. In the second formulation, we use the position and velocity of the observed satellite and its position and velocity relative to the center of mass of the system as variables. The second formulation provides equations that may be solved approximately for small libration angles to obtain an analytical solution that describes the motion better than a similar solution based on the first formulation. However, both formulations provide essentially the same orbit determination results.

Introduction

The task of estimating the motion of a tethered satellite system (TSS) is important for several reasons. Not only is it desired to track the behavior of a "known" TSS after deployment, but it is also vital to be able to identify an "unknown" object in space as tethered or untethered, and to predict as much about the object's motion as possible. It is a well-known fact that the motion of each satellite in a TSS in the Earth s gravitational field is non-Keplerian [1]. This is due to the force transmitted to each satellite through

_____

[*] Professor and Head, Department of Aerospace Engineering, Fellow, AAS.

[+] Formerly, Graduate Reasearch Assistant; curently, Member of Research Staff, Electronics and Telecommunications Research Institute, Taejon, South Korea.

[#] Graduate Research Assistant, Department of Aerospace Engineering.

[‡] Professor, Department of Aerospace Engineering, , Member, AAS

1

the tether, which not only affects the orbital motion of each satellite, but also can induce librational motion of the system. Librational motion is characterized by one of the satellites "leading" the other, thus yielding a nonzero angle between the tether and the local vertical (a line between the Earth and the lower satellite). This non-Keplerian behavior presents a significant problem, in the sense that the orbit predicted for a tethered object as a result of a state estimation process may differ greatly from its true orbit [2,3]. The dynamic model used in an estimation process to identify and/or determine the motion of a tethered system will have a large impact on whether this problem can be alleviated. Previously [4, 5], a model has been developed that incorporates both orbital and librational states of a TSS. However, when this model is used in a routine to estimate the motion of a TSS from observation data, several shortcomings can result. This is because the elements of the information matrix corresponding to the librational motion of the system are generally relatively small, leading to large condition numbers.

In the past, difficulties in acquiring information on librational motion have motivated a quest for analytical approximations for the orbital and librational motions of tethered satellite systems [6,7]. In [8], an analytical solution for the magnitude of the position vector of a tethered satellite was determined from a restricted set of equations obtained by assuming planar, non-librating motion. Since the analytical solution is in terms of elliptic functions, it is analytically tractable, but a more simple approximation is desired for use in completing the solution by integrating the relative motion equations.

Although it may be advisable to consider the motion of one of the satellites and the relative motion of the other as was done by Cho et al. [5], it is obvious that the motion of the observed satellite of a TSS appears to be an elliptical orbit that is either enclosed by, or encloses, the trajectory of the center of the mass of the system. This is interesting because the motion of the center of mass of the system of a TSS is much closer to Keplerian behavior than that of either of the two satellites. It follows that it should be possible to approximate the motion of the observed tethered satellite by using the solution in terms of elliptic functions, *or* by using a suitably adjusted solution to the center of mass motion. Mathematically, this means that all of the elliptic functions can probably be approximated by much simpler functions.

The objectives of this paper are (1) to formulate the equations of motion for a TSS by using the position and velocity of the center of mass of the system as state variables, (2) to obtain an approximate

solution to these equations, and (3) to see if this approach will improve the performance of an estimation algorithm used to determine the state of the system from observations of one satellite.

Equations of Motion of a Tethered Satellite System

The coordinate systems and position vectors used to describe the motion of the system are depicted in Fig. 1. **Exyz** represents a geocentric-equatorial coordinate system with origin at the center of the Earth, which is modeled as a point mass. The vector **r** defines the position of perturbed satellite m with respect to Earth, and the position of the perturbing satellite m_p with respect to Earth is defined by $\mathbf{r_p}$. The vector $\mathbf{r_{CM}}$ represents the position vector of the center of mass of the system. The mass of the tether is neglected to emphasize the motions of the two satellites. The $u_1 u_2$ plane is the osculating plane in which m is moving at time t. The orientation of the osculating plane is defined by Ω and i, the longitude of the ascending node and inclination, respectively. For the following development, it will be assumed that mass m is constrained to lie in this plane. Fig. 2 describes a vector ρ which represents the motion of the satellite m_p with respect to the satellite m. Fig. 2 shows the angles θ_3 and θ_2, which define in-plane motion and out-of-plane motion, respectively, of m_p with respect to m. The vector equations of motion for satellite m and the motion of the satellite m_p relative to m may be written in the rotating frames $\mathbf{Eu_1u_2u_3}$ and $\mathbf{Ee_1e_2e_3}$, respectively [5],

$$\ddot{\mathbf{r}} = \overset{\circ\circ}{\mathbf{r}} + \overset{\circ}{\lambda} \times \mathbf{r} + 2\lambda \times \overset{\circ}{\mathbf{r}} + \lambda \times \lambda \times \mathbf{r} = -\mu \frac{\mathbf{r}}{r^3} + \frac{\mathbf{F_T}}{m} \tag{1}$$

$$\ddot{\varrho} = \overset{\circ\circ}{\varrho} + \overset{\circ}{\omega} \times \varrho + 2\omega \times \overset{\circ}{\varrho} + \omega \times \omega \times \varrho = \Delta\mathbf{g} - \mathbf{F_T} \frac{M}{m\,m_p}. \tag{2}$$

Here, $\overset{\circ}{(\ )}$ represents differentiation with respect to time in the respective rotating coordinate system. In equations (1)-(2), μ is the gravitational parameter for the Earth, $M = m + m_p$, and $\Delta\mathbf{g} \equiv -\dfrac{\mu}{r_p^3}\mathbf{r_p} + \dfrac{\mu}{r^3}\mathbf{r}$. In equation (1), λ is the inertial angular velocity of the $\mathbf{Eu_1u_2u_3}$ coordinate system and ω, which appears in equation (2), is the inertial angular velocity of the $\mathbf{Ee_1e_2e_3}$ coordinate system. In the right-hand-sides of

3
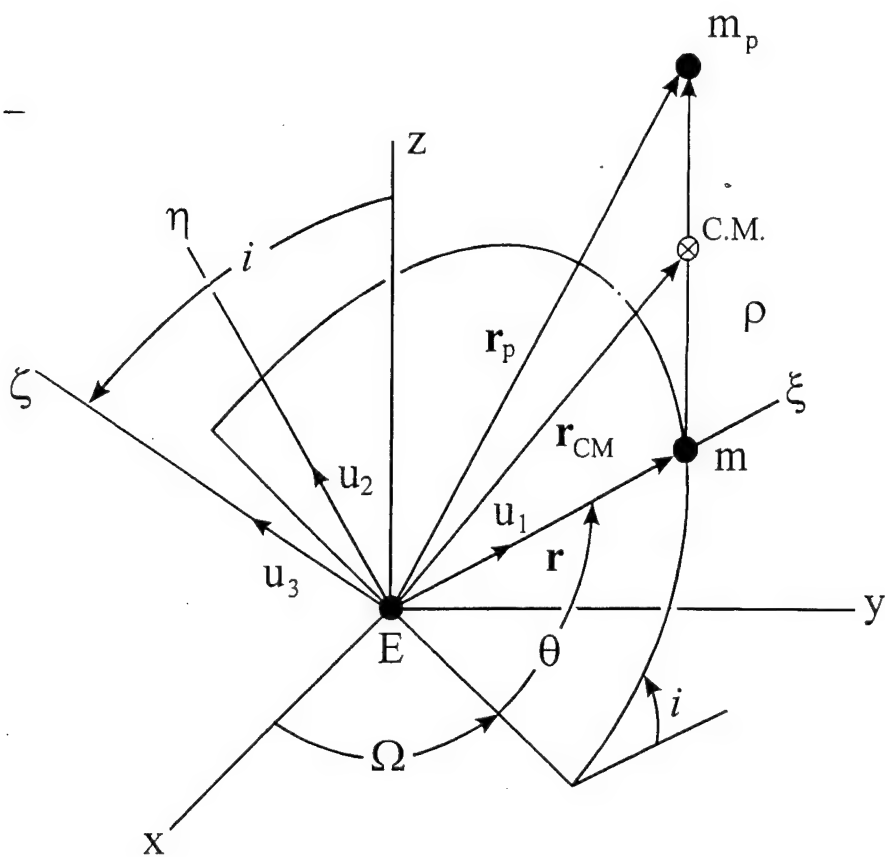
Fig. 1. Osculating Orbit Plane.
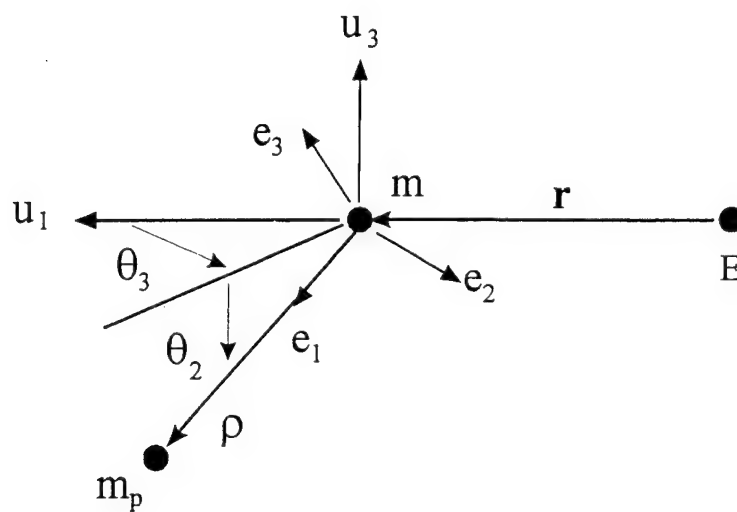
Fig. 2. Relative Motion of m_p w.r.t. m.

equations (1)-(2), $\mathbf{F}_T$ is the tension force due to the tether. It was shown in [5] that if the tether is considered inelastic, $\mathbf{F}_T$ can be expressed as

$$\mathbf{F}_T = \frac{mm_p}{M}\rho\left[\omega_2^2 + \omega_3^2 + \frac{\mu}{r^3}(3\cos^2\theta_2\cos^2\theta_3 - 1)\right]\mathbf{e}_1 \tag{3}$$

Center of Mass Approach

Alternatively, the above equations can be expressed in coordinate frames with origin at the center of mass. The equation of motion for the center of mass of the system can be obtained by noting that

$$\mathbf{r}_{CM} = \mathbf{r} + \frac{m_p}{M}\varrho \tag{4}$$

Differentiating equation (4) twice and inserting equations (1)-(2) gives

$$\ddot{\mathbf{r}}_{CM} = -\frac{\mu}{M}\left(\frac{\mathbf{r}}{r^3}m + \frac{\mathbf{r}_p}{r_p^3}m_p\right) \tag{5}$$

Of course, the tether perturbing force does not appear in this equation because it is an "internal" force. Furthermore, equation (5) is valid even if the satellites are not tethered. The only evidence of a tether is circumstantial, since $\mathbf{r}$ and $\mathbf{r}_p$ are related by the tether length and direction.

Akin to the $\mathbf{Eu_1u_2u_3}$ frame of Fig. 1, consider now a rotating frame $\mathbf{Eu_{CM1}u_{CM2}u_{CM3}}$ that defines an osculating plane $u_{CM1}u_{CM2}$ in which the center of mass moves, whose orientation is described by Ω_{CM} and i_{CM}. Equation (5) can now be written as

$$\overset{\circ\circ}{\mathbf{r}}_{CM} + \overset{\circ}{\boldsymbol{\lambda}}_{CM}\times\mathbf{r}_{CM} + 2\boldsymbol{\lambda}_{CM}\times\overset{\circ}{\mathbf{r}}_{CM} + \boldsymbol{\lambda}_{CM}\times\boldsymbol{\lambda}_{CM}\times\mathbf{r}_{CM} = -\frac{\mu}{M}\left(\frac{\mathbf{r}}{r^3}m + \frac{\mathbf{r}_p}{r_p^3}m_p\right) \tag{6}$$

where $(\overset{\circ}{\,})$ represents differentiation with respect to time in the $\mathbf{Eu_{CM1}u_{CM2}u_{CM3}}$ frame, and $\boldsymbol{\lambda}_{CM}$ is the inertial angular velocity of the frame. Likewise, Fig. 3 depicts the librational motion of the TSS with respect to the center of mass, with ϕ_3 and ϕ_2 being the in-plane and out-of-plane angles, respectively, that the tether makes with the $\mathbf{u}_{CM1}$ axis. With the $\mathbf{Ee_{CM1}e_{CM2}e_{CM3}}$ frame defined in the Figure, equation (2) may then be written as

$$\ddot{\varrho} + \dot{\omega}_{CM} \times \varrho + 2\omega_{CM} \times \dot{\varrho} + \omega_{CM} \times \omega_{CM} \times \varrho = \Delta g - F_T \frac{M}{m\, m_p} \tag{7}$$

where $(\,\dot{}\,)$ represents differentiation with respect to time in the $E e_{CM1} e_{CM2} e_{CM3}$ frame, and ω_{CM} is the inertial angular velocity of the frame.

Fig. 3. Librational Motion about the Center of Mass.

By substituting $r = r_{CM} - (m_p / M)\varrho$ and $r_p = r_{CM} + (m/M)\varrho$ into equation (6), expressing all vectors in the $E u_{CM1} u_{CM2} u_{CM3}$ frame, and expanding the denominators in terms of ρ / r_{CM} (retaining terms through $(\rho / r_{CM})^2$), the following scalar equations of motion for the center of mass can be written:

$$\ddot{r}_{CM} = \lambda_{CM3}^2 r_{CM} - \frac{\mu}{r_{CM}^2} - 3\mu \frac{m\, m_p}{M} \frac{\cos\phi_2^2 \cos\phi_3^2}{r_{CM}^2} \left(\frac{\rho}{r_{CM}} \right)^2 \tag{8}$$

$$\dot{\lambda}_{CM3} = -\frac{1}{r_{CM}} \left[2\lambda_{CM3}\, \dot{r}_{CM} + 3\mu \frac{m\, m_p}{M} \frac{\cos\phi_2^2 \cos\phi_3 \sin\phi_3}{r_{CM}^2} \left(\frac{\rho}{r_{CM}} \right)^2 \right] \tag{9}$$

$$0 = \frac{1}{r_{CM}} \left[\lambda_{CM1}\, \lambda_{CM3}\, r_{CM} - 3\mu \frac{m\, m_p}{M} \frac{\cos\phi_2^2 \sin\phi_2 \cos\phi_3}{r_{CM}^2} \left(\frac{\rho}{r_{CM}} \right)^2 \right] \tag{10}$$

The last equation arises due to the fact that λ_{CM2} must be zero because the center of mass is constrained to lie in the osculating plane.

6

By performing the same three steps with regard to equation (7), the scalar equations that govern the motion of m_p with respect to the center of mass can be written as

$$\ddot{\rho} = (\omega_{CM2}^2 + \omega_{CM3}^2)\rho - \frac{\mu}{r_{CM}^3}\left(1 - \frac{3\cos\phi_2{}^2\cos\phi_3{}^2}{r_{CM}^2}\right)\left(\frac{\rho}{r_{CM}}\right) \cdot$$
$$- \frac{3\mu}{r_{CM}^2}\frac{m_p^2 - m^2}{M^2}\frac{\cos\phi_2\cos\phi_3}{r_{CM}^2}\left(\frac{\rho}{r_{CM}}\right)^2 - F_T\frac{M}{m\,m_p}$$

(11)

$$\dot{\omega}_{CM3} = -\frac{1}{\rho}\left[2\omega_{CM3}\,\dot{\rho} + \omega_{CMI}\,\omega_{CM2}\rho + \frac{3\mu\cos\phi_2\cos\phi_3\sin\phi_3}{r_{CM}^2}\left(\frac{\rho}{r_{CM}}\right)\right]$$

(12)

$$\dot{\omega}_{CM2} = -\frac{1}{\rho}\left[2\omega_{CM2}\,\dot{\rho} - \omega_{CMI}\,\omega_{CM3}\rho + \frac{3\mu\cos\phi_2\sin\phi_2\cos\phi_3{}^2}{r_{CM}^2}\left(\frac{\rho}{r_{CM}}\right)\right]$$

(13)

The tether related terms in the right-hand-sides of equations (8)-(10) are very small since $(\rho/r_{CM})^2$ is very small. Thus, the equations of motion predict that the center of mass of a tethered satellite system will move in essentially a two-body orbit about the Earth.

/

Approximate Motion of the Satellites in the Tethered System

The equations of motion presented in [5] and those given above provide two different avenues for reaching an approximate solution for the system motion. In [8], the equations for the motion of m were approximated for small libration angles by a set of equations that may be solved analytically in terms of elliptic functions. This solution is referred to as a "restricted tether motion" solution because libration is neglected in order to obtain it. An approximate analytical solution for the in-plane libration angle was also provided in [8]. Here a similar approach is used that relies on the center of mass equations for the orbital motion.

Restricted Tether Motion

As stated above, by neglecting the librational motion of the system, a "restricted tether problem" was defined in [8]. The restricted tether motion embodies the dominant characteristics of the tether perturbed orbital motion from the point of view of one of the satellites. The equations for the restricted tether motion are:

$$\ddot{r} = r\dot{\theta}^2 - \frac{\mu}{r^2} + \frac{m_p}{M}\rho\left(\dot{\theta}^2 + 2\frac{\mu}{r^3}\right) \tag{14}$$

and

$$\ddot{\theta} = \frac{-2\dot{\theta}\dot{r}}{r} \tag{15}$$

where r is the radial distance of the satellite from the center of the Earth and θ is the true anomaly of its orbital path. In [8], these equations were solved analytically using elliptic functions and elliptic integrals. The solution was shown to be a good approximation to the tethered satellite's orbital motion.

Adjusted Center of Mass Motion

As noted above, the tether perturbation terms in equations (8)-(10) are second order in ρ/r_{CM} and are therefore very small, even for long tethers. Thus, whether the librational motion is small or not, we can assume that the center of mass motion is Keplerian with little error. Then, when the librational motion is small, the motion of the observed satellite can be approximated by the center of mass motion with an appropriate radial offset.

From equations (8)-(9), non-librating motion can be described by

$$\ddot{r}_{CM} = \dot{\theta}_{CM}^2\, r_{CM} - \frac{\mu}{r_{CM}^2} \tag{16}$$

and

$$\ddot{\theta}_{CM} = \frac{1}{r_{CM}}\left(-2\dot{\theta}_{CM}\,\dot{r}_{CM}\right). \tag{17}$$

where r_{CM} and θ_{CM} are radial distance and true anomaly, respectively, of the center of mass. We can solve the "two-body problem" represented by equations (16)-(17) and use $r = r_{CM} - \rho(m_p/M)$ to find r. Alternatively, we can use $r_{CM} = r + \rho(m_p/M)$ and derive another set of equations for r. Because $\dot{r}_{CM} = \dot{r}$ and $\ddot{r}_{CM} = \ddot{r}$ when there is no librational motion, then by neglecting the $(\rho/r_{CM})^2$ term in equations (8)-(9) and assuming that $\theta_{CM} \approx \theta$, equations (16)-(17) become

$$\ddot{r} = \dot{\theta}^2\left(r + \frac{m_p}{M}\rho\right) - \frac{\mu}{\left(r + \frac{m_p}{M}\rho\right)^2} \tag{18}$$

and

$$\ddot{\theta} = -2\,\dot{\theta}\,\dot{r}\,\frac{1}{\left(r + \dfrac{m_p}{M}\rho\right)}. \qquad (19)$$

Note that if the term $1/\left[r + (m_p/M)\rho\right]$ in equations (18)-(19) is expanded in a binomial series in

$\left(\dfrac{\rho}{r}\right)\left(\dfrac{m_p}{M}\right)$, the equations become

$$\ddot{r} = r\dot{\theta}^2 - \frac{\mu}{r^2} + \frac{m_p}{M}\rho\left(\dot{\theta}^2 + 2\,\frac{\mu}{r^3}\right) \qquad (20)$$

and

$$\ddot{\theta} = -2\,\dot{\theta}\,\dot{r}\,\frac{1}{r}\left(1 - \frac{\rho}{r}\frac{m_p}{M}\right). \qquad (21)$$

where, although equations (14) and (20) are the same, equation (21) contains a term not present in equation (15).

For several cases of TSS motion, comparisons of errors in radial distance of the two approximate motions are provided in Figs. 4 - 7. In each case, the center of mass is on a circular orbit of radius 6621 km. The quantity r_T represents the "true" motion, obtained by numerical integration of equations (1) and (2); r_R represents restricted tether motion, obtained by numerically solving equations (14)-(15); and r_{CM} is the adjusted center of mass motion described above, corresponding to equations (18)-(19). Fig. 4 shows that both approximations are very good for the case of the near-circular orbit, a relatively short tether and a small amount of librational motion. In Fig. 5, a longer tether and more librational motion are introduced for the near circular orbit. (The mass ratio is reduced in order to keep the value of the tether parameter

$\left(\dfrac{\rho}{r_E}\right)\left(\dfrac{m_p}{M}\right)$ constant for all cases.) This is seen to increase the error for both approximations. Although

both approximations are very good in Figs. 4 and 5, the adjusted motion contains significantly smaller errors than the restricted tether motion does. For cases of elliptical orbit motion, the error increases in all cases except r_{CM} for the long tether case (Figs. 5 and 7), in which case the error is roughly the same or decreases slightly. From the results in Figs. 4-7 it can be concluded that the adjusted center of mass motion, which uses simpler equations, approximates the orbital motion of a TSS better than restricted tether motion.

9
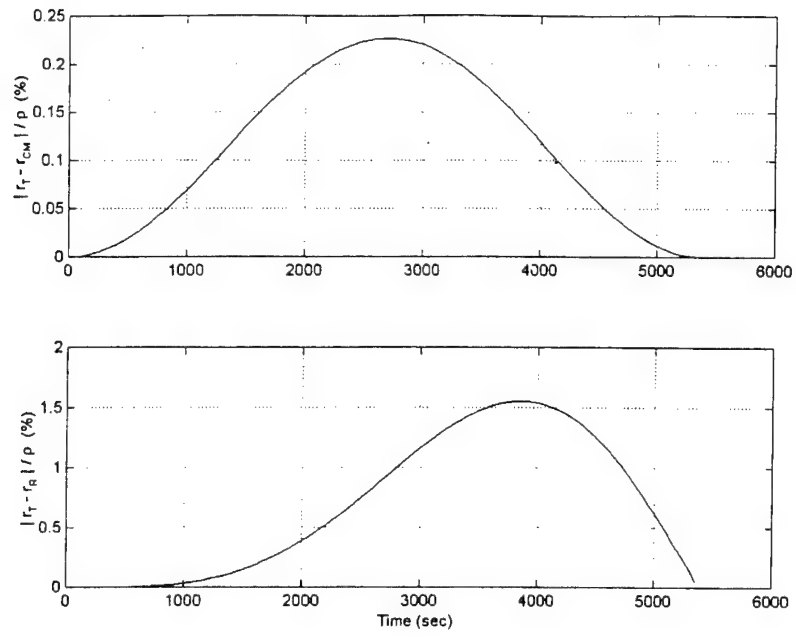
Fig. 4. Errors in Approximate r (% of tether length)
(Near Circular, m/m_p=1, tether length=10km, and θ_{30} =0.0 rad)
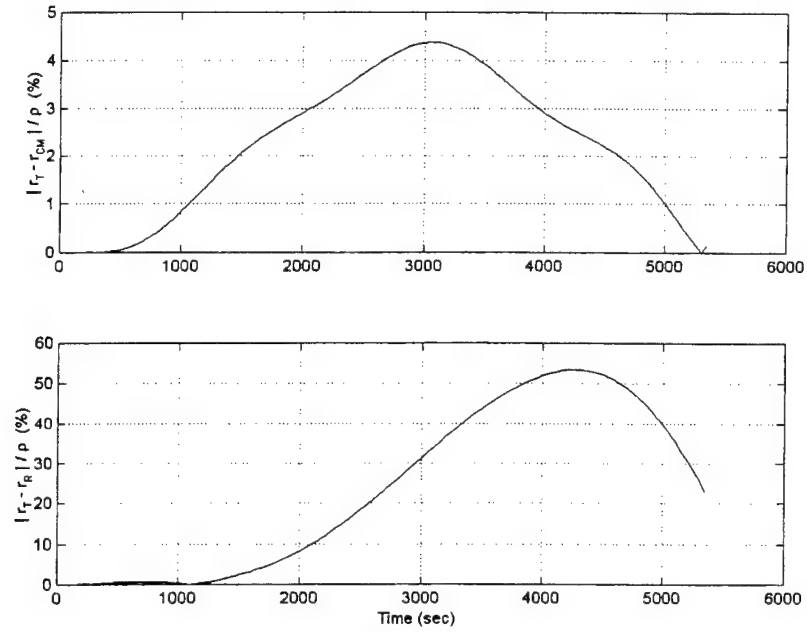
Fig. 5. Errors in Approximate r (% of tether length)
(Near Circular, m/m_p=0.1, tether length=100km, and θ_{30} =0.1 rad)

10
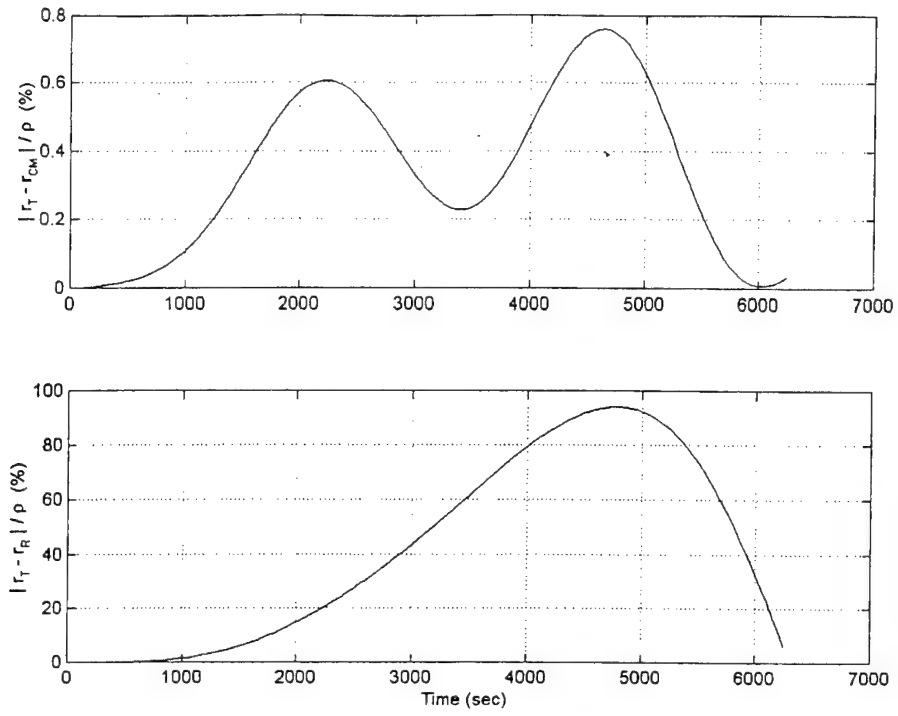
Fig. 6. Errors in Approximate r (% of tether length)
(Elliptic, m/m_p=1, tether length=10km, and θ_{30} =0.0 rad)
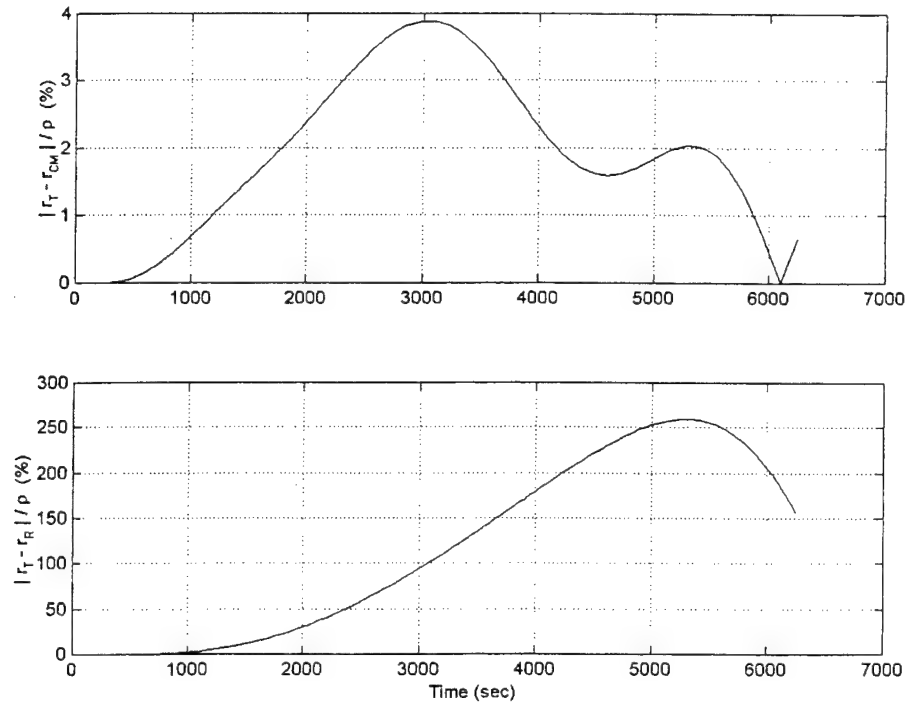
Fig. 7. Errors in Approximate r (% of tether length)
(Elliptic, m/m_p=0.1, tether length=100km, and θ_{30} =0.1 rad)

11

Librational Motion

In Figs. 2 and 3, the motion of the satellite m_p is described as relative motion with respect to the satellite m and the center of mass, respectively. This librational motion will be discussed here. For most cases of tethered motion, the libration perpendicular to the orbital plane is much less significant than the in-plane component. Thus, the motion of the TSS will be assumed planar. Fig. 8 illustrates the motion of a TSS in its orbital plane. Here θ and θ_3 are the true anomaly and libration angle relative to mass m, while θ_{CM} and φ_3 are the same quantities relative to the center of mass. Equations of in-plane motion for satellite m are [8]

$$u'' + u = \frac{\mu}{h^2} - \frac{m_p}{M}\rho\left[u\left(\theta_3' + 1\right)^2 + \frac{2\mu}{h^2}\right]\left(\theta_3 u' + u\right) \tag{22}$$

$$h' = \frac{m_p}{M}\rho\left[u\left(\theta_3' + 1\right)^2 + \frac{2\mu}{h^2}\right]\theta_3 h \tag{23}$$

and

$$\theta_3'' = -\frac{2u'}{u}\left(\theta_3' + 1\right) - \frac{3\mu}{h^2 u}\theta_3 - \frac{m_p}{M}\rho\left[u\left(\theta_3' + 1\right)^2 + \frac{2\mu}{h^2}\right]\theta_3\left(\theta_3' + 1\right) \tag{24}$$

where the variables r and $\dot{\theta}$ have been transformed by using $u = 1/r$ and $h = r^2\dot{\theta}$. The time variable t has been replaced by a time-like variable τ defined by $\dot{\tau} = hu^2$. In equations (22)-(24), $(\ )' = d(\ )/d\tau$. The analytical solution to equation (24) is provided in [8]. Alternatively, the librational motion can be solved for by writing equations (22)-(24) for the center of mass:

$$u''_{CM} + u_{CM} = \frac{\mu}{h_{CM}^2} \tag{25}$$

$$h'_{CM} = 0.0 \tag{26}$$

and

$$\phi_3'' = -\frac{2\,u_{CM}'}{u_{CM}}\left(\phi_3' + 1\right) - \frac{3\mu}{h_{CM}^2\,u_{CM}}\phi_3 \tag{27}$$

As a result, equations (25)-(27) are much simpler than equations (22)-(24).

The libration equation (27) is a second-order, non-homogeneous, linear differential equation with variable coefficients, i.e., it is of the form

$$\phi_3'' + 2P(\tau)\phi_3' + R^2(\tau)\phi_3 = Q(\tau) \tag{28}$$

where

$$P(\tau) = \frac{u_{CM}'}{u_{CM}} \tag{29}$$
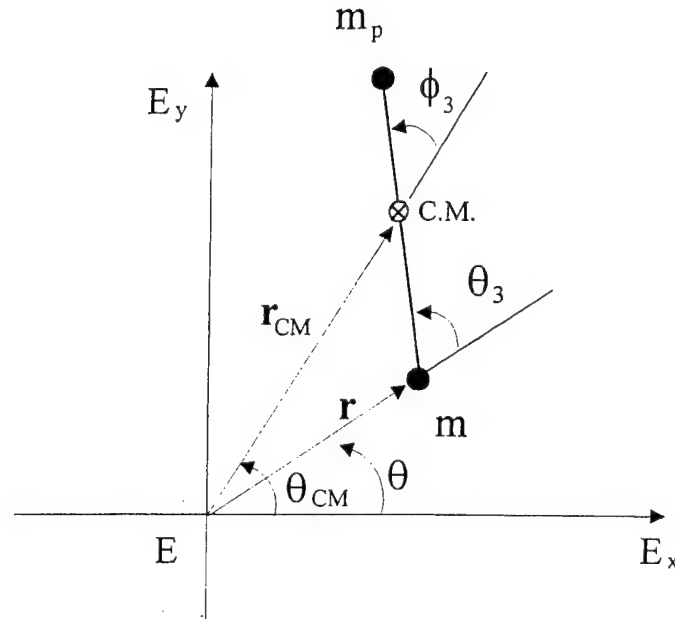
Fig. 8. Motion in Orbital Plane.

$$R^2(\tau) = \frac{3\mu}{h_{CM}^2\,u_{CM}} \tag{30}$$

13

and

$$Q(\tau) = -2\frac{u'_{CM}}{u_{CM}} .$$

(31)

In the first approximation, u_{CM} and u'_{CM} may be replaced in equations (29)-(31) by the solution to equation (25), which is

$$u_{CM} = \gamma \cos(\tau + \xi) + \frac{\mu}{h_{CM}^2}$$

(32)

and

$$u'_{CM} = -\gamma \sin(\tau + \xi)$$

(33)

where γ and ξ are constants determined by the initial conditions on u_{CM} and u'_{CM}. Then, to solve equation (28), the variable ϕ_3 is first transformed to a new variable η defined by

$$\eta = \phi_3 \, e^{\int P(\tau)d\tau} = \phi_3 u_{CM}$$

(34)

or

$$\phi_3 = \eta \, e^{\int -P(\tau)d\tau} = \frac{\eta}{u_{CM}}$$

(35)

Equation (28) can now be expressed in the simpler form

$$\eta'' + G(\tau)^2 \eta = Q^*(\tau)$$

(36)

where

$$G(\tau)^2 = R^2 - P^2 - P'$$

(37)

and

$$Q^*(\tau) = Q(\tau) \, e^{\int P d\tau} = -2u'_{CM}$$

(38)

Substituting equations (32)-(33) into equations (29)-(31) and (37), using a Taylor series expansion for G about $\gamma = 0$, and neglecting terms of order γ^2 or higher, we obtain the following expression:

$$G(\tau) \approx \Omega_0 \left[1 - \frac{1}{3}\frac{h^2\gamma}{\mu}\cos(\tau + \xi) \right]$$

(39)

where $\Omega_0 = \sqrt{3}$. Since G executes small changes about its mean value Ω_0, the WKBJ approximation [9] can be used to obtain the following two (approximate) linearly independent homogeneous solutions to equation (36):

$$x_1 = \frac{1}{\sqrt{G}} \cos \zeta \tag{40}$$

—

$$x_2 = \frac{1}{\sqrt{G}} \sin \zeta \tag{41}$$

where

$$\zeta(\tau) = \int G \, d\tau \tag{42}$$

Using the method of variation of parameters, we seek a particular solution of the form

$$\eta(\tau) = \alpha \, x_1 + \beta \, x_2 \tag{43}$$

where α and β must satisfy

$$\alpha' = \frac{-Q^{\bullet} x_2}{x_1 \, x_2' - x_2 \, x_1'} \tag{44}$$

and

$$\beta' = \frac{Q^{\bullet} x_1}{x_1 \, x_2' - x_2 \, x_1'} . \tag{45}$$

By integrating equations (44) and (45), we obtain the following solutions for α and β (again, neglecting terms of order γ^2 or higher):

$$\alpha = -\frac{\gamma}{\sqrt{\Omega_0}} \left\{ \frac{\sin \left[(1 - \Omega_0) \tau + \xi \right]}{1 - \Omega_0} - \frac{\sin \left[(1 + \Omega_0) \tau + \xi \right]}{1 + \Omega_0} \right\} + C_{\alpha} \tag{46}$$

and

$$\beta = -\frac{\omega \gamma}{\sqrt{\Omega_0}} \left\{ \frac{\cos \left[(1 - \Omega_0) \tau + \xi \right]}{1 - \Omega_0} + \frac{\cos \left[(1 + \Omega_0) \tau + \xi \right]}{1 + \Omega_0} \right\} + C_{\beta} \tag{47}$$

where the constants of integration C_{α} and C_{β} are chosen such that

$$\eta(0) = \alpha(0) x_1(0) + \beta(0) x_2(0) = \varphi_3(0) u_{CM}(0) \tag{48}$$

and

$$\eta'(0) = \alpha'(0) x_1(0) + \alpha(0) x_1'(0) + \beta'(0) x_2(0) + \beta(0) x_2'(0)$$

$$= \varphi_3'(0) u_{CM}(0) + \varphi_3(0) u'_{CM}(0) \tag{49}$$

The solution for ϕ_3 is then found by substituting η into equation (35):

15

$$\phi_3 = (\alpha x_1 + \beta x_2)\frac{1}{u_{CM}} \qquad (50)$$

It should be mentioned that the preceding solution is valid only for circular or near-circular TSS orbits. This is because the effect of γ in equation (32) is to add eccentricity to the circular orbit, and in the foregoing analysis γ was assumed to be small.

Results obtained from the analytical solution above are shown along with numerical simulation results (equations (25)-(27)) in Figs. 9 and 10. The tether lengths used for the results of Figs. 9 and 10 are 10km and 100km, respectively. Again the mass ratio is reduced in order to keep the same value of $\left(\frac{\rho}{r_E}\right)\left(\frac{m_p}{M}\right)$. For both cases, the initial radius is 6621 km and center of mass eccentricity is 0.02. In each case, three different initial librational angles (0, 0.1, and 0.2 rad) are compared. The results from the approximate analytical solution to the librational motion are seen to match those from the numerical simulation very well for small ϕ_3. The results in Fig. 10 are slightly less accurate because of the larger perturbation induced by the tether.

The analytical solution for ϕ_3 can be converted to θ_3 by the geometry of Fig. 8, which indicates that

$$\theta_3 = \varphi_3 + \theta_{CM} - \theta \qquad (51)$$

In [8] an analytical solution for θ_3 was obtained by manipulating equations (22)-(24) and using the WKBJ approximation as was done here for equations (25)-(27). In Fig. 11, the means of obtaining θ_3 described above (referred to as the "calculated solution") is compared with the analytical solution from [8] as well as θ_3 obtained by numerical integration of equations (22)-(24). The initial conditions used are the same as for the case in Fig. 9 where initial libration angle is 0. The calculated θ_3 from the analytical ϕ_3 solution is seen to be closer to the true (numerically integrated) θ_3 than the analytical θ_3 solution from [8].
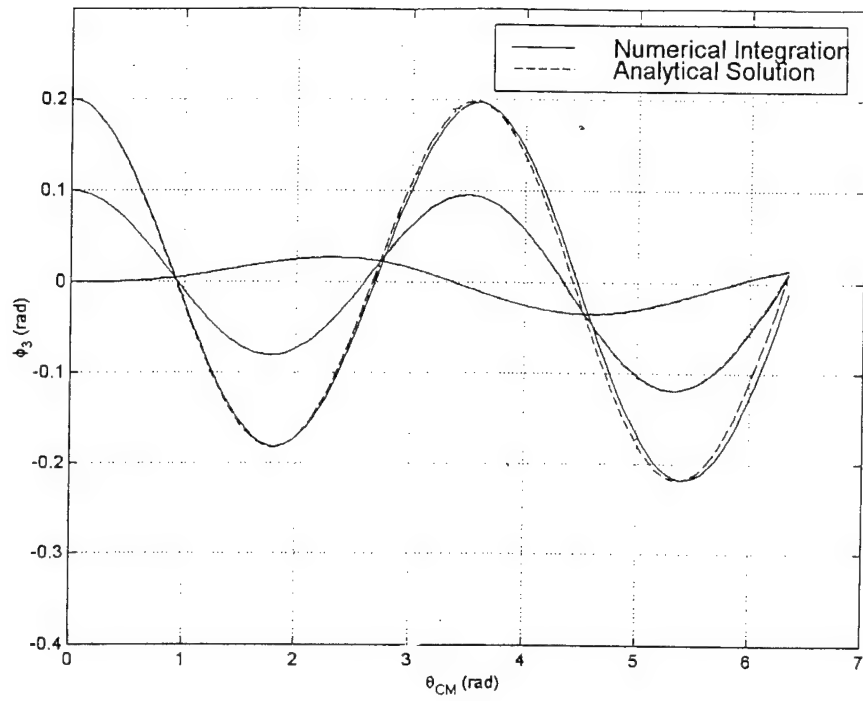
Fig. 9. Comparison of Analytical and Numerical Results.
(Tether Length=10 km and m / m_p = 1.0)
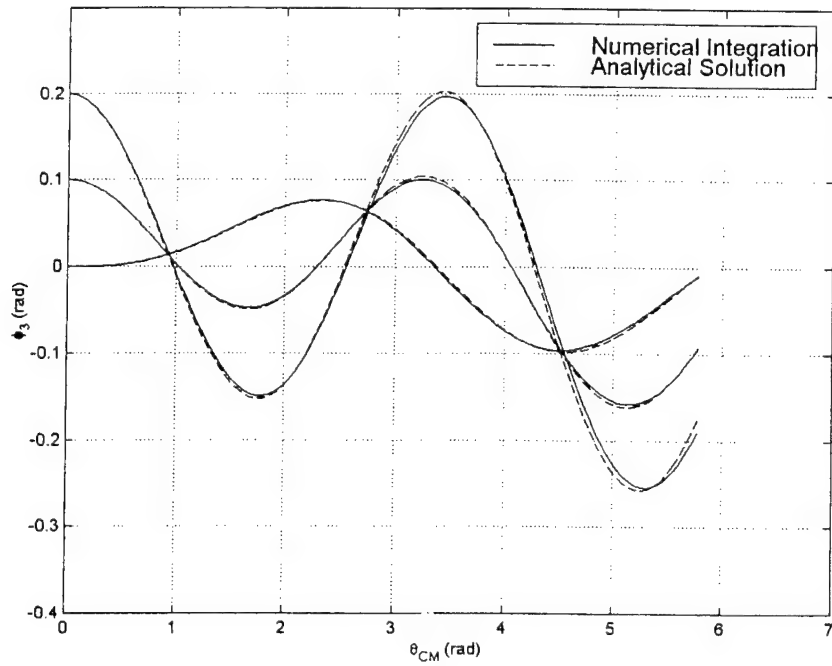
Fig. 10. Comparison of Analytical and Numerical Results.
(Tether Length=100 km and m / m_p = 0.1)

17
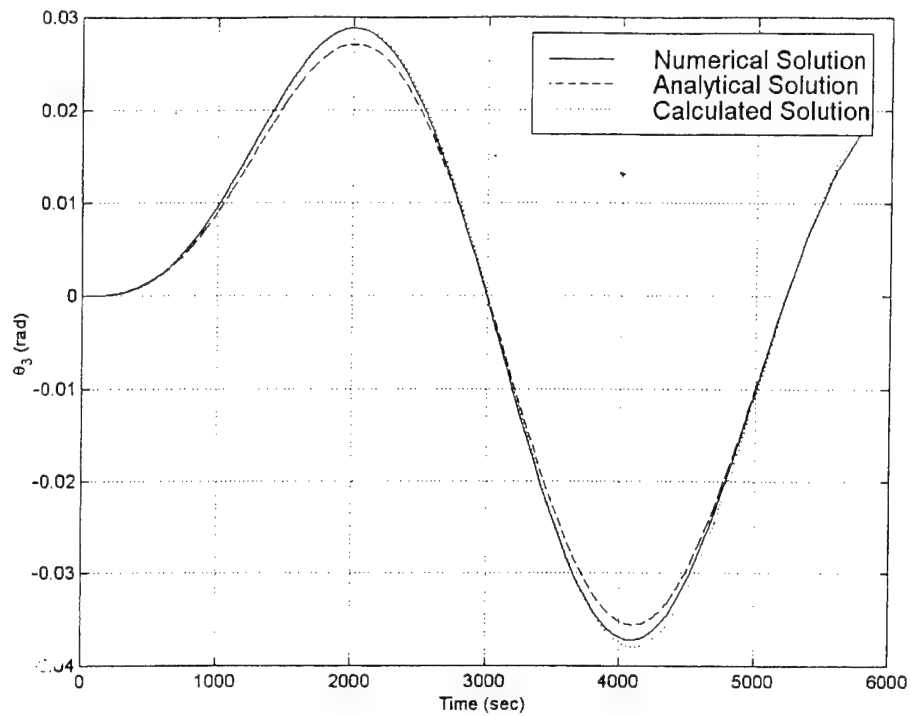
Fig. 11. Angle θ_3 as Calculated by Three Different Methods.

Detection and State Estimation

In [5,10] a state estimation process to identify a TSS by observing only one of the satellites in the TSS was tested. Difficulties encountered included: (a) The state estimation process, including states for the libration angle, fails when a short observation period is used; (b) very accurate guesses for the initial states are needed for successful convergence; (c) initial states for the libration angle cannot be obtained *a priori*. These problems are caused by the fact that no direct information on the librational motion is provided in the observations, and because the effects of libration on the observed satellite are often very small.

The success of the identification process seems to require a trade-off between performance in detecting the effect of the tether force on the observed satellite and achieving completeness of system identification. If detection is the main objective, neglecting states that govern the librational motion should be acceptable, if the libration is small in amplitude and/or the tether length is small (say, less than 20 km). It follows that ignoring the libration states in the equations of motion (as is done with the restricted tether motion formulation) may improve the performance of an estimator without significant loss of accuracy.

18

A method of identification of a TSS based on the above consideration was proposed in [11]. In this process, various formulations of the equations of motion for a tethered body are used in a batch filter. The method is constructed in three stages, two of which will be discussed here.

First Stage

As stated above, by neglecting the librational motion of the system, a "restricted tether problem" was In the first stage, a state estimation technique using the equations for two-body motion is applied with limited observation data. Only one of the satellites in a tethered system is observed and the observation period is limited to a short arc. The state vector to be estimated in the first stage is

$$X = \begin{bmatrix} r & \theta & \dot{r} & \dot{\theta} & \mu \end{bmatrix}^T \tag{52}$$

From this first stage, three different results are possible:

1) **The states will be estimated with high accuracy.** This will likely be the case if the observed satellite is a single (untethered) satellite. In addition, it is likely that the estimated value of μ will be very close to the true gravitational constant for Earth.

2) **The estimation process converges, but the results contain significant error.** This may be the case if the observed satellite is tethered. As a check, the estimated value of μ will likely *not* be close to the true value—nor will it be close to the estimated value of μ for a case where the observed satellite is known to be untethered.

3) **The estimation process fails to converge.** In this case, the observed satellite is most likely a member of a TSS, and the effect of the tether force causes the body's motion to differ significantly from two-body motion.

For all of the above cases, more steps are needed to complete the identification.

Second Stage

In the second stage, equations for the restricted tether motion are applied to verify and improve the results. If the states are estimated successfully in the first stage, these estimates may be used as an initial guess of the second stage. The state vector for the second stage is

19

$$X = \begin{bmatrix} r & \theta & \dot{r} & \dot{\theta} & \varepsilon \end{bmatrix}^T \tag{53}$$

Where ε is the tether parameter, a combination of a mass ratio and a non-dimensional tether length (ρ/r_E, where r_E is the radius of the Earth). This parameter is defined as

$$\varepsilon = \frac{m_p \rho}{M r_E} \tag{54}$$

The tether parameter can be obtained from the first stage results by [4,5]

$$\varepsilon \approx \frac{r}{r_E} \frac{\mu - \mu_e}{\mu_e + 2\mu} \tag{55}$$

where μ_e is the estimated value for the gravitational constant. If the estimation process of the second stage is successful, the estimated state vector identifies a TSS more completely.

Results

In previous sections, the restricted tether motion and adjusted center of mass motion formulations have been compared numerically and analytically. The adjusted center of mass motion equations were shown to provide a simpler formulation as well as a more accurate analytical solution. The purpose of this section is to determine if the adjusted center of mass motion equations can be used to improve the accuracy of the second stage of the aforementioned algorithm. For several cases of TSS motion, the first stage of the algorithm was performed, after which the restricted tether motion equations ((14)-(15)) and adjusted center of mass motion equations ((18)-(19)) are applied separately to the second stage. For both models, the results of the first stage were used as initial guesses for the second stage. Six example cases, with and without libration, were chosen. These are listed in Table 1. For each case, the center of mass is traveling on a circular orbit. Cases C-1 and C-2, represent motion without libration, one having a larger tether parameter than the other. Cases C-3 and C-4 are examples of small in-plane libration for the same tether parameters as in cases C-1 and C-2. Cases C-5 and C-6 include large in-plane libration. All observation data were generated by numerical integration of the equations for complete three-dimensional motion. Radial distance and orbital angle (true anomaly) were used for the observation data set. The observation period was 350 seconds, about 1/16 of the orbital period. Each data set was collected every 5 seconds, for a total of 70 data

However, in modeling the orbital motion of a tethered object, both formulations provide practically the same detection/state estimation results for short observational periods. These formulations could play a vital role in an algorithm whose purpose is to classify an orbiting object as tethered or untethered, and, if tethered, to determine as much about the orbital and librational motion of the object as possible. Based on the results presented herein, a dynamical model based on center of mass motion is to be preferred in fulfilling that role, due to its simplicity and high degree of accuracy.

Acknowledgement

References

[1] Beletsky, V. V., and Levin, E. V., *Dynamics of Space Tether Systems*, Vol. 83, Advances in the Astronautical Sciences, AAS, San Diego, CA, 1993, p. 76.

[2] Hoots, F. R., Roehrich, R. L., and Szebehely, V. G., "Space Shuttle Tethered Satellite Analysis," Technical Report #83-5, Directorate of Astrodynamics, Peterson Air Force Base, CO, August 1983.

[3] Asher, T. A., D. G. Boden, and R. J. Tegtmeyer, "Tethered Satellites: The Orbit Determination Problem and Missile Early Warning Systems," AIAA 88-4284 1988.

[4] Cochran, J. E., Jr., Cho, S., Cheng, Y-M., and Cicci, D. A., "Dynamics and Orbit Determination of Tethered Satellite Systems", AAS 96-147, *AAS/AIAA Space Flight Mechanics Meeting*, Austin, TX, February 12-15, 1996.

[5] Cho, S., Cochran, J.E., Jr., and Cicci, D. A., "Identification and Orbit Determination of Tethered Satellite System", AAS 98-101, *AAS/AIAA Space Flight Mechanic: Meeting*, Monterey, CA, February 9-11, 1998.

[6] Von Flotow, A. H., " Some Approximations for the Dynamics of Spacecraft Tethers," AIAA 87-0821, *AIAA Dynamics Specialists Conference*, Monterey, CA, Apr. 9-10, 1987.

[7] Nacozy, P. E., " Dynamics Analysis of Electrodynamic Satellite Tethers. Equations of Motion and Numerical Solution Algorithms for the Tether," NASA-CR-171777, Jan. 1984.

[8] Cho, S., Cochran, J.E., Jr., and Cicci, D. A., "Approximate Solutions for Tethered Satellite Motion", AAS 99-193, *AAS/AIAA Space Flight Mechanics Meeting*, Breckenridge, CO., February 7-10, 1999.

[9] Cunningham, W. J., *Introduction to Nonlinear Analysis*, McGraw-Hill, New York, 1958, pp. 253-257.

[10] Cochran, J. E., Jr., Cho, S., Lovell, A., and Cicci, D. A., "On the Information Contained in the Motion of One Satellite of a Two-Satellite Tethered System," AIAA-98-4555, *AIAA/AAS Astrodynamics Specialist Conference and Exhibit*, Boston, MA, 1998.

[11] Cho, S., "Analysis of Orbital motion of a Tethered Satellite System," Ph. D. Dissertation, Auburn University, 1999.

Table 1. Example Cases.

Case	m_p/m	ρ (km)	ε	θ_{30} (rad)
C-1	1.0	10	7.8394E-04	0.0
C-2	10.0	100	1.4254E-02	0.0
C-3	1.0	10	7.8394E-04	0.1
C-4	10.0	100	1.4254E-02	0.1
C-5	1.0	10	7.8394E-04	1.0
C-6	10.0	100	1.4254E-02	1.0

Table 2. Estimation Results for Case C-1.

State		Dynamic Model					
		Two-body Motion		Restricted Motion		CM Motion	
	True	Guess	Result	Guess	Result	Guess	Result
r	1.047E+00	1.000E+00	1.047E+00	1.047E+00	1.047E+00	1.047E+00	1.047E+00
θ	3.491E-01	0.000E+00	3.491E-01	3.491E-01	3.491E-01	3.491E-01	3.491E-01
$\dot{r}$	0.000E+00	0.000E+00	8.604E-16	8.604E-16	-3.268E-10	8.604E-16	-3.265E-10
$\dot{\theta}$	9.323E-01	1.000E+00	9.323E-01	9.323E-01	9.323E-01	9.323E-01	9.323E-01
ε	7.839E-04		7.834E-04	7.833E-04	7.839E-04	7.833E-04	7.845E-04
μ	3.986E+14	3.986E+14	3.977E+14				

Table 3. Estimation Results for Case C-2.

State		Dynamic Model					
		Two-body Motion		Restricted Motion		CM Motion	
	True	Guess	Result	Guess	Result	Guess	Result
r	1.047E+00	1.000E+00	1.047E+00	1.047E+00	1.047E+00	1.047E+00	1.047E+00
θ	3.491E-01	0.000E+00	3.491E-01	3.491E-01	3.491E-01	3.491E-01	3.491E-01
$\dot{r}$	0.000E+00	1.000E-01	-7.597E-16	0.000E+00	1.350E-09	0.000E+00	1.333E-09
$\dot{\theta}$	9.144E-01	1.000E+00	9.144E-01	9.144E-01	9.144E-01	9.144E-01	9.144E-01
ε	1.425E-02		1.425E-02	1.425E-02	1.425E-02	1.425E-02	1.445E-02
μ	3.986E+14	3.986E+14	3.825E+14				

Table 4. Estimation Results for Case C-3.

State		Dynamic Model					
		Two-body Motion		Restricted Motion		CM Motion	
	True	Guess	Result	Guess	Result	Guess	Result
r	1.047E+00	1.000E+00	1.047E+00	1.047E+00	1.047E+00	1.047E+00	1.047E+00
θ	3.491E-01	0.000E+00	3.352E-01	3.352E-01	3.491E-01	3.352E-01	3.491E-01
$\dot{r}$	0.000E+00	0.000E+00	2.825E-07	2.825E-07	-1.423E-6	2.825E-07	-1.429E-6
$\dot{\theta}$	9.313E-01	1.000E+00	9.960E-01	9.960E-01	9.313E-01	9.960E-01	9.313E-01
ε	7.839E-04		-4.702E-2	-4.702E-2	7.447E-04	-4.702E-2	7.452E-04
μ	3.986E+14	3.986E+14	4.548E+14				

Table 5. Estimation Results for Case C-4.

State		Dynamic Model					
		Two-body Motion		Restricted Motion		CM Motion	
	True	Guess	Result	Guess	Result	Guess	Result
r	1.047E+00	1.000E+00		1.000E+00	1.047E+00	1.000E+00	1.047E+00
θ	3.491E-01	0.000E+00	**(FAILED)**	0.000E+00	3.490E-01	0.000E+00	3.490E-01
$\dot{r}$	0.000E+00	1.000E-01		0.000E+00	-2.545E-5	0.000E+00	-2.544E-5
$\dot{\theta}$	9.128E-01	1.000E+00		1.000E+00	9.135E-01	1.000E+00	9.135E-01
ε	1.425E-02			1.000E-03	1.353E-02	1.000E-03	1.371E-02
μ	3.986E+14	3.986E+14					

Table 6. Estimation Results for Case C-5.

State		Dynamic Model					
		Two-body Motion		Restricted Motion		CM Motion	
	True	Guess	Result	Guess	Result	Guess	Result
r	1.047E+00	1.000E+00	1.047E+00	1.047E+00	1.047E+00	1.047E+00	1.047E+00
θ	3.491E-01	0.000E+00	3.312E-01	3.312E-01	3.491E-01	3.312E-01	3.491E-01
$\dot{r}$	0.000E+00	0.000E+00	3.755E-07	0.000E+00	-3.132E-6	0.000E+00	-3.105E-6
$\dot{\theta}$	9.313E-01	1.000E+00	1.015E+00	1.015E+00	9.314E-01	1.015E+00	9.314E-01
ε	7.839E-04		-6.510E-2	-6.510E-2	7.394E-05	-6.510E-2	7.389E-05
μ	3.986E+14	3.986E+14	4.729E+14				

Table 7. Estimation Results for Case C-6.

State		Dynamic Model					
		Two-body Motion		Restricted Motion		CM Motion	
	True	Guess	Result	Guess	Result	Guess	Result
r	1.047E+00	1.000E+00	1.047E+00	1.047E+00	1.047E+00	1.047E+00	1.047E+00
θ	3.491E-01	0.000E+00	3.150E-01	3.150E-01	3.490E-01	3.150E-01	3.490E-01
$\dot{r}$	0.000E+00	1.000E-01	1.097E-05	1.097E-05	-5.082E-5	1.097E-05	-4.661E-5
$\dot{\theta}$	9.313E-01	1.000E+00	1.070E+00	1.070E+00	9.141E-01	1.070E+00	9.141E-01
ε	7.839E-04		-1.231E-1	-1.231E-1	1.280E-03	-1.231E-1	1.273E-03
μ	3.986E+14	3.986E+14	5.392E+14				

EVALUATION OF THE INFORMATION CONTAINED IN THE MOTION OF ONE SATELLITE OF A TWO-SATELLITE TETHERED SYSTEM

J. E. Cochran[*], Jr., S. Cho[+], T. A. Lovell[#], and D. A. Cicci[‡]

Abstract

This paper addresses the problem of characterizing the information available in observations of one of the satellites of a two-satellite tethered system. Generally, both satellites in a two-satellite tethered system are observed if it is known *a priori* that the two satellites are tethered together. However, in some cases, the fact that an observed satellite is a member of a tethered system may not be known, and conventional orbit determination methods may predict motion of the observed satellite that differs significantly from its actual motion. When mathematical models of a two-satellite tethered system are used to study the characteristics of the satellite's motion, it becomes evident that librational motion is much less observable than translational motion. Thus, the information contained in observations of one of the satellites is studied in detail in order to learn how such information can be use·' to determine the motion of the system. Both analytical and numerical methods are used to determine the observability of the dynamic states of a tethered satellite system, and a batch state estimation example is provided.

[*] Professor and Head, Department of Aerospace Engineering, Auburn University, Alabama 36849; Fellow, AAS.
[+] Senior Member of Research Staff, Electronics and Telecommunications Research Institute, Taejon, Korea.
[#] Graduate Research Assistant, Department of Aerospace Engineering, Auburn University, Alabama 36849.
[‡] Professor, , Department of Aerospace Engineering, Auburn University, Alabama 36849; Member, AAS.

Introduction

Tethered satellite systems (TSS) have been advocated [1] for over 100 years, studied [2,3] for over two decades, and a number of tethered systems have been constructed and flown. Numerous uses for tethered systems have been identified. One is the generation of electrical power using a conducting tether that interacts with the Earth's magnetic field. Another is the disposal of waste from an orbiting space station by lowering a capsule into the outer fringes of the Earth's atmosphere, cutting the tether and allowing it to reenter the Earth's atmosphere.

Mathematical interest in TSS has been stimulated by their unique dynamics. In the absence of perturbing forces the motion of the center of mass of a deployed two-satellite tethered system is essentially Keplerian. However, the motion of one or both of the satellites in the system may depart significantly from Keplerian motion. As a result, many investigations have centered on the relative motion of these systems, including the dynamics of deployment and retrieval.

In tracking satellites and suborbital objects, the non-Keplerian nature of the orbital dynamics of tethered satellites poses some interesting problems. An example is that the motion of the lower satellite in the system may appear to be that of an untethered satellite moving on a reentry trajectory [4]. Current orbit determination methods are probably sufficient if there is *a priori* knowledge that the observed satellite is part of a TSS and special provisions are made within the orbit determination algorithms. However, the probable increase in tethered systems in the future and the lack of *a priori* information on some make the consideration of the motion of the individual satellites in the system more important from the standpoint of detection and tracking.

Previous papers [5-7] have addressed the problem of "detecting" tethered satellites by using tethered satellite models in the orbit determination scheme. In [5], a simple planar model

with an inextensible tether and no librational motion was used to study the effects of tether length and drag on the determination process. In [6], the planar motion of a two-satellite tethered system was considered, again with an inextensible tether, as a new type of perturbed satellite problem by writing the equations of motion in such a way that the motion of one satellite could be considered perturbed by the other through the tension in the tether. It was shown that the magnitude of the perturbing effect of the second satellite is proportional to a non-dimensional "tether parameter" containing the ratio of the masses of the satellites and the tether length. Examples were presented to show that this parameter, and the entire state of the system, could be determined from ideal, model-generated "observations" of only the perturbed satellite. In [7], more general motion of the perturbing satellite was considered, which allowed for its motion both in and out of the orbital plane of the perturbed satellite. For large out-of-plane libration angles, the tether parameter and the state of the system were able to be determined, again from ideal observations. In both [6] and [7], the models were such that the masses of the satellites and the tether length could not be calculated except as part of the tether parameter combination. Therefore, while it could be determined that the observed satellite was part of a TSS, the precise location of the second (perturbing) satellite could not be calculated. Furthermore, the batch-type filter used in the orbit determination process did not exhibit good convergence properties. This, along with the desire to be able to determine the tether length and perhaps the ratio of the masses of the satellites, has motivated a more detailed investigation of the dynamical characteristics of TSS.

In this work, a two-satellite tethered system is considered as a particular case of an observed nonlinear system. The primary purpose of this study is to determine the characteristics of the information available in observations of one of the satellites. This is done in two ways.

3

First, the model presented in [7] is used to calculate the normal matrices for the associated linear systems that arise in the orbit determination process. These are then analyzed to determine the quality and quantity of the information that may be extracted. Second, a more general model is used that includes atmospheric drag and the Earth's oblateness in order to study different types of actual motion (e.g., initial libration and initial center of mass motion) and different TSS characteristics.

Normal Matrices

Three conclusions can be made regarding the information that may be extracted from measurements of the motions of a dynamical system. First, only information that is present may be extracted. Second, the model used to extract the information must contain some representation of that information. This representation may take the form of complex expressions, such as the geopotential of a planet, or simple expressions, such as constant "unmodeled accelerations." Third, a piece of information must be independent of other information sought if it is to be extracted. An example of a piece of information that is not generally independent is the tether length, if the equations of motion of the tethered satellite model used contain the tether length only in combination with the masses of the satellites.

One way to quantify the information available in observations of a nonlinear system is to determine the information matrix $\mathbf{H}$ of a local linear representation of the system. To do this, let the nonlinear system be represented by the autonomous matrix differential equation

$$\dot{\mathbf{X}} = \mathbf{f}(\mathbf{X}) \tag{1}$$

where $\mathbf{X}$ is an n-vector of states and $\mathbf{f}$ is an n-vector of nonlinear functions. Also, let the (perfect) observations be represented by the equation

4

$$Y = h(X) \qquad (2)$$

where **Y** is an m-vector and **h** is an m-vector of nonlinear functions. If equations (1) and (2) are linearized about some nominal solution **X***(t), which is obtained using a set of initial conditions on the states that are not necessarily the true ones, then we may obtain linear equations of the form

$$\dot{\mathbf{x}} = \mathbf{A}(t)\mathbf{x} \qquad (3)$$

$$\mathbf{y} = \mathbf{H}(t)\mathbf{x} \qquad (4)$$

where, $\mathbf{x} = \mathbf{X} - \mathbf{X}^{*}$, $\mathbf{y} = \mathbf{Y} - \mathbf{Y}^{*}$, $\mathbf{Y}^{*} = \mathbf{h}(\mathbf{X}^{*}(t))$, $\mathbf{H} = \left(\dfrac{\partial \mathbf{h}}{\partial \mathbf{X}}\right)_{\mathbf{X} = \mathbf{X}^{*}}$ and $\mathbf{A} = \left(\dfrac{\partial \mathbf{f}}{\partial \mathbf{X}}\right)_{\mathbf{X} = \mathbf{X}^{*}}$. The

solution to equation (3) is

$$\mathbf{x}(t) = \Phi(t, t_0)\mathbf{x}_0 \qquad (5)$$

where $\Phi(t, t_0)$ is the state transition matrix and $\mathbf{x}_0$ is the value of **x** at the initial time t_0. The measured output of the linear system is

$$\mathbf{y} = \mathbf{H}(t)\,\Phi(t, t_0)\mathbf{x}_0 \qquad (6)$$

The observability Grammian or "normal" matrix [8] for the continuous linear system is

$$N(t_f, t_0) = \int_{t_0}^{t_f} \Phi^{T}(\tau, t_0)\, \mathbf{H}^{T}(\tau, t_0)\, \mathbf{H}(\tau, t_0)\, \Phi(\tau, t_0)\, d\tau \qquad (7)$$

Since observations are usually made at discrete times, a normal matrix for a discrete representation of the continuous linear system can be written as

$$N(k_f, 0) = \sum_{k=0}^{k_f} \Phi^{T}(k,0)\, \mathbf{H}^{T}(k,0)\, \mathbf{H}(k,0)\, \Phi(k,0) \qquad (8)$$

The linear system is observable if $N(k_f, 0)$ is nonsingular. The elements of $N(k_f, 0)$ provide information regarding "the effects of the initial conditions on the observations." If the rank of

5

$N(k_f, 0)$ is less than n, then, obviously, some of the initial conditions do not affect the observations and hence are not observable.

TSS Models

Two models of a two-satellite tethered system were used to study the information available in observations of one of the satellites. The first model is that described by Cho, et al. [7], with the exception that the tether is considered to be inextensible. The second model is more general in that it contains representations of the atmospheric drag and the effects of the Earth's oblateness. The equations of motion applicable to both models are provided in the Appendix; but only the more general model is described, since the first model is a special case of the second (general) model, i.e., accelerations due to drag and oblateness are set to zero. Modeling of the atmospheric drag effects is detailed in [9].
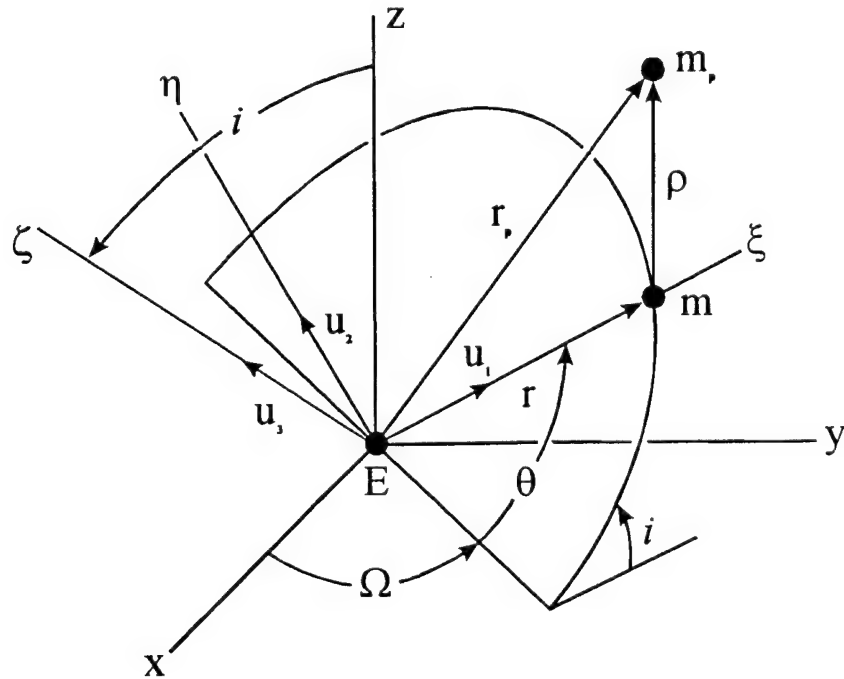
Fig. 1a. Osculating Orbit Plane (u_1, u_2, u_3).

The geometry of the model described in [7] is shown in Fig. 1a, where E is the center of the Earth, m is the observed satellite and m_p is the unobserved "perturbing" satellite. The position vector of m is $\mathbf{r}$ and that of m_p is $\mathbf{r} + \boldsymbol{\rho}$. The observed satellite is moving in an osculating orbit, the orientation of which is defined by the inclination (i), the longitude of the ascending node (Ω), and the sum of the true anomaly and argument of perigee (θ). The position vector, $\mathbf{r}$, and the velocity vector, $\mathbf{v} = \dot{\mathbf{r}}$, lie in the plane of the orbit. Two angles, θ_2 (out-of-plane) and θ_3 (in-plane), are used to define the direction of $\boldsymbol{\rho}$ relative to the direction of $\mathbf{r}$, i.e., the motion of m_p relative to m. These angles are indicated in Fig. 1b. The unit vector triad $(\mathbf{u_1,u_2,u_3})$ is obtained from the geocentric equatorial $(\mathbf{xyz})$ frame via a 3-1-3 rotation sequence through Ω, i, and θ. Likewise, the triad $(\mathbf{e_1,e_2,e_3})$ is obtained from $(\mathbf{u_1,u_2,u_3})$ via a 3-2 rotation sequence through θ_3 and θ_2. The $\mathbf{u_1,u_2,u_3}$ and $\mathbf{e_1,e_2,e_3}$ frames follow the motion of m and m_p, respectively. The angular velocity components of the $(\mathbf{u_1,u_2,u_3})$ system are given by λ_j, $j=1,2,3$, and the angular velocity components of $(\mathbf{e_1,e_2,e_3})$ by ω_j, $j=1,2,3$. The state variables for both models are r, Ω, i, θ, θ_2, θ_3, $\dot{r}$, λ_3, ω_2, and ω_3.

Although the matrices $\mathbf{A}$ and $\mathbf{H}$ are not simple, algebraic manipulation software such as Mathematica® may be used to obtain analytical expressions for the partial derivatives needed to form $\mathbf{A}$ and $\mathbf{H}$. This method is used only for the first (simpler) model.
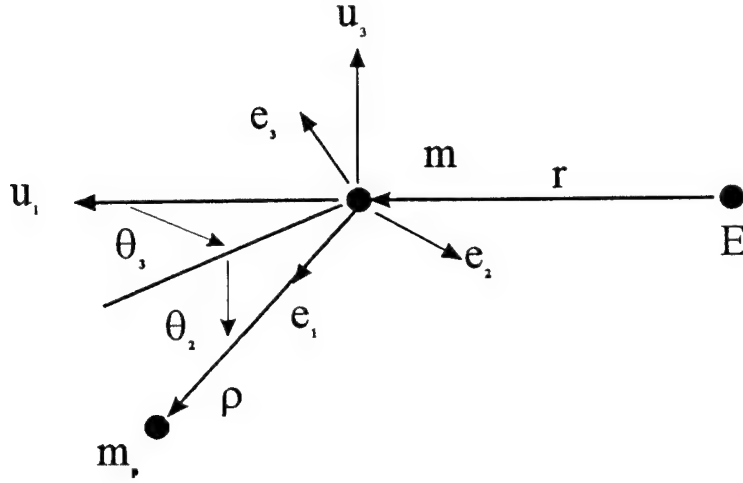
Fig. 1b. Relative Motion of m_p with respect to m (e_1, e_2, e_3).

Results from the First Model

One purpose of the examples given in this section is to show that the choices of models, states, and observations can significantly affect the information available. For the equations of motion based on the first model, it was shown in [7] that the only way ρ, m, and m_p appear is in the combination

$$\varepsilon = \frac{m_p}{(m + m_p)} \frac{\rho}{R_\oplus} \tag{9}$$

where $R_\oplus$ is the radius of the Earth. This is because in order to obtain the equations of motion, the difference in the gravitational forces on the satellites was expanded in powers of ρ/r and terms of second order or higher were neglected. Except for very long tethers, these neglected terms are extremely small. Thus, it is not any more likely that these parameters would be observable independently of one another if the full expression for the difference were used, rather than the aforementioned truncated expression.

Table 1. Test Cases.

8

Case	Mass Ratio (m_p/m)	Tether Length $(\rho$ km$)$	Tether Parameter (ε)	Observation time (Orbital period)	Libration Angle	
					θ_3 (In-plane)	θ_2 (out-plane)
1	0.1	1	1.4254E-05	1/16	0	0
2	10.0	100	1.4254E-02	1/16	0	0
3	0.1	1	1.4254E-05	1/16	Small	Small
4	10.0	100	1.4254E-02	1/16	Small	Small
5	0.1	1	1.4254E-05	1/16	Large	Large
6	10.0	100	1.4254E-02	1/16	Large	Large
7	0.1	1	1.4254E-05	1/16	Large	0
8	10.0	100	1.4254E-02	1/16	Large	0
9	0.1	1	1.4254E-05	1/16	Small	Large
10	0.1	1	1.4254E-05	1.0	Small	Small

Table 2. Condition Number of Normal Matrices for Test Cases.

Case	Range Condition Number	r, α, and δ Condition Number
1	5.8E+18	1.8E+16
2	3.7E+12	2.0E+10
3	3.5E+18	2.1E+16
4	7.7E+14	2.1E+10
5	5.0E+20	1.0E+17
6	5.3E+15	2.6E+11
7	5.0E+19	6.1E+16
8	3.9E+14	1.3E+11
9	5.9E+18	8.6E+16
10	2.3E+15	1.5E+14

The first model was used to calculate the normal matrix for numerous cases. The estimation state vector consisted of the 10 state variables plus ε. The parameters and results for several cases are summarized in Tables 1 and 2. An appropriate way to determine the observability of states in an estimation problem, and thus the feasibility of solution, is by calculating the condition number of the normal matrix. This is defined as the ratio of the maximum eigenvalue to the minimum

eigenvalue. Results in the form of condition numbers of the normal matrices were calculated using ten different nominal motions and two types of observations. For all cases, initial conditions were applied such that the mass m was on a near circular orbit and near its perigee location. In Table 1, the zero libration cases were obtained by using the equilibrium angular velocity of the system and zero initial libration angles. "Small" libration involved libration angles less than 0.1 (rad). "Large" libration was initiated by setting, $\theta_{20} = 1.0$ (rad) and $\theta_{30} = 1.0$ (rad) with zero angular rate. Two types of observation sets were used. The first set consisted only of the range, R, to the mass m from a ground station. The second type consisted of the position vector of m defined by the radial distance, r, the right ascension, α, and the declination, δ. For all cases except Case 10, the total observation time was $1/16^{th}$ of an orbital period. During this period of time 171 observations were processed. For Case 10, it was assumed that the observed satellite could be tracked over an entire orbit.

Cases 1 and 2 in Table 1 are for small and large tether perturbations, respectively, and no initial libration. For the smaller value of ε (Case 1), the condition number of the normal matrix is very large, indicating an ill-conditioned problem. For the larger value of ε (Case 2), the matrix condition numbers are six orders of magnitude smaller.

Cases 3-9 are similar to Cases 1 and 2 except that these cases include librational motions. Intuitively, one might think that these cases should be richer in information because libration of the tether is included in the nominal motion. However, the condition numbers do not change significantly from the Case 1 and Case 2 values.

A comparison of the results of Case 10 with those of Case 3 show that increasing observation time (and thus the number of observations) can improve the conditioning of the

problem considerably. In addition, it is noted that the condition numbers are much smaller when processing r, α, and δ observations than when only the range observations are used.

Results From the General Model

For the more general tethered satellite model, forces due to Earth's oblateness and atmospheric drag were included because it is believed that these phenomena will produce effects that will increase the information available in the motion of the observed satellite. The former effects were included because for short tether lengths, the perturbing effects of the Earth's oblateness are of the same order of magnitude as the tether "perturbations." By including drag forces on each satellite, the quantities m, m_p, and ρ no longer appear strictly in the combined form of the tether parameter ε in the equations of motion. Thus, for this general model, two different combinations of m, m_p, and ρ which yield the same value of ε may affect the system motion differently. Drag forces were modeled on each satellite as well as on the tether itself. Although the mass of the tether is only a fraction of that of the satellites, its frontal area (for a typical tether length and thickness) is generally much larger, making tether drag a significant portion of the total atmospheric drag. Numerical experiments were conducted using the more general model for data generation, in order to see if the sensitivity of the motion to changes in the masses of the satellites and the tether length is significant.

Calculation of Normal Matrix

In contrast to the analytical method of obtaining the normal matrix in the previous section, an alternate approach often used in "sensitivity studies" involves numerical approximation by finite difference. The procedure includes: (1) integrating the nonlinear equations using nominal

11

values, (2) making small changes in each of the states or parameters and integrating the nonlinear equations, and (3) calculating the changes in the observed quantities due to the changes in the states and parameters. Due to the complexities involved in the partial derivatives that form the normal matrix, this numerical method was used to approximate the normal matrix using the general model.

For this model, the estimation state vector consists of the 10 state variables listed previously, as well as the two masses and the tether length. The initial conditions on the states were identical to those given in the previous section for "small" libration, and the values used for the masses and tether length were m = 10 kg, m_p = 100 kg, and ρ = 100 km. As in the previous section, the total observation time was $1/16^{th}$ of an orbital period, during which time 171 observations were obtained. For a particular tracking station location and using range as the only observation, the state transition matrix and normal matrix were numerically approximated at several times along the trajectory. That is, the orbit initial conditions, as well as values for the masses and the tether length, were perturbed slightly one at a time and the change in system states and the calculated range at various times was noted. Of particular interest is the calculation of the H matrix, where:

$$H(t_1) = \frac{\partial R(t_1)}{\partial x(t_o)} \qquad\qquad (10a)$$

$$H(t_2) = \frac{\partial R(t_2)}{\partial x(t_o)} \qquad\qquad (10b)$$

etc.

For the first model (without drag or oblateness effects), the elements of H obtained in this numerical fashion agreed to a high degree of accuracy with those obtained in the previous section, as shown in Table 3. Here, the first ten elements of H, calculated both analytically and

12

numerically, are shown at the final time. (In this table J_2 is the gravitational harmonic coefficient accounting for Earth's oblateness, and C_D is the drag coefficient assumed in the model.) The elements of $H(t_f)$ are the partial derivatives of the range with respect to each state, with the states ordered as described in a previous section. The values for the elements of H at several times along the trajectory were then obtained in the same manner using a model which allows for oblateness effects as well as aerodynamic drag on the end masses and tether. Figure 2 depicts the values of the elements of $H(t_f)$ in the trajectory calculated using each of these models. The first ten elements of H_f are the partial derivatives ordered as given above, while the last three elements are defined as follows:

$$H_{f11} = \frac{\partial R(t_f)}{\partial m} \tag{11a}$$

$$H_{f12} = \frac{\partial R(t_f)}{\partial m_p} \tag{11b}$$

$$H_{f13} = \frac{\partial R(t_f)}{\partial \rho} \tag{11c}$$

Table 3. Comparison of Analytically and Numerically Obtained Values
for H at 1/16th Period. ($J_2 = C_D = 0$)

Element of H	Analytical	Numerical
Hf1	0.62217	0.62211
Hf2	0.53908	0.53911
Hf3	0.38619	0.38622
Hf4	0.74800	0.74793
Hf5	-0.00117	-0.00115
Hf6	0.00261	0.00257
Hf7	0.10560	0.10558
Hf8	0.37447	0.37446
Hf9	-0.0001092	-0.0001081

13

Hf10	0.0011088	0.0011018
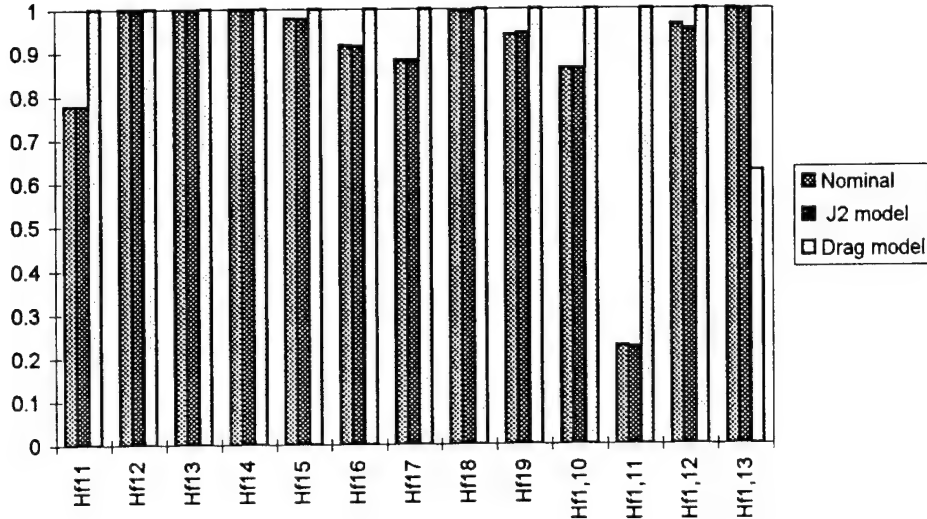
Fig. 2. Effect of Oblateness and Drag on Magnitude of each Element of $\mathbf{H_r}$ Matrix.
(Range observations for $1/16^{th}$ period. Estimation vector $\mathbf{x} = [r \; \Omega \; i \; \theta \; \theta_2 \; \theta_3 \; \dot{r} \; \lambda_3 \; \omega_2 \; \omega_3 \; m \; m_p \; \rho]$)

While the inclusion of oblateness effects in the model does not tend to affect the $\mathbf{H}$ matrix, several elements are significantly affected by the inclusion of drag. In particular, the partial derivatives of range with respect to the masses and tether length are significantly different from those of the nominal case. The fact that the range observation (and system motion in general) is significantly more sensitive to changes in mass m using the drag model, but only slightly more sensitive to changes in mass m_p, is best explained by the fact that m_p is at a much higher altitude where drag can be several orders of magnitude lower. Also, because mass m is being observed, slight changes to m_p will not significantly affect this observation. However, system motion is less sensitive to changes in tether length when drag is present in the model. This is not surprising, considering that drag has a dissipative effect on the tether, decreasing its "tether-perturbing" capability on mass m.

As mentioned previously, the inclusion of drag forces on each satellite means that the quantities m, m_p, and ρ no longer appear in the equations of motion strictly in the form of the tether parameter ε, but rather, each of these quantities enters separately into the equations of motion as well. If this were not the case, it is expected that addition of drag effects to the nominal model would affect H_{fl1}, H_{fl2}, and H_{fl3} all in generally the same manner. However, as seen in Fig. 2, H_{fl1} increases sharply, H_{fl3} decreases, and H_{fl2} remains about the same. Thus, for this general model, m, m_p, and ρ can each affect the system motion (the range in particular) independently. This indicates that m, m_p, and ρ might be estimated independently of one another, i.e., more information can be gained beyond estimation of the tether parameter, if a more general filter model is used.

Conditioning Study

Calculating the **H** matrix at various times in the trajectory using the numerical approximation described above proved to be a much quicker and more expedient method than the analytical means described earlier and used with the first model. Consequently, a larger body of results was generated for this study. First, the condition number of the normal matrix $\mathbf{H^T H}$ was calculated for different choices of the estimation state vector. These results are detailed in Tables 4-6 for the case of a model without oblateness or drag, a model including oblateness effects, and a model including both oblateness and drag. As explained previously, in the absence of drag effects, the quantities m, m_p, and ρ are not independent; therefore, for models not accounting for drag, only one of these three can be included in the estimation state vector. Thus, for the first two models, the full estimation state vector consists of the 10 dynamic states plus ρ, while for the third model it consists of the 10 states plus m, m_p, and ρ. In each table, results are shown for the

15

utilization of range observations only, as well as for the utilization of range plus range-rate observations. In addition, results obtained with observation data from a single tracking station as well as from three tracking stations are shown. The following observations can be made regarding the results:

- For most choices of the estimation state vector, the addition of oblateness effects to the nominal model caused little or no change in condition number, while the addition of drag to the model improved conditioning.

- Processing range-rate observations together with range observations generally decreases the condition number, sometimes by an order of magnitude or more; while processing data from multiple tracking stations may decrease condition number by *several* orders of magnitude.

- For the third model, the condition number of the estimation state vector containing m, m_p, and ρ takes on "reasonable" values, implying that it may be possible to estimate each of these three parameters individually, as postulated earlier.

- Although not shown in the tables, it was found that increasing the observation time for the numerical study resulted in lower condition numbers, as expected. When the observation time was increased from $1/16^{th}$ to $1/4^{th}$ period, condition numbers generally were reduced by approximately 50%.

Table 4a. Condition Numbers of Numerically Constructed Normal Matrix for 1/16th Period Observations (Range & Range Rate) of a Tethered Mass ($J_2 = C_D = 0$).

STATES	CONDITION NUMBER OF H^TH MATRIX			
	1st tracking station		all 3 tracking stations	
	range only	range+r.r.	range only	range+r.r.
$r\ \Omega\ i\ \theta\ \dot{r}\ \lambda_3$	9.29E+04	2.34E+04	4.96E+02	4.78E+02
$r\ \Omega\ i\ \theta\ \dot{r}\ \lambda_3\ \rho$	1.21E+05	2.99E+04	5.86E+02	4.80E+02
$r\ \Omega\ i\ \theta\ \dot{r}\ \lambda_3\ m$	1.15E+05	3.10E+04	6.25E+02	6.08E+02
$r\ \Omega\ i\ \theta\ \dot{r}\ \lambda_3\ m_p$	1.15E+05	3.10E+04	6.25E+02	6.08E+02
$r\ \Omega\ i\ \theta\ \theta_2\ \theta_3\ \dot{r}\ \lambda_3\ \omega_2\ \omega_3$	7.59E+05	1.92E+05	2.30E+03	3.41E+03
$r\ \Omega\ i\ \theta\ \theta_2\ \theta_3\ \dot{r}\ \lambda_3\ \omega_2\ \omega_3\ \rho$	8.39E+05	2.05E+05	2.49E+03	3.42E+03

Latitude and longitude of single station: 60 deg N, 120 deg E
**Latitude and longitude of 2 additional stations: 60 deg N, 132 deg E; 54 deg N, 120 deg E*

Table 4b. Eigenvalues of Numerically Constructed Normal Matrix Using the Full 11-State Model ($J_2 = C_D = 0$).

	EIGENVALUES OF H^TH (all 11 states)			
	1st tracking station		all 3 tracking stations	
	range only	range+r.r.	range only	range+r.r.
MAX. EIGENVALUE:	6.96E+00	4.80E+00	6.02E+00	4.33E+00
	2.36E+00	4.02E+00	2.17E+00	3.05E+00
	9.64E-01	1.07E+00	1.01E+00	1.13E+00
	4.05E-01	7.90E-01	9.47E-01	9.91E-01
	1.94E-01	1.63E-01	3.96E-01	6.43E-01
	5.65E-02	8.47E-02	2.37E-01	4.95E-01
	2.92E-02	3.51E-02	1.06E-01	1.73E-01
	1.99E-02	1.28E-02	7.43E-02	1.17E-01
	6.56E-03	2.36E-02	3.18E-02	5.12E-02
	6.39E-04	1.33E-04	7.89E-03	2.88E-02
MIN. EIGENVALUE:	8.30E-06	2.34E-05	2.41E-03	1.26E-03
STD. DEVIATION:	2.0043874	1.6514088	1.7080741	1.3467464

Table 5a. Condition Numbers of Numerically Constructed Normal Matrix for 1/16th Period Observations (Range & Range Rate) of a Tethered Mass ($J_2 = .00108$, $C_D = 0$).

STATES	CONDITION NUMBER OF H^TH MATRIX			
	1st tracking station		all 3 tracking stations	
	range only	range+r.r.	range only	range+r.r.
$r\ \Omega\ i\ \theta\ \dot{r}\ \lambda_3$	9.68E+04	1.84E+04	5.00E+02	4.53E+02
$r\ \Omega\ i\ \theta\ \dot{r}\ \lambda_3\ \rho$	1.13E+05	1.92E+04	6.16E+02	5.21E+02
$r\ \Omega\ i\ \theta\ \dot{r}\ \lambda_3\ m$	9.86E+04	1.85E+04	7.18E+02	4.68E+02
$r\ \Omega\ i\ \theta\ \dot{r}\ \lambda_3\ m_p$	9.87E+04	1.85E+04	7.16E+02	4.68E+02
$r\ \Omega\ i\ \theta\ \theta_2\ \theta_3\ \dot{r}\ \lambda_3\ \omega_2\ \omega_3$	1.91E+06	1.92E+05	2.41E+03	5.72E+03
$r\ \Omega\ i\ \theta\ \theta_2\ \theta_3\ \dot{r}\ \lambda_3\ \omega_2\ \omega_3\ \rho$	2.24E+06	2.03E+05	2.81E+03	6.29E+03

Latitude and longitude of single station: 60 deg N, 120 deg E
**Latitude and longitude of 2 additional stations: 60 deg N, 132 deg E; 54 deg N, 120 deg E*

Table 5b. Eigenvalues of Numerically Constructed Normal Matrix Using the Full 11-State Model ($J_2 = .00108$, $C_D = 0$).

	EIGENVALUES OF H^TH (all 11 states)			
	1st tracking station		all 3 tracking stations	
	range only	range+r.r.	range only	range+r.r.
MAX. EIGENVALUE:	6.58E+00	4.54E+00	5.96E+00	4.84E+00
	2.07E+00	3.35E+00	2.01E+00	1.91E+00
	1.46E+00	1.44E+00	1.35E+00	1.31E+00
	4.47E-01	8.37E-01	9.06E-01	1.09E+00
	2.81E-01	3.61E-01	3.02E-01	8.48E-01
	8.46E-02	1.67E-01	2.57E-01	5.78E-01
	4.63E-02	1.99E-01	9.74E-02	1.70E-01
	2.12E-02	9.25E-02	3.07E-02	1.34E-01
	4.44E-03	1.55E-02	7.60E-02	7.82E-02
	5.30E-04	1.60E-04	6.43E-03	3.69E-02
MIN. EIGENVALUE:	2.94E-06	2.24E-05	2.12E-03	7.70E-04
STD. DEVIATION:	1.8846579	1.4710474	1.6884572	1.3514679

Table 6a. Condition Numbers of Numerically Constructed Normal Matrix for 1/16th Period Observations (Range & Range Rate) of a Tethered Mass (J_2 = .00108, C_D = 2.7).

STATES	CONDITION NUMBER OF H^TH MATRIX			
	1st tracking station		all 3 tracking stations	
	range only	range+r.r.	range only	range+r.r.
$r\ \Omega\ i\ \theta\ \dot{r}\ \lambda_3$	6.30E+04	2.05E+04	5.19E+02	4.80E+02
$r\ \Omega\ i\ \theta\ \dot{r}\ \lambda_3\ \rho$	1.15E+05	2.54E+04	5.21E+02	6.35E+02
$r\ \Omega\ i\ \theta\ \dot{r}\ \lambda_3\ m$	1.49E+05	2.92E+04	7.58E+02	6.12E+02
$r\ \Omega\ i\ \theta\ \dot{r}\ \lambda_3\ m_p$	1.52E+05	2.94E+04	7.54E+02	6.13E+02
$r\ \Omega\ i\ \theta\ \theta_2\ \theta_3\ \dot{r}\ \lambda_3\ \omega_2\ \omega_3$	7.80E+05	9.22E+04	2.34E+03	4.45E+03
$r\ \Omega\ i\ \theta\ \theta_2\ \theta_3\ \dot{r}\ \lambda_3\ \omega_2\ \omega_3\ \rho$ $\rho\ m\ m_p$	1.25E+06	1.54E+05	1.44E+04	1.67E+04

Latitude and longitude of single station: 60 deg N, 120 deg E
**Latitude and longitude of 2 additional stations: 60 deg N, 132 deg E; 54 deg N, 120 deg E*

Table 6b. Eigenvalues of Numerically Constructed Normal Matrix Using the Full 11-State Model (J_2 = .00108, C_D = 2.7).

	EIGENVALUES OF H^TH (all 11 states)			
	1st tracking station		all 3 tracking stations	
	range only	range+r.r.	range only	range+r.r.
MAX. EIGENVALUE:	6.78E+00	5.88E+00	6.01E+00	5.24E+00
	3.46E+00	4.23E+00	3.52E+00	3.27E+00
	1.16E+00	1.39E+00	1.30E+00	1.45E+00
	7.29E-01	9.94E-01	8.96E-01	9.88E-01
	4.68E-01	2.94E-01	5.47E-01	9.01E-01
	1.77E-01	9.00E-02	3.28E-01	7.85E-01
	1.16E-01	6.70E-02	1.92E-01	1.64E-01
	9.00E-02	2.82E-02	8.05E-02	9.38E-02
	1.33E-02	1.80E-02	6.64E-02	5.89E-02
	3.12E-03	1.33E-02	1.58E-02	3.62E-02
	4.48E-04	3.97E-04	9.43E-03	1.98E-02
	3.24E-04	1.51E-04	1.81E-03	6.99E-04
MIN. EIGENVALUE:	5.42E-06	3.82E-05	4.20E-04	3.13E-04
STD. DEVIATION:	1.9036467	1.807332	1.7283949	1.5100749

Another difference between this study and the study performed for the simpler model, besides the fact that the partial derivatives were calculated numerically rather than analytically, was that the normal matrix was put into correlation form [10] after it was calculated. For an $n \times n$ matrix in correlation form, the sum of its eigenvalues is n. Given this fact, several observations can be made:

1. Since the condition number is the ratio of maximum eigenvalue to the minimum eigenvalue, a perfectly conditioned correlation matrix (i.e., a condition number of 1) would have each eigenvalue equal to 1.

2. The maximum value any eigenvalue of a correlation matrix can approach is n

3. The mean of the eigenvalues of any matrix in correlation form is 1.

These observations explain why the condition numbers in Tables 4-6 are so much lower than those obtained in the previous section, where the normal matrix was not put into correlation form. In terms of the order of magnitude of condition number that would be expected for a problem of this type, the results for each case presented in the tables are very reasonable. In [11], in which a class of estimation problems was posed with various levels of ill-conditioning, cases in which the normal matrix in correlation form had a condition number less than 10^8 made for an accurate solution.

In addition to condition numbers, Tables 4-6 display the eigenvalues of H^TH for the largest choice of estimation state vector. (For Tables 4 and 5 this entails 11 states, while for Table 6 it entails 13 states). At the bottom of each list of eigenvalues the standard deviation of the eigenvalue spectrum (from the mean of 1) is presented. Again, one can see the effect of utilizing multiple observation types as well as multiple tracking stations. Both of these effects tend to yield a normal matrix whose eigenvalues "deviate" less from those of a perfectly

conditioned matrix in correlation form (all eigenvalues equal to 1). In fact, it may be argued that the standard deviation of the eigenvalues is a better measure of the observability than condition number. Consider, for example, the full estimation state vector for nonzero J_2 and C_D (Table 6). For the case of both single and multiple tracking stations, the addition of range-rate to the observational data increases the condition number, contrary to what would be expected. Yet the standard deviation of the eigenvalue spectrum actually *decreases*, indicating greater observability of the states.

Batch Estimation Example

Given the encouraging results of the conditioning study, an example problem was constructed in order to demonstrate batch estimation of the state vector of a TSS. For this example, numerical calculation of the **H** matrix was used, as before, and the observation data was generated for mass m. Both range and range-rate data from three tracking stations were processed for $1/8^{th}$ of an orbital period. The general model was used, and both oblateness and drag effects were included. Results are provided in Table 7 for three different choices of the estimation state vector. In all cases, the initial conditions were generated by perturbing the "exact" initial conditions (those generated by each model) by 1%. The RMS error shown is the difference between the "observed" range values (calculated using the exact initial conditions) and the range values calculated using the estimated values of the initial states. The results of this example imply that accurate state estimation may be possible for the general motion of a tethered satellite pair from observations of only one of the satellites.

Table 7. Results of Batch Estimation Example Using Numerically Constructed Normal Matrix for 1/8th Period Observations (J_2 = .00108, C_D = 2.7).

Case 1: $\mathbf{x} = [r\ \Omega\ i\ \theta\ \dot{r}\ \lambda_3]$

Case 2: $\mathbf{x} = [r\ \Omega\ i\ \theta\ \theta_2\ \theta_3\ \dot{r}\ \lambda_3\ \omega_2\ \omega_3]$

Case 3: $\mathbf{x} = [r\ \Omega\ i\ \theta\ \theta_2\ \theta_3\ \dot{r}\ \lambda_3\ \omega_2\ \omega_3\ \rho\ m\ m_p]$

	True State	Estimated Values (Case 1)	Estimated Values (Case 2)	Estimated Values (Case 3)
r (m)	6.618900000000E+06	6.618900000000E+06	6.618900000000E+06	6.618899975573E+06
Ω (rad)	1.974100000000E+00	1.974100000000E+00	1.974100000000E+00	1.974099989511E+00
i (rad)	1.105100000000E+00	1.105100000000E+00	1.105100000000E+00	1.105100002018E+00
θ (rad)	1.713000000000E+00	1.713000000000E+00	1.713000000000E+00	1.713000007106E+00
θ_2 (rad)	-9.822600000000E-02		-9.822599999084E-02	-9.822722882874E-02
θ_3 (rad)	-9.856800000000E-02		-9.856800000089E-02	-9.859407246329E-02
$\dot{r}$ (m/sec)	-2.231400000000E+00	-2.231400000009E+00	-2.231400000004E+00	-2.231028679703E+00
λ_3 (rad/sec)	1.149200000000E-03	1.149200000000E-03	1.149200000000E-03	1.149199959313E-03
ω_2	5.138600000000E-05		5.138599997979E-05	5.137740562792E-05
ω_3	1.120400000000E-03		1.120400000000E-03	1.120379213851E-03
ρ (m)	1.000000000000E+05			9.948264816649E+04
m (kg)	1.000000000000E+01			9.958891361665E+00
m_p (kg)	1.000000000000E+02			1.055287839197E+02
RMS		1.885152908903E-08	6.189755061858E-08	3.736840807377E-04

Both range & range rate data processed.

**Latitude and longitude of 3 tracking stations: 60 deg N, 120 deg E; 60 deg N, 132 deg E; 54 deg N, 120 deg E*

Conclusions

The problem of estimating the state of a two-satellite tethered system using information available in the observations of one of the satellites has been investigated by using a combination of analytical and numerical methods. The tether length, masses of the satellites, observation time, types of observation, and features of the dynamical model all strongly affect the conditioning of the normal matrix and the accuracy of the results. In problems where the condition number of the matrix is large, substantial error can exist in the estimation results. For the analytical study performed using a simple model (i.e., without oblateness or drag effects) and with the normal matrix calculated analytically, the problem was found to be more well-conditioned when the value

of the tether parameter is large. For a more general model, a study showed was performed involving calculation of the normal matrix by numerical approximation. In contrast to the unwieldy analytical calculations, this method of calculation allowed results to be generated in a more expedient manner and in greater detail. This study showed that the inclusion of drag effects in the model, as well as the use of observational data from multiple tracking stations, improved conditioning. In both studies, improved conditioning was achieved by increasing the observation time, as well as by utilizing additional types of observations. Using the general model and numerical calculation of the normal matrix, an example batch estimation problem that included tether length and the satellite masses as states, was successfully solved. Thus, in problems which are constructed to be reasonably well-conditioned, the estimation of the state vector of a two-satellite tethered system using observations of only one of the satellites appears to be feasible.

Acknowledgments

References

1. Tsiolkovsky, K. E., "Speculation between Earth and Sky," Isd-vo AN-SSR, 1895, p. 35 (reprinted 1959).

2. Columbo, G., Gaposchkin, E. M., Grossi, M. D., and Weiffenbach, G. C., "The Skyhook: A Shuttle-borne Tool for Low Orbital Altitude Research," *Meccanica*, Vol. 10, 1975, pp. 3-20.

3. Belesky, V. V., *Dynamics of Space Tether Systems*, Advances in the Astronautical Sciences, American Astronautical Society, San Diego, CA, 1993.

4. Hoots, F. R., Roehrich, R. L., and Szebehely, V. G., "Space Shuttle Tethered Satellite Analysis," *Directorate of Astrodynamics*, Peterson AFB, CO, August 1983.

5. Kessler, S. A., and Cicci, D. A., "Filtering Methods for the Orbit Determination of a Tethered Satellite," *Journal of the Astronautical Sciences*, Vol. 45, No. 3, pp. 263-278, July-September 1997.

6. Cochran, J. E., Jr., Cho, S., Cheng, Y-M., and Cicci, D. A., "Dynamics and Orbit Determination of Tethered Satellite Systems," *Journal of the Astronautical Sciences*, Vol. 46, No. 2, pp. 177-194, April-June 1998.

7. Cho, S., Cochran, J. E., Jr., and Cicci, D. A., "Identification and Orbit Determination of Tethered Satellite Systems," AAS 98-101, *AAS/AIAA Space Flight Mechanics Meeting*, Monterey, CA, February 9-11, 1998.

8. Stengel, R. F., *Stochastic Optimal Control*, John Wiley & Sons, Inc., New York, 1986, pp. 142-153.

9. Cochran, J. E., Jr., Cho, S., Lovell, A., and Cicci, D. A., "On The Information Contained In The Motion Of One Satellite Of A Two-Satellite Tethered System," AIAA 98-4555, *AAS/AIAA Astrodynamics Specialist Conference*, Boston, MA, August 10-12, 1998.

10. Cicci, D. A. *Optimal* a priori *Covariance Selection for the Solution of Ill-Conditioned Nonlinear Inverse Problems*. Ph.D. Thesis, University of Texas, August 1987, pp. 33-35.

$$(\omega_2{}^2 + \omega_3{}^2)\rho + \Delta g_1 - F_{T_1}\frac{M}{m\,m_p} + \frac{1}{2}\left(\frac{dC_DAV_rV_{r_1}}{m} - \frac{d_pC_{D_p}A_pV_{r_p}V_{r_{p_1}}}{m_p}\right) + a_{op1,e} - a_{o1,e} = 0$$

<div align="right">(A-10)</div>

Also, λ_j, $j=1,2,3$, are the components of the angular velocity of the unit vector triad $(\mathbf{u}_1,\mathbf{u}_2,\mathbf{u}_3)$ associated with the position vector of m; ω_j, $j=1,2,3$, are the components of the angular velocity of the unit vector triad $(\mathbf{e}_1,\mathbf{e}_2,\mathbf{e}_3)$ associated with the position vector of m_p; $\mu = Gm_{\otimes}$, where G is the universal gravitation constant and $m_{\otimes}$ is the mass of the Earth; $\Delta \mathbf{g}$ is the difference between the gravitational acceleration on m and on m_p; d is the atmospheric density; C_D and C_{Dp} are the drag coefficients of the satellites; A and A_p are the average cross-sectional (frontal) areas of the satellites; and V_r and V_{rp} are the magnitudes of the relative velocity of the atmosphere seen by the satellites; a_{o_j} and a_{op_j}, $j=1,2,3$, are the components of the accelerations on the masses due to Earth's oblateness; and ω_e is the rate of rotation of the Earth. (For the oblateness terms, the *u* subscript denotes components expressed in the $\mathbf{u}_1,\mathbf{u}_2,\mathbf{u}_3$ frame, and the *e* subscript represents those expressed in the $\mathbf{e}_1,\mathbf{e}_2,\mathbf{e}_3$ frame.) Drag on the tether is included in the tether force $\mathbf{F}_T$. Further development of these equations, as well as discussion of the drag model and the atmospheric density model used in this study, is found in [9].

IDENTIFICATION AND ORBIT DETERMINATION OF

A TETHERED SATELLITE SYSTEM

S. Cho[1], J. E. Cochran, Jr.[2] and D. A. Cicci[3]

Department of Aerospace Engineering
Auburn University, Alabama 36849-5338

Abstract

Orbital motion of a tethered satellite system, composed of two satellites and an inextensible tether, is considered by using a perturbed two-body model. This approach is adopted so that the determination of the orbit of one of the satellites can be attempted without using observations of the motion of the other satellite in the system. The identification of the tethered condition of the system using observations of only one of the satellites in the tethered satellite system is considered. The characteristics of the "tether perturbed" motion of the observed satellite are investigated. Estimation of the state of the system using near perfect data is also illustrated. Observations of one satellite provide the

[1] Graduate Student
(E-mail:chosung@eng.auburn.edu, Tel:334-844-6806,Fax:334-844-6803)
[2] Professor and Head
[3] Associate Professor

entire state of the system and a parameter involving the ratio of the masses of satellites and the tether length.

1. Introduction

Since the concept of tethered satellite systems was proposed [1,2], numerous types of tethered satellite systems and their dynamic behaviors have been investigated. Dynamics and control problems such as the stability of the systems, deployment and retrieval of tethers, and vibration of tethers have been studied by using various tether models [3]. These are categorized as attitude dynamics problems of the tethered satellite system. Another category of dynamics in tethered satellite system encompasses their orbital motion.

One of the interesting dynamic characteristics of a "general tethered satellite system" (GTSS) consisting of the two satellites and a tether is the non-Keplerian orbital motion of each of the satellites and the center of mass of the system. This non-Keplerian motion may present significant problems to those who are tasked with detecting, identifying and tracking space objects [4,5]. Although conventional orbit determination processes do account for some sources of non-Keplerian motion, such as the oblateness of the Earth, they were not constructed with GTSS in mind. Thus, new methods of identification and orbit determination are needed that will accommodate GTSS.

Due in part to the small number of tethered satellite systems that have orbited the Earth, attempts to solve the identification and tracking problems have been rare and usually the results obtained are restricted. Kessler and Cicci [6] considered using a

2

procedure in which an apparent gravitational parameter was estimated as a means of identifying tethered satellite system. Their model was that of a "gravity-gradient stabilized" two-body system with a non-extensible tether. That is, the two satellites always remained along a local vertical. Cochran, et al.[7], considered the motion of one of the satellites in a two-body GTSS as being perturbed by the presence of the other. This point of view appears to be necessary if the orbits of the satellites in such a system are to be determined correctly when it is not known a priori that they are tethered together. A simple expression for the apparent gravitational constant was derived in [7] for a non-librating two-satellite GTSS. A two-stage process was subsequently applied to (1) detect that the observed satellite is tethered and (2) predict the motion of the two-body GTSS in a fixed orbital plane.

For the problem of identification of GTSS described above, the idea treating the tether effects as perturbations of the orbit of one of the satellite in the GTSS is very useful. Relatively less attention has given to this type of problem compared to that applied to the perturbed single satellite problem. In this paper, we consider the characteristics embodied in non-Keplerian motion of GTSS and extended the result of Ref [7] to study the problems of identification and orbit determination of a GTSS which includes the out-of-plane libration.

2. Equations of Motion

The motion of a single satellite in earth orbit can be divided into two categories: orbital dynamics and attitude dynamics. As in the case of conventional satellites, orbital dynamics deals with the translational motion of satellite, while attitude dynamics focuses on the changes in it's orientation in inertial space. Often the two types of motion are not strongly coupled and can be separated for purposes of analyses. This is the case for conventional satellites. Separation of the problems makes each less complicated. For orbital dynamics purposes, a satellite can usually be modeled as a particle, i.e., a point mass. In attitude dynamics, a satellite is generally modeled as a rigid or flexible body, or a combination of rigid and flexible bodies. The configuration of a tethered satellite system makes it less reasonable to consider the motion of the system center of mass and motion about it as separate problems. However, because of the large size of a deployed GTSS it is reasonable to treat each satellite as a point mass.

The coordinate systems and position vectors used to describe the motion of a two-satellite GTSS are depicted in Fig. 1. The mass of the tether is neglected to emphasize the motions of the two satellites. The origin of the fixed **Exyz** system is the Earth, modeled as a point mass.

Figure 1. Osculating Orbit Plane.

In Fig. 1, the plane $\xi\eta$ is the osculating plane in which m, the tethered satellite of

principal interest, is moving at some point of time. The orientation of the osculating plane

is defined by Ω and i, the longitude of the ascending node and inclination, respectively.

The vector **r** defines the position of perturbed satellite, m, with respect to E and the

position of the perturbing satellite, m_p, with respect to E is defined by $\mathbf{r_p}$. The equations of

motion for the satellites m and m_p are

$$\ddot{\mathbf{r}} = -\mu \frac{\mathbf{r}}{r^3} + \frac{\mathbf{F_T}}{m} + \mathbf{a} \tag{1}$$

$$\ddot{\mathbf{r}}_p = -\mu \frac{\mathbf{r}_p}{r_p^{\;3}} - \frac{\mathbf{F_T}}{m_p} + \mathbf{a}_p \tag{2}$$

In the right-hand-side of the Eqs. (1) and (2), $\mathbf{F_T}$ is the force on the satellite m due to the tether, and $\mathbf{a}$ and $\mathbf{a}_p$ are accelerations of m and m_p, respectively, due to forces not modeled by the dominant term in the gravitational attraction and $\mathbf{F_T}$.

In Fig. 1, the vector ρ is the relative position vector of m_p with respect to m. By using equations (1) and (2) we may then write

$$\ddot{\rho} = \mathbf{g} - \frac{M}{mm_p} \mathbf{F_T} + \mathbf{a}_p - \mathbf{a} \tag{3}$$

where $M = m + m_p$ and $\Delta \mathbf{g} \equiv -\frac{\mu}{r_p^{\;3}} \mathbf{r}_p + \frac{\mu}{r^3} \mathbf{r}$.

Figure 2 shows the angles θ_3 and θ_2, which define in-plane and out-of-plane motion, respectively, of the perturbing body, m_p, with respect to m.
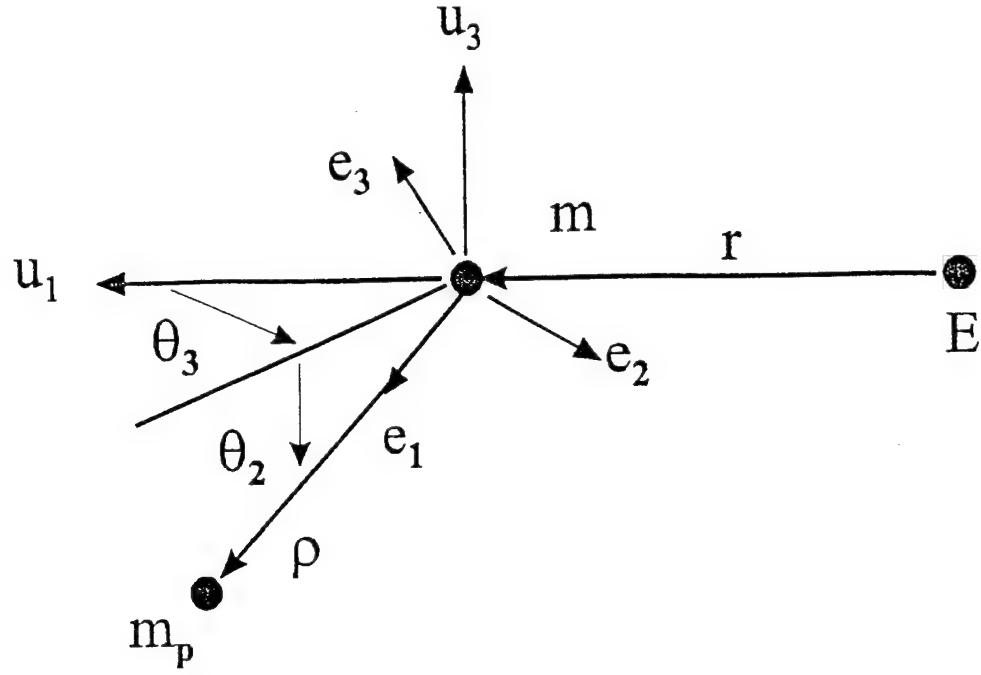
Figure 2. Relative Motion of m_p w.r.t. m.

Using Figs. 1 and 2, and Eqs.(1) and (3), we may express the equations of motion

for m and m_p in the rotating frames $E\xi\eta\zeta$ and $Ee_1e_2e_3$ as

$$\ddot{r} + \dot{\lambda} \times r + 2\lambda \times \dot{r} + \lambda \times \lambda \times r = -\mu\frac{r}{r^3} + \frac{F_T}{m} + a \tag{4}$$

$$\ddot{\rho} + \dot{\omega} \times \rho + 2\omega \times \dot{\rho} + \omega \times \omega \times \rho = \Delta g - F_T \frac{M}{m\,m_p} + a_p - a \tag{5}$$

respectively. In the Eq. (4), λ is the angular velocity of the $E\xi\eta\zeta$ coordinate system.

Also, in Eq.(5), ω is the angular velocity of the $Ee_1e_2e_3$ coordinate system.

7

We can use Eqs. (4), and (5) to get the following scalar equations for the motion of m:

$$\ddot{r} = (\lambda_2^2 + \lambda_3^2)r - \frac{\mu}{r^2} + \mathbf{u}_1 \cdot \left(\frac{\mathbf{F_T}}{m} + \mathbf{a}\right) \tag{6}$$

$$\dot{\lambda}_3 = \frac{1}{r}\left(-2\lambda_3\dot{r} - \lambda_1\lambda_2 r + \mathbf{u}_2 \cdot \left(\frac{\mathbf{F_T}}{m} + \mathbf{a}\right)\right) \tag{7}$$

$$\dot{\lambda}_2 = \frac{1}{r}\left(-2\lambda_2\dot{r} + \lambda_1\lambda_3 r + \mathbf{u}_3 \cdot \left(\frac{\mathbf{F_T}}{m} + \mathbf{a}\right)\right) \tag{8}$$

$$\dot{\Omega} = \lambda_1 \sin\theta / \sin i \tag{9}$$

$$\frac{di}{dt} = \lambda_1 \cos\theta \tag{10}$$

$$\dot{\theta} = \lambda_3 - \lambda_1 \sin\theta\cos i / \sin i \tag{11}$$

Note that, since we have described the motion of perturbed satellite m in the osculating plane $\xi\eta$, $\lambda_2 \equiv \dot{\lambda}_2 \equiv 0$. Then, we may write λ_1 by using Eq.(8) as

8

$$\lambda_1 = \frac{1}{\lambda_3 r} \mathbf{u}_3 \cdot \left(\frac{\mathbf{F_T}}{m} + \mathbf{a} \right) \tag{12}$$

Similarly, the equations of motion for the perturbing satellite m_p can be written as

$$\ddot{\rho} = (\omega_2^2 + \omega_3^2)\rho + \mathbf{e}_1 \cdot \Delta \mathbf{g} + \mathbf{e}_1 \cdot \left(-\mathbf{F_T} \frac{M}{m\,m_p} + \mathbf{a}_p - \mathbf{a} \right) \tag{13}$$

$$\dot{\omega}_3 = \frac{1}{\rho} \left(-2\omega_3 \dot{\rho} - \omega_1 \omega_2 \rho + \mathbf{e}_2 \cdot \Delta \mathbf{g} + \mathbf{e}_2 \cdot \left(-\mathbf{F_T} \frac{M}{m\,m_p} + \mathbf{a}_p - \mathbf{a} \right) \right) \tag{14}$$

$$\dot{\omega}_2 = \frac{1}{\rho} \left(-2\omega_2 \dot{\rho} + \omega_1 \omega_3 \rho - \mathbf{e}_3 \cdot \Delta \mathbf{g} - \mathbf{e}_3 \cdot \left(-\mathbf{F_T} \frac{M}{m\,m_p} + \mathbf{a}_p - \mathbf{a} \right) \right) \tag{15}$$

$$\dot{\theta}_2 = \omega_2 + \lambda_1 \sin \theta_3 \tag{16}$$

$$\dot{\theta}_3 = (\omega_3 - \lambda_1 \sin \theta_2 \cos \theta_3) / \cos \theta_2 - \lambda_3 \tag{17}$$

For tethered satellites, the gravity-gradient $\Delta \mathbf{g}$ in Eqs. (13) - (15) can be approximated [7] by

9

$$\Delta g \cong \frac{\mu}{r^3} \rho \begin{bmatrix} 3\cos^2\theta_2 \cos^2\theta_3 - 1 \\ -3\cos\theta_2 \cos\theta_3 \sin\theta_3 \\ 3\cos\theta_2 \cos^2\theta_3 \sin\theta_3 \end{bmatrix} \qquad (18)$$

3. Characteristics of GTSS Motion

The difference between GTSS and normal satellite dynamics is the existance of the tether force between two of the bodies that is non-gravitational. In Eqs. (1) and (2), the perturbations by F_T, a and a_p cause non-Keplerian motion of the GTSS. The effects of acceleration a and a_p are well developed by theories in orbital mechanics. Here, we neglect a and a_p to concentrate on the tether perturbation, which is provided by F_T.

If the tether is modeled as inextensible, then we can use the fact that $\ddot{\rho} \equiv 0$ to obtain the tether force from the Eq.(12) as

$$F_T = \frac{mm_p}{M} \rho [\omega_2^2 + \omega_3^2 + \frac{\mu}{r^3}(3\cos^2\theta_2 \cos^2\theta_3 - 1)] e_1 \qquad (19)$$

if the right-hand side of Eq. (19) is greater than zero, and $F_T = 0$ otherwise.

If we substitute Eq.(18) into Eqs. (6) - (12) then we have equations of motion for satellite m perturbed only due to the motion of tethered satellite m_p. To study characteristics of the highly non-linear tether perturbed motion in detail, we separate the analysis into non-librating and librating perturbations. If we assume near zero libration ($\theta_2 \approx \theta_3 \approx 0$), then the perturbing force vector becomes

$$F_T = \frac{mm_p}{M} \rho [\lambda_3^2 + 2\frac{\mu}{r^3}] e_1 \qquad (20)$$

Equations of motion of the perturbed satellite then become

$$\ddot{r} = \dot{\theta}^2 r \left[1 + \frac{m_p \rho}{Mr} \right] - \frac{\mu}{r^2} \left[1 - 2 \frac{m_p \rho}{Mr} \right] \qquad (21)$$

$$\ddot{\theta} = \frac{1}{r}\left(-2\dot{\theta}\dot{r} \right) \qquad (22)$$

since $\lambda_3 = \dot{\theta}$. Also $\lambda_1 = 0$, hence the orientation of the orbit plane remains constant

($\dot{\Omega} = 0$ and $\frac{di}{dt} = 0$). Equations (21) and (22) present a form of single satellite equations of

motion with the perturbing factors in equation in the radial direction. In Ref [7], an

"apparent gravitational constant", μ^*, was derived for the circular orbit ($\dot{r} = \ddot{r} = 0$) from

Eq.(21).

$$\mu^* = \mu \left[1 - 2 \frac{m_p \rho}{Mr} \right]\left[1 + \frac{m_p \rho}{Mr} \right]^{-1} \qquad (23)$$

For the pure Keplerian orbit, angular momentum is invariant, i.e., $\dot{\mathbf{h}} = 0$. In case of

the tether perturbed motion, the libration of the tethered satellite causes an angular

momentum change. The unit mass angular momentum vector for the perturbed satellite m

can be expressed as

$$\mathbf{h} = \mathbf{r} \times \dot{\mathbf{r}} \qquad (24)$$

By taking the derivative of Eq. (24) with respect to time, we get

$$\dot{h} = \begin{bmatrix} 0 \\ -\lambda_1\lambda_3 r^2 \\ \dot{\lambda}_3 r^2 + 2\lambda_3 r\dot{r} \end{bmatrix} \qquad (25)$$

We can substitute Eqs.(7) and (12) into Eq.(25) to obtain

$$\dot{h} = \begin{bmatrix} 0 \\ \dfrac{m_p}{M}\rho r \sin\theta_2 \left[\omega_2^2 + \omega_3^2 + \dfrac{\mu}{r^3}(3\cos^2\theta_2\cos^2\theta_3 - 1)\right] \\ \dfrac{m_p}{M}\rho r \cos\theta_2 \sin\theta_3 \left[\omega_2^2 + \omega_3^2 + \dfrac{\mu}{r^3}(3\cos^2\theta_2\cos^2\theta_3 - 1)\right] \end{bmatrix} \qquad (26)$$

Equation (26) is the time rate of change of angular momentum vector for the tether perturbed satellite. The second and third rows represent perturbations due to the out-of-plane libration and the in-plane libration, respectively.

Simulation results for an example of the tether perturbed orbital motion of the one of the satellites in a GTSS (based on the model described above) are illustrated in Fig. 3. System parameters selected are: m (perturbed satellite) = 1000 Kg, m_p (perturbing satellite) =100,000 Kg, tether length = 100 Km. The perturbing satellite's initial orbit is elliptical (e=0.3). The two satellites are positioned so that initially $\theta_3 = 0$ and $\theta_2 = 0.1$.
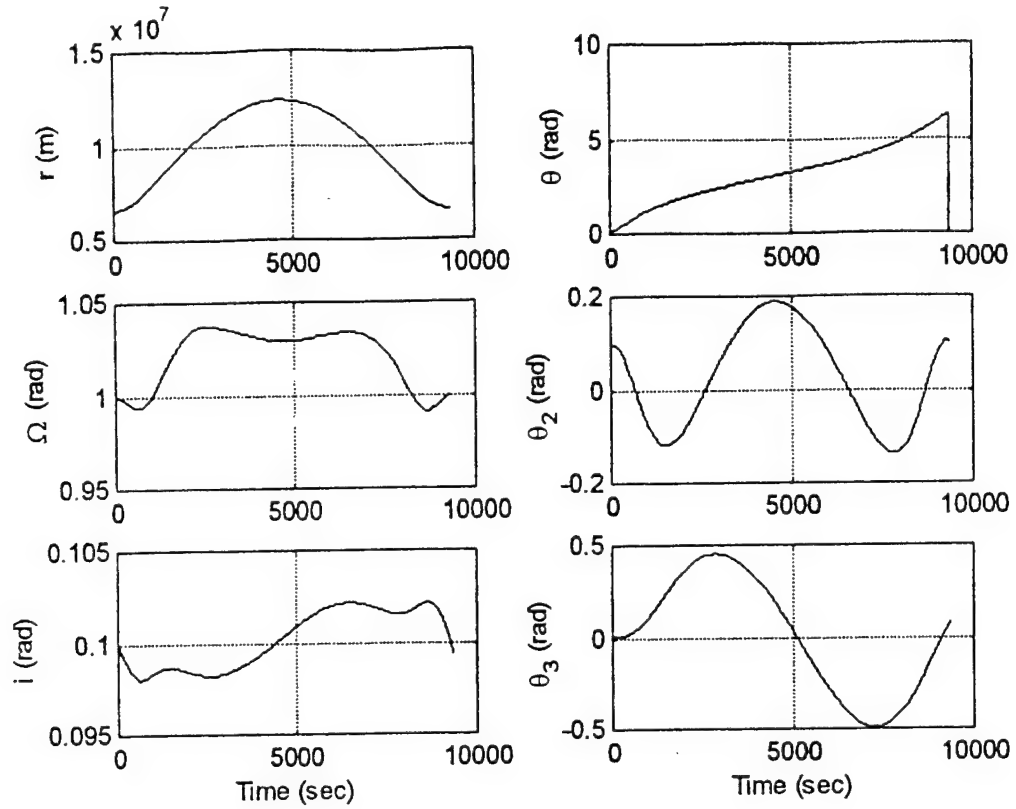
Figure 3. Tether Perturbed Motion of One of the Satellite of a GTSS.

Figure 3 shows the time variations of the longitude of the ascending node (Ω) and the inclination (i) due to the presence of the tethered satellite. The magnitudes of the perturbations in Ω and i are about 0.05 radian (3 degrees) and 0.005 radian (0.3 degree), respectively. Perturbations of the orbit parameters are small, but still may be large enough to cause problems for an identification and tracking process that uses a conventional method.

4. GTSS Identification

The problem considered in this paper is that of identifying an orbiting object as a tethered satellite. The interest in the identification of GTSS was initiated in early 1980's [4,5]. The main concern that motivated investigations was the possibility of a tethered satellite being mistaken for a ballistic missile if only one of the satellites in a tethered satellite system was observed.

In a Ref[5], the motion of tethered satellite was limited to planar motion and small libration angle so that the observation data could be applied to conventional estimation process, which estimated apparent gravitational constants (Eq. 22). From the estimated apparent gravitational constant, the tether parameter, $(m_p \rho)/M$, can be extracted and used to verify the orbit using the tethered satellite estimator. However for the more general case, the out-of-plane libration will cause changes in the orbital plane of the observed satellite, and the tracking process for a single satellite probably cannot be used for pre-process. Hence, the identification process has to be done by a single process.

As in Ref[7], non-dimensional equations are used. The non-dimensional time is defined as

$$\tau = t[\mu / r_\oplus^3]^{\frac{1}{2}} \tag{27}$$

Then, the non-dimensional equations for the satellite m are

14

$$r'' = \lambda_3^2 \, r - \frac{1}{r^2} + \varepsilon \cos\theta_2 \cos\theta_3 \, [\omega_2^2 + \omega_3^2 + \frac{1}{r^3}(3\cos^2\theta_2\cos^2\theta_3 - 1)] \qquad (28)$$

$$\lambda_3' = \frac{1}{r}\left(-2\lambda_3 \, r' + \varepsilon \cos\theta_2 \sin\theta_3 [\omega_2^2 + \omega_3^2 + \frac{1}{r^3}(3\cos^2\theta_2\cos^2\theta_3 - 1)] \right) \qquad (29)$$

$$\Omega' = \lambda_1 \sin\theta / \sin i \qquad (30)$$

$$\frac{di}{d\tau} = \lambda_1 \cos\theta \qquad (31)$$

$$\theta' = \lambda_3 - \lambda_1 \sin\theta \cos i / \sin i \qquad (32)$$

$$\lambda_1 = -\varepsilon \sin\theta_2 \frac{1}{\lambda_3 r}[\omega_2^2 + \omega_3^2 + \frac{1}{r^3}(3\cos^2\theta_2\cos^2\theta_3 - 1)] \qquad (33)$$

where ε, the "GTSS parameter", is defined as

$$\varepsilon \equiv \left[\frac{m_p \rho}{M r_\oplus} \right] \qquad (34)$$

Also, non-dimensional equations of motion for the perturbing satellite m_p can be written by

$$\omega_3' = -\omega_1 \omega_2 - \frac{1}{r^3}(3\cos\theta_2 \cos\theta_3 \sin\theta_3) \qquad (35)$$

$$\omega_2' = \omega_1 \omega_3 - \frac{1}{r^3} (3 \cos\theta_2 \cos^2\theta_3 \sin\theta_2) \tag{36}$$

$$\theta_2' = \omega_2 + \lambda_1 \sin\theta_3 \tag{37}$$

$$\theta_3' = (\omega_3 - \lambda_1 \sin\theta_2 \cos\theta_3) / \cos\theta_2 - \lambda_3 \tag{38}$$

here $(\ )' = d(\ )/d\tau$ and all variables in Eqs.(28)-(33) and (35)-(38) are in non-dimensional units.

The state vector to be estimated for the model is

$$X = \begin{bmatrix} r & \Omega & i & \theta & \theta_2 & \theta_3 & r' & \lambda_3 & \omega_2 & \omega_3 & \varepsilon \end{bmatrix}^T \tag{39}$$

The GTSS parameter ε in Eq. (39) plays a very important role for the identification problem. We consider a situation that we have a set of tracking data of an unknown object, which may be a single satellite, a tethered satellite, or a ballistic missile. If the object is tethered satellite system, then we obtain a non-zero ε by the estimation process. Theoretically, for a single satellite or a ballistic missile, ε is zero. However the estimation process which implements the GTSS dynamics cannot provide correct estimation results for a single satellite motion, since a singularity in the normal matrix occurs due to the tether dependent states in Eq. (39).

Once we estimate all states in Eq. (39), we may predict the satellite's motion. The parameter ε provides the information of the ratio of the masses of satellites and the tether length if the observed satellite is in a tethered satellite system. Also, $R_\oplus * \varepsilon$ is the position of the center of mass of the system. The tether length or mass ratio of the system cannot be obtained separately from observation of one of the satellite. Observations of both satellites are needed in order to obtain tether length or the mass ratio of the GTSS.

5. Simulation Results

Here, we present an example of the identification of the GTSS. Table 1 shows estimation results of a dumbbell type, two-satellite tethered system ($m = m_p = 100,000$ Kg and tether length = 10 Km) for different observation period. The states of the system and ε are estimated. We use a basic least-square batch estimator to determine the initial states given tracking data of one of the satellite (m). Near perfect tracking data generated by computer simulation is used. In this type of estimator, initial guess is critical for good results. The initial guess for states r, Ω, i, θ, and λ_3 can roughly be obtained and computed [8] from observation data. The states θ_2, θ_3 and ω_2 are guessed by assuming that they are normally expected to be small. If θ_3 remains small, then ω_3 should be close to λ_3. For the tether parameter ε, Table 2 provides a sample combination of the tether length and mass ratio and corresponding ε value. From Table 2, ε can be selected in $10^{-2} - 10^{-4}$ for the initial guess.

17

Table 1. Estimation Example (all numbers are Non-dimensional).

State	True State	Initial Guess	Observation Time (Orbital Period)			
			1	1/2	1/8	1/16
r	1.0549364	1.054	1.054936	1.054936	1.054936	1.054936
Ω	1.0	0.1	1.000000	1.000000	1.000000	1.000000
I	0.1	0.2	0.100000	0.100000	0.100000	0.100000
θ	0.0	0.5	0.296442e-8	0.221701e-8	0.861685e-8	0.213889e-8
θ_2	0.1	0.05	0.100000	0.100000	0.099996	0.099998
θ_3	0.0	0.1	0.111681e-5	0.169969e-5	-0.12611 e-4	-0.13267 e-3
r'	0.0	0.001	0.359428e-9	-0.67603 e-8	0.120944e-8	0.231482e-8
λ_3	1.0522822	1.0	1.052282	1.052282	1.052282	1.052282
ω_2	0.0	0.1	-0.11286 e-6	-0.14016 e-6	0.312860e-5	0.206399e-4
ω_3	1.0522822	1.0	1.052283	1.052276	1.052304	1.052592
ε	7.8480615e-4	1.0e-3	7.848070e-4	7.848036e-4	7.847946e-4	7.845962e-4

Table 2. Sample Tether Parameter ε.

		Tether Length ρ (Km)		
		100	10	1
m_p/M	1 ($m_p \gg m$)	1.57e-2	1.57e-3	1.57e-4
	0.5 ($m_p = m$)	7.85e-3	7.85e-4	7.85e-5
	0.1 ($m_p \ll m$)	1.57e-3	1.57e-4	1.57e-5

6. Conclusions

The identification and orbit determination of the general tethered satellite system using observations of only one of the satellites in the system has been considered. The parameter ε, which involves the ratio of the masses of satellites and the tether length, can be used to identify a satellite as a potential member of a tethered satellite system. A least-square batch-type estimator was used to determine the three-dimensional tether perturbed orbital motion. The entire state of the system and the ε may be estimated with long enough observation data sets. However, a more robust estimator will be needed for a quick identification of a satellite which is part of a GTSS.

7. Acknowledgement

8. References

[1] Tsiolkovsky, K. E., "Speculation between Earth and Sky," Isd-vo AN-SSR, 1895, p. 35 (reprinted 1959)

[2] Belesky, V. V., *Dynamics of Space Tether Systems*, Advances in the Astronautical Sciences, American Astronautical Society, San Diego, CA, 1993.

[3] Misra, A. K. and Modi, V. J.,"Survey on the Dynamics and Control of Tethered Satellite Systems," *Advanced in the Astronautical Sciences*, American Astronautical Society, Vol. 62, San Diego, CA,1986, pp.667-719.

[4] Hoots, F. R., Roehrich, R. L., and Szebehely, V. G., "Space Shuttle Tethered Satellite Analysis," Directorate of Astrodynamics, Peterson AFB, CO, August 1983.

[5] T.A. Asher, D.G. Boden, and R.J. Tegtmeyer, "Tethered satellites: The orbit Determination problem and Missile Early Warning Systems,"AIAA PAPER 88-4284, *AIAA/AAS Astrodynamics Conference*, Minneapolis, MN, August 15-17, 1988

[6] Kessler, S. A., and Cicci, D. A., "Filtering Methods for Orbit Determination of a Tethered Satellite," *Journal of the Astronautical Sciences*, Vol. 45, No. 3, July-September 1997, pp. 263-278.

[7] Cochran, J. E., Jr., Cho, S., Cheng, Y-M., and Cicci, D. A., "Dynamics and Orbit Determination of Tethered Satellite Systems," AAS 96-147, *AAS/AIAA Space Flight Mechanics Meeting*, Austin, TX, February 12-15, 1996.

[8] Escobal, P. R., *Methods of Orbit Determination*, John Wiley & Sons, Inc., New York, 1976.

A LOOK AT TETHERED SATELLITE IDENTIFICATION USING RIDGE-TYPE ESTIMATION METHODS

D. A. Cicci[1], C. Qualls[2], and T. A. Lovell[2]
Auburn University, Alabama

Recent studies of ill-conditioned orbit determination problems have demonstrated that ridge-type estimation methods have the capability to provide increased solution accuracy over classical estimation techniques. These advanced estimation methods add a small amount of bias to the solution in order to decrease the total variance of the estimates. Even though the addition of bias to the solution results in a slightly poorer data fit, the overall solution accuracy can be improved in certain types of ill-conditioned problems. One application in which the usefulness of ridge-type estimation methods has been demonstrated is the problem of quick-look orbit determination, i.e., the problem of accurately determining the trajectory of a spacecraft using only a short arc of observational data.

One similar type of orbit determination problem which has received renewed interest lately is that of the identification of a satellite to be part of a tethered satellite system without prior knowledge that it is so. A batch filter has recently been developed which has the capability of identifying a satellite to be tethered, however the accuracy of this filter is highly dependent on the amount of observational data being processed. The performance of this filter has indicated that the shorter the data arc, the more ill-conditioned the problem, thereby resulting in inaccurate solutions.

This paper applies ridge-type estimation methods to the problem of identifying a tethered satellite using short arcs of observational data. Performance of the ridge-type filter is evaluated for cases of differing tether lengths, tether orientations, levels of observation error, and observation span. Results will be compared to those obtained from classical minimum variance methods with special attention being given to the speed at which the identification of a tethered satellite can take place.

INTRODUCTION

Renewed interest in the use of tethered satellites has motivated recent studies addressing the problem of how to accurately track, identify, and predict the motion of a tethered satellite system (TSS) [1-6]. If the motion of a TSS is not analyzed accurately, a tethered satellite could

---

be incorrectly identified as a ballistic threat, causing military measures to be taken in response. This is due to the fact that the force in the tether creates perturbations on the satellite causing a tethered satellite to behave differently from an untethered one in that it will deviate from the Keplerian-like motion followed by an untethered satellite [1].

Classical orbit determination methods do not possess the capabilities to determine whether or not a tracked satellite is part of a tethered system. Such methods will therefore identify and track the satellite as if it were an untethered one, which will likely cause an inaccurate prediction of the trajectory and perhaps a false identification of the vehicle if it is indeed tethered. The problem of identification is compounded by the fact that this process must be performed quickly using as short of an arc of observational data as possible. These 'quick-look' orbit determination problems tend to be highly ill-conditioned due to an inadequate observation sample, which is generally caused by too few, too 'noisy', or inadequately spaced observations. It is well known that conventional estimation techniques such as least squares and minimum variance methods perform poorly in ill-conditioned problems. The estimates can be unreasonable in value and even have the incorrect sign, even though they would satisfy the basic premise of the minimization of the sum of the squared observation residuals. Of additional concern in many quick-look applications is the unreliable performance of predictions, beyond the fit interval, based upon these inaccurate estimates.

A class of biased estimation methods, which are based upon the theory of 'ridge regression,' has been shown by Hoerl and Kennard [7, 8] to yield more accurate solutions in ill-conditioned problems of this type. Cicci and Tapley [9] have developed modifications to the classical ridge regression theory, termed 'ridge-type' estimation methods, which provide solutions in both ill-conditioned and unobservable problems, i.e., problems in which the normal matrix is singular. In addition, Cicci [10] has developed ridge-type methodology to incorporate multiple types of observations, having differing accuracies, into the solution process.

This study presents the application of ridge-type estimation methods to the quick-look orbit determination of a TSS. Performance of the ridge-type filter is evaluated for cases of differing tether lengths, tether orientations, levels of observation error, and observation span. Results are compared to those obtained using conventional minimum variance techniques.

TETHERED SATELLITE SYSTEM MODEL

The description of the TSS model used in this study and described here was previously presented by Cicci et al [11].

The coordinate systems and position vectors used to describe the motion of a two-satellite TSS are depicted in Figure 1. The Earth (E), the observed "daughter" satellite (m), and the unobserved "parent" satellite (m_p) are all modeled as point masses, while the mass of the tether is neglected. The origin of the fixed xyz system is the Earth, as well as the coordinate system defined by unit vectors u_1, u_2, and u_3. The u_1u_2 plane is the osculating plane in which mass m is

2

moving at some point in time. The orientation of the osculating plane is defined by Ω and i, the longitude of the ascending node and inclination, respectively. The vector **r** defines the position of satellite m with respect to Earth while the vector $\mathbf{r_p}$ defines the position of satellite m_p with respect to Earth. For the TSS model used in this study, the forces considered on each satellite are due only to the inverse-squared gravitational attraction of the Earth, and the force due to the tension in the tether. Thus, the equations of motion for the satellites m and m_p become

$$\ddot{\mathbf{r}} = -\mu \frac{\mathbf{r}}{r^3} + \frac{\mathbf{F_T}}{m} \tag{1}$$

$$\ddot{\mathbf{r}}_p = -\mu \frac{\mathbf{r}_p}{r_p^{\ 3}} - \frac{\mathbf{F_T}}{m_p} \tag{2}$$

where the tether tension force $\mathbf{F_T}$ is positive in the direction from m to m_p.

Figure 1. Osculating Orbit Plane

In Figure 1, the vector ρ is the relative position vector of m_p with respect to m. By using equations (1) and (2), we may then write

3

$$\ddot{\rho} = \Delta g - \frac{M}{m\,m_p} F_T \qquad (3)$$

where, $$M = m + m_p \qquad (4)$$

and $$\Delta g \equiv -\frac{\mu}{r_p^3} r_p + \frac{\mu}{r^3} r . \qquad (5)$$

To describe the motion of m_p with respect to m, Figure 2 shows a third coordinate system, $e_1e_2e_3$. The orientation of $e_1e_2e_3$ with respect to $u_1u_2u_3$ is given by the angles θ_3 and θ_2, which are termed the in-plane and out-of-plane libration angles, respectively.

Figure 2. Relative Motion of m_p with respect to m

We may express the equations of motion for m and m_p in the rotating frames $u_1u_2u_3$ and $e_1e_2e_3$, respectively, as

$$\ddot{r} + \dot{\lambda} \times r + 2\lambda \times \dot{r} + \lambda \times \lambda \times r = -\mu \frac{r}{r^3} + \frac{F_T}{m} \qquad (6)$$

$$\ddot{\rho} + \dot{\omega} \times \rho + 2\omega \times \dot{\rho} + \omega \times \omega \times \rho = \Delta g - F_T \frac{M}{m\,m_p} \qquad (7)$$

where λ in equation (6) is the angular velocity of the $u_1u_2u_3$ coordinate system., and ω in equation (7) is the angular velocity of the $e_1e_2e_3$ coordinate system.

Equations (6) and (7) can be used to obtain the following scalar equations for the motion of m:

4

$$\ddot{r} = (\lambda_2^2 + \lambda_3^2)r - \frac{\mu}{r^2} + \mathbf{u}_1 \cdot \frac{\mathbf{F}_T}{m} \tag{8}$$

$$\dot{\lambda}_3 = \frac{1}{r}\left(-2\lambda_3\,\dot{r} - \lambda_1\,\lambda_2\,r + \mathbf{u}_2 \cdot \frac{\mathbf{F}_T}{m}\right) \tag{9}$$

$$\dot{\lambda}_2 = \frac{1}{r}\left(-2\lambda_2\,\dot{r} + \lambda_1\,\lambda_3\,r + \mathbf{u}_3 \cdot \frac{\mathbf{F}_T}{m}\right) \tag{10}$$

$$\dot{\Omega} = \lambda_1\,\sin\theta\,/\sin i \tag{11}$$

$$\frac{di}{dt} = \lambda_1 - \cos\theta \tag{12}$$

$$\dot{\theta} = \lambda_3 - \lambda_1\,\sin\theta\,\sin i\,/\cos i \tag{13}$$

Since we have described the motion of the daughter satellite in the $\mathbf{u}_1\mathbf{u}_2$ osculating plane, $\lambda_2 \equiv \dot{\lambda}_2 \equiv 0$. By using equation (10), λ_1 can be written as

$$\lambda_1 = \frac{1}{\lambda_3 r}\mathbf{u}_3 \cdot \frac{\mathbf{F}_T}{m} \tag{14}$$

Similarly, the equations of motion for satellite m_p can be written as

$$\ddot{\rho} = (\omega_2^2 + \omega_3^2)\rho + \mathbf{e}_1 \cdot \Delta \mathbf{g} + \mathbf{e}_1 \cdot \mathbf{F}_T\frac{M}{m\,m_p} \tag{15}$$

$$\dot{\omega}_3 = \frac{1}{\rho}\left(-2\omega_3\,\dot{\rho} - \omega_1\,\omega_2\,\rho + \mathbf{e}_2 \cdot \Delta \mathbf{g} + \mathbf{e}_2 \cdot \mathbf{F}_T\frac{M}{m\,m_p}\right) \tag{16}$$

$$\dot{\omega}_2 = \frac{1}{\rho}\left(-2\omega_2\,\dot{\rho} + \omega_1\,\omega_3\,\rho - \mathbf{e}_3 \cdot \Delta \mathbf{g} + \mathbf{e}_3 \cdot \mathbf{F}_T\frac{M}{m\,m_p}\right) \tag{17}$$

$$\dot{\theta}_2 = \omega_2 + \lambda_1\,\sin\theta_3 \tag{18}$$

$$\dot{\theta}_3 = (\omega_3 - \lambda_1\,\sin\theta_2\,\cos\theta_3)/\cos\theta_2 - \lambda_3 \tag{19}$$

5

If the tether is modeled as inextensible, then $\ddot{\rho} \equiv 0$ and F_T will always be in the e_1 direction. This eliminates the F_T term from equations (16) and (17) and, in the case where the right-hand side of equation (20) is greater than zero, allows us to obtain the tether force from equation (15) as

$$\mathbf{F}_T = \frac{m\,m_p}{M}\,\rho\,[\omega_2^2 + \omega_3^2 + \frac{\mu}{r^3}\,(3\,\cos^2\theta_2\,\cos^2\theta_3 - 1)]\,\mathbf{e}_1 \qquad (20)$$

Otherwise, the value of F_T is zero. In order to simulate the dynamic motion of a particular tethered system using the above model, the quantities m, m_p and ρ must be specified, as well as initial conditions on r, Ω, i, θ, θ_2, θ_3, $\dot{r}$, λ_3, ω_2, and ω_3.

FILTER DESCRIPTION

A batch-type filter will be used to estimate the state of the satellite which is being tracked by processing observational data in one group or batch. In order for this filter to be capable of distinguishing between a tethered satellite and an untethered one however, the effects of the tether force must be accounted for within the filter's dynamical model. This will require inclusion of tether specific parameters in the filter which will allow the filter to distinguish between Keplerian-like motion and modified Keplerian motion.

The major difference between the motion of a tethered satellite and an untethered one is that its velocity is affected by the parent satellite due to the tether force between the bodies. Unless the filter model is able to account for these differing velocities, inaccurate state estimates of the tethered satellite will be obtained. Figure 3 shows a tethered (daughter) satellite, m, and the effective tether force, F, due to the presence of the parent satellite, m_p.

The effect of the tether force on the motion of a satellite can be easily seen by considering the separate effects of the radial and tangential force components, F_r and F_t, respectively. These force components will tend to change the acceleration on the satellite in their respective directions, thereby altering the satellite's velocity. The presence of F_r, for example, will change the radial acceleration which is normally determined by the gravitational constant, μ. This acceleration component will reduce the radial acceleration on the satellite if the orbit of the daughter is lower than that of the parent and increase the radial acceleration on the satellite if the daughter's orbit is higher than the parent's. A reduced radial acceleration will result in a smaller velocity for the daughter than that of an untethered satellite, while an increased radial acceleration will result in a larger velocity for the daughter than that of an untethered satellite. Similarly, the presence of F_t, has the effect of decreasing the velocity of the daughter satellite when it leads the parent satellite, whereas it increases the daughter satellite's velocity when it lags behind the parent satellite.

6
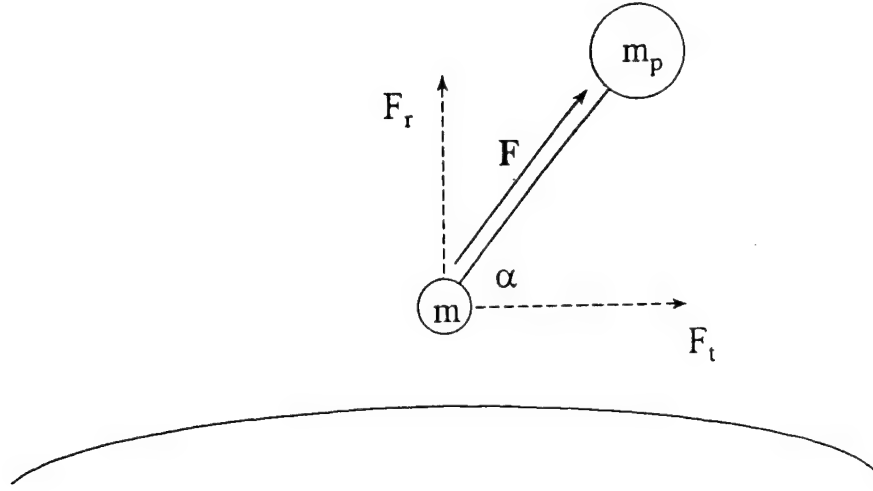
Figure 3. Tethered Satellite System

Two tether specific acceleration parameters, a_r and a_t, resulting from the tether force, can be included in the state vector of the filter, and estimation of these parameters can then be used to indicate the existence of a tether force acting on the satellite. If these terms are computed to be zero, no tether force will be present and the satellite can be considered to be an untethered one. Therefore, a state vector, $\mathbf{X}$, can be defined to include the satellite's position and velocity components in Cartesian form, in addition to a_r and a_t, as shown by

$$\mathbf{X} = \begin{bmatrix} x \\ y \\ z \\ \dot{x} \\ \dot{y} \\ \dot{z} \\ a_r \\ a_t \end{bmatrix} = \begin{bmatrix} X_1 \\ X_2 \\ X_3 \\ X_4 \\ X_5 \\ X_6 \\ X_7 \\ X_8 \end{bmatrix} \tag{21}$$

The state equations for this filter will take the form

$$\dot{\mathbf{X}} = \mathbf{F}(\mathbf{X}, t), \qquad \mathbf{X}(t_k) = \mathbf{X}_k \tag{22}$$

7

where t_k indicates the epoch time, and the force vector, $\mathbf{F(X,}t)$ can be represented by the equations

$$\mathbf{F(X,}t) = \begin{bmatrix} X_4 \\ X_5 \\ X_6 \\ \dfrac{-\mu X_1}{|\mathbf{r}|^3} + \dfrac{a_r X_1}{|\mathbf{r}|} - \dfrac{a_t X_4}{|\mathbf{v}|} \\ \dfrac{-\mu X_2}{|\mathbf{r}|^3} + \dfrac{a_r X_2}{|\mathbf{r}|} - \dfrac{a_t X_5}{|\mathbf{v}|} \\ \dfrac{-\mu X_3}{|\mathbf{r}|^3} + \dfrac{a_r X_3}{|\mathbf{r}|} - \dfrac{a_t X_6}{|\mathbf{v}|} \\ 0 \\ 0 \end{bmatrix} \tag{23}$$

Here, $|\mathbf{r}|$ is the magnitude of the position vector and $|\mathbf{v}|$ is the magnitude of the velocity vector.

In order to estimate the initial conditions of the state vector, measurements of the satellite's range, range-rate, azimuth, and/or elevation are made over a given time frame. The observations are then mapped backward to the initial time. The expression for mapping observations to the desired epoch time is given by

$$\mathbf{y = Hx + \varepsilon} \tag{24}$$

where $\mathbf{y}$ is an (mx1) vector of observation residuals, $\mathbf{H}$ is an (mxn) mapping matrix, $\mathbf{x}$ is an (nx1) vector of corrections to the state vector, and ε is a (mx1) vector of measurement errors. The $\mathbf{H}$ matrix is a function of the state transition matrix, which allows the state vector to be mapped from one time to another. The measurement errors are assumed to be random and have a Gaussian (normal) distribution with zero mean and (m x m) covariance matrix equal to $\mathbf{R}$.

The method used here is to estimate the corrections to the nominal state vector, x_k, at the epoch time. The conventional minimum variance solution for the state correction is provided by Tapley and Szebehely [12] as

$$\mathbf{\hat{x} = (H^T R^{-1} H)^{-1} H^T R^{-1} y} \tag{25}$$

This solution form is used in order to achieve solution convergence, in the non-linear sense, prior to application of the ridge-type estimation methods to be described below.

8

The ridge-type estimator which will be used in this analysis was presented by Cicci [10] and considers the solution form

$$\hat{x}_N^{\bullet} = \left(H_N^T H_N + K \right)^{-1} H^T R^{-1} y \tag{26}$$

where

$$\hat{x}^{\bullet} = D_R \hat{x}_N^{\bullet} \tag{27}$$

$$H_N^T H_N = D_R H^T R^{-1} H D_R \tag{28}$$

and D_R is an (n x n) diagonal matrix whose i^{th} diagonal element is the reciprocal of the square root of the corresponding element of $H^T R^{-1} H$. Also, K is the (n x n) diagonal matrix of biasing parameters k_i, $i = 1 \rightarrow n$. The state correction obtained from equation (26) will attempt to improve the state correction obtained using the minimum variance solution of equation (25).

The covariance matrix of the ridge-type solution provided by equations (26) and (27) is given as

$$P(\hat{x}^{\bullet}) = (H^T R^{-1} H + D_R^{-1} K D_R^{-1})^{-1} H^T R^{-1} H (H^T R^{-1} H + D_R^{-1} K D_R^{-1})^{-1} \tag{29}$$

and the total variance of the solution will be

$$V(\hat{x}^{\bullet}) = tr \, [P(\hat{x}^{\bullet})] \tag{30}$$

The diagonal elements of K, i.e., each k_i, are optimally chosen to minimize the Mean Square Error (MSE) of the solution which is given by

$$MSE = tr(H_N^T H_N + K)^{-1} H_N^T H_N (H_N^T H_N + K)^{-1}$$

$$+ x_N [H_N^T H_N (H_N^T H_N + K)^{-2} H_N^T H_N - H_N^T H_N (H_N^T H_N + K)^{-1}$$

$$- (H_N^T H_N + K)^{-1} H_N^T H_N + I_n] x_N \tag{31}$$

The MSE consists of the sum of the total variance of the solution and the square of the bias introduced by the inclusion of K in the solution process. The minimization process leads to an iterative solution, as shown by Cicci [10], known as the multiple biasing parameter solution as

9

$$k_i = (\hat{x}_{n_i}^\bullet)^{-2} \quad, \quad i = 1 \to n \tag{32}$$

This iterative solution terminates with stability in the quantity: $(\hat{x}_N^\bullet)^T (\hat{x}_N^\bullet)$

Two variations for the computation of the biasing parameters are provided by Cicci and Hall [13] as follows:

1. The averaging of the biasing parameter over all variables comprising the state vector, i.e., single biasing parameter solution, giving

$$K = k\, I_n \quad, \quad k = \frac{n}{(\hat{x}_N^\bullet)^T (\hat{x}_N^\bullet)} \tag{33}$$

2. The averaging of the biasing parameters over different types of model variables, e.g., position components as one type, velocity components as another, etc., i.e. variable-type biasing parameter solution, giving

$$k_i = \frac{q_i}{\sum\limits_{j=q_1+q_2+\ldots+q_{i-1}+1}^{q_1+\ldots+q_i} (\hat{x}_{N_j}^\bullet)^2} \quad, \quad i = 1 \to q \tag{34}$$

where q is the number of different types of variables in the model, and $q_1, q_2, \ldots, q_q$ are the number of model variables of each type, respectively. Equation (34) assumes that variables of the same type are grouped together within the state vector.

Including the biasing parameters in the solution process will increase the size of each eigenvalue of the normal matrix and allow the system to behave as a more well-conditioned system. The effect this will have on the solution is to decrease the total variance while increasing the RMS.

This batch filter will be used to determine the state of the observed satellite at the initial time. Once the parameters, a_r and a_t, are obtained, several determinations can be made as described by Cicci et al [11].

1. If both a_r and a_t are equal to zero, it can be assumed that the satellite is not part of a tethered system and its motion can be analyzed using standard techniques.

2. If a_r and a_t are not equal to zero:

    (a) Their values can be used to determine the tether orientation angle, α, from

10

$$\alpha = \tan^{-1}(a_r / a_t) \tag{35}$$

(b) The magnitude of the tether force (per unit mass) can be calculated by

$$F/m = [a_r^2 + a_t^2]^{1/2} \tag{36}$$

(c) The apparent value of the gravitational parameter, $\mu*$, can be determined from the expression

$$\mu^* = \mu - a_r r^2 \tag{37}$$

This $\mu*$ can then be used along with the position and velocity vectors to determine the orbital element set which fully describes the satellite's orbit.

(d) The value of $\mu*$ can be used to determine ρ_{cm}, the distance the tethered satellite is located above or below the center-of-mass of the system. An approximation for $\mu*$ was provided in [4] in terms of ρ_{cm} as

$$\rho_{cm} = \left(\frac{\mu - \mu^*}{2\mu + \mu^*} \right) r \tag{38}$$

when the daughter satellite is below the parent satellite, and

$$\rho_{cm} = \left(\frac{\mu^* - \mu}{2\mu + \mu^*} \right) r \tag{39}$$

when the daughter satellite is above the parent satellite. Since ρ_{cm} approaches the actual tether length as the ratio of the daughter mass to the parent mass gets small, ρ_{cm} can be a very useful parameter to estimate.

3. If a_t is equal to zero but a_r is not, the satellite will be tethered and the orientation of the system will be vertical, i.e., $\alpha = 0°$ or $180°$.

4. If a_r is equal to zero but a_t is not, the satellite will be tethered and the orientation of the system will be horizontal, i.e., $\alpha = 90°$ or $270°$.

11

RESULTS

In order to evaluate the filter's performance, the TSS model was used to generate simulated observational data for a single (Keplerian) satellite as well as several tethered configurations. For discussion of the results it is most useful to define a "baseline" TSS configuration and to construct all other configurations as modifications to this baseline. Consider a tethered pair with the following parameters and initial state values:

$$m = 10 \text{ kg} \qquad \theta_2 = 0 \text{ rad}$$
$$m_p = 100 \text{ kg} \qquad \theta_3 = 0 \text{ rad}$$
$$r = 6621000 \text{ m} \qquad \dot{r} = 0 \text{ m/sec}$$
$$\Omega = 0.1 \text{ rad} \qquad \lambda_3 = 1.17164 \times 10^{-3} \text{ rad/sec}$$
$$i = 0.1 \text{ rad} \qquad \omega_2 = 0 \text{ rad/sec}$$
$$\theta = 0 \text{ rad} \qquad \omega_3 = 1.17164 \times 10^{-3} \text{ rad/sec}$$

Note that the initial values for the in-plane and out-of-plane libration angles, θ_3 and θ_2, respectively, are zero. This indicates a vertical orientation of mass m being directly above or below mass m_p. This initial orientation will change due to the presence of the Earth's oblateness in the dynamical model, however the small changes that result will not have a major effect on the analysis. This baseline configuration can then be modified by varying the following parameters:

    (a) types of measurements utilized by the filter,
    (b) tether length and orientation,
    (c) observation error level, and
    (d) observation span

In the results that follow, the performance of the filters are evaluated for a single satellite, the baseline TSS scenario, and several variations, based on the above modifications. Results are obtained for the conventional minimum variance solution as well as for the three ridge-type filter solutions described earlier. These solutions will be designated as MV (minimum variance), R-S (ridge, single biasing parameter), R-M (ridge, multiple biasing parameter), and R-VT (ridge, variable-type biasing parameter).

Initial Conditions

Table 1 provides the true initial conditions for a single satellite and for the various TSS configurations addressed in this study. The initial guess in each case, **X***, was constructed by perturbing the true state by the amounts shown in Table 2. This small amount of perturbation was chosen to be within the radius of convergence required for the linear estimation procedures to be used in this study.

State	Single Satellite	TSS			
		1km	10 km	50 km	1 km lib
x (m)	6587922.5783058	6587922.5783058	6587922.5783058	6587922.5783058	6587922.5783058
y (m)	660997.0516186	660997.0516186	660997.0516186	660997.0516186	660997.0516186
z (m)	0.0000000	0.0000000	0.0000000	0.0000000	0.0000000
v_x (m/s)	-770.7400449	-770.5813356	-769.1555950	-762.8760417	-770.8988131
v_y (m/s)	7681.6919707	7680.1101714	7665.9003211	7603.3142464	7683.2743566
v_z (m/s)	774.6098678	774.45C.016	773.0174624	766.7063800	774.7694331
a_t (m/s^2)	0.0000000	0.00?0?00	0.0000000	0.0000000	0.0000000
a_r (m/s^2)	0.0000000	0.0037443	0.0373460	0.1849707	-0.0037465
ρ_{cm} (m)	---	909.0909100	9090.9091000	45203.2505417	909.0909100

Table 1. True Initial Conditions for Single Satellite and TSS Configurations.

State	Perturbation
x	100.0 m
y	-100.0 m
z	100.0 m
v_x	- 0.25 m/s
v_y	- 0.25 m/s
v_z	0.25 m/s
a_t	1.0×10^{-5} m/s^2
a_r	0.01 m/s2

Table 2. Initial Condition Perturbations.

Types of Measurements Utilized by the Filter

The filter will process a combination of range, azimuth, and elevation angle measurements simultaneously at each observation time.

Tether Length and Orientation

Four different selections of tether length and satellite orientation will be considered. Tether lengths of 1 km, 10 km, and 100 km where the daughter satellite is positioned below the parent satellite, and a tether length of 1 km lib (up) where the daughter satellite is positioned above the parent satellite will be evaluated in the analysis. Considering orientation of the TSS and the size of the masses being used in the model, the resulting true values of ρ_{cm} will be: 1 km (ρ_{cm} = 909.1 m), 10 km (ρ_{cm} = 9,090.1 m), 100 km (ρ_{cm} = 90,909.1 m).

13

Observation Error Level

Three levels of observation error for each type of measurement will be added as Gaussian noise to the perfect observations generated by the TSS model. These noise levels will be classified as high, medium, and low and the standard deviations, σ, of these errors are provided in Table 3.

	Measurement Type	
Noise Level	Range Error	Angles Error
High	50 m	0.02 deg
Medium	25 m	0.01 deg
Low	5 m	0.002 deg

Table 3. Standard Deviation of Observation Error Levels.

Observation Span

In order to demonstrate the quick-look orbit determination capabilities of the filters, four observation spans will be considered. These arc lengths will be 5 min, 10 min, 15 min, and 20 min. The first ten minutes of observational data will be provided by one tracking station while the second ten minutes of data will be provided by a second tracking station. The data-sampling rate will be 5 seconds in all cases.

Using the combinations described above, a total of 192 runs were made and the results are provided in Tables 4-7. Each table includes the minimum variance and three ridge-type solutions for four data arcs considering each of the three levels of measurement error. The results which are presented include the RMS of the solution, a calculated value of the length of the tether to the TSS center-of-mass ρ_{cm}, and the difference between the true ρ_{cm} and calculated ρ_{cm}. The accuracy of this quantity will be a strong indication whether the satellite being tracked is part of a TSS or is a single satellite.

14

	High Noise	MV	R - S	R - M	R - VT
5 min obs	RMS	1.016	1.050	1.042	1.047
	ρ_{cm} (m)	-10520.875	487.876	45.893	143.549
	$\rho_{cm} - \rho_{cm}*$ (m)	11429.965	421.215	863.198	765.542
10 min obs	RMS	1.020	1.031	1.023	1.028
	ρ_{cm} (m)	1784.782	558.813	1214.130	1204.260
	$\rho_{cm} - \rho_{cm}*$ (m)	875.692	350.278	305.039	295.169
15 min obs	RMS	1.007	1.011	1.010	1.013
	ρ_{cm} (m)	806.770	1036.586	1285.450	1283.151
	$\rho_{cm} - \rho_{cm}*$ (m)	102.321	127.493	376.359	374.060
20 min obs	RMS	0.996	1.000	1.001	1.005
	ρ_{cm} (m)	406.236	776.510	660.888	900.668
	$\rho_{cm} - \rho_{cm}*$ (m)	502.855	132.581	248.202	8.423

	MediumNoise	MV	R - S	R - M	R - VT
5 min obs	RMS	1.016	1.052	1.031	1.047
	ρ_{cm} (m)	-4810.979	545.087	31.374	48.897
	$\rho_{cm} - \rho_{cm}*$ (m)	5720.070	364.004	877.717	860.194
10 min obs	RMS	1.020	1.026	1.024	1.026
	ρ_{cm} (m)	1348.041	842.442	1254.448	1258.261
	$\rho_{cm} - \rho_{cm}*$ (m)	438.950	66.649	345.357	349.170
15 min obs	RMS	1.027	1.027	1.027	1.028
	ρ_{cm} (m)	1223.747	1170.796	1245.642	1295.419
	$\rho_{cm} - \rho_{cm}*$ (m)	314.656	261.705	336.551	386.328
20 min obs	RMS	1.032	1.032	1.032	1.033
	ρ_{cm} (m)	1054.815	1066.370	1097.533	1167.822
	$\rho_{cm} - \rho_{cm}*$ (m)	145.724	157.279	188.442	258.732

	Low Noise	MV	R - S	R - M	R - VT
5 min obs	RMS	1.016	1.027	1.021	1.019
	ρ_{cm} (m)	-234.323	884.202	9.985	11.435
	$\rho_{cm} - \rho_{cm}*$ (m)	1143.414	24.886	899.106	897.656
10 min obs	RMS	1.020	1.021	1.021	1.022
	ρ_{cm} (m)	998.637	964.728	1052.959	1045.460
	$\rho_{cm} - \rho_{cm}*$ (m)	89.546	55.637	143.868	136.369
15 min obs	RMS	1.027	1.027	1.028	1.028
	ρ_{cm} (m)	974.145	964.112	971.222	978.747
	$\rho_{cm} - \rho_{cm}*$ (m)	65.054	55.022	62.131	69.656
20 min obs	RMS	1.032	1.031	1.031	1.031
	ρ_{cm} (m)	940.742	943.840	948.414	955.626
	$\rho_{cm} - \rho_{cm}*$ (m)	31.651	34.749	39.323	46.535

Table 4. Range and Angle Measurements, 1 km Tether Length ($\rho_{cm} = 909.1$ m).

	High Noise	MV	R - S	R - M	R - VT
5 min obs	RMS	1.016	1.042	1.047	1.052
	ρ_{cm} (m)	-2400.054	5718.181	117.757	125.214
	$\rho_{cm} - \rho_{cm}*$ (m)	11490.963	3372.728	8973.152	8965.695
10 min obs	RMS	1.020	1.021	1.024	1.027
	ρ_{cm} (m)	9972.480	8913.378	9917.115	9442.339
	$\rho_{cm} - \rho_{cm}*$ (m)	881.571	177.531	826.206	351.430
15 min obs	RMS	1.027	1.037	1.047	1.045
	ρ_{cm} (m)	9728.969	9287.654	9332.418	9275.027
	$\rho_{cm} - \rho_{cm}*$ (m)	638.060	196.745	241.509	184.118
20 min obs	RMS	1.032	1.035	1.041	1.040
	ρ_{cm} (m)	9393.218	9650.520	9569.441	9703.003
	$\rho_{cm} - \rho_{cm}*$ (m)	302.309	559.611	478.532	612.094

	Medium Noise	MV	R - S	R - M	R - VT
5 min obs	RMS	1.016	1.030	1.035	1.038
	ρ_{cm} (m)	3342.404	7206.493	9024.762	9316.317
	$\rho_{cm} - \rho_{cm}*$ (m)	5748.505	1884.416	66.148	225.408
10 min obs	RMS	1.020	1.021	1.023	1.026
	ρ_{cm} (m)	9535.943	9218.481	9454.881	9470.850
	$\rho_{cm} - \rho_{cm}*$ (m)	445.034	127.572	363.972	379.941
15 min obs	RMS	1.027	1.032	1.038	1.031
	ρ_{cm} (m)	9416.476	9049.048	9032.391	9168.080
	$\rho_{cm} - \rho_{cm}*$ (m)	325.567	41.861	58.518	77.171
20 min obs	RMS	1.032	1.036	1.089	1.033
	ρ_{cm} (m)	9250.906	9460.220	9467.507	9347.343
	$\rho_{cm} - \rho_{cm}*$ (m)	159.997	369.311	376.598	256.434

	Low Noise	MV	R - S	R - M	R - VT
5 min obs	RMS	1.016	1.016	1.021	1.022
	ρ_{cm} (m)	7945.140	7922.591	8727.462	9015.994
	$\rho_{cm} - \rho_{cm}*$ (m)	1145.769	1168.318	363.447	74.915
10 min obs	RMS	1.020	1.020	1.022	1.021
	ρ_{cm} (m)	9186.702	9227.317	9336.347	9295.080
	$\rho_{cm} - \rho_{cm}*$ (m)	95.793	136.408	245.438	204.171
15 min obs	RMS	1.027	1.027	1.029	1.027
	ρ_{cm} (m)	9166.443	9139.598	9124.178	9154.019
	$\rho_{cm} - \rho_{cm}*$ (m)	75.534	48.689	33.269	63.110
20 min obs	RMS	1.032	1.032	1.032	1.032
	ρ_{cm} (m)	9137.043	9159.726	9141.980	9141.956
	$\rho_{cm} - \rho_{cm}*$ (m)	46.134	68.817	51.071	51.047

Table 5. Range and Angle Measurements, 10 km Tether Length (ρ_{cm} = 9,090.1 m).

16

	High Noise	MV	R - S	R - M	R - VT
5 min obs	RMS	1.016	1.017	1.030	1.026
	ρ_{cm} (m)	77585.959	76996.375	89280.030	89198.267
	$\rho_{cm} - \rho_{cm}{}^*$ (m)	13323.132	13912.716	1629.061	1710.824
10 min obs	RMS	1.020	1.032	1.028	1.034
	ρ_{cm} (m)	90632.005	94204.125	93568.007	94020.249
	$\rho_{cm} - \rho_{cm}{}^*$ (m)	277.086	3295.034	2658.916	3111.158
15 min obs	RMS	1.026	1.028	1.030	1.028
	ρ_{cm} (m)	90464.755	90461.721	90436.447	90434.873
	$\rho_{cm} - \rho_{cm}{}^*$ (m)	444.336	447.370	472.644	474.218
20 min obs	RMS	1.031	1.037	1.035	1.039
	ρ_{cm} (m)	90124.727	89510.929	89589.173	89407.108
	$\rho_{cm} - \rho_{cm}{}^*$ (m)	784.364	1398.162	1319.918	1501.983

	Medium Noise	MV	R - S	R - M	R - VT
5 min obs	RMS	1.016	1.018	1.030	1.027
	ρ_{cm} (m)	83656.682	83111.226	89655.261	89730.343
	$\rho_{cm} - \rho_{cm}{}^*$ (m)	7252.409	7797.865	1253.830	1178.748
10 min obs	RMS	1.020	1.022	1.023	1.022
	ρ_{cm} (m)	90197.568	90828.553	91099.233	90817.237
	$\rho_{cm} - \rho_{cm}{}^*$ (m)	711.523	80.538	190.142	91.854
15 min obs	RMS	1.026	1.027	1.027	1.027
	ρ_{cm} (m)	90135.568	90188.269	90102.602	90102.759
	$\rho_{cm} - \rho_{cm}{}^*$ (m)	773.523	720.822	806.489	806.332
20 min obs	RMS	1.031	1.037	1.033	1.035
	ρ_{cm} (m)	89986.688	89661.627	89832.979	89764.906
	$\rho_{cm} - \rho_{cm}{}^*$ (m)	922.403	1247.464	1076.112	1144.185

	Low Noise	MV	R - S	R - M	R - VT
5 min obs	RMS	1.016	1.044	1.032	1.036
	ρ_{cm} (m)	88522.328	89377.588	90047.589	90215.175
	$\rho_{cm} - \rho_{cm}{}^*$ (m)	2386.763	1531.503	861.502	693.916
10 min obs	RMS	1.021	1.021	1.021	1.021
	ρ_{cm} (m)	89850.006	89872.366	89873.677	89871.759
	$\rho_{cm} - \rho_{cm}{}^*$ (m)	1059.085	1036.725	1035.414	1037.332
15 min obs	RMS	1.007	1.007	1.007	1.007
	ρ_{cm} (m)	89809.871	89816.310	89780.011	89780.878
	$\rho_{cm} - \rho_{cm}{}^*$ (m)	1099.220	1092.781	1129.080	1128.213
20 min obs	RMS	1.002	1.002	1.002	1.002
	ρ_{cm} (m)	89794.796	89787.745	89791.293	89788.958
	$\rho_{cm} - \rho_{cm}{}^*$ (m)	1114.295	1121.346	1117.798	1120.133

Table 6. Range and Angle Measurements, 100 km Tether Length ($\rho_{cm} = 90,909.1$m).

	High Noise	M V	R - S	R - M	R - VT
5 min obs	RMS	1.016	1.062	1.052	1.056
	ρ_{cm} (m)	12328.540	65.577	6.367	63.926
	$\rho_{cm} - \rho_{cm}*$ (m)	11419.449	843.513	902.724	845.165
10 min obs	RMS	1.020	1.031	1.026	1.024
	ρ_{cm} (m)	37.732	348.370	13.247	19.794
	$\rho_{cm} - \rho_{cm}*$ (m)	871.359	560.721	895.844	889.297
15 min obs	RMS	1.027	1.029	1.028	1.033
	ρ_{cm} (m)	288.005	225.410	286.865	394.541
	$\rho_{cm} - \rho_{cm}*$ (m)	621.086	683.681	622.226	514.550
20 min obs	RMS	1.032	1.034	1.033	1.034
	ρ_{cm} (m)	626.955	355.914	597.682	474.637
	$\rho_{cm} - \rho_{cm}*$ (m)	282.136	553.177	311.409	434.454

	Medium Noise	M V	R - S	R - M	R - VT
5 min obs	RMS	1.016	1.062	1.065	1.052
	ρ_{cm} (m)	6625.873	247.122	11.144	64.472
	$\rho_{cm} - \rho_{cm}*$ (m)	5716.782	661.969	897.947	844.619
10 min obs	RMS	1.020	1.025	1.025	1.022
	ρ_{cm} (m)	474.518	366.379	534.879	385.559
	$\rho_{cm} - \rho_{cm}*$ (m)	434.573	542.712	374.212	523.532
15 min obs	RMS	1.027	1.028	1.027	1.028
	ρ_{cm} (m)	599.864	414.720	567.227	499.921
	$\rho_{cm} - \rho_{cm}*$ (m)	309.227	494.371	341.864	409.170
20 min obs	RMS	1.032	1.034	1.032	1.034
	ρ_{cm} (m)	769.585	598.485	698.024	646.718
	$\rho_{cm} - \rho_{cm}*$ (m)	139.506	310.605	211.067	262.373

	Low Noise	M V	R - S	R - M	R - VT
5 min obs	RMS	1.016	1.031	1.034	1.041
	ρ_{cm} (m)	2055.007	540.210	698.399	599.755
	$\rho_{cm} - \rho_{cm}*$ (m)	1145.917	368.881	210.692	309.336
10 min obs	RMS	1.020	1.022	1.025	1.023
	ρ_{cm} (m)	823.959	682.551	666.200	727.726
	$\rho_{cm} - \rho_{cm}*$ (m)	85.132	226.540	242.891	181.364
15 min obs	RMS	1.027	1.027	1.027	1.027
	ρ_{cm} (m)	849.390	832.380	843.650	836.774
	$\rho_{cm} - \rho_{cm}*$ (m)	59.701	76.711	65.440	72.317
20 min obs	RMS	1.032	1.031	1.031	1.032
	ρ_{cm} (m)	883.701	875.511	878.338	870.837
	$\rho_{cm} - \rho_{cm}*$ (m)	25.390	33.580	30.753	38.254

Table 7. Range and Angle Measurements, 1 km lib (up) Tether Length (ρ_{cm} = 909.1 m).

Analysis of the results shown above indicates that ridge-type estimation methods tend to improve the results of the minimum variance method for shorter tether lengths, higher noise

18

levels, and shorter observation spans. This is an expected result since for these types of scenarios the estimation problem would likely be more ill-conditioned than for those with longer tether lengths, lower noise levels, and longer observation spans. This would indicate that the ridge-type filters do indeed provide more accurate estimates in such ill-conditioned problems. Overall, however, there is no clear indication of one method which provides the best results for all cases.

The results also indicate that each method presented has the capability to determine if the observed satellite is part of a TSS. Once this determination is made a more sophisticated dynamical model and filter can be used for precise orbit determination of the satellite.

CONCLUSIONS

The performance of both minimum variance and ridge-type estimation methods was investigated for the purpose of identifying an observed satellite as being tethered or untethered. The filter estimates the satellite's position and velocity components as well as the radial and tangential acceleration components due to the tether force. Using observation data generated from a simplified dynamic model including the effects of Earth's gravity and the tether force, the filter was used to obtain solutions for two masses with varying configurations of tether length and orientation, varying observation error levels, and four observation spans between 5 and 20 minutes in length. From the results of the estimation process it should be easy to determine whether the observed satellite is a tethered satellite or not. If the body is determined to be tethered, a calculation can be made to determine the length of the tether (from the center-of-mass of the system). In all of the cases investigated in this study, the particular filter showed promising results, in terms of the necessary observation time and the level of observation error for which the filter can produce a satisfactory solution.

This study is a work-in-progress, however. Further work needs to be done in refinement of the ridge-type filters as well as in the analysis of the filters' performance on a wider range of scenarios. In addition, scenarios involving both in-plane and out-of-plane libration should be evaluated and specific recommendations regarding the use of these filters need to be forthcoming in order for practical use of these methods to be worthwhile.

ACKNOWLEDGEMENT

REFERENCES

1. Hoots, F. R., R. L. Roehrich, and V. G. Szebehely, "Space Shuttle Tethered Satellite Analysis," Directorate of Astrodynamics, Peterson AFB, CO, August 1983.

2. Kessler, S. A., and D. A. Cicci, "Filtering Methods for the Orbit Determination of a Tethered Satellite," *The Journal of Astronautical Sciences*, Vol. 45, No. 3, July-September 1997, pp. 263-278.

3. Cochran, J. E. Jr., S. Cho, Y-M Cheng, and D. A. Cicci, "Dynamics and Orbit Determination of Tethered Satellite Systems," AAS 96-147, AAS/AIAA Space Flight Mechanics Meeting, Austin, TX, Feb. 12-15, 1996.

4. Cho, S., J. E. Cochran, Jr., and D. A. Cicci, "Identification and Orbit Determination of Tethered Satellite System," AAS 98-101, AAS/AIAA Space Flight Mechanics Meeting, Monterey, CA, Feb. 9-11, 1998.

5. S. Cho, J. E. Cochran, Jr., and D. A. Cicci, "Approximate Solutions for Tethered Satellite Motion," AAS/AIAA Space Flight Mechanics Meeting, Breckenridge, CO, Feb. 7-10, 1999.

6. Cochran, J. E., Jr., S. Cho, A. Lovell, and D. A. Cicci, "On the Information Contained in the Motion of One Satellite of a Two-Satellite Tethered System," AIAA 98-4555, AIAA/AAS Astrodynamics Specialist Conference, Boston, MA, August 10-12, 1998.

7. Hoerl, A. E., and Kennard, R. W., "Ridge Regression: Biased Estimation for Non-Orthogonal Problems," *Technometrics*, Vol. 12, No. 1, February 1970, pp. 55-67.

8. Hoerl, A. E., and Kennard, R. W., "Ridge Regression: Applications to Non-orthogonal Problems," *Technometrics*, February 1970, pp. 69-82.

9. Cicci, D. A., and Tapley, B. D., "Optimal Solutions of Unobservable Orbit Dtermination Problems," *Celestial Mechanics*, 44, pp. 339-363, December 1988.

10. Cicci, D. A., "Use of Multiple Observation Types in Ridge-Type estimation Methods," *The Journal of the Astronautical Sciences*, Vol. 38, No. 2, April-June 1990, pp. 215-227

11. Cicci, D. A., Lovell, A., and Qualls, C., "A Method for the Identification of a Tethered Satellite," Paper AAS 99-196, presented at the AAS/AIAA Space Flight Mechanics Meeting, Breckenridge, CO, Feb. 7-10, 1999.

12. Tapley, B. D. and V. Szebehely, "Recent Advances in Dynamical Astronomy," Proceedings of the NATO Advanced Study Institute in Dynamical Astronomy, Cortina D'Ampezzo, Italy, August 1972.

13. Cicci, D. A., and Hall, R. L., "Improved Estimation/Prediction in Quick-Look Orbit Determination Problems," *The Journal of the Astronautical Sciences*, Vol. 40., No. 1, pp. 91-106, January-March 1992.

APPROXIMATE SOLUTIONS FOR
TETHERED SATELLITE MOTION[1]

S. Cho[2]
Electronics and Telecommunications Research Institute
Taejon, Korea

T. A. Lovell[3], J. E. Cochran Jr.[4], and D. A. Cicci[5]
Department of Aerospace Engineering
Auburn University, Alabama

Abstract

This paper involves the formulation of approximate solutions to equations that embody the

dominant characteristics of the orbital motion of a two-satellite tethered system. The orbital

motion of the system is viewed as perturbed two-body motion and a "restricted tether problem" is

obtained by neglecting librational motion. An exact analytical solution to this restricted problem

in terms of elliptic functions is presented. An approximate solution to the restricted tether

problem obtained by applying the method of averaging is also provided. An approximation for

small-amplitude librational motion is formulated, whose solution is based on methods for solving

equations with variable coefficients. The analytical solutions are good approximations to the

orbital motion of the tether-perturbed satellite and the librational motion of the system when the

libration is small. The restricted tether motion approximation is then utilized to solve the

identification problem of a tethered satellite system.

Nomenclature

a^{*}	= apparent semi-major axis
e^{*}	= apparent eccentricity
F	= incomplete elliptic integral of the first kind
g	= Jacobi's nome
h	= non-dimensional angular momentum
K	= complete elliptic integral of first kind
K'	= associate complete elliptic integral of first kind
k	= modulus of Jacobian elliptic functions and integral
k'	= complementary modulus of Jacobian elliptic functions and integral
m, m_p	= masses of satellites
r_E	= radius of the Earth (6,378,000 m)
r	= non-dimensional radial distance (r = radial distance/ r_E)
t,	= time
t^{*}	= $t \sqrt{\dfrac{\mu}{r_E^3}}$ = t x 0.0012394, non-dimensional time
μ	= gravitational Constant of the Earth
u	= 1/r
sn	= Jacobian elliptic function

X = state vector

α, β, γ, and ξ = variable coefficients

ε = $\dfrac{m_p \rho}{(m + m_p) r_E}$, tether parameter

φ and $\dot{\varphi}$ = amplitudes

θ = orbital angle (true anomaly)

θ_2 = out-of-plane libration angle

θ_3 = in-plane libration angle

ρ = tether length

ω = orbital frequency

I. Introduction

It is a well-known fact that the motion of each satellite in a tethered satellite system (TSS) in the Earth's gravitational field is non-Keplerian[1]. This characteristic may present problems to those who are detecting, identifying and tracking space objects. Cho, et al.[2], showed that identification and estimation of the states of a two-satellite tethered system using observations of the one of the satellite in the system is possible. However, they found that estimation of the librational motion using observations over a short period of time is difficult. These results motivated Cochran, et al.[3] to investigate the problem of characterizing the information available in observations of one of the satellites of a two-satellite tethered system. They showed that the magnitude of the tether parameter (a combination of the tether length and the masses of the end bodies[2]) strongly affects the conditioning of the information matrix, as does the type of observations available. The

3

elements of the information matrix corresponding to the librational motion of the system are generally relatively small, leading to large condition numbers. Difficulties in acquiring information on librational motion have motivated a quest for analytical approximations for the orbital and librational motions of TSS[4,5].

In this paper, a "restricted tether motion" equation is obtained that embodies the dominant characteristics of the orbital motion of the TSS and approximate analytical solutions to the orbital and librational equations of motion for a TSS are presented. First, the equations that govern planar motion of a two-satellite tethered system given in Ref. 2 are discussed. These equations are then transformed by a change of variables, as in the classical two-body problem. The transformed equations are solved approximately by using a combination of methods. Comparisons of analytical results with numerical solutions are made. Then, the use of the restricted tether motion equations as part of a three-stage identification algorithm for TSS is discussed.

II. Equations of Motion

A two-satellite tethered system is depicted in Fig. 1. The vector **r** defines the position of satellite m with respect to the point mass Earth, E, and m_p is a satellite connected to m by the tether. For the dynamic model employed herein, the mass of the tether is assumed to be distributed equally to m and m_p. General non-dimensionalized equations of motion for this system were derived in Ref.2. There it was shown that the out-of-plane librational motion of a TSS is generally small, and has less effect on orbital motion than in-plane libration because the velocity it produces is orthogonal to the orbital velocity. Thus, the planar motion for satellite m can be described by the following non-dimensional equations:

$$\ddot{r} = \dot{\theta}^2 r - \frac{1}{r^2} + \varepsilon\left[\left(\dot{\theta}_3 + \dot{\theta}\right)^2 + \frac{1}{r^3}(3\cos^2\theta_3 - 1)\right]\cos\theta_3 \tag{1}$$

$$\ddot{\theta} = \frac{-2\dot{\theta}\dot{r}}{r} + \varepsilon\left[\left(\dot{\theta}_3 + \dot{\theta}\right)^2 + \frac{1}{r^3}(3\cos^2\theta_3 - 1)\right]\sin\theta_3 . \tag{2}$$

Relative motion of the tethered satellite m_p with respect to satellite m is described by the in-plane librational angle θ_3 as shown in Fig. 1. The equation for the librational motion is

$$\ddot{\theta}_3 = -\ddot{\theta} - 3\frac{1}{r^3}\cos\theta_3 \sin\theta_3 . \tag{3}$$

In Eqs. (1) - (3), $\dot{(\ )} = \frac{d(\ )}{dt^*}$. The tether parameter ε, defined in the Nomenclature section, is a combination of a mass ratio and a non-dimensional tether length (ρ/r_E).
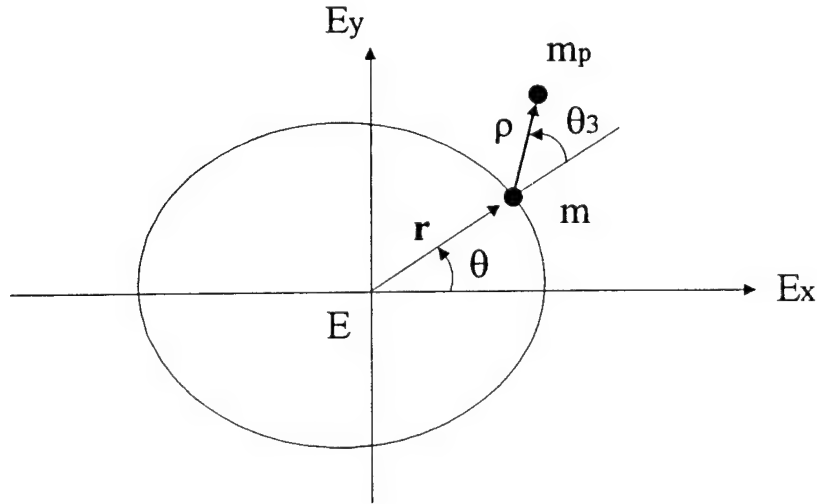
Fig. 1. TSS Motion on Orbit Plane.

III. Tether Perturbed Motion

The terms that include the tether parameter on the right-hand side of Eqs. (1) and (2) represent forces due to the mass m_p in addition to those which cause Keplerian motion. Since the tether parameter is small, in general, we may treat the additional forces as small perturbations to the Keplerian motion of satellite m that would occur if the tether were cut. The perturbations are mainly the gravity-gradient force due to the mass, m_p. Also the librational motion can often be considered as a perturbation, especially when the magnitude of the libration angle, θ_3, is small as it is for a typical tethered system.

Eqs. (1) – (3) may then be transformed by replacing the variable r by $u = 1/r$ and using $h = r^2 \dot{\theta}$ instead of $\dot{\theta}$, for mathematical convenience. The time variable t^* can be replaced by a time-like variable τ defined by $\dot{t} = h u^2$. Note that this is similar to the classical transformation made in solving the two-body problem. Then, Eqs. (1)-(3) can be rewritten as

$$u'' + u = \frac{1}{h^2} + \varepsilon\left(-u\left(\theta_3' + 1\right)^2 - \frac{2}{h^2}\right)\left(\theta_3 u' + u\right) \tag{4}$$

$$h' = \varepsilon\left(u\left(\theta_3' + 1\right)^2 + \frac{2}{h^2}\right)\theta_3 h \tag{5}$$

and

$$\theta_3'' = -\frac{2u'}{u}\left(\theta_3' + 1\right) - \frac{3}{h^2 u}\theta_3 + \varepsilon\left(-u\left(\theta_3' + 1\right)^2 - \frac{2}{h^2}\right)\theta_3\left(\theta_3' + 1\right) \tag{6}$$

where $( )' = \dfrac{d( )}{d\tau}$. In Eqs. (4)-(6), sinusoidal terms in θ_3 have been approximated by Taylor series expansions assuming a small libration angle, θ_3.

Restricted Tether Orbital Motion

By neglecting librational motion, a "restricted tether problem" may be defined that embodies the dominant characteristics of the tether perturbed orbital motion. Equations for the restricted tether motion are obtained by neglecting θ_3 and its derivatives in Eqs. (4) – (5):

$$u'' + u = \frac{1}{h^2} + \varepsilon\left(-u - \frac{2}{h^2}\right)u \qquad (7)$$

and

$$h' = 0 \ . \qquad (8)$$

An exact solution to the restricted tether problem may be found as follows. A first-order differential equation for u is obtained by multiplying Eq. (7) by u and integrating once:

$$u' = 2\sqrt{-\varepsilon\frac{u^3}{3} - \left(1 + \frac{2\varepsilon}{h^2}\right)\frac{u^2}{2} + \frac{u}{h^2} + E} \ . \qquad (9)$$

This may be rewritten as

$$\sqrt{D}\int_{\tau_0}^{\tau} d\tau = \int_{u_0}^{u} \frac{du}{\sqrt{-u^3 - \dfrac{B}{D}u^2 + \dfrac{C}{D}u + \dfrac{2E}{D}}} \qquad (10)$$

where

$$B = 1 + \frac{2\varepsilon}{h^2}$$

$$D = \frac{2}{3}\varepsilon$$

$$C = \frac{2}{h^2}$$

and

$$E = \frac{1}{2}\left(\frac{du}{d\tau}\right)_0 + \frac{1}{3}\varepsilon u_0^3 + \frac{1}{2}\left(1 + \frac{2}{h^2}\varepsilon\right)u_0^2 - \frac{1}{h^2}u_0.$$

We can put Eq. (10) into a standard form,

$$\sqrt{D}\int_{\tau_0}^{\cdot} d\tau = \int_b^u \frac{du}{\sqrt{(a-u)(u-b)(u-c)}} - \int_b^{u_0} \frac{du}{\sqrt{(a-u)(u-b)(u-c)}} \tag{11}$$

where a, b, and c are constants that satisfy the relation, $a \geq u > b > c$. We can use elliptic

functions[6] to evaluate the integral in Eq. (11). The solution is

$$\sqrt{D}(\tau - \tau_0) + gF(\varphi^*, k) = g\,sn^{-1}(\sin\varphi) \tag{12}$$

where $g = \frac{2}{\sqrt{a-c}}$, $k^2 = \frac{a-b}{a-c}$, and F is the incomplete elliptic integral of the first kind. The

amplitudes φ and φ^* are obtained from

$$\varphi = \sin^{-1}\left(\sqrt{\frac{(a-c)(u-b)}{(a-b)(u-c)}}\right) \tag{13}$$

and

$$\varphi^* = \sin^{-1}\left(\sqrt{\frac{(a-c)(u_0-b)}{(a-b)(u_0-c)}}\right), \tag{14}$$

respectively.

8

By Using (13) and (14), we can obtain the following expression for u (τ)

$$u(\tau) = \frac{c\,k^2\,sn^2\left(\dfrac{\sqrt{D}\,\tau}{g} + F\left(\varphi^{\bullet}, k\right)\right) - b}{k^2\,sn^2\left(\dfrac{\sqrt{D}\,\tau}{g} + F\left(\varphi^{\bullet}, k\right)\right) - 1}. \tag{15}$$

The Jacobian elliptic function sn( ) can be expressed as a rapidly convergent series expansion,

$$sn(x) = \frac{2\pi}{kK} \sum_{m}^{\infty} \frac{q^{m+\frac{1}{2}}}{1 - q^{2m+1}} \sin\left[(2m+1)\frac{\pi x}{2K}\right] \tag{16}$$

where $q = e^{-\pi\frac{K'}{K}}$ is Jacobi's nome. In Eq. (16), K is the complete integral of the first kind of modulus k. Also, K' which appears in the definition of q is the associated complete integral of the first kind.

Apparent Orbit

From the analytical solution to the restricted tether problem, an equation can be found for the radial distance of m from the Earth in the form of the classical two-body equation. From Eq. (15), this distance is

$$r(\tau) = \frac{k^2\,sn^2\left(\dfrac{\sqrt{D}\,\tau}{g} + F\left(\varphi^{\bullet}, k\right)\right) - 1}{c\,k^2\,sn^2\left(\dfrac{\sqrt{D}\,\tau}{g} + F\left(\varphi^{\bullet}, k\right)\right) - b}\,r_E. \tag{17}$$

By using the properties of the elliptic function sn(·) and given that $0 < k^2 < 1$, $c < 0$, and $b > 0$, the maximum and minimum radial distances of the object for restricted tether motion are found to be

9

$$r_{max} = \frac{1}{b} r_E \tag{18}$$

$$r_{min} = \frac{k^2 - 1}{c\,k^2 - b} r_E \tag{19}$$

These distances may then be used to define an apparent semi-major axis

$$a^* = \frac{1}{2} \left[\frac{1}{b} + \frac{k^2 - 1}{c\,k^2 - b} \right] r_E . \tag{20}$$

and Eq. (20) may be used to derive an apparent eccentricity

$$e^* = \sqrt{1 - \frac{h^2}{\mu a^*}} \tag{21}$$

By substituting a^* and e^* in the standard two-body equation for r, an equation for a "Keplerian-like" orbit is obtained:

$$r_{apparent} = \frac{a^* (1 - e^{*2})}{1 + e^* \cos\tau} \tag{22}$$

Though this concept of an "apparent orbit" will not be pursued further, comparison of Eq. (17) with Eq. (22) for several different cases shows that this method can be a good approximation to restricted tether motion.

Approximate Solution to the Restricted Tether Problem

Although Eq. (15) is an exact solution to the restricted tether motion equations, its form in terms of the elliptic functions limits its usefulness. In some cases approximate solutions may be more convenient in analyzing the dynamic behavior of m. An approximate solution to Eq. (15) can be obtained by applying the general method of averaging[7]. We may rewrite Eq. (7) as

$$u'' + \omega^2 u = \frac{1}{h^2} - \varepsilon u^2 \quad , \tag{23}$$

where $\omega = \sqrt{1 + \frac{2}{h^2}\varepsilon}$. If we assume that the solution to Eq. (23) has the form of the solution to

the linear term in Eq. (23), then we have

$$u = \gamma \cos(\omega \tau + \xi) + \frac{1}{h^2 \omega^2} . \tag{24}$$

Note that coefficients γ and ξ are variables to be determined to take into account the non-linear

term in Eq. (23). We may derive differential equations for the parameters γ and ξ by using the

method of variation of parameters[7]. These equations are

$$\gamma' = \varepsilon \left(\begin{array}{l} \dfrac{\gamma^2}{\omega} \sin(\omega\tau + \xi)\cos^2(\omega\tau + \xi) + \dfrac{1}{h^4\omega^5}\sin(\omega\tau + \xi) \\ \\ \quad + \dfrac{2\gamma}{h^2\omega^3}\sin(\omega\tau + \xi)\cos(\omega\tau + \xi) \end{array} \right) \tag{25}$$

and

$$\xi' = \varepsilon \left(\frac{\gamma}{\omega}\cos^3(\omega\tau + \xi) + \frac{1}{\gamma h^4\omega^5}\cos(\omega\tau + \xi) + \frac{2}{h^2\omega^3}\cos^2(\omega\tau + \xi) \right) . \tag{26}$$

Solutions to Eqs. (19) and (20) may be assumed in the forms

$$\gamma = \overline{\gamma} + \varepsilon\widetilde{\gamma} \tag{27}$$

and

$$\xi = \overline{\xi} + \varepsilon\widetilde{\xi} \tag{28}$$

where, $\bar{\gamma}$ and $\bar{\xi}$ are smoothly varying terms and $\varepsilon\tilde{\gamma}$ and $\varepsilon\tilde{\xi}$ are small harmonic terms. By substituting Eqs. (27) and (28) into Eqs. (25) and (26), averaging over one period ($2\pi/\omega$), and solving the averaged equations, we get

$$\bar{\gamma} = \gamma_0 \tag{29}$$

and

$$\bar{\xi} = \frac{\varepsilon}{h\omega}\tau + \xi_0 \ . \tag{30}$$

where γ_o and ξ_o represent the values these variables take on at $\tau \cdots 0$. Expressions for the oscillatory terms can also be obtained

$$\tilde{\gamma} = -\frac{\bar{\gamma}^2}{4\omega^2}\left(\cos\left(\omega\tau + \bar{\xi}\right) + \frac{1}{3}\cos 3\left(\omega\tau + \bar{\xi}\right)\right)$$
$$-\frac{1}{h^4\omega^6}\cos\left(\omega\tau + \bar{\xi}\right) - \frac{\bar{\gamma}}{2h^2\omega^4}\cos 2\left(\omega\tau + \bar{\xi}\right) + C_\gamma \tag{31}$$

and

$$\tilde{\xi} = \frac{\bar{\gamma}^2}{4\omega^2}\left(3\sin\left(\omega\tau + \bar{\xi}\right) + \frac{1}{3}\sin 3\left(\omega\tau + \bar{\xi}\right)\right)$$
$$+\frac{1}{\bar{\gamma}h^4\omega^6}\sin\left(\omega\tau + \bar{\xi}\right) + \frac{1}{2h^2\omega^4}\sin 2\left(\omega\tau + \bar{\xi}\right) + C_\xi \tag{32}$$

The constants of the integration C_γ and C_ξ in Eqs. (25) and (26) are such that $\tilde{\gamma} = \tilde{\xi} = 0$ at $\tau = 0$. That is:

$$C_\gamma = \frac{\gamma_0^2}{4\omega^2}\left(\cos\xi_0 + \frac{1}{3}\cos 3\xi_0\right) + \frac{1}{h^4\omega^6}\cos\xi_0 + \frac{\gamma_0}{2h^2\omega^4}\cos 2\xi_0 \tag{33}$$

12

$$C_\xi = -\frac{\gamma_0^2}{4\omega^2}\left(3\sin\xi_0 + \frac{1}{3}\sin 3\xi_0\right) - \frac{1}{\gamma_0 h^4 \omega^6}\sin\xi_0 - \frac{1}{2h^2\omega^4}\sin 2\xi_0 \qquad (34)$$

Example results for a TSS orbit are obtained by evaluating both the exact solution (Eq. (15)) and the approximate solution (Eq. (24)) to the restricted tether problem, and by numerically integrating Eqs. (4)-(6). These results are shown in Fig. 2. The initial conditions used are: $r_0 = 6621$ km, $\dot{r}_0 = 0$, $\theta_0 = 0$, $\dot{\theta}_0 = 1.1835E\text{-}3$ rad/sec, tether length = 10 km, mass ratio $m/m_p = 0.1$, and tether parameter $\varepsilon = 1.4254E\text{-}3$. The parameters a, b, c, from Eq. (11) are the zeros of the cubic function that appears under the radical in Eq. (10), and in this example are given by: a = 1.5103E-7, b = 1.4392E-7, c = -1.6574E-4. Also, the values of γ_0 and ξ_0 are determined by evaluating Eq. (24) and its derivative at $\tau = 0$ and applying the initial conditions on u and u'. For this case, $\gamma_0 = 2.1424E\text{-}2$ and $\xi_0 = 0.0$.

The fact that all three of the above-mentioned curves lie practically on top of one another demonstrates that both the exact and approximate solutions to the restricted tether problem are very good approximations to the TSS orbit solution obtained by numerical integration. The result for a Keplerian orbit with the same initial conditions is provided in Fig. 2 as well, to show how it differs from the tether perturbed orbit.

IV. Relative Motion of the Tethered Mass

Relative motion of the tethered satellite m_p is described by Eq. (6), which is a second-order differential equation with a small non-linear term. Note that Eq. (5) can be rearranged as

$$\frac{h'}{h} = \varepsilon \left(u \left(\theta_3{}' + 1 \right)^2 + \frac{2}{h^2} \right) \theta_3 \qquad (35)$$

and inserted into Eq. (6) to give

$$\theta_3{}'' = -\frac{2u'}{u} \left(\theta_3{}' + 1 \right) - \frac{3}{h^2 u} \theta_3 - \frac{h'}{h} \left(\theta_3{}' + 1 \right) \qquad (36)$$

Fig. 2. Comparison of Solutions for TSS Orbital Radius.
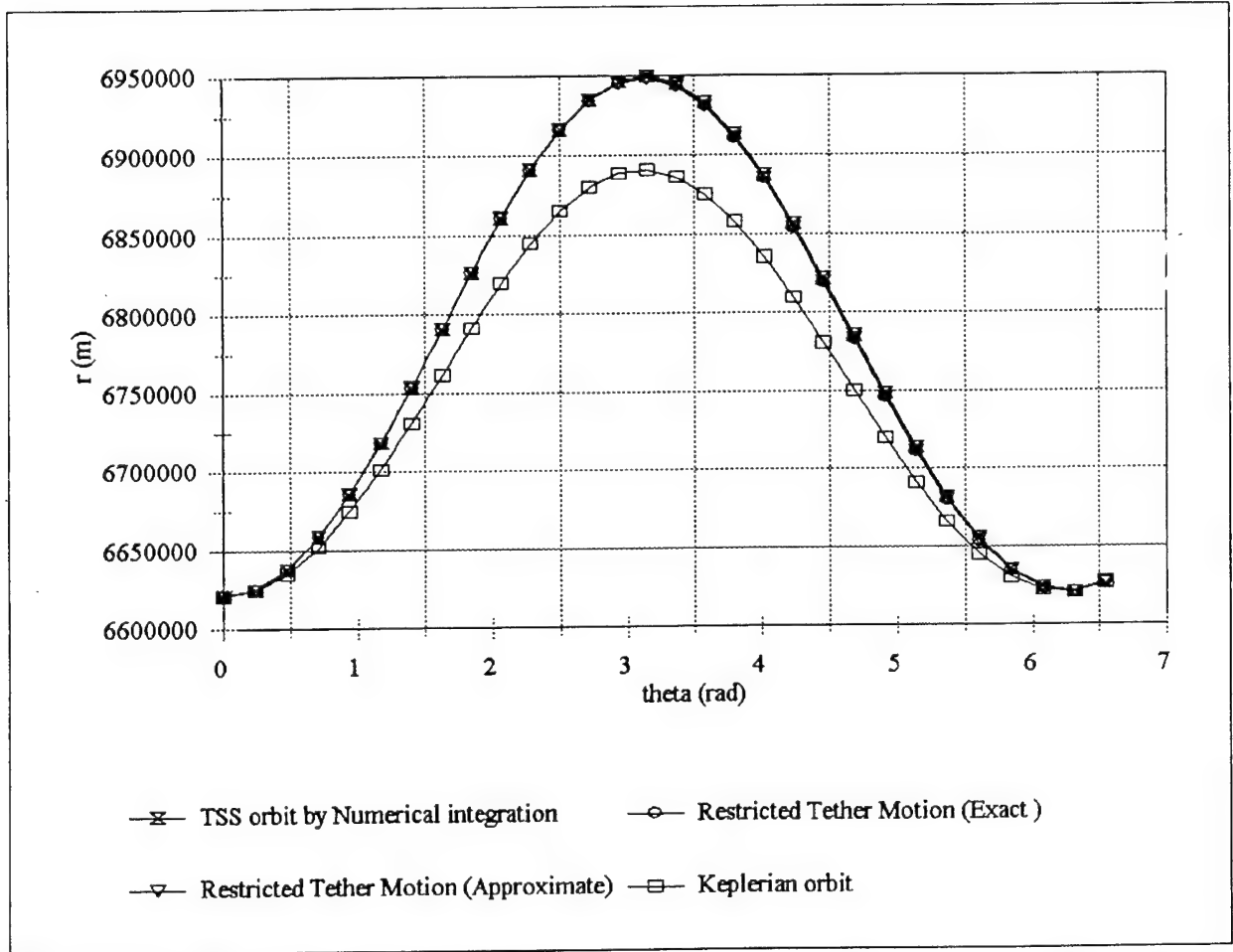
Since the orbital motion approximation is based on h' = 0, it is consistent to neglect the last term

14

on the right hand side in the process of finding an approximate solution for θ_3. The solution

will be zeroth order in ε, and thus will not depend on the tether length. Equation (6) then

becomes a second-order, non-homogeneous, linear differential equation with variable coefficients:

$$\theta_3'' + 2P(\tau)\theta_3' + R^2(\tau)\theta_3 = Q(\tau) \tag{37}$$

where

$$P(\tau) = \frac{u'}{u} \tag{38}$$

$$R(\tau)^2 = \frac{3}{h^2 u} \tag{39}$$

$$Q(\tau) = -2\frac{u'}{u} \quad . \tag{40}$$

In Eqs. (38)-(40), equations for u and u' may be expressed by the zeroth order (in ε) solution in

Eq. (24). They are

$$u \approx \gamma_0 \cos(\omega\tau + \xi_0) + \frac{1}{h^2 \omega^2} \tag{41}$$

$$u' \approx -\omega\gamma_0 \sin(\omega\tau + \xi_0). \tag{42}$$

To solve Eq. (37), first the variable θ_3 is transformed to a new variable ϕ which is defined by

$$\varphi = \theta_3 e^{\int P(\tau)d\tau} = \theta_3 u \tag{43}$$

or

$$\theta_3 = \varphi e^{\int -P(\tau)d\tau} = \frac{\varphi}{u} \tag{44}$$

15

Then, Eq. (37) can be expressed in the simpler form

$$\varphi'' + G(\tau)^2 \varphi = Q^{\bullet}(\tau) \tag{45}$$

where

$$G(\tau)^2 = R^2 - P^2 - P' \tag{46}$$

$$Q^{\bullet}(\tau) = Q(\tau) e^{\int P d\tau} = -2u' \tag{47}$$

By substituting Eqs. (41) and (42) into Eqs. (38) - (40) and (46), using a Taylor series expansion for G about $\gamma_0 = 0$, and neglecting terms of order γ_0^2 or higher, we obtain the following expression:

$$G(\tau) \approx \Omega_0 \left(1 - \frac{1}{3}h^2 \omega^2 \gamma_0 \cos(\omega \tau + \xi_0)\right) \tag{48}$$

where $\Omega_0 = \omega \sqrt{3}$. Since G executes small changes about its mean value Ω_0, the WKBJ approximation[8] can be used to obtain the following two linearly independent homogeneous solutions to Eq. (45):

$$x_1 = \frac{1}{\sqrt{G}} \cos \zeta \tag{49}$$

$$x_2 = \frac{1}{\sqrt{G}} \sin \zeta \tag{50}$$

where

$$\zeta(\tau) = \int G \, d\tau \tag{51}$$

Using the method of variation of parameters, we seek a particular solution of the form

$$\varphi(\tau) = \alpha x_1 + \beta x_2 \tag{52}$$

where α and β must satisfy

16

$$\alpha' = \frac{-\overset{\bullet}{Q} x_2}{x_1 x_2' - x_2 x_1'} \tag{53}$$

and

$$\beta' = \frac{\overset{\bullet}{Q} x_1}{x_1 x_2' - x_2 x_1'} . \tag{54}$$

By integrating Eqs. (53) and (54), we obtain the following solutions for α and β (again, neglecting terms of order γ_0^2 or higher):

$$\alpha = -\frac{\omega \gamma_0}{\sqrt{\Omega_0}} \left(\frac{\left[\sin \left(\omega - \Omega_0 \right) \tau + \xi_0 \right]}{\omega - \Omega_0} - \frac{\left[\sin \left(\omega + \Omega_0 \right) \tau + \xi_0 \right]}{\omega + \Omega_0} \right) + C_\alpha \tag{55}$$

and

$$\beta = -\frac{\omega \gamma_0}{\sqrt{\Omega_0}} \left(\frac{\left[\cos \left(\omega - \Omega_0 \right) \tau + \xi_0 \right]}{\omega - \Omega_0} + \frac{\left[\cos \left(\omega + \Omega_0 \right) \tau + \xi_0 \right]}{\omega + \Omega_0} \right) + C_\beta \tag{56}$$

where the constants of integration C_α and C_β are chosen such that

$$\phi(0) = \alpha(0) x_1(0) + \beta(0) x_2(0) = \theta_3(0) u(0) \tag{57}$$

and

$$\phi'(0) = \alpha'(0) x_1(0) + \alpha(0) x_1'(0) + \beta'(0) x_2(0) + \beta(0) x_2'(0)$$

$$= \theta_3'(0) u(0) + \theta_3(0) u'(0) \tag{58}$$

Finally, we may find the solution for θ_3 by substituting ϕ into Eq. (44).

$$\theta_3 = \left(\alpha x_1 + \beta x_2 \right) \frac{1}{u} \tag{59}$$

It should be mentioned that the preceding solution is valid only for near-circular orbits. This is because the effect of γ in Eq. (24) is to add eccentricity to the circular orbit, and in the

foregoing analysis γ was assumed to be small. Results obtained from the analytical solution in Eq. (59) are compared with numerical simulation results in Fig. 3. The same initial conditions for the results in Fig. 2 were used to obtain Fig. 3. It is seen that the results from the approximate analytical solution to the librational motion match those from the numerical simulation very well; in fact, the maximum difference in the value of θ_3 obtained by the two methods is less than 0.002 rad. Thus, for small eccentricities and small libration amplitude, the analytical solution may be used to accurately predict libration of a tether-connected satellite.
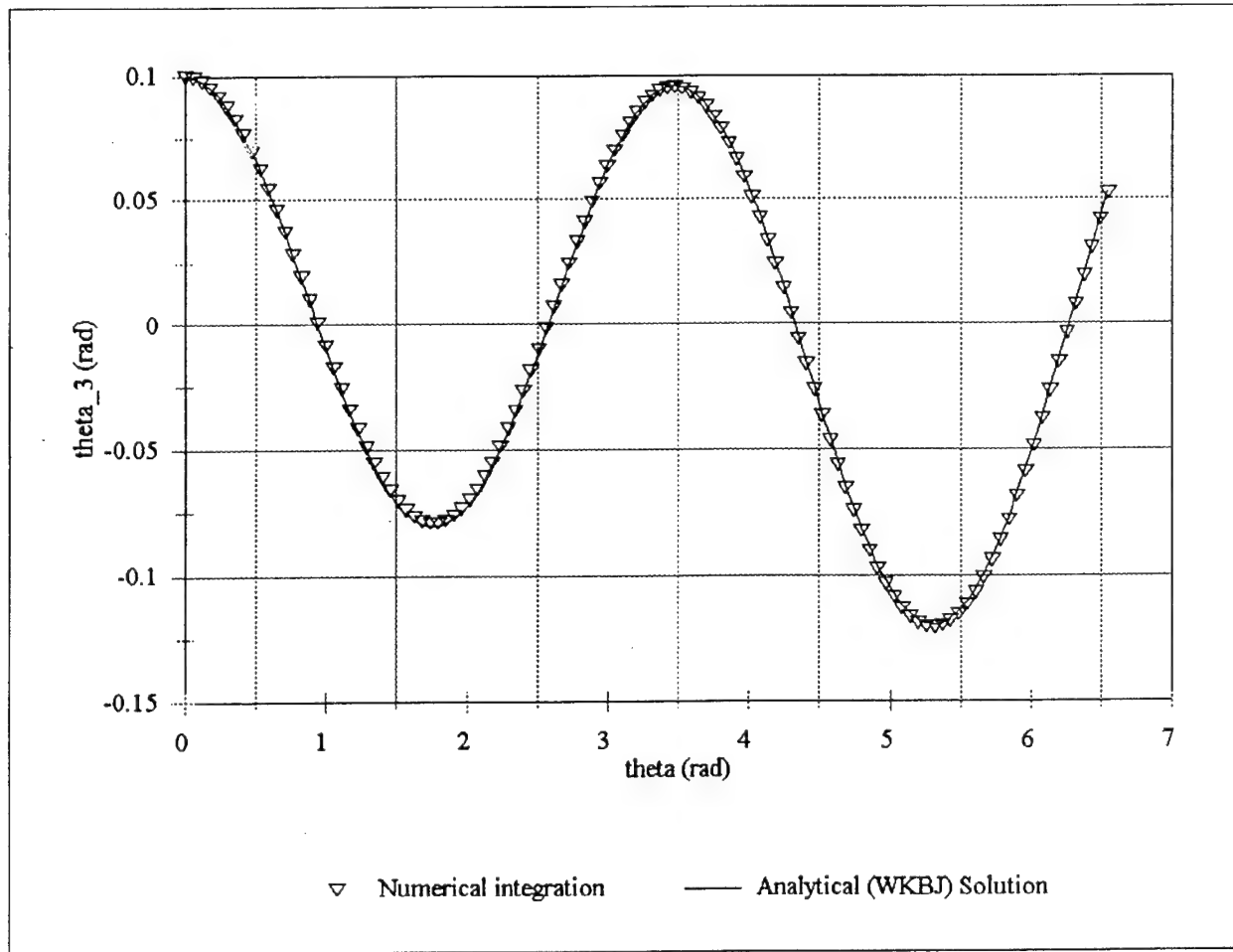
Fig. 3. Comparison of Solutions for Librational Motion.

V. Identification of a Tethered Satellite System

The solutions obtained in this paper may be useful in predicting the orbital motion and libration of a two-satellite tethered system. Here a solution to the identification problem is posed by using equations for the restricted tether motion. In Refs. 2 and 3, a state estimation process to identify a TSS by observing only one of the satellites in the TSS was tested. Difficulties encountered in Refs. 2 and 3 were: (a) The state estimation process, including states for the libration angle, fails when a short observation period is used; (b) very accurate guesses for the initial states, that must be determined by a preliminary orbit determination process, are needed for successful convergence; (c) initial states for the libration angle cannot be obtained *a priori*. These problems are caused by the fact that no direct information on the librational motion is provided in the observations, and because the effects of libration on the observed satellite are often very small.

The success of the identification process seems to require a trade-off between performance in detecting the effect of the tether force on the observed satellite and achieving completeness of system identification. If detection is the main objective, neglecting states that govern the librational motion should be acceptable, if the libration is small in amplitude and/or the tether length is small (say, less than 20 km). It follows that ignoring the libration states in the equations of motion may improve the performance of an estimator without a significant loss of accuracy. In Fig. 2, it was shown that the equations of motion with zero libration described the orbital motion of a two-satellite tethered system very well in cases of small amplitude librational motion. Thus, by ignoring the states about which we have little information, we may eliminate some difficulties.

A method of identification of a TSS based on the above consideration is proposed. In this process, the equations for the restricted tether motion are used in a batch filter. The method is constructed in three stages similar to the method used in Ref. 9. First, a state estimation technique using the equations for two-body motion is applied with limited observation data. Only one of the satellites in a tethered system is observed and the observation period is limited to a short arc. The state vector to be estimated in the first stage is

$$X = \begin{bmatrix} r & \theta & \dot{r} & \dot{\theta} & \mu \end{bmatrix}^T . \tag{60}$$

In Eq. (60), r is radial distance, θ is true anomaly, and μ is the gravitational constant. From this first stage, three different results are expected. If the observed satellite is a single satellite, the states should be estimated with high accuracy. This can be verified by comparing the estimated value of μ with the true gravitational constant. If the observed satellite is a member of a TSS, then the estimation process may be successful or not. That is, although the procedure estimates the state vector successfully, the results may be in error. An estimated gravitational constant may be used to detect errors in results. If the process fails to converge, the observed satellite may be a member of a TSS for which the dynamics of two-body motion is not a good model. For all of the above cases, more steps are needed to complete the identification.

Equations for the restricted tether motion are applied in the second stage to verify and improve the results. The restricted tether motion describes the gross orbital motion of a TSS. As mentioned previously, neglecting the librational motion provides an advantage in the estimation process.

If the states are estimated successfully in the first stage, these estimates may be used as an initial guess of the second stage. The state vector for the restricted tether motion is

$$X = \begin{bmatrix} r & \theta & \dot{r} & \dot{\theta} & \varepsilon \end{bmatrix}^T \quad (61)$$

where ε is the tether parameter. The tether parameter can be obtained from the first stage results, since we can write[2,10]

$$\varepsilon \approx \frac{r_0}{r_E} \frac{\mu - \mu_e}{\mu_e + 2\mu} \quad (62)$$

where μ_e is the estimated value for the gravitational constant. If the second stage is successfully finished, the estimated state vector identifies a TSS more completely.

The third stage employs the two-dimensional motion of a TSS, i.e., the state vector contains the in-plane librational variables. Thus, the state vector is defined as

$$X = \begin{bmatrix} r & \theta & \theta_3 & \dot{r} & \dot{\theta} & \dot{\theta}_3 & \varepsilon \end{bmatrix}^T \quad (63)$$

where θ_3 is the in-plane libration angle. Although this stage may not always be necessary for identification of a TSS, it completes the identification with higher confidence.

To illustrate this identification process, several circular and elliptical orbit conditions, with and without libration, were chosen. Table 1 provides parameters and initial conditions for ten different cases. Initial (non-dimensional) radial distance for all cases is 1.047. For the cases labeled C, initial osculating eccentricity is zero, while the cases labeled E have an eccentricity of 0.2. Cases C-1 and C-2, representing circular orbits of m and m_p without librational motion, were obtained by applying the circular equilibrium angular rate (given in the fifth column of Table 1). Cases C-3 and C-4 are examples of small in-plane libration, one having a larger tether parameter than the other. Cases C-5 and C-6 include large in-plane libration for the same tether parameters as in cases C-3 and C-4, respectively. Cases E-3 to E-6 are similar to cases C-3 to C-6, except the initial angular rate is that which provides an eccentricity of 0.2. All data were generated by

21

numerical integration of the equations for complete three-dimensional motion. The observation period is about 1/16 of the orbital period. Data points were collected every 5 seconds, for a total of about 70 data points. Tables 2 to 11 show results of the identification process via the three-stage method; the stages are labeled, "Two-body Motion," "Restricted Motion," and "Plane TSS," respectively. Values are all in non-dimensional units except the gravitational constant, μ.

In Case C-1 (Table 2), the first stage converges, with the estimated gravitational constant indicating a possible tethered satellite. Therefore, the second stage is performed and verifies the tethered satellite motion of the object. The results of the third stage show estimated values of the librational states as well. Table 3 presents Case C-2, for which identification is similarly successful.

Case C-3 (Table 4) includes small libration. For this case, the first stage cannot provide a good estimate of the tether parameter. However, the second stage provides accurate estimates of ε and of the restricted tether motion states. The third stage then provides very good estimates of all states.

In case C-4 (Table 5), the first stage estimation process failed. This is likely because the effect of the tether caused the mass to deviate too much from two-body motion. This is illustrated in Fig. 4, which presents simulation results of Cases C-4, C-6, restricted tether motion, and two-body motion. (In all cases, the initial radius, orbital angle, and angular rate are the same.) In Fig. 4, it is clear that C-4 cannot be tracked well at all by using equations for two-body motion. By contrast, Fig. 5 shows results for the cases with much smaller tether parameter. Although two-body motion is not necessarily "close" to the motion of C-3, the magnitude of the difference is much smaller than in Fig. 4.

In Cases C-5 and C-6 (Tables 6 and 7), all states in the first-stage process are estimated successfully except for the value of μ; in the second stage, the value of μ is greatly refined; and finally, in the third stage, all states in the two-dimensional motion of the TSS are successfully estimated, including librational motion.

Tables 8 to 11 present estimation results for Cases E-3 to E-6. For each of these cases, the success of all three stages of the identification process is equal to or better than that of the near-circular case with the same tether parameter and initial libration (i.e., Cases E-3 to E-6), with the lone exception that the third stage process fails for Case E-4.

VI. Conclusions

Approximate analytical solutions to the equations of planar motion of a two-satellite tethered system have been obtained. An exact solution to a restricted tether problem obtained by neglecting libration was found in terms of elliptic functions and integrals. This solution provides results that agree very well with exact results obtained by numerically integrating the complete equations for the two-satellite tethered system. The concept of an apparent orbit, which is a projection of the tethered satellite motion onto a Keplerian orbit, was also discussed. An approximate solution to the restricted tether problem was also found by applying the general method of averaging. A solution to the equation that governs librational motion was then found. The solutions derived in this work provide considerable insight regarding the principal motion of tethered satellite systems.

The three-stage method proposed for identification was used to obtain definitive results for several different cases of tethered satellite motion. It was shown that this method can be used

23

successfully when only a short period of observation time and relatively imprecise initial state information are available. The restricted tether motion model may prove useful in addressing the state estimation problem for tethered satellite systems, since this model is a good approximation to the orbit of a two-satellite tethered system and it neglects the libration that causes numerical problems in the estimation process.

Acknowledgement

References

1. Beletsky, V. V., and Levin, E. V., *Dynamics of Space Tether Systems*, Vol. 83, Advances in the Astronautical Sciences, AAS, San Diego, CA, 1993, p. 76.

2. Cho, S., Cochran, J.E., Jr., and Cicci, D. A., "Identification and Orbit Determination of Tethered Satellite System", AAS 98-101, *AAS/AIAA Space Flight Mechanics Meeting*, Monterey, CA, February 9-11, 1998.

3. Cochran, J. E., Jr., Cho, S., Lovell, A., and Cicci, D. A., "On the Information Contained in the Motion of One Satellite of a Two-Satellite Tethered System," AIAA-98-4555, *AIAA/AAS Astrodynamics Conference*, Boston, MA, August 10-12, 1998 (submitted for publication).

4. Von Flotow, A. H., " Some Approximations for the Dynamics of Spacecraft Tethers," AIAA 87-0821, *AIAA Dynamics Specialists Conference*, Monterey, CA, Apr. 9-10, 1987.

5. Nacozy, P. E., " Dynamics Analysis of Electrodynamic Satellite Tethers. Equations of Motion and Numerical Solution Algorithms for the Tether," NASA-CR-171777, Jan. 1984.

6. Byrd, P. F., and Friedman, M. D., *Handbook of Elliptic Integrals for Engineers and Scientists*, Springer-Verlag, New York, 2nd Edition, 1971.

7. Sanders, J. A., and Verhulst, F., *Averaging Methods in Nonlinear Dynamical Systems*, Springer-Verlag, New York, 1985.

8. Cunningham, W. J., *Introduction to Nonlinear Analysis*, McGraw-Hill Inc., New York, 1958.

9. Cho, S., "Analysis of Orbital motion of a Tethered Satellite System", Ph.D. Dissertation, Auburn University, 1999.

10. Cochran, J. E., Jr., Cho, S., Cheng, Y-M., and Cicci, D. A., "Dynamics and Orbit Determination of Tethered Satellite Systems," AAS 96-147, *AAS/AIAA Space Flight Mechanics Meeting*, Austin, TX, February 12-15, 1996.
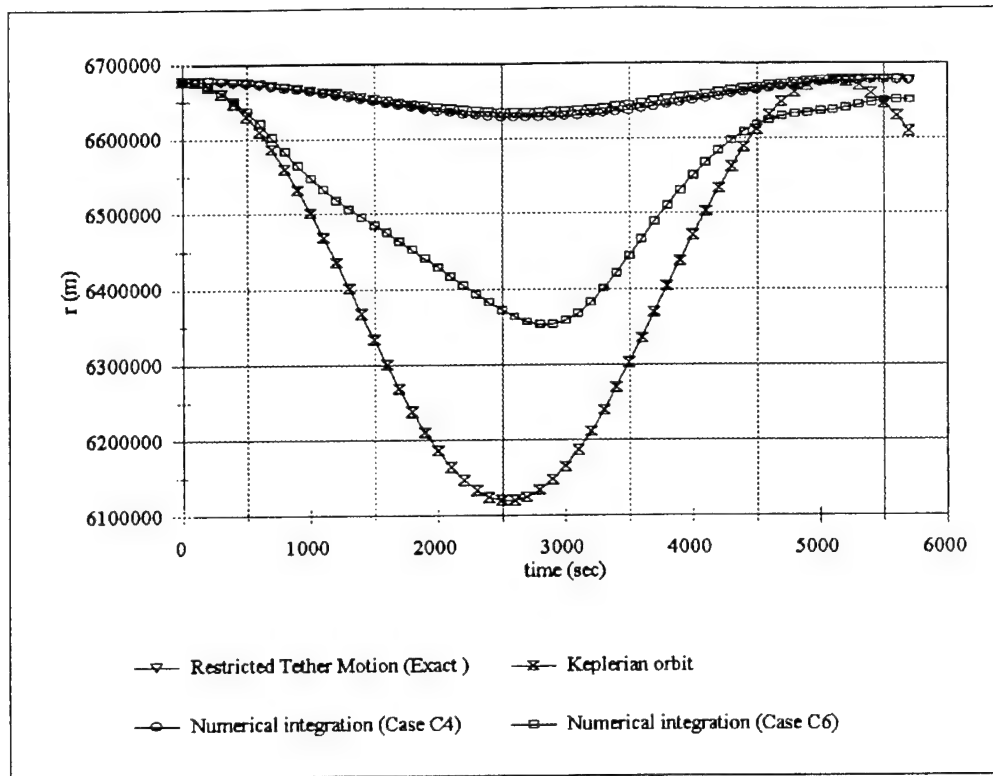
Fig. 4. Radial Distance for Near Circular Orbit and Large Tether Parameters.
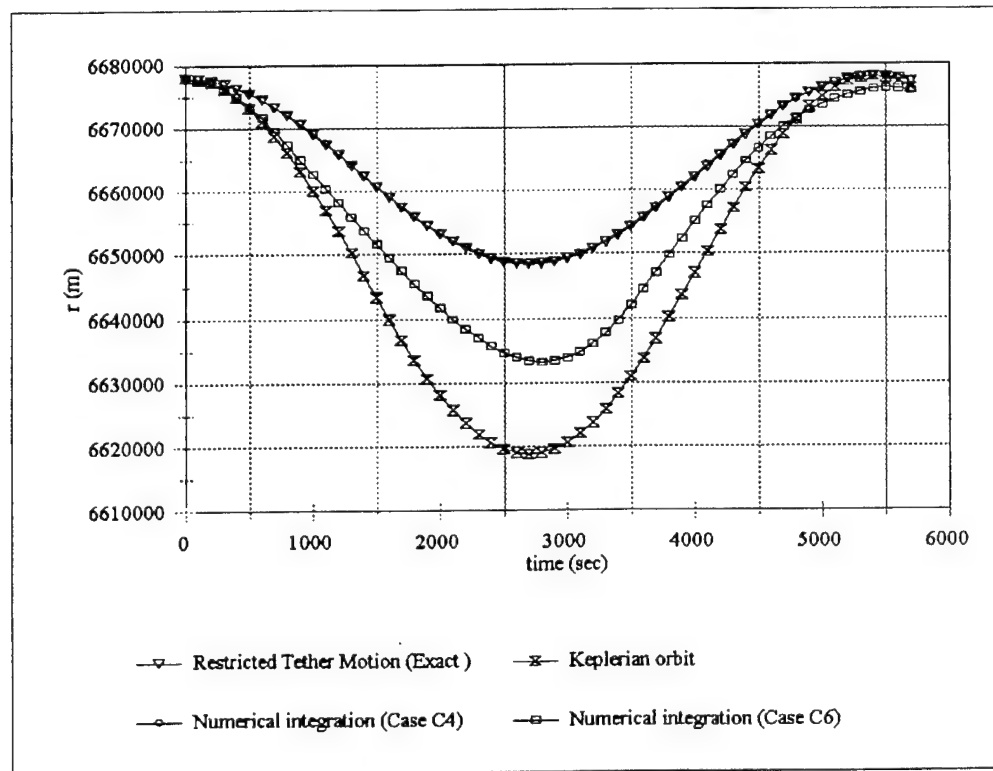
Fig. 5. Radial Distance for Near Circular Orbit and Small Tether Parameters.

Table 1. Example Cases.

Case	m_p/m	ρ (km)	ε	$\dot{\theta}_0$	θ_{30}
C-1	1.0	10	7.8394E-04	9.3233E-01	0.0
C-2	10.0	100	1.4254E-02	9.1438E-01	0.0
C-3	1.0	10	7.8394E-04	9.3128E-01	0.1
C-4	10.0	100	1.4254E-02	9.1280E-01	0.1
C-5	1.0	10	7.8394E-04	9.3128E-01	1.0
C-6	10.0	100	1.4254E-02	9.1280E-01	1.0
E-3	1.0	10	7.8394E-04	1.0202E+00	0.1
E-4	10.0	100	1.4254E-02	9.9992E-01	0.1
E-5	1.0	10	7.8394E-04	1.0202E+00	1.0
E-6	10.0	100	1.4254E-02	9.9992E-01	1.0

Table 2. Estimation Results for Case C-1.

State		Dynamic Model					
		Two-body Motion		Restricted Motion		Plane TSS	
	True	Guess	Result	Guess	Result	Guess	Result
r	1.047E+00	1.000E+00	1.047E+00	1.047E+00	1.047E+00	1.047E+00	1.047E+00
θ	3.491E-01	0.000E+00	3.491E-01	3.491E-01	3.491E-01	3.491E-01	3.491E-01
$\dot{r}$	0.000E+00	0.000E+00	8.604E-16	8.604E-16	-3.268E-10	0.000E+00	2.801E-13
$\dot{\theta}$	9.323E-01	1.000E+00	9.323E-01	9.323E-01	9.323E-01	9.323E-01	9.323E-01
θ_3	0.000E+00					0.000E+00	8.269E-05
$\dot{\theta}_3$	0.000E+00					9.323E-01	-4.040E-04
ε	7.839E-04		7.834E-04	7.833E-04	7.839E-04	7.840E-04	7.842E-04
μ	3.986E+14	3.986E+14	3.977E+14				

Table 3. Estimation Results for Case C-2.

State		Dynamic Model					
		Two-body Motion		Restricted Motion		Plane TSS	
	True	Guess	Result	Guess	Result	Guess	Result
r	1.047E+00	1.000E+00	1.047E+00	1.047E+00	1.047E+00	1.047E+00	1.047E+00
θ	3.491E-01	0.000E+00	3.491E-01	3.491E-01	3.491E-01	3.491E-01	3.491E-01
$\dot{r}$	0.000E+00	1.000E-01	-7.597E-16	0.000E+00	1.350E-09	0.000E+00	7.610E-11
$\dot{\theta}$	9.144E-01	1.000E+00	9.144E-01	9.144E-01	9.144E-01	9.144E-01	9.144E-01
θ_3	0.000E+00					1.000E+00	-1.580E-05
$\dot{\theta}_3$	0.000E+00					9.144E-01	6.613E-05
ε	1.425E-02		1.425E-02	1.425E-02	1.425E-02	1.425E-02	1.425E-02
μ	3.986E+14	3.986E+14	3.825E+14				

Table 4. Estimation Results for Case C-3.

State		Dynamic Model					
		Two-body Motion		Restricted Motion		Plane TSS	
	True	Guess	Result	Guess	Result	Guess	Result
r	1.047E+00	1.000E+00	1.047E+00	1.047E+00	1.047E+00	1.047E+00	1.047E+00
θ	3.491E-01	0.000E+00	3.352E-01	3.352E-01	3.491E-01	3.491E-01	3.491E-01
$\dot{r}$	0.000E+00	0.000E+00	2.825E-07	2.825E-07	-1.423E-06	0.000E+00	1.081E-07
$\dot{\theta}$	9.313E-01	1.000E+00	9.960E-01	9.960E-01	9.313E-01	9.313E-01	9.313E-01
θ_3	1.000E-01					1.000E+00	1.010E-01
$\dot{\theta}_3$	0.000E+00					9.313E-01	-4.453E-03
ε	7.839E-04		-4.702E-02	-4.702E-02	7.447E-04	7.447E-04	7.864E-04
μ	3.986E+14	3.986E+14	4.548E+14				

Table 5. Estimation Results for Case C-4.

State		Dynamic Model					
		Two-body Motion		Restricted Motion		Plane TSS	
	True	Guess	Result	Guess	Result	Guess	Result
r	1.047E+00	1.000E+00		1.000E+00	1.047E+00	1.047E+00	1.047E+00
θ	3.491E-01	0.000E+00		0.000E+00	3.490E-01	3.490E-01	3.491E-01
$\dot{r}$	0.000E+00	1.000E-01		0.000E+00	-2.545E-05	1.000E-04	-2.686E-08
$\dot{\theta}$	9.128E-01	1.000E+00		1.000E+00	9.135E-01	9.135E-01	9.128E-01
θ_3	1.000E-01		(FAILED)			1.000E-00	1.000E-01
$\dot{\theta}_3$	0.000E+00					9.135E-01	-7.388E-05
ε	1.425E-02			1.000E-03	1.353E-02	1.353E-02	1.425E-02
μ	3.986E+14	3.986E+14					

Table 6. Estimation Results for Case C-5.

State		Dynamic Model					
		Two-body Motion		Restricted Motion		Plane TSS	
	True	Guess	Result	Guess	Result	Guess	Result
r	1.047E+00	1.000E+00	1.047E+00	1.047E+00	1.047E+00	1.047E+00	1.047E+00
θ	3.491E-01	0.000E+00	3.312E-01	3.312E-01	3.491E-01	3.491E-01	3.491E-01
$\dot{r}$	0.000E+00	0.000E+00	3.755E-07	0.000E+00	-3.132E-6	-3.132E-6	7.577E-08
$\dot{\theta}$	9.313E-01	1.000E+00	1.015E+00	1.015E+00	9.314E-01	9.314E-01	9.313E-01
θ_3	1.000E+00					1.000E-01	1.001E+00
$\dot{\theta}_3$	0.000E+00					9.314E-01	3.854E-03
ε	7.839E-04		-6.510E-2	-6.510E-2	7.394E-05	7.394E-05	7.801E-04
μ	3.986E+14	3.986E+14	4.729E+14				

Table 7. Estimation Results for Case C-6.

State		Dynamic Model					
		Two-body Motion		Restricted Motion		Plane TSS	
	True	Guess	Result	Guess	Result	Guess	Result
r	1.047E+00	1.000E+00	1.047E+00	1.047E+00	1.047E+00	1.047E+00	1.047E+00
θ	3.491E-01	0.000E+00	3.150E-01	3.150E-01	3.490E-01	3.490E-01	3.491E-01
$\dot{r}$	0.000E+00	1.000E-01	1.097E-05	1.097E-05	-5.082E-5	-5.082E-5	7.698E-08
$\dot{\theta}$	9.128E-01	1.000E+00	1.070E+00	1.070E+00	9.141E-01	9.141E-01	9.128E-01
θ_3	1.000E+00					1.000E-01	1.000E+00
$\dot{\theta}_3$	0.000E+00					9.141E-01	-2.598E-04
ε	1.425E-02		-1.231E-1	-1.231E-1	1.280E-03	1.280E-03	1.427E-02
μ	3.986E+14	3.986E+14	5.392E+14				

Table 8. Estimation Results for Case E-3.

State		Dynamic Model					
		Two-body Motion		Restricted Motion		Plane TSS	
	True	Guess	Result	Guess	Result	Guess	Result
r	1.047E+00	1.000E+00	1.047E+00	1.047E+00	1.047E+00	1.047E+00	1.047E+00
θ	3.491E-01	0.000E+00	3.492E-01	3.492E-01	3.491E-01	3.491E-01	3.491E-01
$\dot{r}$	0.000E+00	0.000E+00	-3.179E-07	-3.179E-07	-7.721E-06	-7.721E-6	7.566E-08
$\dot{\theta}$	1.020E+00	1.000E+00	1.020E+00	1.020E+00	1.020E+00	1.020E+00	1.020E+00
θ_3	1.000E-01					1.000E+00	1.001E-01
$\dot{\theta}_3$	0.000E+00					1.020E+00	-1.997E-04
ε	7.839E-04		1.256E-03	1.256E-03	7.441E-04	7.441E-04	7.840E-04
μ	3.986E+14	3.986E+14	3.971E+14				

Table 9. Estimation Results for Case E-4.

State	True	Two-body Motion		Restricted Motion		Plane TSS	
		Guess	Result	Guess	Result	Guess	Result
r	1.047E+00	1.000E+00	1.047E+00	1.047E+00	1.047E+00	1.047E+00	
θ	3.491E-01	0.000E+00	3.519E-01	3.519E-01	3.490E-01	3.490E-01	
$\dot{r}$	0.000E+00	1.000E-01	-6.280E-06	-6.280E-06	-1.387E-04	-1.387E-04	
$\dot{\theta}$	9.999E-01	1.000E+00	9.913E-01	9.913E-01	1.001E+00	1.001E+00	
θ_3	1.000E-01					1.000E+00	
$\dot{\theta}_3$	0.000E+00					1.001E+00	
ε	1.425E-02		2.166E-02	2.166E-02	1.351E-02	1.351E-02	
μ	3.986E+14	3.986E+14	3.738E+14				

Table 10. Estimation Results for Case E-5.

State	True	Two-body Motion		Restricted Motion		Plane TSS	
		Guess	Result	Guess	Result	Guess	Result
r	1.047E+00	1.000E+00	1.047E+00	1.047E+00	1.047E+00	1.047E+00	1.047E+00
θ	3.491E-01	0.000E+00	3.502E-01	3.502E-01	3.491E-01	3.491E-01	3.491E-01
$\dot{r}$	0.000E+00	1.000E-01	-8.798E-07	-8.798E-07	-1.577E-05	-1.577E-5	-1.723E-07
$\dot{\theta}$	1.020E+00	1.000E+00	1.017E+00	1.017E+00	1.020E+00	1.020E+00	1.020E+00
θ_3	1.000E+00					5.000E-01	9.986E-01
$\dot{\theta}_3$	0.000E+00					1.020E+00	2.046E-03
ε	7.839E-04		3.157E-03	3.157E-03	8.525E-05	8.525E-05	7.776E-04
μ	3.986E+14	3.986E+14	3.949E+14				

Table 11. Estimation Results for Case E-6.

State	True	Two-body Motion		Restricted Motion		Plane TSS	
		Guess	Result	Guess	Result	Guess	Result
r	1.047E+00	1.000E+00	1.047E+00	1.047E+00	1.047E+00	1.047E+00	1.047E+00
θ	3.491E-01	0.000E+00	3.755E-01	3.755E-01	3.489E-01	3.489E-01	3.491E-01
$\dot{r}$	0.000E+00	1.000E-01	-3.225E-07	-3.225E-07	-2.721E-04	-2.721E-04	-1.283E-7
$\dot{\theta}$	9.999E-01	1.000E+00	9.135E-01	9.135E-01	1.002E+00	1.002E+00	9.999E-01
θ_3	1.000E+00					1.000E-01	9.999E-01
$\dot{\theta}_3$	0.000E+00					1.002E+00	2.962E-05
ε	1.425E-02		6.891E-02	6.891E-02	1.478E-03	1.478E-03	1.425E-02
μ	3.986E+14	3.986E+14	3.199E+14				

A FILTERING METHOD FOR THE IDENTIFICATION OF A TETHERED SATELLITE

D. A. Cicci[1], T. A. Lovell[2], and C. Qualls[2]
Auburn University, Alabama

Abstract

The dynamics of a tethered satellite are greatly affected by the perturbing force transmitted to the satellite through the tether. The existence of this tether force causes the satellite to behave in a non-Keplerian manner. Classical orbit determination methods are unable to account for this modified Keplerian motion and the subsequent estimation procedure will commonly result in an inaccurate prediction of the satellite's trajectory. The predicted trajectory in such cases could appear to be ballistic in nature. In such cases, the speed at which an accurate identification of the satellite can be made may also be very important. In order to distinguish between the motion characteristic of a single (untethered) satellite and that of a tethered satellite, and to correctly identify a satellite as being tethered, a batch-type filter has been developed for use in the orbit determination process. This filter includes the effect the tether force has on the motion of the satellite. The filter's performance is also evaluated in this study. Results are presented for cases of differing tether lengths, tether orientations, and types of observations being processed. In addition, results are presented using actual TSS data obtained from the Tether Physics and Survivability Experiment.

[1] Associate Professor, Department of Aerospace Engineering, Member AAS .
  Email: dcicci@eng.auburn.edu. Phone: (334) 844-6820, FAX: (334) 844-6803.
[2] Graduate Student, Department of Aerospace Engineering.

1

Introduction

The concept behind tethered satellites is to control the motion of two satellites relative to one another by connecting them with a tether. In such a tethered satellite system (TSS), one satellite is often much larger than the other and is referred to as the 'parent' satellite. The second satellite, or 'daughter,' is usually smaller than the parent and can be located in either a higher, lower, or the same orbit as the parent.

The prospect of tethered satellites being used more frequently by both the public and private sectors brings with it renewed interest in the ability to accurately track, identify, and predict the motion of a TSS. Failure to accurately analyze the motion of these systems could result in a tethered satellite being incorrectly identified as a ballistic threat. A tethered satellite behaves differently from an untethered one due to the force present in the tether. This tether force creates perturbations on the satellite which cause it to deviate from the Keplerian-like motion followed by an untethered satellite [1]. Specifically, if the tethered body is in a lower orbit than the center-of-mass of the system, its velocity will be smaller in magnitude than that predicted by Keplerian theory for an untethered satellite. Similarly, if the tethered body is in a higher orbit than the center-of-mass of the system, its velocity will be larger in magnitude than that of an untethered satellite. Subsequent calculations of the satellite's trajectory will therefore be inaccurate.

Satellite identification and orbit prediction is performed by utilizing tracking station measurements of the satellite's motion. These measurements typically include range, azimuth, and/or elevation, which are obtained by the use of radar, infrared, radio and/or optical techniques. The first few measurements can be used in an initial orbit determination (IOD) procedure, which will establish

a set of initial conditions for the prediction of the satellite's trajectory. A larger set (or batch) of these measurements, which are obtained from one or more tracking stations, are then processed using a batch filter in order to more accurately determine the satellite's initial conditions, which will subsequently be used to predict the satellite's future trajectory. Classical orbit determination methods can not be used tc determine if a tracked satellite is part of a tethered system because they will identify and track the satellite as if it were an untethered one. Application of such methods will likely cause an inaccurate prediction of the satellite's trajectory and perhaps a false identification of the vehicle.

Several recent studies have addressed the orbit determination of a tethered satellite. Kessler and Cicci [2] evaluated the performance of eight different batch-type filters in the estimation of the state of a tethered satellite. This work considered a simple two-dimensional dynamical model of a TSS, which maintained a vertical orientation of the inextensible, massless tether and its two end masses. The model used did not include libration of the system. These filters were developed to investigate their ability to identify a tethered satellite using a short arc of observational data. Once a satellite was identified, more complex models could then be used to predict its future motion. Subsequent effoits by Cochran, et al. [3], Cho, et al. [4,5], and Cochran, et al [6], have resulted in a more sophisticated dynamical model of a TSS to be used in the trajectory prediction phase of the problem. These enhanced dynamical models and accompanying filtering techniques presented are more useful when long arcs of observational data are available.

This study represents a continuation of the research presented in [2]. Specifically, filter modifications are included which provide for a simple, yet more complete dynamical model. These modifications allow the filter to include libration of a TSS to process multiple types of measurement

data, and also determine the tether force as well as the distance the tethered satellite is located above or below the center-of-mass of the system. The performance of this filter is evaluated through the analysis of simulated data using various tether lengths, tether orientations, and observation types, as well as actual observation data obtained for a TSS from the Tether Physics and Survivability Experiment. Results of the performance of the filter are presented along with several conclusions and recommendations for further research.

Tethered Satellite System Model

The coordinate systems and position vectors used to describe the motion of a two-satellite TSS are depicted in Figure 1. The mass of the tether is neglected to emphasize the motions of the two satellites. The Earth (E), the observed "daughter" satellite (m), and the unobserved "parent" satellite (m_p) are all modeled as point masses.

In Figure 1, the origin of the fixed **xyz** system is the Earth, as well as the coordinate system defined by unit vectors u_1, u_2, and u_3. The u_1u_2 plane is the osculating plane in which mass m is moving at some point in time. The orientation of the osculating plane is defined by Ω and i, the longitude of the ascending node and inclination, respectively. The vector **r** defines the position of satellite m with respect to Earth while the vector r_p defines the position of satellite m_p with respect to Earth. For the model described in this study, the forces considered on each satellite are due only to the inverse-squared gravitational attraction of the Earth, and the force due to the tension in the tether. Thus, the equations of motion for the satellites m and m_p are

$$\ddot{\mathbf{r}} = -\mu \frac{\mathbf{r}}{r^3} + \frac{\mathbf{F}_T}{m} \tag{1}$$

$$\ddot{\mathbf{r}}_p = -\mu \frac{\mathbf{r}_p}{r_p^{\;3}} - \frac{\mathbf{F}_T}{m_p} \tag{2}$$

where $\mathbf{r}$ and $\mathbf{r}_p$ are defined to be positive outward from the Earth, and tether tension force $\mathbf{F}_T$ is positive in the direction from m to m_p.
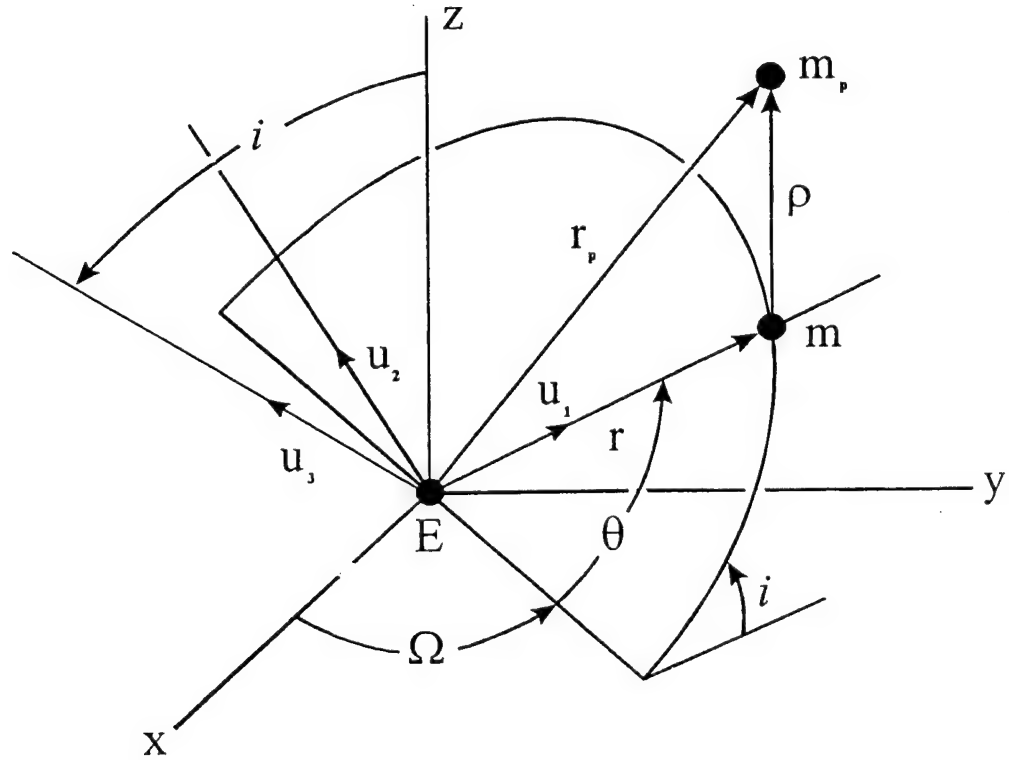
Figure 1. Osculating Orbit Plane

In Figure 1, the vector ρ is the relative position vector of m_p with respect to m. By using equations (1) and (2), we may then write

$$\ddot{\rho} = \Delta g - \frac{M}{m\,m_p}\mathbf{F}_T \qquad (3)$$

where

$$M = m + m_p \qquad (4)$$

and

$$\Delta g \equiv -\frac{\mu}{r_p^3}\mathbf{r}_p + \frac{\mu}{r^3}\mathbf{r} . \qquad (5)$$

To describe the motion of m_p with respect to m, Figure 2 shows a third coordinate system, $e_1e_2e_3$. The orientation of $e_1e_2e_3$ with respect to $u_1u_2u_3$ is given by the angles θ_3 and θ_2, which are termed the in-plane and out-of-plane libration angles, respectively.
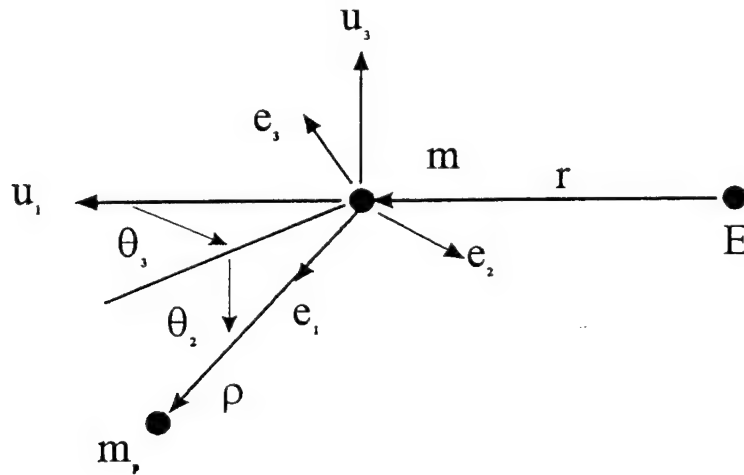
Figure 2. Relative Motion of m_p with respect to m

Using Figures 1 and 2, and equations (1) and (3), we may express the equations of motion for m and m_p in the rotating frames $u_1u_2u_3$ and $e_1e_2e_3$, respectively, as

$$\ddot{\mathbf{r}} + \dot{\boldsymbol{\lambda}} \times \mathbf{r} + 2\boldsymbol{\lambda} \times \dot{\mathbf{r}} + \boldsymbol{\lambda} \times \boldsymbol{\lambda} \times \mathbf{r} = -\mu \frac{\mathbf{r}}{r^3} + \frac{\mathbf{F_T}}{m} \tag{6}$$

$$\ddot{\boldsymbol{\rho}} + \dot{\boldsymbol{\omega}} \times \boldsymbol{\rho} + 2\boldsymbol{\omega} \times \dot{\boldsymbol{\rho}} + \boldsymbol{\omega} \times \boldsymbol{\omega} \times \boldsymbol{\rho} = \Delta \mathbf{g} - \mathbf{F_T} \frac{M}{m\,m_p} \tag{7}$$

where λ in equation (6) is the angular velocity of the $u_1u_2u_3$ coordinate system., and ω in equation (7) is the angular velocity of the $e_1e_2e_3$ coordinate system.

We can use equations (6) and (7) to obtain the following scalar equations for the motion of m:

$$\ddot{r} = (\lambda_2^2 + \lambda_3^2)r - \frac{\mu}{r^2} + \mathbf{u}_1 \cdot \frac{\mathbf{F_T}}{m} \tag{8}$$

$$\dot{\lambda}_3 = \frac{1}{r}\left(-2\lambda_3\,\dot{r} - \lambda_1\,\lambda_2\,r + \mathbf{u}_2 \cdot \frac{\mathbf{F_T}}{m}\right) \tag{9}$$

$$\dot{\lambda}_2 = \frac{1}{r}\left(-2\lambda_2\,\dot{r} + \lambda_1\,\lambda_3\,r + \mathbf{u}_3 \cdot \frac{\mathbf{F_T}}{m}\right) \tag{10}$$

7

$$\dot{\Omega} = \lambda_1 \sin\theta / \sin i \tag{11}$$

$$\frac{di}{dt} = \lambda_1 \cos\theta \tag{12}$$

$$\dot{\theta} = \lambda_3 - \lambda_1 \sin\theta \cos i / \sin i \tag{13}$$

Note that, since we have described the motion of the daughter satellite in the $\mathbf{u_1 u_2}$ osculating plane, $\lambda_2 \equiv \dot{\lambda}_2 \equiv 0$. We may then write λ_1 by using equation (10) as

$$\lambda_1 = \frac{1}{\lambda_3 r} \mathbf{u}_3 \cdot \frac{\mathbf{F}_T}{m} \tag{14}$$

Similarly, the equations of motion for satellite m_p can be written as

$$\ddot{\rho} = (\omega_2^2 + \omega_3^2)\rho + \mathbf{e}_1 \cdot \Delta\mathbf{g} + \mathbf{e}_1 \cdot \mathbf{F}_T \frac{M}{m\, m_p} \tag{15}$$

$$\dot{\omega}_3 = \frac{1}{\rho}\left(-2\omega_3 \dot{\rho} - \omega_1 \omega_2 \rho + \mathbf{e}_2 \cdot \Delta\mathbf{g} + \mathbf{e}_2 \cdot \mathbf{F}_T \frac{M}{m\, m_p} \right) \tag{16}$$

$$\dot{\omega}_2 = \frac{1}{\rho}\left(-2\omega_2 \dot{\rho} + \omega_1 \omega_3 \rho - \mathbf{e}_3 \cdot \Delta\mathbf{g} + \mathbf{e}_3 \cdot \mathbf{F}_T \frac{M}{m\, m_p} \right) \tag{17}$$

8

$$\dot{\theta}_2 = \omega_2 + \lambda_1 \sin \theta_3 \tag{18}$$

$$\dot{\theta}_3 = (\omega_3 - \lambda_1 \sin \theta_2 \cos \theta_3)/\cos \theta_2 - \lambda_3 \tag{19}$$

If the tether is modeled as inextensible, $\ddot{\rho} \equiv 0$ and $\mathbf{F}_T$ will always be in the $\mathbf{e}_1$ direction. This eliminates the $\mathbf{F}_T$ term from equations (16) and (17) and allows us to obtain the tether force from equation (15) as

$$\mathbf{F}_T = \frac{m \, m_p}{M} \rho [\omega_2^2 + \omega_3^2 + \frac{\mu}{r^3}(3 \cos^2 \theta_2 \cos^2 \theta_3 - 1)] \mathbf{e}_1 \tag{20}$$

if the right-hand side of equation (20) is greater than zero; otherwise $\mathbf{F}_T = 0$. In the equation above, an approximation for $\Delta \mathbf{g}$ is used, which was derived in [3] assuming small libration angles. In order to simulate the dynamic motion of a particular tethered system using the above model, the quantities m, m_p and ρ must be specified, as well as initial conditions on r, Ω, i, θ, θ_2, θ_3, $\dot{r}$, λ_3, ω_2, and ω_3. Observational data of the daughter satellite at each time step can then be generated by taking the states pertaining to the motion of mass m (r, Ω, i, θ, $\dot{r}$, λ_3) and converting to range, azimuth, and elevation.

Filter Description

9

The state of a satellite can be estimated by processing observational data in one group using a batch filter. However, in order for the filter to be capable of distinguishing between a tethered satellite and an untethered one, the potential effects of the tether force must be accounted for in the filter's dynamical model. This will require a modification to standard filter models to include tether specific parameters which will allow the filter to distinguish between Keplerian-like motion and modified Keplerian motion.
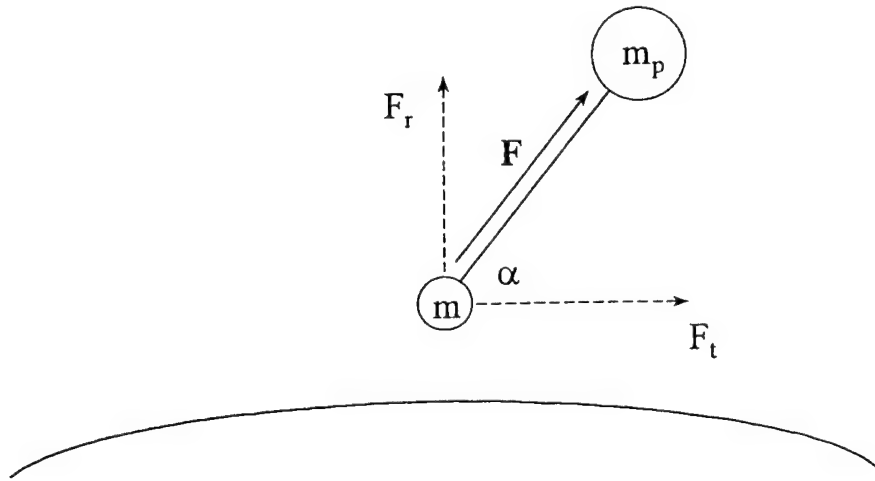
Figure 3. Tethered Satellite System

The most evident characteristic of a tethered satellite's motion is that its velocity is affected by the parent satellite due to the presence of the force in the tether connecting the bodies. The filter model must be able to account for these differing velocities, otherwise inaccurate state estimates of the tethered satellite will be obtained. Figure 3 shows a tethered (daughter) satellite, m, and the

10

effective tether force, **F**, due to the presence of the parent satellite, m_p. Assuming planar motion of the TSS, α is the angle the tether makes with the local horizontal (i.e., with respect to the daughter mass's location above the Earth).

The effect that the tether force will have on the motion of a satellite can be more easily visualized by studying the separate effects of the radial and tangential force components, F_r and F_t, respectively. Both of these force components will tend to change the acceleration on the satellite in their respective directions, thereby altering the satellite's velocity. For example, the presence of F_r will change the radial acceleration, which is normally determined by the Earth's gravitational constant, μ. This radial acceleration component will reduce the total radial acceleration on the satellite if the orbit of the daughter is lower than that of the parent and increase the total radial acceleration if the daughter's orbit is higher than the parent's. A reduced total radial acceleration will result in a smaller velocity for the daughter than that of an untethered satellite, while an increased radial acceleration will result in a larger velocity for the daughter than that of an untethered satellite. The tangential tether force, F_t, has the effect of decreasing the velocity of the daughter satellite when it "leads" the parent satellite, whereas it increases the daughter satellite's velocity when it lags behind the parent satellite. Note that in the former case, F_t has an effect on the satellite similar to atmospheric drag.

It follows from the preceding discussion that two tether specific parameters, namely a radial acceleration term, a_r, resulting from F_r, and a tangential acceleration term, a_t, resulting from F_t, can be included in the state vector of the filter. If one or more of these parameters is estimated by the filter to be nonzero, this should indicate the existence of a tether force acting on the satellite. Likewise, if these terms are estimated to be zero, the satellite can be considered to be an untethered one. To account for a_r and a_t, an augmented state vector, **X**, can be defined for the batch filter. This

11

(8 x 1) state vector consists of the satellite's position and velocity components in Cartesian form, as well as the tether parameters, a_r and a_t, as shown by

$$\mathbf{X} = \begin{bmatrix} x \\ y \\ z \\ \dot{x} \\ \dot{y} \\ \dot{z} \\ a_r \\ a_t \end{bmatrix} = \begin{bmatrix} X_1 \\ X_2 \\ X_3 \\ X_4 \\ X_5 \\ X_6 \\ X_7 \\ X_8 \end{bmatrix} \tag{21}$$

The state equations for this filter take the form

$$\dot{\mathbf{X}} = \mathbf{F}(\mathbf{X}, t), \qquad \mathbf{X}(t_k) = \mathbf{X}_k \tag{22}$$

where t_k indicates the epoch time, and the force vector, $\mathbf{F}(\mathbf{X}, t)$ can be represented by the equations

12

$$F(X, t) = \begin{bmatrix} X_4 \\ X_5 \\ X_6 \\ \dfrac{-\mu X_1}{|r|^3} + \dfrac{a_r X_1}{|r|} - \dfrac{a_t X_4}{|v|} \\ \dfrac{-\mu X_2}{|r|^3} + \dfrac{a_r X_2}{|r|} - \dfrac{a_t X_5}{|v|} \\ \dfrac{-\mu X_3}{|r|^3} + \dfrac{a_r X_3}{|r|} - \dfrac{a_t X_6}{|v|} \\ 0 \\ 0 \end{bmatrix} \tag{23}$$

Here, $|r|$ is the magnitude of the position vector and $|v|$ is the magnitude of the velocity vector.

In order to determine the state vector at a specific time, measurements of the satellite's range, azimuth, and/or elevation are made over a given time frame. These observations are then "mapped" to the desired epoch time. The expression for a linear mapping of the observations to the desired epoch time is given by

$$y = Hx + \varepsilon \tag{24}$$

where y is an (mx1) vector of observation residuals, H is an (mxn) mapping matrix, x is an (nx1) vector of corrections to the state vector, and ε is a (mx1) vector of measurement errors. The H matrix is a function of the state transition matrix, which allows the state vector to be mapped from one time to another [7].

The method used here to estimate the corrections to the state vector at the epoch time, x_k,

13

is the minimum variance solution. This method uses statistical information concerning the observation errors in the solution process. The observational errors are assumed to be random, having a Gaussian (normal) distribution with zero mean and a known covariance, $\mathbf{R}$. The minimum variance solution is given [8] as

$$\hat{\mathbf{x}}_k = (\mathbf{H}^T \mathbf{R}^{-1} \mathbf{H})^{-1} \mathbf{H}^T \mathbf{R}^{-1} \mathbf{y} \tag{25}$$

The covariance matrix provides a measure of the uncertainty in this solution and is given by

$$\mathbf{P}_k = (\mathbf{H}^T \mathbf{R}^{-1} \mathbf{H})^{-1} \tag{26}$$

This batch filter will determine the state of the observed satellite at the epoch time. Once the parameters, a_r and a_t, are calculated through the estimation process, several determinations can be made.

1. If both a_r and a_t are equal to zero, to within some specified tolerance, it can be assumed that the satellite is not part of a tethered system and its motion can be analyzed using standard techniques.

2. If a_r and a_t are not equal to zero:

    (a) Their values can be used to determine the tether orientation angle, α, from

14

$$\alpha = \tan^{-1}(a_r / a_t) \tag{27}$$

(b) The magnitude of the tether force (per unit mass) can be calculated by

$$F/m = [\, a_r^2 + a_t^2\,]^{1/2} \tag{28}$$

(c) The apparent value of the gravitational parameter, $\mu*$, can be determined from the expression

$$\mu^* = \mu - a_r r^2 \tag{29}$$

This $\mu*$ can then be used along with the position and velocity vectors to determine the orbital element set which fully describes the satellite's orbit.

(d) The value of $\mu*$ can be used to determine ρ_{cm}, the distance the tethered satellite is located above or below the center-of-mass of the system. An approximation for $\mu*$ was provided in [4] in terms of $\rho_{cm.}$. If libration is negligible, this equation is

$$\mu^* = \mu \left[1 - 2\frac{\rho_{cm}}{r} \right]\left[1 + \frac{\rho_{cm}}{r} \right]^{-1} \tag{30}$$

15

or

$$\rho_{cm} = \left(\frac{\mu - \mu^*}{2\mu + \mu^*} \right) r \qquad (31)$$

when the daughter satellite is below the parent satellite, and

$$\mu^* = \mu \left[1 + 2\frac{\rho_{cm}}{r} \right] \left[1 - \frac{\rho_{cm}}{r} \right]^{-1} \qquad (32)$$

or

$$\rho_{cm} = \left(\frac{\mu^* - \mu}{2\mu + \mu^*} \right) r \qquad (33)$$

when the daughter satellite is above the parent satellite. Since ρ_{cm} approaches the actual tether length as the ratio of the daughter mass to the parent mass gets small, ρ_{cm} can be a very useful parameter to estimate.

3. If a_t is equal to zero but a_r is not, the satellite will be tethered and the orientation of the system will be vertical, i.e., $\alpha = 0°$ or $180°$.

4. If a_r is equal to zero but a_t is not, the satellite will be tethered and the orientation of the system will be horizontal, i.e., $\alpha = 90°$ or $270°$.

16

The following is a brief description of how the initial guess for the state vector $\mathbf{X}^*$ was determined in order to obtain the results given in the next section. As mentioned previously, the TSS simulation model contains the equations for the position and velocity of the masses in terms of the orbital elements, whereas the model contained within the filter expresses position and velocity of the observed mass in terms of Cartesian inertial coordinates. The goal of the filter is to estimate the true position (x, y, z) and velocity $(\dot{x}, \dot{y}, \dot{z})$ of mass m, as well as the acceleration components (a_t and a_r) due to the tether. Initial values for $(x, y, z, \dot{x}, \dot{y}, \dot{z})$ are found by converting the initial orbital elements to Cartesian form; while a_t and a_r are calculated at the beginning of the simulation, using equation (20). The initial guess $\mathbf{X}^*$ was then constructed by taking these "exact" values, and perturbing each value by a certain percentage.

Results

To investigate the filter's performance on sample observation data, the model described herein was used to simulate both a single (Keplerian) satellite and several tethered configurations. (For simulation of single-satellite motion, only the states pertaining to mass m $(r, \Omega, i, \theta, \dot{r}, \lambda_3)$ were integrated and the tether force, F_T, was set to zero in the fundamental equations of motion.) From these simulation results, position data, as a function of time, for the daughter mass m was translated into range, azimuth, and elevation data (relative to a tracking station at a chosen location on the Earth) to be utilized by the filter.

17

For discussion of the results obtained, it is most useful to define a "baseline" TSS configuration and to consider all other configurations as modifications to this baseline. Consider a tethered pair with the following parameters and initial state values:

$$m = 10 \text{ kg} \qquad \theta_2 = 0 \text{ rad}$$

$$m_p = 100 \text{ kg} \qquad \theta_3 = 0 \text{ rad}$$

$$r = 6621000 \text{ m} \qquad \dot{r} = 0 \text{ m/sec}$$

$$\Omega = 0.1 \text{ rad} \qquad \lambda_3 = 1.17164 \times 10^{-3} \text{ rad/sec}$$

$$i = 0.1 \text{ rad} \qquad \omega_2 = 0 \text{ rad/sec}$$

$$\theta = 0 \text{ rad} \qquad \omega_3 = 1.17164 \times 10^{-3} \text{ rad/sec}$$

Note that the initial values for the in-plane and out-of-plane libration angles are zero. This indicates a vertical orientation of mass m being directly "below" mass m_p. The initial angular velocities λ_3 and ω_3 are such that the masses remain in this vertical orientation. This is only possible with the "simple" dynamic model described in this simulation, and adding any features to the model, such as the Earth's oblateness or aerodynamic drag, would upset this equilibrium. For the baseline scenario, the range, azimuth, and elevation relative to a particular tracking station were recorded for the daughter mass at five-second intervals for 335 seconds (approximately 1/16th period). The initial guess X* was constructed by taking the eight "exact" values, and perturbing each value by 1%.

This baseline equilibrium configuration can then be modified in several ways by varying the following parameters:

(a) tether length and orientation of the masses

(b) observation time/ sampling rate

(c) types of observational quantities utilized

(d) amount of initial in-plane (θ_3) or out-of-plane (θ_2) libration

In addition, the observational data can be corrupted with various levels of Gaussian noise in order to simulate the measurement error inherent in all tracking stations. In the results that follow, the performance of the filter is evaluated for a single satellite, the baseline TSS scenario, and several "offshoot" scenarios, based on the above modifications.

Baseline Performance

Table 1 indicates the filter's performance for a single satellite and the "baseline" (1km tether) TSS configuration. For both cases, in accordance with the discussion above, the filter processed range, azimuth, and elevation data for $1/16^{th}$ period. The initial guess, $\mathbf{X}^*$ was constructed by perturbing the exact $\mathbf{X}^*$ by 1%. The estimated state and parameter values show excellent agreement with the actual values, in most cases to eight significant digits or better. The RMS error shown is the error between the Cartesian coordinates of the daughter mass's actual position at each observation time and the coordinates of its position as predicted by the filter, based on the estimated value of the state at the final iteration. The filter was allowed to run until the change in RMS from one iteration to the next was less than .001%. In addition, Table 1 shows the calculated value of ρ_{cm} resulting from the state estimate obtained from equations (29)-(31).

19

Varying Tether Length

Table 2 shows the results on four slightly modified TSS configurations. As before, all configurations are deployed with initial conditions such that the TSS is in a vertical equilibrium orientation. For the first two cases (tether lengths of 10 km and 100 km), the orientation of the TSS is the same as that of the baseline, with mass m below m_p; while for the third case (tether length of 1 km), mass m is above m_p. In each case, 1/16th period of data was processed, and the initial guess, $\mathbf{X}^*$, was constructed by perturbing the exact $\mathbf{X}^*$ by 1%.

In general, for all three configurations the filter performs as well as for the baseline case. It was shown in [3] that the force on m due to the tether is proportional to tether length, and thus it would seem at first that the larger disturbances to the system by longer tethers would present more of a problem to the system. However, it should be pointed out that since all cases represent an idealized vertical equilibrium motion, accelerations a_t and a_r remain constant throughout each simulation (a_t being zero and a_r proportional to tether length). Thus, it follows that the filter's performance should be about the same for these several cases.

Varying Observation Time/ Sampling Rate

For the baseline case described above, the time between observations was increased from 5 seconds to 10, 20, and eventually 100 seconds. In each case, the filter yielded a solution with almost identical accuracy to that obtained with a five-second sampling interval. At this point it was found that an accurate solution could be obtained with as few as three observation times spread over the 1/16th-period time window. Given that there are eight parameters to be estimated, this is the minimum number of observations necessary if range, azimuth, and elevation measurements are being

20

processed at each observation time. This is, of course, the ideal case of no libration, in which case a_t and a_r are constant.

In order to determine the effect of a decreased observation span on the solution, the filter processed increasingly smaller batches of observation data, all of which were subsets of the full set of data used in the baseline case. (The sampling interval, in all cases, was maintained at 5 seconds.) It was found that $1/16^{th}$ period is the minimum observation time required for an acceptably accurate solution.

Varying Number of Observation Types

In the event that angle data cannot be obtained by a tracking station, a version of the filter which utilizes range measurements only was executed on several of the above configurations. These solutions are depicted in Table 3. For each case, the true state values are shown in Tables 1 and 2. In comparing these results with those above, the RMS error has increased and the accuracy of the solution, in terms of agreement between the actual and predicted states, has decreased to approximately six significant digits.

Observation Error

In order to simulate tracking station error, each piece of observation data for the baseline case was corrupted with a Gaussian noise component having a standard deviation compatible with the accuracy of tracking station sensors. To this end, the error in range, azimuth, and elevation measurements for typical stations are shown in Table 4. To simulate a "worst-case" scenario, the standard deviation for noise in each observation type was chosen to be equal to the maximum error

21

among those listed in Table 4; i.e., 45m for range and .023deg for the angles. The filter was run with each noise component added separately, then with all three combined. Table 5 contains the results of the filtering process for these four cases. The solution in each case was acceptably accurate, however in all but one case a $1/4^{th}$-period observation time was required. The RMS error is the average error between the Cartesian coordinates of the daughter mass's position as indicated by the observation data, and the coordinates of its position as determined by the filter. Both the RMS error and the estimated ρ_{cm} indicate the degree to which error in each of the observation types affects the solution. Namely, range error degrades the accuracy the least, while error in the two angle quantities both have about the same effect on the solution in terms of RMS. The error in azimuth, however, degrades the estimate of ρ_{cm} slightly more than error in elevation.

Libration

If the baseline TSS scenario is modified by setting the initial in-plane libration angle θ_3 to some nonzero value, the resulting librational motion induces periodic variation in several quantities, including the tether accelerations a_t and a_r. Note that in all the previous cases a_t and a_r are constant, and are assumed to be such by the model contained in the filter. Figures 4a-4d depict a_t and a_r for $1/16^{th}$ of an orbital period, given an initial in-plane libration angle of 1° and 5°, as well as for an initial out-of-plane libration angle of 1°. In all three instances, a_t and a_r will vary periodically about their "constant" value corresponding to the equilibrium configuration (0 and .00374 m/sec² respectively). It was found that a nonzero initial out-of-plane libration angle will induce a certain amount of in-plane libration as well.

22

Table 6 shows the results of the filter's performance, given $1/16^{th}$ period of observation data, for these various initial values of θ_3 and θ_2. Comparing a_t and a_r in the solutions with the "true" results of Figures 4a-4d, we see that their converged values in each case appear to very accurately estimate the average value of the "true" a_t and a_r over the observation time. As expected, the accuracy of the solution degrades with enhanced in-plane libration, as is evident by the increasing RMS error. In addition, the accuracy is less for initial out-of-plane libration than for an equivalent amount of initial in-plane libration, since the filter model assumes planar motion.
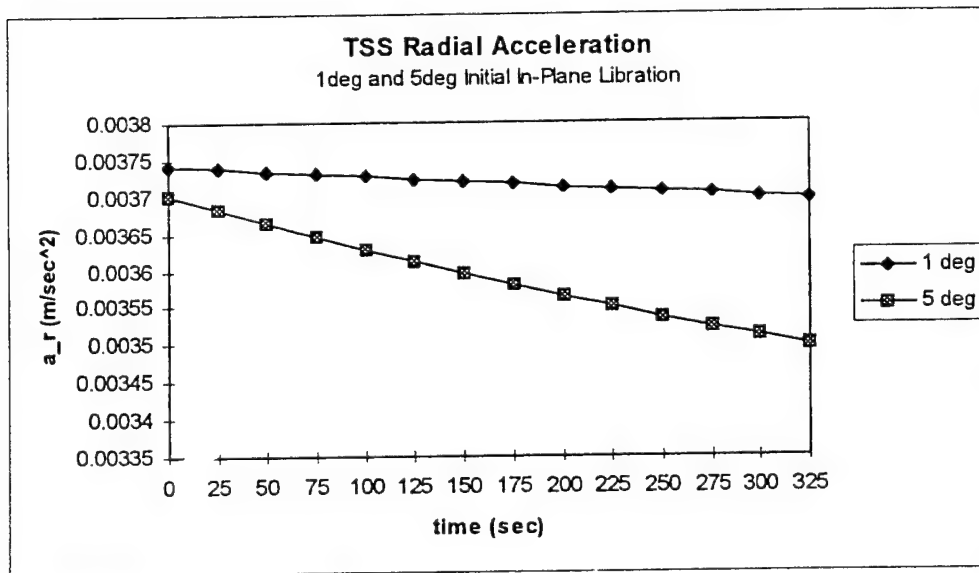
Figure 4a. TSS Radial Acceleration with In-Plane Libration
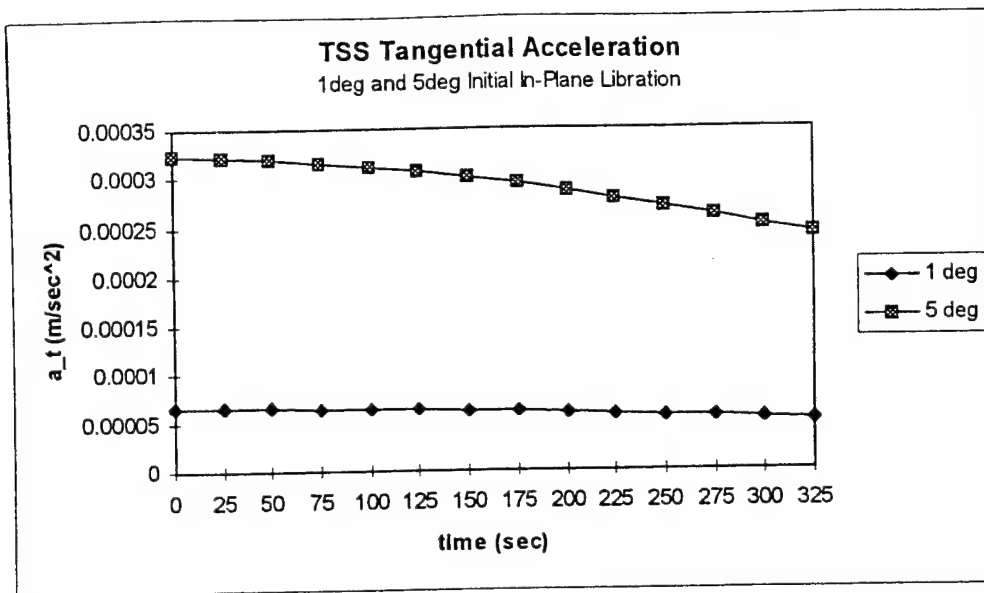
Figure 4b. TSS Tangential Acceleration with In-Plane Libration
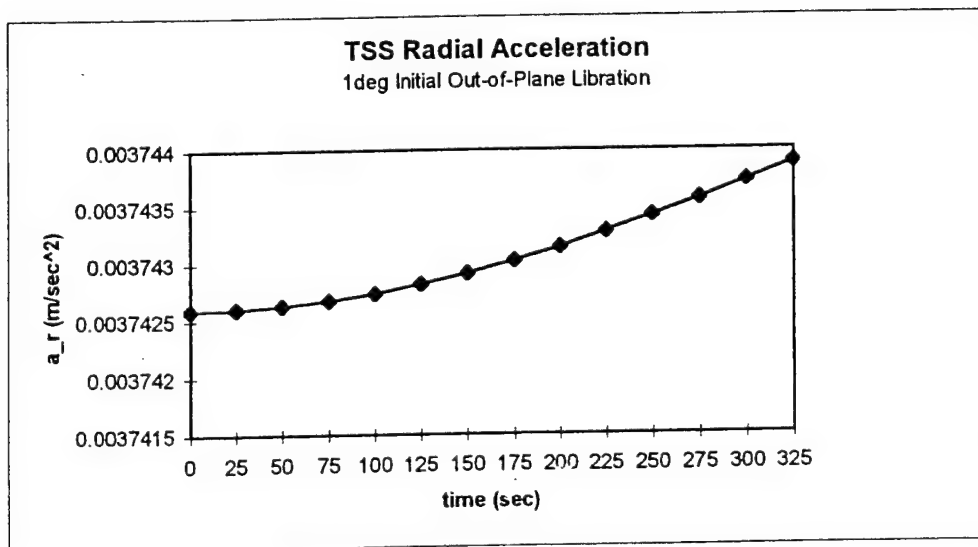
Figure 4c. TSS Radial Acceleration with Out-of-Plane Libration

24

TSS Tangential Acceleration

1deg Initial Out-of-Plane Libration
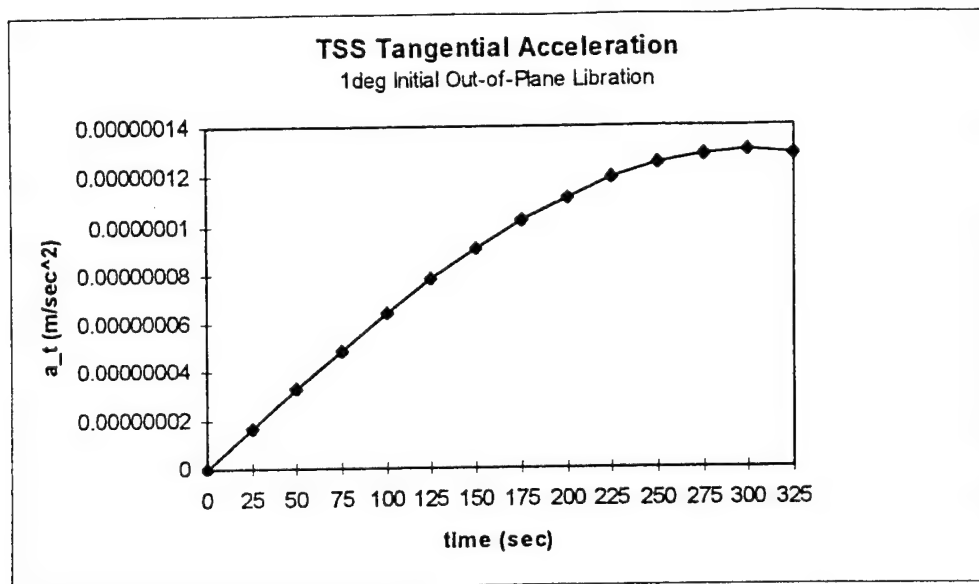
Figure 4d. TSS Tangential Acceleration with Out-of-Plane Libration

Application to Actual TSS Data

Having tested the filter successfully on several cases of model-generated data, the estimation routine was then performed on a batch of actual tracking data obtained for the lower mass of a TSS. The TSS under study is known as TiPS (Tether Physics and Survivability Experiment), which was deployed on 20 June 1996 at an altitude of 1,022 kilometers. The data processed by the filter consisted of a 600-second batch of range, azimuth, and elevation data obtained for the TiPS lower mass from a single tracking station during 1996. The geodetic latitude and longitude, and geodetic height of the tracking station are 42.6174351deg, 288.5091034deg, and 125.6m, respectively. The average sampling interval for this batch is approximately 8.5 seconds.

Since this data is not model-generated, the "correct" initial conditions (i.e., true state) for the mass's motion are not known. Therefore, an estimate of the initial conditions (initial orbit

determination) is obtained as follows. The range, azimuth, and elevation values for the first three observation times (call them t_1, t_2, and t_3) are converted to the Cartesian position coordinates of the satellite via the method described in [9]. The mass' velocity at time t_2 is then approximated by

$$\dot{\mathbf{x}}(t_2) = \frac{\Delta\mathbf{x}}{\Delta t} = \frac{\mathbf{x}(t_3) - \mathbf{x}(t_1)}{t_3 - t_1} \tag{31}$$

In order to approximate a_r and a_t, libration is assumed to be negligible, in which case a_t is assumed to be zero and a_r is assumed to act along the local vertical, i.e., opposing the gravitational acceleration. If it is further assumed that the mass's orbit is nearly circular, the apparent value of the gravitational parameter, $\mu*$, can be determined from

$$\mu* = v_c^2 r \tag{32}$$

where r and v_c are the magnitude of the position and velocity vectors, respectively, at t_2. Equating this expression for $\mu*$ to that in equation (29) yields an estimate of a_r. An initial orbit determination of the mass' state at the "epoch" time t_2 can then be obtained.

Table 7 displays the initial guess of the state obtained by the method above, as well as the converged solution. As was done with the model-generated data cases, equations (29)-(31) were used to determine ρ_{cm}. The resulting value, 4.596km, compares reasonably well to the actual value of 3.109km. Given the values of the TiPS masses (37.7kg and 10.8kg), the estimate of ρ_{cm} yields a tether length of approximately 5.9km, compared to the actual value of 4km.

26

Conclusions

A batch filtering technique was investigated for the purpose of identifying an Earth-orbiting satellite as being tethered or untethered. The filter estimates the satellite's position and velocity components as well as the radial and tangential acceleration components due to the tether force. Using observation data generated from a simplified dynamic model including the effects of Earth's gravity and the tether force, the filter was used to obtain solutions for two masses with varying configurations of tether length and orientation. The effects of several modifications to the filtering process were also explored. These included reduced observation time and sampling interval, introduction of Gaussian error to the observation data, and libration (non-equilibrium motion) in the tethered system. In all cases, the filter showed promising results, in terms of the necessary observation time, the level of measurement noise, or the amount of libration for which the filter can produce a satisfactory solution. Finally, the filter was used to estimate the state of an actual tethered satellite, using real observation data of the lower mass. As a verification of the method, the resulting calculation of the tether length proved to be fairly close to the actual value.

Acknowledgement

in the preparation of this work.

References

1. Hoots, F. R., R. L. Roehrich, and V. G. Szebehely, "Space Shuttle Tethered Satellite Analysis," Directorate of Astrodynamics, Peterson AFB, CO, August 1983.

2. Kessler, S. A., and D. A. Cicci, "Filtering Methods for the Orbit Determination of a Tethered Satellite," *The Journal of Astronautical Sciences*, Vol. 45, No. 3, July-September 1997, pp. 263-278.

3. Cochran, J. E. Jr., S. Cho, Y-M Cheng, and D. A. Cicci, "Dynamics and Orbit Determination of Tethered Satellite Systems," AAS 96-147, AAS/AIAA Space Flight Mechanics Meeting, Austin, TX, Feb. 12-15, 1996.

4. Cho, S., J. E. Cochran, Jr., and D. A. Cicci, "Identification and Orbit Determination of Tethered Satellite System," AAS 98-101, AAS/AIAA Space Flight Mechanics Meeting, Monterey, CA, Feb. 9-11, 1998.

5. S. Cho, J. E. Cochran, Jr., and D. A. Cicci, "Approximate Solutions for Tethered Satellite Motion," AAS/AIAA Space Flight Mechanics Meeting, Breckenridge, CO, Feb. 7-10, 1999.

6. Cochran, J. E., Jr., S. Cho, A. Lovell, and D. A. Cicci, "On the Information Contained in the Motion of One Satellite of a Two-Satellite Tethered System," AIAA 98-4555, AIAA/AAS Astrodynamics Specialist Conference, Boston, MA, August 10-12, 1998.

7. Gelb, A., J. F. Kasper, Jr., R. A. Nash, Jr., C.F. Price, and A. A. Sutherland, Jr., *Applied Optimal Estimation*, The M.I.T. Press, Cambridge, MA, 1982.

8. Tapley, B. D. and V. Szebehely, "Recent Advances in Dynamical Astronomy," Proceedings of the NATO Advanced Study Institute in Dynamical Astronomy, Cortina D'Ampezzo, Italy, August 1972.

9. Bate, R. B., D. D. Mueller, and J. E. White, *Fundamentals of Astrodynamics*, Dover, New York, NY, 1971, pp. 83-86.

	Single Satellite		Baseline TSS	
	True State	Estimated Values	True State	Estimated Values
x (m)	6.5879225783306E+06	6.5879225783309E+06	6.5879225783306E+06	6.5879225783306E+06
y (m)	6.6099705161886E+05	6.6099705161300E+05	6.6099705161886E+05	6.6099705161311E+05
z (m)	0.00000000000000E+00	-6.099135609409E-07	0.00000000000000E+00	-5.596768671864E-07
v_x (m/s)	-7.7074004494957E+02	-7.7074004506911E+02	-7.7058133356314E+02	-7.7058133357330E+02
v_y (m/s)	7.681691970741E+03	7.681691971957E+03	7.6801110171439E+03	7.6801110172626E+03
v_z (m/s)	7.74609867819E+02	7.746098679425E+02	7.7445036163386E+02	7.7445036175811E+02
a_t (m/s^2)	0.00000000000000E+00	-4.2021028007111E-11	0.00000000000000E+00	6.724600917431E-11
a_r (m/s^2)	0.00000000000000E+00	-1.888271960329E-10	3.7442976362252E-03	3.744297434029E-03
RMS (m)	---	2.845468051330E-08	---	1.036318750471E-09
ρ_{cm} (m)	---	---	9.09090909090909E+02	9.08953560940903E+02

Table 1. Performance of Filter for Single Satellite and "Baseline" TSS Configuration

	Tether Length = 10 km		Tether Length = 100 km		Tether Length = 1 km (m above mp)	
	True State	Estimated Values	True State	Estimated Values	True State	Estimated Values
x (m)	6.5879225783306E+06	6.5879225783306E+06	6.5879225783306E+06	6.5879225783306E+06	6.5879225783306E+06	6.5879225783306E+06
y (m)	6.6099705161886E+05	6.6099705161311E+05	6.6099705161886E+05	6.6099705161886E+05	6.6099705161886E+05	6.6099705161886E+05
z (m)	0.00000000000000E+00	-5.543636105906E-07	0.00000000000000E+00	1.245401217021E-10	0.00000000000000E+00	2.635252665324E-10
v_x (m/s)	-7.6915559449612E+02	-7.6915559505615E+02	-7.5515544403972E+02	-7.5515544404037E+02	-7.7089881310791E+02	-7.7089881311151E+02
v_y (m/s)	7.6659003221138E+03	7.6659003223151E+03	7.5263657587291E+03	7.5263657587971E+03	7.6832743565591E+03	7.6832743566341E+03
v_z (m/s)	7.7301746244407E+02	7.7301746255921E+02	7.5894701424311E+02	7.5894701425001E+02	7.7476943314351E+02	7.7476943315111E+02
a_t (m/s^2)	0.00000000000000E+00	6.676063044581E-11	0.00000000000000E+00	8.194254676729E-13	0.00000000000000E+00	1.041870784922E-12
a_r (m/s^2)	3.7346040994371E-02	3.7346040768411E-02	3.639949182599E-01	3.639949182331E-01	-3.7464575112441E-03	-3.746457522102E-03
RMS (m)	---	1.769662622967E-10	---	2.925015549524E-09	---	2.469023125850E-09
ρ_{cm} (m)	9.09090909090909E+03	9.0771874305451E+03	9.09090909090909E+04	8.9544984189071E+04	9.09090909090909E+02	9.0922822467981E+02

Table 2. Performance of Filter for TSS Configurations of Various Tether Lengths

30

	Baseline TSS	Tether Length		
		10km	100km	1 km (m above m_p)
x (m)	6.587922577752E+06	6.587922574775E+06	6.587922547563E+06	6.587922578407E+06
y (m)	6.609971385133E+05	6.609971472780E+05	6.609972275480E+05	6.609971365843E+05
z (m)	-1.141254459464E-01	-1.289680622234E-01	-2.648032885981E-01	-1.108587738544E-01
v_x (m/s)	-7.705813695162E+02	-7.691556365638E+02	-7.551555512793E+02	-7.708988452906E+02
v_y (m/s)	7.680109627894E+03	7.665899775495E+03	7.526365194185E+03	7.683273813476E+03
v_z (m/s)	7.744504288009E+02	7.730175394919E+02	7.589471794447E+02	7.747694981238E+02
a_t (m/s^2)	-2.355257872642E-10	2.519779181179E-11	2.121628463537E-09	-2.936487118764E-10
a_r (m/s^2)	3.745519370517E-03	3.734726409236E-02	3.639961530448E-01	-3.745236069387E-03
RMS (m)	1.384957717803E-04	1.363858833731E-04	1.095966990840E-04	1.389347046617E-04
ρ_{cm} (m)	9.092502392237E+02	9.077485174966E+03	8.954529205946E+04	9.089318366401E+02

Table 3. Performance of Filter for Several TSS Configurations, Using Range-Only Observations

Site	σ_{range} (m)	σ_{az} (deg)	σ_{elev} (deg)
CAV (396)	45	0.009	0.01
EGL (399)	21	0.019	0.023
FYL (346)	18	0.014	0.009

Table 4. Sensor Accuracies for Several Tracking Stations

31

σ_a (m)	σ_a (deg)	σ_e (deg)	Observation Time (sec)	RMS (m)	ρ_{cm} (m)
45	0	0	670	2.7089981677754E+01	8.839299991318E+02
0	0.02	0	1340	8.523381227729E+02	7.634261239021E+02
0	0	0.02	1340	9.056157841005E+02	8.611636798857E+02
45	0.02	0.02	1340	1.243663468348E+03	7.191546577227E+02

Table 5. Performance of Filter for Baseline TSS Configuration with Observation Error

	θ_{30} = 1 deg	θ_{30} = 5 deg	θ_{20} = 1 deg
x (m)	6.587922534010E+06	6.587922381251E+06	6.587922585548E+06
y (m)	6.609970281489E+05	6.609969274358E+05	6.609969922418E+05
z (m)	-1.899360251617E-03	-1.042374751311E-02	5.993279293452E-01
v_x (m/s)	-7.705797780651E+02	-7.705743127046E+02	-7.705814800457E+02
v_y (m/s)	7.680110892090E+03	7.680114063920E+03	7.680111215138E+03
v_z (m/s)	7.744504179819E+02	7.744506798914E+02	7.744397668810E+02
a_t (m/s^2)	6.005134855208E-05	2.905779845706E-04	1.110708739232E-07
a_r (m/s^2)	3.717822655992E-03	3.586099159832E-03	3.743034434837E-03
RMS (m)	9.979140279686E-03	4.588424953238E-02	1.443204401469E-01
ρ_{cm} (m)	9.026089001177E+02	8.705447303360E+02	9.086469214628E+02

Table 6. Performance of Filter for Baseline TSS Configuration, Given Initial Libration Angle

	Initial Guess	Converged Values
x (m)	4.2943419661544E+06	4.2938635268809E+06
y (m)	-5.3552676765491E+06	-5.3556653565964E+06
z (m)	2.7702168014134E+06	2.7685460623977E+06
v_x (m/s)	1.2765671638871E+03	1.2569437066422E+03
v_y (m/s)	4.0138731077791E+03	4.0881184152001E+03
v_z (m/s)	5.7778676341951E+03	5.9771723509991E+03
a_t (m/s^2)	0.0000000000000E+00	-1.8462548706201E-02
a_r (m/s^2)	3.6791366379551E-01	1.3545915228621E-02
RMS (m)	----	4.2720847595821E+02

Table 7. Performance of Filter on TiPS Observation Data

33

EXISTENCE OF PERIODIC MOTIONS OF A TETHER TRAILING SATELLITE

E. V. Rossi[*], D. A. Cicci[†] and J. E. Cochran Jr.[‡]
Auburn University, Alabama[§]

ABSTRACT

Tethered satellite systems are becoming more widely used in space explorations. In this analytical study, the dynamics of a satellite trailing a tether are addressed. More precisely, we derive the conditions for existence of periodic motions about the relative equilibrium states of the tethered system. The system is considered to be affected by the atmospheric drag and nonspherical Earth. The mathematical proof of the existence result is based on the Leray-Schauder degree theory. Main conclusions can be easily generalized for any bounded forcing and/or forces with linear growth.

INTRODUCTION

The goal of this study is to better understand the dynamics of a satellite trailing a tether. Such a scenario may occur when the tether connecting two satellites is cut as a result of an accident or a planned maneuver. The dynamics of such a system are extremely complicated. However, the relative equilibrium states of the tether trailing satellite can be obtained numerically, and in some cases, even analytically. The problem of predicting of motion of such a system can be significantly aided if the tether trailing satellite was known to admit periodic motions about such states. In this study, the conditions for the existence of such motions are derived analytically.

The main objective here is to apply some recent advances in the theory of nonlinear partial differen-

tial equations to an applied problem in dynamics. The well-known Leray-Schauder degree theory[4,7] is the main tool used in obtaining the results.

The degree theory was first applied to prove existence of solutions of nonlinear PDEs in 1970's by E. M. Landesman and A. C. Lazer. At first, the theory was used to research elliptic PDEs, which are mostly used to describe chemical processes. However, recently[5] it was implemented to prove periodic solvability of parabolic and hyperbolic PDEs, which are widely used in dynamic modeling. Here the Leray-Schauder degree theory is employed to prove the existence of periodic solutions for a system of perturbed hyperbolic PDEs, which model the motion of a linearly extensible tether in a rotating coordinate system. The tethered system is assumed to be influenced by the Earth's gravitational attraction, nonspherical Earth and atmospheric drag.

EQUATIONS OF MOTION

The following basic assumptions of the mathematical model are made:

- The Earth-centered coordinate system is inertial.

- The satellite is modeled as a point mass.

- The tether is homogeneous with uniform density ρ.

- Torsional and transverse vibrations of the tether are neglected, and tether elasticity is modeled by Hooke's Law[6,11].

The equations describing the motion of a tether trailing satellite are based on a well-known wave equation[9,11]. They consist of the partial and ordi-

[*]Graduate Student, Department of Aerospace Engineering, Student Member, AIAA

[†]Associate Professor, Department of Aerospace Engineering, Member, AAS; Associate Fellow, AIAA

[‡]Professor and Head, Department of Aerospace Engineering, Fellow, AAS; Associate Fellow, AIAA

1
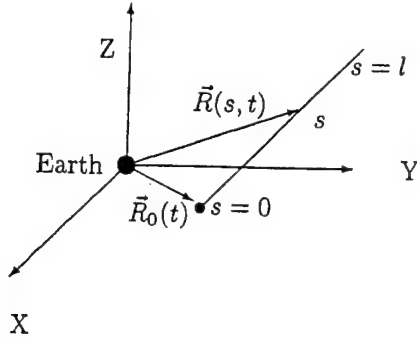
Figure 1: Tether Trailing Satellite in Earth-Centered Coordinate System
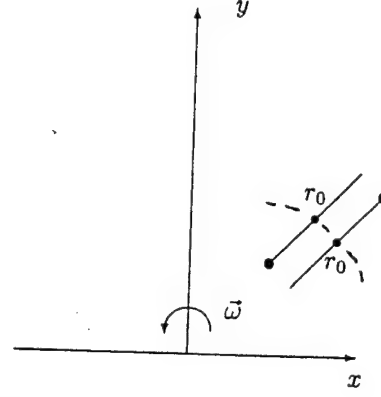
Figure 2: Radial Relative Equilibrium Configurations

nary differential equations:

$$\vec{R}_{tt} = \frac{k}{\rho}\vec{R}_{ss} - \mu\frac{\vec{R}}{R^3} + \frac{1}{\rho}\vec{F}(s,t),$$
$$m(\vec{R}_0)_{tt} = -m\mu\frac{\vec{R}_0}{R_0^3} + k\vec{T}_0 + \vec{F}_0, \qquad (1)$$
$$\vec{T}_0 = \vec{R}_s(0,t), \ \vec{F}_0 = \vec{F}(0,t),$$

where $\vec{R}(s,t)$ is the geocentric radius vector to the point s on the tether (see Figure 1), $\vec{R}_0(t) = \vec{R}(0,t)$, ρ is the uniform density of the tether, k is a constant Young's modulus of the tether, μ is the Earth's gravitational constant, m is the mass of the satellite, and $\vec{F}(s,t)$ includes the effects of atmospheric drag and nonspherical Earth. Similar equations were used by V. Beletskii and E. Levin[2].

The atmospheric drag forces are modeled[2] by

$$\vec{F}_{drag} = -\frac{1}{2}cdp_a|\vec{v}_{rel}|\vec{v}_{rel},$$
$$\vec{F}_{0,drag} = -\frac{1}{2}c_0S_0p_a|\vec{v}_{0,rel}|\vec{v}_{0,rel}, \qquad (2)$$

where $\vec{v}_{rel}(s,t)$ is the velocity of the tether point relative to the atmosphere, $\vec{v}_{0,rel}(t)$ is the velocity of the satellite relative to the atmosphere, d is the tether diameter, c is the tether drag coefficient, c_0 is the satellite drag coefficient, S_0 is the satellite reference area, and p_a is the atmospheric pressure.

In the Earth-centered coordinate system, the force due to the nonspherical Earth potential can be written[8]

$$\vec{F}_{obl} = -\mu J_2 R_e^2 \frac{3R_z}{R^5}\vec{k}$$
$$-\mu J_2 R_e^2\left(\frac{3}{2R^5} - \frac{15R_z^2}{2R^7}\right)\vec{R}, \qquad (3)$$

where $\vec{R} = (R_x, R_y, R_z)$, R_e is the equatorial radius of the Earth and J_2 is the *oblateness term*, $J_2 \approx 1.093 \times 10^{-3}$.

EXAMPLES OF RELATIVE EQUILIBRIUM STATES

Under certain assumptions, it is possible to analyze the relative equilibrium states of the tether trailing satellite. Assume that the tethered system rotates as a solid body around the Earth's OZ-axis with a constant angular velocity ω. There will be a point on the system[1] where $\vec{F}_{gravitational} + \vec{F}_{centrifugal}$ equals zero. A mass at this point is in a zero-g condition and experiences no net force in the radial direction, and will move therefore in circular orbit about the Earth. For short tethers, r_0 is located in the vicinity of the center-of-mass of the system. However, this is no longer true for long tethers[1]. The location of this point can be found by equating the gravitational and centrifugal forces resulting in

$$r_0 = \left(\frac{\mu}{\omega^2}\right)^{1/3}. \qquad (4)$$

In geocentric axes $Oxyz$ which rotate about $OZ = Oz$ with the same angular velocity ω, such stationary motion is observed as a relative equilibrium and is time-independent.

Assume that $\vec{F} = \vec{F}_0 = \vec{0}$ for all s and t, i.e. the system is influenced by tension and gravitational forces only. Then the equation for the tether can be written in component form as follows:

$$\frac{k}{\rho}x_{ss} - \frac{\mu x}{(x^2 + y^2 + z^2)^{3/2}} + x\omega^2 = 0, \qquad (5)$$

$$\frac{k}{\rho}y_{ss} - \frac{\mu y}{(x^2 + y^2 + z^2)^{3/2}} + y\omega^2 = 0, \qquad (6)$$

2

American Institute of Aeronautics and Astronautics
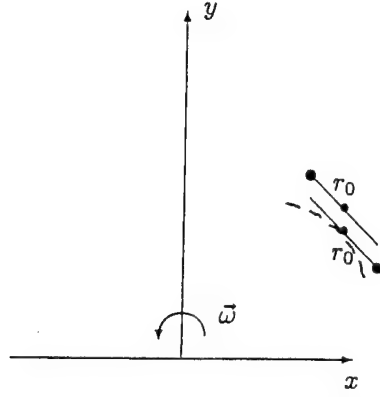
Figure 3: 'Nearly Circular' Equilibrium Configurations

Figure 4: Out-of-Plane Relative Equilibrium Configuration

$$\frac{k}{\rho}z_{ss} - \frac{\mu z}{(x^2 + y^2 + z^2)^{3/2}} = 0, \qquad (7)$$

where $\vec{R} = (x, y, z)$. Analysis of equations (5)-(7) gives rise to two obvious cases:

Case 1: $z = 0$: The system moves in the orbital plane. In this case a few configurations are possible.

(i) Radial configuration (see Figure 2). Every point of the tethered system moves in concentric circular orbits. When viewed in the rotating coordinate system, the satellite and the tether are aligned along local vertical, with tether either 'ahead' or 'behind' the satellite. Since the whole system rotates as a solid body with constant velocity ω, all the points of the system must be collinear. The behavior of relatively short tethers can be described by $r_{ss} = 0$, resulting in straight line configurations.

When the tether is extremely long, or if a more accurate description of the motion is desired, the tether can be described by the equation

$$\frac{k}{\rho}r_{ss} + 3\omega^2 r = 0, \qquad (8)$$

which will give the tether a wave-like periodic configuration rather than a straight line.

(ii) 'Nearly circular' configuration, which occurs when $(x^2 + y^2)^{1/2} = r_0$ for all points on the tether. This configuration of the tether is determined by

$$x_{ss} = 0, \qquad y_{ss} = 0, \qquad (9)$$

which gives a straight line shape tangent to the circular orbit of r_0, as shown in Figure 3. Two situations are possible: the satellite is either 'ahead' or 'behind' the tether.

Similarly to the previous case, the straight line shape will become wave-like periodic for extremely long tethers.

Case 2: $z \neq 0$, i.e. the out-of-plane motion is permitted. Short tethers will have a straight-line projection onto the xy-plane and wave-like $\frac{2\pi\sqrt{k}}{\omega\sqrt{\rho}}$-periodic configuration in z-direction (see Figure 4). The system is perpendicular to the orbital plane. For long tethers, the projection onto the xy-plane is also wave-like.

It is also possible to analyze the relative equilibrium states without neglecting the atmospheric drag forces[2].

PERIODIC MOTIONS UNDER THE INFLUENCE OF AIR DRAG FORCES

Here it is assumed that $\vec{R}(s, t)$ is the relative equilibrium state which satisfies the following equations:

$$\begin{aligned}
\vec{\omega} \times (\vec{\omega} \times \vec{R}) + \frac{\mu\vec{R}}{R^3} - \frac{k}{\rho}\vec{R}_{ss} - \frac{1}{\rho}\vec{F}_{drag} &= 0, \\
\vec{\omega} \times (\vec{\omega} \times \vec{R}_0) + \frac{\mu\vec{R}_0}{R_0^3} - \frac{k}{m}\vec{T}_0 - \frac{1}{m}\vec{F}_{0,drag} &= 0,
\end{aligned} \qquad (10)$$

where $\vec{R}_0 = \vec{R}(0, t)$ and $\vec{F}_{drag}$ is given by the equation (2). It is important to explore the motion of the system about the relative equilibrium points, i.e. the solution of the form $\vec{R} + \vec{u}$, where $\vec{u}$ is the deviation from equilibrium.

Expanding the atmospheric drag forces in Taylor series about $\vec{R}$, letting $\vec{u} = (x, y, z)$, and letting

3

ω_e denote the Earth's angular rotation rate, gives the variational equation of motion about the relative equilibrium state:

$$\vec{u}_{tt} + 2\vec{\omega} \times \vec{u}_t + \vec{\omega} \times (\vec{\omega} \times \vec{u}) - \frac{\mu}{R^3}\vec{R}$$
$$+\frac{\mu}{|\vec{R}+\vec{u}|^3}(\vec{R}+\vec{u}) - \frac{k}{\rho}\vec{u}_{ss} - \frac{1}{\rho}\delta\vec{F} = 0. \quad (11)$$

Also assume that one end of the tether is free, which results in no tension when $s = l$

$$\vec{u}_s(l,t) = 0. \quad (12)$$

Additionally, assume that the satellite remains in an equilibrium orbit

$$\vec{u}(0,t) = 0. \quad (13)$$

Finally, consider the solvability of the equation (11) with the following boundary and initial conditions:

$$\vec{u}_s(l,t) = \vec{u}(0,t) = 0, \text{ for all } t \in [0,T]$$
$$\vec{u}(s,0) = \vec{u}(s,T), \text{ for all } s \in [0,l] \quad (14)$$
$$\vec{u}_t(s,0) = \vec{u}_t(s,T), \text{ for all } s \in [0,l].$$

Equation (11) leads to the following matrix operator equation:

$$A\vec{u} - \omega^2\vec{u} + B\vec{u} + G(\vec{u}) - \delta F = 0, \quad (15)$$

where $\vec{u} = (x,y,z)^T$, A s a telegraph operator in the form

$$A_{11} = \frac{\partial^2}{\partial t^2} + 2\omega\frac{\partial}{\partial t} - \frac{k}{\rho}\frac{\partial^2}{\partial s^2},$$
$$A_{22} = \frac{\partial^2}{\partial t^2} + 2\omega\frac{\partial}{\partial t} - \frac{k}{\rho}\frac{\partial^2}{\partial s^2},$$
$$A_{33} = \frac{\partial^2}{\partial t^2} + 2\omega\frac{\partial}{\partial t} - \frac{k}{\rho}\frac{\partial^2}{\partial s^2}, \quad (16)$$

$$A_{ij} = 0, \qquad i \neq j, \ 1 \leq i,j \leq 3.$$

B is a pseudo-gyroscopic operator in the form

$$B = \begin{pmatrix} -2\omega\frac{\partial}{\partial t} & -2\omega\frac{\partial}{\partial t} & 0 \\ 2\omega\frac{\partial}{\partial t} & -2\omega\frac{\partial}{\partial t} & 0 \\ 0 & 0 & -2\omega\frac{\partial}{\partial t} \end{pmatrix}, \quad (17)$$

G is the nonlinear gravitational operator

$$G(\vec{u}) = \begin{pmatrix} -\frac{\mu}{R^3}R_x + \frac{\mu(R_x+x)}{\bar{R}+\vec{u}|^3} \\ -\frac{\mu}{R^3}R_y + \frac{\mu(R_x+y)}{|R+\vec{u}|^3} \\ -\frac{\mu}{R^3}R_z + \frac{\mu(R_z+z)}{|\vec{R}+\vec{u}|^3} \end{pmatrix}, \quad (18)$$

and

$$\delta F = \frac{1}{\rho}(\delta F_x, \delta F_y, \delta F_z)^T. \quad (19)$$

Letting $Q = [0,l] \times [0,T]$, then the $L^2(Q)$-inner product can be expressed as follows

$$\langle x_1, x_2 \rangle_0 = \int_0^l \int_0^T x_1(s,t)x_2(s,t)dtds, \quad (20)$$

for all $x_1, x_2 \in L^2(Q)$. Also, letting x, y and z belong to the Hilbert space $H^2(Q)$[5], then $\vec{u}$ belongs to the product space $H^2(Q) \times H^2(Q) \times H^2(Q)$ with the inner product

$$\langle \vec{u}, \vec{v} \rangle = \int_0^l \int_0^T u_x(s,t)v_x(s,t)dtds$$
$$+ \int_0^l \int_0^T u_y(s,t)v_y(s,t)dtds$$
$$+ \int_0^l \int_0^T u_z(s,t)v_z(s,t)dtds$$
$$= \langle u_x, v_x \rangle_0 + \langle u_y, v_y \rangle_0$$
$$+ \langle u_z, v_z \rangle_0,$$

and the norm

$$\|\vec{u}\|^2 = \langle \vec{u}, \vec{u} \rangle$$
$$= \langle u_x, u_x \rangle_0 + \langle u_y, u_y \rangle_0 + \langle u_z, u_z \rangle_0$$
$$= \|u_x\|_0^2 + \|u_y\|_0^2 + \|u_z\|_0^2.$$

Properties of such spaces are discussed in detail[10,13].

Now, the telegraph operator A is acting from $H^2(Q) \times H^2(Q) \times H^2(Q)$ into $L^2(Q) \times L^2(Q) \times H^2(Q)$ and is self-adjoint, i.e.

$$\langle A\vec{u}, \vec{v} \rangle = \langle \vec{u}, A\vec{v} \rangle, \quad (21)$$

for all $\vec{u}, \vec{v} \in H^2(Q) \times H^2(Q) \times H^2(Q)$.

Assume that λ is a (3×3) diagonal constant matrix. It can be shown that the problem

$$A\vec{u} = \lambda\vec{u}, \text{ in } Q, \quad (22)$$

with initial and boundary conditions (14) has a non-trivial solution $\vec{u} \in H^2(Q) \times H^2(Q) \times H^2(Q)$ if and only if the time-independent problem

$$A_0\vec{u} = -\lambda\vec{u}, \text{ on } [0,l], \quad (23)$$

$$\vec{u}_s(l) = \vec{u}(0) = 0 \quad (24)$$

has a non-trivial solution $\vec{u} \in H^2(Q) \times H^2(Q) \times H^2(Q)$, where

$$A_0 = \begin{pmatrix} \frac{k}{\rho}\frac{d^2}{ds^2} & 0 & 0 \\ 0 & \frac{k}{\rho}\frac{d^2}{ds^2} & 0 \\ 0 & 0 & \frac{k}{\rho}\frac{d^2}{ds^2} \end{pmatrix}. \quad (25)$$

4

(A similar result was recently obtained by M. R. Grossinho and M. N. Nkashama[5].)

Consequently, the telegraph operator A is positive definite, i.e.

$$\langle A\vec{u}, \vec{u} \rangle \geq \frac{\pi^2 k}{4l^2 \rho} \|\vec{u}\|^2, \qquad (26)$$

for all $\vec{u} \in H^2(Q) \times H^2(Q) \times H^2(Q)$.

Assume that

$$|\vec{R}_t + \vec{u}_t| \leq v_{max} < c \qquad (27)$$

where c is the speed of light. Then it can be shown that the operator $\omega^2 Id - B - G + \delta F$ is bounded[13] as an operator from $L^2(Q) \times L^2(Q) \times L^2(Q)$ into $L^2(Q) \times L^2(Q) \times L^2(Q)$.

In particular, boundedness of the mentioned operators implies that for all $u \in L^2(Q) \times L^2(Q) \times L^2(Q)$ we have

$$\|B\vec{u}\| \leq \omega(v_{max})\sqrt{8lT}, \qquad (28)$$

$$\|G(\vec{u})\| \leq \frac{2\mu\sqrt{lT}}{R_e^2}, \qquad (29)$$

$$\|\delta F\vec{u}\| \leq \frac{1}{\rho} c d p_a |\vec{V}_{rel,max}| \Big[(v_{max})^2 lT$$

$$+ \omega_e^2 \|\vec{u}\|^2 + 2\omega_e(v_{max})\|\vec{u}\| \Big]^{1/2}, \qquad (30)$$

where $|\vec{V}_{rel,max}|$ is the maximal speed relatively to the rotating atmosphere which is attained by the relative equilibrium state.

The following is one of the main results of this study:

Under the assumptions made in this section, there exists at least one solution to the equation (11) with the boundary and initial conditions given by the equations (14), provided that the following inequality holds

$$\int_0^l \int_0^T (\delta F\vec{u} \cdot \vec{u}) \, dt ds$$

$$< \left(\frac{\pi^2 k}{4l^2 \rho} - \omega^2 \right) \|\vec{u}\|^2 \qquad (31)$$

for all $\vec{u} \in L^2(Q) \times L^2(Q) \times L^2(Q)$.

The proof of this existence result is based on the homotopy invariance property of the Leray-Schauder degree theory[7]. Consider the homotopy $H : [0,1] \times$

$(L^2(Q) \times L^2(Q) \times L^2(Q)) \longrightarrow L^2(Q) \times L^2(Q) \times L^2(Q)$ given by

$$H(\tau, \vec{u})$$

$$= \tau A^{-1} \left[\omega^2 \vec{u} - B\vec{u} - G\vec{u} + \delta F\vec{u} \right], \qquad (32)$$

for $\tau \in [0,1]$. It is known[3,12] that the operator A^{-1} is compact as an operator from $L^2(Q) \times L^2(Q) \times L^2(Q)$ into $L^2(Q) \times L^2(Q) \times L^2(Q)$ due to Sobolev embedding theorems. From inequalities (28)-(30) it follows that the operator in brackets is bounded. Therefore, the homotopy H is compact. The homotopy equation for which a solution is sought is

$$\vec{u} - H(\tau, \vec{u}) = 0, \qquad \tau \in [0,1]. \qquad (33)$$

Note that if $\tau = 0$, equation (33) becomes $\vec{u} = 0$, which has a unique trivial solution. If $\tau = 1$, then (33) yields the problem under consideration. The homotopy invariance property will imply solvability of the equation in question provided that there exists a real number M such that if $\vec{u}$ satisfies (33), then $\|\vec{u}\| \leq M$.

On the contrary, assume that there exist sequences $\{\vec{u}_n\}$ and $\{\tau_n\}$ such that $\lim_{n\to\infty} \tau_n = \theta$, $0 \leq \theta \leq 1$, $\lim_{n\to\infty} \|\vec{u}_n\| = \infty$, and $\vec{u}_n, \tau_n$ satisfy (33) for all n.

Combining the estimates (27)-(30) gives for all n,

$$\langle \delta F\vec{u}_n, \vec{u}_n \rangle \geq \left(\frac{\pi^2 k}{4l^2 \rho} - \omega^2 \right) \|\vec{u}_n\|^2$$

$$- \left(\omega(v_{max})\sqrt{8lT} + \frac{2\mu\sqrt{lT}}{R_e^2} \right) \|\vec{u}_n\|. \qquad (34)$$

Dividing both sides of (34) by $\|\vec{u}_n\|^2$ and letting $n \to \infty$, we obtain

$$\lim_{n\to\infty} \frac{\langle \delta F\vec{u}_n, \vec{u}_n \rangle}{\|\vec{u}_n\|^2} \geq \frac{\pi^2 k}{4l^2 \rho} - \omega^2. \qquad (35)$$

Thus, there exists a natural number N_0 such that

$$\langle \delta F\vec{u}_n, \vec{u}_n \rangle \geq \left(\frac{\pi^2 k}{4l^2 \rho} - \omega^2 \right) \|\vec{u}_n\|^2,$$

for all $n \geq N_0$, which is a contradiction to the assumption (31). Therefore, all solutions of the homotopy equation (33) are bounded, and a periodic solution exists.

The above result has an important corollary:

Under the assumptions made in this section, and if $\delta F\vec{u} = 0$ (no drag), there exists at least one solution to the equation (11) with the boundary and

initial conditions (14), provided that the following inequality holds

$$\omega^2 < \frac{\pi^2 k}{4l^2 \rho}$$

for all $\vec{u} \in L^2(Q) \times L^2(Q) \times L^2(Q)$.

PERIODIC MOTION UNDER THE INFLUENCE OF NONSPHERICAL EARTH

In the further discussion, assume that $\vec{F}(s,t)$ is described by equation (3). Then the variational equations can be written as follows:

$$\vec{u}_{tt} + 2\vec{\omega} \times \vec{u}_t + \vec{\omega} \times (\vec{\omega} \times \vec{u}) - \frac{\mu}{R^3}\vec{R}$$
$$+\frac{\mu}{|\vec{R}+\vec{u}|^3}(\vec{R}+\vec{u}) - \frac{k}{\rho}\vec{u}_{ss} - \frac{1}{\rho}\vec{F} = 0. \quad (36)$$

Similarly to the previous section, consider the solvability of the equations (36) with the initial and boundary conditions (14).

Consider the following matrix operator equation:

$$A\ddot{\vec{u}} - \omega^2\vec{u} + B\vec{u} + G(\vec{u}) + F(\vec{u}) = 0, \quad (37)$$

where A, B and $G(\vec{u})$ are defined by the relations (16), (17) and (18), respectively, and

$$F(\vec{u}) = \frac{1}{\rho}(F_x, F_y, F_z)^T.$$

In addition to the inequalities (28)-(30), it can be shown that the nonlinear oblateness operator $F(\vec{u})$ is bounded, and for all $\vec{u} \in L^2(Q) \times L^2(Q) \times L^2(Q)$,

$$\|F(\vec{u})\| \le \frac{18\mu J_2\sqrt{lT}}{R_e^2}. \quad (38)$$

Similarly to the previous section, the main result is:

Under the assumptions made in this section, there exists at least one solution to the equations (36) with the boundary and initial conditions (14), provided that the following inequality holds

$$\omega^2 < \frac{\pi^2 k}{4l^2 \rho} \quad (39)$$

for all $\vec{u} \in L^2(Q) \times L^2(Q) \times L^2(Q)$.

The final result of this study is the solvability condition for the following problem:

$$\vec{u}_{tt} + 2\vec{\omega} \times \vec{u}_t + \vec{\omega} \times (\vec{\omega} \times \vec{u}) - \frac{\mu}{R^3}\vec{R}$$
$$+\frac{\mu}{|\vec{R}+\vec{u}|^3}(\vec{R}+\vec{u}) - \frac{k}{\rho}\vec{u}_{ss} - \frac{1}{\rho}(\vec{F}+\delta\vec{F}) = 0, \quad (40)$$

where $\vec{F}$ is the effect of Earth oblateness, and $\delta\vec{F}$ is the linearized effect of atmospheric drag.

There exists at least one solution to the equation (40) with the boundary and initial conditions (14), provided that the following inequality holds

$$\int_0^l \int_0^T (\delta F\vec{u} \cdot \vec{u})\,dt\,ds < \left(\frac{\pi^2 k}{4l^2\rho} - \omega^2\right)\|\vec{u}\|^2$$

for all $\vec{u} \in L^2(Q) \times L^2(Q) \times L^2(Q)$.

CONCLUSIONS

The primary result of this study is that the modern theory of nonlinear partial differential equations was applied to analyze dynamics of a tether trailing satellite. Moreover, the gravitational and oblateness forces did not have to be linearized about the relative equilibrium states. Analysis produced several important results:

- In the case when the system is influenced exclusively by the gravitational and oblateness forces, existence of periodic solutions does not depend on the relative equilibrium state. Existence of such motions depends solely on the physical characteristics of the tether (density, length, flexibility), and the system's rotational speed. It is evident that less flexible, shorter tethers will admit periodic motions about their equilibrium states.

- If atmospheric drag is influencing the system, then the effects of drag must be bounded for the system to have a periodic motion. In this case, periodic behavior of the tether trailing satellite will heavily depend on the equilibrium state, as well as on tether parameters.

- The difference in the above results can be easily explained by the fundamental properties of the forces involved. The effect of gravitational and oblateness forces is *uniformly bounded* independently of position of an object in space, i.e.

$$|\vec{F}_{grav,obl}(\vec{R})| \le C_{grav,obl},$$

where $\vec{R}$ denotes position, and C is a positive constant. However, the drag forces do not follow the same pattern, and consequently required *linearization* about the equilibrium states.

6

- The obtained mathematical results can be easily generalized in the case of *any* bounded forcing and/or forces with *linear growth*:

$$|\vec{F}(\vec{R})| \leq C|\vec{R}|.$$

Existence of periodic motions with bounded forces will depend on tether parameters only, and in the case of unbounded (linear growth) will depend on equilibrium states.

REFERENCES

1. D. A. Arnold, *The Behavior of Long Tethers in Space*, Journal of the Astronautical Sciences, 35 (1987), 3-18.

2. V. V. Beletskii, E. M. Levin, *Dynamics of the Orbital Cable System*, Acta Astronautica, 12(5) (1985), 285-291.

3. H. Brezis, L. Nirenberg, *Characterizations of the Range of Some Nonlinear Operators and Applications to Boundary Value Problems*, Ann. Scuola Norm. Sup. Pisa, 5 (1978), 225-326.

4. K. Deimling, "Nonlinear Functional Analysis", Springer-Verlag, 1985.

5. M. R. Grossinho, M. N. Nkashama, *Periodic Solutions of Parabolic and Telegraph Equations with Asymmetric Nonlinearities*, Nonlinear Analysis, Theory, Methods and Applications, 33(2) (1998), 187-210.

6. K. D. Kopke, L. E. Herder, C. L. Trowbridge, T. J. Eller, *Newtonian Derivation of the Equations of Motion for a Tethered Satellite System*, AIAA-90-2989-CP.

7. N. Lloyd, "Degree Theory", Cambridge University Press, 1978.

8. J. E. Prussing, B. A. Conway, "Orbital Mechanics", Oxford University Press, 1993.

9. Reiko Sakamoto, "Hyperbolic Boundary Value Problems", Cambridge University Press, 1982.

10. S. L. Sobolev, "Some Applications of Functional Analysis in Mathematical Physics", American Mathematical Society, 1991.

11. A. N. Tikhonov, A. A. Samarskii, "Equations of Mathematical Physics", New York: Macmillan, 1963.

12. O. Vejvoda, "Partial Differential Equations: Time-periodic Solutions", Martinus Nijhoff Publishers, 1982.

13. K. Yosida, "Functional Analysis", Springer-Verlag, 1974.

A STUDY OF THE RE-ENTRY ORBIT DISCREPANCY INVOLVING TETHERED SATELLITES

T. Alan Lovell[#], John E. Cochran, Jr.[*] and David A. Cicci[**]
Department of Aerospace Engineering
211 Aerospace Engineering Bldg
Auburn University, Alabama 36849-5338

Sungki Cho[‡]
Electronics and Telecommunications Research Institute
Taejon, Korea

ABSTRACT

This paper describes an investigation of the motion of objects in near-Earth orbit that have a high probability of being identified as re-entering the Earth's atmosphere. In the case of two or more satellites tethered together, each object's motion deviates from the traditional Keplerian-like motion of a single untethered body, due to the tension force in the tether. Consequently, classical identification and motion prediction techniques applied to a tethered object may produce results that indicate that the object is on course to re-enter when it actually is not, or vice-versa. In this study the factors that cause tethered bodies to behave differently than expected, and how significant these factors must be to cause a discrepancy regarding re-entry, are determined. A candidate re-entry identification methodology based on this foundation is then formulated.

1. INTRODUCTION

One of the interesting dynamic characteristics of a tethered satellite system (TSS) consisting of two satellites and a tether is the non-Keplerian orbital motion of each of the satellites. This is due

---

[#] Graduate Research Assistant and Ph.D. Candidate.
[*] Professor and Department Head.
[**] Professor.
[‡] Senior Member of Research Staff.

to the perturbational forces on each mass caused by the tension force in the tether and may present problems to those who are tasked with tracking, detecting, and identifying space objects. The center of mass of a TSS generally exhibits Keplerian motion. However, unless one of the masses is significantly larger than the other, the center of mass lies at a point along the tether and thus cannot be physically observed by tracking equipment. In fact, oftentimes there may be observation data for only one of the masses of a TSS available for processing. Although conventional orbit determination processes do account for some sources of non-Keplerian motion, such as the oblateness of the Earth, they were not constructed with TSS in mind.

In [1] a tethered satellite system model without libration is used to show how the radial tether force combines with the standard two-body gravitational force to create an "apparent" gravitational force. The magnitude of this force is less than the conventional gravitational force for the lower mass of a TSS, while for the upper mass the magnitude is greater. A conventional satellite estimation technique does not account for tether force, and thus will interpret the lower mass of a TSS as being on a smaller orbit (smaller semi-major axis) than it actually is, and the upper mass as being on an orbit larger than its true orbit. For an identification method equipped with only a conventional filter, this can lead to a major discrepancy:

The lower mass of a TSS that is not going to re-enter the atmosphere can be mistaken for an untethered satellite that is on a re-entry trajectory.

This situation, which will be referred to herein as the "re-entry discrepancy," was illustrated in [2,3] for the case of circular motion of the center of mass of a TSS with no libration. In [4] the possibility of a re-entry orbit was further explored by investigating apparent elliptical trajectories

resulting from varying such properties as tether orientation, mass ratio of the end bodies, and impact altitude. In [5] a similar study was performed for non-circular TSS orbits. This paper expands on the work of [2,3,4,5] by considering the impact that librational motion of the TSS, the gravitational force due to oblateness of the Earth, and other phenomena can have on the re-entry discrepancy. Namely, several different cases of TSS motion are investigated to determine the value of the tether length above which the discrepancy will occur. In the spirit of previous work [6,7], analytical results are generated whenever possible. Some of the cases, however, involve numerical simulation in order to include as many aspects of the motion as possible. Furthermore, a new type of filtering technique is proposed—one that is applicable to tethered satellites rather than a conventional filter—for the purpose of alleviating the re-entry discrepancy. In [8] a classical orbit determination technique was modified for application to TSS. This method, rather than having a TSS dynamic model embedded within it, employs a Keplerian model of an untethered satellite, with the tether effects treated as perturbational accelerations. The technique estimates position and velocity of the mass being observed, as well as the tangential and radial components of tether acceleration. It was shown in [8] that the magnitude of the tether force increases with the length of the tether from the observed mass to the center of mass of the TSS. Hence, from the radial tether acceleration, this length can be estimated. However, since the filter does not contain a full dynamic model of a TSS, certain finer aspects of tethered motion, such as librational motion, cannot be captured. Thus, it is important in the present analysis to determine the effects of libration and other characteristics of tethered systems on the re-entry discrepancy.

2. RE-ENTRY DETECTION ANALYSIS

Here, the discrepancy between the actual motion of a tethered mass and its motion as predicted by an orbit determination technique is investigated for four different scenarios.

Scenario 1: circular motion of the center of mass of the TSS, without libration

Scenario 2: circular motion of the center of mass with libration

Scenario 3: elliptical motion of the c.m. (at perigee or apogee) without libration

Scenario 4: general motion of the TSS (elliptical motion of the c.m., with libration)

Each scenario involves a different set of assumptions regarding the motion. For all scenarios, the condition of re-entry will be defined as follows:

A body exhibiting Keplerian motion is said to be on a re-entry path if the following condition holds:

$$r_p < r_E \tag{1}$$

or equivalently

$$2a < r_a + r_E \tag{2}$$

where r_p is the perigee radius and r_E is a radius to be chosen on the basis of atmospheric drag considerations.

2.1. Circular Motion Without Libration

For the first scenario, the following assumptions are made:

1. The motion of the TSS is planar.

2. The TSS center of mass is traveling on a circular (Keplerian) orbit.

3. The libration angle of the TSS is negligible.

4. The libration rate is negligible.

Because the system is not librating and the center of mass travels in a circle, both endmasses (members of the system) do as well. Figure 1 depicts the motion of the system in this scenario, whereby the center of mass (solid line) and the two endmasses (dotted lines) all travel in concentric circles. The speed of the center of mass is that corresponding to a circular Keplerian orbit:

$$V_{cm} = \sqrt{\frac{\mu}{r_2 + \rho_2}} \tag{3}$$

Thus the angular speed of the center of mass (and the entire system) is

$$\omega_{cm} = \frac{V_{cm}}{r_2 + \rho_2} \tag{4}$$

The speed of the lower mass is then

$$V_2 = V_{cm}\left(\frac{r_2}{r_2 + \rho_2}\right) = \sqrt{\frac{\mu r_2^2}{(r_2 + \rho_2)^3}} \tag{5}$$

This, however, is *less* than the velocity of a body exhibiting circular Keplerian motion at the altitude determined by r. Since the observed mass's position and velocity vectors are perpendicular, a classical (Keplerian) orbit determination method will predict the mass to be at the apogee position of an elliptical orbit. The question is then, will a classical filtering technique predict the object to be on a re-entry orbit?

To answer this question, it must be determined what (elliptical) path the mass would follow if it were an untethered (Keplerian) body, with the observed radial distance and velocity of the mass at perigee. Applying the energy equation for elliptical orbits

$$\frac{v^2}{2} - \frac{\mu}{r} = -\frac{\mu}{2a} \tag{6}$$

to the lower mass, it is found that

$$a^* = \frac{\mu r_2}{2\mu - r_2 v_2^2} = \frac{r_2}{2 - \left(\dfrac{r_2}{r_2 + \rho_2}\right)^3} \qquad (7)$$

where a* denotes the "apparent" semi-major axis of the lower mass's orbit, as estimated by a classical (Keplerian) technique. Applying then the condition of re-entry given above, the path of the mass will be assessed as a re-entry orbit if

$$\frac{2 r_2}{2 - \left(\dfrac{r_2}{r_2 + \rho_2}\right)^3} < r_2 + r_E \qquad (8)$$

which agrees with the result given in [2]. This inequality can be rearranged to provide a condition on the distance from the body to the center of mass:

$$\rho_2 > r_2 \left(\sqrt[3]{\frac{r_2}{2 r_E} + \frac{1}{2}} - 1 \right) \qquad (9)$$

In terms of the lower mass's altitude h ($\approx r_2 - r_E$), this equation can be written as:

$$\rho_2 > (r_E + h) \left(\sqrt[3]{1 + \frac{h}{2 r_E}} - 1 \right) \qquad (10)$$

The value of ρ_2 for which the two sides of (10) are equal represents a threshold value above which the mass will be "mis-assessed" as a re-entry object. This value is denoted $\rho_{2,th}$. Figure 2 depicts this value for a range of orbital altitudes. The results of this figure are very similar in order of magnitude to results presented in [4] that were obtained in a similar fashion.

The TSS orbit determination technique described in [8] can approximate ρ_2 for a tethered object by estimating the tether force. Because orbit determination of a tethered satellite involves the estimation of more parameters than that of an untethered one, more observation data is generally required for sufficiently accurate determination of the state of a TSS. Therefore, a candidate identification method for re-entering objects might involve: (1) use of a conventional filter to make a rapid orbit determination of an object's motion assuming that it is untethered; (2) assessment of whether or not such an untethered satellite is on a re-entry path; and (3) after more observation data is obtained, refining this assessment via the TSS filter detailed in [8]. Unfortunately, this technique is based on the assumption that libration of the object, if tethered, is negligible. If libration is significant (as may often be the case with TSS), the scheme fails to provide an accurate assessment of the path of a tethered body due to the fact that neither of the aforementioned filtering techniques accounts for librational motion. The significance of this is illustrated in the next section.

2.2. Circular Motion With Libration

A TSS may experience appreciable libration, especially in the initial stages after deployment. For example, the TiPS system initially had a maximum libration angle on the order of 40 degrees [9]. In this scenario, assumptions 1, 2, and 3 above are adopted. The instantaneous libration angle is small, but libration rate of the TSS is no longer assumed negligible; i.e. the TSS is near the vertical portion of its "swing." In such a case, it is possible for libration rate to cause an incorrect assessment to be made concerning the anticipated path of the object being tracked by adding a component of velocity to the object that is not part of its gross orbital motion. Figure 3 depicts a librating TSS.

The libration rate $\dot{\phi}_3$ is defined to be positive when the smaller mass is "swinging" in the direction of orbital motion. Then, the velocity of the lower mass can be expressed as the sum of a component due to the orbital motion of the TSS (as in the above section) and a component due to libration:

$$v_2 = \sqrt{\frac{\mu r_2^{\,2}}{(r_2 + \rho_2)^3}} + \rho_2 \dot{\phi}_3 \tag{11}$$

The development in [10] regarding pendular oscillations of a tethered system yields, after making simplifications appropriate to this scenario, the following expression for libration rate:

$$\dot{\phi}_3 = \pm \sqrt{\frac{3}{2}} n \sqrt{\cos 2\phi_3 - \cos 2\phi_{30}} \tag{12}$$

where ϕ_{30} is the libration angle corresponding to zero libration rate. If instantaneous libration angle is small,

$$\dot{\phi}_3 = \pm \sqrt{\frac{3}{2}} n \sqrt{1 - \cos 2\phi_{30}} \tag{13}$$

The value of the instantaneous libration rate will then vary from $-\sqrt{3}n$ to $\sqrt{3}n$, depending on initial libration angle and whether the mass is swinging "toward" or "away from" its orbital path. Since the center of mass is in a circular orbit, the mean motion n is simply the angular velocity of the center of mass from the above section. Instantaneous libration rate can then be expressed as

$$\dot{\phi}_3 = \pm \sqrt{\frac{3}{2}} \sqrt{\frac{\mu}{(r_2 + \rho_2)^3}} \sqrt{1 - \cos 2\phi_{30}} = \beta \sqrt{\frac{\mu}{(r_2 + \rho_2)^3}} \tag{14}$$

where β is a function of ϕ_{30} and can take on values ranging from $-\sqrt{3}$ to $\sqrt{3}$. Inserting this expression into that for v_{m2} above and then into Equation (6) in the previous section yields

$$a* = \frac{r_2}{2 - \dfrac{r_2(r_2 + \beta\rho_2)^2}{(r_2 + \rho_2)^3}} \qquad (15)$$

Applying the condition of re-entry, as in the previous section, it is seen that the path of the

mass will be assessed by a classical orbit determination technique to be a re-entry orbit if

$$\frac{2r_2}{2 - \dfrac{r_2(r_2 + \beta\rho_2)^2}{(r_2 + \rho_2)^3}} < r_2 + r_E \qquad (16)$$

which simplifies to

$$\frac{\left(1 + \dfrac{\rho_2}{r_2}\right)^3}{\left(1 + \dfrac{\beta\rho_2}{r_2}\right)^2} > \frac{r_2}{2r_E} + \frac{1}{2} \qquad (17)$$

or, in terms of the lower mass's altitude:

$$\frac{\left(1 + \dfrac{\rho_2}{r_E + h}\right)^3}{\left(1 + \dfrac{\beta\rho_2}{r_E + h}\right)^2} > 1 + \frac{h}{2r_E} \qquad (18)$$

The inequality (18) is a function of altitude, tether length (from lower mass to c.m.), and β.

Again, the threshold value of ρ_2 is that for which the two sides of (18) are equal. Figure 4 shows

the value of $\rho_{2,th}$ versus altitude for various values of β (corresponding to various values of initial

libration angle). As can be seen here, for a given altitude, the presence of negative libration rate

decreases $\rho_{2,th}$ from that of the previous section. That is, because a negative libration rate reduces

the lower mass's total velocity (which is its apparent orbital velocity as predicted by classical

means), less tether force is needed to cause its trajectory to be assessed as a re-entry path.

Conversely, a much longer tether is required to cause the re-entry discrepancy for positive libration rates; so much longer, in some cases, as to essentially preclude the possibility of re-entry discrepancy altogether.

Considering that libration can contribute so significantly to the discrepancy stated in the Introduction, it is hypothesized that libration might possibly cause the same problem for the *upper* mass. That is, although the upper mass's velocity without libration is greater than that for a circular Keplerian orbit at that altitude, libration in the direction opposite the orbital motion may cause enough of a decrease in the mass's total velocity to make it look like an untethered body on a re-entry path. Toward this end, the same investigation performed above for the lower mass was performed for the upper mass. The equation representing a re-entry condition is similar to that above. It was found that this discrepancy *is* possible for the upper mass due to libration, but only for unrealistically long tethers, and at near the maximum possible libration rate. Nonetheless, in this section it has been clearly shown that in order to avoid the possibility of re-entry discrepancy caused by a tethered body, the orbit determination technique used must not only provide an estimate tether length, but libration rate as well.

2.3. Elliptical Motion (at Perigee or Apogee) Without Libration

While it has often been assumed that most practical applications of TSS will involve the center of mass traveling on an essentially circular orbit, the possibility of elliptical orbits should not be ruled out. In the following scenario, assumptions 1, 3, and 4 above are adopted. The TSS center of mass is on an elliptical orbit with semi-major axis a and eccentricity e, and is at the perigee position. This motion is depicted in Figure 5. The radius of the orbit of the center of mass, in terms of a and e, is

$$r_{cm} = a(1-e) \tag{19}$$

Likewise, in terms of the position of the lower mass and the tether length, r_{cm} is given by

$$r_{cm} = r_2 + \rho_2 \tag{20}$$

Combining these equations gives

$$a = \frac{r_2 + \rho_2}{1 - e} \tag{21}$$

By inserting this expression for a into Equation (6), the speed of the center of mass may be expressed as

$$V_{cm} = \sqrt{\frac{\mu(1+e)}{r_2 + \rho_2}} \tag{22}$$

The speed of the lower mass is

$$V_2 = V_{cm} \left(\frac{r_2}{r_2 + \rho_2} \right) = \sqrt{\frac{\mu(1+e)r_2^{\,2}}{(r_2 + \rho_2)^3}} \tag{23}$$

Inserting this into Equation (6) and rearranging gives

$$a^* = \frac{r_2}{2 - (1+e)\left(\dfrac{r_2}{r_2 + \rho_2} \right)^3} \tag{24}$$

as the "apparent" semi-major axis of the lower mass's orbit, as estimated by a classical (Keplerian) technique. The path of the mass will then be assessed as a re-entry orbit if

$$\frac{2r_2}{2 - (1+e)\left(\dfrac{r_2}{r_2 + \rho_2} \right)^3} < r_2 + r_E \tag{25}$$

or

$$\rho_2 > r_2 \left(\sqrt[3]{\left(\frac{r_2}{2r_E} + \frac{1}{2} \right)(1+e)} - 1 \right) \tag{26}$$

or, in terms of the lower mass's altitude:

$$\rho_2 > (r_E + h) \left(\sqrt[3]{\left(1 + \frac{h}{2r_E} \right)(1+e)} - 1 \right) \tag{27}$$

Note that the threshold value of ρ_2 is approximately a linear function of h, due to the fact that h $\ll r_E$. Figure 6 depicts the value of $\rho_{2,th}$ as a function of altitude for varying eccentricity.

If the center of mass is at its apogee position, the re-entry condition is obtained by interchanging 1-e for 1+e in the above inequality. The results are in Figure 7. A comparison of the two figures illustrates how increasing eccentricity of the center of mass makes it less likely to mistake a tethered body's orbit as a re-entry path when the TSS is at perigee, but more likely to experience this discrepancy when the TSS is at apogee. This is due to the fact that increasing eccentricity increases the perigee velocity of the center of mass and decreases its apogee velocity. The velocity of the lower mass will then increase or decrease proportionally to that of the center of mass, and of course, the slower the velocity at a given position, the greater the likelihood that the re-entry discrepancy will occur. This result is consistent with [5], in which the re-entry discrepancy for an eccentric TSS orbit is investigated at several locations in the orbit, including apogee and perigee.

Note that, for a given eccentricity and altitude, $\rho_{2,th}$ takes on its highest value when the center of mass is at perigee and its lowest value when it is at apogee. Thus, Figures 6 and 7 depict the upper and lower bounds, respectively, on $\rho_{2,th}$ during the course of a particular (non-circular) orbit. Consider a slightly elliptical TSS orbit, one in which the altitude of the lower mass does not change significantly. Given the eccentricity and altitude of this orbit, the upper and lower bounds

on $\rho_{2,th}$ can immediately be read from Figures 6 and 7. If the tether length is greater than the upper bound, the re-entry discrepancy is guaranteed to occur everywhere in the orbit, while if the tether length is less than the lower bound, the discrepancy is guaranteed *not* to occur *anywhere* in the orbit. If the tether length is in between these values, the discrepancy will occur only at some points in the orbit.

One final observation to be made in this section is as follows. For a TSS on an elliptical orbit with the center of mass at apogee, the possibility of actual re-entry of the lower mass must be considered. That is, the altitude of the center of mass upon reaching perigee may be less than the tether length. This is the case if

$$r_{cm,perigee} < r_E + \varrho_2 \tag{28}$$

or

$$(r_2 + \varrho_2)\left(\frac{1-e}{1+e}\right) < r_E + \varrho_2 \tag{29}$$

or, in terms of the lower mass's altitude:

$$\varrho_2 > \left(\frac{1-e}{2e}\right)h - r_E \tag{30}$$

Equation (30) indicates a threshold tether length of a different sort: the value above which an apparent re-entry is in fact an actual re-entry. This tether length is depicted in Figure 8 (the steeper of the two curves) for an eccentricity of 0.05, along with $\rho_{2,th}$ for the same eccentricity (center of mass at apogee). These curves naturally divide the tether length vs. altitude space into three distinct regions: the region to the left of the curve resulting from Equation (30); the region to the right of the $\rho_{2,th}$ curve; and the region between the two curves. The first region indicates a lower mass that will re-enter and is predicted to do so. The second region indicates a lower mass

that will not re-enter, nor is it predicted to do so. And the third region indicates a lower mass that is predicted to re-enter, but will not (the true "re-entry discrepancy").

2.4. General Motion of the TSS

For the final scenario, the re-entry condition was determined numerically rather than analytically. The model used is described in [1]. Any general orbit of a TSS can be simulated, and libration is accounted for. Thus, *none* of the assumptions listed earlier were adopted in this scenario. The investigation proceeded as follows: a set of initial conditions was chosen specifying a particular (generally elliptical) orbit for the TSS center of mass. Once this "baseline" set of values was fixed, the tether length, eccentricity, and initial libration angle—all of which can impact the re-entry discrepancy—were varied. By this process, results for several cases were generated. These cases are listed in Table 1. For each case, the TSS motion was simulated for one orbit of the center of mass (approximately 5000 sec) and the position and velocity vectors of the lower mass were recorded continuously during this time span. This data was then manipulated in two ways:

1. Assuming the observed (lower) mass to be an *untethered body exhibiting Keplerian motion,* each pair of position and velocity vectors was converted to a set of orbital elements, from which the perigee radius was calculated.

2. Again the lower mass was assumed to be untethered. Taking the position and velocity of the lower mass recorded at the first time step to be "initial" values, the motion of the lower mass was simulated for one orbit, using equations that account for forces due to Earth's oblateness.

This simulation was repeated, using each pair of position and velocity vectors, in turn, as the "initial" position and velocity. For each simulation, the minimum radius attained over the orbit was recorded.

Each of the two procedures provided a history of the "apparent perigee radius" over one orbit of the center of mass for each of the cases in Table 1. The results for cases A-D are shown in Figures 9-12, respectively. Dotted curves denote the apparent perigee radius obtained via the first procedure (Keplerian motion assumed), while the solid curves were obtained via the second procedure (oblateness effects included). In each plot the mean radius of the Earth is indicated (approximately 6378000 m), in order that it may be clearly seen whether, and at what times during the orbit, the mass is perceived to be on a re-entry path. Clearly, all three parameters that were varied have a significant effect on whether the mass is perceived as one that is about to re-enter. (It should be mentioned that none of the cases in Table 1 correspond to actual re-entry of the lower mass at any point in the orbit.)

3. DISCUSSION

Figures 9-12 in many ways corroborate the results from the previous three scenarios, which were obtained analytically and under several assumptions. For example, Figure 9 illustrates how increasing tether length tends to decrease the apparent perigee radius, thus making the re-entry discrepancy more likely. This is in keeping with the analytical result shown in Figure 2. Consider also Figure 10. The peaks in the curves are points in the orbit where libration rate is maximum and positive, i.e., in the direction of orbital motion. These indicate the location of highest

apparent perigee radius, where the re-entry discrepancy is least likely to occur. The reverse is true for the trough in each curve, corresponding to maximum negative libration rate. The figure depicts a set of curves with increasing value of initial libration angle which, according to Equation (12), increases the amplitude of libration rate. This then exaggerates both the highest apparent perigee radius at the peaks and the lowest highest apparent perigee radius at the trough. This agrees with the trend evident in Figure 4; that is, increasing negative libration rate increases the likelihood of the re-entry discrepancy, whereas the opposite is true for increasing positive libration rate. Finally, Figure 11 depicts how, when the TSS is simulated from the perigee point of an eccentric orbit, increasing eccentricity essentially translates the curve of apparent perigee radius upward. Likewise in Figure 12, when the TSS is simulated from the apogee point, increasing eccentricity translates the curve downward. These trends agree with those of Figures 6 and 7. That is, $\rho_{2,th}$ increases with eccentricity for TSS motion at the perigee point, and decreases with eccentricity for motion at the apogee point. In all the curves it is noted that, when calculating the apparent orbit based on the assumption of an untethered body, taking Earth's oblateness into account results in a lower apparent perigee radius, i.e., a more likely occurrence of the re-entry discrepancy.

It is instructive to consider what would occur if the tether were to be severed, either intentionally or unintentionally. In such a case, if one of the end masses becomes free of the other end mass as well as the tether, it then exhibits motion characteristic of an untethered satellite, with its orbit determined by its position and velocity at the instant the tether was cut. The path of the observed mass as predicted by classical means (i.e., assuming it is untethered), which was incorrect in each of the above scenarios, will now be the *correct* path of the object. Further, the object's orbital velocity will be the sum of its orbital velocity as part of the TSS, plus any

significant component of librational velocity the object may have when the tether breaks. (Recall that, at the time the object was tethered, libration did *not* contribute directly to the object's gross orbital motion.)

4. ALGORITHM FOR RE-ENTRY DETERMINATION

The previous sections have shown that both tether length and libration can play a large role in effecting the re-entry discrepancy associated with a tethered object. As mentioned earlier, the TSS orbit determination technique detailed in [8] provides a means of approximating tether length but cannot assess librational motion. However, a filtering technique that does include an estimate of libration angle and libration rate has been developed and applied experimentally in [1,7]. With the premise that both this technique and a conventional Keplerian-based filter are available, a method for determining the possibility of re-entry of an object can be formulated. First, a fundamental difference between the motion of tethered and untethered objects should be pointed out. For an untethered object exhibiting Keplerian motion, both the argument of perigee and eccentricity are constant for a given orbit. If oblateness is taken into account in modeling the motion of that body, it causes slight perturbations to both quantities over the course of one orbit. In contrast, given the position and velocity vectors of a tethered body during its orbit, as in the last section, the "apparent" argument of perigee and eccentricity vary significantly over the course of an orbit. Figures 13 and 14 bear this out, for the data of Case A1 from Table 1. Although the exact behavior of these apparent quantities may differ for different cases of tethered motion, their deviations from the true values for an untethered body are apparent. With these deviations in mind, a candidate algorithm for re-entry detection is as follows:

1. Given a batch of tracking data for an object, process a small portion of the data via classical orbit determination methods to estimate the object's position and velocity at a particular time. Convert these quantities to orbital elements.

2. If the calculated perigee radius indicates the object is on a re-entry trajectory, process more data to estimate its position and velocity at several times.

3. From these quantities, calculate the argument of perigee and eccentricity of the body at each time, and look for significant deviations from untethered behavior, as in Figures 13 and 14.

4. If no significant deviations are detected, it can be concluded that the object is untethered, the perigee raduis corresponding to the estimated position and velocity is correct, indicating a re-entry trajectory, and the assessment is complete. Otherwise, conclude that the object is the lower mass of a TSS and proceed to the next step.

5. Use the TSS orbit determination scheme to estimate the state of the tethered object, including position, velocity, tether length, libration angle, and libration rate, at a particular time. The position of the center of mass can then be calculated by the following vector equation:

$$\mathbf{r}_{cm} = \mathbf{r}_2 + \rho_2 \mathbf{u}_\rho \tag{31}$$

where r_2 and ρ_2 are known from the state estimate, and $\mathbf{u}_\rho$ is a unit vector in the direction of the tether, whose components can be found knowing ϕ_3. Also, the velocity of the center of mass is calculated by

$$\mathbf{v}_{cm} = \left(\mathbf{v}_2 - \rho_2 \dot{\phi}_3 \mathbf{u}_\phi\right)\left(\frac{r_2 + \rho_2}{r_2}\right) \tag{32}$$

which is essentially Equation (11) rearranged and expressed in vector form. Here $\mathbf{u}_\phi$ is a unit vector perpendicular to the direction of the tether (i.e., perpendicular to $\mathbf{u}_\rho$), and all other quantities are known from the state estimate.

6. Convert position and velocity of the center of mass into orbital elements. Calculation of the perigee radius will then determine the re-entry status of the tethered object.

The above steps are illustrated in the flow chart of Figure 15. Note that the above calculations are based on the assumption of Keplerian motion (two-body force only) for either the untethered object or the center of mass of the TSS. For the general motion cases of Figures 9-12, it is seen that including higher-order gravity effects tends to decrease the apparent perigee radius. For this reason, if Keplerian considerations lead to the conclusion that the object (tethered or untethered) is set to re-enter, then it is certain that the same conclusion would be arrived at by accounting for higher-order effects. If, on the other hand, a Keplerian-based procedure assesses the body to be a tethered object NOT on a re-entry path, then further analysis may be necessary for an unambiguous determination to be made.

5. CONCLUSIONS

The problem of quickly identifying whether an object in near-Earth orbit is a candidate to re-enter the Earth's atmosphere has been considered, including tethered satellites as possibilities. By investigating several particular cases of tethered satellite motion, it was found that both the force due to the tether and the librational motion of a TSS can play a significant role in causing a tethered body to appear to be on a re-entry path, even though it in fact is not. Consequently, a successful re-entry identification methodology must utilize an orbit determination method that can distinguish between tethered and untethered objects, as well as estimate the tether length and librational motion, if the object is tethered; otherwise the results of such an assessment may be ambiguous or inconclusive. A candidate algorithm was then formulated utilizing such a technique in conjunction with a conventional orbit determination method, that is, one based on a two-body (Keplerian) motion model.

REFERENCES

1. Cho, S., Cochran, J. E., Jr., and Cicci, D. A., Identification and orbit determination of tethered satellite systems. Accepted for publication in *Journal of Applied Mathematics and Computation*, 2000.

2. Hoots, F. R., Roehrich, R. L., and Szebehely, V. G., Space shuttle tethered satellite analysis. Technical Report #83-5, Directorate of Astrodynamics, Peterson Air Force Base, CO, August 1983.

3. Asher, T. A., D. G. Boden, and R. J. Tegtmeyer, Tethered satellites: the orbit determination problem and missile early warning systems, AIAA 88-4284 1988.

4. Racca, R. A., Liu, J. J. F., and Feldman, J. K., Conditions for apparent Earth-impacting orbits of tethered space objects. Technical Report #97-22, Directorate of Analysis and Engineering, Falcon Air Force Base, CO, January 1998.

5. Racca, R. A., and Feldman, J. K., Eccentricity effects on apparent Earth-impacting orbits of tethered space objects. Technical Report #98-9, Directorate of Analysis and Engineering, Falcon Air Force Base, CO, April 1998.

6. Cho, S., Cochran, J. E., Jr., and Cicci, D. A., Approximate solutions for tethered satellite motion. Accepted for publication in *Journal of Guidance, Control, and Dynamics*, 2000.

7. Cho, S., Cochran, J. E., Jr., and Cicci, D. A., Modeling tethered satellite systems for detection and orbit determination, AAS 99-416 1999.

8. Cicci, D. A., Lovell, T. A., and Qualls, C., A method for the identification of a tethered satellite, AAS 99-196 1999.

9. *TiPS: Tether Physics and Survivability Satellite Experiment* web page, Naval Center for Space Technology, http://hyperspace.nrl.navy.mil/TiPS/data.html

10. Beletsky, V. V., and Levin, E. V., *Dynamics of Space Tether Systems*, Vol. 83, Advances in the Astronautical Sciences, AAS, San Diego, CA, 1993, p. 76.

APPENDIX

Nomenclature

a	semi-major axis of a Keplerian orbit
e	eccentricity of a Keplerian orbit
h	orbital altitude
m_1	upper mass of tethered satellite system
m_2	lower mass of tethered satellite system
r_1	distance from Earth's center to the upper mass
r_2	distance from Earth's center to the lower mass
r_a	apogee radius of a Keplerian orbit
r_{cm}	distance from Earth's center to the center of mass
r_E	radius denoting re-entry into Earth's atmosphere
r_p	perigee radius of a Keplerian orbit
v_1	velocity of the upper mass
v_2	velocity of the lower mass
v_{cm}	velocity of the center of mass
ϕ_3	libration angle with respect to the center of mass
$\dot{\phi}_3$	libration rate about the center of mass
μ	Earth's gravitational parameter
ρ_1	tether length from center of mass to upper mass
ρ_2	tether length from center of mass to lower mass
ω_{cm}	angular velocity of the center of mass

Table 1. List of Cases for Numerical Results. (For all cases, m_1=100kg, m_2=10kg, initial radius of TSS orbit = 6600km.)

Case	Tether length (km)	Initial lib. Angle (deg)	Eccentricity
A1	10	15	0
A2	30	15	0
A3	50	15	0
B1	30	5	0
B2	30	20	0
B3	30	35	0
C1	20	10	.005*
C2	20	10	.01*
C3	20	10	.015*
D1	20	10	.005**
D2	20	10	.01**
D3	20	10	.015**

*c.m. initially at perigee
**c.m. initially at apogee
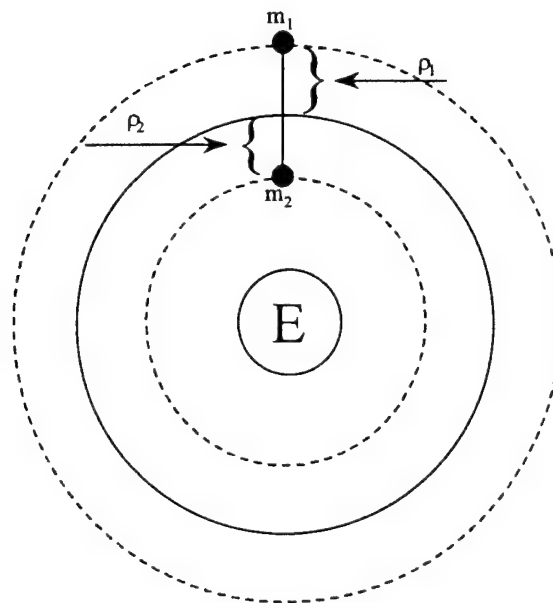
Figure 1. Center of Mass in a Circular Orbit, no Libration.
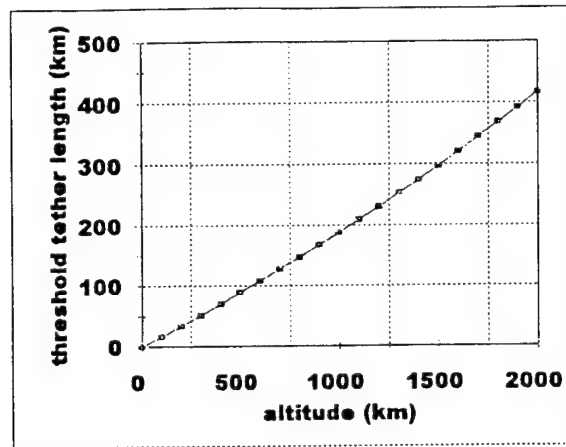
Figure 2. Threshold Value of ρ_2.
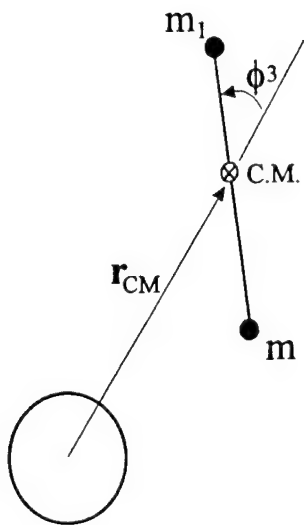
Figure 3. Librating TSS.
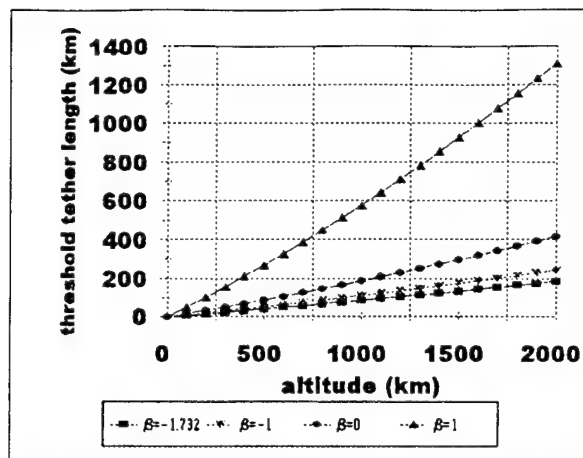
Figure 4. Value of $\rho_{2,th}$ as a Function of Libration Rate.
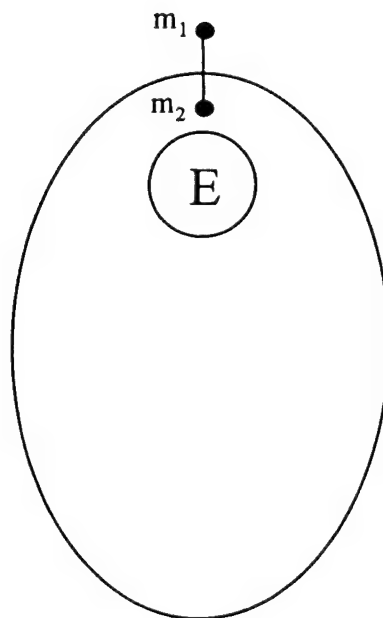
Figure 5. Center of Mass in an Elliptical Orbit at Perigee, no Libration.
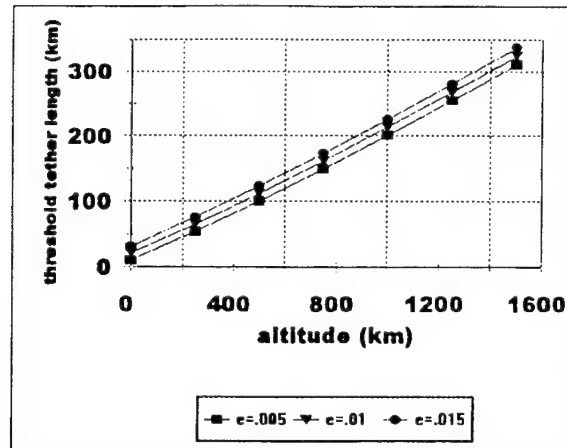
Figure 6. Value of $\rho_{2,th}$, Center of Mass in an Elliptical Orbit at Perigee, no Libration.
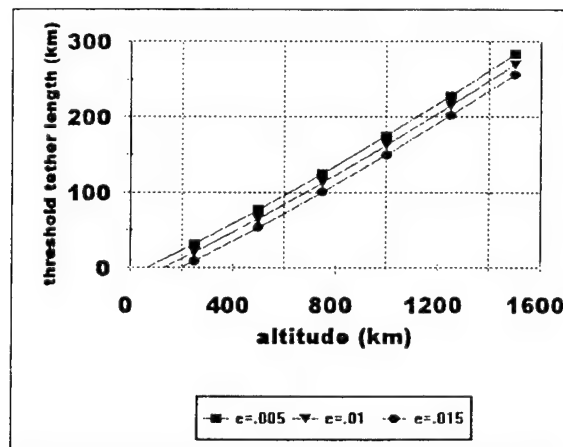
Figure 7. Value of $\rho_{2,th}$, Center of Mass in an Elliptical Orbit at Apogee, no Libration.
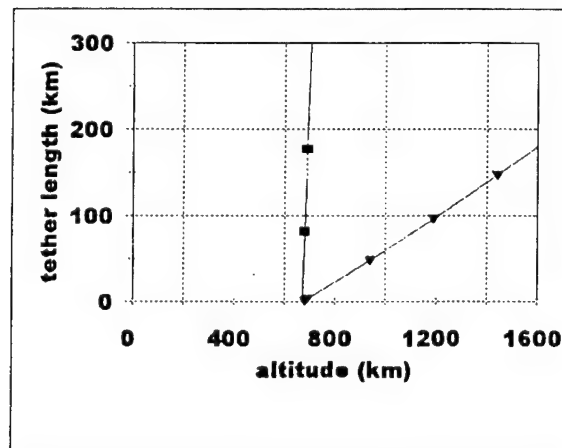
Figure 8. Delineation Between Areas of Actual Re-entry, Apparent Re-entry, and No Re-entry.
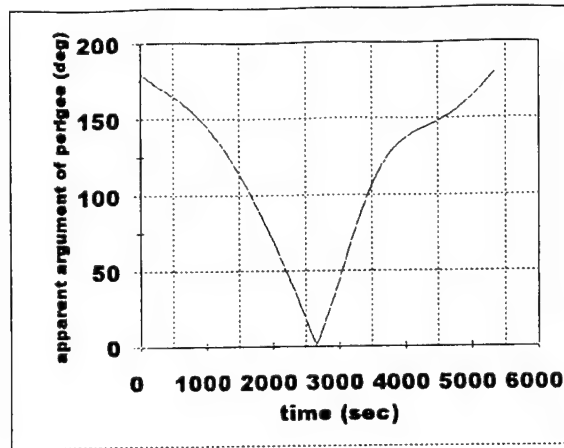
Figure 13. "Apparent" Value of Argument of Perigee, for the Orbit of Case A1.
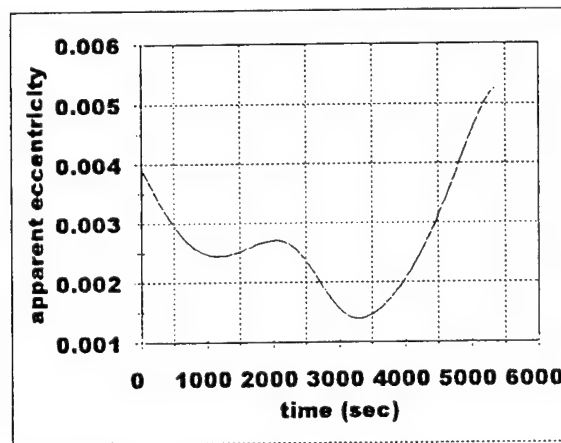
Figure 14. "Apparent" Value of Eccentricity, for the Orbit of Case A1.

PRELIMINARY ORBIT DETERMINATION
OF A TETHERED SATELLITE

C. Qualls[1] and D. A. Cicci[2]
Auburn University, Alabama

A renewed interest in the deployment of tethered satellites has led to a need for preliminary orbit determination methods which are capable of distinguishing tethered satellites from untethered ones. A number of current preliminary orbit determination methods, which are used for Keplerian satellites, generally require two or more position vectors along with their respective observation times in order to determine a preliminary orbital element set. These conventional methods, however, are unable to distinguish between Keplerian and tethered satellites, whose motion is modified due to the presence of a tether force. The use of these conventional methods will result in the calculation of inaccurate orbital elements if the observed satellite is part of a tethered satellite system. Modifications have been made to four classical preliminary orbit determination methods in order to allow for the identification of tethered satellites. These modifications allow for the calculation of a gravitational parameter, in addition to a set of orbital elements, which can be used to distinguish between a tethered satellite and an untethered one. This paper applies these modified preliminary orbit determination methods to the problem of the identification of a tethered satellite. The performance of these methods is evaluated through scenarios of differing tether lengths and levels of observation error. Due to the desire for the preliminary orbit determination to be achieved quickly, only small radius vector spreads were considered. Results are compared in order to determine the most accurate method. A description of how this preliminary orbit information can be used to obtain tether parameters for the subsequent differential correction process is also provided.

INTRODUCTION

The method of orbit determination of a space vehicle is defined to include both preliminary (or initial) orbit determination (POD) and orbit improvement using a differential correction procedure [1]. POD, which considers only two-body, i.e., Keplerian, dynamics uses the first few observations of the vehicle's motion to calculate a first estimate of the orbit. This 'preliminary' orbit is then used as a set of initial conditions for the differential correction process. The differential correction phase

[1] Graduate Student, Department of Aerospace Engineering, Student Member, AIAA.
[2] Associate Professor, Department of Aerospace Engineering, Member, AAS; Associate Fellow, AIAA.
Email: dcicci@eng.auburn.edu. Phone: (334) 844-6820, FAX: (334) 844-6803.

typically includes dynamical models which consider the perturbation effects on the space vehicle in order to improve the solution accuracy obtained by the POD procedure. This is achieved by processing, i.e., filtering, additional observational data obtained from tracking stations and will generally continue as long as the vehicle's motion is being observed.

A number of recent studies [2-8] have addressed the difficulties encountered in identifying a satellite as part of a tethered satellite system (TSS) without prior knowledge that it is so. These difficulties arise from the fact that the dynamics of a tethered satellite are greatly affected by the force present in the tether. This force causes a tethered satellite to behave in a non-Keplerian manner. Since classical orbit determination methods are unable to account for this modified Keplerian motion, the calculation of the orbital elements by these methods will likely produce large errors. Errors in the determination of the orbital elements can cause the predicted trajectory of the satellite to appear sub-orbital in nature [9].

In order to distinguish between the different motions of a tethered and untethered satellite a batch-type filter has been developed [5,8] to be used in the differential correction process. This filter includes the effect of the tether force on the dynamics of the satellite and therefore can be used to identify a tethered satellite through observations of the satellite's motion. However, the potential for the misidentification of a tethered satellite as a sub-orbital object emphasizes the need for the orbit determination to be performed quickly. As a result, tethered satellite identification should be possible using only a short arc of observational data, which unfortunately creates an ill-conditioned estimation problem. Ridge-type estimation methods have been proposed [6] in order to improve the 'quick-look' capabilities of the differential correction process in these types of problems. These filtering methods have proven to be very effective in tethered satellite identification. However, improvements in the filtering process can be achieved through the development and use of POD methods capable of providing an improved preliminary orbit, including information on tether specific parameters, as initial conditions in the differential correction phase.

POD methods have been developed which use various types of observational data to calculate the preliminary orbit. For example, measurements of range, range-rate, azimuth and elevation angles, or position vectors, in addition to the times of the measurements, are used in various POD methods. This study focuses on four conventional POD methods which use position vectors and time data from at least two observation points which are provided or easily calculated since this type of data is generally available for tethered satellites. The POD methods addressed in this study include: the Herrick-Gibbs method, the true anomaly iteration technique, the p (semi-parameter) iteration technique, and an f and g series iteration method, which are described in [10]. These are the methods which will be modified to include the capability to distinguish between a tethered satellite and an untethered one using only the first few observations.

The modification required for each of the classical POD methods is to include the calculation of a gravitational parameter which can account for the non-Keplerian motion of a tethered satellite. This gravitational parameter will be calculated to be different from the standard gravitational parameter in the case that the observed satellite is part of a TSS. A smaller-than-standard value of this parameter will indicate that the observed satellite is the lower satellite of a two-satellite TSS while a larger-than-standard value will indicate that the observed satellite is the upper satellite of the TSS. In the case of a Keplerian satellite the calculated value of the gravitational parameter will be equal to the standard value. From this calculated value a determination can be made as to how far below or above the TSS center-of-mass the observed satellite is located. This information, in addition to the orbital element set, is then provided as part of the initial conditions to the differential correction phase of the identification process.

The sections below discuss each of the four classical POD methods addressed in this study and the required modifications to these methods. Through the use of simulated data, the performance of these modified POD methods are evaluated for differing tether lengths and levels of observation error. Results are compared and recommendations are made for the use of these POD methods in the process of the identification of a tethered satellite. A description of how the tether specific information is obtained from the calculated gravitational parameter is also provided.

CLASSICAL POD METHODS

The classical POD methods addressed in this study are outlined below and include the following: the Herrick-Gibbs method, the true anomaly iteration technique, the p (semi-parameter) iteration technique, and an f and g series iteration method. These methods are presented in detail by Escobal [10], and each assumes that position vectors and time data from at least two observation points are provided or easily calculated.

The Herrick-Gibbs Method

Using three given position vectors and times, the Herrick-Gibbs method is able to compute the velocity vector at t_2. The computation of this vector allows the determination of the orbital elements by standard techniques [11] since the position vector at t_2 was given. In order to solve for $\dot{r}_2$ the following equations are used:

$$G_1 = \frac{t_3 - t_2}{(t_2 - t_1)(t_3 - t_1)} \tag{1}$$

$$G_3 = \frac{t_2 - t_1}{(t_3 - t_2)(t_3 - t_1)} \tag{2}$$

$$G_2 = G_1 - G_3 \tag{3}$$

3

$$H_1 = \frac{\mu(t_3 - t_2)}{12} \tag{4}$$

$$H_3 = \frac{\mu(t_2 - t_1)}{12} \tag{5}$$

$$H_2 = H_1 - H_3 \tag{6}$$

where μ is the gravitational parameter. Using the preceding equations, the coefficients

$$d_i = G_i + \frac{H_i}{r_i^3}, \quad i = 1, 2, 3 \tag{7}$$

can be calculated, which are used to determine the velocity vector, $\dot{\mathbf{r}}_2$, as follows:

$$\dot{\mathbf{r}}_2 = -d_1 \mathbf{r}_1 + d_2 \mathbf{r}_2 + d_3 \mathbf{r}_3 \tag{8}$$

True Anomaly Iteration Technique

The true anomaly iteration technique requires two position vectors and their respective times. If the equation of a conic is written for the two times given, it is possible to write

$$r_1 (1 + e \cos \upsilon_1) = r_2 (1 + e \cos \upsilon_2) \tag{9}$$

from which, the eccentricity can be calculated. In order to calculate the eccentricity, an initial approximation of the true anomaly at t_1 must be made and the angle between the radius vectors must be determined. Once the eccentricity has been computed the semi-major axis can be found. The eccentric anomalies are then computed using

$$\sin E_i = \frac{\sqrt{1 - e^2} \sin \upsilon_i}{1 + e \cos \upsilon_i}, \quad i = 1, 2 \tag{10}$$

$$\cos E_i = \frac{\cos \upsilon_i + e}{1 + e \cos \upsilon_i}, \quad i = 1, 2 \ . \tag{11}$$

Once the eccentric anomalies have been determined the mean anomaly can be calculated using Kepler's Equation and the iterative function, F, can be written as

4

$$F = \tau - \left(\frac{M_2 - M_1}{n} \right) k \qquad (12)$$

where τ is the modified time variable and n is the mean motion. If F is greater than the specified tolerance, υ_1 is slightly increased and the elements are then recalculated. The Secant (or similar) root-finding method can then be used with the iterative function to determine an accurate value of υ_1, which in turn, leads to accurate estimates of the orbital elements.

p-Iteration Technique

As in the true anomaly iteration technique, the p-iteration technique requires two position vectors and their respective times. From the position vectors, it is possible to compute two unit vectors along the corresponding radius vectors. Using these unit vectors, one can find the difference in true anomalies between the two radius vectors. An estimate of the semi-parameter, p, is then used, along with the difference in the true anomalies and the trajectory equation, to obtain the orbital eccentricity and semi-major axis. After calculating the eccentricity, the trajectory equation may again be used to find the true anomalies for each position vector. The eccentric anomalies are then found using the following equations:

$$\cos E_i = \frac{r_i}{p} (\cos \upsilon_i + e), \quad i = 1, 2 \qquad (13)$$

$$\sin E_i = \frac{r_i}{p} \sqrt{1 - e^2} \sin \upsilon_i, \quad i = 1, 2 \qquad (14)$$

The eccentric anomalies, along with the eccentricity, are then used in Kepler's equation to calculate the difference in the mean anomalies. The iterative function, F, can be expressed again using Equation (12). This iterative function is also used with the Secant (or similar) root-finding method to calculate an accurate value of p.

f and g Series Iteration Method

Using two position vectors and times provided, one is able to calculate approximations of the position and velocity vectors, $\mathbf{r}_o$ and $\dot{\mathbf{r}}_o$, at an arbitrarily selected epoch time, t_o. These first approximations are computed through linear combinations of the position vectors. Improvements can now be made to $\mathbf{r}_o$ and $\dot{\mathbf{r}}_o$ by evaluating the f and g series at t_1 and t_2 as follows:

$$\mathbf{r}_0 = \frac{g_2}{f_1 g_2 - f_2 g_1} \mathbf{r}_1 + \frac{-g_1}{f_1 g_2 - f_2 g_1} \mathbf{r}_2 \qquad (15)$$

5

$$\dot{\mathbf{r}}_0 = \frac{-f_2}{f_1 g_2 - f_2 g_1} \mathbf{r}_1 + \frac{f_1}{f_1 g_2 - f_2 g_1} \mathbf{r}_2 \tag{16}$$

The new improved values of $\mathbf{r}_o$ and $\dot{\mathbf{r}}_o$ can then be used to calculate $\dot{\mathbf{r}}_1$ by using the following linear combination:

$$\dot{\mathbf{r}}_1 = \dot{f}_1 \mathbf{r}_0 + \dot{g}_1 \dot{\mathbf{r}}_0 \tag{17}$$

Upon obtaining the converged value of this vector, standard techniques [11] are used to convert to the orbital elements.

MODIFICATIONS TO THE CLASSICAL METHODS

In order for the four classical POD methods to be able to distinguish between Keplerian and tethered satellites, several modifications must be made. The classical POD methods previously described were originally written to be used with Keplerian satellites only and therefore, all methods use the standard value for the gravitational parameter, μ, in the calculations. It is known that the presence of a tether force creates a radial acceleration component on the tethered satellite thereby resulting in non-Keplerian motion of the satellite. The effect that this additional acceleration component has on the satellite's motion can be effectively modeled by a modified gravitational parameter, μ^* [10]. The value of this parameter will be different from the standard value and will depend on the satellite's location and the length of the tether. Therefore, the use of the standard value of the gravitational parameter in the various POD methods will not allow for an accurate determination of the orbital parameters of a tethered satellite.

In order to determine the value of μ^* for an observed tethered satellite, all equations in the four POD methods were rewritten as functions of the gravitational parameter. The purpose of rewriting the equations in this form is to allow the value of μ^* to be determined by iteration. The Secant root-finding technique was used to perform this iteration. In order for the Secant method to be able to iterate, an initial estimate of μ^* is required. The initial estimate chosen was the standard value of μ. This is because since details of the satellite's configuration are not known beforehand, one must assume a Keplerian satellite. The iterative function used by the Secant method is the differenced Kepler's equation. Once enough iterations on μ^* have been performed to meet the specified tolerance, the process is stopped and the value of the gravitational parameter is considered to be determined.

The Herrick-Gibbs and f and g series methods require additional changes. Due to the fact that neither of these two methods estimates more than one position and velocity vector, additional input is required. In order to use the differenced Kepler's equation, at least two position and velocity vectors must be estimated. To obtain the additional

6

position and velocity vectors the Herrick-Gibbs method is initially provided with four position vectors and their respective times. Using these four position vectors allows for the orbit to be determined at both t_2 and t_3 and thus allows for the use of the differenced Kepler's equation. Similarly, the f and g series is provided with position vectors at three times instead of two. This allows the orbit to be determined at two arbitrarily selected epoch times, one between t_1 and t_2 and the other between t_2 and t_3.

In both the Herrick-Gibbs method and the f and g series method, the resulting position and velocity vectors are converted to orbital elements by conventional algorithms [11]. All equations used in the conversion from vectors to orbital elements use the iterating value of μ^* during the solution process.

TETHER SPECIFIC PARAMETERS

A simplified, two-satellite TSS was presented in [5] and is shown in Figure 1 below. Here, the 'daughter' satellite, m, is connected by a tether to the 'parent' satellite, m_p, with the effective tether force acting on m as indicated by **F**. This tether force on the daughter satellite can be resolved into radial and tangential components, F_r and F_t, respectively, as indicated.
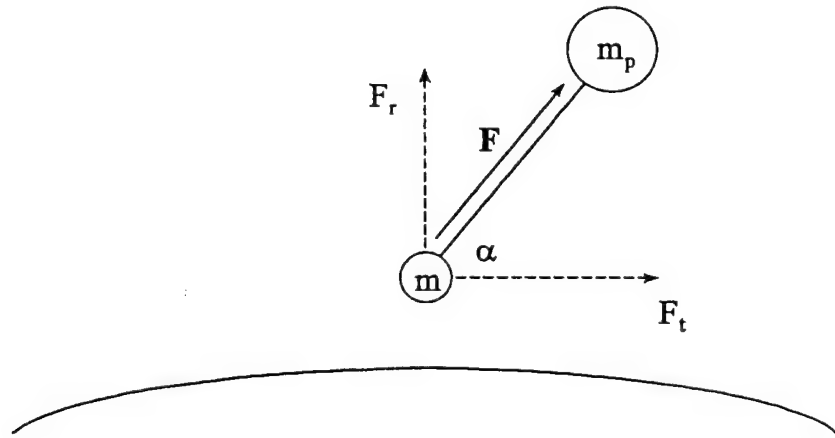
Figure 1. Tethered Satellite System

Assuming that the motion of the TSS is planar, α is the angle the tether makes with the local horizon relative to the daughter mass' location above the Earth. These force components tend to change the acceleration on the satellite thereby altering its velocity. The radial force component will reduce the total radial acceleration on the satellite if the

daughter satellite is in a lower orbit than the parent satellite and increase the total radial acceleration if the daughter is in a higher orbit than the parent. The tangential force component will create a tangential acceleration component, a_t, and will tend to decrease the velocity of the daughter when it 'leads' the parent, whereas it increases the daughter's velocity when it 'trails' the parent.

An accurate POD of a tethered satellite can provide useful information in the determination of the radial component of the tether force. Specifically, the calculation of the modified gravitational parameter, μ^*, can be used to determine the radial acceleration component using the following expression presented in [5].

$$\mu^* = \mu - a_r r^2 \tag{18}$$

Along with the position and velocity vectors obtained from the orbital element set, the calculated value of a_r will be supplied as initial conditions to the differential correction phase of the orbit determination process. Furthermore, the distance that the daughter satellite is located above or below the center-of-mass of the TSS, assuming negligible libration, can also be calculated using expressions presented in [5] as follows:

$$\rho_{cm}^* = [(\mu - \mu^*) / (2\mu + \mu^*)] \, r \tag{19}$$

if the daughter is below the parent, and

$$\rho_{cm}^* = [(\mu^* - \mu) / (2\mu + \mu^*)] \, r \tag{20}$$

if the daughter is above the parent. The value of ρ_{cm} will approach the actual tether length as the ratio of the daughter mass to the parent mass gets small.

SIMULATION DESCRIPTION

In order to test the accuracy of the modified POD methods, a simulation was developed using both Keplerian and tethered satellite data. The data was generated using the baseline circular orbit whose elements are provided in Table 1.

Orbital Elements	
a	6621 km
e	0.00
i	5.73 deg
Ω	5.73 deg

Table 1. Baseline Orbit for Data Generation.

The tether lengths considered were 0 km (Keplerian), 1 km, 10 km, 100 km, and 1 km up (daughter satellite above parent). Both uncorrupted and three levels of corrupted (Gaussian) Keplerian and tethered data were used. The levels of noise applied to the position vectors used in this simulation are provided in Table 2. Twenty cases were analyzed for each of the four POD methods.

Noise Level	Position Error
High	10 m
Medium	5 m
Low	1 m

Table 2. Standard Deviation of Observation Error Levels.

Since the goal was to achieve a POD as quickly as possible, only small radius vector spreads were considered. The smallest possible observation time spans between data points that can be used to obtain accurate results are provided in Table 3.

Method	Δt (sec)	Data Points	Total Time (sec)
Herrick-Gibbs	5	4	15
True Anomaly	200	2	200
p-Iteration	200	2	200
f and g Series	5	3	10

Table 3. Minimum Time Spans.

Observation time spans of less than 200 seconds for the true anomaly and p iteration methods produce inaccurate results and are not recommended.

RESULTS

Tables 4-8 below present the results of the cases described above. Each table provides the calculated values of the modified gravitational parameter, μ^*, the calculated distance of the observed satellite from the center-of-mass of the TSS, ρ_{cm}^*, and the error in this calculation, $\rho_{cm} - \rho_{cm}^*$.

High Noise	Herrick-Gibbs	v-Iteration	p-Iteration	f-g Series
$\overset{*}{\mu}$ (kg*m^3/s^2)	398645.1693	398580.5195	398602.8198	398599.6779
$\overset{*}{\rho_{cm}}$ (m)	247.6719	110.2768	13.1986	4.1976
$\rho_{cm} - \overset{*}{\rho_{cm}}$ (m)	247.6719	110.2768	13.1986	4.1976

Medium Noise	Herrick-Gibbs	v-Iteration	p-Iteration	f-g Series
$\overset{*}{\mu}$ (kg*m^3/s^2)	398628.3274	398590.4778	398601.6279	398599.6775
$\overset{*}{\rho_{cm}}$ (m)	154.4270	55.1379	6.5993	4.1998
$\rho_{cm} - \overset{*}{\rho_{cm}}$ (m)	154.4270	55.1379	6.5993	4.1998

Low Noise	Herrick-Gibbs	v-Iteration	p-Iteration	f-g Series
$\overset{*}{\mu}$ (kg*m^3/s^2)	398601.7690	398598.4444	398600.6744	398599.6772
$\overset{*}{\rho_{cm}}$ (m)	7.3809	11.0275	1.3199	4.2015
$\rho_{cm} - \overset{*}{\rho_{cm}}$ (m)	7.3809	11.0275	1.3199	4.2015

Uncorrupted	Herrick-Gibbs	v-Iteration	p-Iteration	f-g Series
$\overset{*}{\mu}$ (kg*m^3/s^2)	398600.4360	398600.4360	398600.4360	398599.2277
$\overset{*}{\rho_{cm}}$ (m)	0.0000	0.0000	0.0000	6.6903
$\rho_{cm} - \overset{*}{\rho_{cm}}$ (m)	0.0000	0.0000	0.0000	6.6903

Table 4. Estimated Gravitational Parameter, Keplerian Satellite ($\rho_{cm} = 0.0$ m).

High Noise	Herrick-Gibbs	v-Iteration	p-Iteration	f-g Series
$\mu^{\cdot}$ (kg* m^3/s^2)	398494.5111	398382.4600	398440.5437	398549.1975
$\rho_{cm}^{\cdot}$ (m)	586.5413	1207.1188	885.4167	283.7115
$\rho_{cm} - \rho_{cm}^{\cdot}$ (m)	322.5487	298.0288	23.6733	625.3785

Medium Noise	Herrick-Gibbs	v-Iteration	p-Iteration	f-g Series
$\mu^{\cdot}$ (kg*m^3/s^2)	398466.3755	398409.3772	398438.4193	398492.3326
$\rho_{cm}^{\cdot}$ (m)	742.3574	1058.0342	897.1851	598.6070
$\rho_{cm} - \rho_{cm}^{\cdot}$ (m)	166.7326	148.9442	11.9049	310.4830

Low Noise	Herrick-Gibbs	v-Iteration	p-Iteration	f-g Series
$\mu^{\cdot}$ (kg*m^3/s^2)	398460.4513	398430.9113	398436.7197	398447.4236
$\rho_{cm}^{\cdot}$ (m)	775.1678	938.7694	906.5999	847.3184
$\rho_{cm} - \rho_{cm}^{\cdot}$ (m)	133.9222	29.6794	2.4901	61.7716

Uncorrupted	Herrick-Gibbs	v-Iteration	p-Iteration	f-g Series
$\mu^{\cdot}$ (kg*m^3/s^2)	398436.5636	398436.2948	398436.2948	398434.4320
$\rho_{cm}^{\cdot}$ (m)	907.4652	908.9536	908.9536	919.2709
$\rho_{cm} - \rho_{cm}^{\cdot}$ (m)	1.6248	0.1364	0.1364	10.1609

Table 5. Estimated Gravitational Parameter, 1 km Tether Length (ρ_{cm} = 909.1 m).

High Noise	Herrick-Gibbs	ν-Iteration	p-Iteration	f-g Series
$\mu^{\cdot}$ (kg* m³/s²)	397007.7825	396977.1387	396962.0155	397075.7446
$\rho_{cm}^{\cdot}$ (m)	8830.0316	9000.2165	9084.1810	8452.7535
$\rho_{cm} - \rho_{cm}^{\cdot}$ (m)	260.0584	89.8735	5.9090	637.3365

Medium Noise	Herrick-Gibbs	ν-Iteration	p-Iteration	f-g Series
$\mu^{\cdot}$ (kg* m³/s²)	396993.5751	396970.2062	396962.6446	397019.2049
$\rho_{cm}^{\cdot}$ (m)	8908.9317	9038.7018	9080.6842	8766.6439
$\rho_{cm} - \rho_{cm}^{\cdot}$ (m)	181.1583	51.3882	9.4058	323.4461

Low Noise	Herrick-Gibbs	ν-Iteration	p-Iteration	f-g Series
$\mu^{\cdot}$ (kg* m³/s²)	396996.9255	396964.6602	396963.1478	396973.7600
$\rho_{cm}^{\cdot}$ (m)	8890.3509	9069.4903	9077.8868	9018.9620
$\rho_{cm} - \rho_{cm}^{\cdot}$ (m)	199.7391	20.5997	12.2032	71.1280

Uncorrupted	Herrick-Gibbs	ν-Iteration	p-Iteration	f-g Series
$\mu^{\cdot}$ (kg* m³/s²)	396963.5127	396963.2737	396963.2737	396962.2296
$\rho_{cm}^{\cdot}$ (m)	9075.8605	9077.1875	9077.1875	9082.9843
$\rho_{cm} - \rho_{cm}^{\cdot}$ (m)	14.2295	12.9025	12.9025	7.1058

Table 6. Estimated Gravitational Parameter, 10 km Tether Length (ρ_{cm} = 9,090.1 m).

High Noise	Herrick-Gibbs	v-Iteration	p-Iteration	f-g Series
μ^{*} $(kg*m^{3}/s^{2})$	382680.5557	382659.5233	382642.0775	382755.0719
ρ_{cm}^{*} (m)	89335.2006	89455.3243	89554.5485	88911.4342
$\rho_{cm} - \rho_{cm}^{*}$ (m)	1573.8905	1453.7667	1354.5425	1997.6568

Medium Noise	Herrick-Gibbs	v-Iteration	p-Iteration	f-g Series
μ^{*} $(kg*m^{3}/s^{2})$	382681.8751	382651.6404	382642.9175	382698.8845
ρ_{cm}^{*} (m)	89327.9438	89500.1539	89549.7663	89231.2086
$\rho_{cm} - \rho_{cm}^{*}$ (m)	1581.1472	1408.9371	1359.3247	1677.8824

Low Noise	Herrick-Gibbs	v-Iteration	p-Iteration	f-g Series
μ^{*} $(kg*m^{3}/s^{2})$	382671.1018	382645.3340	382643.5895	382654.4704
ρ_{cm}^{*} (m)	89389.4132	89536.0181	89545.9406	89484.0034
$\rho_{cm} - \rho_{cm}^{*}$ (m)	1519.6778	1373.0729	1363.1504	1425.0876

Uncorrupted	Herrick-Gibbs	v-Iteration	p-Iteration	f-g Series
μ^{*} $(kg*m^{3}/s^{2})$	382644.0620	382643.7574	382643.7574	382640.8593
ρ_{cm}^{*} (m)	89543.2520	89544.9842	89544.9842	89561.4677
$\rho_{cm} - \rho_{cm}^{*}$ (m)	1365.8390	1364.1068	1364.1068	1347.6233

Table 7. Estimated Gravitational Parameter, 100 km Tether Length (ρ_{cm} = 90,909.1 m).

High Noise	Herrick-Gibbs	ν-Iteration	p-Iteration	f-g Series
$\overset{\bullet}{\mu}$ (kg* m^3/s^2)	398494.3193	398382.1260	398769.3965	398549.2039
$\overset{\bullet}{\rho_{cm}}$ (m)	587.6035	1208.9730	935.3786	283.6765
$\rho_{cm} - \overset{\bullet}{\rho_{cm}}$ (m)	321.4865	299.8830	26.2886	625.4135

Medium Noise	Herrick-Gibbs	ν-Iteration	p-Iteration	f-g Series
$\overset{\bullet}{\mu}$ (kg* m^3/s^2)	398466.4544	398400.8644	398767.6551	398492.3536
$\overset{\bullet}{\rho_{cm}}$ (m)	741.9204	1105.1858	925.7403	598.4909
$\rho_{cm} - \overset{\bullet}{\rho_{cm}}$ (m)	167.1696	196.0958	16.6503	310.5991

Low Noise	Herrick-Gibbs	ν-Iteration	p-Iteration	f-g Series
$\overset{\bullet}{\mu}$ (kg* m^3/s^2)	398460.5385	398415.8552	398766.2619	398447.4565
$\overset{\bullet}{\rho_{cm}}$ (m)	774.6847	1022.1579	918.0296	847.1361
$\rho_{cm} - \overset{\bullet}{\rho_{cm}}$ (m)	134.4053	113.0679	8.9396	61.9539

Uncorrupted	Herrick-Gibbs	ν-Iteration	p-Iteration	f-g Series
μ (kg* m^3/s^2)	398436.6640	398419.6029	398765.9136	398434.4305
$\overset{\bullet}{\rho_{cm}}$ (m)	906.9088	1001.4012	916.1020	919.2787
$\rho_{cm} - \overset{\bullet}{\rho_{cm}}$ (m)	2.1812	92.3112	7.0120	10.1887

Table 8. Estimated Gravitational Parameter, 1 km up Tether Length (ρ_{cm} = 909.1 m).

Analysis of the results in Tables 4-8 shows that the p-iteration technique consistently produced smaller errors that the other POD methods evaluated. As expected, the size of the error generally increased with the length of the tether and the level of observation error. Evaluating the error as a percentage of ρ_{cm}, however, indicates that the error is typically only on the order of 1-2% of ρ_{cm} for all cases studied. By using the p-iteration technique, the determination of whether or not the satellite is part of a TSS can be made in the 200 second observation span required for that method. If a quicker identification is required, either the Herrick-Gibbs method or the f and g series method can be used, however the errors obtained from these methods will be much larger, especially in the cases of Keplerian satellites or short tethers.

CONCLUSIONS

From the results presented above it can be concluded that the while all of the POD methods studied are able to distinguish between a tethered and an untethered satellite, the p-iteration technique clearly produced the most accurate results for the cases studied. However, further studies are needed in order to evaluate the effectiveness of this method on different types of orbits. Specifically, these additional studies should include both circular and elliptical orbits of varying altitudes, orbital inclinations and observation

noise levels in order to determine how well this POD method will perform on a wide range of possible TSS orbits and tracking scenarios.

ACKNOWLEDGEMENTS

REFERENCES

1. Snow, D. E., and Kaya, D. A., "Short Arc Orbit Determination Using Angles-Only Space Based Observations," Paper AAS 92-112, AAS/AIAA Space Flight Mechanics Meeting, Colorado Springs, CL, Feb. 24-26, 1992.

2. Cho, S., Cochran, J. E., Jr., "Identification an Orbit Determination of a Tethered Satellite System," *Advances in the Astronautical Sciences*, Vol. 99, Part 1, pp. 21-34, proceedings of the AAS/AIAA Space Flight Mechanics Meeting, Monterey, CA, Feb. 9-11, 1998.

3. Cochran, J. E., Jr., Cho, S., Lovell, A., and Cicci, D. A., "On the Information Contained in the Motion of One Satellite of a Two-Satellite Tethered System," *A Collection of Technical Papers*, pp. 422-431, proceedings of the AIAA/AAS Astrodynamics Specialist Conference, Boston, MA, Aug. 10-12, 1998.

4. Cho, S., Cochran, J. E., Jr., and Cicci, D. A., "Approximate Solutions for Tethered Satellite Motion," *Advances in the Astronautical Sciences*, Vol. 102, Part 2, pp. 1345-1360, proceedings of the AAS/AIAA Space Flight Mechanics Meeting, Breckenridge, CO, Feb. 7-10, 1999.

5. Cicci, D. A., Lovell, T. A., and Qualls, C., "A Filtering Method for the Identification of a Tethered Satellite," *Advances in the Astronautical Sciences*, Vol. 102, Part 2, pp. 1399-1418, proceedings of the AAS/AIAA Space Flight Mechanics Meeting, Breckenridge, CO, Feb. 7-10, 1999.

6. Cicci, D. A., Qualls, C., and Lovell, T. A., "A Look at Tethered Satellite Identification Using Ridge-Type Estimation Methods," Paper AAS 99-415, AAS/AIAA Space Flight Mechanics Meeting, Girdwood, AK, Aug. 16-19, 1999.

7. Cochran, J. E., Jr., Cho, S., Lovell, A., and Cicci, D. A., "Modeling Tethered Satellite Systems for Detection and Orbit Determination," Paper AAS 99-416, AAS/AIAA Space Flight Mechanics Meeting, Girdwood, AK, Aug. 16-19, 1999.

8. Kessler, S. A., and Cicci, D. A., "Filtering Methods for the Orbit Determination of a Tethered Satellite," *The Journal of Astronautical Sciences*, Vol. 45, No. 3, July-September 1997, pp. 263-278.

9. Hoots, F. R., Rodhrich, R. L., and Szebehely, ·V. G., "Space Shuttle Tethered Satellite Analysis," Directorate of Astrodynamics, Peterson AFB, CO, August 1983.

10. Escobal, P., *Methods of Orbit Determination*, John Wiley & Sons, Inc., New York, NY, 1965.

11. Bate, R. R., Mueller, D. D., and White, J. E., *Fundamentals of Astrodynamics*, Dover Publications, Inc., New York, NY, 1971.

QUICK-LOOK IDENTIFICATION AND ORBIT DETERMINATION OF A TETHERED SATELLITE

D. A. Cicci[1], J. E. Cochran, Jr.[2], C. Qualls[3] and T. A. Lovell[3]

A renewed interest in the deployment of tethered satellites has motivated recent studies addressing the problem of the accurate identification, orbit determination, and motion prediction of a tethered satellite system (TSS). If the motion of a TSS is not analyzed accurately, a tethered satellite could be incorrectly identified as an object on a re-entry trajectory. Classical orbit determination methods do not possess the capabilities to determine whether or not a tracked satellite is part of a TSS. The problem of identification is compounded by the fact that this process must be performed quickly using a short arc of observational data. Once this "quick-look" identification is achieved, it is also important to have the capabilities to precisely determine the orbit of the TSS for future tracking and orbit prediction purposes. This paper presents a three-stage methodology which has been developed to address the accurate identification, orbit determination, and long-term orbit prediction of a TSS. The first stage uses recently developed preliminary orbit determination (POD) methods which have the capability to determine whether an observed satellite is part of a TSS or not using only a few observations. The second stage utilizes ridge-type estimation methods, which have been shown to be capable of obtaining a more accurate state of the observed satellite using a short arc of observational data. The third-stage analysis utilizes an enhanced tether satellite dynamical model suited for the long-term orbit determination and motion prediction. The effectiveness of this proposed three-stage method is demonstrated using both simulated tether satellite data and actual data obtained from the Tether Physics Survivability (TiPS) Experiment.

INTRODUCTION

The possibility of the increased future use of tethered satellites has renewed the interest in the ability to accurately track, identify, and predict the motion of a tethered satellite system (TSS). The inability to accurately determine the motion of such systems may result in the satellite being incorrectly identified as one which is on a re-entry trajectory [1]. This is due to the fact that the force within the tether creates perturbations on the satellite causing it to behave differently from an untethered one [2]. Specifically, if the tethered body occupies a lower orbit than the center-of-mass of the TSS, its velocity will be smaller in magnitude than

[1]Professor, Aerospace Engineering Department, Auburn University; Member, AAS; Associate Fellow, AIAA.
Email: dcicci@eng.auburn.edu. Phone: (334) 844-6820, FAX: (334) 844-6803.
[2]Professor and Head, Aerospace Engineering Department, Auburn University; Fellow, AAS; Associate Fellow, AIAA.
[3]Graduate Student; Aerospace Engineering Department, Auburn University; Student Member, AIAA.

the velocity predicted by Keplerian theory for an untethered satellite. Similarly, if the tethered satellite occupies a higher orbit than the TSS center-of-mass, its velocity will be larger in magnitude than that predicted for an untethered satellite. Subsequent calculation of the tethered satellite's trajectory will be inaccurate since Keplerian theory can no longer describe the perturbed motion resulting from the existence of the tether force.

Classical orbit determination and filtering methods are not capable of determining whether or not a satellite being tracked is part of at TSS. These methods will therefore identify a tracked satellite as if it were an untethered one and subsequently cause errors in the prediction of its trajectory. Since the predicted trajectory may appear to be a re-entry trajectory, the identification of the tracked satellite as part of a TSS must be performed quickly. This need for "quick-look" identification creates a problem which is ill-conditioned due to the short arc of observational data available with which to make such a determination. Furthermore, once it is determined that a satellite is tethered, classical methods are not able to predict its long-term motion, again due to the perturbations created on each member of the TSS by the tether force.

Recent studies have addressed the different aspects of the TSS identification problem. Modified methods for the preliminary orbit determination (POD) of a tethered satellite were presented in [3], while new methods for the quick-look identification and orbit prediction aspects were presented in [4-6]. In addition, filtering techniques which use enhanced dynamical models capable of the long-term motion prediction of a TSS were presented in [7-11]. The feasibility of each of these techniques was demonstrated on a number of TSS scenarios in each particular study.

This paper combines the methods presented in these previous studies in order to formulate a three-stage orbit determination methodology capable of both the quick identification and long-term motion prediction of a TSS. These three stages include the POD (1st Stage), quick-look identification (2nd Stage), and the long-term orbit determination and motion prediction filter (3rd Stage). The performance of this combined filtering methodology is demonstrated on a series of simulated cases with varying TSS geometry and observation noise levels, as well as on real TSS data obtained from the Tether Physics and Survivability Experiment (TiPS) Program [12]. Results of these studies are presented along with several conclusions and recommendations for future research. In addition, the sections below present a brief description of the TSS models used in the filter as well as provide further discussion of the three stages comprising this filtering method.

THREE-STAGE TSS ORBIT DETERMINATION METHOD

The proposed three-stage orbit determination method uses three different TSS dynamical models. A simple dynamical TSS model is used for the POD (1st Stage), while enhanced dynamical models are used for both the quick-look identification (2nd Stage) and long-term orbit determination and motion prediction (3rd Stage). These three models, while related, are each specifically designed for the particular stage in order to give the most accurate results within the observation span being considered. For example, the POD phase

2

is designed to occur using only the first few observations, the quick-look identification phase is designed to be accomplished using up to 15 minutes of observational data, and the long-term orbit determination and motion prediction phase is implemented when a long-arc of observational data, e.g., a half-period or more, is available. Output from each stage of the filter is then used as input into the next stage. A flow chart of the three-stage method is shown in Figure 1, and a general description of each stage is provided in the paragraphs that follow. Full descriptions of the model details are available from the cited reference.
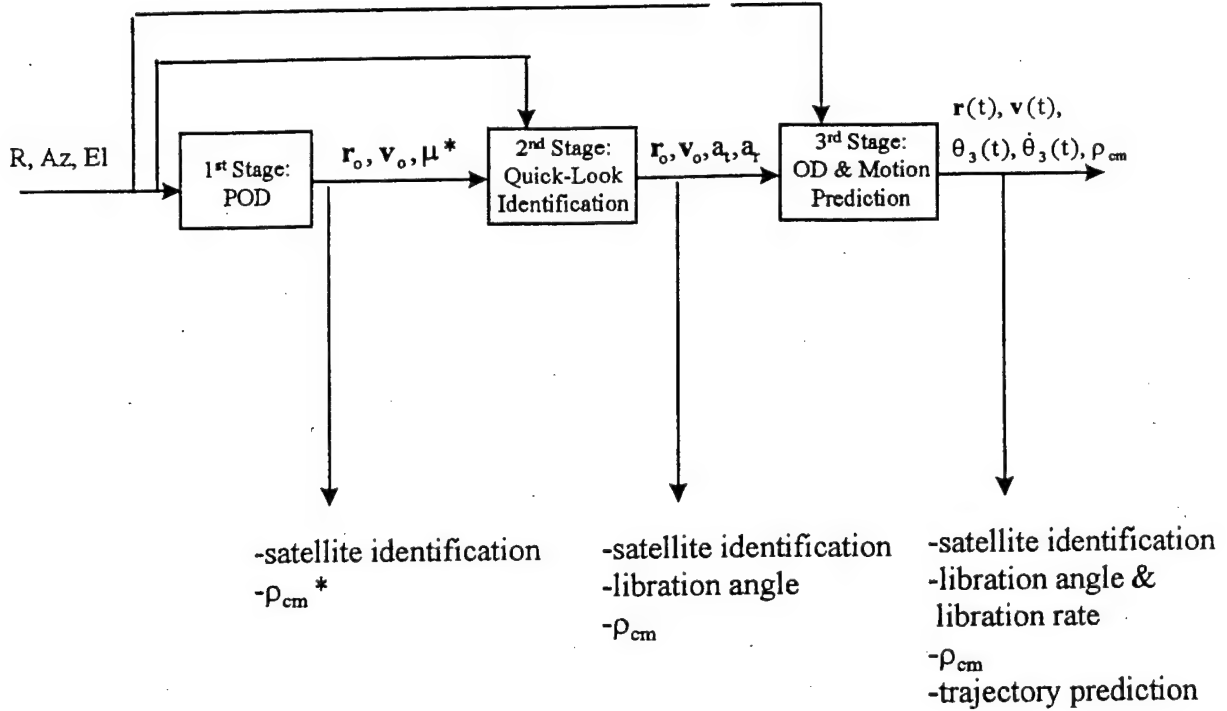
Figure 1. Three-Stage TSS Identification and Orbit Determination Method

1st Stage - Preliminary Orbit Determination

The simplified, two-satellite TSS model used in this stage is shown in Figure 2 and described in [3]. In this model the 'daughter' satellite, m, is connected by a tether to the 'parent' satellite, m_p, and both are considered to be point masses. In this study, it will generally be assumed that the daughter satellite is the one whose motion is being observed. The parent and daughter satellites are connected by a massless tether and the effective tether force acting on the daughter satellite is indicated by the vector **F**. The dynamical model for this TSS considers only two-body forces and the tether force to be acting on each satellite. Modeling librational motion of the TSS is not possible in this POD analysis.

3
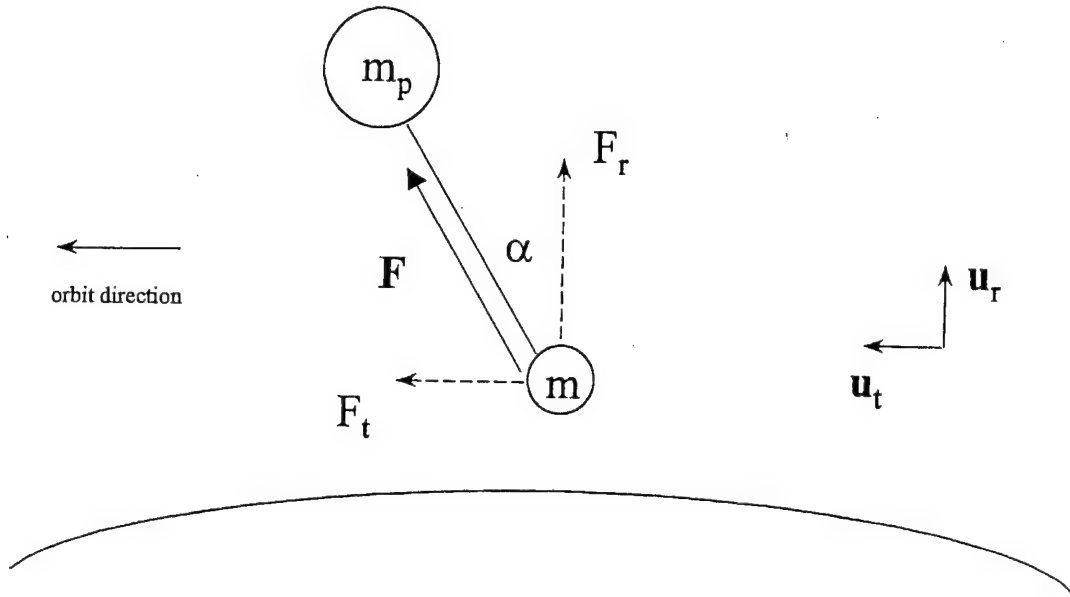
Figure 2. TSS Model

The tether force acting on the daughter satellite can be resolved into radial and tangential force components, F_r and F_t, respectively, as indicated in Figure 2. These force components will alter the acceleration on the satellite and subsequently change its velocity. The radial force component will create a radial acceleration, a_r, acting on the daughter satellite and tend to reduce the daughter's velocity if it is in a lower orbit than the parent satellite and increase the daughter's velocity if it is in a higher orbit than the parent. Similarly, the tangential force component of the tether force will create a tangential acceleration, a_t, acting on the daughter which will tend to decrease the daughter's velocity if it leads the parent and increase the daughter's velocity if it trails the parent. The opposite of these dynamical characteristics will be true if the motion of the parent mass is being observed.

Figure 2 also illustrates the libration angle, α, which is defined as the angle between the tether and the local vertical. The libration angle shown is positive and less than 90°, with the parent mass above the daughter mass and 'leading' the daughter mass slightly in the direction of orbital motion. In addition, Figure 2 shows the radial and tangential directional unit vectors, with radial defined as positive from the center of the Earth toward the daughter mass, and tangential defined as positive in the direction of orbital motion. The instantaneous value of α will therefore indicate the signs of both F_r and F_t.

The POD of a tethered satellite can provide information in determining the radial acceleration on the observed satellite created by the tether force. Specifically, a modified gravitational parameter, μ^*, can be calculated during the POD process, which represents a combination of both the standard gravitational parameter, μ, and the radial acceleration component provided by the tether force. The relationship between these parameters is presented in [3] as

4

$$\mu^* = \mu - a_r r^2 \qquad (1)$$

where r is the distance from the Earth's center to the daughter satellite.

Once μ^* is obtained from the POD process, it can be used to approximate the distance that the daughter satellite is located above or below the center-of-mass of the TSS. This distance, measured along the tether length, is designated ρ_{cm}. In cases where libration of the TSS is present, this quantity will represent the projection of ρ_{cm} in the radial direction and is designated ρ_{cm}^*. The expression for this approximation during the POD process was presented in [3] as

$$\rho_{cm}^* = [(\mu - \mu^*) / (2\mu + \mu^*)] \, r \qquad (2)$$

This quantity will be positive if the daughter is below the parent, i.e., $\mu > \mu^*$, and negative if the daughter is above the parent, i.e., $\mu^* > \mu$. A negative value of ρ_{cm} will therefore indicate a TSS orientation such that the satellite being observed is above (or up) from the parent satellite. In addition, the value of ρ_{cm}, and ρ_{cm}^* in the case where no libration is present, i.e., $\alpha = 0°$, will approach the actual tether length as the ratio of masses, m/m_p, approaches zero.

Four classical POD methods have been modified to include capabilities to determine μ^* for a TSS as described in [3]. These classical methods include the v-iteration, p-iteration, 9th order f and g series, and the closed-form f and g series techniques. Each modified method uses only a few observations of the daughter satellite in order to determine its components of position and velocity along with the value of μ^*. The choice of which particular method to use in the POD process is automatically determined in order to achieve the most accurate results. The 9th order f and g series is initially used to calculate an estimate of ρ_{cm}^*, which, along with the value of Δt, is used to select the appropriate POD method.

Since only a few observations are used in the POD process, the value of μ^* can be used to quickly determine if this observed satellite is part of a TSS. Output from this 1st Stage POD process, in the form of position and velocity components and a_r, which is obtained from μ^* using Eq. (1), is then used as input into the 2nd Stage Quick-Look Identification phase. Since no information can be obtained regarding a_t during the 1st Stage analysis, a value of zero is assumed for input into the 2nd Stage.

2nd Stage - Quick-Look Identification

An enhanced dynamical model is used for the 2nd Stage analysis and is presented in detail in [5]. This model considers an inextensible tether and has the capabilities to include the effects of in-plane libration in the TSS dynamics. In order to include these effects, however, the values of the libration angle, both masses, and the tether length must be available. In most cases, however, this information is unknown. In such cases a default model will be used which only considers two-body point mass effects as was done in the POD model.

In order to determine the dynamical characteristics of the TSS being observed, a batch-type filter is used to estimate the daughter satellite's state vector as described in [5]. This state vector includes the position and velocity components of the satellite as well as the acceleration components provided by the tether force, a_r and a_t, as shown in Figure 2. For the short observation arcs used in this stage, a_r and a_t are both assumed to not change significantly and are therefore modeled as constants. Inclusion of these tether specific parameters will allow the filter to distinguish between a tethered and untethered satellite. If these acceleration components are determined to be zero, no tether force is present and the satellite can be considered to be an untethered one. Nonzero acceleration terms will indicate that the satellite is indeed tethered. The values of these acceleration components can then be used to determine the libration angle, α, of the TSS.

In order to perform the 2nd Stage process quickly and be able to identify the observed satellite in as short of a data arc as possible, ridge-type estimation methods have been incorporated into the filter. These methods achieve increased accuracy in ill-conditioned problems where only short data arcs are available, as demonstrated in [6], through the addition of biasing parameters into the filtering process which improve the conditioning of the problem. The particular form of the ridge-type estimator used in this 2nd Stage consists of a combination of single and multiple biasing parameters for better solution stability. A thorough discussion of ridge-type estimation methods is presented in [12].

Several determinations can be made from the results obtained from this filter. These include:

1. If both a_r and a_t are equal to zero, it can be assumed that the satellite is not part of a tethered system and its motion can be analyzed using standard techniques.

2. If a_r and a_t are both nonzero:

(a) The libration angle, α, can be determined from

$$\alpha = \tan^{-1} (a_t / a_r) \tag{3}$$

where the signs of a_r and a_t will determine the appropriate quadrant for α.

(b) The magnitude of the tether force (per unit mass) can be calculated by

$$F_T/m = [a_r^2 + a_t^2]^{1/2} \tag{4}$$

(c) Using the value of a_r, Eqs. (1)-(2) can be used to approximate the radial projection of the tether length, to the center-of-mass of the TSS, ρ_{cm}^*. This approximation can then be used to calculate the tether length to the TSS center-of-mass, ρ_{cm}, using the expression

$$\rho_{cm} = \rho_{cm}^* / \cos \alpha \tag{5}$$

6

3. If a_t is equal to zero but a_r is not, the satellite will be tethered and the orientation of the system will be vertical, i.e., $\alpha = 0°$ if $a_r > 0$, or $180°$ if $a_r < 0$.

4. If a_r is equal to zero but a_t is not, the satellite will be tethered and the orientation of the system will be horizontal, i.e., $\alpha = 90°$ if $a_t > 0$, or $270°$ if $a_t < 0$.

Output from this 2nd Stage Quick-Look Identification process in the form of the initial position and velocity components, a_r, and a_t is then used as input into the 3rd Stage Long-Term Orbit Determination and Motion Prediction phase of the analysis.

3rd Stage - Long-Term Orbit Determination and Motion Prediction

Once accurate information on the initial conditions and tether specific parameters is obtained from the 2nd Stage filter, a long-term orbit determination filter using an enhanced dynamical model for a more exact solution is used to predict the future motion of the TSS. The enhanced model is based on the model presented in [7] and [8] and accounts for both the in-plane libration and libration-rate. In addition, the effects of the non-spherical Earth have also recently been added to the model.

This 3rd Stage process is designed to use a substantial set of observational data encompassing at least one-half of an orbital period or longer. As a result, a standard minimum variance batch filter can be used without the need to incorporate ridge-type estimation methods as was done in the 2nd Stage process described above. The state vector for this filter consists of the initial position and velocity components, the in-plane libration angle, the in-plane libration-rate, and $\rho_{cm}{}^*$. Once these accurate estimates of the initial conditions are obtained in the filtering process, these quantities can subsequently be used in the dynamical model to predict the long-term motion beyond the observation arcs which are available.

TEST CASES

In order to demonstrate the feasibility of this Three-Stage TSS Identification and Orbit Determination Method, test cases using both simulated data and data from an actual TSS were evaluated. The TSS data used for this portion of the analysis was obtained from the Tether Physics and Survivability Satellite (TiPS) Experiment [13].

For the test cases using simulated data, the performance of the method was evaluated for a total of 108 TSS scenarios involving differing tether lengths, orientations, observation noise levels, and observation arcs. The value of 10 for the mass ratio m_p/m was used and measurements were provided in the form of range, azimuth angle, and elevation angle for all cases studied. The particular test case combinations which were evaluated are shown in Table 1 below.

7

Table 1. Simulated Data Test Cases

Tether Lengths (ρ)	0 km, 1 km, 10 km, 50 km, 1 km up
Observation Error (σ), Range/Angles	5 m/0.002° (low), 25 m/0.01°(med), 50 m/0.02° (high)
In-Plane Libration Angle (α)	0°, 5°, 10°
Observation Arc (Δt)	5 min, 10 min, 15 min

The TiPS Experiment is described in [13] and consists of two end masses having the mass ratio m_p/m of 3.65, which are connected by a 4 km tether weighing 12.0 lbs. This geometry results in a value of 3024 m for ρ_{cm}. TiPS was launched in June 1996 into an orbit having an altitude of 1022 km.

Unfortunately, only a limited amount of TiPS data was available and only four different data sets could be analyzed. The particular cases evaluated consisted of range, azimuth, and elevation angles which were recorded over various observation spans obtained from different tracking stations having differing measurement accuracies. All data used was recorded in mid-to-late 1996. The particular TiPS data test cases evaluated are summarized in Table 2 below.

Table 2. TiPS Data Test Cases

Case	Tracking Stations	Mass Observed	Observation Span	Number of Observations
1	A, B	lower	350 sec	36
2	C	lower	410 sec	42
3	C	upper	410 sec	42
4	D	lower	626 sec	72

8

RESULTS

Simulated Data Test Cases

The results presented provided in Tables 3-15 below include the values of $\rho_{cm}{}^*$ for the 1st Stage and the values of Root Mean Square (RMS) error and ρ_{cm} for the 2nd Stage and 3rd Stage processes. The RMS calculations were normalized using the known observation error statistics so that all values approximately equal to 1.0 indicate a good solution fit with the data. The values of $\rho_{cm}{}^*$ and ρ_{cm} reported provide an indication of the overall solution accuracy as well as the ability of each particular phase to identify whether an observed satellite is part of a TSS.

The 1st Stage - POD portion of the filter requires three position vectors which are each 60 to 80 seconds apart in order to obtain the best results. A time span smaller than this is not recommended. As can be seen from the results, there is significant error present in the calculation of $\rho_{cm}{}^*$ and definitive identification is generally not possible. However, the results obtained during the POD do provide a sufficiently accurate set of initial conditions input into the 2nd Stage - Quick-Look Identification phase which can be used to obtain a substantially more accurate solution.

The 2nd Stage of the filter was tested using three different time spans: 5, 10, and 15 minutes of observational data. The results show that the filter produces the most accurate results when using 10 or 15 minutes of data. For the shorter tether lengths a 10 minute time span produces the best result while the 10 km and 50 km tethers require 15 minutes of data when libration is included. The filter is able to produce accurate results regardless of the observation error level or the amount of libration present. Time spans of 5 minutes or less are not recommended due to sufficiently inaccurate results. If at least 10 minutes of data is processed, identification of the tracked satellite as to whether or not it is part of a TSS can almost certainly be made, as can be seen by comparing the calculated value of ρ_{cm} with the actual value. In addition, the RMS of the solution indicates the fit to the observational data is quite good for this phase and provides a substantially improved set of initial conditions for input into the 3rd Stage - Long-Term Orbit Determination and Motion Prediction.

The 3rd Stage of the filter performs a long-term orbit determination when data beyond the 10-15 minutes used in the 2nd Stage is available. To demonstrate the effectiveness of this stage, data arcs equal to ½ the orbital period and a full orbital period are processed. Results show that, if the initial conditions used were obtained from 10-15 minutes of data during 2nd Stage processing, solution accuracies are quite good for all noise levels and libration angles considered. The state vector, ρ_{cm}, and the libration parameters are accurately determined and the resulting RMS of the fit is quite close to 1.0. The accurate prediction of the future motion of the TSS can subsequently be achieved.

9

Table 3. Simulated Data: No tether, $\rho_{cm} = 0$ m

| | POD | | Quick-Look | | Long-Term | | | |
| | | | | | ½ period | | 1 period | |
	$\rho_{cm}{}^*$(m)	Δt	RMS	ρ_{cm}(m)	RMS	ρ_{cm}(m)	RMS	ρ_{cm}(m)
σ = low:	2856	5 min:	1.021	-116	0.987	19	0.989	0
		10 min:	1.025	310	0.986	16	0.989	2
		15 min:	1.006	152	0.986	16	0.989	2
σ = med:	15679	5 min:	1.042	4246	1.027	5	1.026	-5
		10 min:	1.021	624	1.027	122	1.026	3
		15 min:	1.011	708	1.027	60	1.027	1
σ = high:	46398	5 min:	1.033	4613	1.040	18	0.999	18
		10 min:	1.021	1400	1.010	18	0.999	18
		15 min:	1.009	1493	1.042	18	0.999	18

Table 4. Simulated Data: $\rho = 1$ km ($\rho_{cm} = 909$ m), σ = low

| | POD | | Quick-Look | | Long-Term | | | |
| | | | | | ½ period | | 1 period | |
α	$\rho_{cm}{}^*$(m)	Δt	RMS	ρ_{cm}(m)	RMS	ρ_{cm}(m)	RMS	ρ_{cm}(m)
0°	-4487	5 min:	1.022	277	2.196	415	14.300	590
		10 min:	1.022	991	0.986	925	0.989	910
		15 min:	1.007	1077	0.986	925	0.989	910
5°	-4470	5 min:	1.022	230	2.204	472	16.130	518
		10 min:	1.022	943	0.986	925	0.989	910
		15 min:	1.008	1028	0.986	925	0.989	910
10°	-7793	5 min:	1.021	260	0.986	925	0.989	910
		10 min:	1.021	956	0.986	925	0.989	910
		15 min:	1.010	979	0.986	925	0.989	910

Table 5. Simulated Data: $\rho = 1$ km ($\rho_{cm} = 909$ m), $\sigma = $ med

| | POD | | Quick-Look | | Long-Term | | | |
| | | | | | ½ period | | 1 period | |
$\underline{\alpha}$	$\underline{\rho_{cm}*(m)}$	$\underline{\Delta t}$	$\underline{RMS}$	$\rho_{cm}(m)$	$\underline{RMS}$	$\rho_{cm}(m)$	$\underline{RMS}$	$\rho_{cm}(m)$
0°	19974	5 min:	1.020	-1318	1.146	78	3.736	53
		10 min:	1.021	1001	1.084	826	1.027	904
		15 min:	1.008	1521	1.027	821	1.027	904
5°	19999	5 min:	1.020	-1364	1.402	7	2.143	373
		10 min:	1.021	950	1.027	822	1.027	905
		15 min:	1.008	1472	1.027	822	1.027	905
10°	-78347	5 min:	1.021	3381	1.517	-7	4.114	32
		10 min:	1.021	1236	1.027	827	1.027	905
		15 min:	1.010	1416	1.027	827	1.027	905

Table 6. Simulated Data: $\rho = 1$ km ($\rho_{cm} = 909$ m), $\sigma = $ high

| | POD | | Quick-Look | | Long-Term | | | |
| | | | | | ½ period | | 1 period | |
$\underline{\alpha}$	$\underline{\rho_{cm}*(m)}$	$\underline{\Delta t}$	$\underline{RMS}$	$\rho_{cm}(m)$	$\underline{RMS}$	$\rho_{cm}(m)$	$\underline{RMS}$	$\rho_{cm}(m)$
0°	-4371	5 min:	1.015	-892	1.039	87	2.086	-47
		10 min:	1.023	840	1.010	854	1.000	928
		15 min:	1.006	1003	1.010	855	1.000	928
5°	50869	5 min:	1.020	-1432	1.027	822	1.027	905
		10 min:	1.021	1096	1.043	594	1.473	-802
		15 min:	1.009	1950	1.010	847	1.000	928
10°	-146423	5 min:	1.021	-8401	1.010	843	1.000	927
		10 min:	1.022	1509	1.010	843	1.000	927
		15 min:	1.011	2196	1.010	843	1.000	927

11

Table 7. Simulated Data: $\rho = 10$ km ($\rho_{cm} = 9091$ m), $\sigma =$ low

| | POD | | Quick-Look | | Long-Term | | | |
| | | | | | ½ period | | 1 period | |
$\underline{\alpha}$	$\underline{\rho_{cm}*(m)}$	$\underline{\Delta t}$	RMS	$\rho_{cm}(m)$	RMS	$\rho_{cm}(m)$	RMS	$\rho_{cm}(m)$
0°	3640	5 min:	1.022	8423	0.986	9107	0.989	9092
		10 min:	1.025	9192	0.986	9107	0.989	9092
		15 min:	1.010	9339	0.986	9107	0.989	9092
5°	3834	5 min:	1.021	7948	0.986	9107	0.989	9057
		10 min:	1.025	8714	0.986	9107	0.989	9092
		15 min:	1.065	8845	0.986	9107	0.989	9092
10°	3807	5 min:	1.021	7444	0.986	9107	0.989	9092
		10 min:	1.195	8406	0.986	9107	0.989	9092
		15 min:	1.028	8267	0.986	9107	0.989	9092

Table 8. Simulated Data: $\rho = 10$ km ($\rho_{cm} = 9091$ m), $\sigma =$ med

| | POD | | Quick-Look | | Long-Term | | | |
| | | | | | ½ period | | 1 period | |
$\underline{\alpha}$	$\underline{\rho_{cm}*(m)}$	$\underline{\Delta t}$	RMS	$\rho_{cm}(m)$	RMS	$\rho_{cm}(m)$	RMS	$\rho_{cm}(m)$
0°	28156	5 min:	1.020	6801	1.027	9001	1.027	9086
		10 min:	1.022	9179	1.027	9001	1.027	9086
		15 min:	1.008	9787	1.027	9001	1.027	9086
5°	28429	5 min:	1.020	6341	1.027	9003	1.027	9087
		10 min:	1.021	8708	1.027	9003	1.027	9087
		15 min:	1.010	9294	1.027	9003	1.027	9087
10°	28473	5 min:	1.020	5842	1.027	9007	1.027	9087
		10 min:	1.022	8274	1.027	9007	1.027	9087
		15 min:	1.016	8855	1.027	9003	1.027	9087

Table 9. Simulated Data: $\rho = 10$ km ($\rho_{cm} = 9091$ m), $\sigma = $ high

$\underline{\alpha}$	POD $\rho_{cm}*$(m)	$\underline{\Delta t}$	Quick-Look RMS	ρ_{cm}(m)	Long-Term ½ period RMS	ρ_{cm}(m)	1 period RMS	ρ_{cm}(m)
0°	3738	5 min:	1.015	7211	1.010	9036	1.000	9110
		10 min:	1.023	8992	1.010	9036	1.000	9110
		15 min:	1.006	9225	1.010	9036	1.000	9110
5°	59491	5 min:	1.020	63٦٦	1.010	9030	1.000	9109
		10 min:	1.021	8888	1.010	9031	1.000	9109
		15 min:	1.010	9791	1.010	9032	1.000	9109
10°	59655	5 min:	1.020	5811	1.010	9026	1.000	9109
		10 min:	1.021	8450	1.010	9027	1.000	9109
		15 min:	1.011	9355	1.010	9027	1.000	9108

Table 10. Simulated Data: $\rho = 50$ km ($\rho_{cm} = 45455$ m), $\sigma = $ low

$\underline{\alpha}$	POD $\rho_{cm}*$(m)	$\underline{\Delta t}$	Quick-Look RMS	ρ_{cm}(m)	Long-Term ½ period RMS	ρ_{cm}(m)	1 period RMS	ρ_{cm}(m)
0°	39754	5 min:	1.022	44523	0.986	45471	0.989	45455
		10 min:	1.027	45385	0.986	45471	0.989	45455
		15 min:	1.023	45659	0.986	45471	0.989	45455
5°	41338	5 min:	1.017	42148	0.986	45471	0.989	45455
		10 min:	1.035	42994	0.986	45471	0.989	45455
		15 min:	1.844	43146	0.986	45471	0.989	45455
10°	41783	5 min:	1.016	39625	0.986	45471	0.989	45455
		10 min:	1.105	40795	0.986	45471	0.989	45455
		15 min:	3.202	40910	0.986	45471	0.989	45455

Table 11. Simulated Data: $\rho = 50$ km ($\rho_{cm} = 45455$ m), $\sigma =$ med

| | POD | | Quick-Look | | Long-Term | | | |
| | | | | | ½ period | | 1 period | |
α	$\rho_{cm}{*}(m)$	Δt	RMS	$\rho_{cm}(m)$	RMS	$\rho_{cm}(m)$	RMS	$\rho_{cm}(m)$
0°	64509	5 min:	1.021	42789	1.027	45365	1.027	45451
		10 min:	1.022	45482	1.027	45365	1.027	45451
		15 min:	1.008	46154	1.027	45365	1.027	45451
5°	66681	5 min:	1.019	40517	1.027	45367	1.027	45451
		10 min:	1.021	43138	1.027	45367	1.027	45451
		15 min:	1.054	43703	1.027	45367	1.027	45451
10°	67694	5 min:	1.019	38056	1.027	45370	1.027	45451
		10 min:	1.022	40931	1.027	45370	1.027	45451
		15 min:	1.178	41358	1.027	45370	1.027	45451

Table 12. Simulated Data: $\rho = 50$ km ($\rho_{cm} = 45455$ m), $\sigma =$ high

| | POD | | Quick-Look | | Long-Term | | | |
| | | | | | ½ period | | 1 period | |
α	$\rho_{cm}{*}(m)$	Δt	RMS	$\rho_{cm}(m)$	RMS	$\rho_{cm}(m)$	RMS	$\rho_{cm}(m)$
0°	95770	5 min:	1.020	42834	1.010	45382	1.000	45471
		10 min:	1.022	45584	1.010	45383	1.000	45471
		15 min:	1.009	46644	1.010	45383	1.000	45471
5°	99001	5 min:	1.019	40629	1.010	45377	1.000	45470
		10 min:	1.021	43221	1.010	45377	1.000	45470
		15 min:	1.022	44137	1.010	45377	1.000	45470
10°	101085	5 min:	1.019	38232	1.010	45374	0.999	45470
		10 min:	1.022	41013	1.010	45374	0.999	45469
		15 min:	1.058	41908	1.010	45374	0.999	45469

14

Table 13. Simulated Data: $\rho = 1$ km up ($\rho_{cm} = -909$ m), $\sigma = $ low

| | POD | | Quick-Look | | Long-Term | | | |
| | | | | | ½ period | | 1 period | |
α	$\rho_{cm}*$(m)	Δt	RMS	ρ_{cm}(m)	RMS	ρ_{cm}(m)	RMS	ρ_{cm}(m)
0°	-6290	5 min:	1.022	-1532	0.986	-893	0.989	-908
		10 min:	1.022	-833	0.986	-893	0.989	-908
		15 min:	1.006	-761	0.986	-893	0.989	-908
5°	-6307	5 min:	1.022	-1484	0.986	-893	0.989	-908
		10 min:	1.022	-785	0.986	-893	0.989	-908
		15 min:	1.006	-712	0.986	-893	0.989	-908
10°	-6302	5 min:	1.022	-1532	0.986	-893	0.989	-908
		10 min:	1.022	-740	0.986	-893	0.989	-908
		15 min:	1.007	-668	0.986	-893	0.989	-908

Table 14. Simulated Data: $\rho = 1$ km up ($\rho_{cm} = -909$ m), $\sigma = $ med

| | POD | | Quick-Look | | Long-Term | | | |
| | | | | | ½ period | | 1 period | |
α	$\rho_{cm}*$(m)	Δt	RMS	ρ_{cm}(m)	RMS	ρ_{cm}(m)	RMS	ρ_{cm}(m)
0°	18159	5 min:	1.020	-3121	1.027	-998	1.027	-914
		10 min:	1.021	-809	1.027	-998	1.027	-914
		15 min:	1.008	-318	1.110	-44C	1.027	-914
5°	18135	5 min:	1.020	-3074	1.027	-997	1.027	-914
		10 min:	1.021	-757	1.027	-997	1.027	-914
		15 min:	1.009	-269	1.112	-493	1.027	-914
10°	18134	5 min:	1.020	-3025	1.027	-995	1.027	-914
		10 min:	1.021	-709	1.027	-994	1.027	-914
		15 min:	1.008	225	1.010	-964	0.999	-891

Table 15. Simulated Data: $\rho = 1$ km up ($\rho_{cm} = -909$ m), $\sigma = $ high

	POD		Quick-Look		Long-Term ½ period		Long-Term 1 period	
α	$\rho_{cm}\!*(m)$	Δt	RMS	$\rho_{cm}(m)$	RMS	$\rho_{cm}(m)$	RMS	$\rho_{cm}(m)$
0°	49000	5 min:	1.020	-3194	1.010	-957	0.999	-890
		10 min:	1.021	-683	1.010	-957	0.999	-890
		15 min:	1.009	-155	1.010	-957	0.999	-890
5°	48965	5 min:	1.020	-3149	1.010	-961	0.999	-890
		10 min:	1.021	-637	1.010	-959	0.999	-890
		15 min:	1.009	203	1.031	-453	1.820	-156
10°	48953	5 min:	1.020	-3100	1.010	-964	0.999	-891
		10 min:	1.021	-593	1.010	-962	0.999	-891
		15 min:	1.008	246	1.070	5	1.109	352

TiPS Data Test Cases

Results of the analysis of the limited amount of TiPS data available are provided in Table 16 below and the results are encouraging. While the POD process did not provide accurate results for $\rho_{cm}\!*$, the Quick-Look results were reasonably accurate and could be used to identify whether the tracked satellite was part of a TSS. The inaccuracies present could well be caused by erroneous data or data which were tagged as being obtained from one satellite when the actual measurement was obtained from the other satellite, which is a common problem among TiPS data sets. Case (4) was the only case which consisted of at least 10 minutes of data, which could also contribute to errors in the solutions for Cases (1)-(3).

The Long-Term Orbit Determination results also shown in Table 16 contain substantial error in Cases (1)-(3) but showed improvement over the Quick-Look solution for Case (4). This is likely due to the longer data arc available for this case. However, these results still contain substantial error in the attempt at accurate orbit determination, thereby demonstrating that a significantly longer arc of data is required to achieve such accuracy.

The low values of the RMS results also presented below (as compared to 1.0) likely indicate that the observations used in the estimation process were of a higher accuracy than the nominal tracking station statistics would indicate.

16

Table 16. TiPS Data: $\rho = 4$ km ($\rho_{cm} = 3024$ m)

Case	POD $\rho_{cm}*(m)$	Δt	Quick-Look RMS	$\rho_{cm}(m)$	Long-Term (through Δt) RMS	$\rho_{cm}(m)$
1	19855	350 sec:	0.403	1075	0.438	24
2	33987	410 sec:	0.200	2228	0.163	-31
3	-25054	410 sec:	0.167	3619	0.178	-24

(upper mass observed: $\rho_{cm} = -3024$ m)

Case	POD $\rho_{cm}*(m)$	Δt	Quick-Look RMS	$\rho_{cm}(m)$	Long-Term (through Δt) RMS	$\rho_{cm}(m)$
4	-4395	626 sec:	4.210	7746	2.375	1979

CONCLUSIONS AND RECOMMENDATIONS

Based on the results obtained in this and previous studies, the three-stage orbit determination method presented in this paper can be used for the POD, quick-look identification, and long-term orbit determination and motion prediction of a TSS. While the best results can certainly be obtained using the most accurate data available, several guidelines can be recommended for the use of this proposed methodology. These guidelines are:

(a) Observations used in the 1st Stage POD process should be taken 60-80 seconds apart.

(b) Observations used in the 2nd Stage Quick-Look Identification process should consist of 10-15 minutes of data taken as often as possible within this time span.

(c) Once the satellite has been identified as being part of a TSS in the 2nd Stage process, longer arcs of data on the order of ½ of an orbital period or more should be used to determine the TSS orbit and generate an accurate prediction of the long-term TSS motion.

While the results presented are very encouraging, additional work is clearly needed in order to verify, test, and develop the techniques presented in this study to achieve a software package which can be operationally useful. Recommendations for future work will therefore include:

(1) extensive testing of the dynamical models and software algorithms which have been developed, i.e., perform parametric studies to quantify model performance in an environment of limited and/or noisy data;

17

(2) investigate the effects of the use of range-rate data on filter/model performance, and investigate the effects of the use of combined data from multiple ground sensors, i.e., stereo viewing, on filter/model performance;

(3) combine the POD, Quick-Look Identification, and Long-Term Orbit Determination and Motion Prediction algorithms to achieve a single, stand-alone, program;

(4) enhance the existing dynamical models to include the incorporation of additional dynamical characteristics, such as massive tethers, out-of-plane libration and libration-rate, etc., into the dynamical and filter models; and

(5) investigate and develop of additional analysis methods for the detection of configuration changes in a TSS.

ACKNOWLEDGMENT

REFERENCES

1. Asher, T. A., D. G. Boden, and R. J. Tegtmeyer, "Tethered satellites: The orbit determination problem and Missile Early Warning Systems,"AIAA PAPER 88-4284, *AIAA/AAS Astrodynamics Conference*, Minneapolis, MN, August 15-17, 1988.

2. Hoots, F. R., Roehrich, R. L., and Szebehely, V. G., "Space Shuttle Tethered Satellite Analysis," Directorate of Astrodynamics, Peterson AFB, CO, August 1983.

3. Qualls, C., and Cicci, D. A. "Preliminary Orbit Determination of a Tethered Satellite," Paper AAS 00-191, presented at the AAS/AIAA Astrodynamics Specialist Conference, Clearwater, FL, Jan. 23-26, 2000.

4. Kessler, S. A., and Cicci, D. A., "Filtering Methods for the Orbit Determination of a Tethered Satellite," *The Journal of the Astronautical Sciences*, Vol. 45, No. 3, July-September 1997, pp. 263-278.

5. Cicci, D. A., Lovell, T. A., and Qualls, C., "A Method for the Identification of a Tethered Satellite," Paper AAS 99-196, presented at the AAS/AIAA Space Flight Mechanics Meeting, Breckenridge, CO, Feb. 7-10, 1999.

6. Cicci, D. A., Qualls, C., and Lovell, T. A., "A Look at Tethered Satellite Identification Using Ridge-Type Estimation Methods," Paper AAS 99-415, presented at the AAS/AIAA Astrodynamics Specialist Conference, Girdwood, AK, Aug. 16-19, 1999.

18

7. Cochran, J. E., Jr., Cho, S., Cheng, Y-M, and Cicci, D. A., "Dynamics and Orbit Determination of Tethered Satellite Systems," *The Journal of the Astronautical Sciences*, Vol. 46, No. 2, pp. 177-194, April-June 1998.

8. Cho, S., Cochran, J. E., Jr., and Cicci, D. A., "Identification and Orbit Determination of Tethered Satellite System," Paper AAS 98-101, presented at the AAS/AIAA Space Flight Mechanics Meeting, Monterey, CA, Feb. 9-11, 1998.

9. Cho, S., Cochran, J. E., Jr., and Cicci, D. A., "Approximate Solutions for Tethered Satellite Motion," Paper AAS 99-193, presented at the AAS/AIAA Space Flight Mechanics Meeting, Breckenridge, CO, Feb. 7-10, 1999.

10. Cho, S., Cochran, J. E., Jr., and Cicci, D. A., "Modeling Tethered Satellite Systems for Detection and Orbit Determination," Paper AAS 99-416, presented at the AAS/AIAA Astrodynamics Specialist Conference, Girdwood, AK, Aug. 16-19, 1999.

11. Cochran, J. E., Jr., Cho, S., Lovell, T. A., and Cicci, D. A., "Evaluation of the Information Contained in the Motion of One Satellite of a Two-Satellite Tethered System," Paper AIAA 98-4555, presented at the AIAA/AAS Astrodynamics Specialist Conference, Boston, MA, Aug. 10-12, 1998.

12. Cicci, D. A., and Tapley, B. D., "Optimal Solutions of Unobservable Orbit Determination Problems," *Celestial Mechanics*, 44, pp. 339-363, December 1988.

13. "TiPS: Tether Physics and Survivability Satellite Experiment" web page, Naval Center for Space Technology, http://hyperspace.nrl.navy.mil/TiPS/data.html.

ON THE INFORMATION CONTAINED IN THE MOTION OF ONE
SATELLITE OF A TWO-SATELLITE TETHERED SYSTEM

J. E. Cochran*, Jr., S. Cho[†], A. Lovell[†], and D. A. Cicci[‡]
Auburn University, Alabama 36849

ABSTRACT

This paper addresses the problem of characterizing the information available in observations of one of the satellites of a two-satellite tethered system. Generally, both satellites in a two-satellite tethered system are observed because it is known a priori that the two satellites are tethered together. However, in some cases, the fact that an observed satellite is a member of a tethered system may not be known a priori. In such cases, conventional orbit determination and tracking methods may predict motion of the observed satellite that differs significantly from its actual motion. Here, we use mathematical models of a two-satellite tethered system to study the characteristics of the information contained in observations of one of the satellites as a prelude to using such information to determine the motion of the system.

INTRODUCTION

Tethered satellite systems have been advocated[1] for over 100 years, studied[2,3] over two decades, and a good many tethered systems have been constructed and flown. Numerous uses for tethered systems have been identified. One is the generation of electrical power using a conducting tether that interacts with the Earth's magnetic field. Another is the disposal of waste from an orbiting space station by lowering a capsule into the outer fringes of the Earth's atmosphere, cutting the tether and allowing it to reenter the Earth's atmosphere.

* Professor and Head, Department of Aerospace Engineering, Associate Fellow

† Graduate Research Assistant, Department of Aerospace Engineering, Student Member

‡ Associate Professor, Department of Aerospace Engineering, Associate Fellow

Mathematical interest in tethered satellite systems has been stimulated by their unique dynamics. In the absence of perturbing forces the motion of the center of mass of a deployed two-satellite tethered system is essentially Keplerian. However, the motion of one, or both, of the satellites in the system may depart significantly from such motion. As a result, hundreds of investigations have centered on the relative motion dynamics of these systems, including especially, deployment and retrieval.

For those with the assignment of tracking satellites and suborbital objects, the non-Keplerian nature of the orbital dynamics of tethered satellites poses some interesting problems not as fully analyzed as the relative motion problems. A prime example is that the motion of the lower satellite in the system may be kinematically the same as that of a free satellite moving continuously at apogee, with a potential perigee below reentry altitude.[4] This is a potential source of false alarms. Tracking algorithms that do not consider tethered systems dynamics as a possibility are probably sufficient if there is a priori knowledge that a tethered system will be orbited and special provisions are made to track the satellites. However, the probable increase in tethered systems in the future and the lack of enough a priori information on some make the consideration of the motion of the individual satellites in the system more important from the standpoints of detection and tracking.

Previous papers[5,6,7] have confronted the problem of "detecting" tethered satellites by using tethered satellite models in the orbit determination process. In Ref. 5 a simple planar model with an inextensible tether and no librational motion was used to study effects of tether length and drag on the determination process. In Ref. 6, we considered the planar motion of a two-satellite tethered system, again with inextensible tether, as a new kind of perturbed satellite problem by writing the equations of motion in such a way that the motion of one

satellite could be considered perturbed by the other through the tension in the tether. We showed that the magnitude of the perturbing effect of the second satellite is proportional to a non-dimensional parameter (the "tether parameter") containing the ratio of the masses of the satellites and the tether length. Examples were presented to show that this non-dimensional parameter, and the entire state of the system, could be determined from near ideal "observations" of only the perturbed satellite, generated using the model. In Ref. 7, we considered more general motion of the perturbing satellite that allowed for its motion both in and out of the orbital plane of the perturbed one. For large enough out of plane libration angles, the tether parameter and the state of the system were determined, again from near ideal observations. In these two investigations, the models were such that the masses of the satellites and the tether length could not be determined except in the "tether parameter" combination. Thus, we could determine that a tether connected the perturbed satellite to another, and we could find the unit vector to the perturbing satellite from the perturbed one, but we could not completely determine the location of the perturbing satellite. Furthermore, the batch least squares process used for state determination did not exhibit good convergence properties. This, plus the desire to determine the tether length and perhaps the ratio of the masses of the satellites motivated a more detailed investigation of the dynamical characteristics of two-satellite tethered systems.

In this paper, we consider a two-satellite tethered system as a particular case of an observed nonlinear system. Our primary purpose is to determine the characteristics of the information available in observations of one of the satellites (the "observed satellite"). We do this in two ways. First, we use the model from Ref. 7 to calculate information matrices for the associated linear systems that arise in the state determination process. These are analyzed to determine the quality and quantity of the information that may be extracted. Second, we use a more general model that includes tether extensibility, atmospheric drag, and the Earth's oblateness to study different types of actual motion (e.g., initial libration and initial center of mass motion) and different system characteristics (e.g., tether length, satellite masses).

INFORMATION MATRICES.

Three conclusions regarding the information that may be extracted from measurements of the motions of a dynamical system are self-evident. First, only information that is present may be extracted. Second, the model used to do the extracting must contain some representation of the information. This representation may take the form of complex expressions, such as the geopotential of a planet, or simple expressions, such as constant "unmodeled accelerations." Third, a piece of information must be independent of other information sought if it is to be extracted. An example of a piece of information that is not generally independent is the tether length, if the tethered satellite model used contains the tether length only in combination with the masses of the satellites.

One way to quantify the information available in observations of a nonlinear system is to determine the information matrix of a local linear representation of the system. Let the nonlinear system be represented by the autonomous matrix differential equation

$$\dot{X} = f(X) \qquad (1)$$

where X is an n-vector of states and f is an n-vector of nonlinear functions. Also, let the (perfect) observations be represented by the equation

$$Y = h(X) \qquad (2)$$

where Y is an m-vector and h is an m-vector of nonlinear functions. If we linearize (1) and (2) about some nominal solution $X^*(t)$, obtained using a set of initial conditions on the states (including extra states representing parameters) which are not necessarily the true ones, then we may obtain linear equations of the form,

$$\dot{x} = A(t)x \qquad (3)$$

$$y = H(t)x \qquad (4)$$

where, $x = X - X^*$, $y = Y - Y^*$, $Y^* = h(X^*(t))$, $H = \left(\dfrac{\partial g}{\partial Y}\right)_{X=X^*}$ and $A = \left(\dfrac{\partial f}{\partial X}\right)_{X=X^*}$. The solution to (3) is, of course,

$$x(t) = \Phi(t, t_0)x_0 \qquad (5)$$

where $\Phi(t, t_0)$ is the state transition matrix and x_0 is the value of x at the initial time t_0. The measured output of the linear system is

$$y = \mathbf{H}(t)\,\Phi(t,t_0)\,\mathbf{x}_0 \qquad (6)$$

The observability Grammian matrix, or "information" matrix, for the continuous linear system is [see, for example, Ref. 8, p. 143]

$$N(t_f,t_0) = \int_{t_0}^{t_f} \Phi^T(\tau,t_0)\,\mathbf{H}^T(\tau,t_0)\,\mathbf{H}(\tau,t_0)\,\Phi(\tau,t_0)\,d\tau$$

$$(7)$$

Usually, observations are made at discrete times. An information matrix for a discrete representation of the continuous linear system is

$$N(k_f,0) = \sum_{k=0}^{k_f} \Phi^T(k,0)\,\mathbf{H}^T(k,0)\,\mathbf{H}(k,0)\,\Phi(k,0) \qquad (8)$$

The linear system is observable if $\mathbf{N}\,(k_f,0)$ is nonsingular. The elements of $\mathbf{N}\,(k_f,0)$ provide information regarding "the effects of the initial conditions on the observations." If the rank of $\mathbf{N}\,(k_f,0)$ is less than n, then, obviously, some of the initial conditions do not affect the observations and hence are not observable.

A more straightforward, but certainly less elegant, method for determining how changes in states, or parameters treated as extra states, affect observed quantities is often used in "sensitivity studies." The procedure followed is to: (1) integrate the nonlinear equations using nominal values, (2) make small changes in each one of the states or parameters and integrate the nonlinear equations, and (3) calculate the changes in the observed quantities due to the changes in the states and parameters. This procedure may be used to generate an approximate information matrix.

TWO-SATELLITE TETHERED SYSTEM MODELS

Two models of a two-satellite tethered system were used to study the information available in observations of one of the satellites. The first model is that described by Cho, et al.[7] The equations of motion are given in Appendix. The second is a more general model that contains representations of the atmospheric drag and the effects of the Earth's oblateness. The latter effects were included because for short tether lengths, the perturbing effects of the Earth's oblateness are of the same order of magnitude as the tether "perturbations." Only the more general

model is described in the Appendix, since the simpler one is a special case of it.
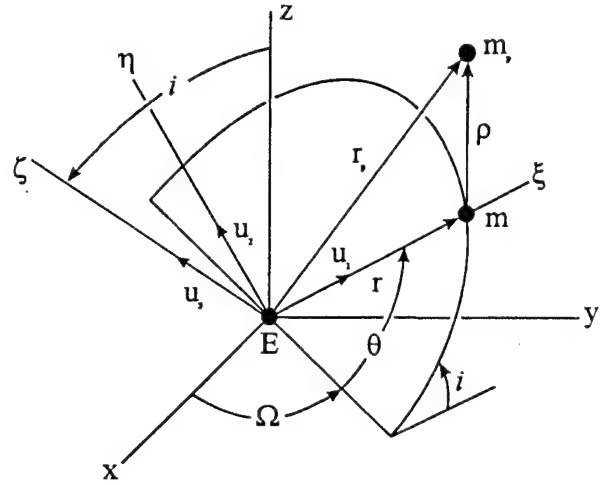
Figure 1. Osculating Orbit Plane

The geometry of the model of Ref. 7 is shown in Figure 1, where E is the center of the Earth, m is the observed satellite and m_p is the unobserved "perturbing" satellite. The position vector of m is $\mathbf{r}$ and that of m_p is $\mathbf{r} + \rho$. The observed satellite is moving in an osculating orbit, the orientation of which is defined by the inclination, i, and the longitude of the ascending node, Ω. The position vector, $\mathbf{r}$, and the velocity vector, $\mathbf{v} = \dot{\mathbf{r}}$, lie in the plane of the orbit. The angle θ is the sum of the true anomaly and the argument of perigee. Two angles, θ_2, out-of-plane, and θ_3, in-plane, are used to define the direction of ρ relative to the direction of $\mathbf{r}$. The state variables are r, Ω, i, θ, θ_2, θ_3, $\dot{r}$, $\dot{\theta}$, $\dot{\theta}_2$, and $\dot{\theta}_3$, since the tether length is constant in this model.

Even for the simpler model the elements of the matrices $\mathbf{A}$ and $\mathbf{H}$ are not simple. However, algebraic manipulation software, such as Mathematica®, may be used to obtain explicit expressions for the partial derivatives needed to form $\mathbf{A}$ and $\mathbf{H}$. Here, we use analytical derivatives only for the simpler model.

RESULTS FROM THE SIMPLER MODEL

One purpose of the examples we give in this section is to show that the choices of models, states,

and observations can significantly affect the information available. From the equations of motion for the simpler model, it is apparent that the only way ρ, m, and m_p appear is in the combination ε. This is because the difference in the gravitational forces on the satellites was expanded in powers of ρ/r and terms of order higher than the first were neglected. However, since the terms of order higher than the first are extremely small except for very long tethers, the fact that these parameters appear only in ε in the model also means that they would probably not be observable if the full expression for the difference were used.

The simpler model was used to calculate numerous information matrices. The parameters and results for twenty of these are summarized in Tables 1 and 2.

Table 1. Test Cases

Case	Mass Ratio (m_p/m)	Tether Length (ρ km)	Tether Parameter (ε)	Observation time (Orbital period)	θ_3 (In-plane)	θ_2 (out-plane)
1	0.1	1	1.4254E-05	1/16	0	0
2	10.0	100	1.4254E-02	1/16	0	0
3	0.1	1	1.4254E-05	1/16	Small	Small
4	10.0	100	1.4254E-02	1/16	Small	Small
5	0.1	1	1.4254E-05	1/16	Large	Large
6	10.0	100	1.4254E-02	1/16	Large	Large
7	10.0	100	1.4254E-02	1/16	Large	0
8	0.1	1	1.4254E-05	1/16	Large	0
9	0.1	1	1.4254E-05	1/16	Small	Large
10	0.1	1	1.4254E-05	1.0	Small	Small

Table 2. Condition Number of Information Matrices for Test Cases

Case	Range Condition Number	Range Rank	r, α, and δ Condition Number	r, α, and δ Rank
1	5.8E+18	7	1.8E+16	9
2	3.7E+12	11	2.0E+10	11
3	3.5E+18	7	2.1E+16	9
4	7.7E+14	10	2.1E+10	11
5	5.0E+20	7	1.0E+17	8
6	5.3E+15	10	2.6E+11	11
7	2.3E+15	10	1.5E+14	11
8	5.0E+19	7	6.1E+16	7
9	5.9E+18	7	8.6E+16	8
10	3.9E+12	11	1.3E+11	11

Results in the form of condition numbers and ranks of the information matrices were calculated using ten different nominal motions and two types of observations. Some of the initial conditions which were the same for all cases are $r_0 = 6.6189E+06$ m, $\theta_0 = 1.7130$ (rad), $\Omega_0 = 1.9741E-03$ (rad), $i_0 = 1.1051$ (rad), $\dot{r}_0 = -2.2314$ (m/sec), and $\lambda_{30} = 1.1492E-03$ (rad/sec) (see the Appendix for definitions).

The initial values of the states θ_2 and θ_3 were changed from zero to produce nominal motion of m in and out of the plane of the motion of m. "Small" libration was produced by using,

$\theta_{20} = -9.8226E-02$ (rad),

$\theta_{30} = -9.8568E-02$ (rad),

$\omega_{20} = 5.1386E-05$ (rad/sec),

and $\omega_{30} = 1.1204E-03$ (rad/sec).

"Large" libration was initiated by setting ,

$\theta_{20} = 1.0$(rad),

$\theta_{30} = 1.0$ (rad),

$\omega_{20} = 0.0$ (rad/sec),

and $\omega_{30} = \lambda_{30}$ (rad/sec).

The zero libration cases were obtained by using the equilibrium angular velocity of the system and zero initial libration angles.

The two types of observations used were the range to m from a ground station (R) and the position vector of m defined by the radial distance, r, the right ascension, α , and the declination, δ.

For all cases except Case 10, the total observation time was $1/16^{th}$ an orbital period of m. During this period of time 171 observations were assumed. For Case 10, we assumed that the observed satellite could be tracked over an entire orbit.

Cases 1 and 2 in Table 1 are for small and large tether perturbations, respectively, and no initial libration. For the smaller value of ε, the condition numbers of the information matrix are both large, indicating ill-conditioning. For the larger value of ε, the matrix condition numbers are two orders of magnitude smaller. The more complete set of observations produces a full rank information matrix in the large ε case (Case 2).

Cases 3 and 4 should be richer in information because small initial libration of the tether is included in the nominal motion. However, the condition numbers do not change very much from the Case 1 and Case 2 values, respectively. The additional nominal motion does increase the rank of the information matrix for the small ε case. (Case 3).

Intuitively, one might think that Cases 5 and 6, for large libration, would produce somewhat better information. Based on a comparison of the condition numbers and ranks for small and large ε, this does not appear to be true. The condition number is much smaller for the position vector observations than when only the range is used for the observation.

Cases 7 and 8 are one in which only in-plane libration is excited initially. Even for a large tether parameter in Case 7, the results for this case are not as good as those for Case 6.

Case 9 includes a small ε and mixed libration, small in-plane and large out-of-plane. The results for this case are not as good as those for Cases 2 , 4, and 6. The ranks of the matrices for both types of observations are less than 11.

Case 10 results show that with a longer total observation time and correspondingly greater numbers of observation, the information matrix quality improves considerably, producing full rank matrices and relatively low condition numbers.

RESULTS FROM THE MORE GENERAL MODEL

Atmospheric drag and the Earth's oblateness will produce effects that will reduce, or increase, the information available in the motion of the observed satellite. To investigate the possibility of getting better information, limited numerical experiments were conducted to see if the sensitivity of the motion generated using the more general model to changes in the relative masses of the satellites and the tether length is significant.
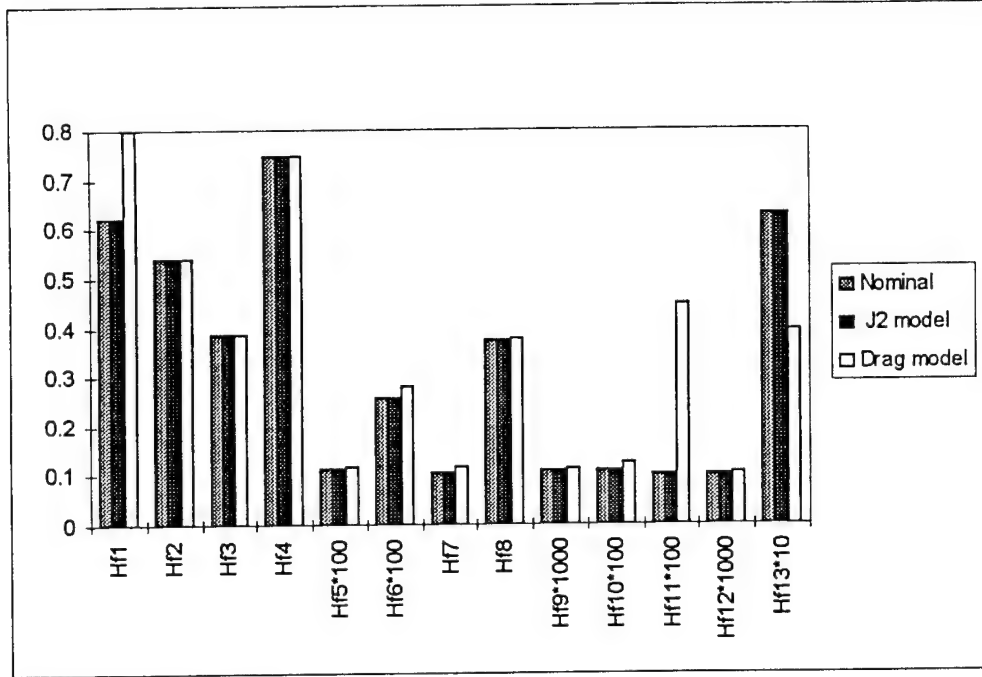
Figure 2. Magnitudes of Elements in H_f Matrix

For this model, the partial derivatives of the states at a particular time with respect to the initial conditions were numerically approximated by simple finite difference. The estimation vector consisted of the 10 state variables listed previously, as well as the two masses and the tether length. The initial conditions on the states were identical to those given in the previous section for "small" libration, and the values used for masses and tether length were m = 10kg, m_p = 100kg, and ρ = 100km. As in the previous section, the total observation time was $1/16^{th}$ an orbital period of m, and during this time 171 observations were made. Using range R as the only observation, the state transition matrix $\Phi(t, t_0)$ and information matrix were numerically approximated at several times along the trajectory: That is, the orbit initial conditions, as well as values for the masses and the tether length, were perturbed slightly one at a time and the change in system states and range observation at various times was noted. Of particular interest is the calculation of the H matrix, where:

$$H(t_1) = \frac{\partial R(t_1)}{\partial x(t_o)} \quad (9)$$

$$H(t_2) = \frac{\partial R(t_2)}{\partial x(t_o)}$$

etc.

For the simple model (without drag or oblateness effects), values obtained in this fashion for elements of H agreed to a high degree of accuracy with those obtained in the previous section. The values for the elements of H at several times along the trajectory were then obtained in the same manner using a model which allows for oblateness effects as well as aerodynamic drag on the end masses and tether. Figure 2 depicts the values of the elements of $H(t_f)$ in the trajectory calculated using each of these models. Here, the first ten elements of H_f are the partial derivative of R with respect to each state, with the states ordered as given in a previous section. Further,

$$H_{f11} = \frac{\partial R(t_f)}{\partial m} \quad (10)$$

$$H_{f12} = \frac{\partial R(t_f)}{\partial m_p}$$

$$H_{f13} = \frac{\partial R(t_f)}{\partial \rho}$$

While the inclusion of oblateness effects in model does not tend to affect the H matrix, several elements are significantly affected by inclusion of drag. In particular, the partial derivatives of range with respect to the masses and tether length are

American Institute of Aeronautics and Astronautics

significantly different from the nominal case. The fact that the range observation (and system motion in general) is significantly more sensitive to changes in mass m using the drag model but only slightly more sensitive to changes in mass m_p is best explained by the fact that m_p is at such a higher altitude where drag can be several orders of magnitude lower. Also, because the observation is of mass m, slight changes to m_p will not significantly affect the observation. However, system motion is less sensitive to changes in tether length when drag is present in the model. This is not surprising, considering that drag has a dissipative effect on the tether, decreasing its "tether-perturbing" capability on mass m. It is important to note that since for the simple model the masses and tether length are related by the tether parameter, the partial derivatives of range with respect to each of these parameters will only differ by a constant factor for given values of the masses and tether length. However, this cannot be the case for the drag model, as seen by the behavior of $H_{\Omega 1}$, $H_{\Omega 2}$, and $H_{\Omega 3}$ in Figure 2. Thus two different combinations of m, m_p, and ρ which yield the same tether parameter value may in fact affect the system motion (the range in particular) differently. The effect of drag on the $\mathbf{H_f}$ matrix indicates that m, m_p, and ρ might be estimated independently of one another, i.e., more information can be gained beyond estimation of the tether parameter, if a more general model is used with good observations.

After calculation of $\mathbf{H}$ at various times on the trajectory, the condition number of the overall information matrix was calculated for different choices of the estimation vector. Generally this vector consisted of the 10 states and some combination of m, m_p, and ρ. Although the condition number in most cases was higher than that obtained in the previous section, the trends were similar:

-For most choices of the estimation vector, condition number calculated using the oblateness model was slightly than for the nominal model, while the value calculated with the drag model was lower still.

-In many cases the addition of one of the system parameters--m, m_p, or ρ--to the estimation vector brought about a lower condition number than that for which the vector consisted of the 10 states alone.

-Condition number tended to decrease as observation time increased, or as the mass ratio or tether length increased.

It should be noted that, in addition to accounting for effects of oblateness and aerodynamic drag, the general model can allow for extensibility of the tether, whereby the tether tension force is given by

$$\mathbf{F_T} = k_s\,(\rho - \rho^*) + c_s\,\dot{\rho} \qquad (11)$$

where k_s and c_s are the tether stiffness and damping. However, for the cases observed in this analysis, the motion of an extensible tether is not significantly different from that of an inextensible tether in terms of overall system motion. For the range of tether stiffness and damping assumed, the oscillatory motion of the tether damps fairly quickly as it reaches an "equilibrium" position whereby the spring tension in the tether approximately equals the tension in an inextensible tether undergoing the same motion.

CONCLUSIONS

The information available in observation of one satellite in a two-satellite tethered system has been investigated by using a combination of analytical and numerical methods. As expected, the magnitude of the tether parameter strongly affects the conditioning of the information matrix, as does the types of observation. Although the information matrix elements corresponding to the motion of the perturbing satellite are generally relatively small and the condition numbers of the matrix large, the estimation of the entire state of a two-satellite tethered system from the observations of one of the satellites appears feasible.

ACKNOWLEDGMENTS

REFERENCES

1. Tsiolkovsky, K. E., "Speculation between Earth and Sky," Isd-vo AN-SSR, 1895, p. 35 (reprinted 1959).
2. Columbo, G., Gaposchkin, E. M., Grossi, M. D., and Weiffenbach, G. C., "The Skyhook: A Shuttle-borne Tool for Low Orbital Altitude Research," *Meccanica*, Vol. 10, 1975, pp. 3-20.
3. Belesky, V. V., *Dynamics of Space Tether Systems*, Advances in the Astronautical Sciences, American Astronautical Society, San Diego, CA, 1993.

4. Hoots, F. R., Roehrich, R. L., and Szebehely, V. G., "Space Shuttle Tethered Satellite Analysis," *Directorate of Astrodynamics*, Peterson AFB, CO, August 1983.

5. Kessler, S., and Cicci, D. A., "Orbit Determination of a Tethered Satellite," AAS 95-350, *AAS/AIAA Astrodynamics Specialist Conference*, Halifax, Nova Scotia, Canada, August 14-17, 1995.

6. Cochran, J. E., Jr., Cho, S., Cheng, Y-M., and Cicci, D. A., "Dynamics and Orbit Determination of Tethered Satellite Systems," AAS 96-147, *AAS/AIAA Space Flight Mechanics Meeting*, Austin, TX, February 12-15, 1996.

7. Cho, S., Cochran, J. E., Jr., and Cicci, D. A., "Identification and Orbit Determination of Tethered Satellite Systems," AAS 98-101, *AAS/AIAA Space Flight Mechanics Meeting*, Monterey, CA, February 9-11, 1998.

8. Stengel, R.F., *Stocastic Optimal Control*, John Wiley & Sons, Inc., New York, 1986, pp. 142-153

9. Hedin, A. E., "Extension of the MSIS Thermospheric Model into the Middle and Lower Atmosphere," *J of Geophys. Res. 96*, 1159,1991

10. Warnock, T. W., and Cochran, J. E. Jr., "Orbital Lifetime of Tethered Satellites," *The Journal of the Astronautical Sciences*, Vol. 41, No. 2, 1993, pp. 165-188.

APPENDIX

Model Equations of Motion

The equations of motion used to obtain the result presented in the body of this paper are summarized here. Only the equations for the more general model are given since they contain the ones used to obtain the results for analytically derived information matrices as a special case.

Motion of Mass m.

$$\ddot{r} = (\lambda_2^2 + \lambda_3^2)r - \frac{\mu}{r^2} + \frac{F_{T_1}}{m} + a_1 - \frac{d}{2m}C_D A V_r \dot{r} \quad (A-1)$$

$$\dot{\lambda}_3 = \frac{1}{r}\left(-2\lambda_3\,\dot{r} - \lambda_1\lambda_2\,r + \frac{F_{T2}}{m}\right) + \frac{1}{r}\left(a_2 - \frac{d}{2m}C_D A V_r(\lambda_3 r - \omega_e r\cos i)\right) \quad (A-2)$$

$$\dot{\lambda}_2 = \frac{1}{r}\left(-2\lambda_2\,\dot{r} + \lambda_1\lambda_3\,r - \frac{F_{T3}}{m} - a_3\right) + \frac{1}{r}\left(\frac{d}{2m}C_D A V_r(\omega_e r\cos\theta\sin i - \lambda_2 r)\right) \quad (A-3)$$

where λ_j, $j=1,2,3$, are the components of the angular velocity of the unit vector triad (u_1, u_2, u_3) associated with the position vector of m; $\mu = Gm_\oplus$, where G is the universal gravitation constant and $m_\oplus$ is the mass of the Earth; F_{T_j}, $j=1,2,3$, are the components of the tether force; d is the atmospheric density; C_D is the drag coefficient of the satellite; A is the reference area of the satellite; V_r is the magnitude of the relative wind seen by the satellite is given by

$$V_r = \sqrt{\dot{r}^2 + (\lambda_3 r - \omega_e r\cos i)^2 + (\omega_e r\cos\theta\sin i - \lambda_2 r)^2} \quad (A-4)$$

where ω_e is the rate of rotation of the Earth. For an osculating orbit, $\lambda_2 \equiv \dot{\lambda}_2 \equiv 0$, so that (A-3) provides

$$\lambda_1 = \frac{1}{\lambda_3 r}\left(\frac{F_{T3}}{m} + a_3\right) + \frac{1}{\lambda_3 r}\left(-\frac{d}{2m}C_D A V_r \omega_e r\cos\theta\sin i\right) \quad (A-5)$$

The equations for Ω, θ, and i may be found by using those angles and θ to write the angular velocity λ. They are

$$\dot{\Omega} = \lambda_1\sin\theta / \sin i \quad (A-6)$$

$$\frac{di}{dt} = \lambda_1\cos\theta \quad (A-7)$$

$$\dot{\theta} = \lambda_3 - \lambda_1\sin\theta\cos i / \sin i \quad (A-8)$$

The acceleration of m_p may be written as

$$\ddot{\rho} + \dot{\omega}\times\rho + 2\omega\times\dot{\rho} + \omega\times\omega\times\rho = \Delta g - F_T\frac{M}{m\,m_p} + a_p - a \quad (A-9)$$

where a_p and a are as yet unspecified accelerations acting on m_p and m, respectively. The accelerations

due to aerodynamic drag may be included in the same manner as $\mathbf{a}_p$ and $\mathbf{a}$, to get

$$\ddot{\boldsymbol{\rho}} + \dot{\boldsymbol{\omega}} \times \boldsymbol{\rho} + 2\boldsymbol{\omega} \times \dot{\boldsymbol{\rho}} + \boldsymbol{\omega} \times \boldsymbol{\omega} \times \boldsymbol{\rho} =$$

$$\Delta \mathbf{g} - \mathbf{F}_T \frac{M}{m\, m_p} + \mathbf{a}_p - \mathbf{a} - \frac{\mathbf{D}_m}{m} + \frac{\mathbf{D}_{m_p}}{m_p} \qquad \text{(A-10)}$$

where

$$\mathbf{D}_{m_p} = -\frac{d_p}{2} C_{D_p} A_p V_{r_p} \mathbf{V}_{r_p} \qquad \text{(A-11)}$$

where d_p is the atmospheric density experienced by m_p, C_{Dp} is its drag coefficient, A_p its wetted area, and $\mathbf{V}_{r_p}$ its velocity relative to Earth's atmosphere. This velocity is defined as

$$\mathbf{V}_{r_p} = \dot{\mathbf{r}} + \dot{\boldsymbol{\rho}} - \boldsymbol{\omega}_e \times (\mathbf{r} + \boldsymbol{\rho}) \qquad \text{(A-12)}$$

where $\boldsymbol{\omega}_e$ is the Earth's rotational velocity vector. Note that $\boldsymbol{\omega}_e$ is expressed in the $\mathbf{E}u_1 u_2 u_3$ system as

$$\boldsymbol{\omega}_e = \mathbf{C}_e \mathbf{C}_u \begin{bmatrix} 0 \\ 0 \\ \omega_e \end{bmatrix} \qquad \text{(A-13)}$$

where $\mathbf{C}_u$ is as defined above and $\mathbf{C}_e$ is the direction cosine matrix from $\mathbf{E}u_1 u_2 u_3$ to $\mathbf{E}e_1 e_2 e_3$, obtained by a 3-2 Euler rotation through the tether angles θ_3 and θ_2, respectively. By defining $\mathbf{C}_{eu} = \mathbf{C}_e \mathbf{C}_u$, we may write the velocity of m_p relative of the Earth's atmosphere as

$$\mathbf{v}_{r_p} = \begin{bmatrix} C_{e_{11}}\dot{r} + C_{e_{12}}(\lambda_3 r - \omega\omega_e r\cos i) + C_{e_{13}}(\omega\omega_e r\cos\theta\sin i - \lambda_2 r) \\ C_{e_{21}}\dot{r} + C_{e_{22}}(\lambda_3 r - \omega\omega_e r\cos i) + C_{e_{23}}(\omega\omega_e r\cos\theta\sin i - \lambda_2 r) \\ C_{e_{31}}\dot{r} + C_{e_{32}}(\lambda_3 r - \omega\omega_e r\cos i) + C_{e_{33}}(\omega\omega_e r\cos\theta\sin i - \lambda_2 r) \end{bmatrix}$$

$$+ \begin{bmatrix} \dot{\rho} \\ \rho(\omega_3 - C_{eu_{33}}\omega_e) \\ \rho(C_{eu_{23}}\omega_e - \omega_2) \end{bmatrix} \qquad \text{(A-14)}$$

Note that $\mathbf{V}_{r_p}$ can be divided into

$$\dot{\mathbf{V}}_r = \dot{\mathbf{r}} - \boldsymbol{\omega}_e \times \mathbf{r} = \begin{bmatrix} C_{e_{11}}\dot{r} + C_{e_{12}}(\lambda_3 r - \omega_e r\cos i) + C_{e_{13}}(\omega_e r\cos\theta\sin i - \lambda_2 r) \\ C_{e_{21}}\dot{r} + C_{e_{22}}(\lambda_3 r - \omega_e r\cos i) + C_{e_{23}}(\omega_e r\cos\theta\sin i - \lambda_2 r) \\ C_{e_{31}}\dot{r} + C_{e_{32}}(\lambda_3 r - \omega_e r\cos i) + C_{e_{33}}(\omega_e r\cos\theta\sin i - \lambda_2 r) \end{bmatrix}$$

$$\text{(A-15)}$$

and

$$\mathbf{V}_{r_p}{}' = \rho\dot{\rho} - \boldsymbol{\omega}_e \times \rho\rho \qquad \text{(A-16)}$$

where $\mathbf{V}_r$ is the relative velocity of mass m as defined above (except here it is expressed in the $\mathbf{E}e_1 e_2 e_3$ system) and $\mathbf{V}_{r_p}{}'$ is the relative velocity of mass m_p as seen from mass m. The expressions for $\mathbf{V}_r$ and $\mathbf{V}_{rp}$ can then be inserted into the above expressions for $\mathbf{D}_m$ and $\mathbf{D}_{mp}$, respectively. Then, inserting $\mathbf{D}_m$ and $\mathbf{D}_{mp}$ into (A-10) and using the approximation for $\Delta \mathbf{g}$ in the $\mathbf{E}e_1 e_2 e_3$ system given by Eq. (18) of Ref. 7, gives the vector equation of motion for mass m_p, the three components of which are

$$\ddot{\rho} = (\omega_2^2 + \omega_3^2)\rho + \Delta g_1 - F_{T_1}\frac{M}{m\,m_p} +$$

$$a_{p_1} - a_1 + \frac{1}{2}(\frac{dC_D A V_r V_{r_1}}{m} - \frac{d_p C_{D_p} A_p V_{r_p} V_{r_{p_1}}}{m_p})$$

$$\text{(A-17)}$$

$$\dot{\omega}_3 = \frac{1}{\rho}\left(-2\omega_3\dot{\rho} - \omega_1\omega_2\rho + \Delta g_2 - F_{T_2}\frac{M}{m\,m_p}\right) +$$

$$\frac{1}{\rho}\left(+a_{p_2} - a_2\right) +$$

$$\frac{1}{\rho}\left(+\frac{1}{2}(\frac{dC_D A V_r V_{r_2}}{m} - \frac{d_p C_{D_p} A_p V_{r_p} V_{r_{p_2}}}{m_p})\right)$$

$$\text{(A-18)}$$

$$\dot{\omega}_2 = \frac{1}{\rho}\left(-2\omega_2\dot{\rho} + \omega_1\omega_3\rho - \Delta g_3 + F_{T_3}\frac{M}{m\,m_p}\right) +$$

$$\frac{1}{\rho}\left(-a_{p_3} + a_3 - \frac{1}{2}(\frac{dC_D A V_r V_{r_3}}{m} - \frac{d_p C_{D_p} A_p V_{r_p} V_{r_{p_3}}}{m_p})\right)$$

$$\text{(A-19)}$$

where

$$V_{r_1} = C_{e_{11}}\dot{r} + C_{e_{12}}(\lambda_3 r - \omega_e r\cos i)$$
$$+ C_{e_{13}}(\omega_e r\cos\theta\cos\theta - \lambda_2 r) \qquad \text{(A-20)}$$

$$V_{r_{p_1}} = C_{e_{11}}\dot{r} + C_{e_{12}}(\lambda_3 r - \omega_e r\cos i)$$
$$+ C_{e_{13}}(\omega_e r\cos\theta\cos\theta - \lambda_2 r) + \dot{\rho}$$

and similarly for V_{r_2}, $V_{r_{p_1}}$, $V_{r_{p_2}}$, and V_{r_3}.

The equations for θ_2, and θ_3 can be found by using λ and ω as

$$\dot{\theta}_2 = \omega_2 + \lambda_1 \sin\theta_3 \qquad \text{(A-21)}$$

$$\dot{\theta}_3 = (\omega_3 - \lambda_1 \sin\theta_2 \cos\theta_3)/\cos\theta_2 - \lambda_3 \qquad (A\text{-}22)$$

If the tether is assumed inextensible, then, in the above equations, $\dot{\rho} \equiv \ddot{\rho} \equiv 0$, and $\mathbf{F_T}$ is constrained to be in the $\mathbf{e_1}$ direction only. Then the $\mathbf{F_T}$ components in (A-2) and (A-3) are zero and Eq. (A-17) reduces to an expression for $\mathbf{F_T}$ given by Eq. (19) on p. 6 of Ref. 7 that can be inserted into the remaining equations.

Drag on the Tether

Consider the modeling of the tether as n massless inextensible segments of equal length. Each segment experiences drag $\mathbf{D_{Ti}}$. Let each $\mathbf{D_{Ti}}$ be a concentrated point force at the midpoint of each ith segment as in Figure 1:

In Ref. 6, the tether force $\mathbf{F_T}$ was constrained to be in the $\mathbf{e_1}$ direction only, such that $\ddot{\rho} = 0$. But with the above assumptions, the tether force is now

$$\mathbf{F_T} = \mathbf{F_T}' + \sum_i \mathbf{D_{T_i}} \qquad (A\text{-}23)$$

where $\mathbf{F_T}'$ represents the tether force expression used in Ref. 6. The equation for the drag on the ith tether segment is

$$\mathbf{D_{T_i}} = -\frac{d_i}{2} C_{D_i} A_i V_{r_{i\perp}} \mathbf{V_{n\perp}} \qquad (A\text{-}24)$$

where d_i is the atmospheric density at the geodetic altitude of the midpoint of the ith segment and C_{Di} is the drag coefficient of the cylindrical segment. A_i is the rectangular cross-sectional area calculated by multiplying the tether diameter by ρ/n. $\mathbf{V_{r_i}}$ is the relative velocity of the midpoint of the ith segment and is similar to the expression for . $\mathbf{V_{r_p}}$ from the previous section:

$$\mathbf{V_{r_i}} = \dot{\mathbf{r}} + \left(\frac{2i-1}{2n}\right)\dot{\rho} - \omega_\bullet \times \left[\mathbf{r} + \left(\frac{2i-1}{2n}\right)\rho\right] \qquad (A\text{-}25)$$

However, $\mathbf{D_{T_i}}$ is a function of the crossflow velocity, i.e. the component of $\mathbf{V_{r_i}}$ perpendicular to the axis of the tether. Thus the $\mathbf{e_1}$ component of $\mathbf{V_{r_i}}$, if any, is set to zero in order to obtain $\mathbf{V_{n\perp}}$.

Since we assume that the tether segments have no mass, we cannot obtain equations of motion for them. However, if we include the tether drag in the

equations for m and m_p, we get a better estimate of the tether force on the satellites

Atmospheric Density Model

The atmospheric density model currently used in the simulations is MSIS-E-90 developed by NASA Goddard[9]. To implement this model, density values were taken at the equator, 0 deg longitude, at a particular day and time, over several altitudes. The density (d) vs. altitude (h) data was then curve-fit by means of a neural network to the following function:

$$\log(d) = \frac{a_1}{1+e^{-(b_1+c_1 h)}} + \frac{a_2}{1+e^{-(b_2+c_2 h)}} + \frac{a_3}{1+e^{-(b_3+c_3 h)}} + a_4$$
$$(A\text{-}26)$$

where h is in km, d is in kg/m^3, and the a, b, and c coefficients were optimized for minimum RMS. error between calculated and "actual" density. The resulting optimized coefficients are

a_1	=	5.91414
a_2	=	2.4841
a_3	=	8.73673
a_4	=	-9.58712
b_1	=	3.97094
b_2	=	1.89697
b_3	=	-1.58299
c_1	=	0.0420787
c_2	=	-0.0849698
c_3	=	0.00583612

This provides a means of quickly calculating density, given the geodetic altitude, at any point in the orbit.

Drag Coefficient Model

The drag coefficient currently used in the simulations is a constant value of 2.7, which according to Warnock,[10] is the approximate maximum value attained by a spherical body from 0 to 200km altitude.

USE OF TETHERED SATELLITE ESTIMATION METHODS IN IDENTIFYING RE-ENTERING OBJECTS

T. A. Lovell[#], S. Cho[#], J. E. Cochran, Jr.[*] and D. A. Cicci[**]
Auburn University, Alabama 36849-5338

ABSTRACT

In this paper an investigation is carried out regarding the motion of objects in near-Earth orbit that have a high probability of being identified as re-entering the Earth's atmosphere. If an object is one of two or more satellites tethered together, this object's motion will deviate significantly from the traditional Keplerian-like motion of a single untethered body, due to the tension force in the tether. Consequently, classical techniques used to identify and predict the motion of orbiting objects will incorrectly predict the path of a tethered body. If the undetected tether force is large enough, an orbit determination procedure may interpret the object to be on course to re-enter when it actually is not, or vice-versa. Indeed, even a method that can estimate the tether force may wrongly assess the situation if libration of the tethered pair is not included in the filter model. In this study it is determined what factors cause tethered bodies to behave so differently than expected, and how significant these factors must be to cause a discrepancy regarding re-entry. A successful re-entry identification methodology must take all of these factors into account.

NOMENCLATURE

a	semi-major axis of a Keplerian orbit
e	eccentricity of a Keplerian orbit
h	orbital altitude
m_1	upper mass of tethered satellite system
m_2	lower mass of tethered satellite system
r	distance from Earth's center to the lower mass
r_1	distance from Earth's center to the upper mass
r_{cm}	distance from Earth's center to the center of mass
r_E	radius denoting re-entry into Earth's atmosphere
r_p	perigee radius of a Keplerian orbit
v_{m1}	velocity of the upper mass

---

[*] Graduate Student, Department of Aerospace Engineering.
[*] Professor and Head, Department of Aerospace Engineering; Fellow; AAS; Associate Fellow, AIAA;
[**] Associate Professor, Department of Aerospace Engineering; Member AAS; Associate Fellow, AIAA

v_{m2}	velocity of the lower mass
v_{cm}	velocity of the center of mass
ϕ_3	libration angle with respect to the center of mass
$\dot{\phi}_3$	libration rate about the center of mass
ϕ_{30}	libration angle corresponding to zero libration rate
μ	Earth's gravitational parameter
ρ_1	tether length from center of mass to upper mass
ρ_2	tether length from center of mass to lower mass
ω_{cm}	angular velocity of the center of mass

INTRODUCTION

One of the interesting dynamic characteristics of a tethered satellite system (TSS) consisting of two satellites and a tether is the non-Keplerian orbital motion of each of the satellites. This is due to the perturbational forces on each mass caused by the tension force in the tether and may present problems to those who are tasked with tracking, detecting, and identifying space objects [1,2]. The center of mass of a TSS generally exhibits Keplerian motion. However, unless one of the masses is significantly larger than the other, the center of mass lies at a point along the tether and thus cannot be physically observed by tracking equipment. In fact, oftentimes there may only be observation data for one of the masses of a TSS available for processing. Although conventional orbit determination processes do account for some sources of non-Keplerian motion, such as the oblateness of the Earth, they were not constructed with TSS in mind.

In [3] a tethered satellite system model without libration is used to show how the radial tether force creates an "apparent mu," denoted μ^*, which effectively incorporates all of the radial acceleration due to the tether force into the standard two-body gravitational force. The μ^* for the lower mass of a TSS is less than the conventional μ, while for the upper mass μ^* is greater than μ. A conventional satellite estimation technique does not account for tether force, thus it perceives a tethered object as an untethered (Keplerian) body whose orbit is governed by μ^*. Hence, such a method will interpret the lower mass of a TSS as being on a smaller orbit (smaller semi-major axis) than it actually is, and the upper mass as being on an orbit larger than its true orbit. For an identification method equipped with only a conventional filter, this can lead to a major discrepancy:

The lower mass of a TSS that is not going to re-enter the atmosphere can be mistaken for an untethered satellite that is on a re-entry trajectory.

This discrepancy was illustrated in [1,2] for the case of circular motion of the center of mass of a TSS with no libration. Part of the analysis presented in this paper is similar to that in [1,2]. However, more general motion of the TSS is modeled and investigated here. In the spirit of previous work [4,5], we desire to generate analytical results, be they approximate or not, whenever possible. Furthermore, several scenarios will be explored

wherein the identification method consists of a filtering technique for tethered satellites, rather than a conventional filter. In [6] a classical orbit determination technique was modified for application to TSS. This method, rather than having a TSS dynamic model embedded within it, employs a simple Keplerian model of an untethered satellite, with the tether effects treated as perturbational accelerations. The technique estimates position and velocity of the mass being observed, as well as the components of tether acceleration tangential and radial to the path of the observed mass. From the radial tether acceleration, the length of the tether from the mass to the center of mass of the TSS can be estimated, as well as μ^*. In many cases, this will allow the above discrepancy to be avoided. However, since the filter does not contain a full dynamic model of a TSS, certain finer aspects of tethered motion, such as librational motion, cannot be captured. Thus, it is important in the present analysis to determine what effect libration and other such effects characteristic of tethered systems could have on the re-entry discrepancy.

RE-ENTRY DETECTION ANALYSIS

Here the discrepancy between the actual motion of a tethered mass and its motion as predicted by an orbit determination technique, will be investigated for four different scenarios.

Scenario 1: circular motion of the center of mass of the TSS, without libration
Scenario 2: circular motion of the center of mass with libration
Scenario 3: elliptical motion of the c.m. (at perigee or apogee) without libration
Scenario 4: general motion of the TSS (elliptical motion of the c.m., with libration)

Each case involves a different set of assumptions regarding the motion. For all scenarios, the condition of re-entry will be defined as follows:

A body exhibiting Keplerian motion is said to be on a re-entry path if the following condition holds:

$$r_p < r_E \tag{1}$$

or equivalently

$$2a < r_a + r_E \tag{2}$$

where r_p is the perigee radius and r_E is a radius to be chosen on the basis of atmospheric drag considerations.

CIRCULAR MOTION WITHOUT LIBRATION

For the first scenario, the following assumptions are made:

1. The motion of the TSS is planar.

3

2. The TSS center of mass is traveling on a circular (Keplerian) orbit.
3. The libration angle of the TSS is negligible.
4. The libration rate is negligible.
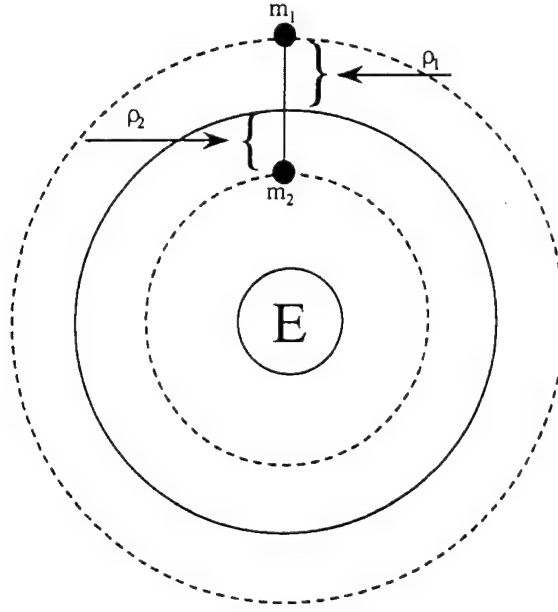
Figure 1. Center of mass in a Circular Orbit, no Libration.

Because the system is not librating and the center of mass travels in a circle, both endmasses (members of the system) do as well. Figure 1 depicts the motion of the system in this scenario, whereby the center of mass (solid line) and the two endmasses (dotted lines) all travel in concentric circles. The velocity of the center of mass is that corresponding to a circular Keplerian orbit:

$$v_{cm} = \sqrt{\frac{\mu}{r + \rho_2}} \tag{3}$$

Thus the angular velocity of the center of mass (and the entire system) is

$$\omega_{cm} = \frac{v_{cm}}{r + \rho_2} \tag{4}$$

The velocity of the lower mass is then

$$v_{m_2} = v_{cm} \left(\frac{r}{r + \rho_2}\right) = \sqrt{\frac{\mu r^2}{(r + \rho_2)^3}} \tag{5}$$

4

This, however, is *less* than the velocity of a body exhibiting circular Keplerian motion at the altitude determined by r. Since the observed mass's position and velocity vectors are perpendicular, a classical (Keplerian) orbit determination method will predict the mass to be at the apogee position of an elliptical orbit. The question is then, will a classical filtering technique predict the object to be on a re-entry orbit?

To answer this question, we must determine what (elliptical) path the mass would follow if it were an untethered (Keplerian) body, knowing the radius and velocity of the mass at perigee. Applying the energy equation for elliptical orbits

$$\frac{v^2}{2} + \frac{\mu}{r} = -\frac{\mu}{2a} \tag{6}$$

to the lower mass, we find that

$$a^* = \frac{\mu r}{2\mu - r v_{m_2}^2} = \frac{r(r + \rho_2)^3}{2(r + \rho_2)^3 - r^3} \tag{7}$$

where a^* denotes the "apparent" semi-major axis of the lower mass's orbit, as estimated by a classical (Keplerian) technique. Applying then the condition of re-entry given above, the path of the mass will be assessed as a re-entry orbit if

$$\frac{2r(r + \rho_2)^3}{2(r + \rho_2)^3 - r^3} < r_a + r_E \tag{8}$$

which agrees with the result given in [1]. This inequality can be simplified to

$$\rho_2 = r\left(\sqrt[3]{\frac{r}{2r_E} + \frac{1}{2}} - 1 \right) \tag{9}$$

or, in terms of the lower mass's altitude h ($\approx r - r_E$):

$$\rho_2 > (r_E + h)\left(\sqrt[3]{1 + \frac{h}{2r_E}} - 1 \right) \tag{10}$$

This then is $\rho_{2,th}$, the threshold value of ρ_2 above which the mass will be "mis-assessed" as a re-entry object. Figure 2 depicts this value for a range of orbital altitudes.

The TSS orbit determination technique described in [6] can in fact approximate ρ_2 for a tethered object by estimating the tether force. But, because orbit determination of a tethered satellite involves the estimation of more parameters than that of an untethered one, more observation data is generally required for sufficiently accurate determination of

5

the state of a TSS. Therefore, a candidate identification method for re-entering objects should involve: (1) use of a conventional filter to make a rapid orbit determination of an
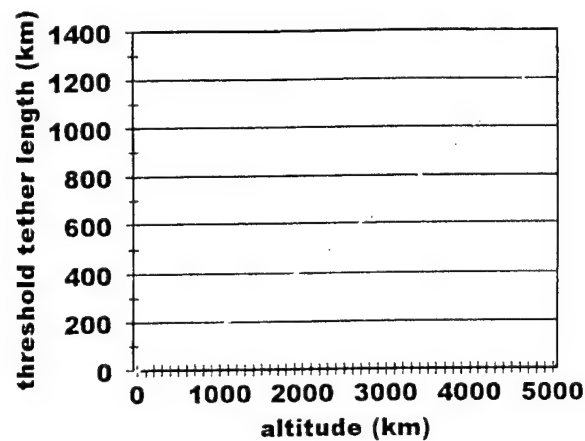
Figure 2. Threshold Value of ρ_2.

object's motion assuming that it is untethered and (2) assessment of whether or not such an untethered satellite is on a re-entry path; and (3) after more observation data is obtained, refining this assessment via the TSS filter. In this manner, a classical (Keplerian motion) estimation technique may be used in conjunction with the modified technique of [6], in this type of scenario, to improve the accuracy of an assessment of the path of an orbiting body.

CIRCULAR MOTION WITH LIBRATION

A TSS may experience appreciable libration, especially in the initial stages after deployment. For example, the TiPS [7] system initially had a maximum libration angle on the order of 40 degrees. In this scenario assumptions #1, 2, and 3 above are adopted. The instantaneous libration angle is small but libration rate of the TSS is no longer assumed negligible; i.e. the TSS is near the vertical portion of its "swing." In such a case, it is possible for libration rate to cause an incorrect assessment to be made concerning the anticipated path of the object being tracked by adding a component of velocity to the object that is not part of its gross orbital motion. Figure 3 depicts a librating TSS.

We define the libration rate $\dot{\phi}_3$ to be positive when the smaller mass is "swinging" in the direction of orbital motion. Then, the velocity of the lower mass can be expressed as the sum of a component due to the orbital motion of the TSS (as in the above section) and a component due to libration:

6

$$v_{m_2} = \sqrt{\frac{\mu r^2}{(r + \rho_2)^3}} + \rho_2\dot{\phi}_3 \qquad (11)$$
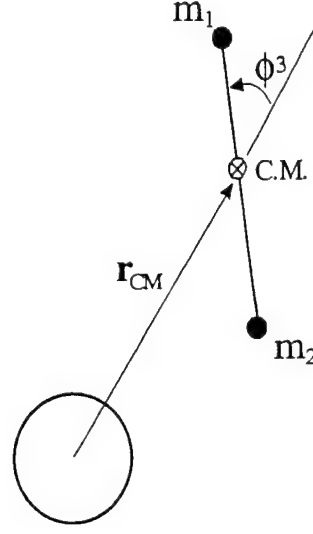
Figure 3. Librating TSS.

The development in [8] regarding pendular oscillations of a tethered system yields, after making simplifications appropriate to this scenario, the following expression for libration rate:

$$\dot{\phi}_3 = \pm\sqrt{\frac{3}{2}}n\sqrt{\cos 2\phi_3 - \cos 2\phi_{30}} \qquad (12)$$

Or, if instantaneous libration angle is small,

$$\dot{\phi}_3 = \pm\sqrt{\frac{3}{2}}n\sqrt{1 - \cos 2\phi_{30}} \qquad (13)$$

As we shall see, libration rate can cause a potential discrepancy for both a classical (Keplerian) and a TSS orbit determination technique.

Keplerian Orbit Determination

The value of the instantaneous libration rate will then vary from $-\sqrt{3}n$ to $\sqrt{3}n$, depending on initial libration angle and whether the mass is swinging "toward" or "away from" its orbital path. Since the center of mass is in circular orbit, the mean motion n is

7

simply the angular velocity of the center of mass from the above section. Instantaneous libration rate can then be expressed as

$$\dot{\phi}_3 = \pm\sqrt{\frac{3}{2}}\sqrt{\frac{\mu r^2}{(r+\rho_2)^3}}\sqrt{1-\cos 2\phi_{30}} = \beta\sqrt{\frac{\mu r^2}{(r+\rho_2)^3}} \tag{14}$$

where β is a function of ϕ_{30} and can take on values ranging from $-\sqrt{3}$ to $\sqrt{3}$. Inserting this expression into that for v_{m2} above and then into Equation (6) in the previous section yields

$$a* = \frac{r(r+\rho_2)^3}{2(r+\rho_2)^3 - r(r+\beta\rho_2)^2} \tag{15}$$

Applying the condition of re-entry, as in the previous section, we see that the path of the mass will be assessed by a classical orbit determination technique to be a re-entry orbit if

$$\frac{r(r+\rho_2)^3}{2(r+\rho_2)^3 - r(r+\beta\rho_2)^2} < r_a + r_E \tag{16}$$

which simplifies to

$$\frac{\left(1+\dfrac{\rho_2}{r_E+h}\right)^3}{\left(1+\dfrac{\beta\rho_2}{r_E+h}\right)^2} < 1 + \frac{h}{2r_E} \tag{17}$$

The inequality (17) is a function of altitude, tether length (from lower mass to c.m.), and β. Figure 4 shows the value of $\rho_{2,th}$ versus altitude for various values of β (corresponding to various values of initial libration angle). As can be seen here, for a given altitude, the presence of negative libration rate decreases $\rho_{2,th}$ from that of the previous section. That is, because a negative libration rate reduces the mass's total velocity (which is its apparent orbital velocity as predicted by classical means), less tether force is needed to cause its trajectory to be assessed as a re-entry path.

8
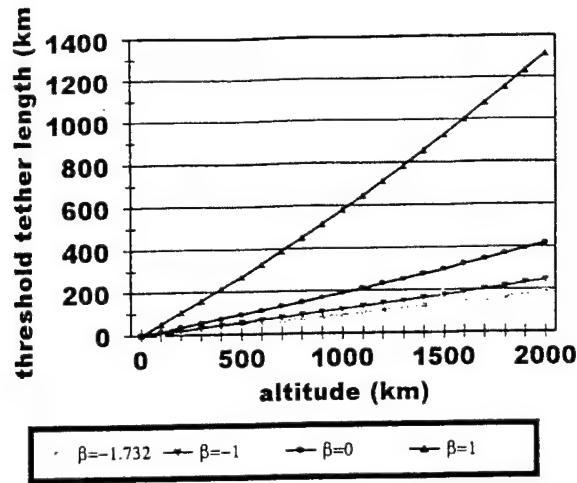
Figure 4. Value of $\rho_{2,\text{th}}$ as a Function of Libration Rate, for Classical Orbit
Determination Applied to Lower Mass.

Considering that libration can contribute so significantly to the discrepancy stated in the Introduction, we hypothesized that libration might possibly cause the same problem for the *upper* mass. That is, although the upper mass's velocity without libration is greater than that for a circular Keplerian orbit at that altitude, libration in the direction opposite the orbital motion may cause enough of a decrease in the mass's total velocity to make it look like an untethered body on a re-entry path. Toward this end, the same investigation performed above for the lower mass was performed for the upper mass. The equation representing a re-entry condition is similar to that above. It was found that this discrepancy *is* possible for the upper mass due to libration, but only for unrealistically long tethers (approximately the same length as the altitude of the mass's orbit!), and at near the maximum possible libration rate.

TSS Orbit Determination

Suppose the TSS orbit determination technique described earlier is estimating the path of the lower mass. This technique provides estimates of position, velocity, and tether force, but not libration rate. Assuming the instantaneous libration angle is small, the velocity of the c.m. can be extrapolated from the estimated velocity of the mass as

$$\dot{v}_{cm} = v_{m_2}\left(\frac{r + \rho_2}{r}\right) \tag{18}$$

or, using the velocity expression of Equation (11) above,

$$\dot{v}_{cm} = \sqrt{\frac{\mu}{r + \rho_2}} + \rho_2\dot{\phi}_3\left(\frac{r + \rho_2}{r}\right) \tag{19}$$

9

where the * indicates the fact that v_{cm} has been arrived at by (incorrectly) assuming no libration. Thus, if libration rate is not accounted for, a state estimate based on observations of the lower mass will cause the TSS to appear to be orbiting faster or slower than it actually is, depending on whether the lower mass is "swinging" in the direction toward, or away from, its orbital motion. If v_{cm}^* is slower than the actual v_{cm} (i.e., negative libration rate), the TSS could in fact appear to be on a re-entry path.

Inserting the expression for v_{cm}^* into Equation (6) in the previous section yields

$$a^* = \frac{(r + \rho_2)}{2 - \left(1 + \frac{\beta \rho_2}{r}\right)^2} \tag{20}$$

Because libration angle is assumed small, the lower mass is said to re-enter if the center of mass comes within a distance ρ_2 of the Earth's surface. Thus, the path of the mass will be assessed as a re-entry orbit if

$$\frac{2(r_E + h + \rho_2)}{2 - \left(1 + \frac{\beta \rho_2}{r_E + h}\right)^2} < 2\rho_2 + 2 r_E + h \tag{21}$$

Again we have an inequality that is a function of altitude, tether length (from lower mass to c.m.), and initial libration angle. Figure 5 charts $\rho_{2,th}$ for various values of h and β. Again we see the negative libration rate decreasing $\rho_{2,th}$, as expected.

In the event that the *upper* mass is being estimated by the TSS orbit determination technique, a similar discrepancy may arise. The equations are not too different from those above, with the re-entry condition being

$$\frac{2(r_E + h - \rho_1)}{2 - \left(1 + \frac{\beta \rho_1}{r_E + h}\right)^2} < 2 r_E + h - \rho_1 \tag{22}$$

where h in this case refers to altitude of the upper mass. Figure 6 depicts this threshold value of tether length, which in this case is $\rho_{1,th}$. Note that at each altitude, threshold tether length for both values of β is slightly less in Figure 6 than in Figure 5. Thus, it is "easier," in terms of less tether force required, for a TSS filtering technique to make a mis-assessment of the path of an upper mass of a TSS, as a result of libration, than for a lower mass.

10
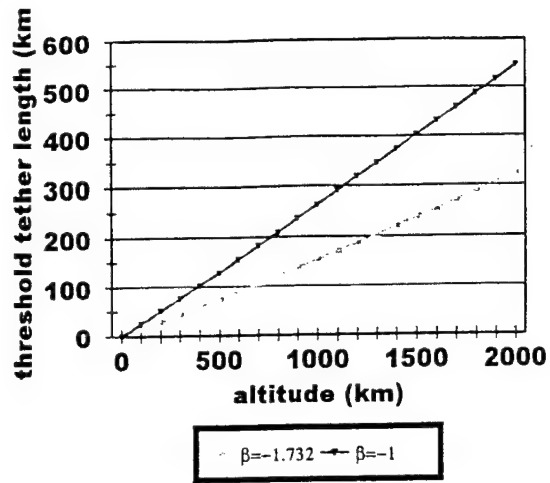
Figure 5. Value of $\rho_{2,th}$ as a Function of Libration Rate, for TSS Orbit Determination.
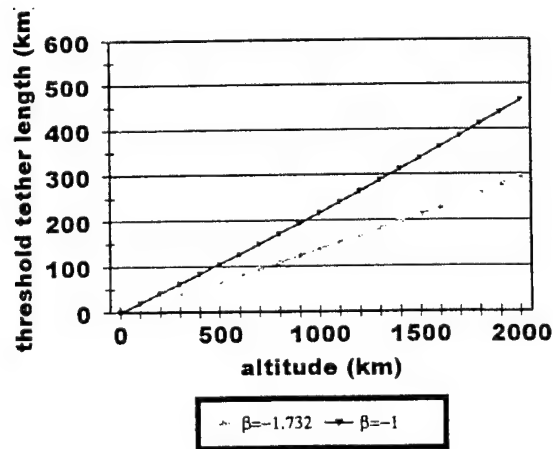
Figure 6. Value of $\rho_{2,th}$ as a Function of Libration Rate, for TSS Orbit
Determination Applied to Upper Mass.

11

ELLIPTICAL MOTION (AT PERIGEE OR APOGEE) WITHOUT LIBRATION

In this scenario assumptions #1, 3, and 4 above are adopted. The TSS center of mass is on an elliptical orbit with semi-major axis a and eccentricity e, and is at the perigee position. This motion is depicted in Figure 7. Then, inserting $r_p = a(1-e)$ into Equation (6), we may express the velocity of the center of mass as
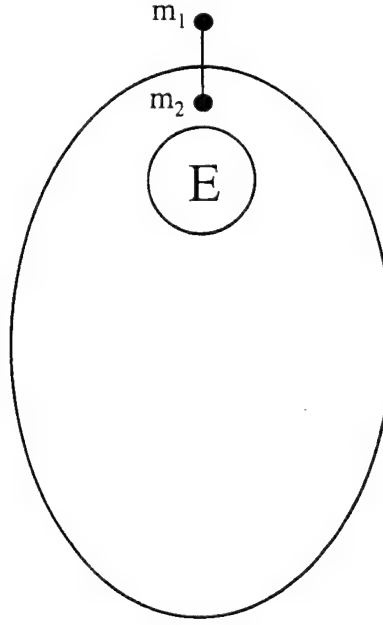
Figure 7. Center of mass in an Elliptical Orbit at Perigee, no Libration.

$$v_{cm} = \sqrt{\frac{\mu}{a} \frac{(1+e)}{(1-e)}} \tag{23}$$

The radius and velocity of the lower mass are

$$r = a(1-e) - \rho_2 \tag{24}$$

$$v_{m_2} = v_{cm} \left(\frac{r}{r + \rho_2}\right) = \sqrt{\frac{\mu}{a} \frac{(1+e)}{(1-e)}} \frac{a(1-e) - \rho_2}{a(1-e)} \tag{25}$$

Inserting these into Equation (6) and rearranging gives

$$a* = \frac{a(1-e) - \rho_2}{2 - (1+e)\left(\dfrac{a(1-e) - \rho_2}{a(1-e)}\right)^3} \tag{26}$$

12

as the "apparent" semi-major axis of the lower mass's orbit, as estimated by a classical (Keplerian) technique. The path of the mass will then be assessed as a re-entry orbit if
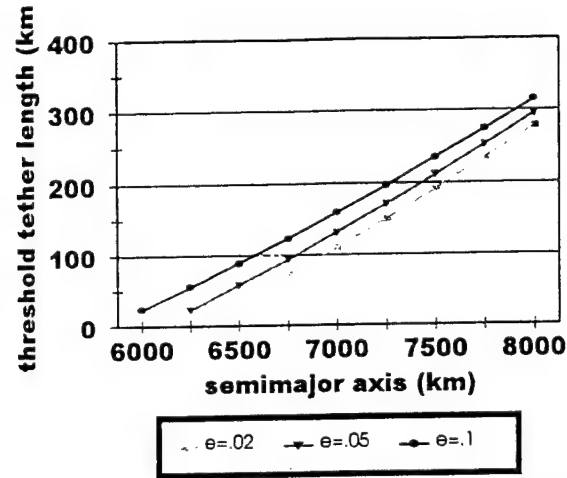
Figure 8. Value of $\rho_{2,th}$, Center of Mass in an Elliptical Orbit at Perigee, no Libration.

$$\frac{2(a(1-e)-\rho_2)}{2-(1+e)\left(\dfrac{a(1-e)-\rho_2}{a(1-e)}\right)^3} < a(1-e)-\rho_2 + r_E \tag{27}$$

This inequality is a function of the semi-major axis of the center of mass, eccentricity of the center of mass, and tether length from the lower mass to the c.m. Figure 8 depicts the value of $\rho_{2,th}$ for various values of a and e.
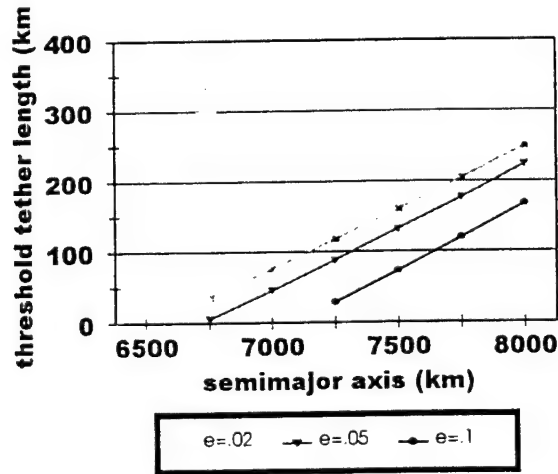
Figure 9. Value of $\rho_{2,th}$, Center of mass in an Elliptical Orbit at Apogee, no Libration.

13

If the center of mass is at its apogee position, the re-entry condition is obtained from the above inequality by interchanging 1+e and 1-e everywhere. The results are in Figure 9. A comparison of the two figures illustrates how increasing eccentricity makes it "harder" to mistake a tethered body's orbit as a re-entry path when the TSS is at perigee, but "easier" to have this discrepancy when the TSS is at apogee. This is likely due to the fact that increasing eccentricity increases the perigee velocity and decreases the apogee velocity, and of course, the slower the orbital velocity at a given position, the greater the chances of re-entry.

GENERAL MOTION OF THE TSS

For the final scenario, the re-entry condition was determined numerically rather than analytically. The model used is described in [3]. Any general orbit of a TSS can be simulated, and both in-plane and out-of-plane libration are accounted for. Thus, *none* of the assumptions listed earlier were adopted in this phase. The investigation proceeded as follows: a set of initial conditions was chosen specifying a particular (elliptical) orbit for the TSS center of mass. Once these variables were fixed, the values of ₋ther length, eccentricity, and initial libration angle—all of which have been shown to have an impact on the re-entry condition—were varied. This generated several cases, which are listed in Table 1. For each case, the TSS motion was simulated for one period (approximately ₋ 5000 sec) and the position and velocity vector of the lower mass were calculated continuously during this time span. From each position and velocity vector, the value of perigee radius *as if the mass were an untethered body exhibiting Keplerian motion* was then calculated. This procedure provided a history of the "perceived r_p" over approximately one-half period of motion of the center of mass for each case. The results for cases A-E are shown in Figures 10-14, respectively. Each plot has the mean radius of the earth marked, in order that it may be clearly seen whether, and at what times during the orbit, the mass is perceived to be on a re-entry path. Clearly, all three parameters that were varied have a significant effect on whether the mass is perceived to re-enter. As expected, when one of the parameters is set to a small or moderate value, another parameter may have to be set rather high in order to bring about the re-entry condition—if it can even do so at all. These figures in many ways corroborate the results from the previous scenarios, which were obtained analytically and under several assumptions.

Table 1. List of Cases for Numerical Results. (For all cases, m_1=100kg, m_2=10kg, perigee radius of TSS orbit = 6600km.)

Case	Tether length (km)	Initial lib. Angle (rad)	Eccentricity
A1	50	.1	0
A2	50	.2	0
A3	50	.3	0
A4	50	.4	0
A5	50	.5	0
B1	20	.3	0
B2	40	.3	0
B3	60	.3	0
B4	80	.3	0
B5	100	.3	0
C1	50	.1	.1
C2	50	.2	.1
C3	50	.3	.1
C4	50	.4	.1
C5	50	.5	.1
D1	20	.3	.1
D2	40	.3	.1
D3	60	.3	.1
D4	80	.3	.1
D5	100	.3	.1
E1	50	.1	.05
E2	50	.2	.05
E3	50	.3	.05
E4	50	.4	.05
E5	50	.5	.05

Finally, for each of the above scenarios, it is instructive to consider what would occur if the tether were to be severed, either intentionally or unintentionally. In such a case, assuming the tether has little effect on either mass once it is cut, the two masses will then exhibit Keplerian motion, with their orbits determined by their position and velocity at the time the tether was cut. The path of the observed mass as predicted by a classical (Keplerian) technique, which was incorrect in each of the above scenarios, will now be the *correct* path of the object. Further, the object's orbital velocity will be the sum of its orbital velocity as part of the TSS, plus any significant component of librational velocity the object may have when the tether breaks. (Recall that, at the time the object was tethered, libration rate did *not* contribute to the object's gross orbital motion.)

CONCLUSIONS

The problem of quickly identifying whether an object in near-Earth orbit is a candidate to re-enter the Earth's atmosphere has been considered. Several particular cases of tethered satellite motion were investigated, assuming an orbit determination method based on a two-body ("Keplerian") motion model, as well as one based on a non-librating tethered satellite model. It was found that both the force due to the tether and the librational motion of a TSS can play a significant role in causing a body to appear as though it were on a re-entry path, even though it in fact is not. Consequently, an orbit determination method that includes libration of a tethered system must be used, and over a sufficiently long period of time, to assure the unambiguous determination of eminent re-entry of a tethered satellite.

ACKNOWLEDGEMENT

REFERENCES

1. Hoots, F. R., Roehrich, R. L., and Szebehely, V. G., "Space Shuttle Tethered Satellite Analysis," Directorate of Astrodynamics, Peterson AFB, CO, August 1983.
2. Asher, T. A., D. G. Boden, and R. J. Tegtmeyer, "Tethered satellites: The orbit Determination problem and Missile Early Warning Systems,"AIAA PAPER 88-4284, *AIAA/AAS Astrodynamics Conference*, Minneapolis, MN, August 15-17, 1988.
3. Cho, S., J. E. Cochran, Jr., and D. A. Cicci, "Identification and Orbit Determination of Tethered Satellite System," AAS 98-101, AAS/AIAA Space Flight Mechanics Meeting, Monterey, CA, Feb. 9-11, 1998.
4. Cho, S., J. E. Cochran, Jr., and D. A. Cicci, "Approximate Solutions for Tethered Satellite Motion," AAS/AIAA Space Flight Mechanics Meeting, Breckenridge, CO, Feb. 7-10, 1999.
5. Cho, S., J. E. Cochran, Jr., and D. A. Cicci, "Modeling Tethered Satellite Systems for Detection and Orbit Determination," AAS/AIAA Astrodynamics Specialist Conference, Girdwood, AK, Aug. 16-19, 1999.
6. Cicci, D. A., Lovell, T. A., and Qualls, C., "A Method for the Identification of a Tethered Satellite," Paper AAS 99-196, presented at the AAS/AIAA Space Flight Mechanics Meeting, Breckenridge, CO, Feb. 7-10, 1999.
7. "TiPS: Tether Physics and Survivability Satellite Experiment" web page, Naval Center for Space Technology, http://hyperspace.nrl.navy.mil/TiPS/data.html
8. Beletsky, V. V., and Levin, E. V., *Dynamics of Space Tether Systems*, Vol. 83, Advances in the Astronautical Sciences, AAS, San Diego, CA, 1993, pp. 76.
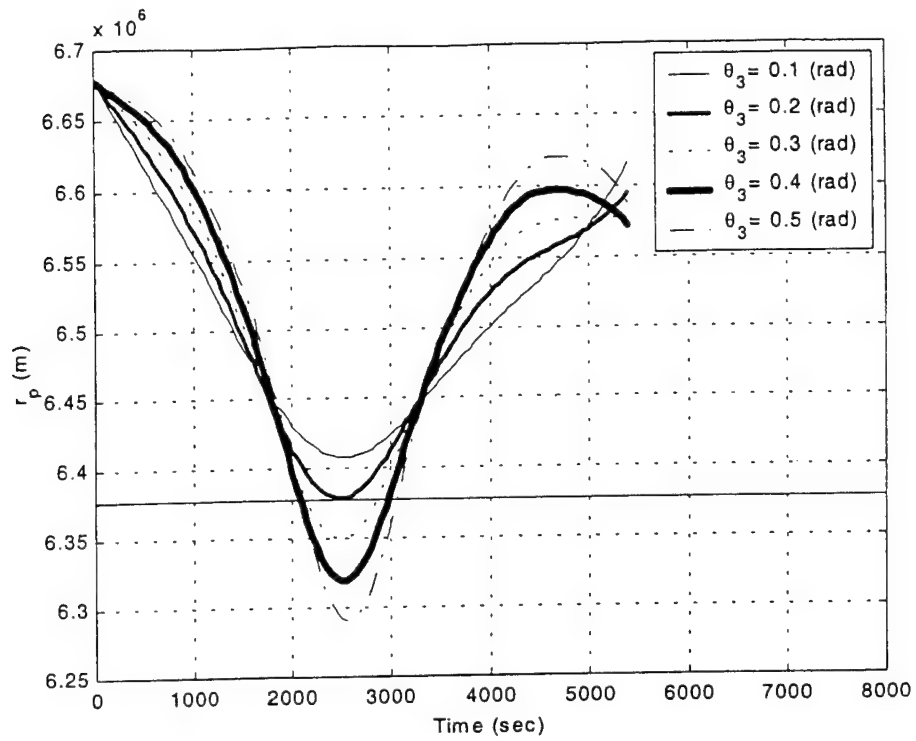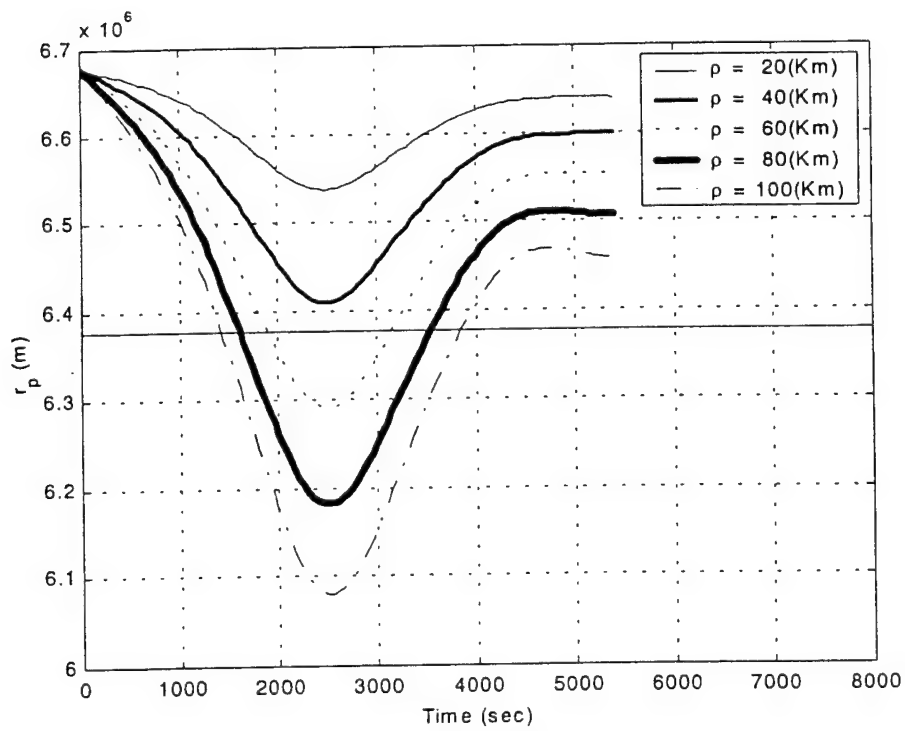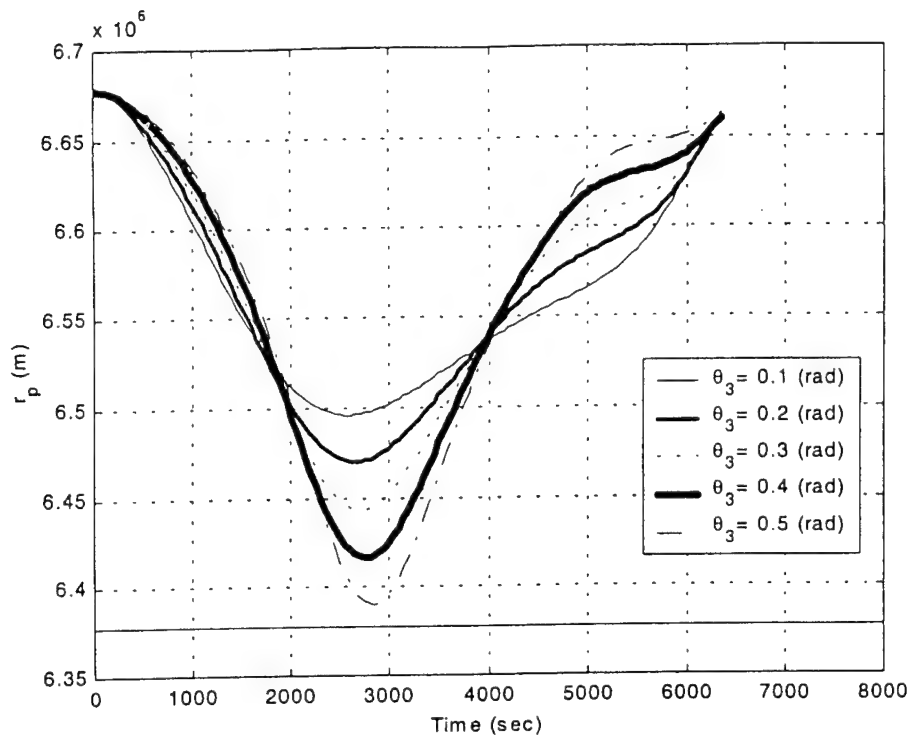
Figure 10. Case A Results.

Figure 11. Case B Results.
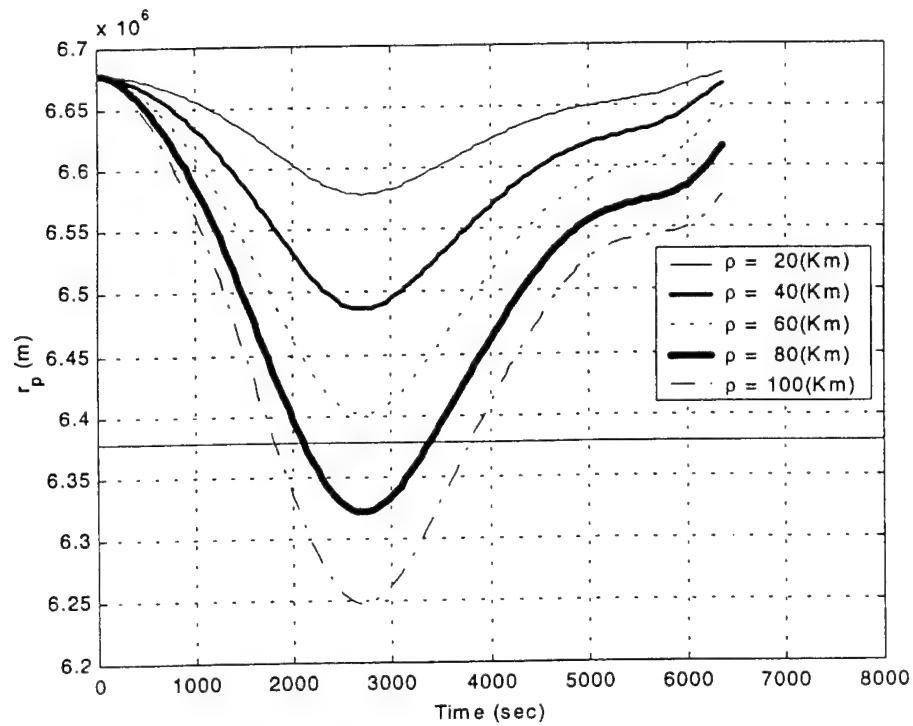
17

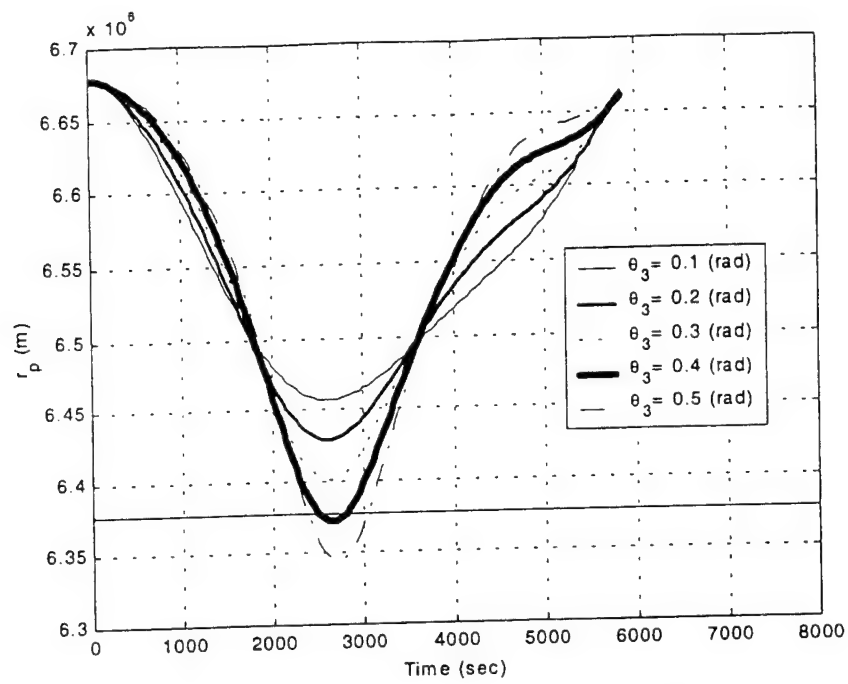Figure 12. Case C Results.

Figure 13. Case D Results.

18

Figure 14. Case E Results.

A COMPARISON OF ORBIT DETERMINATION AND LONG-TERM PREDICTION METHODS FOR TETHERED SATELLITE SYSTEMS

T. A. Lovell,[#] J. E. Cochran, Jr.,[*] and D. A. Cicci[**]
Auburn University, Alabama 36849-5338

ABSTRACT

A renewed interest in the deployment of tethered satellites has motivated recent research with regard to both the modeling of the dynamics of a tethered satellite system and the development of filtering techniques for the orbit determination and long-term prediction of the motion of such a system. An issue that is pertinent to both of these areas is the formulation of the dynamic model to be employed by the filter. Because every dynamic model embodies a tradeoff between accuracy and complexity, the most appropriate model to include within the filter is that which represents the best compromise in terms of these two qualities. In this paper a standard batch filter algorithm is used, within which several different choices of dynamic models are investigated. These candidate models vary in complexity in terms of the way various physical phenomena are accounted for in the equations of motion. In one of the models, an artificial neural network is used to emulate the tethered satellite dynamics. The performance of these candidate schemes is then compared in terms of orbit determination accuracy, long-term orbit prediction accuracy, computational speed, robustness in the face of sparse or noisy observation data, and overall ease of use.

INTRODUCTION

It is well-krc.wn that the motion of each satellite in a tethered satellite system (TSS) deviates from the traditional Keplerian-like motion of a single untethered body [1]. Although the motion of the center of mass of a TSS is nearly Keplerian, this point in space cannot be physically observed by satellite tracking equipment. Rather, it is only the end masses of the TSS that can be observed. Consequently, classical orbit determination techniques that can accurately identify and predict the motion of untethered objects, will incorrectly predict the path of a tethered body [2-3]. In order for a filtering technique to successfully perform the task of TSS orbit determination, the dynamic model employed within the filter must accurately represent the numerous phenomena that influence TSS motion. For example, a filter incorporating a model that includes the tension force in the tether may inaccurately assess the system's motion if it does not account for libration of the TSS as well.

The challenge, then, is to determine as much information as possible regarding the orbital motion (e.g., position and velocity at epoch time), librational motion, and physical

characteristics (e.g., tether length, mass ratio) of the system as a whole based only on observations (e.g., range, azimuth angle, elevation angle) of one of the end masses. With this goal in mind, extensive model development for a generic TSS configuration has been performed in [4-6], while the work of [7-11] focuses on the design of filtering techniques for orbit determination. Although most of the filters detailed therein are intended simply for the quick identification of an orbiting object as tethered or untethered, the need is also discussed for an orbit estimate encompassing longer observation spans and lending itself to prediction of the system's future motion. It is this long-term filtering task that will be investigated here. As such, several "candidate" filtering techniques are proposed, each of which represents an extension of the work detailed above.

One of the candidate filters is based on a decidedly different approach to the problem. This filter will employ an artificial neural network (ANN) to represent the dynamics of a TSS. In the past few years, ANN's have been used for an increasing number of applications in several engineering fields [12-13]. Based on the major fundamental strengths of ANN's (e.g., model emulation, pattern recognition, outcome prediction) they would seem to be ideal for such tasks as "recognizing" the orbital path of a satellite, predicting its future motion, and determining whether it is a single body or one of two or more bodies tethered together.

In this paper, a brief background of the previous model and filtering development is first given. Then the candidate filtering schemes currently under study are discussed. This is followed by a description of the test cases used to demonstrate each filter's performance. The results of these tests are then presented, and an assessment of the comparative feasibility of the various filters is made.

GENERAL MODEL DEVELOPMENT AND FILTERING SCHEME

The model development of [4-5] assumed a TSS consisting of two point masses connected by a massless inextensible tether. This formulation employs a sufficient number of states to account for the motion of the system as a whole, including both the gross orbital motion and in-plane and out-of-plane librational motion. The state variables for orbital motion closely resemble standard orbit elements for untethered satellites. The forces assumed on each mass include the two-body (inverse-squared) gravitational force of the Earth, the gravitational force due to the oblateness of the Earth, and the tension force in the tether. In [6] the model was extended to account for the aerodynamic drag force on both the masses and the tether. Figure 1 is a basic sketch of a TSS configuration pertinent to the aforementioned development.

The orbit determination filtering scheme detailed in [7-9] is of the "quick-look" variety, i.e., designed to process a very short arc of observational data (usually a small fraction of a full orbital period). For the dynamic model contained in this type of filter, the orbital motion state variables consist of position and velocity of the observed mass in cartesian coordinates. The estimate obtained by the quick-look filter consists of the state values at epoch time, plus a calculation of the libration angle, which is assumed constant. For a short observation time, this assumption may be valid. However, for long-term prediction of TSS motion, it is expected that a filter must account for the periodic changes in the libration angle, which would necessitate the inclusion of a time-varying tether force in the model. Toward this end, a batch-type filtering scheme was introduced

in [10] that estimates position and velocity of the observed mass, libration angle and rate, and the distance from the observed mass to the TSS center of mass (which is proportional to tether length). Although this too is a cartesian formulation, it draws heavily on the development of [4-5]. The methodology of [10] involved obtaining an estimate with a quick-look filter for a short arc of observational data; then using a long-term filter to process a longer arc of data, with the quick-look estimate serving as the initial guess of the epoch conditions. The long-term filter then yields both a refined estimate of the state of the TSS and a prediction of its long-term behavior. These two tasks are depicted in the block diagram of Figure 2.

The analysis of this paper will determine the best possible long-term filtering technique for performing the tasks indicated in Figure 2. A number of candidate filters will be formulated. The "baseline" filter is similar to that of [10] and contains a dynamic model that accounts for in-plane libration, the two-body gravitational force of the Earth, and the tension force in the tether. The other candidate filters will function in generally the same way as the baseline, but will contain dynamic models of varying complexity. These include:

-A model that accounts for the phenomena in the baseline filter, plus the gravitational force due to the oblateness of the Earth
-One that accounts for the phenomena in the baseline filter, plus aerodynamic drag (on both the satellites and the tether)
-One that accounts for the phenomena in the baseline filter, plus out-of-plane libration of the TSS
-One that encompasses ALL of the aforementioned phenomena
-One that employs an artificial neural network representation of TSS dynamics

DISCUSSION OF TEST CASES

In order to demonstrate the performance of the various techniques, each will be employed in a battery of test cases, involving both simulated observational data and actual TSS data. In each case, the observations will be of only one of the end masses and will be in the form of range, azimuth angle, and elevation angle. To generate the simulated data, the formulation of [6] will be used, which represents the most comprehensive model of the development alluded to above ([4-6]). This model encompasses such features as in-plane and out-of-plane libration, the force due to the oblateness of the Earth, and aerodynamic drag. Each data set will be generated with the same set of initial conditions, except for the following parameters, which will be varied with each case: tether length, initial altitude of the observed mass, initial in-plane libration angle, initial out-of-plane libration angle, total observation time, and amount of observation error added to the data. Each of these parameters will be varied over a particular range one at a time, with the other parameters remaining constant. In this way a matrix of test cases will be built up. Table 1 lists both the minimum and maximum value each parameter is expected to take on.

Table 1.

	minimum value	maximum value
tether length	1km	100km
initial altitude (observed mass)	20km	200km
initial in-plane libration angle	5°	20°
initial out-of-plane libration angle	5°	20°
observation error (range/angles)	5m/0.002°	50m/0.02°
total observation time	1/4 orbital period	1 orbital period

EXPECTED RESULTS

A total of six candidate filters are proposed, including the baseline scheme. Each filter will be used to process the observation data in the test cases outlined above and then evaluated in terms of the following performance indices:

-ability to yield a state estimate of the system (i.e., successful convergence)
-computation time required to yield a state estimate
-accuracy of the estimate

In addition, once a state estimate in each case is obtained, these values will be used to propagate the motion of the TSS for several orbital periods, using the dynamic model contained within the filter. Each filter can then be further evaluated in terms of the following:

-computation time required to yield a prediction of the "future" orbit
-accuracy of the predicted orbit

From these results, very definitive conclusions can be drawn regarding which phenomena (e.g., in-plane or out-of-plane libration, aerodynamic drag) it is necessary to account for in the dynamic model contained within a filtering scheme, and more generally, what constitutes the most feasible filtering technique for orbit determination and long-term motion prediction of tethered satellites.

REFERENCES

1. Beletsky, V. V., and Levin, E. V., *Dynamics of Space Tether Systems*, Vol. 83, Advances in the Astronautical Sciences, AAS, San Diego, CA, 1993, pp. 76.
2. Hoots, F. R., Roehrich, R. L., and Szebehely, V. G., "Space Shuttle Tethered Satellite Analysis," Directorate of Astrodynamics, Peterson AFB, CO, August 1983.
3. Asher, T. A., D. G. Boden, and R. J. Tegtmeyer, "Tethered satellites: The orbit Determination problem and Missile Early Warning Systems," AIAA PAPER 88-4284, presented at the AAS/AIAA Astrodynamics Conference, Minneapolis, MN, August 15-17, 1988.
4. Cochran, J. E., Jr., Cho, S., Cheng, Y-M., and Cicci, D. A., "Dynamics and Orbit Determination of Tethered Satellite Systems," *Journal of the Astronautical Sciences*, Vol. 46, No. 2, pp. 177-194, April-June 1998.
5. Cho, S., Cochran, J. E., Jr., and Cicci, D. A., "Identification and Orbit Determination of Tethered Satellite System," AAS 98-101, AAS/AIAA Space Flight Mechanics Meeting, Monterey, CA, Feb. 9-11, 1998.
6. Cochran, J. E., Jr., Cho, S., Lovell, A., and Cicci, D. A., "Evaluation of the Information Contained in the Motion of One Satellite of a Two-Satellite Tethered System," *Journal of the Astronautical Sciences*, Vol. 48, No. 4, October-December 2000.
7. Kessler, S. A., and Cicci, D. A., "Filtering Methods for the Orbit Determination of a Tethered Satellite," *Journal of the Astronautical Sciences*, Vol. 45, No. 3, pp. 263-278, July-September 1997.
8. Cicci, D. A., Lovell, T. A., and Qualls, C., "A Method for the Identification of a Tethered Satellite," Paper AAS 99-196, presented at the AAS/AIAA Space Flight Mechanics Meeting, Breckenridge, CO, Feb. 7-10, 1999.
9. Cicci, D. A., Qualls, C., and Lovell, T. A., "A Look at Tethered Satellite Identification Using Ridge-Type Estimation Methods," Paper AAS 99-415, presented at the AAS/AIAA Astrodynamics Specialist Conference, Girdwood, AK, Aug. 16-19, 1999.
10. Cicci, D. A., Cochran, J. E., Jr., Qualls, C., and Lovell, T. A., "Quick-Look Identification and Orbit Determination of a Tethered Satellite," Paper AAS 01-232, presented at the AAS/AIAA Space Flight Mechanics Meeting, Santa Barbara, CA, Feb. 11-15, 2001.
11. Qualls, C., and Cicci, D. A., "Preliminary Orbit Determination of a Tethered Satellite," Paper AAS 00-191, presented at the AAS/AIAA Space Flight Mechanics Meeting, Clearwater, FL, Jan. 23-26, 2000.
12. Faller, W.E., Smith, W.E., and Huang, T.T., "Applied Dynamic System Modeling: Six Degree-of-Freedom Simulation of Forced Unsteady Maneuvers Using Recursive Neural Networks," presented at the 35th AIAA Aerospace Sciences Meeting, Reno, NV, 1997.
13. Jaw, L.C., "Neural Network Modeling of Engine Tip Clearance," presented at the 33rd AIAA Joint Propulsion Conference, Seattle, WA, 1997.
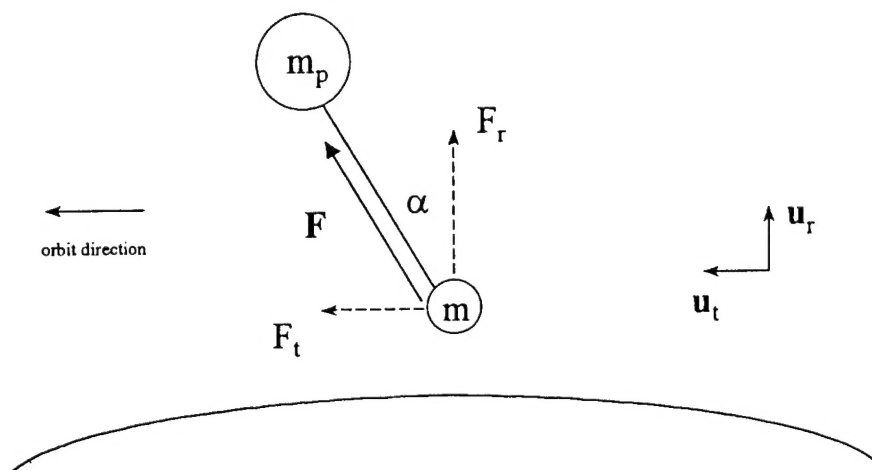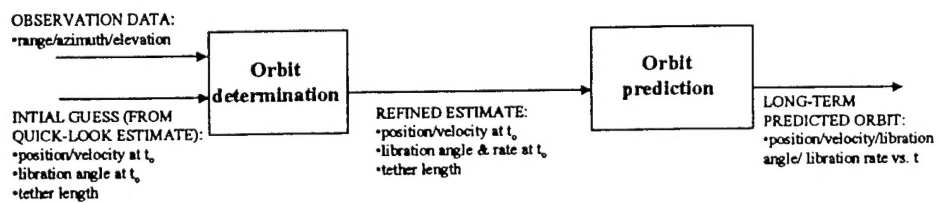
Figure 1. TSS Model.

Figure 2. Orbit Determination and Prediction Tasks as Performed by a Long-Term Filter.